HIGH RESOLUTION PALAEOENVIRONMENTAL ANALYSES OF COASTAL WETLAND SEDIMENTS FROM SOUTH EAST SICILY

A thesis submitted for the degree of Doctor of Philosphy

by

Simon David Turner

Department of Geography & Earth Sciences, Brunel University

October 1999 2000

ABSTRACT

HIGH RESOLUTION PALAEOENVIRONMENTAL RECORDS OF COASTAL WETLAND SEDIMENTS FROM SOUTH EAST SICILY.

by Simon David Turner

This study examines the sedimentology of salt marshes and lagoonal sediments from coastal wetland settings in south east Sicily. Palaeoenvironmental studies have been carried out to assess the recent evolution of disturbed coastal wetlands, and to examine the sensitivity of these depositional settings in recording historical environmental change.

The evolution of Recent coastal wetland environments in the region can be related to anthrpogenic disturbance phases in drainage catchments due to changes in land-use. Archaeo-historical changes to the coastal topography are identified, in relation to the development of present-day coastal wetland areas in south east Sicily. The impact of 19th-early 20th century salt workings is recognised as a major and continuing factor in the condition of present day wetlands.

Measurement of ^{210}Pb, ^{137}Cs, pollen content, major and trace elements, loss on ignition and other sedimentological features generates valuable information on depositional processes that have occurred over the last 100-150 years. Sub-surface sedimentological changes recognised in cores extracted from shallow sediment sequences (< 50 cm) can be related to coastal wetland land-use changes and hydrological flood events. A 30 cm depth sediment sequence analysed from the Mulinello estuary records the interaction between estuarine channel processes, following embankment construction and the variable influence of catchment-generated flood episodes. A clearly identifiable change in accretion and core composition occurred during the mid-late 1940's and early 1950's which coincides with recorded peaks in monthly rainfall totals. The impact of marsh development, flooding and recovery is highlighted by the variable abundance of dominant pollen types. A marked increase of ruderal pollen types during periods of channel-dominated deposition is contrasted with an abundance of halophyte pollen during low-energy phases of organic marsh sedimentation.

The two lagoonal cores from Pantano Piccolo record successive hydrological changes, due almost certainly to artificial enclosure in the late 18th to early 19th century. The apparent change in water levels dramatically affected marginal salt marsh communities. Artificial impoundment generated a lagoonal setting conducive to the accumulation of local and extra-local sources of pollen, reflecting the re-establishment of salt marsh vegetation. Although

largely separated from catchment-overland flow patterns during the 20th century, large magnitude rainfall events were recorded in lagoonal accretion patterns. ^{210}Pb-derived sediment accretion rates and estimated pollen accumulation rates have enabled the response and sensitivity, of coastal wetland and nearby plant communities to phases of disturbance and recovery, to be determined. Due to artificial impoundment of the lagoon, fringing-halophyte communities and organic accretion migrated outwards to occupy their present marginal position.

To aid the interpretation of pollen encountered in estuarine and lagoonal settings, soil samples from nearby land surfaces around Pantano Piccolo were analysed for pollen content. Soil surfaces reflected the dominance of gravity fallout from surface vegetation and the accumulation of pollen from regional-atmospheric sources.

The reliability of the multi-proxy approach and palaeoenvironmental analyses used, indicate that coastal wetlands in south east Sicily have evolved in a dynamic system of punctuated equilibria, due to climatic events and human activity over the last 100-150 years. Their current status reflects the continued pressure on coastal systems by anthropogenic development and recent conservation measures.

CONTENTS

CONTENTS

LIST OF FIGURES

Chapter Six

Chapter Seven

LIST OF TABLES

LIST OF PLATES

LIST OF APPENDICES

ACKNOWLEDGEMENTS

The completion of this thesis would not have been possible without the assistance provided by various people and institutions. Firstly I would like to thank Brunel University for providing the funding that made this work possible. The help and encouragement provided by all of the staff in the Department of Geography & Earth Sciences has been greatly appreciated, with special thanks to Dr. A. Patterson for maintaining a link to the real world. I am indebted to Dr. A. B. Cundy, Dr. P. E. F. Collins and Dr. C. Firth for support, practical advice and assistance throughout this period of research. Special thanks are due to Dr. I. W. Croudace at the Geosciences Advisory Unit at the Southampton Oceanography Centre for the use of the XRF and obtaining geochemical data. I would like to thank various field assistants for their time spent watching a fool wade around in slightly warm mud; thank you Stella Kortekaas, Sean McHugh and Martyn Graham.

This research would certainly not have been possible without the permission of the Ispettorato Ripartimentale delle Foreste Siracusa, who permitted access to the Vendicari reserve in south east Sicily.

Finally my thanks and love go to Sherie and my family who have been continually supportive and encouraging during the last few years. This thesis is dedicated to Patrick and his certain future with a close affinity to mud.

Chapter One

Introduction to the Study

1.1 Introduction to the Study

Present day salt marshes and coastal wetlands are threatened by continued human development and the potential future impact of predicted sea level changes in the next century (Tooley & Jelgersma, 1992). In the Mediterranean region where the human impact on the environment, particularly on fluvial and coastal systems has been extensive, coastal wetlands developed at the interface of these two systems have had to adjust to new hydraulic regimes imposed by anthropogenic controls.

The following study examines the palaeoenvironmental record of wetland sediments from estuarine and lagoonal settings in the coastal zone of south east Sicily. High resolution, multi-proxy sedimentological analyses were conducted on a number of sediment cores to assess the recent environmental evolution of present day microtidal, estuarine and lagoonal salt marsh habitats and the effectiveness of palaeoenvironmental investigation techniques in disturbed coastal wetland settings.

Since the timescale over which human activity, in conjunction with the susceptible terrain and climate characteristic of the Mediterranean has affected the evolution and interaction of fluvial and coastal processes, present day coastal wetlands should exist in dynamic equilibrium with the cumulative effect of anthropogenic and natural environmental factors. How dependent the evolution of present day wetland communities in south east Sicily has been on a variety of factors, particularly direct local anthropogenic controls, more distant anthropogenically influenced factors or non-human affected processes, e.g. neotectonic motion, has important implications for the continued existence of coastal wetlands in the Mediterranean.

Coastal wetland sediment sequences can provide high resolution records of material inputs from coastal and terrestrial sources, provided that the supply of materials to the wetland has been effectively continuous and there has been little in the way of post-depositional mobility. To determine these effects, radiometric dating techniques of short-lived isotopes (^{210}Pb and ^{137}Cs) are used in this study to provide a chronological control of variations in core sedimentology. Sediment accumulation rates calculated by radiometric dating for the sequences used in this study, provide a record of depositional changes over the last 100-150 years; a period that has seen extensive land use changes in upstream catchments and widespread disturbance to low-lying coastal areas occupied by present-day coastal wetlands.

1.2 Site selection process

The south east region of Sicily was identified prior to this study (Firth *et al.* 1996; Stewart *et al.* 1997) as being under-represented in records of Holocene-Recent sea level changes. The difference in coastal tectonic regime between north east and eastern Sicily (neotectonic uplift) down to Augusta-Siracusa, and the south east corner of the island (neotectonic stability-net subsidence) was identified as a limit to further investigation of measuring elevated Holocene coastal features. Initial results from the preliminary investigation of a depositional coastal wetland (Cundy *et al.* 1998) at the River Mulinello estuary at Augusta (15°15'E 37°15'N) generated the stimulus for further research (this study included) into the Holocene evolution of coastal depositional settings in south east Sicily.

During fieldwork the suitability of wetland sites for palaeoenvironmental research was based on four main criteria: firstly, that the depositional setting appeared active (to permit ^{210}Pb dating); that the site has remained affected by either/or coastal and hydrological processes (generating a definable stratigraphy); at the site or in the locality, archaeological or historical evidence of occupation/land-use existed; and finally that core material was readily extractable. As disturbance was likely to have been an inherent controlling factor during the accretion of the studied sequences, a distinct aim of this study was to test the effectiveness of recognised palaeoenvironmental techniques in recording dynamic, short-lived environmental changes. These criteria and the notion that sea level change and other broader scale environmental controls on deposition, could only be identifiable if other local effects were accounted for, provided the initiative to find suitable coastal wetland settings in southern and eastern Sicily.

At the River Platani coastal floodplain, on the south coast of Sicily, near Agrigento (Figure 1.1.) coring took place at the wetland to the rear of the beach, developed in a back barrier environment. The artificially channelised and intensively cultivated floodplain is overlooked by the Ancient Greek (6th century BC) archaeological site *Heraclea Minoa.* Short cores (40 cm) at the river mouth comprised of sand and mud, probably related to variations in channel-flooding and the construction of a barrier across the river mouth during periods of low discharge/high wave activity. Coring also took place inland away from the main meandering channel in a preserved cut-off channel. A thick (3 m) sequence of alluvial sediments extracted from the site analysed for loss on ignition, indicated an initial period of organic-enhanced accretion followed by the deposition of low-organic content alluvium. Initial pollen investigations revealed that the sediments were dominated by *Pinus* and Lactuceae, reflecting the sites position near a coastal pine plantation and the

Figure 1.1 Location map of Sicily (inset) and core extraction sites

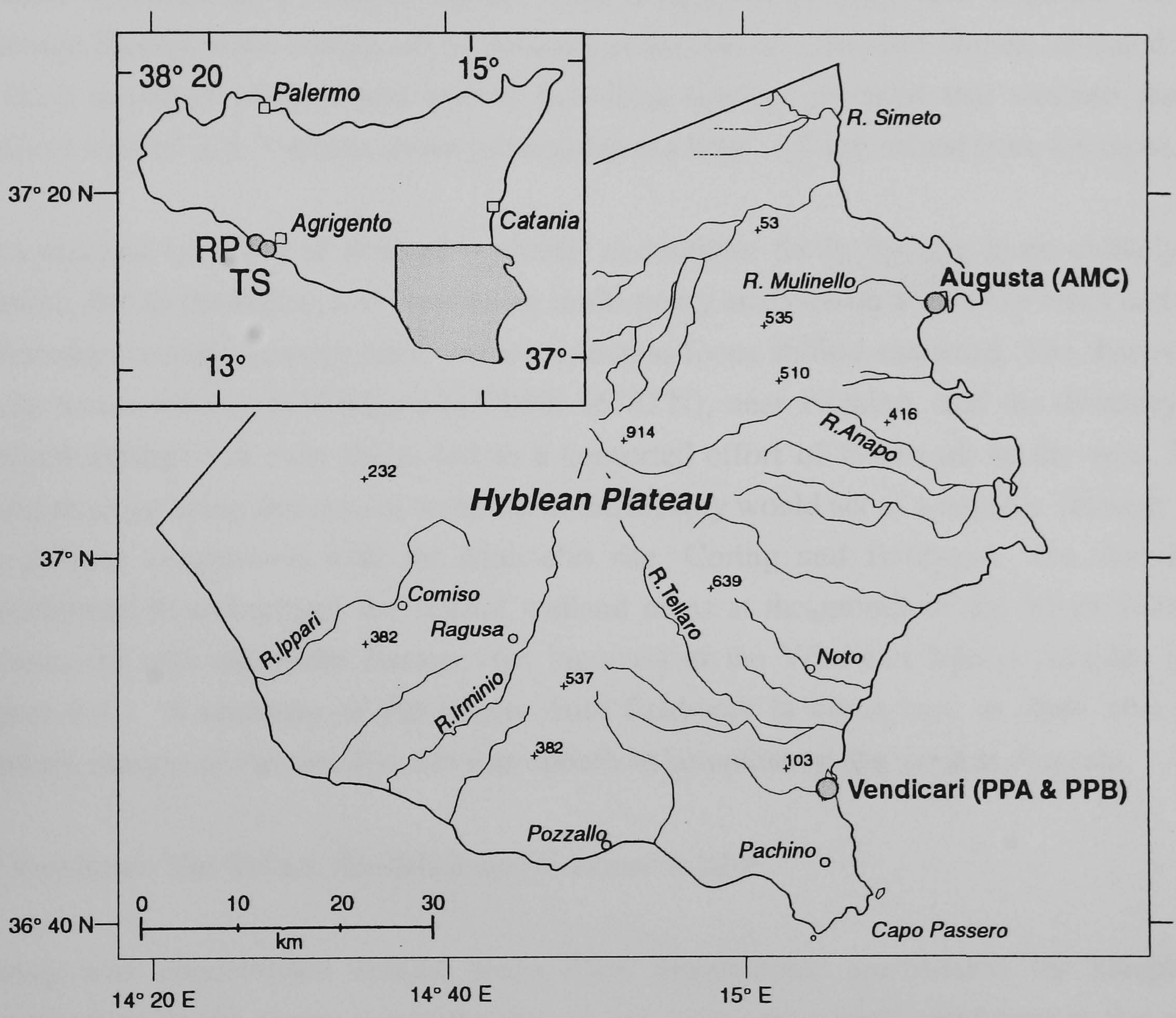

Spot heights in m

○ Study sites and core abbreviations

RP River Platani

TS Torre Salso

sites fluvial-dominated setting. Problems in the retrieval of surface sediments, the logistics of analysing metre scale cores at a high resolution (1 cm) and the scale of the Platani catchment/local alluvial-coastal sediment architecture (in relation to identifying and attempting to correlate local/regional environmental changes with depositional records) dissuaded further sedimentological investigations at the site for this thesis.

A riparian wetland site (Torre Salso) was also investigated in southern Sicily, near to Agrigento, 8 km south east of the River Platani (Figure 1.1.). Although containing a wetland flora typical of coastal halophyte communities, the brackish-saline nature of the wetland appeared to be caused by the local (evaporite) geology and impeded coastal drainage. Coring at the margin of the wetland, at the foot of cultivated slopes, revealed a 2 m thick sequence of mud and gravel. Levelling surveys revealed that wetland marsh surfaces existed at 6-7 metres above present day sea level, 1-2 km inland from the coast.

As a regional synthesis of wetland evolution in southern Sicily became more unlikely to achieve, due to the logistics of conducting multi-proxy analyses on a series of cores and the differences in scale between sites, the site-selection focus shifted eastward. The discovery of the nature reserve at Vendicari (15°05'E 36°47'N), near Pachino, and the diversity of wetland settings that exist there, led to a concerted effort of fieldwork in the area. The initial strategy being that coastal wetlands in the locality would act as a suitable (though not too distant) comparison with the Mulinello site. Coring and fieldwork was therefore concentrated in and around the coastal wetland areas at the mouth of the River Tellaro, Calamosche and within the *Pantani* (or lagoons) of the Vendicari lagoon complex (see Figure 6.4.). A summary of the results from fieldwork is given here to show how the northern margin of Pantano Piccolo was chosen to complement the work at Augusta.

(a) Vendicari: The Tellaro floodplain and Calmosche inlet.

Coring was concentrated around water filled depressions, surrounded by halophyte communities, in the centre and to the rear of the dune and coastal sand area at the river mouth of the Tellaro floodplain. A number of morphological features in the area at the rear of the beach suggested a past channel configuration/ contemporary flood outlet of the embanked Tellaro channel. Ponds and depressions surrounded by halophyte vegetation exposed in their banks, sequences of grey clay-rich mud. Coring in the area was limited seaward by beach/dune sand and landward by walled and cultivated fields, resulting in a number of cores being investigated on a W-E transect and others scattered around the site. Vertical changes in sediment sequences were capable of being traced across the site. Similar to the Mulinello estuary, deeper cores revealed a sequence of fine-grained organic and clay-rich muds apparently deposited in a low-energy coastal environment. Due to the

environmental setting and historical background to the site it was assumed be that these sequences represented a past period of more dynamic estuarine-floodplain period of the Tellaro outlet (see Section 4.12.).

Attempts at developing a stratigraphy for the Calamosche coastal inlet (see Fig. 6.4.) repeatedly failed, due to the abundance of sand and varying groundwater levels. Preliminary coring in September 1996 was hindered by sand and saturated conditions at depth, retrieving dark brown, peaty mud overlain by dune sand. On a return to conduct more extensive stratigraphic studies in April 1998, winter-spring precipitation had raised the water table to form open pools. Apart from the difficulty in conducting coring in open water, the now completely saturated overlying sand prevented core penetration in the rear beach area due to sand continually entering the sides of the borehole, when the gouge was retracted. A cored transect attempted in April 1998, N-S across the inlet retrieved only dune sand.

At both the Tellaro floodplain and Calamosche it was clear that fine-grained and organic sediments were representative of historical coastal environments. It was also apparent that because of this, their suitability for reflecting active coastal wetland deposition and recent environmental changes was reduced.

(b) Vendicari: Pantano Sichilli, Pantano Vendicari and Pantano Grande (Fig. 6.4.)

A number of exploratory cores were undertaken around the Vendicari lagoons to determine suitable sites for further investigation. Pantano Grande was not investigated due to restricted access, enforced so as to prevent disturbance to migratory and native wildfowl.
Between Pantano Grande and Pantano Vendicari, ground conditions were unfavourable for the gouge collection of sediments; in the area between and the back-barrier dune lagoonal area of Pantano Vendicari due to saturated sand and in Pantano Sichilli, due to dried and hardened lagoonal muds.
A mudflat exposed at the landward extent of Pantano Sichilli, during low water levels in September 1996, was investigated with a number of shovel-dug pits. A 45 cm depth monolith was removed, which comprised of homogenous brown-grey mud, with abundant *Cerastoderma glaucum* valves and other shell fragments. The hardened mud had developed a fractured fabric, presumably as a result of successive seasonal exposure and inundation, maintaining sun-crack tensional features in the sediment fabric. This sediment fabric and the abundance of shell material (i.e. active bioturbation) through the core was felt to be disadvantageous for time-depth signatures in the sequence.
The cores extracted from the northern margin of Pantano Piccolo (see section 6.2) were therefore viewed initially as a compromise; between extracting longer term (and possibly

fragmentary) records of coastal change and generating a comparable record with the Augusta-Mulinello core. The comparative ease with which complete surface-to depth sequences of soft mud were extracted was a significant factor in using cores from Pantano Piccolo for further sedimentological analyses.

Though the contemporary environment suggested that a coastal wetland had existed at the setting for some time (allowing ^{210}Pb to be used and a before-present chronology to be developed), the visible stratigraphy of the cores indicated that the setting had undergone significant depositional changes in the recent past. Walls and structures in fields surrounding the lagoon and within the lagoon itself were taken as evidence of historical land-use in the local area. Archaeological and historical remains in the vicinity of Vendicari, were considered to have ensured that the setting had also been affected (directly and indirectly) by human activity for a considerable period of time.

1.3 Objectives

The objectives of this thesis are therefore:

- to assess the applicability of a multi-proxy approach combining stratigraphic, ^{210}Pb and ^{137}Cs analyses, pollen and sediment geochemistry analyses to provide data on recent coastal wetland evolution in SE Sicily.
- to interpret this data in relation to temporal patterns of wetland environmental change and their recent dynamics
- to use records of environmental change in the identification and differentiation between regional, extra local and local controlling factors on depositional records
- to examine the sensitivity and resilience of coastal wetlands in the coastal zone of south east Sicily to environmental change.

1.4 Form of the Thesis

Chapter Two examines the dynamics of coastal wetlands and the practical and theoretical aspects of recording recent environmental changes through multi-proxy lines of evidence.

Chapter Three provides the context of broader scale Mediterranean patterns of climate change, landscape evolution and the impact of human activity on fluvial and coastal systems in the region, during the Late Quaternary (especially within the last 200 years) up to the present.

Chapter Four provides a background to the environmental evolution of south east Sicily. The regional climate, geology and tectonic structure are discussed in relation to coastal and fluvial processes. An outline of the main archaeological and historical patterns during the Holocene is used in conjunction with other documented sources as evidence of coastal changes in south east Sicily.

Chapter Five outlines the methodological procedures used to obtain the results from the sediment cores used in this study. Full laboratory procedures for pollen, geochemistry and ^{210}Pb dating and loss on ignition are presented in the Appendices.

Chapter Six is in four parts, comprising of results obtained from multi-proxy analyses of cores taken from the Mulinello estuary and Pantano Piccolo. The environmental background of each core setting is discussed before the results from the three selected cores used are presented. The final part of the chapter is the results from a preliminary study undertaken to determine spatial differences of pollen deposition in the Pantano Piccolo locality with a comparison of surface pollen with present land-surface vegetation.

Chapter Seven provides a synthesis of the results from the individual cores. Core AMC, from the Mulinello estuary is discussed firstly on its own due to its separate location and physiographic setting. Depositional changes observed in the two cores from Pantano Piccolo (PPA and PPB) are characterised individually, before being used jointly to interpret temporal and spatial relationships of sediment horizons encountered at the northern lagoon margin of Pantano Piccolo. The results from the Mulinello core is then discussed in relation to results obtained from Pantano Piccolo.

The final part of chapter seven is concerned with the implications of the core results in terms of the vulnerability of the settings in relation to disturbance, recovery and survival of future coastal wetlands in the Mediterranean.

Chapter Eight summarises the results and conclusions obtained in the study and consequently identifies further possible avenues of further research.

In the appendices are reproductions of historical maps discussed in Chapter 4 along with the full procedures of sample preparation for the multi-proxy analyses in the study. Tables outlining the stratigraphy of cores taken during site investigation and transects are also shown.

Chapter Two

Recording environmental change in coastal wetland sediments

2.1 Introduction

Coastal wetlands exist at the physical, biological and chemical interface between terrestrial and marine systems. They are an expression of both the fragility and resistance of natural systems to evolution within a dynamic, transitional environment. The ecology of coastal wetlands inherently reflects this by species and habitats adapted to dynamic environmental changes (e.g. sediment stabilisation, tidal activity) and to often widely variable salinity conditions.

Coastal wetlands have primarily been classified by their coastal geomorphological setting and hydraulic regime which control the diversity of vegetation types, landforms and biogeochemical processes. Large scale controls on coastal wetland evolution such as climate change, tectonic activity, sea level change or human interaction may directly impact wetland dynamics (e.g. earthquake-induced coastal flooding) or are more subtle. These provide the backdrop upon which smaller scale morphological and biogeochemical wetland systems operate.

Three main types of coastal wetland occur on a global scale which are determined by latitudinal position and vegetation communities found there (Viles & Spencer, 1995). Mangrove replaces salt marsh vegetation within sub-tropical latitudes, while in regions of increased aridity and salinity (e.g. along the southern coastline of the Mediterranean, Red Sea and Arabian Gulf), greater rates of evapotranspiration can result in the formation of low gradient salt marshes and sabkhas (e.g. Abdel-Razik & Ismail, 1990; Sadek & El-Darier, 1995; Böer, 1996). Mediterranean-type coastal salt marshes in the classification proposed by Dijkema (1987) are also sub-divided into two inter-related categories of settings:

- salt marshes fringing lagoonal and sedimentary shores, e.g. in the protected margins of barrier lagoon systems and;

- estuarine salt marsh communities developed at the distal extent of drainage catchments subjected to microtidal coastal processes.

Due primarily to the relief, climate and microtidal conditions of the Mediterranean, but also greatly exacerbated by anthropogenic interference and destruction, coastal wetlands within the region are some of the most threatened by predicted sea level increases within the next century (Tooley & Jelgersma, 1992).

A global similarity of coastal wetlands is the colonisation of areas by plant species tolerant to saline-brackish water inundation. The surface-resistance generated by plant growth

encourages the accumulation of mineral sediment in the coastal zone. Plant growth also generates the accumulation of *in situ* sediments (e.g. autocthonous salt marsh peat) by wetland biogeochemical processes. By raising the wetland surface elevation above tidal influence and adapting to hydrological-marine influences, coastal wetlands inherently exhibit a suite of largely depositional landforms and a range of salt-tolerant and non-marine habitats.

Although often situated within dynamic tidal and fluvial sedimentary environments, the relative stability afforded by colonising marsh vegetation usually encourages fine-grained sediment accretion and by doing so preserves previously deposited sediments.

Once a sheltered growing substrate has been colonised by saline/inundation tolerant plant species, the elevation of the marsh surface and continued accretion is dependent on a positive balance of sediment supply. Continued deposition or erosion is usually only limited by physiographic controls, i.e. the upper limit of tidal activity, rates of coastal subsidence/uplift or changes to coastal landforms, e.g. dune barriers, that initially created the low energy environment. These are widely recognised responses in recent and longer-term coastal wetland evolution (e.g. Clark, 1986b; Oenema & DeLaune, 1988; French *et al.,* 1990; Craft *et al.,* 1993; Cahoon & Lynch, 1997).

The physical accumulation of sediments forms the basis of palaeoenvironmental investigations in coastal wetland sediments as the nature of sediments at a wetland surface, at any given time, represents the culmination of longer term, regional processes and local physiographic and biogeochemical processes.

Inherent controls on wetland evolution are therefore largely favourable to the deposition and preservation of sedimentological components, for example the mutual retention and preservation of surface-derived organic matter and some metal species in wetland sediments occurs as a consequence of saturated and subsurface anoxic soil-conditions (e.g. Jenne & Zachara, 1987; Gambrell, 1994; Williams *et al.,* 1994). As accretion occurs over a period of time, sediments deposited should be progressively buried and preserved, unless erosion occurs. The characteristics of the deposited sediments should theoretically be representative of palaeoenvironmental conditions. However as deposited sediments form the substrate for ongoing wetland processes, physical, chemical and biological processes do not cease in the sub-surface; rather they have the potential to alter sedimentological characteristics developed or incorporated at the surface, through early diagenesis and bioturbation. The longer the time that subsurface conditions can alter the surface record, i.e. in slowly accreting settings or shallow depth sequences, the greater the potential exists of not being able to distinguish between what is strictly past evidence or contemporary information on coastal wetland processes.

Though the existence of both large and small coastal wetlands require the presence and continuation of permanent to semi-permanent saturation, a positive sediment budget, availability of nutrients, etc., the spatial extent of an individual wetland may be a significant control on the life span and sensitivity of the wetland to environmental changes, especially over comparatively short periods of time. On a geological timescale, coastal wetlands can only be considered to act as a temporary sink for sediments, organic matter and nutrients in the coastal zone. Larger coastal wetlands are likely to have a greater potential of resisting short-term changes and of recovery from disturbance, while smaller wetlands may be irrecoverably damaged during a similar event or phase of degradation, e.g. storm damage to a narrow vegetated wetland margin.

Changes to the depositional environment are recognised in sediments by identifiable textural, temporal and spatial differences between sediment units and their relationship to other units. A vertical sequence of sediments therefore represents the depositional culmination of environmental processes responsible for the setting and transportation of materials to the core site in co-operation with processes at the locality during deposition. Due to a small horizontal surface area, a vertical core taken of wetland sediments can be expected not be representative of spatial differences across the entire marsh. Where over short distances the depositional environment can be significantly different, for example at marginal environments, multiple cores are a necessary requirement to identify broader scale marsh wide changes. Logistically however, this is often not achievable, so individual cores used for further analyses should be as representative of sequences nearby.

2.2 Multi-proxy records of environmental change in coastal wetland sediments

Due to the effectiveness of wetlands as sinks of alluvial, marine and atmospheric derived materials, many studies of past environmental changes have been conducted in coastal wetland depositional settings. Coastal wetland sediment sequences and preserved remnants have contributed greatly to the understanding of Quaternary sea level change and coastal wetland evolution globally in a multitude of settings (e.g. Dupré *et al.,* 1988; Davis, 1992; Plater & Shennan, 1992; Jennings *et al.,* 1993; Guntenspergen *et al.,* 1995; Dubar & Anthony, 1995; Ellison, 1996; Nelson *et al..,* 1996; Kelsey *et al.,* 1998; Rull *et al.,* 1999). Late Holocene sediment sequences have also been widely utilised in interpreting the long-term impact of human activity on fluvial catchments and the coastal zone (e.g. Clark & Patterson, 1985; Davis, 1992) especially in the Mediterranean (e.g. Kraft *et al.,* 1975; Kraft *et al.,* 1977; Delano-Smith, 1979; Bottema, 1980; Baeteman, 1985; Yll *et al.,* 1997). Coastal wetland sediments deposited in the historical period have also been used

extensively to document the release of contaminants into the environment, changing patterns of industrialisation and subsequent contaminant loading of estuarine and coastal wetland settings (e.g. McCaffrey & Thompson, 1980; ValetteSilver, 1993; Zwolsman *et al.,* 1993; Daoust *et al.,* 1996; Cundy & Croudace, 1995; Callaway *et al.,* 1998; Cochran *et al.,* 1998; Grousset *et al.,* 1999). Significantly, depositional changes recognised in sediment sequences deposited in the last few centuries, have also been correlated with observational and quantitative records of controlling influences, i.e. hydrology, changing land use, storm events, and other human impacts (e.g. Sheffield *et al.,* 1995; Cahoon *et al.,* 1996; Niemi & Hall, 1996; Roman *et al.,* 1997; Cundy *et al.,* 1998).

A wide range of analytical techniques have been used in the investigation of environmental changes and coastal wetland evolution. Palaeoenvironmental analyses of coastal wetland sediments have primarily involved the extraction of components from the sediment fabric, (i.e. the physico-chemical composition - stratigraphy, grain size, mineral, trace element and pore water chemistry) and ecological remains (e.g. pollen, foraminifera, diatoms, macro fauna) and placing them within a chronostratigraphic framework (e.g. McCaffrey & Thompson, 1980; Stevenson, 1985; Clark, 1986a; Jennings *et al.,* 1993; Daoust *et al.,* 1996; Roman *et al.,* 1997).

Palaeoenvironmental investigation of sediments have invariably used at least two reconstructive tools, e.g. pollen and diatoms, foraminifera and sediment chemistry, etc., so changes detected in the results from one technique are reflected in the other. A preference has usually been made for sources of data generated by contrasting environmental factors, e.g. pollen deposition and radionuclide incorporation, which are capable of testing the interpretation made from the individual analyses used. This criteria has been particularly important for dating sediment sequences, i.e. validating calibrated ^{14}C dates with recognised environmental horizons (i.e. varves and tephras).

As a result of the diversity of controlling and interacting processes, a multi-proxy approach to palaeoenvironmental investigation is therefore vital to link possibly disparate controls on sedimentation; reflecting environmental changes at both the core site and within the boundaries of the catchment. A multi-proxy approach has therefore been used in the present study consisting of:

- an initial core sediment description and determination of local stratigraphy,
- ^{210}Pb [and ^{137}Cs*] analysis and dating for the determination of past depositional dynamics and a chronology for deposited sediments,
- loss on ignition as a measurement of the organic content of the sediment,

• major [and trace*] element geochemistry to establish the chemical composition and potential source of the deposited sediments and assess post-depositional geochemical changes and,

• pollen [and diatom*] analysis; to determine vegetation and palaeoecological changes in the surrounding area.

[*] Analyses used for one core only (Ch. 6.1., core AMC)

2.3 Physical sedimentology and stratigraphy

Although groundwater conditions may allow the establishment of wetland vegetation on a coarse clastic substrate, e.g. a sheltered position to the rear of a barrier-dune complex, coastal wetlands in protected, low-energy depositional settings are invariably developed on a fine-grained, variably organic substrate; usually an accumulation of both allochthonous (catchment-derived) and autochthonous materials (Orme, 1990). Local and recent differences in the substrate of coastal wetlands therefore reflect both temporal and spatial variations in the provenance of sediment materials, the hydrodynamics of the depositional setting and climatic-hydrological factors and events (e.g. French & Spencer, 1993; Cundy & Croudace, 1995; Benson *et al.*, 1997). Subsequently, wetland sediments contained within, or comprising entirely, longer-term lithostratigraphic successions reflect both local controls and larger scale controls on coastal evolution, e.g. catchment denudation rates, relative sea level changes and crustal motion (e.g. Baeteman, 1985; Belloti *et al.*, 1995; Nelson *et al.*, 1996; Viñals & Fumanal, 1996).

Physical characteristics and stratigraphic successions observed in coastal wetland sediments, can initially provide a considerable amount of information on the depositional evolution of the site, e.g. inter-layered peat and sand units indicating flood events, grain size and sorting, macrofaunal remains, etc. The physical characteristics of sediment horizons and their spatial extent should provide the basis for more detailed analysis of sediment units.

2.4 ^{210}Pb analysis: Chronological control for coastal wetland sediments.

The technique of ^{210}Pb-dating has proven to be a valuable tool in identifying recent sediment dynamics for coastal wetlands and other depositional settings over the last 100-150 years. ^{210}Pb has been used in floodplain, salt marsh, estuarine and mudflat settings to determine recent trends in relative sea-level (e.g. Cundy & Croudace, 1996; Cahoon & Lynch, 1997), spatial patterns of sediment deposition (e.g. He & Walling, 1996; Roman *et*

al., 1997), to date industrial/contaminant inputs (e.g. McCaffrey & Thomson, 1980; Alexander *et al.*, 1993; Zwolsman *et al.*, 1993; Cundy & Croudace, 1995; Cochran *et al.*, 1998; Grousset *et al.*, 1999) and in the interpretation of land-use history/ecological disturbance and degradation (e.g. Pennington *et al.*, 1976; Gale *et al.*, 1995; Sheffield *et al.*, 1995; Szeicz *et al.*, 1998; Brezonik & Engstrom, 1998; El-Daoushy & Eriksson, 1998). ^{210}Pb dating only partially spans the gap between short-term monitoring studies and the minimum of longer-term ^{14}C based studies, which is accepted as being prior to AD 1640).

The period capable of being dated by ^{210}Pb (optimally 100-150 years) coincides with the most recent advances in agricultural land-use, industrialisation, population growth and widespread landscape degradation. In Mediterranean Europe (including the coastal zone of south east Sicily) the intensity and spatial extent of these changes are unparalleled compared to any previous time period. Consequently, sediment deposition at coastal wetland sites during this period have responded to catchment-driven and site dependent processes, often as a clear consequence of anthropogenic activity.

However the technique may be limited by disturbance processes and events affecting the depositional environment. Irregular rates of sediment accretion, post-depositional mobility and changes in sediment composition have been observed to be a significant influence on ^{210}Pb activity profiles and the choice of dating model used to obtain time-depth values.

2.4.1 Principles of ^{210}Pb dating

^{210}Pb is a naturally occurring isotope derived from the ^{238}U radioactive decay series. ^{238}U in crustal materials decays through a series of intermediate isotopes to the solid ^{226}Ra (half-life = 1602 y), which in turn decays to the inert gas ^{222}Rn (3.82 days), which diffuses into the atmosphere and hydrosphere. ^{222}Rn continues to decay via a series of short-lived daughter isotopes to ^{210}Pb, a solid with a decay half-life of 22.26 years. As an aerosol in the atmosphere, ^{210}Pb is washed out by precipitation or by dry-fallout onto the earth's surface. The fate of ^{210}Pb once deposited from the atmosphere is largely dependent on the nature of the surface environment; the isotope is rapidly scavenged from water bodies by adsorption onto particulate matter and incorporated into lacustrine, estuarine and coastal marine sediments (Benninger *et al.*, 1979; Cochran *et al.*, 1998; Kirchner & Ehlers, 1998) or just as rapidly retained in surface soil materials within catchment areas (Nozaki *et al.*, 1978). Transport within the catchment (and the continued mobility) of ^{210}Pb towards a depositional setting at this stage is controlled by the physical transport of ^{210}Pb-labelled sediments, being mobilised by erosion and transported into depositional settings with suspended sediment loads (e.g. El-Daoushy & Eriksson, 1998). The crustal production,

release and atmospheric deposition thereby provides a continuous input of ^{210}Pb to surface environments, compared to the intermittent release of anthropogenically-associated radioactive isotopes (e.g. ^{134}Cs, ^{137}Cs, ^{60}C). The formation, transport and potential re-distribution of ^{210}Pb in a depositional environment is depicted in Figure 2.1.

^{210}Pb incorporated into sediment sequences as a result of direct and reworked atmospheric fallout is known as *unsupported* or $^{210}Pb_{excess}$ distinguishing it from ^{210}Pb produced by the *in situ* decay of ^{226}Ra present in crustal materials. The latter ^{210}Pb activity is known as the *supported* component and is in decay equilibrium with the parent ^{226}Ra activity. The supported component may therefore be determined in sediments by measurement of its ^{226}Ra parent directly (e.g. Pennington *et al.,* 1976; Gale *et al.,* 1995) or approximated by measuring the background unsupported component (at depth where the exponential decay curve levels off). $^{210}Pb_{excess}$ activity is commonly derived therefore, by subtracting either the measured ^{226}Ra activity from the total ^{210}Pb activity or by approximating the supported component from unsupported activity at depth (e.g. Appleby & Oldfield, 1992; Kirchner & Ehlers, 1998) in sediments older than ~150 years.

The primary assumption of an unsupported ^{210}Pb derived chronology assumes a relatively constant, time-averaged, supply and incorporation of $^{210}Pb_{excess}$ into a vertical sediment sequence. Once incorporated into the sediment column, $^{210}Pb_{excess}$ activity continues to decay with a half-life of 22.26 years. The measured unsupported activity of a buried sediment horizon at depth may therefore be assigned a palaeo-surface date (Fig. 2.2) using simple, or more complicated dating models, which take account of the supply and burial of unsupported ^{210}Pb (Appleby & Oldfield, 1992). A simple activity/depth sequence assumes therefore that *unsupported* ^{210}Pb activity at depth has remained isolated since burial, protecting sediments from the further incorporation of $^{210}Pb_{excess}$ activity *via* sediment mixing i.e. mechanical disturbance (e.g. Gardner *et al.,* 1987) and diagenetic movements (e.g. Cundy & Croudace, 1995).

2.4.2 Deposition, incorporation and potential mobility of ^{210}Pb

A considerable problem in ^{210}Pb dating is the accumulation of errors achieved by assumptions made on operating environmental controls and sediment characteristics. Complex depositional regimes may be expected to produce more complicated sediment sequences, where cumulative errors may be expected to be significant, due to a diversity of transport pathways and differing phases of sediment stability. The impact of more "open" depositional systems are evident in ^{210}Pb activity-depth profiles from environments which have been subject to hydrological and sediment-input variations, e.g. fluvial-affected coastal wetlands (Sheffield *et al.,* 1995; Roman *et al.,* 1997; Brezonik & Engstrom, 1998;

Figure 2.1. ^{210}Pb formation, transport and incorporation in sediment sequences

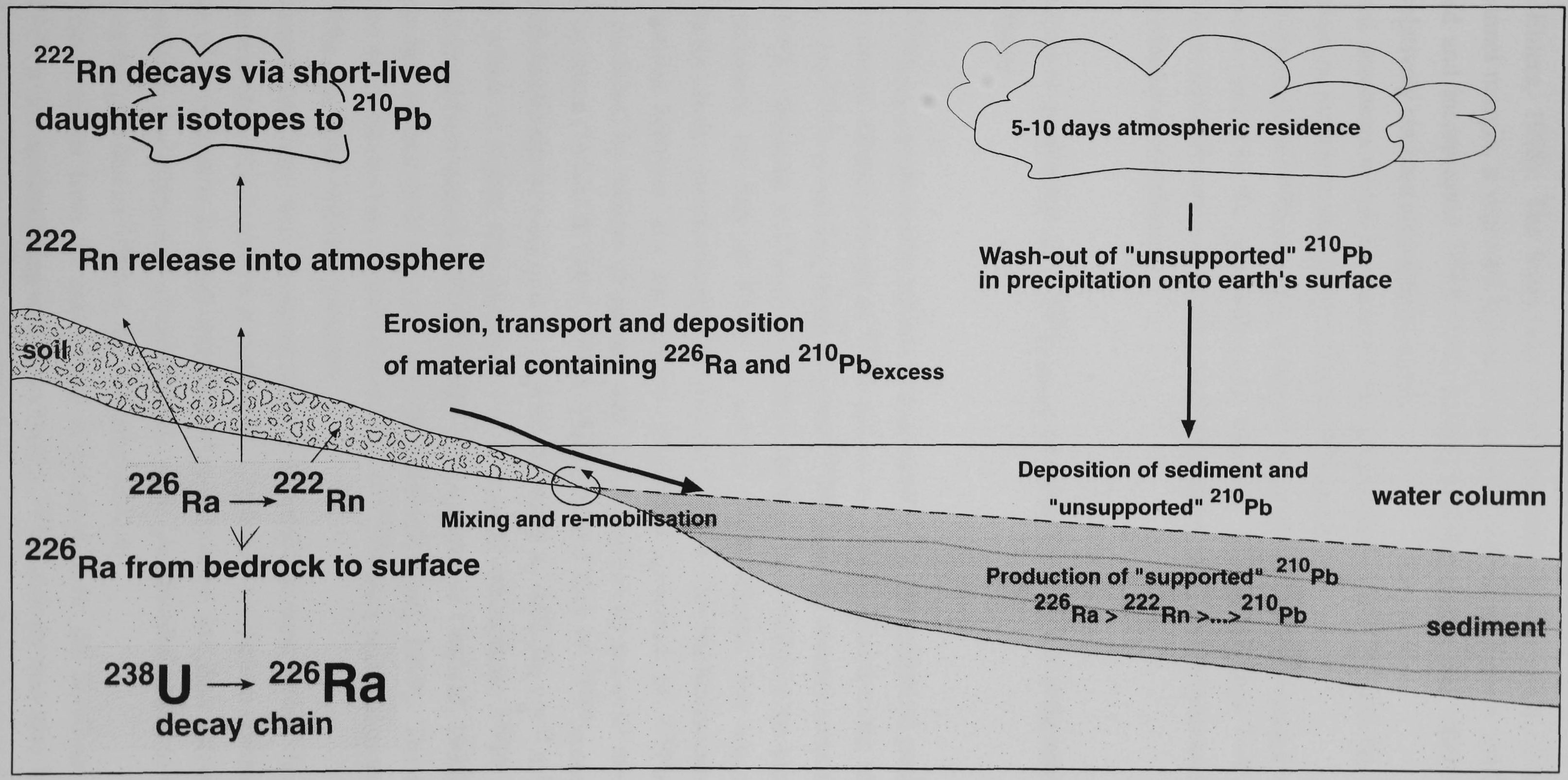

(After Wise. 1980)

Kirchner & Ehlers, 1998). The three core sequences used in this study; a microtidal estuarine channel margin, a vegetated lagoon margin and a fronting lagoon mudflat, will have received and incorporated ^{210}Pb from locality-specific inputs and others that are regional or relatively constant atmospheric input.

Environmental processes which have altered the incorporation of ^{210}Pb into the sediment should therefore be evident in the core profiles of ^{210}Pb activity.

Controlling influences on ^{210}Pb deposition may be sub-divided into two categories: firstly those that have controlled the generation and transport of *unsupported* ^{210}Pb to the sediment surface; and differences in activity caused by sediment characteristics and the sub-surface biogeochemical environment.

2.4.3 Transport pathways of $^{210}Pb_{excess}$ to coastal wetland sediment surfaces

The flux of $^{210}Pb_{excess}$ to the earth's surface is dependant on the geographical position and climatic environment. Global patterns in ^{210}Pb fallout are largely related to the movement of air masses over ^{210}Pb-generating continental and ^{210}Pb-depleted oceanic areas (Appleby & Oldfield, 1992). Regional and local atmospheric factors may therefore be expected to measurably influence the flux of ^{210}Pb to surface environments. For example, an influencing factor on the annual atmospheric flux of ^{210}Pb in the Mediterranean may be seasonal variations between dry atmospheric deposition (potential of ^{210}Pb-labelled Saharan dust particles) by African air-masses and wet deposition by seasonal mid-latitude depressional systems (Tadjiki & Erten, 1994). The calculated flux of $^{210}Pb_{excess}$ for the marsh at the Mulinello site in south east Sicily was calculated as 0.02 Bq cm^{-2} a^{-1} (Cundy *et al.*, 1998) which is higher than estimates for the typical atmospheric ^{210}Pb input to northern continental land-masses (0.014 Bq cm^{-2} a^{-1}, Appleby & Oldfield, 1992) and the Mediterranean Sea surface (0.01 Bq cm^{-2} a^{-1}, (Radakovitch *et al.*, 1999). The increased flux at the core site indicates that a significant amount of $^{210}Pb_{excess}$ was transported to the setting as $^{210}Pb_{excess}$ labile sediment particles.

Any core features associated with changing rates of atmospheric input would therefore be expected to be represented in sediment sequences as a regional, ubiquitous climatic signal. However due to the variation in cored sediment sequences used and their environmental setting, it is unlikely that differences of atmospheric input are identifiable due to dominant local factors on the past flux of ^{210}Pb to the sediment surface.

Though the direct fallout from the atmosphere is assumed to be the dominant input of unsupported ^{210}Pb into accumulating sediments, excess ^{210}Pb activity may also be derived from ^{222}Rn-rich groundwater entering the hydrological system. Groundwater may add a

significant amount of the total ^{210}Pb supply to a water body (e.g. Norton *et al.*, 1985) contributing to the influx of ^{226}Ra materials derived from catchment sources.

Because of the spatial and temporal diversity of morphological, hydrological and ecological systems in coastal wetlands affected by human activity, a constant rate of $^{210}Pb_{excess}$ incorporated into the sediment is unlikely to have been guaranteed for the period of time effective for ^{210}Pb dating. In many cases the expected exponential decline in unsupported $^{210}Pb_{excess}$ in the sediment will be offset by variations in sediment composition and $^{210}Pb_{excess}/^{210}Pb_{supported}$ activity. The introduction of material caused by the re-mobilisation and incorporation of sediment with an older ^{210}Pb signature, for example, may violate the basic assumption of ^{210}Pb dating models (see below) that the exponential decline with depth is a consequence of dominantly atmospheric input. Even assuming a constant rate of atmospheric flux to a marsh surface, the sediment component of $^{210}Pb_{excess}$ may be transported laterally and be subject to depositional focusing, depleting some areas of $^{210}Pb_{excess}$ that would otherwise be incorporated vertically to accentuate deposition at a nearby sediment surface.

In a dynamic hydrological regime (for example the evolutionary gradient from a mudflat to high brackish marsh) wetland surfaces may be expected to have been exposed to temporal variations in the flux of atmospheric $^{210}Pb_{excess}$ from the inwash of ^{210}Pb-labelled sediment. The expansion of wetland vegetation not only creates preferential zones for sediment accretion brought into coastal systems during inundation periods (e.g. French & Stoddart, 1992; Craft *et al.*, 1993; French & Spencer, 1993; Callaway *et al.*, 1998) but by the same process, generates highly suitable organo-chemical conditions for the adsorption of radionuclides (e.g. Church *et al.*, 1981).

Calculated fluxes of $^{210}Pb_{excess}$ have been observed to vary across marsh areas, with high flux rates occurring at the marsh front (which are most likely added to by the tidal input of re-mobilised $^{210}Pb_{excess}$ associated with sediment particles) and lower fluxes at the rear of the marsh reflecting the decreased tidal input of minerogenic material (e.g. Cundy & Croudace, 1995).

From the same study, cores from a mudflat environment which was subject to erosion (supplying sediment to higher marsh areas) exhibited low $^{210}Pb_{excess}$ inventories (0.001-0.003 $Bq/cm^2\ a^{-1}$) and low apparent annual fluxes (0.03-0.1 Bq/cm^2).

The stability of a marsh surface (near or outside the regime of constant sediment supply) and the growth of vegetation may be expected therefore to lead to an increase of ^{210}Pb activity in near-surface horizons. As the minerogenic supply diminishes, the duration of surface exposure and $^{210}Pb_{excess}$ accumulation of a potential buried horizon may be increased, as a constant rate of $^{210}Pb_{excess}$ is deposited directly from the atmosphere onto the sediment surface. Conversely without burial, the surface sediments may be more susceptible to erosion and disturbance from surface processes. A period of prolonged

sediment surface stability should theoretically be identifiable therefore in a sediment sequence as a significant, even organically associated (due to the growth of surface vegetation) peak in $^{210}Pb_{excess}$ activity, or a reduction in activity caused by erosion.
Whether $^{210}Pb_{excess}$ has been derived from atmospheric fallout, from the decay of ^{226}Ra-^{222}Rn in water masses or from re-mobilised ^{210}Pb-labelled materials derived from the catchment, if the total flux of unsupported ^{210}Pb to a depositional setting has been constant, conventional models of ^{210}Pb dating remain valid. However, if a significant input of total ^{210}Pb has been derived from re-worked sediment particles an extra consideration has to be whether the $^{210}Pb_{excess}$ has been incorporated at a steady rate (fulfilling the requirement of a constant rate of ^{210}Pb flux) or been interrupted by sedimentary processes. Problems occur (as with the choice and operation of the suitable model) when sediment accretion has been accompanied with phases of erosion and the introduction of older supported ^{210}Pb material (El-Daoushy & Eriksson, 1998; Kirchner & Ehlers, 1998). Critically, once interred, palaeo-surface sediments incorporating $^{210}Pb_{excess}$ activity should have had the opportunity to decay, without further disturbance from the mechanical incorporation of mixed-age $^{210}Pb_{excess}$ and by biogeochemical processes of vertical transport and movement.

2.4.4 Sediment characteristics and sub-surface biogeochemical conditions on the post-depositional redistribution of ^{210}Pb.

The potential impact of post depositional movement is clearly dependent on the magnitude, frequency and effectiveness of disturbance processes affecting the sediment sequence. An extreme scenario would involve the entire mixing of sediments deposited in the last 150-200 years prior to sampling. In contrast, changing geochemical conditions may shift the concentration of $^{210}Pb_{excess}$ across a boundary of a few millimetres-centimetres (e.g. Hardaway *et al.*, 1998). The impact of physical mixing on a $^{210}Pb_{excess}$ profile/sediment sequence may be expected to have been proportional to the depth of sediment deposited, the energy of the process imposed on the sequence and the resistance of the deposited sediment to erosion-disturbance. Likewise the impact of changing biogeochemical conditions on potential mixing processes is dependent on the biogeochemical environment and the chemical properties (i.e. bounding states with other materials) of ^{210}Pb in the deposited sediment.
Although infrequent and large magnitude mixing processes may severely upset the pattern of $^{210}Pb_{excess}$ activity with depth, small scale and more frequent mixing (occurring within the sediment-water interface and the most recently deposited sediments) may also significantly affect $^{210}Pb_{excess}$ core inventories. During the deposition of $^{210}Pb_{excess}$ to the

Figure 2.2 ^{210}Pb activity in accreted sediments and age-depth relationships.

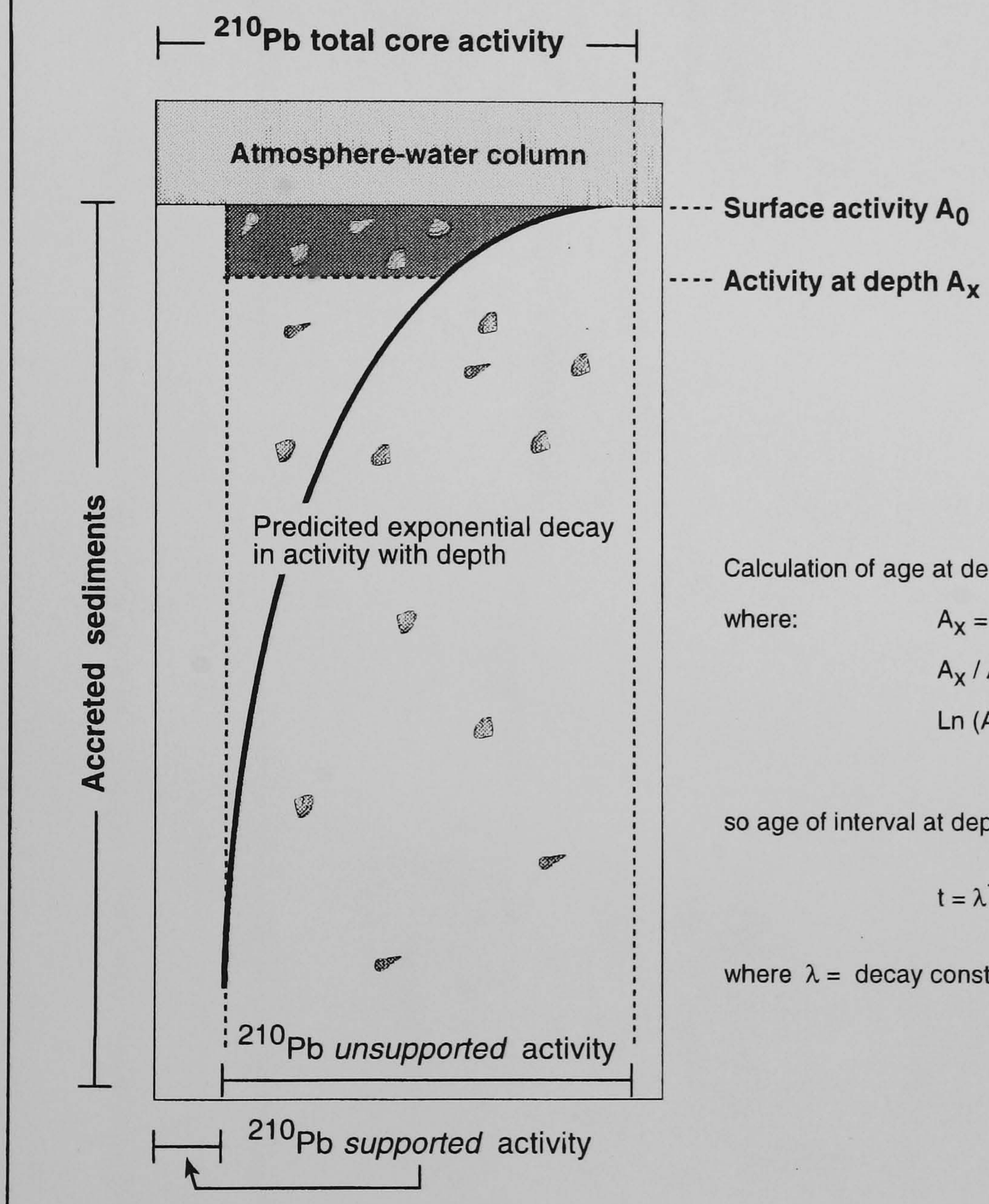

Calculation of age at depth using ^{210}Pb

where: $A_x = A_0 e^{-\lambda t}$

$A_x / A_0 = e^{-\lambda t}$

$Ln (A_x / A_0) = -\lambda t$

so age of interval at depth x:

$$t = \lambda^{-1} ln (A_x / A_0)$$

where λ = decay constant of ^{210}Pb ($0.03114\ yr^{-1}$)

Figure 2.3. Depositional scenarios resulting in vertical redistribution and non-exponential decline of ^{210}Pb with depth

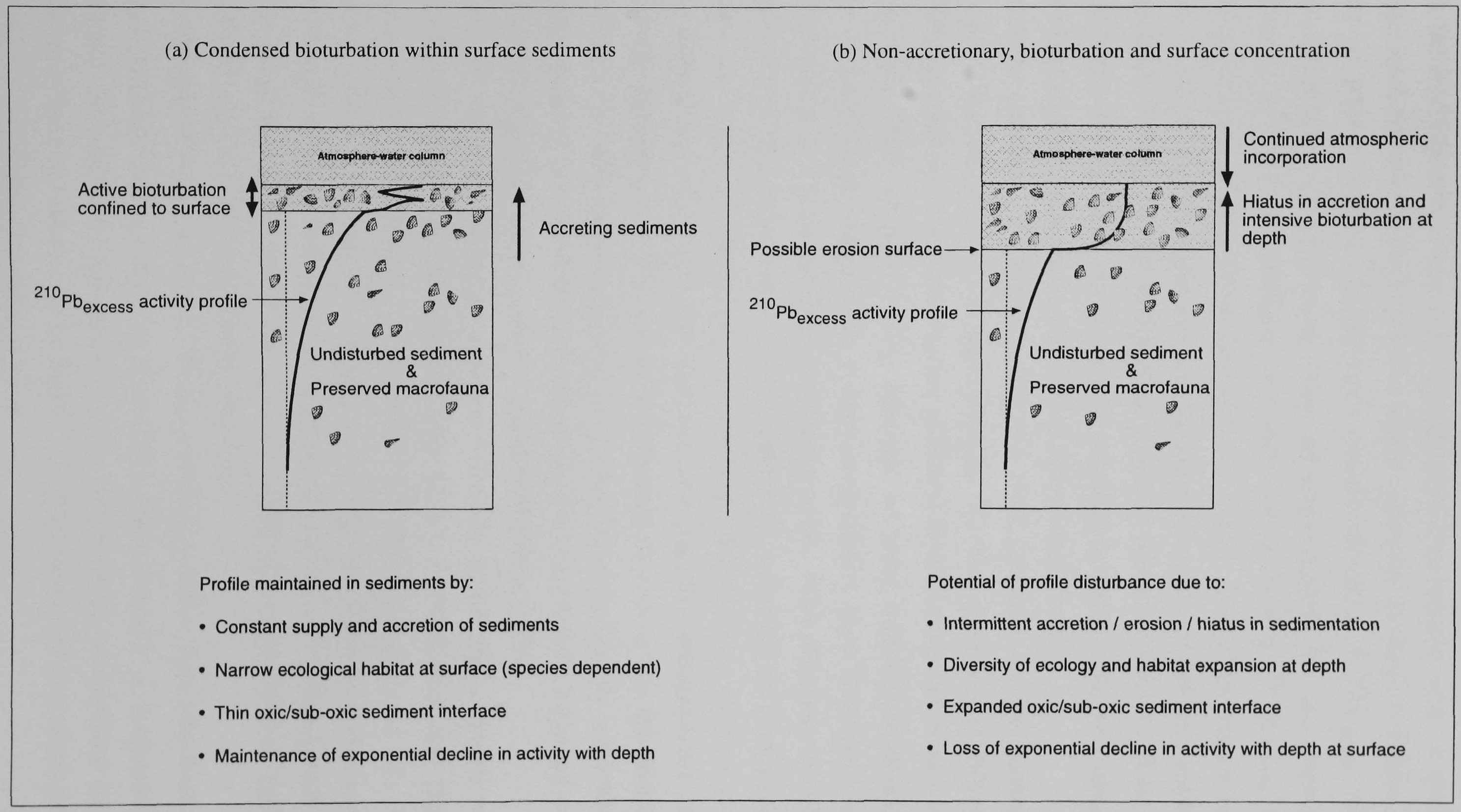

sediment surface, previously deposited $^{210}Pb_{excess}$ at the surface has the potential to be in a more favourable position to be re-mobilised.

Depending on the hydrodynamics and the deposition-erosion balance (e.g. a sheltered micro tidal water level elevation compared with a heavy rainstorm induced, sediment laden flood) a lesser or greater amount of previously surface-entrapped $^{210}Pb_{excess}$ will be available for re-mobilisation and deposition. Wave activity especially has the potential of almost continuously re-suspending surface sediments and mobilising $^{210}Pb_{excess}$ when covered by a shallow depth of water (Lund-Hansen *et al.* 1998). In shallow lagoon waters subject to water level variation this process may be expected to be significant; entraining previously deposited $^{210}Pb_{excess}$ and transporting it within the water column along with suspended sediments. Rising water levels may be expected to radiate this re-suspension outwards to the lagoon margin and *vice versa* during falling water levels.

The sediment-water interface of wetland sediments often provides a rich habitat for macrofaunal and molluscan ecology. A high potential for bioturbation and differential mixing of $^{210}Pb_{excess}$ activity exists in estuarine sediment settings (e.g. Benninger *et al.*, 1979; Gardner *et al.*, 1987; Heijnis, 1987), although in many intertidal vegetated salt marsh settings sediments have remained (or at least interpreted to have remained) largely undisturbed (McCaffrey & Thomson, 1980; Zwolsman *et al.*, 1993; Kirchner & Ehlers, 1998). The intensity of this bioturbation will be limited by a number of ecological and physical factors; the habits of individual mud-dwelling species (e.g. surface grazing gastropods or burrowing crabs) and the chemical and organic characteristics of the substrate and overlying water mass. The timing and intensity of activity (i.e. the number of individuals, resident or advantageous species, etc.) may therefore greatly influence the temporal re-distribution of radionuclides and other sediment components deposited during a limited time period, e.g. soil organic matter (e.g. Bhiry & Filion, 1996).

Bioturbation may be expected to remain confined within an active zone, though with a propensity to move physically and in intensity with relation to ecological and physical stresses in the sediment or overlying water mass (e.g. De Casabianca *et al.*, 1997; Tagliapietra *et al.*, 1998). If bioturbation in the past has been confined to a continuously active zone in the surface of an actively accreting sediment sequence, $^{210}Pb_{excess}$ may have been interred at a time-dependent rate below an active depth of re-mobilisation, fulfilling the necessary burial rate for $^{210}Pb_{excess}$ dating (Fig.2.3).

Less apparent ecological bioturbation of $^{210}Pb_{excess}$ activity profiles may also have been caused by faunal activity (bird and fish species with a high diversity of mud-associated feeding techniques) even by large mammals/humans. For example, water-filled imprints left in intertidal muds by fishermen at the Mulinello site were measured to a depth of 5-10 cm, while grazing cattle left imprints up to 20 cm.

Natural environmental change and anthropogenic activity aside, a potential exists of random, non-documented disturbance events to have greatly affected $^{210}Pb_{excess}$ activity with depth, disrupting an ideal progressive model of sedimentation.

As with other chemical species in wetland sediments, a potential exists for $^{210}Pb_{excess}$ to be mobilised and transported by changing biogeochemical conditions; altering the vertical distribution and concentration of $^{210}Pb_{excess}$ in the sediment column following burial. Although generally accepted that the mobility of $^{210}Pb_{excess}$ is limited in estuarine and wetland sediments it has been suggested that $^{210}Pb_{excess}$ may be mobilised from highly reduced marsh sediments, under water saturated conditions and re-precipitated in overlying sediment horizons (e.g. Cundy & Croudace, 1995). Similarly in lacustrine sediments the distribution of ^{210}Pb has been shown to largely correlate with Eh and pH conditions coincidental with the mobility of Pb (Hardaway *et al.,* 1998). A sequence of sediments of varying organic content and affected by alternating oxic/anoxic conditions (brought on by hydrological differences) may therefore be expected to have some effect on the vertical distribution of ^{210}Pb, along with redox sensitive elements such as Mn and Fe (see below).

Over a period of time therefore, both the depth of mobilisation and re-precipitation may be expected to move, and may (as in the case of seasonally, irregularly inundated sediments) cloud a clear relationship between $^{210}Pb_{excess}$ activity and redox conditions. Plant-derived organic material incorporated into accreting sediments, also provides highly receptive surfaces for ^{210}Pb adsorption during initial deposition and diagenetic mobility (Armentano & Woowell, 1975; Cundy & Croudace, 1995).

Although it is less complicated to assume that an activity profile of unsupported ^{210}Pb with depth has only been affected by previous environmental and physical depositional processes, the influence of the contemporary biogeochemical environment is a vital consideration, especially sediments forming the substrate of vegetated, microtidal, low accretion settings, e.g. Mediterranean climate salt marshes.

2.4.5 Models of ^{210}Pb dating used: the CF:CS & CRS models

Horizon ages are ascribed within vertical sequences of sediment by mathematical models which describe the activity at depth in relation to the known decay rate of $^{210}Pb_{excess}$ and flux of $^{210}Pb_{excess}$ to the sediment surface (Fig. 2.2). As a result of the relationship between depositional processes and incorporation of $^{210}Pb_{excess}$, the choice of ^{210}Pb dating model should be based on prior knowledge of processes governing the accumulation of $^{210}Pb_{excess}$ and on the assessment of ^{210}Pb activity data derived from the sediment sequence (Appleby & Oldfield, 1992). Clearly in settings subject to unsteady patterns in deposition and the flux of ^{210}Pb to the accreting sediments, the assumption that the

atmospheric flux of unsupported ^{210}Pb has remained constant over time is stretched to its limits; as is the applicability of simple models of ^{210}Pb dating.

2.4.6 The Constant Flux: Constant Sedimentation (CF:CS) or "simple" model

The exponential decline of $^{210}Pb_{excess}$ activity caused by a constant flux of unsupported ^{210}Pb to a steadily accreting sequence, plotted on a logarithmic scale may be used to determine mean accretion rates; being the basis of the "simple" constant flux - constant sedimentation (CF:CS) model (Appleby & Oldfield, 1992). The average sediment accumulation rate S is estimated by the CF:CS model by a best-fit straight-line equation describing radioactive decay with depth (McCaffrey & Thomson, 1980);

$$\ln A_z = \ln A_0 - (\lambda / S)_z$$

where: A_z is activity at depth z, A_0 is the initial activity (assumed equal to surface activity, if the flux of ^{210}Pb to the sediment has been constant), λ is the decay constant of $^{210}Pb_{excess}$ (0.03114 yr^{-1}) and S is the rate of sediment accumulation (cm/yr^{-1}). Mean sediment accretion rates were determined by plotting $\ln A$ (specifically $\ln\ ^{210}Pb_{excess}$) against core depth. A fitted least squares regression line provided an equation describing the gradient of the line $y = mx + c$ or:

$$\ln A_z = -(\lambda/s)_z + \ln A_0$$

where: $\ln A_0$ is the constant "c" and λ/s is the gradient "m". The decay rate (λ) for ^{210}Pb is 0.03114 yr^{-1}, so the sediment accretion rate S is given as λ/m. A least squares regression of normal log values of $^{210}Pb_{excess}$ activity against depth may therefore be determined for each core. For this study the linear regression facility in SPSS for Windows Version 8 provided the best line fit (mean gradient) within a 95% confidence interval, which was used to calculate the mean accretion rate (cm/yr^{-1}) of the individual cores.

Understandably, given the dynamic nature of sedimentation in marginal systems such as coastal wetlands, the flux of unsupported ^{210}Pb will almost certainly have been affected by varying rates of sediment accretion, not least by the high disturbance potential of interrupted and accelerated sedimentation due to human activity, negating a constant rate of accretion . More useful therefore in these circumstances are dating models developed to account for significant variations in sediment accumulation rates and the varying influx of

unsupported ^{210}Pb into lacustrine settings (e.g. Pennington *et al.*, 1976; Appleby & Oldfield, 1978) and overbank floodplain deposits (He and Walling, 1996).

To account for variations in sediment supply, the constant initial concentration (CIC) model (e.g. Krishnaswamy *et al.*, 1971) assumes constant initial unsupported activity incorporated into the surface horizon, independent of any changes in sedimentation rate. The model assumes that increased sediment supply will automatically lead to greater rates of available $^{210}Pb_{excess}$ being scavenged from the water column, thereby maintaining a constant initial concentration at the surface (Appleby & Oldfield, 1992). Decreasing exponentially with increasing depth, the slope of a fitted regression line provides a mean sedimentation rate (e.g. Zwolsman *et al.*, 1993).

2.4.7 The Constant Rate of Supply (CRS) model

The CRS (constant rate of supply) model of ^{210}Pb dating has been widely used in a variety of environmental settings which have been subject to variable rates of sedimentation (Allen *et al.*, 1993; Gale *et al.*, 1995; Sheffield *et al.*, 1995; Alvisi & Frignani, 1996; Roman *et al.*, 1997; Kirchner & Ehlers, 1998; Thorndycraft *et al.*, 1998). The CRS model accommodates the dilution of ^{210}Pb concentration by accelerated sedimentation (Appleby & Oldfield, 1978). Accounted for in the model is that unsupported ^{210}Pb activity will vary inversely with the mass accumulation rate/bulk density of the host sediment.

The sediment age at any given depth calculated by the CRS model is calculated as the ratio of *unsupported* ^{210}Pb below a depth interval to the total *unsupported* ^{210}Pb activity in the sediment column (the ^{210}Pb core inventory) or:

$$t_z = \lambda^{-1} \log_n (A_z/A_{total})$$

where t_z = age at depth z, $\lambda = {}^{210}Pb$ constant (0.03114/ yr^{-1}), A_z is the *unsupported* ^{210}Pb activity below depth z and A_{total} is the total core ^{210}Pb inventory (Appleby & Oldfield, 1978; Gale *et al.*, 1995). Calculated using an inventory of ^{210}Pb activity in the horizon below depth z, sample points on an age depth curve derived from the CRS model, represent differing periods of accretion rate. Inflections in an age-depth curve derived from CRS models are indicative therefore of changing rates of accretion, while major breaks clearly represent hiatuses in sediment deposition and possible erosional phases (Brezonik & Engstrom, 1998). The CRS model allows for increased sedimentation rates by diluting $^{210}Pb_{excess}$ activity, though the model may be detrimentally disrupted by aged material at depth. In the event of this the basic assumption of the CRS model, that the deviation of

$^{210}Pb_{excess}$ activity at depth is due to variations in past sedimentation rates, may therefore be violated (Kirchner & Ehlers, 1998).

Without the benefit of long-term monitoring of depositional patterns and $^{210}Pb_{excess}$ incorporation, activity profiles extracted from cored sediments can only provide an approximation of the sequence of events that have led to the present-day pattern of deposited sediments. The dating of sediments using unsupported ^{210}Pb activity therefore requires a rigorous consideration of the factors that have influenced the activity profile measured in the deposited sediments. This has been commonly achieved by comparison with other lines of dating and independent verification through other lines of multi-proxy evidence.

2.5 ^{137}Cs relative dating of wetland sediments

^{137}Cs is an artificial radionuclide (half-life of 30.2 years) that only exists in the global environment as a consequence of atmospheric nuclear weapons testing and discharges (accidental or otherwise) from nuclear energy and military facilities. Strongly sorbed onto fine-grained mineral sediments in soils (e.g. Cremers *et al.,* 1988) and relatively inert to subsequent depositional translocation in coastal wetland settings (e.g. Kirchner & Ehlers, 1998; Orson *et al.,* 1998), the isotope has proved to be of widespread use in interpreting recent sediment dynamics.

Peak levels of ^{137}Cs were released into the atmosphere by above-ground nuclear weapons testing prior to the signing of the Limited Test Ban Treaty (1963). This period of peak fallout provided an activity maximum of ^{137}Cs in sediments accreted at the same time which has been used, often in conjunction with ^{210}Pb, to estimate both, recent rates of sediment flux in coastal wetland (e.g. De Laune *et al.,* 1978; Battiston *et al.,* 1988; Oenema & DeLaune, 1988; Ehlers *et al.,* 1993; Cundy & Croudace, 1995; Roman *et al.,* 1997; Orson *et al.,* 1998), marine (e.g. Tadjiki & Erten, 1994; Radakovitch *et al.,* 1999) and fluvial-lacustrine sediments (e.g. Pennington *et al.,* 1976; Robbins *et al.,* 1978; Battiston *et al.,* 1988; El-Daoushy & Eriksson; Grousset *et al.,* 1999) and rates of soil erosion (e.g. Ritchie *et al.,* 1974; Quine *et al.,* 1994; Zhang *et al.,* 1998). Although the move to underground testing reduced the amount of the isotope in the atmosphere, ^{137}Cs has continued to be released into the environment from point sources; either controlled over a period of time, e.g. from Sellafield in NW England (e.g. Hutchinson & Prandle, 1994) or nuclear power stations on the River Rhône in southern France (e.g. Radakovitch *et al.,* 1999); or accidentally released, i.e. from Chernobyl, Ukraine (1986) and Three Mile Island, U.S.A. (1979).

As with ^{210}Pb in sediment sequences, errors are compounded in ^{137}Cs relative dating by preferential sorption onto fine-grained (clay) material (e.g. Cremers et al., 1988; Dumat *et al.*, 1997), post-depositional mobility (e.g. Hardaway *et al.*, 1998; Kirchner & Ehlers, 1998) and physical sediment re-working (e.g. Ely *et al.*, 1992; Walling *et al.*, 1992). As identifying a sharp peak in concentration at depth, attributable to a known period of release, is the primary calculation for ^{137}Cs dating, the blurring of any peaks understandably lessens the precision. The use of ^{137}Cs in wetlands benefits from the assumption that the isotope is comparatively redox insensitive, unlike ^{210}Pb which can undergo chemical re-mobilisation (and therefore vertical mobility) under more reduced conditions.

2.6 Loss on ignition as a proxy measurement of organic content for wetland soils

Loss on ignition (LOI) is a simple and relatively efficient technique to quantify the organic component of a sediment sample. Results from loss on ignition analyses may be viewed therefore as proxy evidence of the variable controls governing the generation and introduction of organic matter into depositing sediments. At its simplest, the technique allows the identification of organic (high ignition loss) and inorganic (lower ignition loss) materials in a sediment sequence. In conjunction with other sedimentological analyses, the technique has been used widely to quantify organic matter within allochthonous terrestrial sediments (e.g. Bierman *et al.*, 1997; Brezonik & Engstrom, 1998; Szeicz *et al.*, 1998). The variable inorganic and organic component measured by LOI has been observed to be significantly influenced by autochthonous "organic" production (e.g. Si produced by diatoms in the water column and sediment) as well as catchment derived allochthonous organic/inorganic materials (e.g. Robinson, 1994, Rhodes & Davis, 1995; Barber *et al.*, 1999).

Having developed at the margin of terrestrial and aquatic/coastal systems, the organic content of buried coastal wetland sediments (e.g. Moore, 1990) can vary as a result of both autochthonous and allochthonous depositional processes: due to net primary marsh productivity (e.g. Hatton *et al.*, 1983; Cundy & Croudace, 1995), low organic decomposition rates due to sub-surface anaerobic conditions (e.g. Craft *et al.*, 1991; Rae and Allen, 1993; Reddy & D'Angelo, 1995); and the allochthonous input of organic matter incorporated into accreting sediments (e.g. Craft *et al.*, 1993; Bierman *et al.*, 1997). Within coastal wetland and estuarine sediments, linear relationships have been observed between organic carbon and loss on ignition (Craft *et al.*, 1991; Cundy, 1994), which validates the techniques use as a simple proxy for organic content.

In bulk sediment samples of a variable nature, attributing the loss on ignition values to specific components remains difficult without complimentary mineralogical and textural analyses (e.g. Rhodes & Davis, 1995; Daoust *et al.,* 1996). The decrease in mass due to thermal combustion, i.e. loss on ignition, will therefore be due to the combustion of variable sediment components at different temperatures. Depending on the porosity and water content of the sediment, some mass will be lost during air drying with the release of H_2O. Following air drying, H_2O and mineral lattice-bound OH will have a greater effect on ignition losses in fine-grained (clay mineral/phyllosilicate) sediments and with hydrous mineral components e.g. gypsum ($CaSO_4(H_2O)$). Loss on ignition at 550° C as a proxy of organic carbon therefore may only be reliable for organic rich sediments as the release of lattice-bound OH and other volatiles will have a relatively greater effect on combustion losses from low organic sediments than materials higher in organic content (Mackereth, 1965; Grimshaw, 1989).

2.7 Salt marsh geochemistry and records of depositional change

The geochemical (major element) composition of wetland sediments is primarily dependent on sediment provenance and the sediment dynamics of the depositional environment. Subsequent post-depositional changes in sediment composition, e.g. trace metal mobility, are often strongly controlled by initial textural and geochemical characteristics determined by the physiographic setting. Differences in major element sediment chemistry (geochemical parameters determined by catchment earth materials and hydrology) have therefore been used extensively (often in conjunction with other types of proxy evidence) in coastal wetland/recent sedimentological investigations; for palaeoenvironmental reconstruction (e.g. Rhodes & Davis, 1995; Siegel *et al.,* 1995; Schütt, 1996; Hölzer & Hölzer, 1998) often in conjunction with historical and contemporary trace element patterns (e.g. McCaffrey & Thomson, 1980; Reboredo & Ribeiro, 1984; Zwolsman *et al.,* 1993; Cundy & Croudace, 1995, 1996; Daoust *et al.,* 1996, Cundy *et al.,* 1998).

The minerals present in the rocks and soils of a catchment are a major control on the distribution of major elements occurring in wetland soils. As a result the release of particulate and dissolved ionic components of weathered bedrock is subject to processes affecting sediment transport within the catchment, i.e. climate, vegetation and hydrology (e.g. Sabater *et al.,* 1990; Rhodes & Davis, 1995; Schütt, 1996). At background concentrations similarly, trace elements in river water and wetland soils also reflect specific aspects of the catchment area geology and hydrology (e.g. Martin & Meybeck, 1979; Windom *et al.,* 1989; Alexander & Windom, 1999). Due to often low background levels,

elevated concentrations of trace elements (e.g. heavy metals) in coastal wetlands and recent alluvial sediments have been able to be closely correlated with spatial and historical variations in anthropogenic contamination (e.g. McCaffrey & Thomson, 1980; Klimek & Zawilinska, 1985; Rozan *et al.,* 1994; Zwolsman *et al.,* 1993; Zwolsman *et al.,* 1996; Callaway *et al.,* 1998; Cochran *et al.,* 1998; Grousset *et al.,* 1999).

The hydraulic evolution of the coastal wetland depositional setting may be viewed as the primary control on sediment geochemistry; largely determining the input of materials and the physical and textural properties (grain size, mineralogy, organic content) of the sediment. The typical combination of fine-grained (< 2μm) mineral (clays especially) and organic matter in coastal marsh and estuarine sediments have been identified as being preferential to the adsorption and retention of metals (e.g. Pb, Cd, Ni, Zn, Cu, Hg) in the aquatic-estuarine environment (e.g. Reboredo & Ribeiro, 1984; Carruesco & Lapaquellerie, 1985; Jenne & Zachara, 1987; Allen *et al.,* 1990; Zwolsman *et al.,* 1993; Cundy & Croudace, 1995; Caçador *et al.,* 1996).

Frequent inundation of wetland soils increases both the potential of aquatic sediment transport, element re-suspension and the development of anoxic soil conditions at depth; all of which are major controls on the vertical distribution of elements found in wetland soils. Although anthropogenic inputs of trace metals are a recognisable cause of elevated concentrations in wetland sediments, their abundance in the sediments may not necessarily reflect historical inputs. Changing post-depositional (early diagenetic) processes also dominate the organic and inorganic biogeochemistry of the sediments, i.e. redox potential, salinity, organic content, pH, microbial activity etc. Ionic species of major elements, trace elements and the mobility of metals in sediments are particularly affected by variations of the *in situ* geochemical environment and overlying water chemistry (e.g. Dongarrá *et al.,* 1985; Gambrell, 1994; Williams *et al.,* 1994; Windom *et al.,* 1999).

The geochemistry of near surface (often rhizospheric) wetland environments are a critical factor for both subsequent geochemical reactions at depth and in determining patterns of surface ecology. i.e. wetland floral and faunal communities. Edaphic, or environmental conditions determined by soil characteristics, is a key feedback process within coastal wetlands between nutrient dynamics and the temporal evolution of marsh plant communities.

Exposure to the atmosphere and different flooding intervals by brackish-saline water, determined by the physiography of the salt marsh and climatic conditions, results in variable interstitial salinities and quantities of salts precipitated in the surface environment. Soil salinities in marshes, even under a temperate climate are often elevated by evapotranspiration (to salinities exceeding that of sea water) to the extent of the formation of a surface saline crust. In more arid, microtidal coastal wetlands especially, e.g. the

Mediterranean, the temporal and spatial variation in the concentration of salts at the surface is the main edaphic variable on the type of species found and their distribution (e.g. Purer, 1942; Basset, 1978; Abdel-Razik & Ismail, 1990; Callaway *et al.*, 1990; Ortiz *et al.*, 1995; Boër, 1996; Sanchez *et al.*, 1998).

The ionic composition of the surface environment for coastal salt marsh plants is dominated by Na^+ and Cl^-, followed by Mg^{2+}, SO_4^{2-}, Ca^{2+} and K^+ reflecting the major constituents of sea water (Adam, 1990). Clear relationships have therefore been found to exist between the content of major ions in the soil and proximity to the sea/water body, climatic conditions and subsequent vegetation communities (e.g. Cooper, 1982; Calvo *et al.*, 1995; Ortiz et al., 1995 Boër, 1996). Although most apparent as spatial differences across a marsh area, the same changes in salinity may also occur vertically in the sub-surface as groundwater levels respond to evapotranspirational gradients and seasonal precipitation (e.g. Basset, 1978).

Plant growth and the incorporation of organic matter also play a highly significant, complex and interactive role in the composition of marsh-surface sediments. The incorporation of macrophytic debris from surface vegetation and detritus derived from the catchment, also introduces a large quantity of carbon, nitrogen and phosphorus to the sediment (e.g. Ranwell, 1964; Nixon *et al.*, 1976). The decomposition of organic matter in the subsurface is seen to control both the recycling of nutrients available to primary productivity (e.g. Jefferies & Perkin, 1977), as well as, subsequent geochemical patterns at depth (see below). A more detailed introduction to nutrient dynamics, phosphorus and nitrogen cycling is provided by Reddy & D'Angelo (1994).

The development of anaerobic conditions at depth is dependent on both the frequency and duration of surface inundation and the hydraulic conductivity of the deposited sediments. Groundwater conductivity in wetland soils is dependent on both the physiographic setting and the permeability/porosity of the sediments (e.g. grain size differences, desiccation cracks, organism burrows) (e.g. Arndt & Richardson, 1993; Harvey *et al.*, 1993; Amiaud *et al.*, 1998). As a result, physical factors such as the temporal and spatial differences in hydraulic conditions in the sediment column, e.g. due to tidal effects or climate-controlled hydrological variations are intimately related to subsurface sediment geochemistry by gas and liquid exchanges across the surface interface.

Anaerobic conditions develop in inundated wetland soils as a response to the decomposition of organic matter by microbial activity. The sharp decrease in dissolved oxygen concentrations with depth in wetland soils are due to: an increase in O_2 consuming organisms; the loss of photosynthetic O_2 production; and the reduced O_2 advection and diffusion between the water column/atmosphere (e.g. Patrick & DeLaune; 1972; Chambers & Odum, 1990). In regularly flooded salt-marsh soils, saturated conditions sharply reduce

the amount of available O_2 within a few millimetres below the surface and dissolved O_2 often becomes undetectable below a few centimetres (e.g. Cartaxana & Lloyd, 1999). As a result, at least three different horizons occur in wetland sediments, due to the favoured thermodynamic sequence of microbiological oxygen utilisation and the use of alternative oxidants: an aerobic zone (usually at the surface) where O_2 is readily available; a variably oxidised and reduced zone (the redoxcline); and a permanently anaerobic zone. Oxidants for the decomposition of organic matter are favoured preferentially through these zones; by thermodynamic stability from aerobic (O_2 reduction) to increasingly anaerobic NO_3^- (nitrate reduction), MnO_2 (manganese reduction), $Fe(OH)_3$ (iron reduction), SO_4^{2-} (sulphate reduction) and CO_2 (methanogenesis) (e.g. Berner, 1981; Lord & Church, 1983; Reddy & D'Angelo, 1994).

The temporal and spatial movement of these zones in the sediment column due to hydraulic variations or physical disturbance (e.g. organism bioturbation or flow re-suspension) within a stable hydraulic regime may result in the exposure of materials to a different redox environment. Upon exposure to less reduced conditions free metal ions released from the decomposition of sulphides and the cation exchange from clay-organic ligand complexes (dependent on the bonding state of metal-organic complexes in the sediment) may be adsorbed onto Mn and Fe oxyhydroxides and re-precipitated in near-surface oxic layers above (e.g. Farmer, 1991, Williams *et al.,* 1994). Although occurring as a widespread phenomenon in wetland soils, the same process also occurs on a much smaller scale, due to rhizospheric activity in waterlogged soils. Capable of operating at a greater depth than direct atmospheric gas exchange, oxygen can be directly transported to sediments at depth via the root-soil-water interface. Oxygen diffusion from rhizomes causes a micro-oxidative environment around root surfaces and the development of a red-brown $Fe(OH)_3$ coating, due to the oxidation of ferrous to ferric iron (e.g. Williams *et al.,* 1994).

Visible stratigraphical changes in coastal marsh sediments usually provide clear evidence of the extent of the contemporary redox environment. A typical sequence involves: a thin oxidised surface layer, rich in plant matter from surface vegetation; an $Fe(OH)_3$ mottled zone of varying thickness (reflecting rhizospheric activity and tidal/hydrological variation in groundwater) subject to shifting oxidising and reduced states; and a dark layer with no mottling, indicating the presence of Fe-sulphides and reduced conditions (e.g. McCaffrey & Thomson, 1980; Zwolsman *et al.,* 1993; Cundy & Croudace, 1995).

The preservation of a chemical time-depth signature in a sediment sequence may therefore be significantly unrepresentative of historical inputs (e.g. Farmer, 1991; Zwolsman *et al.,* 1993), especially due to the localised effects of vegetation and rhizospheric activity, i.e. the association of trace metals ions with Fe-Mn oxyhydroxide and organic complexes (e.g. Jenne & Zachara, 1987; Gambrell, 1994; Caçador *et al.,* 1996).

A measure of the influence on the sediment chemistry of external (allocthonous-minerogenic) and internal (autochthonous-biogenic-organic) depositional factors can be had by determining the Fe:Mn ratio of samples at depth. Variations in the amount of Fe and Mn found in depositional settings, e.g. lakes, are determined by the mineral content and redox environment of catchment soils and redox conditions of the water body (e.g. Mackereth, 1966). Under moderately reducing conditions Mn is readily leached from sediments while strongly reducing conditions are required for the re-mobilisation of Fe. Inputs of Fe and Mn from soils and sediments therefore should reflect local redox conditions in the catchment, i.e. reduced wetland soils should release more Fe compared with more oxic, dry land soils. As Mn will be mobilised in catchment soils and released towards depositional environments more easily, over a wider range of Eh/pH conditions compared with Fe, the Fe:Mn ratio of sediments in cored lacustrine sequences can be used as evidence of variations in (Fe) sediment loads derived from the erosion of minerogenic soils (e.g. Brugam, 1978; Thorndycraft, *et al.* 1998). Problems occur with this assumption when reducing conditions occur at the sediment-water interface or within the deposited sediment (e.g. Bennet *et al.* 1992), when Fe and Mn concentrations respond to the *in situ* redox environment. This effect can be expected to be particularly compounded in the development of organic salt marsh soils; which are inherently diminished in minerogenic input and can contain strongly reducing sub-surface redox conditions.

2.8 Palynological records of environmental change: vegetation dynamics and pollen taphonomy in coastal wetlands

The pollen content of wetland soils and sediments is ultimately due to the characteristics of vegetation in the local area and catchment. Although sediment pathways and depositional controls play a major role in determining the final assemblage of pollen in wetland sediments (discussed below), the type and abundance of palynomorphs found is a result of contemporary vegetation dynamics. To use pollen as a reconstructive tool for palaeo-vegetational dynamic it is necessary to understand both the controls that determine the spatial and temporal evolution of coastal wetland surface vegetation, i.e. disturbance and intrinsic factors of pollen production, dispersal and deposition.

2.8.1 Vegetation dynamics in coastal wetlands

The spatial distribution of plant communities in salt marsh habitats are determined by interacting physiographic and ecological processes. Surface vegetation is clearly indicative

of the symbiotic relationship between abiotic controls of the depositional environment and the response of plant communities to the growing environment.

The spatial pattern of salt marsh plant zonation in macro and mesotidal wetlands has primarily been attributed to gradients developed in edaphic factors, due to the gradual elevation of marsh surfaces and subsequent variations in tidal inundation frequency and depth (e.g. Chapman, 1960; Ranwell, 1972; Redfield, 1972; Oenema and DeLaune, 1988). Although tidal status may be considered the primary control on lateral and vertical vegetation zonation in macro-tidal salt marsh settings, e.g. around the North Sea, local scale physiographic features also complicate the distribution of species across marshes (Table 2.1.), e.g. at the margin of creek or barrier-dune systems where better drained, sandy soil often favours the growth of *Atriplex portulacoides* (e.g. Cooper, 1982; French *et al.*, 1990).

Subsurface interactions between soil conditions and vegetation zonation become more complex however, with decreased tidal status, as the diversity of climatic, physico-chemical and ecological controls on plant distribution take precedent. Plant communities in microtidal and Mediterranean-climate salt marshes are greatly influenced by salinity gradients and other edaphic conditions (e.g. Purer, 1942; Costa & Boira, 1981; Pennings & Callaway, 1992; Ortiz *et al.*, 1995; Sanchez *et al.*, 1998). Compared with more frequent changes of salinity as a consequence of tidal inundation, Mediterranean-type climatic conditions (mild, wet winters and hot dry summers) induce a marked seasonality in soil (euryhaline) conditions and subsequent patterns of plant growth and zonation. For example, stress induced in perennial plant communities, during periods of high soil-salinity, i.e. the migration of salts to the surface due to summer evapotranspiration, has been suggested to explain a concomitant increase in winter annuals during successive winter months of higher precipitation and lower soil salinity (Callaway *et al.*, 1990). Other biotic controls on plant distribution patterns in coastal salt marshes have also been recognised; principally vegetation zonation due to inter-specific competition and adaptive strategies of individual species to marsh disturbance (e.g. Silander & Antonovics, 1982; Bertness & Ellison, 1987).

Pennings & Callaway (1992) indicate that the zonation of marsh plants in Mediterranean-climate salt marshes may be considered as similar to the zonation of species in an inter-tidal rock-pool. Species are replaced by a competitive superior in the most physically favourable conditions, while at the opposite end of the gradient, will be limited by its tolerance to physical conditions. This pattern is also suggested to be further complicated in Mediterranean-type salt marsh plant zonation because of the difficulty in separating the cause of physical condition extremes, i.e. phenological stresses induced due to microtidal flooding often being in close proximity to euryhaline conditions invoked by seasonal

temperature-precipitation patterns (e.g. Callaway *et al.,* 1990; Ortiz et al. 1990; Pennings & Callaway, 1992).

Physical disturbance to vegetation, can therefore be viewed as an inherent, though relative factor in the evolution of coastal wetland communities. The impact of disturbance processes on marsh communities should be considered in terms of the spatial and temporal context of the environmental setting. Research on the status of marsh communities affected by disturbance events, e.g. hurricane landfall, storm surges and alluvial flooding, has identified that they are often crucial for the longer-term survival of the coastal wetland (e.g. Guntenspergen *et al.* 1995; Hensel *et al.* 1999).

The response of marsh surfaces and vegetation to physical disturbance in coastal marshes may therefore be considered as being dependent on three inter-related variables: the initial resistance of the depositional environment to disturbance (threshold physiographic/biotic limits); the timing, scale and magnitude of the disturbance process/event; and available biotic resources/growing conditions for recovery following disturbance (Allison, 1996).

Disturbance in salt marsh communities is invariably used to describe a sudden change in growing conditions that are reflected by an equally detectable change in plant populations/community structure (e.g. Beeftink, 1979; Bertness & Ellison, 1987; DeLaune *et al.,* 1994; Baldwin & Mendelssohn, 1998). In coastal salt marshes disturbance in this sense usually occurs in three ways; the rapid accretion of sediment on the marsh surface covering existing vegetation, the removal of surface vegetation by erosion/die-off, or a sudden change in the edaphic environment, e.g. rapid subsidence/uplift. The general result of these scenarios, results in the generation of areas available for the re-establishment of vegetation capable of adapting to new hydraulic conditions.

Table 2.1. Typical distribution of vegetation and pollen types in estuarine-salt marsh settings.

Palynomorph	Environment
Abundance of Hystricospheres and *Pinus*	Tidal channel and mudflats (saline)
Ruppia	Aquatic-submerged salt-marsh
Potamogeton -Triglochin	Freshwater-Brackish marsh
Chenopodiaceae (e.g. *Atriplex, Salicornia*)	Low - High elevation salt marsh
Poaceae - Cyperaceae (e.g. *Phragmites*)	High salt marsh - brackish/freshwater
Asteraceae (Lactuceae-Asteroideae)	High salt marsh - brackish/freshwater
Terrestrial species	Rear marsh (non-saline)

After Jennings *et al.* (1993)

Available surfaces for re-colonisation by erosion and deposition may be generated as a result of catchment flooding of marsh surfaces (e.g. Zedler, 1986; Allison, 1995, 1996; Cahoon *et al.,* 1996; Cundy *et al.,* 1998) or high energy coastal processes, i.e. storm driven sedimentation and coastal erosion (e.g. Nyman *et al.,* 1994; Guntenspergen *et al.,* 1995; Roman *et al.* 1997). Disturbance and the creation of available surfaces may also occur due to lower magnitude, high frequency intrinsic wetland dynamics, operating at a more local scale, e.g. creek margin collapse, salt pan development and vegetation die-off caused by the dumping of uprooted vegetation (wrack) on marsh surfaces (Bertness & Ellison, 1987).

The timescale and spatial extent of marsh vegetation re-establishment following disturbance has been observed largely to correspond with a number of factors: the status of the plant community prior to disturbance, e.g. the maturity of plants, size of population, seasonal phenological differences; differences in marsh physiography and soil conditions brought about by disturbance (e.g. Guntenspergen *et al.,* 1995; Allison, 1996) and the individual species phenological response to colonise available surfaces, i.e. via rhizospheric offshoots or seedlings (e.g. Purer, 1942; Ranwell, 1964; Bertness & Ellison, 1987; Pennings & Callaway, 1992). The recovery of salt marsh vegetation to pre-disturbance levels has been observed to be rapid (*circa* 1-2 years) where disturbance has generated growing conditions suitable for either for the germination of seedlings (e.g. Allison, 1996) or the establishment of a different plant community after an extreme event (Guntenspergen *et al.,* 1995). Experimental plots indicate that existing plant species (*Arthrocnemum* and *Salicornia*) can expand by as much as 300% over the period of a year (Pennings & Callaway, 1992).

The most extreme disturbance to marsh surfaces has often been a result of anthropogenic activity, either for an indefinite period due to drainage, reclamation and re-surfacing (e.g. Purer, 1942) or as recoverable disturbance due to the re-establishment of marsh vegetation and hydraulic conditions following disturbance to coastal marsh areas for reclamation, agriculture and other industrial activities (e.g. Heijnis *et al.* 1987; Bressolierbousquet, 1991; Esselink *et al.,* 1998).

As present-day coastal salt marshes have evolved invariably over timescales ranging between *circa* 1-10^3 years, vegetation-associated accretion rates at a fixed point in space may have potentially been affected by repeated patterns of short-term (seasonal-yearly-decadal) disturbance depending on the historical stability of the marsh surface and wider environmental controls on wetland development. The timing and magnitude of disturbance events and subsequent rates of recovery, therefore, are a critical factor for the palaeoenvironmental interpretation of salt marsh sediments, especially when using a vegetation-dependent palaeoecological technique like pollen analysis.

2.8.2 Pollen production and transport in coastal wetlands

The pollination energetics and dispersal patterns of salt marsh species is complicated by two principal factors, which have led to pollen production and transport within salt marsh areas being poorly understood: namely spatial and temporal differences in the flooding of marsh surfaces during flowering periods and the uncertainty with many species as to whether they disperse pollen by wind or visiting insects (Adams, 1990). An investigation by Manso & Andres (1993) on the pollinic characters found in Mediterranean salt marsh plants identified a relationship between phenological differences and pollination mechanism. Findings from the study indicated that anemophilous (wind-transported) pollinators were associated with non-colourful flowers (Poaceae, Chenopodiaceae, Juncaceae and Cyperaceae) producing multi-aperture, spherical pollen types, while entomophilous pollinated (insect transported) species had more colourful flowers producing irregularly shaped and ornamented grains (e.g. Tamaricaceae, Compositae and Plumbaginaceae).

When salt marsh vegetation is flooded, pollen is likely to be transported directly from flower heads and from plant surfaces. Plant surfaces regularly inundated by floodwater may provide a temporary storage for pollen from the initial plant as well as grains introduced into the marsh area within the water column. Successive flooding may be expected to transport grains further, compared with precipitation and gravity fallout which is more likely to distribute grains directly beneath the surface vegetation.

The effectiveness of salt marsh habitats to act as a sink for the flux of materials transported to and within the coastal zone is emphasised by pollen assemblages found in salt marsh sediments. Although initially a result of the production and dispersal of pollen from plant communities in the catchment and local vegetation, assemblages of pollen grains incorporated into accreted sediments are also highly indicative of sediment dynamics within coastal wetland systems (e.g. Stevenson, 1985; Clark & Patterson, 1985; Clark, 1986a, 1986b). Research to determine spatial and temporal variations of pollen assemblages encountered in coastal wetlands has highlighted a number of factors which have important consequences for the use of pollen as a proxy of vegetation change in coastal salt marsh, estuarine and lagoonal sediments.

Compared with terrestrial aquatic environments where the most extensive sources of pollen are *via* atmospheric transport or a relatively definable catchment (e.g. Pennington, 1979; Stevenson & Battarbee, 1991; Gale *et al.*, 1995; Parizzi *et al.*, 1998; Waller, 1998), the supply of pollen to coastal wetlands (both fringing estuarine, mangrove and lagoonal environments) has a massive potential of being complicated by the aquatic supply of catchment pollen and reworking of previously deposited pollen within coastal-marine environments (e.g. Planchais & Parravergara, 1984; Sheffield *et al.*, 1995; Ellison, 1996;

Woo *et al.,* 1998). The use of "local", "extra-local" and "regional" as terms to describe the source and distance travelled by pollen grains to a marsh surface are clearly relative being dependent on the size of the marsh, scale of the catchment area, potential transport sources to and within the marsh area and the pollen taphonomic characteristics of plant species in the catchment (e.g. Clark & Patterson, 1985; Waller, 1998). Regional and extra-local pollen may be differentiated by the latter having been derived from within the hydrological catchment area. Brush and DeFries (1981) determined that sediments from an estuarine setting contained only tree pollen assemblages that were representative of a band of local channel-side populations. Pollen assemblages from tree types found upstream above the tidal limit of the estuary were particularly under-represented.

The timing and supply of regional pollen to an estuary or coastal wetland can therefore be expected to be complicated by an indefinite number of factors, e.g. tidal obstruction, floodplain-channel storage, to an extent that all pollen types clearly unrepresentative of the local coastal wetland vegetation may be considered regional. In large deltaic or estuarine wetlands these sources can be extremely distant, e.g. Ethiopian upland pollen types in Nile delta lagoonal deposits (Leroy, 1990). Any supply of pollen-containing sediment from the marine-coastal environment, incorporating regional, long-range transported grains from adjacent drainage catchments and coastal vegetation may therefore be best considered as an undefinable extra-local source (Fig. 2.4). Pollen types such as *Pinus* (because of its buoyant nature) and resistant types such as Lactuceae clearly come under this category.

Although the local, extra-local and regional sources of pollen may be considered relative factors to the supply of pollen to a marsh surface, the intensity of potential re-suspension, mobility and surface-assemblage homogenisation has been observed to occur as a direct consequence of the physiographic-hydraulic regime. The dimensions of most pollen grains (0.01 - 0.05 mm) makes them theoretically susceptible to the same transport, re-suspension and depositional processes as fine-grained (silt-size) clastic sediment.

As a result, even without a change in local/extra-local vegetation, changing physiographic factors on sediment transport may significantly influence the pollen record of local/extra-local types transported to the sediment surface (e.g. Davis, 1992; Jennings *et al.,* 1993; Sheffield *et al.,* 1995; Woo *et al.,* 1998). In shallow bodies of water, e.g. coastal lagoons, mudflats and inundated marsh surfaces, wave-induced turbulence has been observed to be especially effective (due to a high sediment surface area-wave activity depth ratio) at winnowing and re-suspending pollen grains, e.g. *Pinus*, from previously deposited sediments (e.g. Chmura & Eisma, 1995;Woo *et al.,* 1998). This also implies that in areas less-affected by active re-working, i.e. at below the depth of active wave re-suspension or in a more sheltered position, pollen accumulation rates may be enhanced by the deposition of re-worked materials (Bonny, 1976), including grains derived from much older deposits.

Figure 2.4. Pollen sources, transport pathways and deposition in a coastal lagoon/estuarine setting

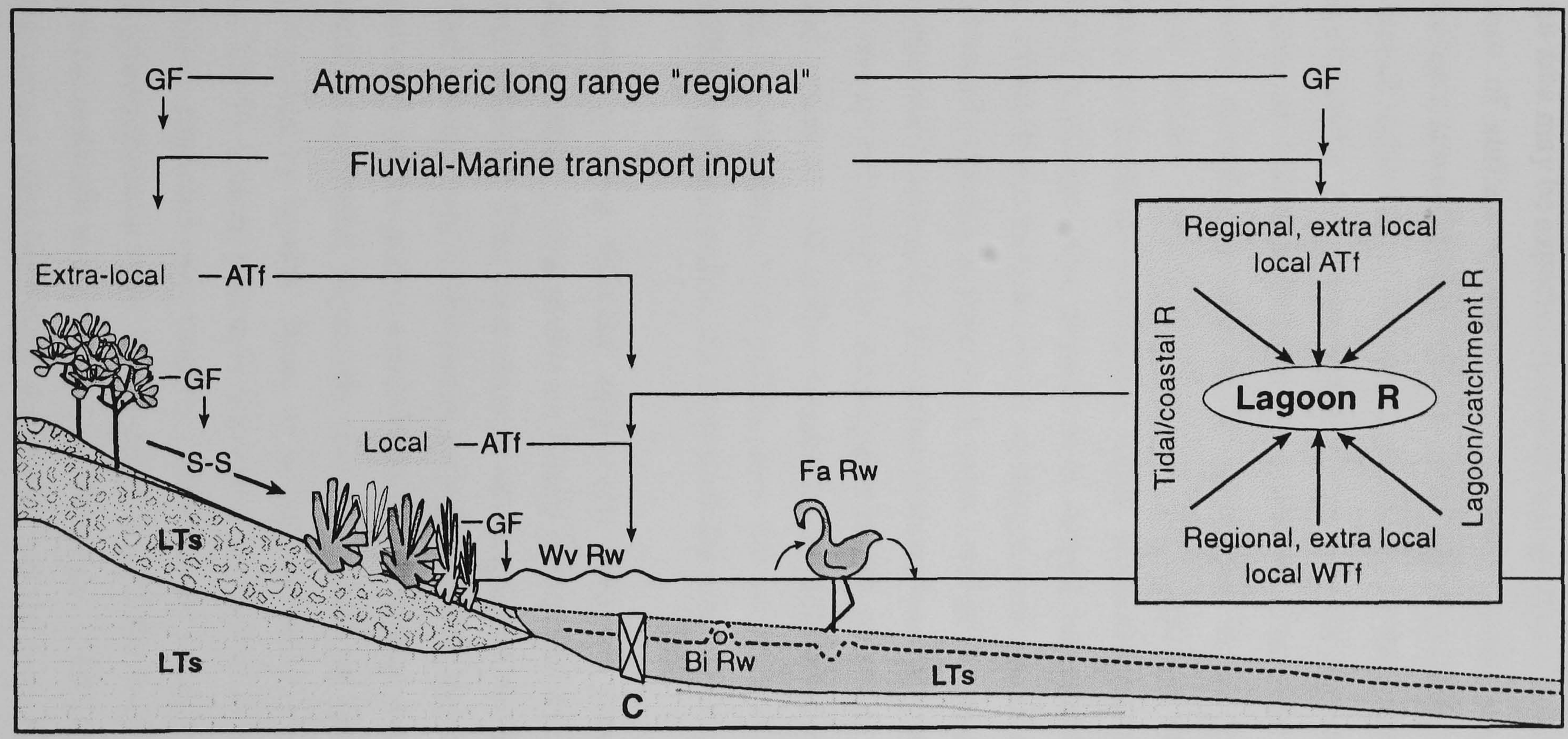

KEY

Local	Pollen sources
S-S	Soil slope transport and tempoary storage
GF	Gravity fallout (direct and via plant surfaces)
Bi Rw	Bioturbation re-working
Fa Rw	Faunal (incl. human) re-working and transport
Wv Rw	Wave action re-working
C	Example core site
ATf	Atmospheric Transport function
WTf	Water-body Transport function
R	Multi-source reservoir
LTs	Longer term storage (sediment deposition)

Pollen assemblages in sediments of coastal wetlands primarily reflect local vegetation patterns, due to direct gravity fallout, canopy wash by precipitation and limited local transport (e.g. Brush & DeFries, 1981; Clark, 1986b; Woo *et al.,* 1998) along with pollen incorporated *via* longer range transport and dispersal. As a result the local pollen content over an area may be expected to exhibit a high spatial variability, related to the presence and response of surface vegetation to growing conditions, e.g. surface vegetation-pollen assemblages across an inter-tidal mudflat-marsh gradient (Table 2.1.).

This spatial variability of wetland vegetation and the gradual development of zones related to physiographic and ecological controls, should theoretically be observable in vertical sequences of marsh sediments. A series of cores for example, representing sediment sequences accreting normal to the principal stress gradient (e.g. seaward-landward transect) should contain a record of the migrating edaphic environments (e.g. tidal influence to brackish-freshwater). These temporal and spatial differences are commonly observed in transgressive sequences of coastal salt marsh deposits (e.g. Redfield, 1972; Clark, 1986). If not representative of longer-term marsh evolution, the sediment sequence should usually contain at least local, extra-local pollen assemblages representative of recent environmental changes, i.e. the influx of extra local pollen due to wetland flooding by river or the sea or reflecting the subsequent marsh recovery. As a result, rather than using wetland sediment and pollen sequences to determine regional patterns of vegetational change, i.e. excluding local pollen from the pollen sum (e.g. Clark & Patterson, 1985) assemblages of local pollen are most usefully representative of local wetland dynamics.

A potentially great time-lag may exist between production, transportation and re-suspension before pollen grains are finally incorporated into a definable estuarine or coastal wetland sequence. This time element also increases the likelihood of pollen grains having travelled a wide range of distances, as well as being successively deposited and reworked. In most cases pollen grains which have been buried and reworked will show some form of structural decay, either physically due to abrasion or chemical damage brought about by being digested by benthic fauna or being successively buried and exhumed (Chmura & Eisma, 1995). Unless pollen is deposited into a low oxygen environment the structure of the grain is degraded over time by oxidation. In an oxic environment the degradation of pollen grains depends upon the susceptibility of the individual taxa, with *Pinus* being one of the most resistant to corrosion (e.g. Havinga, 1984), though not to mechanical stresses with the saccae often becoming detached from the body (Chmura & Eisma, 1995).

As both dispersal rates and the time difference between pollen production and sediment incorporation can be expected to be greater for vegetation communities at a distance, the accuracy of recording vegetational changes distant from a particular core site may also be expected to decrease. The relationship between pollen content and distance from production

is not aided in lagoonal-estuarine settings by the fact that different types of pollen grains have different buoyancy characteristics, which are affected by varying hydraulic conditions. Bi-saccate *Pinus* pollen in particularly is often over-represented in lagoonal-estuarine sediments (in terms of actual nearby tree population) due to the initial atmospheric dispersal of the grains and subsequent buoyancy in aquatic environments (e.g. Woo *et al.* 1998). Similarly the over-representation of other grains, such as Lactuceae can occur not due to being more efficiently transported but by having a resistant exine, capable of surviving long-term transport and re-working in both the fluvial and marine environment.

2.9 Summary

Coastal wetland sediment sequences require a multi-proxy approach to sedimentological analyses to identify depositional changes over space and time in relation to environmental change. As closely inter-related physical, geochemical and ecological processes control the deposition of coastal wetland sediments, the choice of palaeoenvironmental investigation techniques used to interpret environmental changes should also reflect the main environmental controls on the evolution of the setting and sequence sedimentology.

On their own they can only provide evidence of a particular component of the development of coastal wetlands, e.g. loss on ignition to determine the organic-inorganic content of salt marsh soil, but used together, the results from the techniques outlined above provide a powerful tool for the palaeoenvironmental interpretation of recent sedimentation in coastal wetlands.

As the final deposition and nature of sediments in coastal wetlands is a consequence of often far-reaching (occasionally disparate) environmental controls (operating on diverse spatial and temporal scales), a multi-proxy palaeoenvironmental approach is clearly vital.

Chapter Three

The environmental evolution of the Mediterranean and its influence on coastal wetlands

"In the time of the Trojan wars the Argive land was marshy and could only support a small population, whereas the land of Mycenae was in good condition (and for this reason Mycenae was the superior). But now the opposite is the case...the land of Mycenae has become...dry and barren, while the Argive land that was formerly barren owing to the water has now become fruitful. Now the same process that has taken place in this small district must be supposed to be going on over whole countries and on a large scale".

Aristotle, from Meteorologica, Book 1, Chapter 14

3.1 Introduction

Coastal wetlands in the Mediterranean region occupy only a very small component of the present-day landscape which has evolved due to the close interaction of geological, climatic, ecological and anthropogenic systems. The Mediterranean basin has long been recognised as a region in which human activity has been both influenced greatly by physical aspects of the landscape and played a dominant role in subsequent environmental changes.

Coastal wetlands are capable of retaining information of progressive and more rapid environmental processes affecting hydrological and coastal systems as they occur at the interface of these and the terrestrial environment. Despite their limited extent, coastal wetlands in the Mediterranean provide highly suitable sites for the investigation of past interactions between natural systems and human activity, not least because of the resources they have provided for human occupation and development.

As a result an introduction to the environmental processes which have shaped the diversity of landscapes (and coastal wetland settings) in the Mediterranean region is required to set the evolution of the south east Sicilian coastal landscape (see following chapter) into its regional context.

3.2 Geology, tectonics and relief of the Mediterranean

The Mediterranean basin primarily represents the lithospheric collision boundary of the African, Eurasian and Arabian plates. Tectonic activity is also complicated by the presence of a number of smaller, intervening micro-plates (e.g. the Aegean and Adriatic plates, Fig.3.1). Continental collision and subduction through the Tertiary between Africa and Eurasia produced the uplift of the Alpine Fold Belt, the high relief mountainous landscapes of the Pyrenees, Maghreb, Alps and Apennines and the subduction-collision associated islands of Sicily, Crete, Cyprus and the Aegean archipelago. Subduction between the African and Eurasian plates and continued crustal motion is confirmed by the geomorphological, archaeological and historical record of high magnitude earthquakes, volcanic activity and active faulting in the region particularly in the Aegean (e.g. Papazachos & Papazachou, 1997), western Turkey (e.g. Altunel, 1999), Sicily and the Aeolian Islands (e.g. Chester *et al.,* 1985).

The complexity of tectonic activity in the Mediterranean, with often dramatically different stress regimes within an active region has been especially apparent in the construction of regional chronologies of long and short-term changes in relative sea level (e.g. Flemming

Figure 3.1. Schematic tectonic map of the Mediterranean region (modified from Robertson & Grasso 1995)

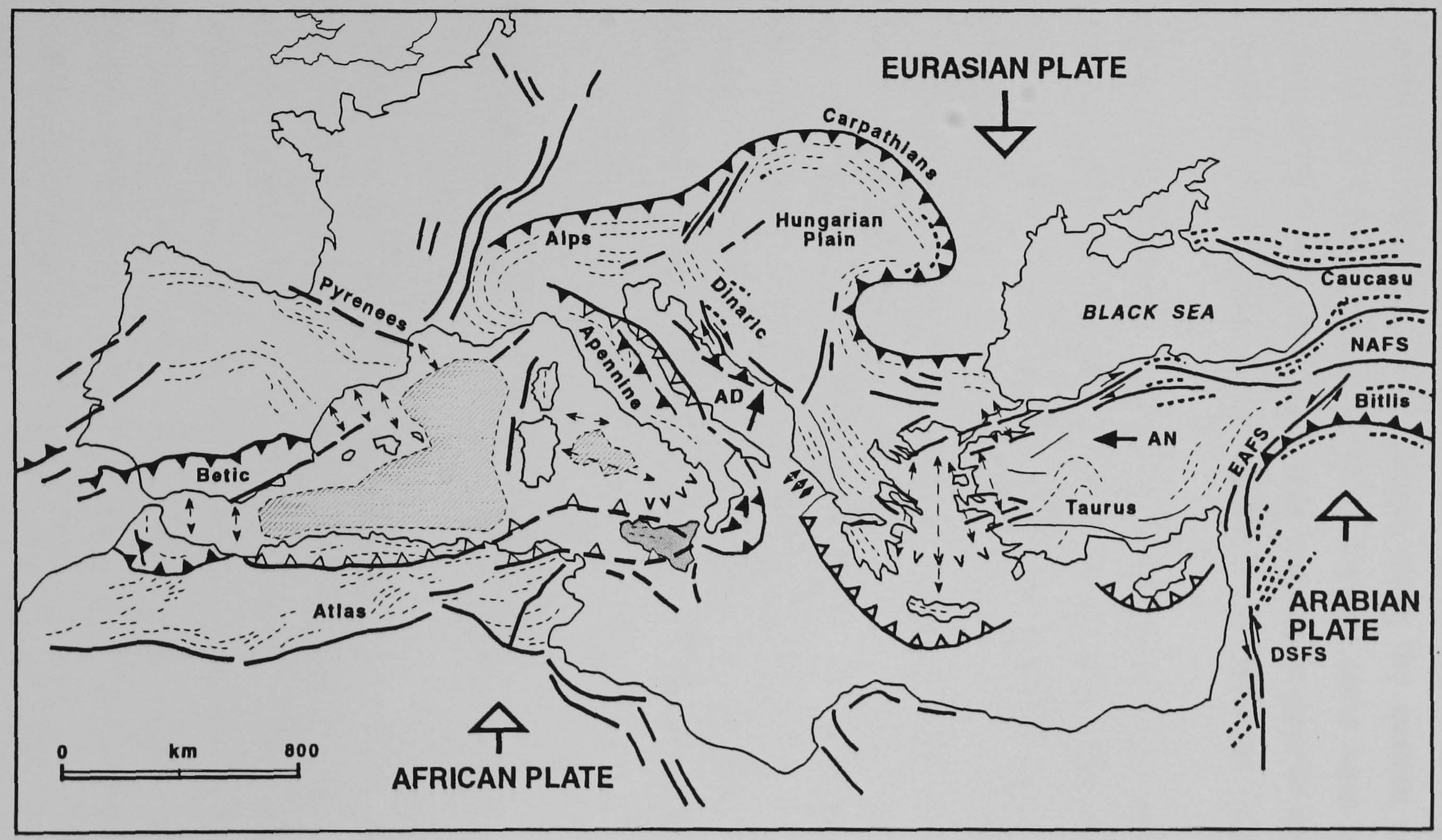

& Webb, 1986; Emery *et al.* 1988; Pirazzoli, 1994; Stewart, 1996; Bordoni & Valensise, 1998) and the effect of tectonic motion on coastal uplift, drainage catchments (e.g. Collier *et al.* 1992) and coastal landforms (e.g. Soter, 1998; Mathers *et al.* 1999).

Mediterranean coastal wetlands situated at river mouths, delta fronts and along low lying coastal areas in active tectonic settings have been shown to have been inundated as a result of rapid coseismic subsidence (e.g. Lekkas *et al.* 1996; Cundy *et al.* in press) and tsunami generated by offshore earthquakes, for example along the eastern coastline of Sicily following the 1908 earthquake (Barrata, 1910). Wetland areas have also been sites of short-lived, dramatic events associated with large magnitude seismic events, for example sand volcano eruptions and thermal-salinity shifts in groundwater (e.g. Schmidt, 1862; Soter, 1999).

Over both long-term timescales of tectonic influence and recent neotectonic motions, evidence of tectonic activity in Mediterranean coastal wetland sediments have only been recognised if they have been distinguishable from other controlling factors on deposition and other high magnitude phases of disturbance. Recent work by Cundy *et al.* (in press) has highlighted difficulties in identifying the signature of historically documented coseismic wetland flooding in coastal sediment sequences from the affected locality, corresponding with the correct age. The nature of coseismic flooding in this event left only slight palaeoecological evidence of immersion, which could have been attributed to a more recurrent non-seismic event, e.g. a breach in the protective shingle barrier due to winter storms, where it not for the measured high resolution ^{210}Pb chronology of the sediment sequence.

3.3 Sea level change in the Mediterranean basin

The Mediterranean sea is the key feature separating the region from other Mediterranean climates found globally at mid-latitudes between 30°-40°(Money, 1965). The sea itself is sub-divided into two basins (Fig 3.2.): the western (max. depth ~3400 m) and eastern (max. depth ~4200 m) by a sill between Sicily and Tunisia with a maximum depth of 400 m and the Strait of Messina (max. depth 120 m) between Sicily and Calabria (Tomczak & Godfrey, 1994). Due to its enclosed nature, another characteristic of the Mediterranean sea is its low tidal range, decreasing from 0.8 m at Gibraltar in the west to 0.4 m at Port Said, Egypt and as low as 0.2 m along the French coast (Pickard & Emery, 1990). The main rivers entering the sea (Nile, Rhône, Ebro, Po) have therefore been able to develop extensive deltaic areas as a response to river discharge, sediment budgets and wave conditions.

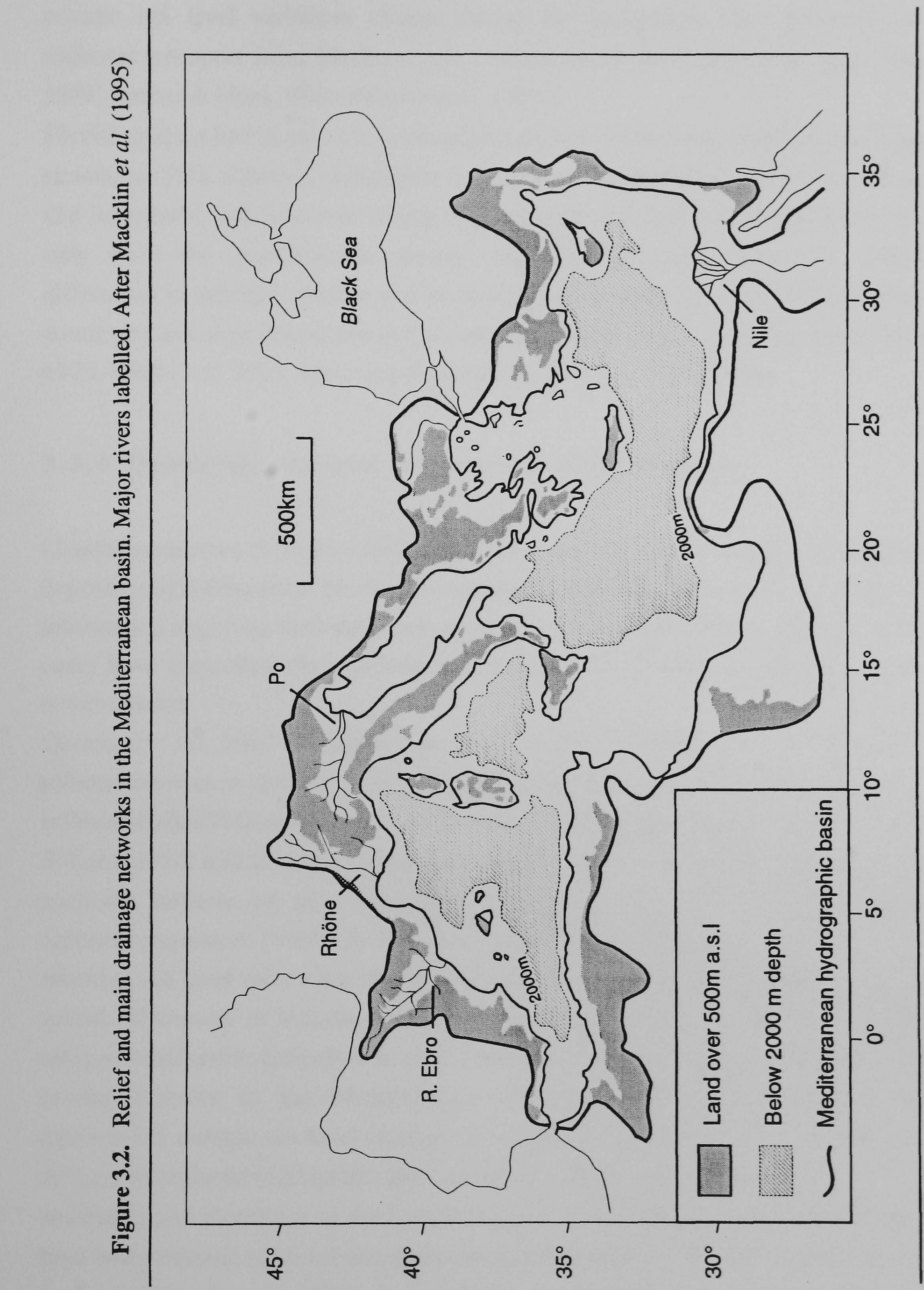

Figure 3.2. Relief and main drainage networks in the Mediterranean basin. Major rivers labelled. After Macklin *et al.* (1995)

Large amplitude changes in sea level, especially those encountered during the Late Quaternary have greatly affected the evolution of present-day Mediterranean coastal landscapes. Combined with climatic and tectonic controls, base level changes due to eustatic sea level variations change during the Quaternary have primarily controlled sediment transport from Mediterranean catchments to the coastal zone (e.g. Vita Finzi, 1969; Barker & Hunt, 1995; Bellotti *et al.* 1995).

Fluvial systems had to adjust to large magnitude base level changes during the Quaternary, creating a cyclic pattern of denudation and incision during falling and low stand sea levels and successive sedimentation during transgressive and high stand sea levels. Generally only since the mid-Holocene eustatic sea level still-stand (Pirazzoli, 1987), have differences in tectonic, climatic and increasingly anthropogenic causal factors been able to dominate catchment denudation and coastal topography (e.g. Flemming, 1969; Kraft *et al.* 1975, Kraft *et al.* 1977; Mourtzas & Marinos, 1994; Lambeck, 1996).

3.3.1 Quaternary sea level trends in the Mediterranean

Coastal landscapes of the present-day Mediterranean are often dominated by landforms and deposits originating from Pleistocene sea level variations. These have not only provided information regarding the longer term evolution of individual coastal settings, but in many cases have controlled the structural and depositional patterns of later Holocene coastal environments.

Quaternary sea level variations are most visibly recorded in the Mediterranean as palaeoshorelines in uplifted areas e.g. along stretches of coastlines in Calabria and Sicily, southern Italy (Di Grande & Raimondo, 1982; Dumas *et al.,* 1993), Almeria, Spain (Goy & Zazo, 1986) and the Ionian Islands, Greece (Pirazzoli *et al.* 1994). Palaeoshorelines and erosional surfaces are also identifiable at the base of estuarine, coastal and offshore sediment sequences (Viñals & Fumanal, 1995; Dubar & Anthony, 1995). The potential record of sea level variation in the Mediterranean is therefore closely linked to temporal and spatial differences in tectonic activity and sedimentation history. Further to this, there remain considerable difficulties in identifying, dating and extrapolating between Quaternary marine deposits in the Mediterranean (Pirazzoli, 1987), even between sediments representing eustatic sea level changes of magnitudes seen in the last 150,000 years, i.e. the Last Interglacial (120 ka BP) and Last Glacial Maximum (c. 18 ka BP).

Sediments and shorelines of the Last Interglacial are recognised around the Mediterranean from when eustatic sea level was approximately between two and five metres above present sea level (Dumas *et al.,* 1993). In the Mediterranean basin these deposits have been given the general term "Tyrrhenian", containing a recognisable warm-water faunal assemblage particularly the abundance of the marine gastropod *Strombus bubonius* Lmk, presently

Figure 3.3. Eustatic sea level changes and extended coastal plains in the Mediterranean

(a) Exposed plains in the central Mediterranean during the Last Glacial Maximum

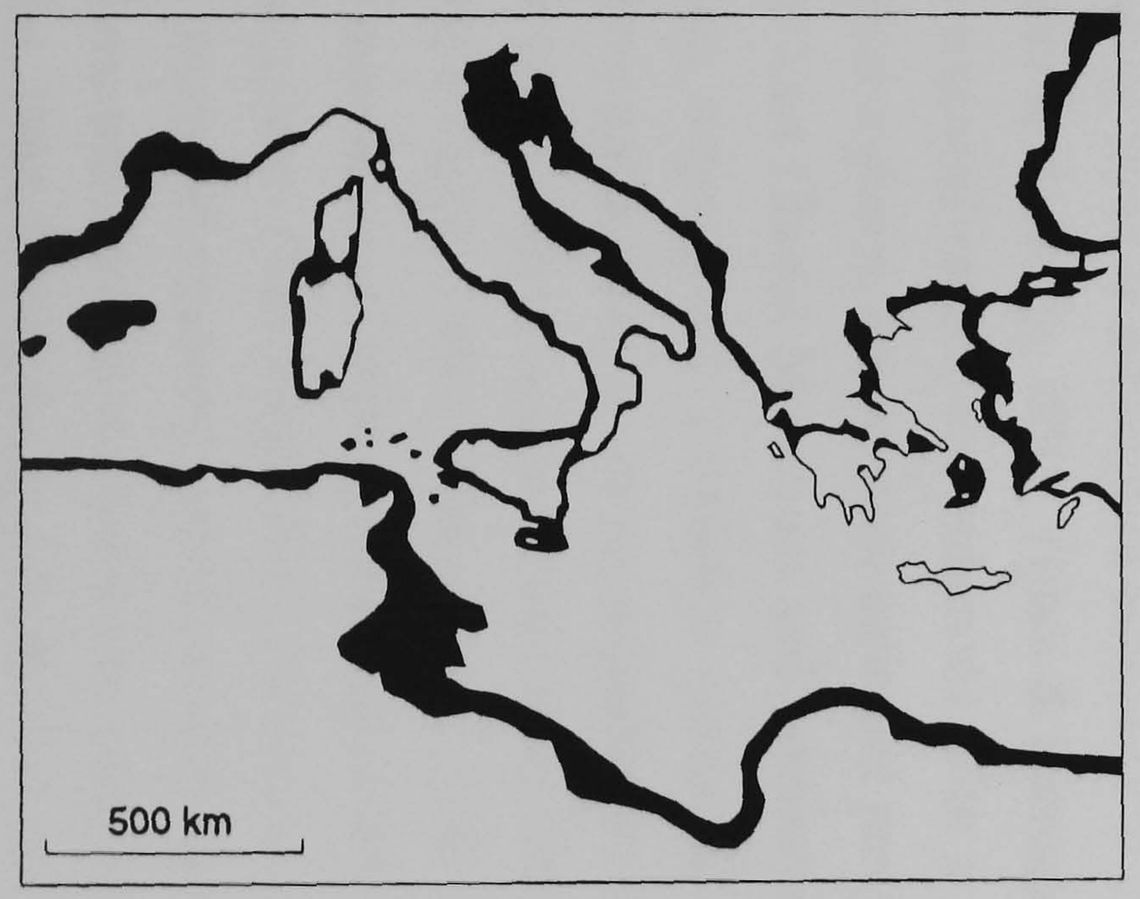

(After Van Andel, 1989)

(b) Estimated eustatic sea level variations over the last 150 ka.

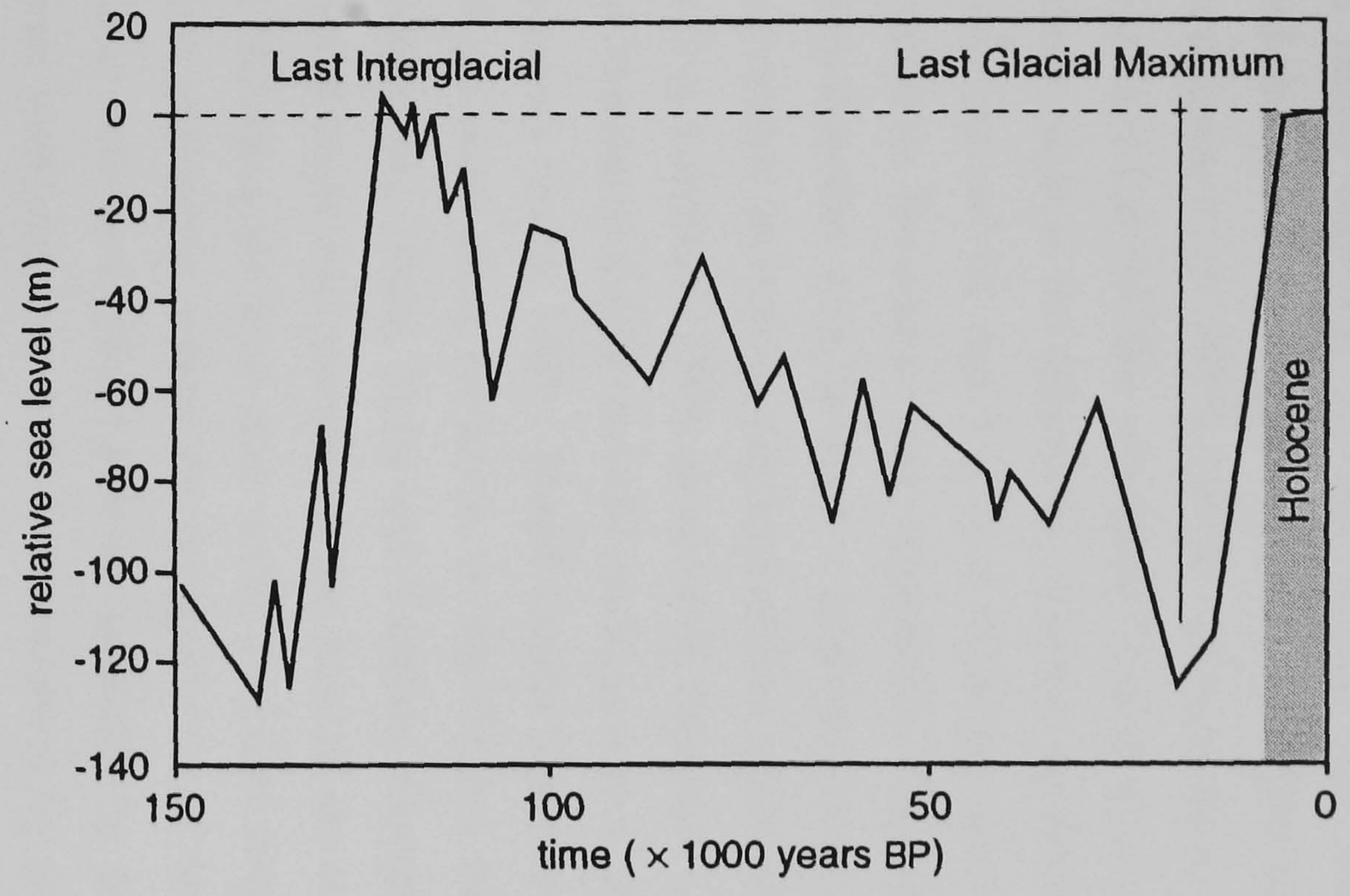

After Lambeck (1996)

found only off the west coast of Senegalese Africa (Pirazzoli, 1987). Similarly with other Quaternary and more recent deposits, tectonic activity has altered the elevation of Tyrrhenian deposits and shorelines. In Reggio Calabria, southern Italy, uplift has elevated deposits to up to 150m (Dumas *et al.*, 1993). On the southern shore of the Gulf of Corinth, Greece, this shoreline is found at 30-70m elevations (Collier *et al.*, 1992), while in other areas of the Mediterranean such as the tectonically inactive Sardinian coastline (Ulzega & Hearty, 1986), this shoreline and its deposits have remained near to sea level (0-10 m) indicative of minimal tectonic movement since deposition. The identification of the last interglacial shoreline may therefore only be used to estimate the extent, though clearly not the entire chronology of vertical tectonic motion and relative sea level over the last 120 000 years between regions (e.g. Lambeck, 1996; Bordoni & Valensise, 1998).

During the Last Glacial Maximum (LGM) eustatic sea level was in the order of 100-120 m below present sea level (van Andel, 1989). Broad coastal plains bordered many areas of the Mediterranean. These were most extensive in the Central Mediterranean (Gulf of Gabes, Tunisia and connecting Malta, Sicily and Calabria, Southern Italy) (Fig.3.3) as well as in the north-west Adriatic and margins of the Aegean sea (e.g. van Andel, 1989). Due to the subsequent Holocene sea level rise, nearly all LGM shorelines currently reside offshore, buried beneath sediments, where the interpretation of beach rock samples and palaeoshorelines found at various depths, has been disrupted by problems in radiometric dating, post-depositional movement, as well as entrainment by postglacial transgressive sedimentation (Pirazzoli, 1987). With the adjustment of fluvial systems to lowered base levels and more extensive coastal areas, earlier Quaternary sediment units in the coastal zone were denuded and incised leading to the deposition of diachronous coarse clastic units, which underlie many areas of subsequent onshore and offshore Holocene deposition (Kraft *et al.*, 1975; Dubar & Anthony, 1995; Viñals & Fumanal, 1995).

During glacial periods seasonal runoff was enhanced with a greater spatial and temporal variability of hydrological regimes, due to snow melt and precipitation patterns (Macklin *et al.*, 1995). During the Last Glacial Maximum and previous stadials, high runoff rates associated with shifting tropospheric circulation patterns, decreased vegetation cover (*Artemisia* steppe) and coastal thalweg incision, adjusting to the fall in sea level, often led to the development of high energy, coarse clastic river environments (Barker & Hunt, 1995; Provansal, 1995; Coltorti, 1997). These were often accompanied with enhanced slope erosion and the deposition of thick colluvial deposits (e.g. Rose *et al.* 1999) and aggradational fluvial sequences (Vita-Finzi, 1969; Harvey *et al.*, 1995).These often coarse, angular deposits were deposited relatively synchronously across the Mediterranean during the Last Glacial-Holocene transition as recognised by early researchers (e.g. Judson, 1963; Eisma, 1964; Vita-Finzi, 1964, 1969), being described as the "Older-Fill". Aside from the chronostratigraphic division, these older fills are distinguishable from successive Holocene

valley fills by prehistoric artefacts (Judson, 1963; Vita-Finzi, 1969) and sedimentological characteristics (e.g. Macleod & Vita-Finzi, 1982).

Early human occupation sites from this time around the Mediterranean, indicate that Palaeolithic populations were adapted to low and rising sea levels and extended alluvial plains, utilising coastal and marine resources during glacial maxima and post glacial sea level rise e.g. at Franchthi Cave in southern Greece (Shackelton & van Andel, 1980). As a result, much of the scattered evidence of human populations at this time occurs offshore (e.g. Flemming, 1998).

3.3.2 Mediterranean sea level trends in the Holocene

Pleistocene-Holocene sea level curves obtained from the Mediterranean show a rapid steady rise in sea levels from the LGM (*circa* 18ka BP) when sea levels were approximately 100m below present to the mid-Holocene (*circa* 6 ka BP) when rapidly rising post-glacial eustatic sea levels started to decelerate (Fig. 3.3a) and attained to a lesser or greater extent, present-day sea level (Kraft *et al.*, 1975, 1980; Dubar & Anthony, 1995; Lambeck, 1996). By the mid-Holocene coastal plains and land bridges developed during the Last Glacial Maximum eustatic sea level low-stand were reduced and severed. This shift between previously rapid rates of early Holocene, postglacial sea level rise (*circa* 10 m ka^{-1}) and decreased rates (*circa* 1 m ka^{-1}) during approximately the last six thousand years was recognised early on in the study of sea level changes in the Mediterranean (e.g. Bintliff, 1975) as a widespread controlling factor of Mediterranean fluvial systems, deltas and alluvial plains. The eustatic component to sea level change since this time has been calculated from archaeological sites in coastal settings (e.g. Flemming & Webb, 1986) and modelling scenarios to have been negligible (e.g. Lambeck, 1996).

Archaeological and geomorphological evidence from around the Mediterranean, however often indicates conflicting variations in sea level (caused by crustal uplift variations) during the later Holocene. At the coast of Dor, Israel, for example, "eustatic" sea level has been recorded to have fluctuated in the last 4 ka BP, between 2 metres below present 4000 years ago, rising to 1 metre below the present level 3000 years ago, and rising to one metre above present sea level 1500 years ago, before dropping to one metre below present level around 800 years ago, before attaining its present position (Sneh & Klein, 1984). Disputable archaeological evidence from the same region further complicates the effect that tectonic activity has had on sea level variation on the Israeli coastline (Vita-Finzi, 1986). Sea level is generally thought to have progressively risen in the Mediterranean during the time of the Roman Empire, reaching a high stand comparable to present-day sea level around AD 400 (Lamb, 1995).

Consequently, determining the timing and rate of any eustatic component of Holocene sea level change is problematical in the Mediterranean due to spatial and temporal differences in sea level records due to local tectonics and uncertainty of archaeological evidence (e.g. Mourtzas & Marinos, 1994). Abrupt sea level change related to tectonic and palaeoseismic events has in some areas rapidly uplifted and submerged coastlines. These have occurred for example, due to regional fault movements in tectonically active areas, e.g. volcanic uplift along the Taormina coastline of north-eastern Sicily (Stewart *et al.,* 1997) and fault block controlled coastal subsidence along the Adriatic coastline of Albania (Mathers *et al.* 1999).

The continued effect of local controls on relative sea level change and the difficulty of ascertaining Mediterranean-wide patterns of sea level change are clearly shown with historically recorded tidal gauge data (Emery *et al.* 1988) and mean sea level (Tsimplis & Spencer, 1997). Measurements in the Mediterranean over the last 100 years give little indication that sea level rise has increased eustatically in recent years and that fluctuations in relative sea level continue to reflect local uplift/subsidence regimes and climatic effects (Pirazzoli, 1987).

3.4 Pleistocene climate change and vegetation dynamics

The present-day characteristic climate of a hot and dry summer and mild winter with moderate rainfall is primarily a consequence of the latitudinal position of the basin, along with differences caused by the Mediterranean sea itself. Situated within the boundary of mid-latitude and subtropical pressure systems, weather systems are seasonally influenced by the expanded sub-tropical high pressure zone during the summer, while winter months reflect the eastward passage of rain-carrying Atlantic depressions and cooler polar air (HMSO, 1964; Perry, 1981). This seasonally skewed distribution of rainfall to autumn-winter months has been conducive to high rates of erosional runoff, exacerbated in the past by climatic, vegetational and land-use changes. Climate changes have also influenced Mediterranean coastal dynamics by the alteration of hydrological regimes and related variations in vegetation cover, leading to changes in landscape denudation and sediment supply to fluvial, as well as, coastal systems (e.g. Paepe *et al.* 1995; Coltorti, 1997; Gutiérrez-Elora & Peña-Monné, 1998; Martín-Consuegra *et al.,* 1998). Increasingly in the Holocene, vegetational systems in the Mediterranean basin have had to respond on much shorter time scales than those determined by climate change.

Mediterranean climate-vegetation organisations were established in the Late Pliocene (2.6 Ma BP) as deduced from pollen data, initiating the style of later Quaternary climate

oscillations and subsequent vegetation dynamics (Suc, 1984). In general, glacial climates in the Mediterranean were characterised by colder winters, more intense precipitation and accentuated summer drought (e.g. Prentice *et al.,* 1992; Peyron *et al.,* 1998), which saw the expansion of *Artemisia*-dominated steppe (e.g. Grüger, 1977; Prentice *et al.,* 1992) and the survival of thermophilous species in refugia (Leroy *et al.* 1994; Carrión *et al.* 1995). At the end of the Last Glacial Maximum, semi-arid/arid conditions appear to have existed at both low and high elevations (Tarasov *et al.* 1998), while grass steppe and evergreen stands existed in more favourable, mid-elevation areas (Rossignol-Strick *et al.,* 1994). During interstadials in areas with favourable growing conditions, forest-steppe through to pine-oak forest communities were able to develop and expand (Tzedakis, 1999). During the last glacial period in southern Mediterranean Europe, climatic and vegetational changes have been shown to have occurred on a centennial-millennial scale of variability, frequently occurring in less than 200 years (Allen *et al.* 1999). Deglaciation at the end of the Last Glacial Maximum and the expansion of deciduous trees (*Quercus* sp. associations) in the grass steppe at low and middle elevations, was interrupted by the re-expansion of cold-arid steppe relating to the Younger Dryas event (11-10,000 ^{14}C uncalib. yrs BP) (Rossignol-Strick, 1995). Following this, the herb-dominated steppe was replaced by an early-mid Holocene expansion of mixed deciduous and evergreen sub-humid forest (Lipschitz & Gideon, 1990; Roberts, 1998).

Changes in large scale atmospheric-oceanic circulation patterns associated with oscillating glacial and interglacial periods have altered Mediterranean climatic patterns through the Quaternary (Macklin *et al.,* 1995). Estimated average latitudes of the controlling subtropical high and sub-polar low pressures have shifted position since the Last Glacial Maximum (Lamb, 1995 p.127).

3.5 Holocene climate changes

In the Holocene, climate appears to have varied in the Mediterranean between relatively dry and humid phases of differing amplitude and duration due to the latitudinal shift and dominance of mid-latitude and sub-tropical tropospheric pressure systems associated with North Atlantic sea-surface temperatures (Lamb *et al.* 1992). The present-day marked seasonality of the Mediterranean was developed progressively from the Last Glacial Maximum, imprinting the climatic pattern of summer drought and winter precipitation (Zonneveld, 1996; Jalut *et al.* 1997) on evolving vegetation communities. At the beginning of the Holocene a more humid climate existed in the Mediterranean, caused by the northward migration of the Azores-Subtropical high pressure zone, which pulled the summer monsoon belt into the sub-tropical Sahara and Mediterranean (Ritchie *et al.,* 1985; Roberts, 1989; Lamb, 1995). Transitional glacial-Holocene phases of cool-humid and

warm-dry periods are recognised around the Mediterranean, identifiable in marine sediments and terrestrial deposits (e.g. Reille & Lowe, 1993; Carrión *et al.* 1995; Paepe *et al.*, 1995; Rossignol-Strick, 1995; Jalut *et al.* 1997), from the Dead Sea and other inland water body levels (Issar & Makover-Levin, 1996; Harrison *et al.* 1996).

The declining strength of Early-Mid Holocene monsoonal weather systems, brought to an end the dominance of sub-humid forest, favouring the development of summer-drought resistant evergreen forest and scrub vegetation (Table 3.1.). Recorded mid-Late Holocene (5000 BP-Present) shifts between colder and wetter periods and warmer and drier periods in Europe may be collectively grouped into four climatic epochs; the cooler and wetter Late Bronze-Iron Age (900-300 BC), the warmer and drier "Roman-Medieval" Optimum (AD 300 BC-1450), including the Medieval Warm Period (AD 1000-1200) and the cooler and wetter Little Ice Age (AD 1450-1850) (Lamb, 1977). The year to year climate during all these periods however appear to have varied considerably, not least due to regional differences but locally-dominant weather systems. In the Mediterranean region, for example during the Roman period, multi-proxy evidence suggests that the period was wetter and cooler (Issar & Makover-Levin, 1996).

Cooler and wetter phases appear to have been caused by a latitudinal shift south of low pressure systems, relating to the expansion of the polar vortex, lowering temperatures in the region and decreasing the marked seasonality of the present-day Mediterranean climate. Conversely warm epochs saw cyclonic pressure systems shift north, allowing a greater sub-tropical anticyclone influence to affect local weather patterns in the region (Lamb, 1995).

3.5.1 Holocene vegetation change and human disturbance

Pollen analysis has been used widely to record the timing and spatial extent of vegetational change in the Mediterranean due to anthropogenic disturbance and climate change. Pollen records from the Mediterranean region provide temporal evidence of widespread spatial variations in vegetation patterns and successive phases of disturbance in one of the earliest regions to be extensively affected by anthropogenically-induced environmental change (e.g. Bottema & Woldring, 1990; Roberts 1990).

Vegetational changes caused by Upper Paleolithic-Neolithic land use in the Mediterranean, however has not been clearly documented by pollen records (e.g. Bottema & Woldring, 1990) even where earlier human occupation has been demonstrated by archaeological evidence (e.g. Carriòn *et al.* 1995). Pollen studies covering this period in the Mediterranean reflect the low population density, their small-scale impact on climate-vegetation patterns already adapted to disturbance as well as the unsuitability of using large

Table 3.1. Mediterranean plant formations and environment typical of region

plant formation	*life-form*	*height (m)*	*understorey*	*environment*
Sub-humid forest	broad-leaved deciduous or coniferous trees	5 up to 30	perennial grasses and herbs; sclerophyllous shrubs on poorer soils	high elevations up to tree line montane forest (e.g. firs) and deciduous tree species
Evergreen forest	broad-leaved evergreen trees	5-30	perennial grasses and herbs; sclerophyllous shrubs on poorer soils	"Mediterranen forest" of *Quercus suber, Q. ilex, Pinus halepensis, P. pinea* and *Olea europea.* Coastal peripheral belt
Open scrub	stunted evergreen trees and sclerophyllous shrubs	2-8	perennial grasses and herbs and chenopods	*macchia* association drought prone areas
Open scrub-heathland	evergreen shrubs	0-2		*garrigue* association, heathland drought prone areas and badlands
Steppic grassland	perennial grasses and herbs	0-1		Mediterranean steppe; tussock grassland cool, dry, high elevations

From di Castri and Mooney (1973)

scale catchment derived pollen assemblages to identify small scale vegetation changes (e.g. Roberts 1990).

As land use intensified and early Holocene vegetation was degraded, pre-disturbance vegetation was replaced in many areas by drought, overgrazing and fire resilient evergreen tree and shrub species (e.g. *Quercus ilex*, *Quercus coccifera*, *Pinus spp*, *Ceratonia siliqua*, *Olea europea* and *Pistacia lentiscus*, Table 3.1) along with a rich diversity of spring and autumn flowering geophytes, grasses and herbaceous annuals (e.g. Bottema, 1980; Atherden *et al.*, 1993; Tivy, 1993).

This distinct ecotype to the Mediterranean (Di Castri & Mooney, 1973) progressively expanded from the west during the Holocene, largely due to the contemporaneous expansion of deforestation, grazing and agricultural land, as well as significant changes in Early to Mid-Holocene climate (Huntley, 1988; Kelly & Huntley, 1991). In the Spanish Balaeric islands, for example, pollen sequences suggest that a change in climate from more temperate conditions and mesophyllous taxa to xerophyllous vegetation and climatic conditions occurred contemporaneously with anthropogenic interference about 6000-5000 uncalib. C^{14} yr. BP., which favoured the expansion of Mediterranean scrub vegetation (Yll *et al.*, 1997).

The controls of climate, relief, growing conditions and history of land use are visible on both regional (Fig. 3.4) and local scales (e.g. Gimingham & Walton, 1954) in the Mediterranean. This diverse mosaic patterning of vegetation communities makes for considerable difficulties in the palaeoenvironmental interpretation and impact of human activity using pollen analysis; not least due to the complicated assessment of the true abundance of species (Delano-Smith, 1979, Fernàndez, 1994). In interpreting evidence of environmental change in the Mediterranean a key consideration must be that vegetation communities have responded to long-term and extensive basin wide changes as well as the often rapid and localised land-use changes caused by anthropogenic activity (e.g. Lyrintzis & Papanastasis, 1995).

Within the last century, the large-scale migration of rural populations away from the countryside and the abandonment of centuries old small-scale agricultural practices has allowed the regeneration of natural vegetation, often over the space of a few decades (e.g. Rackham, 1990). In fallow areas the establishment of *macchia-garrigue* associations in areas once cultivated or extensively grazed has seen the natural regeneration of degraded soils (e.g. Ruecker *et al.* 1998) and the expansion of forested areas in less accessible areas (e.g. Debussche *et al.* 1999). Degradation and regeneration processes in the Mediterranean region however, continue to show an enormous spatial variability, with degraded areas often found adjacent to less disturbed habitats (Hill *et al.* 1998).

The timescales of degradation, recovery and the development of complex vegetation mosaics, due to anthropogenic disturbance, recognised in the last century will have

Figure 3.4. Distribution of principal vegetation zones in the Mediterranean basin.

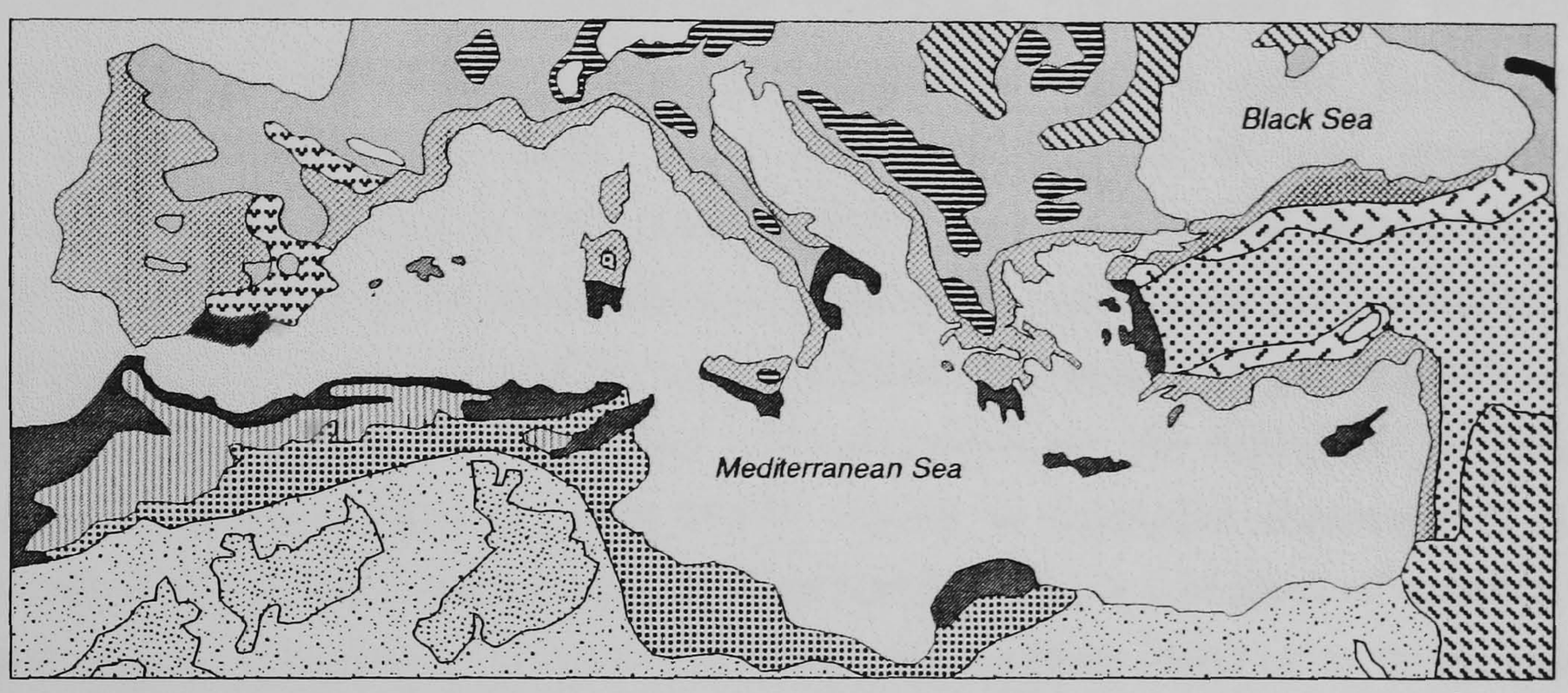

After Eyre (1968) & Macklin *et al.* (1995)

certainly occurred in the region throughout the Holocene. It is apparent therefore that the understanding of contemporary environmental changes in the Mediterranean, can provide much relevant information for palaeoenvironmental research in the region.

3.6 Mediterranean soil types and processes

Soils are similar to vegetation in that they are particularly indicative of local climatic and geomorphological controls. However the response of soils (in development terms) to environmental change is much greater than vegetation. Consequently the rapidity of vegetational change which has affected the region has been a major factor in the degradation of Mediterranean soils, being unable to respond to new geomorphic-vegetational settings, leading to their susceptibility to soil erosion and destruction (e.g. Woodward, 1995) and their existence often as a relic of past environmental conditions.

Four attributes may be determined in having affected the nature of the region's soils: climate and soil processes; the underlying geological substrate; the deposition of Saharan dust; and anthropogenic factors (Yaalon 1997). Similar to vegetation communities in the Mediterranean, the pedogenesis of soils and their distribution are a product of regional and local processes, in operation at present (e.g. wetland-floodplain soils) or as in the case of the common *terra rossa* soils found in limestone areas, are a result of palaeo-pedogenesis (Delano-Smith, 1979; Van Andel *et al.* 1990).

The characteristic reddening of Mediterranean soil B-horizons (*terra rossa* / Fersiallitic) is a product of the skewed seasonality of rainfall and high rates of soil evapotranspiration. Iron compounds [Fe-oxyhydroxides] released from surface weathering are re-precipitated and strongly bound to clays (Duchafour, 1977). Depending on the intensity of rainfall, dissolved carbonate may also be re-precipitated lower in the profile, producing calcitic horizons and calcrete where conditions are particularly semi-arid. Significantly the occurrence of these red soils in the region usually indicates there has been considerable soil erosion and the removal of the overlying brown earth A horizon (Delano-Smith, 1979), which would have supported pre-disturbance vegetation. Under stable conditions however Mediterranean soils that have resisted degradation generally have properties favourable to plant growth; surface crumb structures provide good aeration and water penetration, as well as favourable biogeochemical factors in humus and mineral cycling (Duchafour, 1977).

Apart from the *in situ* geological, climatological and vegetational controls on soil development, a feature of Mediterranean soils has been the significant addition of aeolian dust, originating from the Saharan desert in soil profiles (Pye, 1991). This input in some

cases results in more than 50% of the fine silt and clay fraction in *terra rossa* soils on limestones having been derived via atmospheric transport (Pye 1991; Yaalon, 1997).

During the Late Quaternary, vegetational changes caused by variations in climate, and especially in the late Holocene by cultural factors, dramatically altered the transport of soil material from slopes into drainage catchments (Macklin *et al.* 1995; Gutiérrez-Elorza & Peña-Monné, 1998). Studies conducted in the Mediterranean reveal that soil-loss from slopes is as a result of a large number of variables, including slope angle and aspect (e.g. Cerda, 1997, 1998a), soil type and structure (e.g. Cerda 1998b), surface vegetation and development stage (e.g. Andreu et al. 1995), fire history (Naveh, 1975) and the intensity / nature of land use e.g. Martinez-Fernandez *et al..*, 1995; Kosmas *et al.,* 1997).

Though physical and geomorphic thresholds controlling soil denudation were clearly overstepped in the past by anthropogenic activity, erosion was also checked by the rapid regeneration of "natural' vegetation and degraded soils (e.g. van Andel, 1990; Ruecker *et al.* 1998). At a catchment scale therefore, soil erosion episodes in the past were unlikely to have occurred synchronously in tributary catchments at the same extent, even during the most expansive periods of degradative land use.

3.7 Holocene Mediterranean fluvial and coastal systems

Although the Mediterranean basin is characterised by high relief and active tectonics, the most dynamic changes in landscape morphology, affecting archaeological and historical human populations of the region has occurred due to drainage catchment erosion, fluvial transport, deposition and sedimentation in the coastal zone, with the development of extensive deltaic lowlands, wetlands and lagoons. Fluvial and coastal processes are extremely sensitive to variations in sediment supply and as coastal alluvial plains and deltas on the whole are sediment sinks for upstream fluvial systems, these areas are an archive of the cumulative effects of upstream changes, even though often having been altered by littoral processes (e.g. Douglas, 1990; Bellotti *et al.* 1995; Viñals & Fumanal, 1995).

3.7.1 Fluvial and coastal environments during the Holocene

The increased flux of sediment, from upland slopes into catchment valleys and into coastal alluvial plains during the Holocene, caused by the destabilisation of soil-slope systems resulted in repeated phases of valley aggradation and the progradation of alluvium into coastal environments. As recognised by Plato (428-348 BC) in Attica, Greece (below) and much later by research into Mediterranean valley alluviation episodes (e.g. Judson, 1963; Vita Finzi, 1969; Bintliff, 1974; Brückner, 1980 etc.) geomorphic thresholds controlling

landscape denudation were frequently exceeded in the past, leading to identifiable phases of slope deposition, valley alluviation (Kraft *et al.,* 1975; Kraft *et al.,* 1977; van Andel *et al.* 1990; Runnels, 1995), delta progradation (Sestini, 1992; Bellotti *et al.* 1995) and widespread coastal infilling (e.g. Delano-Smith, 1979).

"In consequence of the successive violent deluges...there has been a constant movement of soil away from high elevations; and, owing to the shelving relief of the coast, this soil, instead of laying down alluvium as it does elsewhere, has been perpetually deposited in the deep sea around the periphery of the country or, in other words, lost... All the rich, soft soil has molted away, leaving a country of skin and bones [so that rainfall] is allowed to flow over the denuded surface directly into the sea..."

Plato, Critias, iii, D-E, (4th century BC)

A cause of considerable concern to Greek-Roman socio-economic systems was the rapid infilling of anchorage sites and harbours e.g. the Kara Menderes-Çayi coastal floodplain, in the vicinity of Ancient Troy (Kraft *et al.,* 1980; Bintliff, 1981), and the Küçük Menderes floodplain, infilling the harbour of the ancient city-port of Ephesus on the Aegean coast of Turkey (Kraft *et al.,* 1977). Rates of coastal progradation of alluvial materials would have been rapid, changing the coastal-land relationship between harbours and ports; the floodplain of the Küçük Menderes extended approximately 3 km seaward in four hundred years (c. 200 BC - c. 200 AD) (Eisma, 1978).

While the "Older-Fill" (Fig. 3.5) was deposited under Late Glacial-Early Holocene climatic and vegetational conditions prior to widespread human influences in the environment, the distribution and timing of erosional and depositional episodes in valley catchments during the Holocene (Younger-Fills), was the co-operative result of both diachronous climate change and anthropogenic activity (e.g. Brückner, 1986). The extent to which each influence was the dominant control on triggering erosional and depositional episodes has been argued since "historical-fills" were recognised in Sicily (Judson, 1963) and elsewhere in the Mediterranean basin (Vita-Finzi, 1969). Initially depicted as a pan-Mediterranean, climatically driven episode of valley aggradation, as Classical-Roman landscapes and fluvial systems responded to a distinct change in climate and socio-economic systems, the deposition of Medieval-Middle Ages historical valley fills has since been observed to correlate to a large extent with periods of human occupation and landscape degradation (Vita-Finzi, 1976; Neboit, 1984; Brückner, 1986; Brückner & Hoffman, 1992; Ballais, 1995; Barker & Hunt, 1995; Hunt & Gilbertson, 1995; Yll *et al.,* 1997).

While confined in upland valleys to terrace sequences, polyphase historical-fill deposits were able to expand areally at the coastline, filling embayments and forming large coastal

Figure 3.5. (i) Proposed model for the timing of Mediterranean valley evolution and deposition of Older and Younger Fill (Vita-Finzi, 1969); and (ii) valley cross section of the Gornalunga River, Eastern Sicily (Judson, 1963)

(i)

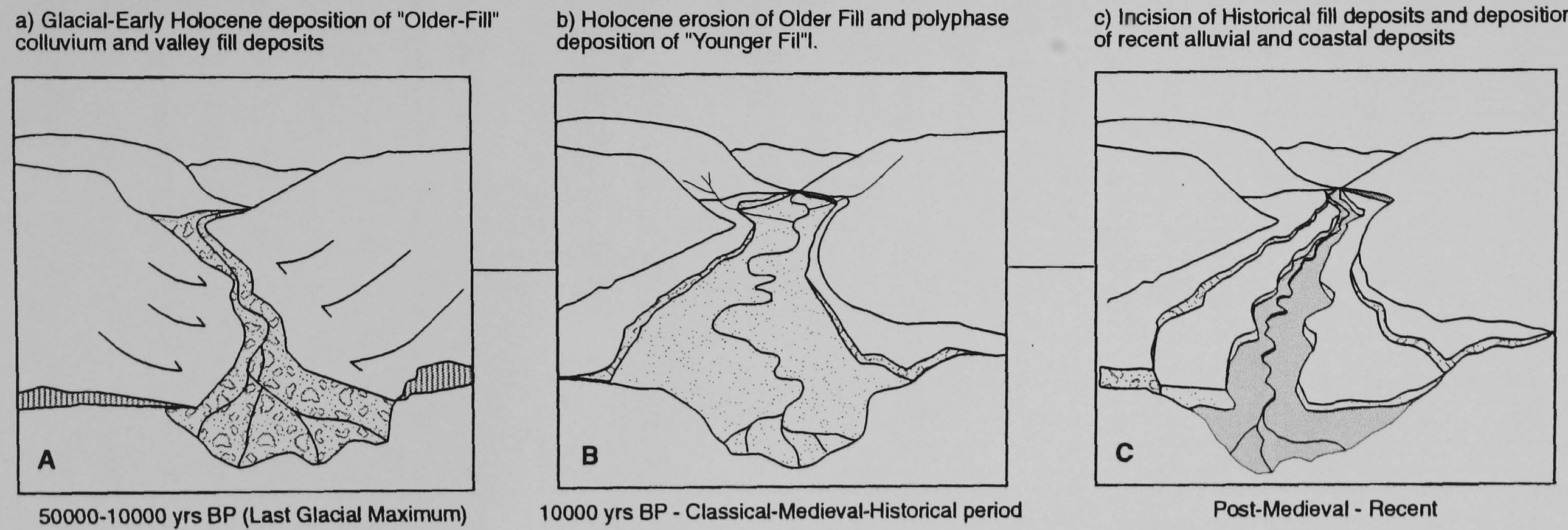

(ii)

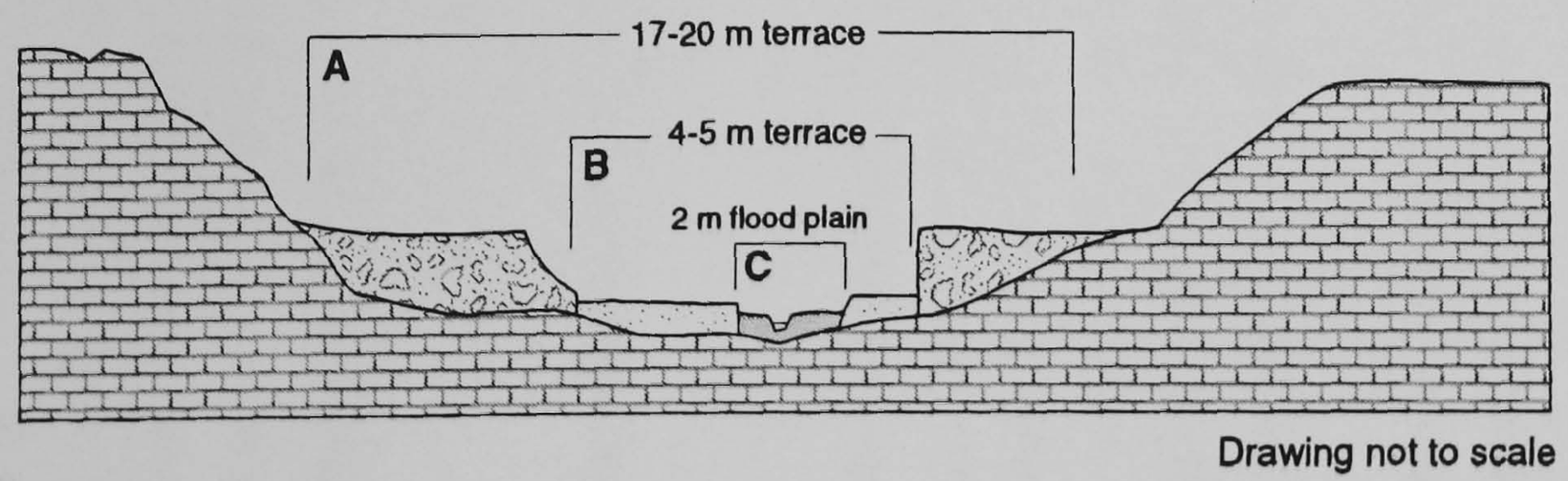

plains and deltas prograding into the Mediterranean along the coastlines of Southern Spain (Hoffmann 1995; Brückner & Hoffmann, 1992), France (Dubar & Anthony, 1995; Provansal, 1995), Italy (Coltorti, 1997; Cencini, 1998) and Greece (Baeteman, 1985; Lambeck, 1996). Aggradation rates were often considerable, for example in southern Italy, as much as 10 m of aggradation over the span of a few centuries occurred, occurring successively during Greek occupation and again during the Middle Ages (Abbot & Valastro, 1995).

The valley surface of historical fills in many Mediterranean valleys (Fig. 3.5) has since been incised, exposing the stratigraphic succession, which is usually predominantly well bedded, buff-grey fine-sandy silts incorporating archaeological remains (Vita-Finzi, 1969; Neboit, 1984). Although initially poorly drained when deposited (favouring wetland development), subsequent incision and the lowering of valley water tables, as well as drainage and irrigation techniques, have led to these areas being the focus of intensive cultivation and settlement in modern times (Bintliff, 1981).

The punctuated nature of diachronistic historical alluviation in the Mediterranean (either due to a regionally synchronous change in the climate or closer interaction between patterns of climate and land-uses) has lent itself to both arguments. Due to a lack of local and correlateable palaeoclimatic data, and the inherent difficulties in distinguishing between anthropogenic and climatic signals this situation is likely to continue (Woodward, 1995), until a comprehensive correlation of regionally-dispersed and local, small-scale temporal and spatial changes is achieved.

3.8 Documentary and instrumental evidence of climatic and environmental change in the Mediterranean

The most recent evolution of Mediterranean landscapes has been a successive continuation of co-operative geological, climatic and biological systems being progressively influenced by anthropogenic processes. These interactive systems have affected different areas at different times and to lesser or greater extents. Fluvial and coastal systems during this most recent phase, have had to respond to either anthropogenic (often climatically-reinforced) environmental regimes or been irreparably altered due to human intervention and control.

To understand the evolution of the modern-day Mediterranean landscape, specifically the rate of change and extent of disturbance to natural systems within the last two hundred years, modern environmental changes have to be considered within a relevant temporal context.

The dynamic nature of climatic and environmental change recognised in the last couple of centuries by documentary and instrumental records can be observed to be primarily an

extension of environmental variations which have affected the region within at least the last 500 years, i.e. the impact and recovery from the globally recognised period of climatic deterioration known as the "Little Ice Age" (LIA) *circa* AD 1450 - AD 1850. The net effect of this period of climatic instability and enhanced rainfall in the Mediterranean being that within both large and small catchments, discharge rates and sediment transport were enhanced. Changes in the landscape however related to changing socio-economic systems and land management techniques both exacerbated, as well as, decreased soil erosion and the extent of valley aggradation. For example during this period of time in southern Spain the cultivation of steep, susceptible slopes to degradation was achieved without significant soil erosion during the Arab phase of occupation (AD 711 - AD 1492/1560) (Brückner & Hoffman, 1992). Imported cultivation techniques, namely extensive areas of agricultural terraces reduced soil erosion, maintained soil fertility and though dramatically altering the natural landscape prevented widespread valley aggradation. The 16th century extradition of Arabs from the region and resettlement by Spanish farmers, less familiar with Arab techniques in irrigation and cultivation, led to an expansion of low-productivity farmland and the destruction of large forested areas. The consequence of this was widespread soil erosion, coastal alluviation and delta progradation which resulted in the present day coastline of embayments infilled since the 15th century (Brückner & Hoffman, 1992).

During the 17th-18th centuries similar progradational changes in the Rhône delta were caused by intensified land settlement and degradational land-use upstream in the catchment and a greater frequency/magnitude of floods in the lower Rhône valley (Arnaud-Fasseta & Provansal, 1999). Likewise in Italy, the number of Tiber river flood events per century in Rome showed a distinct increase during this period greater than previous centuries since the Roman period (Pavese *et al.* 1995).

Documentary evidence of the climate at the time in the eastern Mediterranean during the Little Ice Age period, for example from the island of Crete indicates a variability of anomalous weather conditions as compared to the twentieth century. Winter and spring rainfall is seen to have been lower in some years, often leading to severe droughts, while in other years, severe winters and excessive snowfalls were documented (Grove & Conterio, 1995). This excess of rainfall led to a significant change in river behaviour on the island, with small upland catchments switching from low rates of sediment transport and channel stability to valley floor and alluvial fan aggradation (Maas *et al.* 1998).

Evidence exists from enough areas to suggest that during the Little Ice Age period the Mediterranean region was subject to climatic anomalies related to variable shifts in the southerly position of depression tracks, caused by weakened circumpolar westerlies and blocking high pressures further north in Europe (Lamb, 1984). Extensive large magnitude floods recorded in Mediterranean Spain during the LIA appear to reflect this prevalence of

southerly-tracking, western and north-western Atlantic frontal systems also affecting catchments elsewhere in the Mediterranean (Benito *et al.* 1996).
Increased valley aggradation and flooding would indicate that coastal and estuarine wetlands during this period were also in receipt of significant amounts of sediment. It is not inconceivable that wetland sediments deposited at the terrestrial interface of hydrological systems over the same period, should contain evidence of LIA (and post-LIA recovery) climate changes and meteorological events in the Mediterranean.

3.8.1 Instrumental and documentary records of climatic variability in the Mediterranean (AD 1800-2000).

The complexity of climates found in the Mediterranean is due to the region being variably dominated by either sub-tropical or mid-latitude weather. Within the last couple of centuries instrumental records of meteorological have verified this control and identified smaller scale fluctuations in climate. Over the last two centuries, the regional climate has been observed to have fluctuated on a decade-yearly timescale, due to a variable dominance of mid-latitude pressure systems. Although too often considered as an isolated climate system meteorological conditions in the basin are a result of the variability of global patterns and within basin interactions with influencing continental-ocean climate systems (Reddaway & Bigg, 1996; Leroux, 1998)

Reliable meteorological monitoring has occurred at a few stations (e.g. Marseilles and Rome) in the Mediterranean region since the start of the 19th century, providing some long records of precipitation and temperature data. 30 yr running averages of precipitation records measured at Rome in the central Mediterranean reveal that winter rainfall totals after *circa* AD 1820 (~380 mm) began a steady decline over the next twenty years. Corresponding with this was a subsequent increase in cooler wet summers (Flohn, 1984). Between circa AD 1840 and the start of the 20th century, Rome winter precipitation totals increase up to nearly the 19th century totals.
Increased summer rainfall is also noticeable from circa AD 1880 up to AD 1900 (Flohn, 1984). In the Eastern Mediterranean (Jerusalem) however annual rainfall totals during the latter half of the 19th century showed a progressive decrease (Issar & Makover-Levin, 1996).
In the western Mediterranean, precipitation patterns have fluctuated over the last century on a *circa* 20 year periodicity between wetter and drier periods (Maheras, 1988). Wetter periods are recorded between 1901 to 1921 and 1930-1941, separated by drier conditions between 1922-1929 and 1942-1954 and a marked decrease in precipitation between 1980-

Figure 3.6. Timing of annual dry and wet phases in the Eastern Mediterranean during the last century. After Kutiel *et al.* 1996

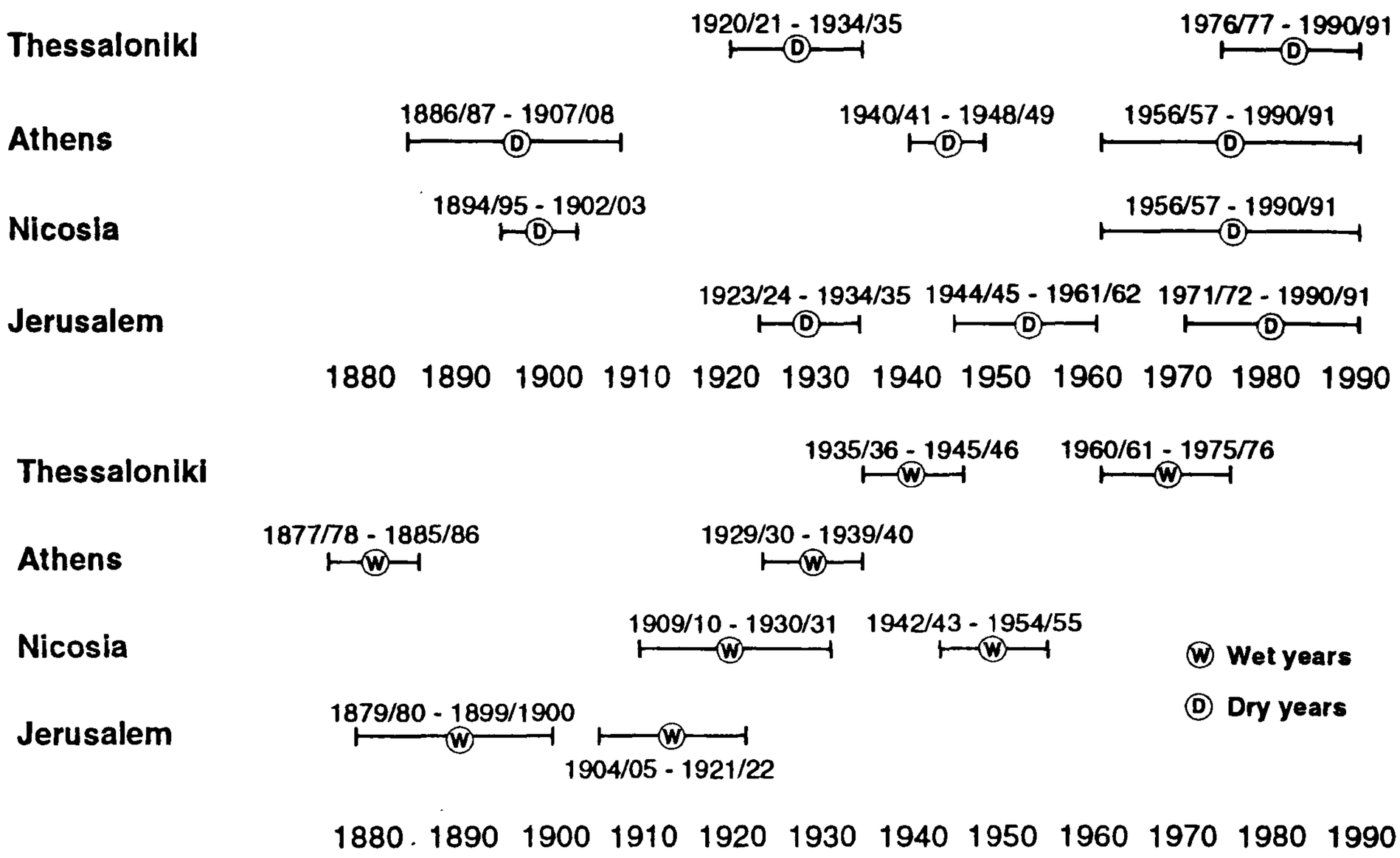

Figure 3.7. West,central and east Mediterranean SST: Frequency percentage difference between warm minus cold months (10 year moving average), for the years 1880-1985. Other y axes indicate corresponding SST temperature. After Metaxas *et al.* 1991

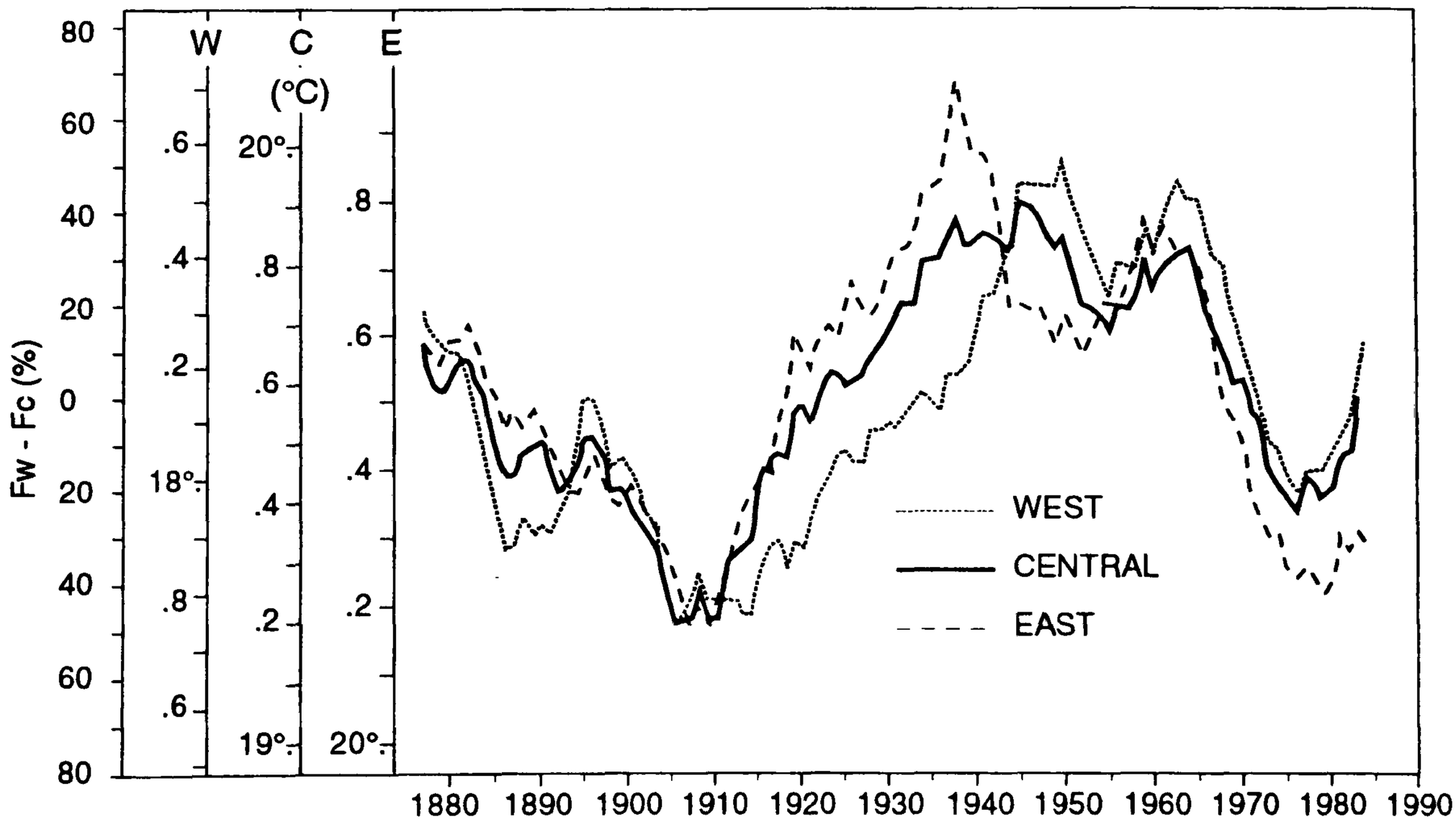

1985 (Fig 3.6.). This pattern is similar to the timing of wetter and drier periods observed in the eastern Mediterranean (Kutiel *et al.* 1996) (Fig. 3.7) and to some extent in Sicily over the same period (see Chapter 4).

In the Eastern Mediterranean however the timing of extremely wet periods as with extremely dry ones, are observed not to be correlatable between stations, being more reliant on local climatic factors and the fact that many of the long-term monitoring stations are now situated within large urban areas (Kutiel *et al.* 1996). The general trend of sea-surface temperatures (SST) saw minimum SST temperatures around 1910 with a maximum around 1940-1965, decreased SST temperatures between 1975-1980, rising up to the present (Metaxas *et al.* 1991), reflecting the last decades phase of increasing temperatures.

Temperature measurements across the Mediterranean during the last century also highlight the difference of climate between the western and eastern basins, i.e. circulation patterns favourable for high temperatures in one basin are not reflected in the other (Kutiel & Maheras, 1998). Climatic conditions and observed changes between the two basins are therefore frequently out-of-phase (Reddaway & Bigg, 1996), the phenomena known as the Mediterranean-Oscillation.

It has also been observed that in the last century the most severe precipitation events in the Mediterranean have occurred when the difference between air-sea surface temperatures are greatest, i.e. Autumn-Winter when the potential of atmospheric disturbance is highest (e.g. Serra, 1973; Perry, 1981). Although heavy and often the cause of destructive flooding, rainfall during the autumn season has been and remains essential in maintaining hydrological systems around the Mediterranean (e.g. Romero *et al.* 1998; Bull *et al.* 1999), as well as the supply of sediment to the coastal zone. This annual period of instability is discussed in Chapter 4 with regards the climatic conditions which have been responsible for destructive flooding in Sicily during the last century.

Documentary evidence of the effect of these measured changes in precipitation patterns appear also in historical records of flood episodes and the stratigraphy of recent sediments deposited following the LIA period of climatic instability in the region.

The increase in precipitation recognised in the Eastern Mediterranean from the latter half of the 19th century and up to the mid-20th century (Kutiel *et al.* 1996) are recognisable. A spate of damaging winter floods in Rome by the River Tiber occurred (AD 1843, 1846, 1855, 1858 and 1870) during this mid-late 19th century phase of increased rainfall (Pavese *et al.* 1995) before new embankments were constructed at the turn of the century to protect the city. In Spain during the later half of the nineteenth century the number of destructive floods also increased in Mediterranean catchments (e.g. Benito *et al.* 1996; López-Avilés *et al.* 1998). In Crete from AD 1871 up to the mid-20th century runoff and valley aggradation

was renewed, depositing coarse grained alluvial and fan sediments (Maas *et al.* 1998) as a result of the enhanced moisture measured in the Eastern Mediterranean.

It is clear therefore that fluvial activity in catchments around the Mediterranean have responded to sub-century scale climatic changes and are comparable to instrumental climate measurements taken in the last 200-150 years. Examples of instrumental and documented evidence indicate that the nature, frequency and magnitude of environmental changes related to these variations in climate have remained spatially and temporally different.
These differences have clearly been a result of the different physical characteristics of catchments around the Mediterranean. What remains unclear, due to a lack of detailed records of land-use changes, is to what extent human activity during the last few centuries have affected individual catchments.

3.8.2 Landscape changes during the last two hundred years (AD 1800-2000).

Even though instrumental records highlight the variability of climate in the Mediterranean over the last two centuries, the effect of subtle climate changes has to be compared with other controlling factors of environmental change. Recognising the effect that climatic changes have had on environmental systems during the last two hundred years, has to be weighed against other systems within a landscape that has been almost totally transformed by the effects of agriculture and human population. A landscape dominated by agriculture and human pressures is as noted by Perez & Remmers (1997), "a social construction..., not static, but a reflection of the balance of social forces which influence the way in which the natural resources of the site are combined".
Documentary evidence of the changing landscape during the last two hundred years (prior to contemporary monitoring) therefore provides a much broader context of environmental changes. These far-reaching human-made controls, e.g. changing agricultural practices, land reclamation, etc., have over the last two hundred years had a more dramatic and prolonged influence on Mediterranean systems than climate change alone. Over this short timescale and period of intense human activity, environments where the effects of climatic change could have been potentially recorded (e.g. wetlands, floodplain sediments) have either been physically erased or their essential components for existence reduced.
The consequence of land-use changes in the Mediterranean can be sub-divided into two environmental change scenarios: those direct changes caused by human activity which exacerbate landscape degradation processes, and changes as a result of human activity

(often inactivity) which has led to post-disturbance recovery and the "natural" regeneration of often susceptible landscapes.

The timing and extent of land-use around the Mediterranean has varied from one region/catchment to another, due to both natural (local climate, relief, soil types, etc.) and socio-economic factors. None the less, in the last two centuries the general agricultural transformation of the Mediterranean has seen an accelerated transformation from extensive to intensive farming, especially since the post-war (AD 1945) period. Combined with this, and often as a consequence of changing agricultural methods, there have also been significant demographic changes.

In many areas of the Mediterranean, land-use since the 18th-19th century up to the mid-20th century was dominated by expansive agriculture and an expanding rural population living within largely self-sufficient rural communities (McNeill, 1992; Perez & Remmers, 1997). In many areas therefore all suitable areas were often under cultivation and those unsuitable for crop growth were grazed by goat and sheep herds. As a result, in areas where extensive cultivation led to soil exhaustion and grazing continued to destabilise slopes by reducing the protective cover of vegetation, large scale soil erosion often occurred, enhanced by late Little Ice Age-climatic conditions (see above) greatly increasing catchment sediment loads (Hunt *et al.* 1992; Puigdefábregas & Mendizabal, 1998).

During the same period however where agricultural techniques were used to prevent soil exhaustion, for example by cultivating terraced hill-slopes, landscapes became stabilised. In the Marche region of Central Italy the introduction of an "alberata" (tree-lined) field system to reduce soil erosion at the start of the 20th century led to dramatic coastal retreat and erosion due to decreased sediment loads (Coltorti, 1997). Similar events also occurred in the Etang de Berre, southern France due to a reduction of agricultural activity on the catchment slopes (Provansal, 1995).

Socio-economic factors accelerating landscape change in the Mediterranean have been particularly acute in the later half of the 20th century. The spatial extent and timing of fluvial and coastal changes brought about by human activity, especially in the last fifty years, has been unique in its rapidity and far-reaching consequences (compared to the lengthy period of human occupation in the Mediterranean). As Barker & Hunt (1995) note... "the equivalence between classical and recent sedimentation....is that one is a record of three or four centuries of agricultural intensification, the other of scarcely a generation". A point emphasised by Coltorti (1997) in the investigation of fluvial and coastal settings, that catchment changes in the last 50 years (due mainly to gravel quarrying) have been of a greater magnitude than those which occurred during the whole Holocene.

Although post-war mechanisation has increased the area of land capable of being cultivated by animals/humans, the agricultural landscape of the Mediterranean has been significantly

affected by land-use deintensification. The widespread migration of rural Mediterranean populations from the countryside, due to mechanisation and modern agricultural techniques, as well as, the post-war attraction of urban areas for employment has led to many areas of the Mediterranean (especially those distant from the most profitable and intensively cultivated areas for cultivation) to regenerate into a natural/semi-natural state (e.g. Rackham, 1990; Debussche *et al.* 1999).

Previous cycles of land abandonment and natural regeneration of vegetation in the past have certainly occurred in the past in the Mediterranean region, due to successive phases of human occupation. The abandonment of cultivated land, particularly terraced-slope field systems in the Mediterranean however is of particular concern because of the potential that unless maintained, traditional land-use practices will be lost, e.g. polyculture production and goat grazing. The renewal of soil erosion is also a primary concern (e.g. Lyrintzis & Papanastasis, 1995; Douglas *et al.* 1996; Green & King, 1996) which is clear, considering that following abandonment and the re-establishment of natural vegetation the land is susceptible to erosion (mainly from short-lived intensive rainfall events) and the longer term threat of desertification (e.g. Ruecker *et al.* 1998; Lasanta *et al.* 2000).

The variability of annual-decadal-century scale environmental changes identified in the Mediterranean by documented and instrumental records, reveals the great complexity of the Mediterranean region especially in terms of the interaction between climate, geomorphology and human activity. Too often in previous palaeogeographic and palaeohydrological studies from the Mediterranean (even with recent instrumental data) the emphasis has been in correlating recorded environmental changes in one area with apparently similar changes in another. Clearly there remains a need for greater multidisciplinary research to identify linkages first at a local, then catchment scale before broader scale interpretations can be made.

To better understand the interaction of these variables in the Mediterranean, both in terms of providing more accurate analogues for past geomorphological processes and the present-day environment, information is required from environments which have been affected by them all and can be compared with historical-instrumental records. The dependence of wetlands on climate, geomorphology and human activity has made them therefore an ideal setting for the recording of recent environmental change in the Mediterranean.

3.9 Physical setting of coastal wetlands in the Mediterranean

Evidence from coastal and alluvial sediment sequences indicates that environmental settings conducive to the development of coastal wetlands have existed throughout the Holocene.

Responding to environmental processes governing the hydrology of catchments and coastal evolution, coastal wetlands have evolved and responded by migration and re-growth. In the last few centuries however destruction and degradation has often irrevocably outpaced the regeneration of wetland systems and coastal habitats in the Mediterranean.

Palaeogeographical studies from the Mediterranean indicate that coastal wetland [swamp, marsh] conditions have often occurred during the transitional phase of embayment-estuarine infilling and more terrestrial conditions (e.g. Kraft *et al.* 1975; Provansal, 1995; Coltorti, 1997; Vinals & Fumanal, 1995). During the rapid sea level rise preceding *c.* 6000 yrs BP, large sub-aerial alluvial areas were diminished due to transgressive, post glacial sedimentation against the previous land-surface. With a levelling-off and decrease in the rate of sea level rise, terrestrial materials deposited in coastal-fluvial settings were effectively prevented from reaching further offshore. Where conditions allowed, e.g. the indented coastline of Greece, this led to the development of wide coastal plains around the Mediterranean, described by Kraft *et al.,* (1975) as "alluvial plains of relatively high angle with terminal swamp areas separated from the sea by a sand and gravel barrier" and the progradation of estuarine-delta areas (Belloti, *et al.* 1995; Dubar & Anthony, 1995). The regional pattern of present-day coastal wetlands around the Mediterranean occur largely as a result of this sequence of events (Sestini, 1992) (Fig. 3.8.) since which time other, more local environmental factors have exerted their dominance (see previous sections).

The effect of a relative sea level still stand and subsequent impacts of local catchment and coastal factors on the development of coastal wetlands are observeable in late Holocene sediment sequences deposited at the margin of coastal embayments and low lying coastal areas in the Mediterranean. Typical facies associations include barrier dune sands, shallow lagoonal, terrestrial and intercalated salinity-dependent wetland marsh deposits, in relation to the local depositional environment and recent evolution (Kraft *et al.,* 1975; Baeteman, 1985; Dupré *et al.,* 1988; Provansal, 1995; Pacheco *et al.,* 1996; Amore *et al.* 1997). In recent sequences the occurrence of peat is a useful indication of organic accumulation and preservation (Reddy & D'Angelo, 1994) and is indicative of relative hydrological-surface stability.

As a consequence of their geological evolution and long-term utilisation of their resources by humans, coastal lowlands surrounding the Mediterranean have been intensively modified by anthropogenic activity. In many instances areas of coastal lowland and wetlands have developed as a consequence (of increased catchment-erosion and coastal siltation) and been successively degraded by human activity. From inception to the final stages of degradation and disappearance, the relationship between natural and human factors on the development of coastal lowlands and wetlands during the later Holocene may often have been inseparable (Delano-Smith, 1979). From the example of the studied coastline in south east Sicily (which may be viewed as fairly representative of other areas in

Figure 3.8. Main alluvial and deltaic areas in the Mediterranean basin. After Sestini (1992)

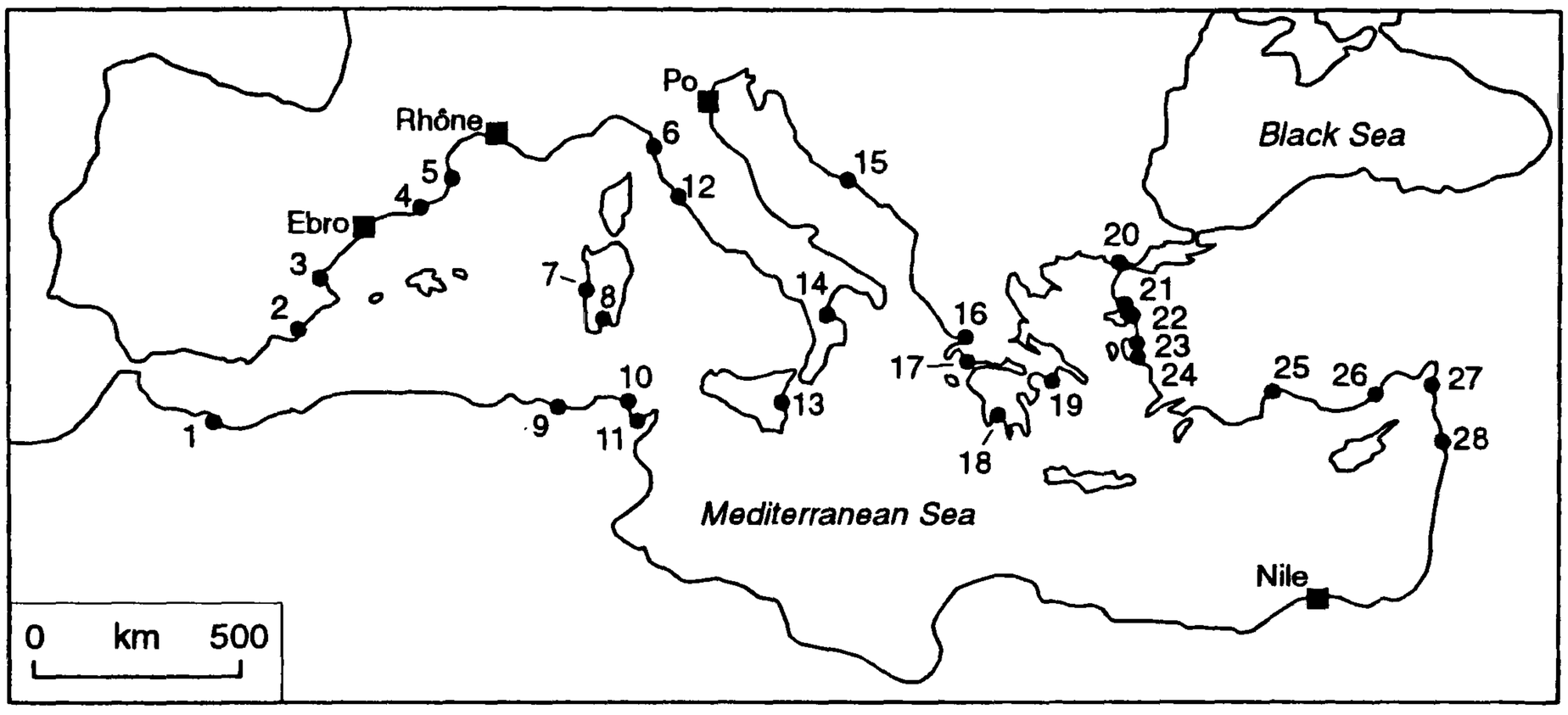

Key to localities around Mediterranean

Morroco

1. *Mar Chica* and *Moulya*

Spain

2. *Mar Menor*
3. *Valencia*
4. *Llobregat*
5. *Rosas*

Italy

6. *Arno*
7. *Oristano*
8. *Cagliari*
14. *Crati, Gulf of Taranto*
12. *Tiber*
13, *Simeto* (Sicily)

Tunisia

9. *Gulf of Annaba*
10. *Medjerda-Birzeta*
11. *Tunis*

Greece

16. *Amvrakia*
17. *Achelaos*
18. *Messenia*
19. *Marathon*

Croatia

15. *Neretva*

Turkey

20. *Evros*;
21. *Edremit*;
22. *Bakir Çay*;
23. *Gediz*;
24. *Kücük and Buyuk Menderes*;
25. *Aksu*;
26. *Goksu*;
27. *Latakia*

Syria

28, *Akkar*

■ Major deltas developed in Holocene

the Mediterranean) the long-term evolution of coastal lowland areas controlled successive patterns of land-use and population. Subsequent environmental changes affecting coastal lowlands have therefore impacted both socio-economic and natural systems.

Because of the often confined nature of coastal lowlands in the Mediterranean (bounded by steep slopes/at the margin of coastal-fluvial systems) natural resources have been increasingly diminished due to expanding populations and industrial development (Tooley & Jelgersma, 1992). As a result environmental changes which have influenced the development of low-lying coastal areas in the Mediterranean, are likely to have an exacerbated effect on the population and socio-economic systems of the region, even if checked by region-wide sustainable development schemes, e.g. The Mediterranean Action Plan (1975) and The Blue Plan (1979) discussed in Stansell (1990). Wetlands as a whole in the Mediterranean region have so far been severely degraded in the last century due to land reclamation for agriculture, settlement expansion and industrialisation, drainage catchment management schemes and groundwater depletion (e.g. Zalidis *et al.* 1997). At the forefront of the disruption to fluvial systems caused by human activities, interior and wetlands have been severely degraded over the last century. Countries surrounding the Mediterranean Sea have witnessed the almost total disappearance of much of their wetland areas. In central-western Spain for example, during the period AD 1896-1996 a calculated 94% of the original wetland areas have been destroyed as a consequence of drainage and subsequent cultivation (Gallego-Fernandez *et al.* 1999).

Having been confined physically by coastal development and reclamation efforts and progressively isolated from controlling inputs for continued existence, i.e. water, silt and nutrients, coastal wetlands will remain increasingly threatened. A clear threat therefore to the spatial extent of present-day microtidal coastal wetlands in the Mediterranean is the predicted sea-level rise in the next century (Corre, 1992; Marino, 1992; Sestini, 1992, Hensel *et al.* 1999).

To predict the extent to which future environmental changes will affect coastal wetlands, an understanding of past events and processes is necessary to place present-day conditions in context. When accounts of recent environmental change in coastal wetlands have been limited by observational or documented records, wetland sediment sequences are the next best source of palaeoenvironmental information for the settings. This alternative timescale of historical environmental change must be considered however in terms of influencing factors controlling the incorporation of proxy sources of information, e.g. pollen, sediment composition, vegetation dynamics and post-depositional processes.

The recent evolution of anthropogenically-modified coastal wetland settings in south east Sicily, are therefore used in this study to investigate historical trends of depositional change and the sensitivity of Mediterranean coastal wetlands to recent environmental changes over the last 150-200 years.

Chapter Four

Environmental change and coastal evolution in South-East Sicily

The term "countryside" implies soil transformed by labour; but the scrub clinging to the slopes was still in the very same state of scented tangle in which it had been found by Phœnicians, Dorians and Ionians when they disembarked in Sicily, that America of antiquity.

The Leopard (di Lampedusa, 1960 p. 96)

4.1 Introduction

The present-day physical environment of south east Sicily has evolved, as in other areas around the Mediterranean, in response to closely interacting geological, climatological and ecological processes. Long-term human occupation has also imprinted itself on the environment, to an extent as to blur the cause and effect of natural and anthropogenic environmental processes observed today.

The island of Sicily is situated at the tectonic suture of the African and Eurasian plates, with regional geological structures and rock types representing the continuing Tertiary-Quaternary collision of the two crustal plates (Figure 3.1). During the Tertiary-Quaternary, climatic and sea level oscillations affected the region as it underwent a gradual tectonic emergence and uplift-driven denudation. During the lowest Quaternary sea level stands, the area was at the centre of an extended "land bridge" connecting mainland Italy with Sicily and Malta, separated from present-day Tunisia by a narrow strait, before rising sea levels during the early Holocene isolated the island.

The pan-Mediterranean pattern of cultural expansion through the Holocene, combined with the post-glacial adjustment of hydrological, vegetational and geomorphological systems led to the expansive and prolonged degradation of susceptible terrain to erosion. Exacerbated denudation of upland catchments due to human activity in the last thousand years has led to dramatic changes in the morphology and dynamics of fluvial and coastal systems due to phases of increased sediment transport and deposition.

Present-day depositional settings in the coastal zone of south east Sicily contain a potential archive of information on the past interaction of Holocene alluviation and coastal processes; depositional settings in which the long-term relationship between anthropogenic and natural controlling processes have also been recently imprinted.

4.2 The physical environment of the south east Sicilian coastline

The relief of the south east corner of Sicily is dominated by the uplifted highland area known as the Hyblean plateau. The highest elevations are found in the centre of the plateau (Mt. Lauro (986 m) and Mt. Contessa (914 m) which descends rapidly to the coastal margin (Fig. 4.1.). Radiating out from the plateau are a number of rivers incised into Tertiary-Quaternary sequences, the larger, i.e. the rivers Irminio, Tellaro, Anapo and Gornalunga, are capable of maintaining flow year-round due to groundwater storage in the permeable Hyblean geology. Smaller rivers (known regionally as *torrente*, with steep

Figure 4.1. Location map of south east Sicily and place names used in text

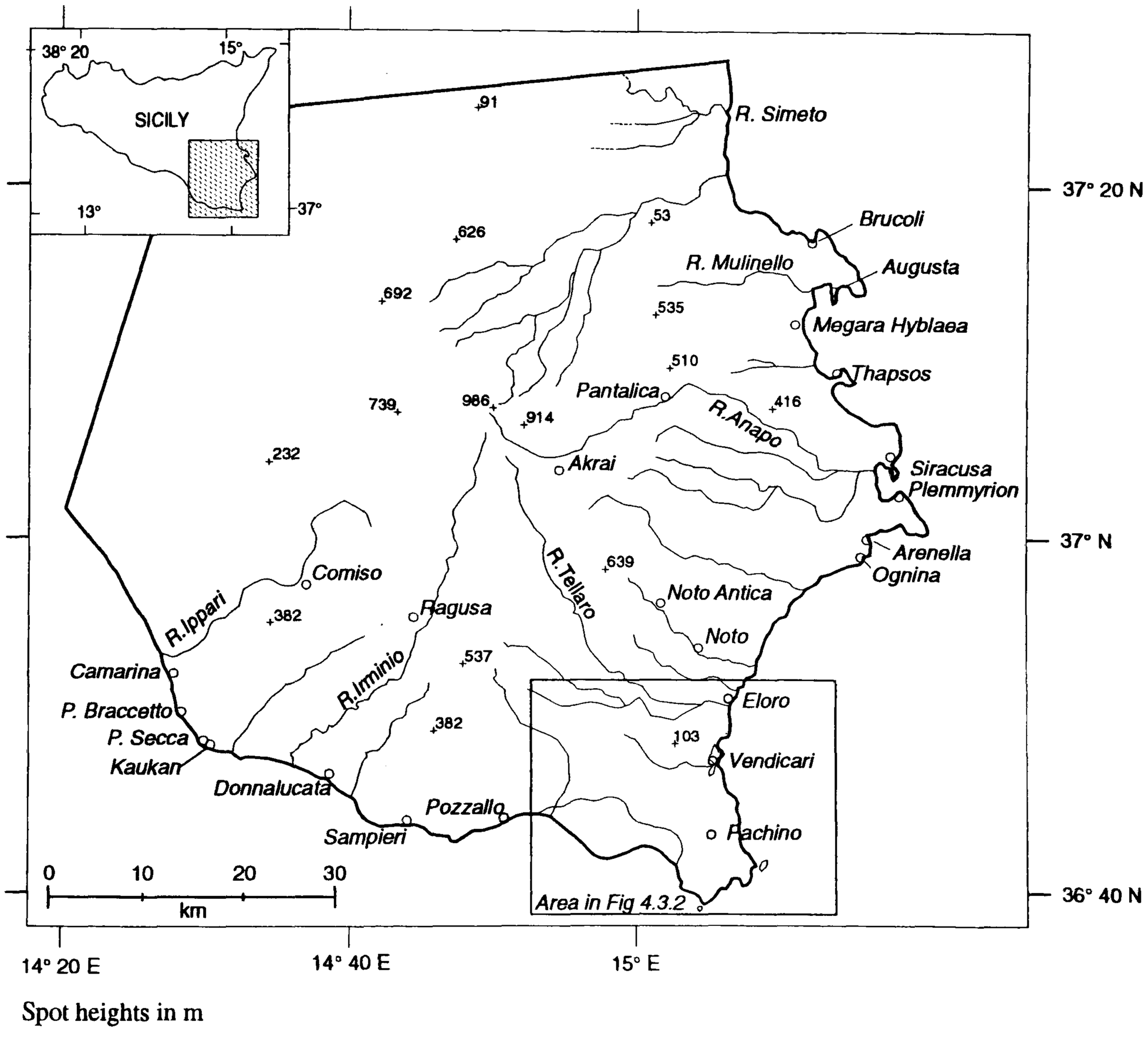

Spot heights in m

gradients and "flashy" hydrographic characteristics) often dry out in the summer months due to their dependence on seasonal-storm rainfall and overland flow rates.

As a consequence of land use and water requirements for irrigation and domestic supply, water courses are now largely managed, especially in coastal areas, where embankments have been constructed to ensure an efficient supply of water to irrigated areas while preventing seasonal flood damage. Straightened and embanked channels constructed this century have led to a reduction in the natural geomorphic activity of lowland floodplains and river channels in the region (e.g. Megiér *et al.* 1997). Catchment-derived sediments suspended in high energy discharge events are currently transferred rapidly across coastal floodplains and into the offshore zone (Amore *et al.* 1990). The progressive human modification of alluvial systems in south east Sicily and the reduction of materials to littoral areas has often resulted in a sedimentation deficit and coastal retreat of clastic shoreline areas (Amore *et al.* 1990).

The geomorphological evolution of the coastline of south east Sicily has, as previously noted, been a consequence of Tertiary-Quaternary sedimentation patterns and local tectonic movements. The coastline south of the River Simeto floodplain to Capo Ognina, consists of a series of coast-parallel, fault-bounded headlands and promontories of Oligocene-Miocene materials, i.e. *Monte Tauro* (Augusta), *Penisola Magnisi, Capo Sta Panagia* (Siracusa), the *Penisola della Maddalena* and *Capo Ognina* (see below). Holocene terrestrial and coastal sediments have been deposited within these embayments, where low energy conditions required for alluvial sedimentation in the coastal zone are found. Protection afforded by these headlands have made them naturally defendable harbour and anchorage sites since the earliest periods of human occupation (Section 4.7).

The coastline between Ognina and Capo Passero (Fig. 4.1.) consists of a low, extensively cultivated, coastal plain backed by the steep slopes of the Hyblean limestone plateau massif. This lowland area is juxtaposed against the Hyblean limestone uplands, by the Pozzallo-Ispica fault escarpment to the west and the Hyblean escarpment of Oligocene-Miocene limestone to the north. The coastal lowland area and rocky coastline of low cliffs and headlands has been dissected by a drainage network radiating off the Hyblean plateau. The largest river, the River Tellaro and other sizeable rivers draining the southern Hyblean plateau have developed dune-fronted floodplains, while less extensive drainage networks in the lowland area south east of the Pozzallo-Ispica escarpment have created a number of barrier dune and coastal lagoon complexes infilling the indented coastline, i.e. between Pozzallo to Capo Passero and from Capo Passero, in more confined valleys towards Siracusa, e.g. Vendicari.

The narrower southern coastal area of the Hyblean plateau between Pozallo and Camarina has been intersected by the River Irminio and a series of fault controlled embayments,

within which a similar distribution of Late Quaternary coastal sediments and Holocene materials have been deposited, repeating patterns seen on the eastern coastline (Lentini, 1987). Draining the south west of the Hyblean plateau, the River Ippari and Acate o Dirillo, have eroded the stratigraphic succession of the Gela Thrust zone and later Quaternary sediments, forming an extensive lowland area (the Piana di Gela) and dune-fronted coastline.

Tidal conditions around the coastline are typically Mediterranean, with a mean tidal range in the area (recorded at Catania) of less than 30 cm (0.3 m springs, 0.1 m neaps; Hydrographer of the Navy, 1996). Despite these microtidal conditions, the fetch afforded by a central Mediterranean location generates a considerable amount of wave activity along the exposed coastline.

Evidence of high-energy wave activity on rocky shorelines manifests itself along the Vendicari coastline for example, by the large accumulation of flotsam found on rock platforms and cliff tops, to the rear of breached dunes and cove accumulations. Flotsam comprising mainly of wood (tree-length boles, branches and drift-scrapwood), reed stems, sea grass fragments and assorted human detritus are found tens of metres inland and on top of cliffs ~5 m above sea level (Plate 4.1.). This last fraction includes plastics (mainly packaging), metal drums, tyres and other waste derived from shipping and dumping in the Mediterranean Sea (e.g. Gabrielides *et al.* 1991). On the same coastal stretch (Plate 4.2.) detached boulders of eroded Pleistocene cliffs, also occur on rock platforms at altitudes that range from near sea level to the rear of rock platforms and on top of cliffs. Often of considerable size (> 2 m) and locally derived, occurring solitary and in imbricated groups their origin is uncertain. Although scars caused by movement during storm activity on surfaces below the boulders were not observed, the presence of faunal burrows in the rock, attesting to an original position at sea level, suggests they may well have been derived from the shore face during high magnitude wave activity. If such examples have been naturally extracted from cliff faces, the imbricated orientation of some blocks resting on one another would indicate wave pressure from the east, coinciding with the prevalent onshore wind direction. It is plausible that odd boulders may have been positioned on rock platforms as a consequence of tsunami waves.

Also at the rear of rock platforms in the Vendicari area, shingle accumulation often occurs as a ridge, coinciding with the main flotsam accumulation (Plate. 4.1.) and the lowest degraded *garrigue* communities. Corresponding with the high wave activity, along the stretch of Vendicari coastline at the headlands of Eloro, Fondo dell'Mosche and the Torre Vendicari peninsular, only a contemporary coastal notch was observed, which suggests that the coastline has not been subjected to recent neotectonic vertical motion.

Plate 4.1. Tree trunks, *Phragmites* stems and flotsam accumulation at rear of rock platform. 500 m south of River Tellaro outlet, Vendicari, SE Sicily. Large boulders incorporated within flotsam + 1m diameter. Base of accumulation was at upper reach of wave-splash zone

Plate 4.2. View north towards Hyblean plateau escarpment (horizon) from abandoned coastguard station, Vendicari Mid-Upper Pleistocene calcarenite peninsula separating Pantano Piccolo (body of water to the left) from sea. Note limit of coastal garrigue species on rock shoreline due to wave generated sea-spray and thin soil.

Plate 4.3. Lagoon water level variations observed at the Foci del Pantano Sicihilli
Both photographs looking west from outlet (Figure 6.4.)

(a) Low levels in September 1996 resulting in shallow anoxic conditions

(b) High water levels resulting in tidal-marine water exchange between lagoon and sea
Flow into picture towards horizon

On exposed clastic-estuarine coastlines, wave activity at river-channel mouths have been observed to shift channel positions on a seasonal basis in relation to channel flow and wave intensity, as well as over longer periods of time, e.g. the mouth of the River Simeto, which was observed to have shifted 1 km south in under 30 years in the late 19th century AD. (Marinelli, 1890) due to meander-channel migration. The mouth of the River Simeto has also been observed to have migrated inland of the order of 200m since 1938 AD, due to wave erosion and decreased sediment loads (Megiér, 1997). Sediment loads have diminished in the upstream catchment of the River Simeto, due to the construction of small dams for water storage and slope reduction. The retreat of the coastline at the Simeto river mouth was also observed to have accelerated after 1970 AD, in relation to dam construction and the use of alluvial sediments for building material.

Smaller scale examples (over a few years and 10's-100's of metres) of channel migration and changing beach morphologies in relation to wave activity and differences in seasonal discharge were also observed at a number of channel mouths and embayments; between periods of fieldwork (Sept. 1996 to April 1998) at the outlets of the River Tellaro, the Foci del Pantano Sichilli (Plate 4.3.) and the River Platani (near Agrigento, south west Sicily).

4.3 South east Sicilian climate and meteorological patterns

..this landscape which knows no mean between sensuous sag and hellish drought; which is never petty, never ordinary, never relaxed, as should be a country made for rational beings to live in;...and when the rains come, they are always tempestuous and set dry torrents to frenzy, drown beast and men on the very spot where two weeks before both had been dying of thirst.

(di Lampedusa, 1960 "The Leopard" p. 167-168)

Precipitation and temperature patterns in south east Sicily, may be viewed as a microcosm of the entire islands climate, typical of the Mediterranean region. The island of Sicily is strongly controlled by seasonal weather patterns, complicated by differences in relief and marine influence. Rainfall totals are distinctly seasonal, with the wettest period extending from October to April caused by depressions tracking across the island from the west and north west (Durbin, 1981). This results in a southerly and altitudinal gradient of decreasing rainfall over the island as the higher relief in the north and north-east of the island, the Nebrodi-Madonie mountains (below 2000 m) & Etna (3340 m) extract much of the available moisture (Fig. 4.2a). The Hyblean plateau acts similarly in the south-east of the island (Fig. 4.2b).

Figure 4.2. (a) Annual precipitation in Sicily and (b)Relief and major drainage patterns in SE Sicily

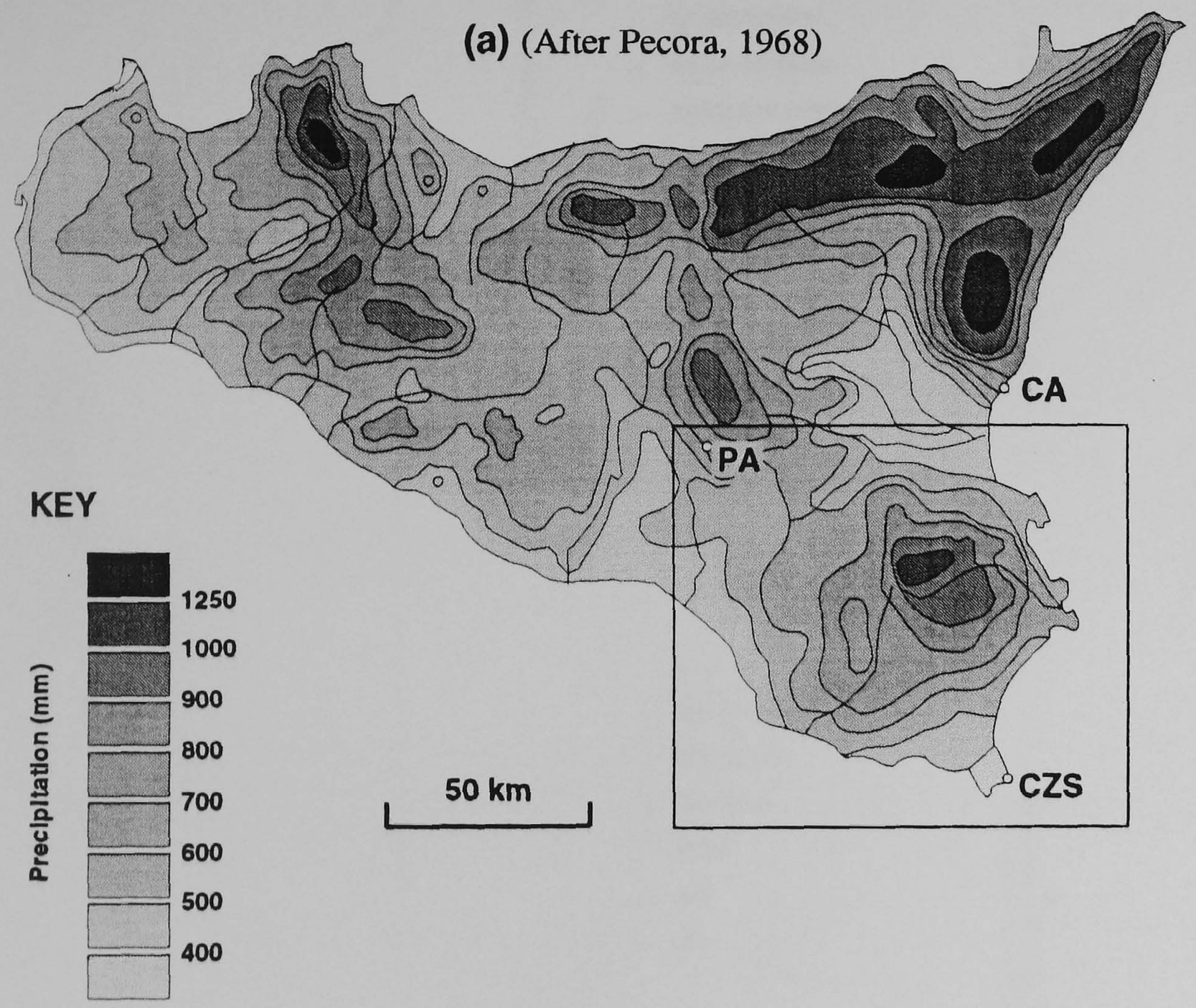

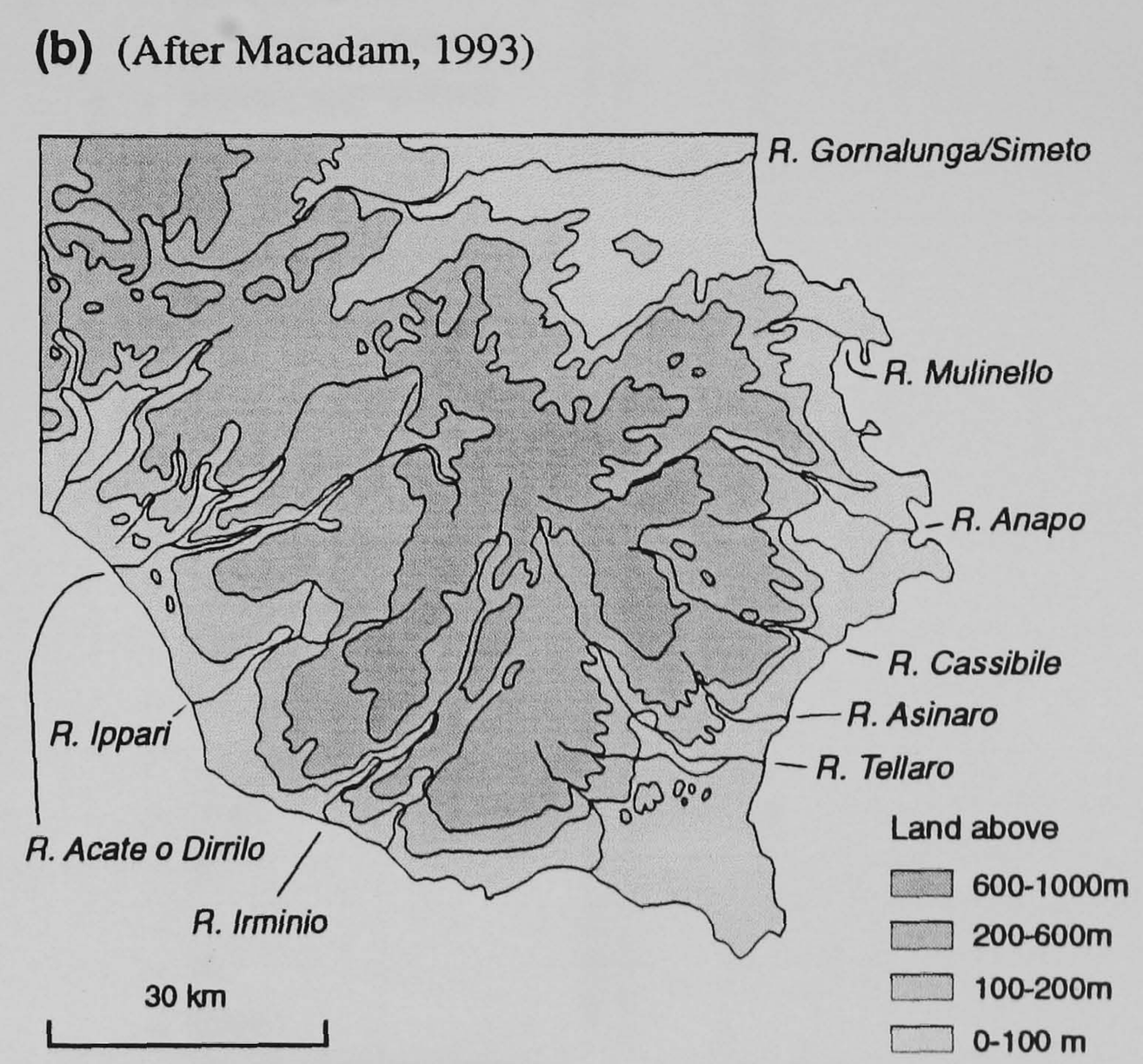

Climate and meteorological record sites (Figures 4.2.1. & 4.2.2.)

CZS = Cozzo Spadoro
CA = Catania
PA = Piazza Armerina

Figure 4.2.1. Annual Temperature and precipitation patterns at (a) Catania and (b) Cozzo Spadoro, SE Sicily

(a)

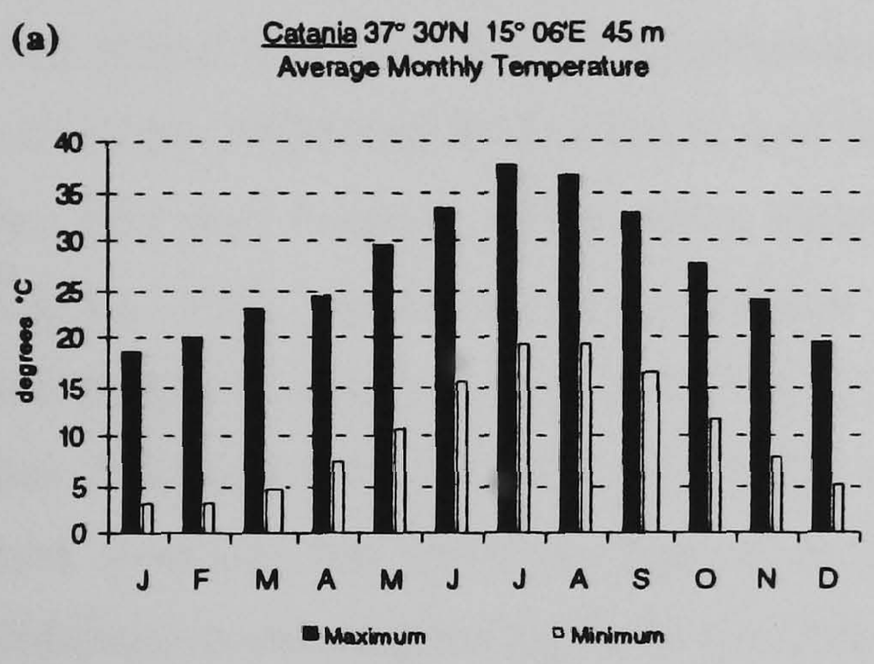

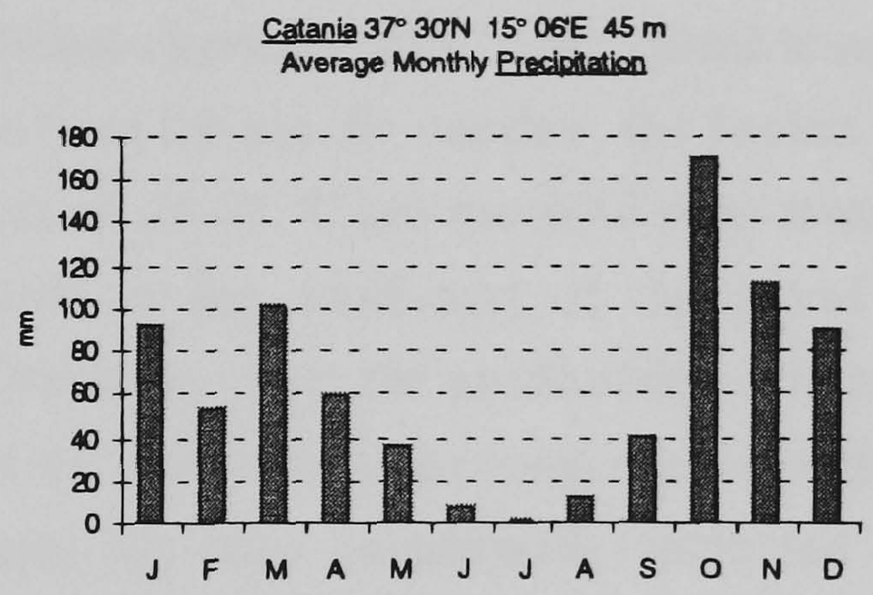

Period of measurement: 1953-68

(b)

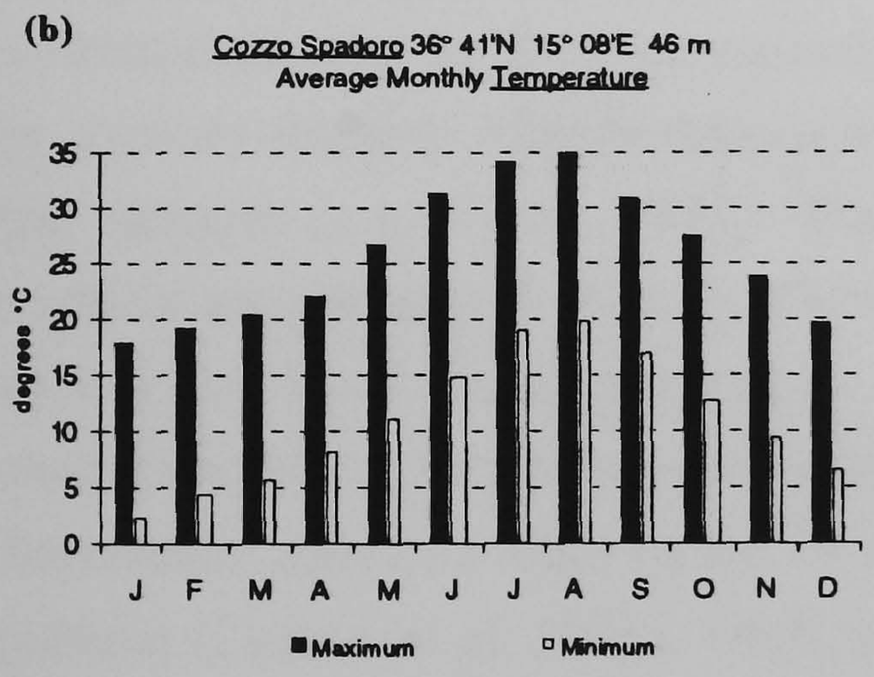

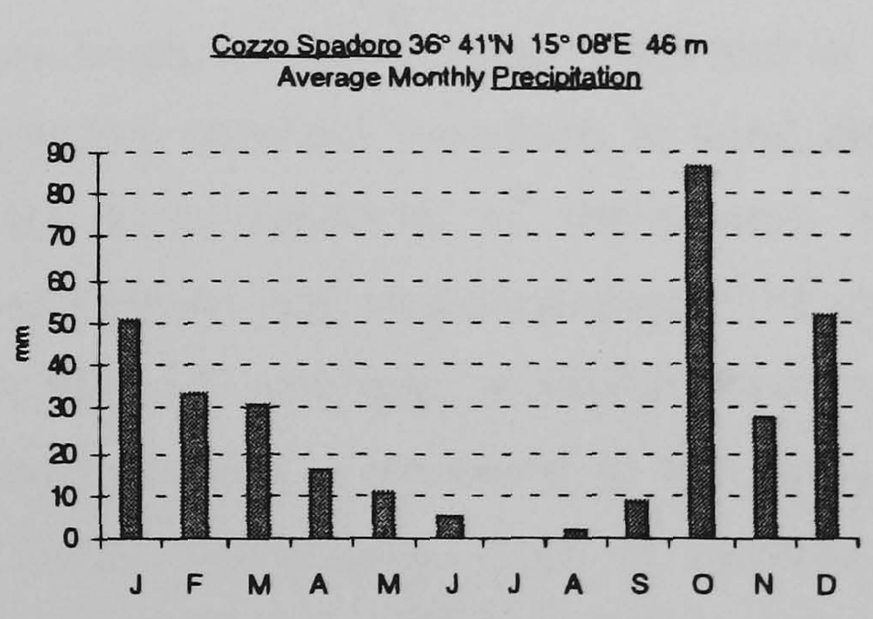

Period of measurement: 1959-68

Source: HMSO (1972)

Subsequently the lowest rainfall totals are recorded along the southern coastline and coastal plains e.g. the Piana di Gela and Piana di Catania, with minimum totals occurring in the extreme south east-Capo Passero peninsula (Fig. 4.2.1). Low rainfall totals are however increased by localised convective rainfall in the Summer (e.g. Ferreri & Ferro, 1990) and in autumn-winter months by the west-east track of Atlantic depressions through the Mediterranean (e.g. Serra, 1973). Sudden flooding of *torrente*, soil erosion and the flooding of lowland areas is a common occurrence in the region (as depicted above by Lampedusa, 1960), during short-term rainfall events (Cannarozzo *et al.* 1995) and from Autumn-Winter month precipitation events.

The island displays distinct Mediterranean climate characteristics, with annual temperature variations reflecting both altitude and distance from the sea. In summer, the hottest months are July and August, when mean temperatures of 24-27 ℃ are recorded over most of the island, with maximum temperatures recorded in the south-east of the island where temperatures may exceed 35-40°C (Pecora, 1968). In winter the ameliorating affects of the sea, maintain temperatures (10-15 °C) around the coastline, decreasing rapidly with height and towards the interior. Spring temperatures are also occasionally increased by the *scirocco* wind originating from the Sahara, although this is felt more on the northern coast, where having descended from the Nebrodi mountains the air mass recuperates much of its arid characteristics (Chester *et al.* 1985).

Wind circulation patterns in the central Mediterranean are dominated by meteorological patterns caused by the summer expansion of sub-tropical high pressure cells and in winter by westerly-tracking Atlantic depressions, producing seasonal variations in wind direction and strength (e.g. Perry, 1981). Predominant wind directions of the eastern Sicilian coastline are prevalently onshore, alternating through the year as a consequence of cyclonic airflow and local coastal topography. At Catania for example, a switch from easterly onshore winds in July to westerlies in the winter months is attributed to the topographic disturbance (elevated relief in the N of the island and nearby Etna) of cyclonic wind patterns (Chester *et al.* 1985). High and persistent wind speeds in south east Sicily are recorded at Cozzo Spadoro (Capo Passero), where north-easterlies to easterlies are most frequent and persistent (Amore *et al.* 1990).

4.3.1 Climate change in south east Sicily during the last century

Monthly precipitation totals recorded over the last century in south-east Sicily, show clearly the yearly-seasonal skewness of winter precipitation (Fig. 4.2.2.). Records also indicate that since the late 19th century, there has been a recurrence of exceptionally wet months, during the Autumn-Winter period when yearly rainfall totals were exceeded during one month, often over a period of a few days. Monthly precipitation totals from Piazza

Figure 4.2.2. Monthly rainfall totals and mean annual precipitation totals between 1891-1980 AD

(a) Monthly rainfall totals 1892-1980 from Catania (CA) and Piazza Armerina (PA) SE Sicily

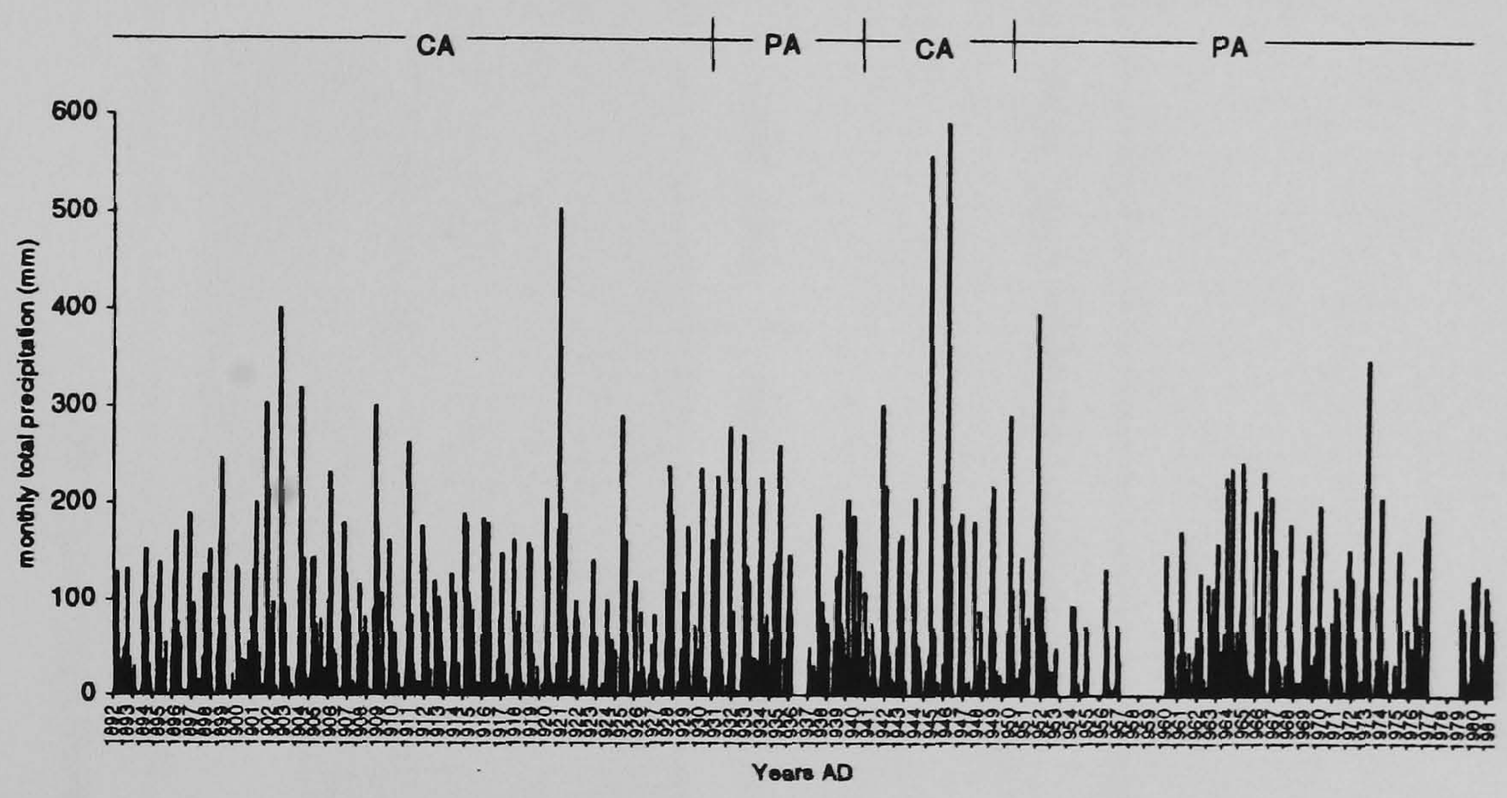

(b). Mean annual precipitation (1892-1980 AD*) from Catania (CA) and Piazza Armerina (PA) SE Sicily

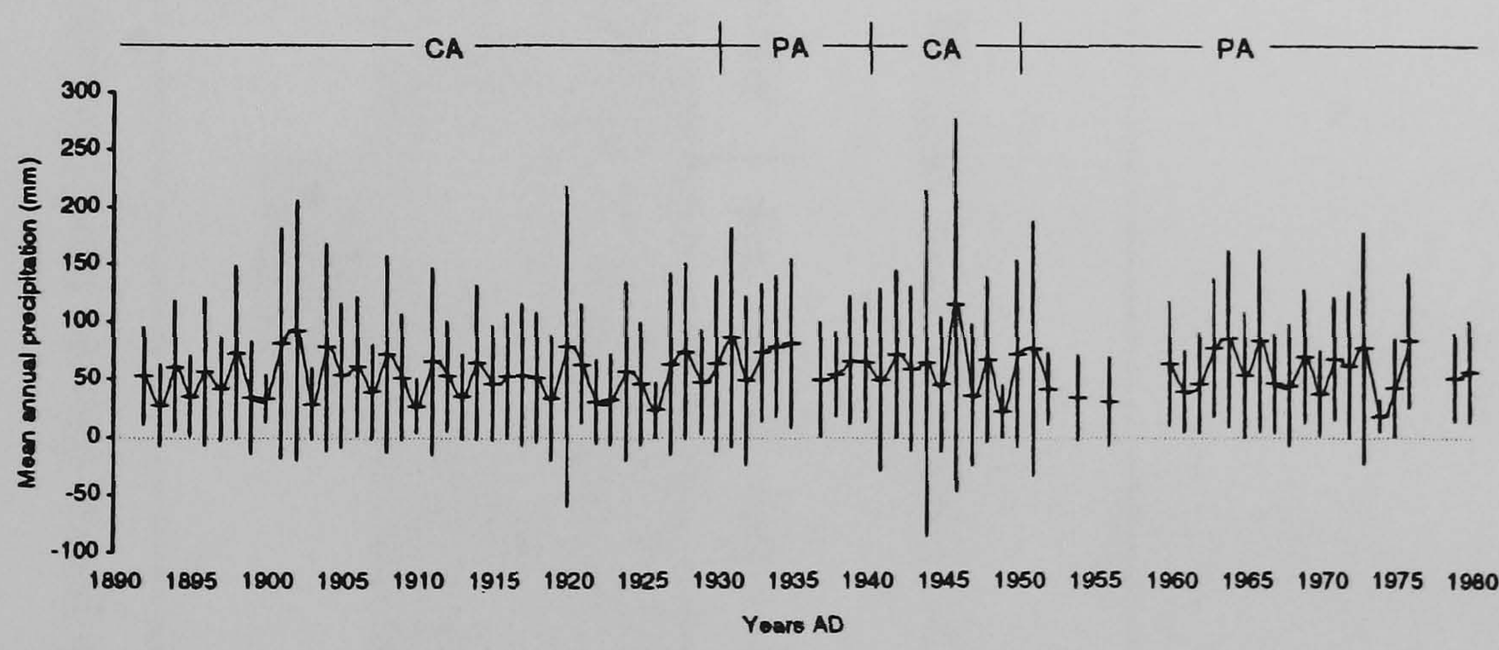

y-error bars indicate 2σ of monthly variations in precipitation totals

** Missing years1936, 1953, 1955, 1957, 1958, 1959, 1977 and 1978*

Sources: Simpson, 1927, 1934; U.S. Dept. Commerce, 1959; Argenti 1997.

Figure 4.2.3. Years with annual rainfall totals greater than the mean (56 mm) for the period 1891-1980 AD

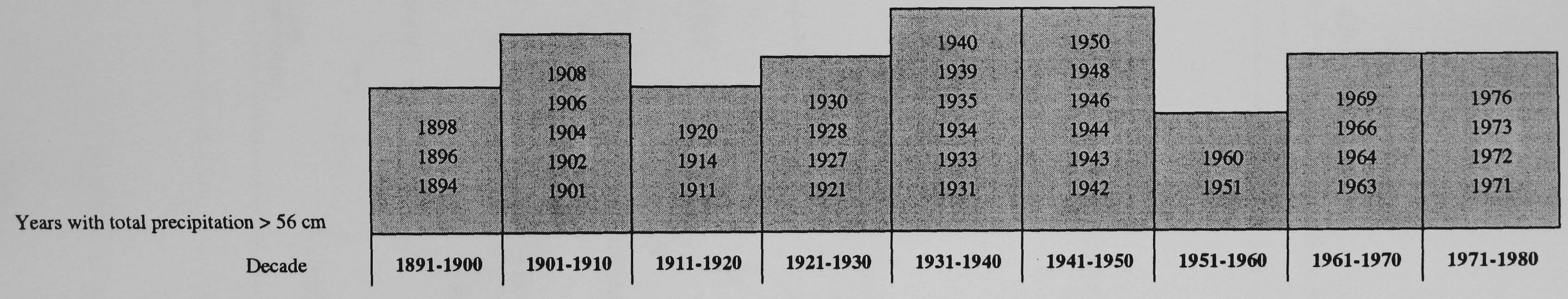

* Missing years from data set: 1936, 1953, 1955, 1957, 1958, 1959, 1977 and 1978.

Sources: Simpson, 1927, 1934; U.S. Dept. Commerce, 1959; Argenti 1997.

Figure 4.2.4. Rainfall totals in eastern Sicily and Calabria, Southern Italy for 11 October 1951 (After Serra, 1973)

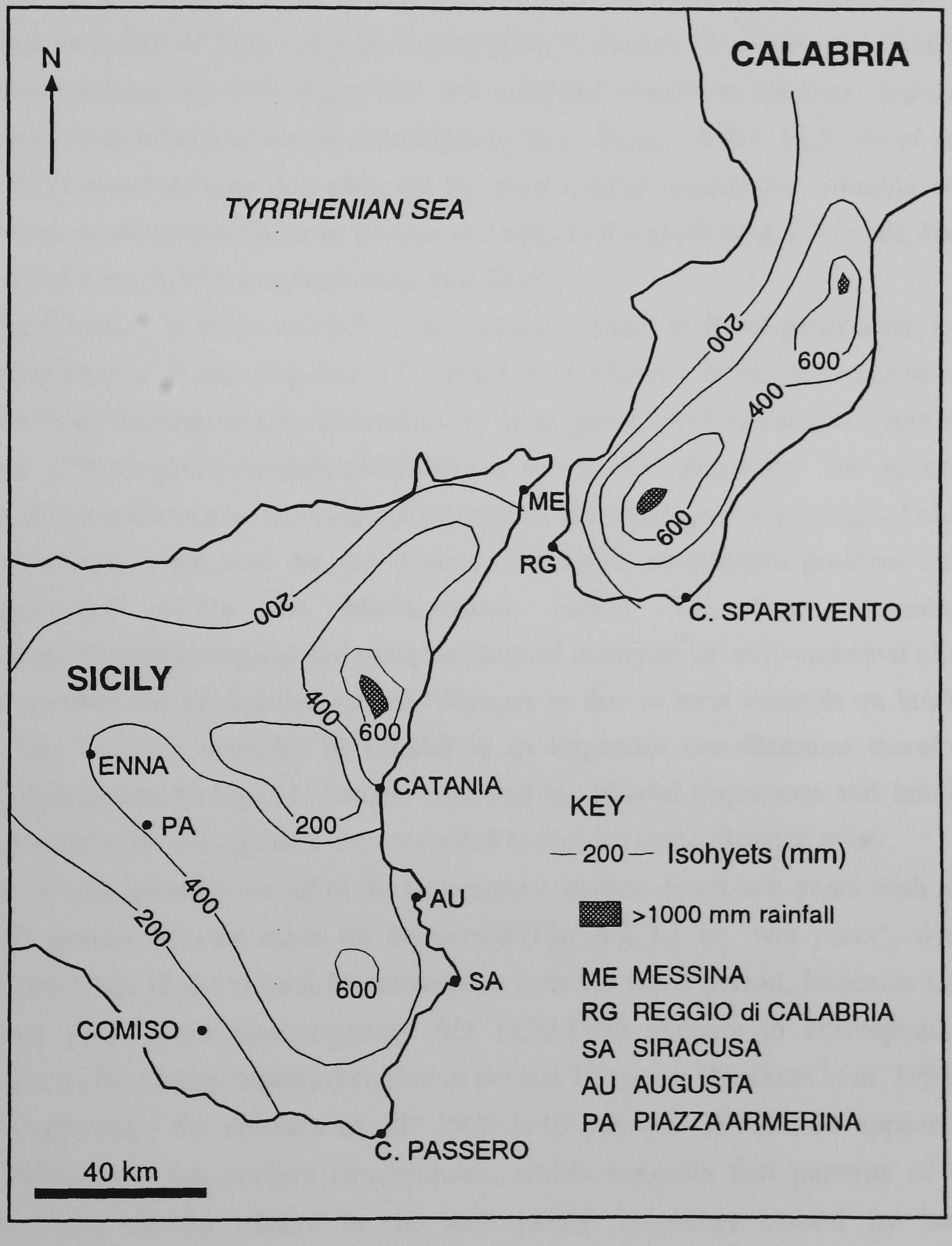

Armerina and Catania combined together, provide an almost complete record of rainfall for the region between 1892 and 1981 (Fig.4.2.2.). No further data was obtainable during the period of this research, though it is certain that data covering the last two decades exists.

The dominance of winter rainfall in the region and its potential of exceeding yearly totals in a one-two monthly period are highlighted by monthly totals at Catania for September 1902 (400 mm), November 1920 (500 mm), December 1944 (559 mm), January 1946 (590 mm), and at Piazza Aremerina in December 1951 (396 mm) and October 1973 (205 mm). The localised intensity of high magnitude precipitation events in south east Sicily, are caused by the passage of abnormally low and southern west-east tracking depressions combined with local relief and sea/air temperatures (e.g. Serra, 1973). Isohyets of rainfall during the 1951 event indicate that although the most intense rainfall was roughly centred on Palazzolo Acreide on the Hyblean plateau and Etna to the north (Fig.4.2.4), the 400 mm isohyet covered a much wider area of south east Sicily.

Although the intensity of storm rainfall is an important aspect of flood generation, it must also be recognised that the response of downstream channel flow, the magnitude of flooding and flood damage is also dependent on other geomorphological and hydrological controls and anthropogenic modification/land-use within the catchment. The uncertainty involved with extrapolating meteorological records to historical geomorphological changes between catchments, even over the last century, highlights an inherent problem that has been encountered within the Mediterranean region, i.e. how representative geomorphological, archaeological and palaeoecological evidence of environmental changes recorded at one site are of regional climatic changes or due to local controls on landscape evolution. The localised intensity of rainfall is an important consideration therefore in correlating past sedimentological changes recorded by alluvial sequences and landforms within the coastal zone and climatic data recorded at stations some distance away.

Comparing the precipitation record of the last century, broken down into years with annual rainfall totals greater than the mean for the period (Fig. 4.2.3.) or "wet-years", with sea surface temperatures of the central Mediterranean over the same period, indicates that the spate of wet years from approximately AD 1930-1950 appears to correspond with maximum sea surface temperatures recorded in the last 100 years (Metaxas *et al.* 1991) (see Fig.3.7.). Conversely the decades of AD 1900-1910 and AD 1970-1980 appear to be associated with lower sea surface temperatures, which suggests that patterns of heavy rainfall are more closely related to the atmospheric instability caused by land-sea temperature differences, rather than the particular temperature of either body. Being dependent on hydrological changes in the catchment and at the local scale, the historical evolution of coastal wetlands in south east Sicily may be expected therefore to have been influenced by these century-decadal climate changes.

A potential certainly exists therefore for hydrologically-influenced depositional settings, i.e. wetlands, to provide a terrestrial archive of climate changes related to central Mediterranean weather systems and sea-surface temperatures.

4.4 Geological evolution and setting

A detailed account of the sedimentary and tectonic evolution of the Hyblaean Plateau from the Late Cretaceous to the Quaternary is provided by Grasso & Lentini (1982), so only a general description of the regional geology of the eastern Hyblaean area is given here (Fig. 4.3.).

The geological stucture of the island of Sicily may be subdivided into four main units; the Hyblean foreland, the Northern Chain (an extension of the Appeninian-Maghrebian mountain belt), the Caltanissetta Basin and Gela-Catania Foredeep (Adorni & Carveni, 1993). The Hyblaean plateau represents a gently deformed segment of the African continental margin, which acted as a foreland during the Late Tertiary period of crustal collision between Eurasia and Africa. To the north and west the plateau is delimited by the Gela nappe system, comprising of thrusted and deformed Miocene and Plio-Quaternary foredeep sediments, and offshore to the east by similar fault structures of the Malta-Siracusa Escarpment (Butler *et al.* 1992; Catalano *et al.* 1995). North of the Hyblaean Foreland, within the regionally compressive tectonic regime of Sicily, fracturing of the continental crust during the Plio-Pleistocene led to basaltic-alkaline magmatism and the development of Mt. Etna (Adorni & Carveni, 1993; Chester *et al.* 1985).

During the Late Cretaceous, submarine volcanism was centred in the area of Capo Passero and between Siracusa and Augusta. At the volcanic centres and within the surrounding shallow marine basins, platform carbonates developed through the Palaeocene-Eocene. During the Oligocene-Miocene shallow marine carbonate sedimentation (Ragusa and Tellaro Formations) occurred with explosive volcanism in the north-east of the area (Lentini *et al.* 1987). Late Miocene-Messinian sediments reflect the regions progressive tectonic emergence, with a succession of shallow marine coquinal limestones, marls and evaporites being deposited. Regional uplift and the dramatic drop in Messinian sea levels led to widespread erosion and karstic unconformities of emerged areas, on top of which Late Messinian continental sediments were deposited (Butler *et al.* 1992).

Although during this period the Hyblaean area was largely emergent, Pliocene sedimentation occurred on the eastern Hyblaean margin, during the post-Messinian salinity-crisis refilling of the Mediterranean basin. South of Siracusa, towards the Capo Passero, Lower Pliocene open marine chalks (Trubi Formation) overlie Messinian marls and evaporites, while north of Siracusa, Pliocene-Pleistocene submarine lavas and sub-

Figure 4.3. Regional geology of south east Sicily (a) and (b) structural units of Sicily.

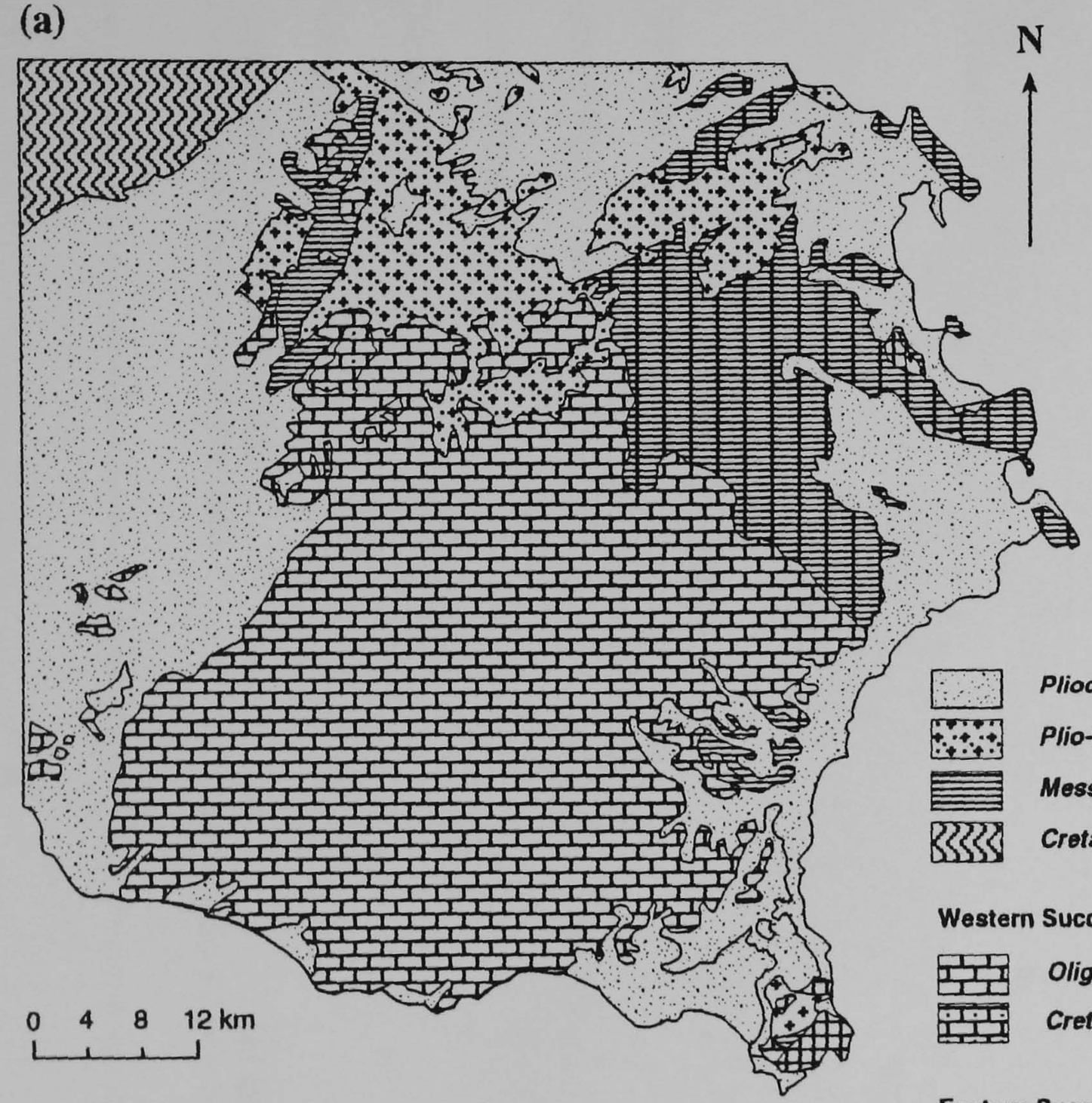

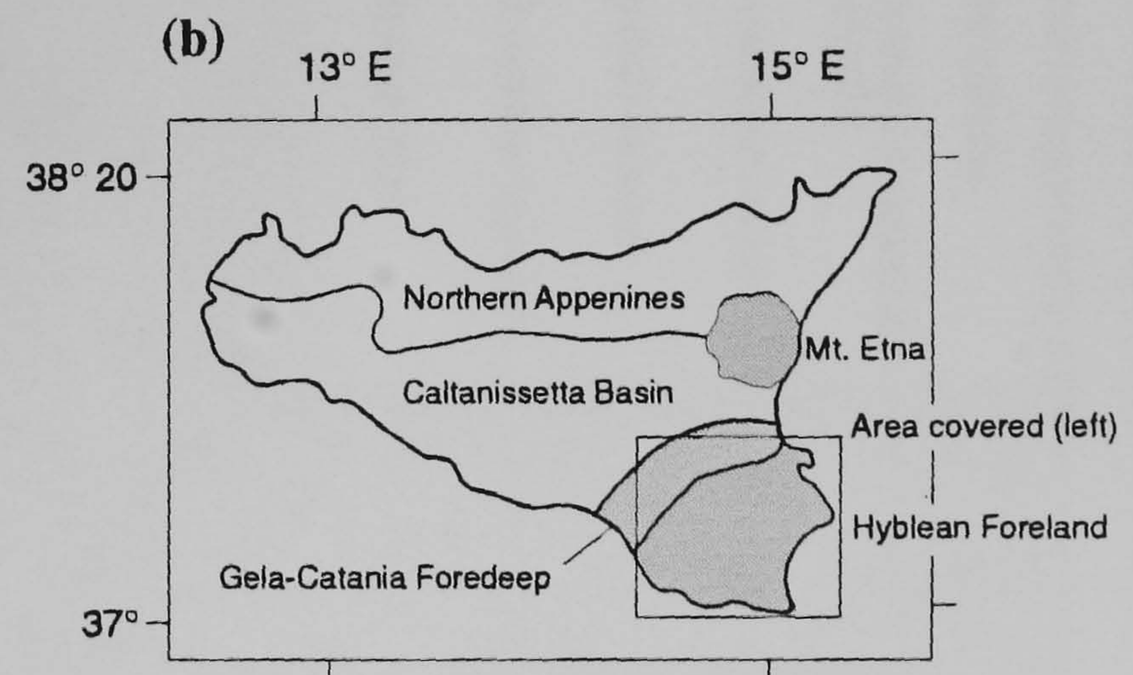

After Adorni & Carveni, 1993

Pliocene-Quaternary - Various marine, coastal and terrestrial deposits

Plio-Pleistocene - Basaltic lava eruptions

Messinian-Pliocene - Evaporites, volcanic products and marine limestones (trubi)

Cretaceous-Pliocene - Stratigraphic and structural units of Gela Thrust

Western Succession

Oligocene-Miocene - Carbonate shelf deposits

Cretaceous -Eocene - Basin carbonates

Eastern Succession

Oligocene-Miocene - Coastal and lagoon carbonate sequences and volcanics

Cretaceous-Eocene - Platform and basin margin carbonates

Cretaceous - Submarine volcanics

From Lentini, 1987

Figure 4.3.1. Geology of Capo Passero area, south east Sicily. After Lentini (1987).

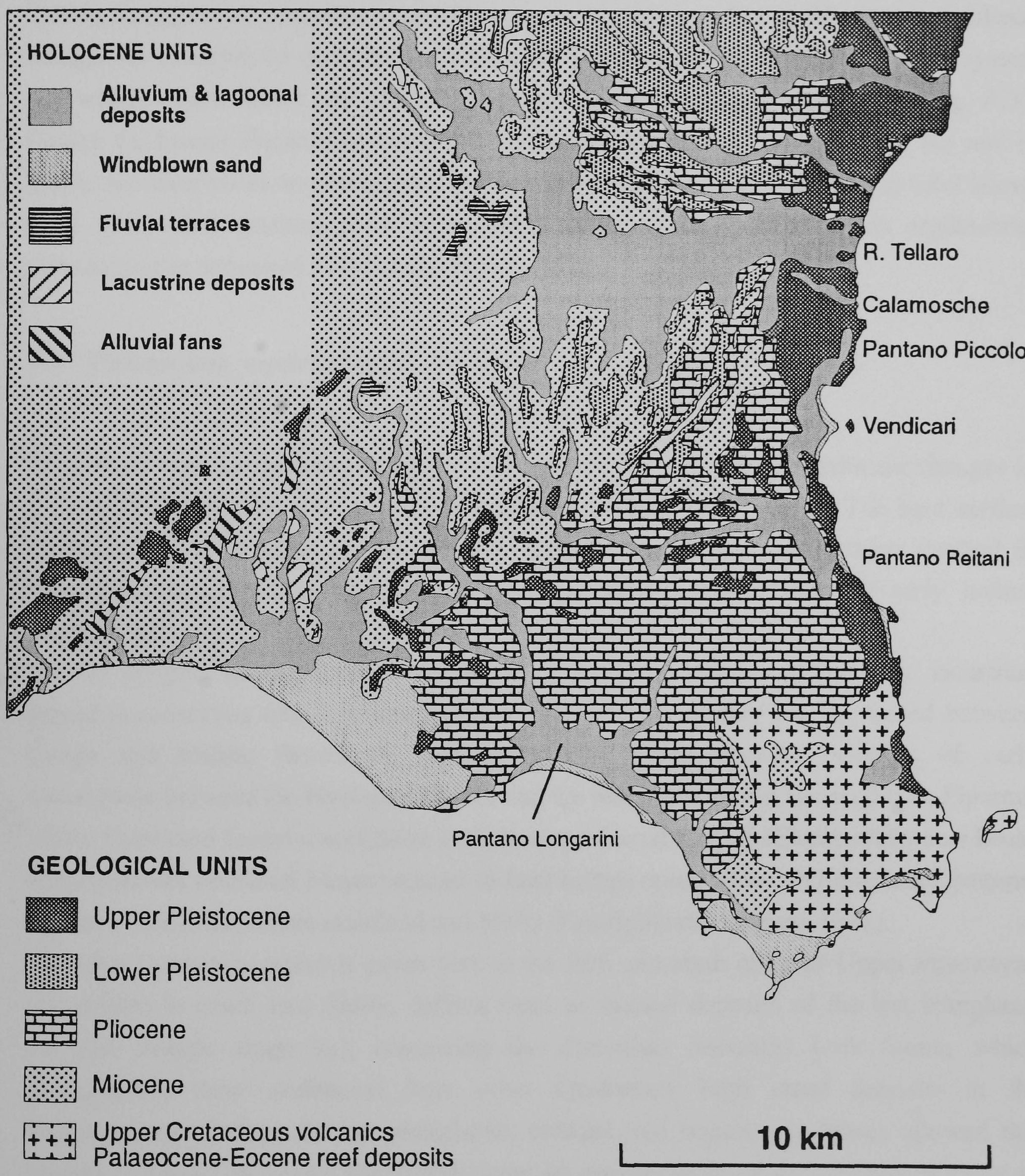

aerial volcanics were erupted (Grasso & Lentini, 1982; Lentini *et al.* 1987; Schminke *et al.* 1997).

Regional tectonic emergence, large amplitude glacio-eustatic sea level oscillations and more localised tectonic movements controlled the distribution and textural characteristics of Quaternary sediments in south east Sicily (Grasso & Lentini, 1982; Lentini *et al.* 1987). During transgressive episodes, sediments were primarily deposited at the eastern Hyblaean margin; for example the downthrown region south-east of the Ispica-Rosolini fault system and within coastal horst and graben structures in the Siracusa-Augusta area (Fig. 4.3). During the Lower Pleistocene when the Hyblaean plateau was isolated from the rest of Sicily, biocalcarenites were deposited in shallow marine basins separated by coastal horsts from deep-water grabens (East of Siracusa and Augusta) within which argillaceous materials were deposited (Grasso & Lentini, 1982).

4.5 Pleistocene environments in south east Sicily

The period saw the initiation of Etnæn volcanic activity and highly significant changes in geographical evolution due to major fluctuations of eustatic sea level. The land surface extension and contraction of the southern Calabria-Sicily-Malta archipelago resulted in successive faunal migrations, and the development of sites suitable for early human populations.

On the margins of the Hyblaean plateau, terrestrial sediments (palaeosols, lacustrine deposits) containing faunal evidence of the early-mid Quaternary are interposed between Lower and Middle Pleistocene marine deposits which provide evidence of early connections between the Hyblaean Plateau and the rest of the island (Bonfiglio & Piperno, 1996). Fossilised faunal associations include mega-faunal species (*Elephas falconeri* Busk, *Hippopotamus pentlandi* Meyer) related to land bridge connections and migratory patterns between Sicily, the Italian mainland and Malta (Bonfiglio and Insacco, 1992).

The term Tyrrhenian which is given here to the fifth and sixth order of Upper Pleistocene calcarenites in south east Sicily, defines them as marine deposits of the last interglacial (oxygen isotope stage 5e), containing the *Strombus bubonius* Lmk fauna, which distinguishes these sediments from other Quaternary high stand deposits in the Mediterranean. During the last interglacial, climatic and oceanic conditions allowed this species to extend its range northwards from its present limit of the north-west coast of Africa into the Mediterranean (Pirazzoli, 1987). *S. bubonius* deposits are reported in the Capo Passero-Pachino area occurring between 10 and 20 m (Malatesta, 1985; Carbone *et al.* 1982; Bordoni & Valensise, 1998). Identified by Colacicchi (1963) in the locality of

Vendicari, the 10 m shoreline neatly follows the pattern of subsequent Holocene deposits to the rear of Pantano Morghella, near Pachino and the fishing village of Marzamemi.

Within Tyrrhenian sediments, palaeosols and lacustrine deposits are occasionally interbedded between shallow-marine calcarenites. The more subdued occurrence of Pleistocene palaeoshorelines in the area along with abrasion surfaces identifiable in Plio-Pleistocene sequences (Grasso & Lentini, 1982) suggests a north-south difference in regional tectonic evolution between the Capo Passero area and the fault-controlled headland/embayment coastline in the area of Augusta and Siracusa.

It is likely that the earliest human groups arrived on the island during the early Pleistocene from the Italian mainland, possibly from Africa (Bonfiglio & Piperno, 1996), aided by low sea level stands which expanded coastal plains and dramatically reduced the width of the Mediterranean between Sicily and Tunisia (e.g. Van Andel, 1989). The earliest settlements are however recorded in the north and west of the island (Monte Pellegrino, Palermo and Levanzo, Egadi Islands) while only scattered remains of the Palaeolithic have been found between Siracusa and Marina di Ragusa in the south east of Sicily (Bonfiglio & Piperno, 1996).

4.6 Early Holocene environmental change

Alluvial sequences representing the environmental transition from the Last Glacial Maximum to the Holocene epoch are found in southern and eastern Sicily. On the southern flanks of Mt. Etna, deposits from this time period, consisting of chaotic assemblages of coarse, poorly sorted gravels with thin lenses of sand and a lack of argillaceous materials, suggest deposition under flash-flood, semi-arid conditions (Chester & Duncan, 1982). Elsewhere in Sicily, terraces 15-20 m above the present-day channel of valley sections of the Gornalunga (Fig. 3.5.), Platani, Salso and Dittaino rivers in Sicily (Judson, 1963; Neboit, 1984, Brückner, 1986), are assumed to represent episodes of river valley aggradation which occurred in the period spanning the Last Glacial maximum and Early Holocene. This assumption has been based on the lack of archaeological evidence contained within the terrace sediments and the incision-alluviation relationship with later terraces. It is likely that these older materials correlate with diachronous deposits of Late Glacial alluviation recognised in the Mediterranean (Vita Finzi, 1969).

Vegetation in Sicily during the glacial to post-glacial climate transition, is thought to have consisted of a *Quercus ilex* association of species (*Quercus ilex, Quercus suber, Pinus pinaster, Pinus pinea, Pinus halepensis* and *Olea europaea*) in areas below 1000 m (Chester and Duncan, 1985). Above this height deciduous trees such as *Fraxinus, Ulmus, Corylus,*

Juglans and *Castanea* reflected the more temperate conditions up to ~1500 m. In the semi-alpine environment below the tree line (approx. 1900 m) *Fagus, Larix, Pinus* and *Picea* grew near the summits of the Nebrodi-Madonie mountains and around the lower flanks of Etna (Poli, 1965). Unaffected by human activity, these altitudinal zones would have fluctuated in elevation and spatial extent during climate change (e.g. Tzedakis, 1999).

In Classical times, the richness of vegetation on the island impressed early writers, for example by Homer (c. 800 BC) and later Strabo (64 BC - AD 23), who were especially impressed by the forests around the flanks of Etna and Nebrodi mountains (Delano-Smith 1979). Widespread deforestation in Sicily appears to have almost certainly been a product of Roman and post-Roman/Medieval clearance for agriculture and the demand for ship construction materials (Thirgood, 1981).

The aridity of the southern coastal zone in Sicily may have led to the development of a natural macchia /*Quercus ilex* association in south east Sicily. The present day macchia association of the area ranges from degraded patches of original *Quercus ilex*-vegetation in less degraded areas to coastal garrigue communities of *Sarcopoterium spinosum* and *Thymus capitatus* (Brullo *et al.* 1980). Coastal and wetland vegetation types are likely to have been similar to present-day habitats, though more extensive and less disturbed by human activity.

4.7 Holocene tectonic activity affecting south east Sicily

Following the rapid post glacial sea level rise and quasi-still stand from the mid-Holocene onwards (*c* . 6-5000 calib.C^{14} yr BP), tectonic uplift of the coastline of south east Sicily, between Augusta and Gela, appears to have been minimal. With some local variations, geomorphological and archaeological evidence of relative sea level change in the region suggests a slow rate of relative sea level rise following the mid-Holocene stabilisation of sea level (Ruggieri, 1959; Coliacchi, 1963; Basile *et al.* 1986; Amore *et al.* 1994). The ria-type coastline of Late Quaternary incised valleys (e.g. the Tellaro, Vendicari and Pantano-Longarini-Cuba complex (Fig. 4.3.1) appears to have been initiated during the post-glacial flooding of coastal valleys. Post inundation/subsidence rates and estuarine transport processes, are likely to have maintained marine access until the flux of later phases of alluviation led to the widespread infilling of estuarine areas and the present-day distribution of Holocene sediments (Fig.4.3.2).

Evidence of slow subsidence and relative sea level rise exists in the form of Neolithic archaeological remains. At Vulpiglia near Pachino, Neolithic (*circa* 3000 BC) post holes have been discovered at 1.7 m below sea level (Guzzardi, 1996), giving a minimum rate of relative sea level rise of ~0.34 mm/yr for the last five thousand years, assuming that the

Plate 4.4. Series of excavated ponds in calcarenite bedrock, extending into sea, Vendicari, SE Sicily. Associated with remains of Greek (Hellenistic) - Roman fish processing industry in area. Near sea level position indicates that relative sea level change has been minimal in area. Torre Vendicari (circa. 15th century AD) in background.

holes were originally at or near sea level. The suggestion of sea level being 4-5 m lower than that of today (Basile *et al.* 1986), around the same period, in the vicinity of Ognina (Fig. 4.1) implies a much greater rate of subsidence (~1 mm yr^{-1}) over the same period. The island of Ognina is situated at the end of a coastal valley (1.6 km width) between two normal faults (Lentini, 1987), which may have locally accelerated the rate of coastal subsidence at the site over approximately the last *circa* 5000 years BP. It would appear clear therefore, that the rate of vertical motion has locally affected coastal settings in south east Sicily to a lesser or greater extent during the Holocene.

Archaeological evidence of late Holocene relative sea level rise may be separated into three areas; around Siracusa, Augusta and Ognina, where Bronze Age, Greek and Roman structures are submerged on the scale of a few metres below present day sea level, then south of Ognina to Capo Passero (Eloro, Vendicari, Marzamemi), where similarly-aged structures, i.e. fish ponds (Plate 4.4.) show a slight (≤ 1m) submergence (Ruggieri, 1959; Lena & Basile, 1986), before the coastal stretch towards Camarina, where as Basile *et al.* (1986) state " on the basis of archaeological data there is no evidence to suppose coastal submersions".

The spatial and temporal pattern of Quaternary shorelines displaced by uplift in the Augusta-Siracusa area compared to the southern coastline and Capo Passero peninsula, suggests that in relation to Quaternary sea level oscillation, the former area has been affected by increased rates of vertical motion. Whether the tectonic signal of these movements represents the local expression of regional crustal tectonics associated with larger scale Calabrian tectonics (e.g. Stewart *et al.* 1997), or due to more local crustal motion remains unclear. Crustal vertical motion during the later Holocene however, appears to have maintained the development of transgressive-high stand sedimentation along low-lying coastal stretches.

Due to the island's continued active tectonic setting, large magnitude earthquakes in the last thousand years have also affected Sicily, causing widespread devastation in the southern and eastern areas of the island (Mulargia *et al.* 1990; Guidoboni & Traina, 1996). Most significantly, in AD 1169, AD 1693 and AD 1908 the region was affected by highly destructive earthquakes. In the case of AD 1693, the seismic event with an estimated magnitude of M = 7.5 caused widespread devastation, largely destroying the cities of Catania (killing 60,000 inhabitants) and Siracusa, Ragusa, levelling Noto Antica (below) and towns throughout the region (Mulargia *et al.* 1990).

"Then came an earthquake so horrible, so ghastly that the soil undulated like the waves of a stormy sea, and the mountains danced as if drunk, and the city collapsed in one terrible moment killing more than a thousand people"

Eyewitness account at Noto Antica during the 1693 event (Facoros & Pauls, 1986)

The tectonic structure responsible for the high magnitude seismic event of 1693 (Mercalli >X) in the region (Mulargia *et al.* 1985) has been determined to have been the Simeto-Scordia-Lentini graben. This graben and an opposing one situated offshore in the Sicily Channel, is connected by a NE-SW right-lateral strike-slip wrench fault which bisects the Hyblaean plateau, parallel to the offshore Hyblaean-Malt escarpment (Mulargia *et al.* 1985; Piatenesi, 1998). A significant decrease in earthquake activity in the last two hundred years, compared to previous centuries in eastern Sicily (Guidoboni & Traina, 1996) suggests an increased likelihood of a high magnitude event occurring in the near future (Mulargia *et al.* 1991). The 1908 earthquake (M = 7) epicentre occurred on a reactivated fault in the Straits of Messina, where the thrust fronts of the Appennine-Calabrian-Maghrebian chains intersect between Sicily and the Italian mainland (Stewart *et al.* 1997). In 1990 a significant earthquake (M = 5.2-5.6 / intensity VII) killed 19 people and left 10-15000 people homeless in the provinces of Syracuse, Catania and Ragusa (Macadam, 1993) and caused much structural damage, especially in the Lentini area.

As well as having caused widespread destruction in the region, seismic events have also been observed to have greatly altered fluvial regimes in upstream catchments due to seismically-induced mass movements (e.g. Nicoletti *et al.* 1998). The two-fold effect of large volumes of soil-sediment injected into channel systems, i.e. the ponding of water upstream and changes in the long profile of the affected river channel have not however been recognised in the catchments used for recent stratigraphical investigation in this study (Nicoletti pers comm). The formation of ponds and depositional areas by seismic activity does however indicate the presence of an archive of geomorphological evidence on the timing and magnitude of seismic activity, which may be compared with, and used in conjunction with archaeo-historical and palaeoenvironmental evidence encountered lower in the catchment or in coastal wetlands.

The large magnitude earthquakes of AD 1693 and AD 1908 both generated tsunami waves, which affected coastal areas in south east Sicily. The AD 1693 earthquake generated a series of tsunami which were recorded in the ports of Augusta and Siracusa, raising and draining harbour waters in Augusta by "*..otto piedi geometrici..*" (eight [geometrical?] feet or 2.44 m ?) (Boccone, 1697) and causing destruction in districts close to the port (Piatenesi and Tinti, 1998). The most documented recent tsunami was that generated by the Messinia earthquake on 28 December AD 1908. This wave caused extensive damage to low lying coastal areas along the eastern coastline of Sicily. At Augusta wave heights of up to 2 m were reported, though inside the "harbour" at the Mulinello salina (presumed to have been near to the Mulinello core site (Section 6.1) the wave was only 60 cm in height (Platania, 1909). Due to the indented nature of the coastline, offshore morphometry and

headland refraction patterns, wave heights and their effects (and in turn observational records) differed along the coastline (Piatenesi & Tinti, 1998).

4.8 Human occupation and landscape alteration

Primarily the archaeohistorical settlement of the south east Sicilian coastline has been a consequence of the island's central Mediterranean position and its changing strategic importance of Sicily to successive Mediterranean civilisations. Before more advanced navigation and maritime transport, the south-east Sicilian coastline provided ports of call for coastal navigation, between the western and eastern Mediterranean and the North African coastline. On a regional and local scale, and from the earliest times of habitation, the coastline has provided shelter, defendable positions for access into the interior and access to the physical and ecological resources of the coastal and marine environment.

During at least the last three thousand years human activity has significantly influenced the coastal geomorphology of south east Sicily through direct human intervention (e.g. the construction of harbours, embankments and the removal of materials for construction) and indirectly by altering the environmental controls on the deposition and transport of upstream alluvial materials and coastal sediments. Archaeological and historical evidence in the coastal zone of south east Sicily therefore allows some assessment of the environmental changes which have impacted late Holocene coastal environments. Artefacts and structures not only reflect past environmental conditions but by their preservation or reconfiguration, provide an archive of subsequent environmental changes.

Throughout the later Holocene, the Mediterranean Sea and its resources have played a major role in the establishment and history of human settlements in the coastal zone of south east Sicily. The coastline before open sea navigation controlled lines of coastal communication, settlement positions, access to coastal and marine resources (such as fisheries and coastal quarries) and provided settings which after having been manipulated, allowed construction of additional resources such as salinas and fish ponds. Communities utilising resources in the marginal coastal environment would not only have been dependent on recognised patterns of environmental conditions e.g. seasonal flooding, coastal sea conditions and harbour water levels but would also have been the most negatively affected by, for example, coastal flooding caused by tsunami events or vessel draft reduction due to excessive estuarine alluviation. Although these events may have had great repercussions for the local economy and community, the most far-reaching consequences of coastal change and human activity are likely to have been those environmental and demographic changes that affected the coastal zone as a whole (Delano-Smith, 1979).

Figure 4.3.2. Holocene deposits and human occupation in the Capo Passero area, SE Sicily

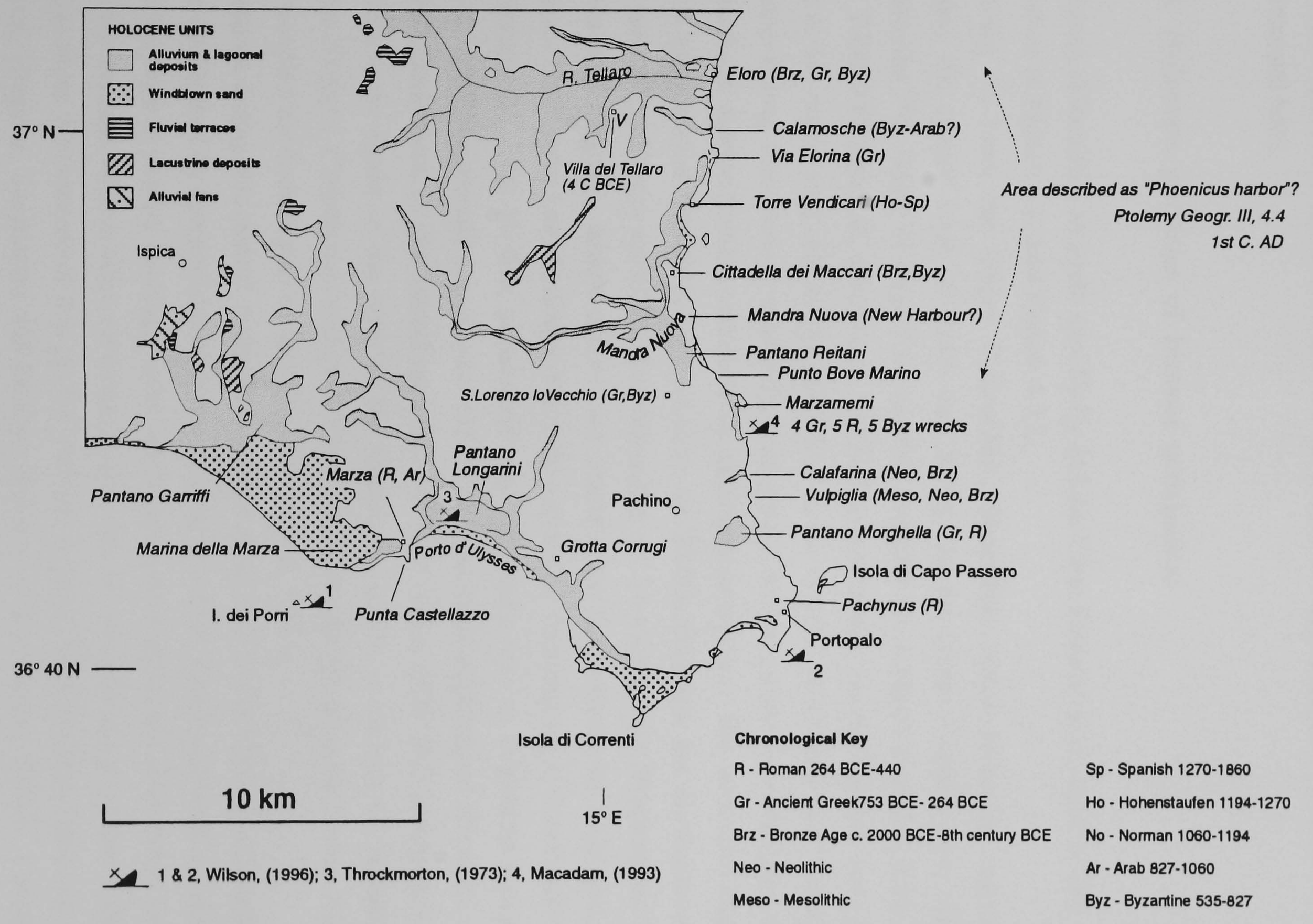

The complex nature of the archaeological and historical heritage in south east Sicily, with many areas displaying an almost continuous occupation from prehistoric times, makes a full account of the archaeohistorical evolution of the region beyond the scope of this research. Consequently only human factors which are likely to have influenced the geomorphological setting of the fieldwork areas and the depositional sequences from them are discussed here.

4.8.1 Holocene patterns of human occupation

The names of localities in south east Sicily and the Capo Passero area, used in this section are shown in Figure 4.1. and Figure 4.3.2.

Following on from the Upper Palaeolithic, Mesolithic hunter-gathering communities occupied the coastal zone of south east Sicily. At the Grotta Carrugi cave site (near Pachino) the ^{14}C dating of large fish vertebra indicates an occupation period from at least *circa.* 7000-5000 years BC (Guzzardi, 1996). The community occupying this cave site and others in the region (e.g. the caves developed in the uplifted shorelines near Siracusa and Augusta) during this period, most likely integrated hunter-gathering techniques of both terrestrial and marine (fishing and shellfish gathering) resources. The westward expansion of early agropastoral, Neolithic cultures from the Middle East saw the development (*circa* 3000 years BC) of larger agricultural communities i.e. Stentinello near Siracusa and Megara Hyblaea near Augusta, which utilised the coastal zone for commercial trade and marine resources. During the Late Neolithic-Early Bronze Age continuing up to Greek colonisation (8th century BC), the Sicilian population was a complex mix of migratory settlers who retained close commercial touch with other Mediterranean populations (Procelli, 1996). The first inhabitants of the island recorded by Thucydides (431 BC) comprised of the Sicanians from Spain in the west of the island, the Elymi, a mixture of Mediterranean peoples (Trojans, Phoenicians and exiled Sicanians), and Sicels, from the Italian mainland, who occupied the eastern part of the island (Macadam, 1993).

Settlements during this period, around the coastal periphery of the Hyblaean plateau, were clearly influenced by morphological features of the coastline. Characteristically, settlements took advantage of natural landing places, sheltered embayments and defendable headlands near river mouths, which allowed easier access into the interior and provided fertile sites for agriculture. Settlements of this period from the Augusta-Siracusa area (Brucoli, Megara Hyblaea, Thapsos, Stentinello and Ognina) down to Capo Passero (Eloro, Cittadella dei Maccari, Vulpiglia) and west along the Ragusan coastal arc (Punta Secca, Camarina) developed in settings with many, if not all, of these coastal landforms (Basile *et al.* 1986; Procelli , 1996).

The extent of trade and communication during this period is expressed by the origin of artefacts found at archaeological sites. Communication and trade during the Late Neolithic-Bronze Age is apparent by the presence of obsidian (from Lipari) and schist (from Messina) as well as Greek-Aegean imports found during excavations in south east Sicily (Guzzardi, 1996). At Ognina and the Cittadella dei Maccari (Vendicari), Mid-Bronze age ceramics originating from Maltese cultures (Tarxien, Borg-in-Nadur) have also been discovered (Basile *et al.*, 1986, Guzzardi, 1996). Harassment by pirates and internal feuding on the island during this period, led to the construction of defensive walls (e.g. at Thapsos) and defendable settlements within the interior. The Sicel settlement at Pantalica near Siracusa in the 13th century BC (*circa* 1270 years BC) for example, saw a Late Neolithic-Bronze Age culture remaining virtually unchanged until the arrival of Greek colonists in the 8th century BC (Macadam, 1993).

In an effort to gain a monopoly on coastal and commercial trade routes, Greek colonisation in the 8th century BC led to the re-colonisation of existing Bronze Age settlements, establishing early Hellenic commercial outposts; the island of Ortigia [Siracusa] (733 BC) and Megara Hyblaea (727 BC), as well as sub-colonies and settlements along coastal and inland trade routes i.e. *Eloro* (8th century BC), *Kamarina* (6th century BC) and *Akrai* [Palazzolo Acreide] (633 BC) (Macadam, 1993). After the turbulent period of Greek rule, conflict between Athens, Carthage and increasingly from Rome (3rd century BC Punic wars), Roman-Byzantine settlements supplanted previously established Greek sites e.g. at Siracusa, Catania and at the other sub-colonies.

The expansion of agricultural land and population centres inland, following Roman occupation (a process which continued through the Mediaeval period), led to the construction of ports and in the increased use of suitable coastal settings for ship anchorage. A contributory factor for moving inland may have been due to malaria. The malaria carrying *Anopheles* sp. mosquito, which may have been introduced into Sicily from North Africa in the fourth century BC (Thirgood, 1981) would certainly have been a contributory factor in the health of the population at the time. These dispersed coastal ports and anchorage sites catered for Mediterranean-wide commercial and military traffic, as well as, the coastal transportation of local resources (see below). Aside from the continued occupation of existing sites (Camarina, Eloro, Ognina, Siracusa), new harbour areas were established under successive Byzantine, Arab, Norman, French and Spanish rule, within coastal embayments that afforded access to the interior (e.g. coastal towns/vilages of Donnalucata, Sampieri, Pozzallo, Marza). Around the Capo Passero peninsula, this expansion led to the development of ports/anchorage sites currently occupied by the wetland areas of the Ambra coastline (Pantano Longarini-Cuba and Pantano Vendicari.

4.8.2 Commercial exploitation of the coastal environment

While providing the environmental settings for prolonged settlement periods, the coastal zone of south east Sicily has also historically, produced commercial resources for trading economies and local inhabitants. Commercial exploitation of the coastal zone has revolved, unsurprisingly around coastal and marine products. The physical morphology of coastal settings have been altered on a range of spatial scales and evidence remains of the extraction of construction materials, the production of salt via evaporation and commercial fisheries.

The combination of a favourable climate and shallow, low energy coastal settings led, most likely, to natural salt accreting environments being adapted for subsistence-peasant economy and commercial salt production by evaporation. Salt production by this means was likely to have been used as a commodity from prehistoric times, becoming an industrial enterprise with the management of suitable settings. Salt production by evaporation is carried out by the relatively simple procedure of concentrating the salinity of a large water mass of relatively low salinity, by stages of evaporation and volumetric reduction, before a desiccated product can be scraped off. Salt production by this method in the coastal zone of Sicily has a long history, with commercial operations existing until the mid-20th century (Naval Intelligence Division, 1945) when economic pressure from large scale operations e.g. at Marsala (western Sicily), war damage and destructive flooding combined to put an end to small scale operations.

In the Greek-Hellenistic-Roman period, salt production and fish processing was closely related to the coastal trading economy. Salt was used as a preservative and in cuisine, being a necessary ingredient for products such as *garum* (fish sauce), a Roman delicacy. Archaeological remains of Hellenistic fish processing structures occur at Vendicari (where Roman fish fattening tanks also exist (Plate 4.4.) and at Pantano Morghella, near Pachino, where a fish processing workshop appears to have been in use for approximately 800 years from the 4th century BC (Wilson, 1996; Bacci, 1983). Industrial salt extraction appears to have been operative at Pantano Morghella during this period also, by utilising the brackish marshes for salinas and salt production (Basile *et al.* 1986). Evidence of cargo-transport of these products comes from the scattered remains of shipwrecks and their cargo around the coastline (Throckmorton & Throckmorton, 1973; Wilson, 1996).

Small-scale salina operations are likely to have expanded commercially in relation to economic pressures and the development of more extensive brackish areas in the coastline due to upstream soil erosion following post Roman-Mediaeval landscape denudation episodes. Larger operations at or near sea level would have required more elaborate controls on the flow of marine-brackish water into the "pans", with channels and embankments being constructed. Salt production sites taking advantage of more open

estuarine settings (River Mulinello, Pantano Grande at Vendicari) would also had to protect the salinas from flooding and the flow of fresh, less-saline water into evaporating pans, necessitating the construction of embankments and flood-defences.

Remains of coastal quarries (*latomies*) are interspersed around the coastline of south east Sicily (Lena & Basile, 1986). Stone extraction from coastal quarries, in general, was made easier as initial work faces presented themselves as cliffs, which allowed specific rock types to be chosen before the removal of unprofitable overburden. Local stone was used extensively in the monumental construction of Greek and Roman settlements (e.g. at Siracusa, Megara Hyblea, Eloro) as well as later constructions, e.g. the use of local marl-limestone in the post 1693 earthquake reconstruction of Noto, due to its hue and suitability for Baroque-style carving and architecture.

Contemporary and earlier Quaternary rocky shorelines in the local area (Di Grande & Raimondo, 1982; Bordonaro *et al.* 1983) must have reduced problems in extracting stone (reduced overburden) and eased transportation by the use of stone-carrying vessels. Remains of extensive coastal quarries are found on the Monte Tauro (Augusta), Siracusa, Plemmyrion headlands and the calcarenite-limestone coastline (e.g. between Eloro, Vendicari and Marzamemi) extending south to Capo Passero (Basile *et al.* 1986; Lena & Basile, 1986).

4.8.3 Late Holocene impacts on alluvial environments in south east Sicily

Changing patterns of land-use have significantly affected the nature of landscape denudation and timing of alluviation in south east Sicilian drainage catchments. A broad outline of land-use changes having occurred within drainage catchments during the late Holocene are shown in Table 4.1.(below). In Sicily three periods of archaeo-historical alluviation have been recognised from upstream river terrace sequences containing archaeological remains; occurring between 2700 and 2300 BP (Neboit, 1984), from circa 400 AD to 1500 AD or "Medieval" and in the 18th-19th century (Judson, 1963). These periods of exacerbated upstream denudation and valley alluviation are likely to have been a major influence on increased deposition in the coastal zone.

The distal, estuarine areas of rivers draining the Hyblaean plateau have certainly undergone considerable hydrological changes in archaeo-historical times largely contemporaneous with episodes of fluvial aggradation. The larger Holocene coastal floodplain areas of the Tellaro, Irminio, Ippari and Anapo rivers, as well as smaller river systems and coastal embayments (e.g. the Mulinello, Asinaro, Saia Scirbia, Cozzo Pantano) display many similarities, in terms of the spatial and temporal decline of navigable channels and shrinkage of estuarine-embayments due to the influx of alluvial sediments.

Table 4.1. Land use changes in drainage catchments in south east Sicily (After Nicoletti & Terranova, 1998).

Time period (Years B.P.)	**Land use**
Early Holocene - 7000	Natural forest cover
7000 - circa. 2700	Natural forest cover with encroaching agriculture (90% forest/10% agricultural)
circa 2700 - 900	50% forest cover - 50% agricultural
900 to present	20% forest - 80% agricultural

Three localities in south east Sicily serve as reliable examples of the timing and nature, of fluvial and coastal changes during the last 2000 years (Fig. 4.1/ Fig. 4.3.2. for locations):-

i) The River Irminio: In Ancient Greek times (c. 2400 yrs BP), the river is reported to have been navigable as far as Ragusa *Hybla* (20km inland) (Amore *et al.* 1997). The infilling of the River Irminio may have followed a similar pattern to the nearby River Ippari, where the port of Kamarina (Camarina) active until the Hellenistic period, was gradually infilled during the Middle Ages (Basile *et al.* 1986). By the Middle Ages (1154), the "port of Ragusa" was situated at the Irminio river mouth (Amore & Randazzo, 1997) due to reduced navigability upstream. During the Norman occupation period (1100-1250 AD), widespread deforestation in the catchment increased upstream sediment loads, burying port constructions at the river mouth, resulting in the formation of "unhealthy lagoon areas" (Amore & Randazzo, 1997).

ii) Eloro: The Syracusan colony of Helorus (Eloro) was founded on an existing mid-Bronze age settlement at the start of the 7th century BC., on a headland overlooking the river mouth of the Tellaro (Helorus) river (Macadam, 1993). The harbour to the colony is assumed to have been to the south of the headland, where the present day beach and floodplain now exists (Basile *et al.* 1986). This river mouth appears to have been mentioned by Virgil (70-19 BC.) some centuries later on a voyage during his circumnavigation of Sicily, which provides an image of the wider river mouth and active floodplain :

"Our voices hailed the great gods of the land with reverent prayer; then skirted we the shore, where smooth Helorus floods the fruitful plain"

Virgil (70-19 BC.) Aenid 3.692 (955)

What the extent and nature of the harbour was like at the time of Late Bronze Age-Greek occupation remains unclear. The sheltered embayment would certainly have been given protection from north east winds by the now more-eroded Eloro headland, though may have been a simple landing stage on the beach at the mouth of the river Tellaro. As Delano-Smith (1979) suggests, what made a good anchorage was the shelter from unfavourable winds and protection from enemies, rather than the construction of complicated structures. Evidence for the estuarine-inlet which formed the landing stage for Eloro is assumed to be at present beneath the cultivated floodplain and beach area formed at the outlet of the embanked River Tellaro (Basile *et al.* 1986).

Preliminary core investigations at the site to the rear of the beach revealed a sequence of organic and grey-blue muds which extended 1-2 m below present day sea level. These would appear to represent a more fine-grained depositional environment, than that which occurs at the present. Further stratigraphic and palaeoenvironmental studies in the area are required before an accurate palaeogeographical reconstruction can be made.

iii) Pantano Longarini: This present day lagoonal and wetland area was known in antiquity as an area of anchorage and harbour, often the last and first port of call from Malta and North Africa. Known under various names, as the anchorage of *Odissea* to Ancient Greeks and *Edissa* during Roman times (Throckmorton & Throckmorton, 1973), it appears to have been known as the *Porto di Ulisses* (Port of Ulysses) until at least the 19th century (Figure 4.4.1.). The embayment would also have provided sheltered anchorage for coastal navigation before or after rounding Capo Passero (known as *Pachynus*). Cicero (106-43 B.C.) describes a pirate attack in the "*Port of Pachynus*" (Against Verres, Ch. 5) occurring in the 1st century B.C., while the remains of a ship discovered during wetland reclamation work (^{14}C dated at AD 500 ± 150) appears to have been a cargo vessel trading between Africa and Sicily (Throckmorton & Throckmorton, 1973).

The present day low-lying area of Pantano Longarini, apparently once an inland extension of the sea, has since been infilled in the last 1000, even 200 years, caused by the increase of sediment in the coastal zone from the degradation of upstream catchments and later land reclamation efforts (Amore *et al.* 1997). On the promontory of Punta Castellazzo nearby are remains of port structures and dwellings associated with cult worship, connected with an invasion of Libyans who were repulsed by a virulent pestilence unleashed by the god *Lybinistus* (though more likely malaria from the nearby marshes) and localised cults connected with the passage of *Ulysses* through Sicily (Basile *et al.* 1986). The nearby

settlement of Marza (in Arabic "*marsa* ") and Portopalo (*Marsa al bawalis*; in Arabic "the port of the swamps") (Basile *et al.* 1986) indicate coastal wetlands were a characteristic feature of the coastal landscape during the period of Muslim-Arab occupation (*circa.* 9th - 11th century AD).

The increase in sediment transport and deposition within the coastal zone, caused by agricultural expansion was almost definitely initiated during the Greek colonial period (8th century BC) onwards. Rather than recovering from the decline in Greek-Roman cultures in the Middle Ages, Sicily was extensively deforested (especially during the Norman period) and turned over to expansive cultivation of crops (wheat especially) and grazing. Increased fluvial sediment loads as a result of unregulated expansion into terrain susceptible to erosion, led to increased alluviation in lower catchment areas; estuarine environments becoming choked flood plains and embayments becoming restricted lagoonal areas. With the loss of their strategic settings and once favourable positions at the mouths of navigable channels, settlements were abandoned.

4.9 Five centuries of changing land use and impacts on coastal environments

Compared to the Italian mainland, especially the industrial and agricultural centres of northern and central Italy, the agricultural economy in southern Italy and Sicily has until only relatively recently, remained fairly antiquated. Long standing feudal agricultural systems and land use (*latifondia*) systems remained in existence until the mid-20th century. Under the rule of the Spanish (1409-1860 AD) the island remained as a grain-producing backwater to the Italian mainland, losing its strategic importance in the central Mediterranean (with the strategic and commercial shift to the Atlantic), governed by corrupt aristocratic rule with feudalism maintained in the country side (Andrews & Brown 1993).

From the 15th-16th century onwards, the agricultural landscape was progressively transformed, with the consolidation and commercialisation of large estates, reclaiming some areas of marshland, though concentrating on the expansion of sheep and pasture, to the detriment of small peasant economies (Woolf, 1979). The expansion of the rural population through the 16th to 19th centuries and the external demands for food products (wheat, oil, citrus fruits, wine etc.) led to the expansion of cultivable areas. This demand was generally not met by improved agricultural productivity, but by the increase in expansive cultivation. The *latifondia* system expanded into previously un-cultivatable areas, which were unsuitable for grazing and low yield grain cultivation, while landowners continued to exploit the abundant and mobile peasant labour (Woolf, 1979; Clark, 1989). During the 19th century therefore the cumulative effects of centuries of extensive

agriculture and expanding cultivation, combined as well with the meteorological variability during the climatic recovery from the Little Ice Age (see Chapter 3), appears to have led to extensive soil erosion in upland areas, downstream valley and estuarine alluviation and coastline progradation, similar to other areas around the Mediterranean. This combination of climate and expanding land use into susceptible terrain was an event that also occurred on the Italian mainland at the Po delta (Cencini, 1998), and in the Molise, Tuscan and Marche regions of central and northern Italy (Barker & Hunt, 1995; Hunt & Gilbertson, 1995; Coltorti, 1997).

4.9.1 Late 17th-19th century maps of the south east Sicilian coastline

During this period of recent historical change in land use, early maps of the island were being constructed. Accounting for errors caused by early attempts at cartographic representation, historical maps obtained of Sicily suggest relatively dramatic changes of the coastline over the last few centuries, especially with the depiction of rivers and presence/absence of islands. These apparent changes need to be set into the context of historical and archaeological records mentioned previously, to avoid over-exaggerating the cartographic depiction of coastal changes. Four maps held in the Map Room at the Royal Geographical Society, London are discussed here: that of G. G. di Rossi (1695), Hubert Iaillot (1700), a German Military map of 1720 and an Admiralty map (Captain Smyth RN, 1826). Photocopied reproductions of the original maps are contained in Appendix I. A coastal outline of each map is shown adjacent to the reproduction for reference to the text below. These coastal outlines are shown together (excluding the 1695 map) in Figure 4.4.

(a) "Italia di Matteo Grerter" G. G. di Rossi (1695)

Preceding the Hubert Iaillot map by five years, the coastal features of the island, depicted on the map (not shown due to poor reproduction of original) display similar inaccuracies in distance and orientation. The coastline around the Capo Passero peninsula is depicted as being far more indented, with the Ambra coastline marked as one large marsh area. The estuary mouth of a river draining the Noto area, is shown much wider with an island, though because of the map accuracy, this could well be the island of Ognina situated 20 km to the north. Many islands are displayed, those offshore of Camarina, discussed below as well as further west, the town of Alicato [*Licata*] is represented clearly as an island at the mouth of the present day River Salso.

(b) Hubert Iaillot 1700 AD (Fig. 4.4./Appendix I)

It is difficult to assess how much of a map constructed during this time was based on measured observation, rather than perhaps pre-1700 historical references, and maps of the calibre of the 1695 G. G. Rossi. The outstanding feature of this map is not necessarily the inaccuracy of scale but, as the previous map showed, the accentuated indentation of the coastline. Both Pantano Longarini and Pantano Morghella can be identified and show open contact with the sea (Fig. 4.4.). The coastline north of the marked fortification of Vendicari is particularly interesting, not only because of the marked estuarine nature of the R. Tellaro-R. Calabernado estuarine area, but the presence of three islands at the river mouth. It is suggested here that these may represent the Pleistocene calcarenite outliers at the River Tellaro mouth (Lentini *et al.* 1987), which are surrounded by Holocene alluvium and coastal sands (Fig.4.3.2.). At the end of the 17th century these may have been separate islands or more discernible as high land in an estuarine-wetland environment. Alternatively the depiction may be evidence of the Tellaro being multi-mouthed depicting its course via the present day 'dead-valley' of Calamosche (1.5 km S). Similarly the small islands represented offshore to the south and east of Camarina (Punta Secca) (PS) appear to coincide with outliers of Late Quaternary calcarenites which at the present-day are surrounded by Holocene alluvium and coastal dunes (Lentini *et al.* 1987). Accounting for cartographic errors in depiction, the overall impression of the map suggests that rivers may have been more dynamic in nature, and embayments between protective headlands were less infilled by coastal deposits at the start of the 18th century.

(c) German Military 1720 AD (Fig. 4.4./Appendix I)

It is unlikely that the more subdued coastal outline depicted on the map, represents widespread coastal alluviation having occurred in 20 years since the previous map. More likely the coastal outline was a less important feature for German military use. The depiction of the early 18th century coastline supports some of the assumptions made from the 1700 Hubert Iaillot map. A chain of islands is recognisable to the south west of Camarina as the present day outcrop pattern of Tyrrhenian calcarenite (Punta Secca and Punta Brucetta), ante-dating the present day expanse of coastal deposits, alluvium and windblown sand (Lentini *et al.* 1987). Lagoons are represented inland on the Capo Passero peninsular, however with a distinct lack of detail. North towards Vendicari, the Punta Bove Marino is marked as well as being slightly to the north a small inlet. This inlet would appear to be the dune and alluvium filled area at the southern end of the Saia Scirbia-Vendicari lagoon complex. The present day area of Pantano Reitani (Fig.4.3.2.) is likely to have evolved contemporaneously with the Vendicari lagoon complex, as a breach in the local Pliocene-Pleistocene geology caused by Late Pleistocene-Holocene fluvial and coastal processes. This outlet may have been a seasonal flood outlet or the primary outlet, before the Saia Scirbia was diverted to the north of the Cittadella headland (e.g. Colacicchi,

Figure 4.4. Coastal outlines of south east Sicily (Capo Passero area) from historical maps *. Inset maps show region of Sicily covered by shaded area.

* Reproductions of original maps used are in Appendix I

Figure 4.4.1. Coastal features of Capo Passero area, south east Sicily depicted in early 19th century compared with present day coastline and Holocene sediments

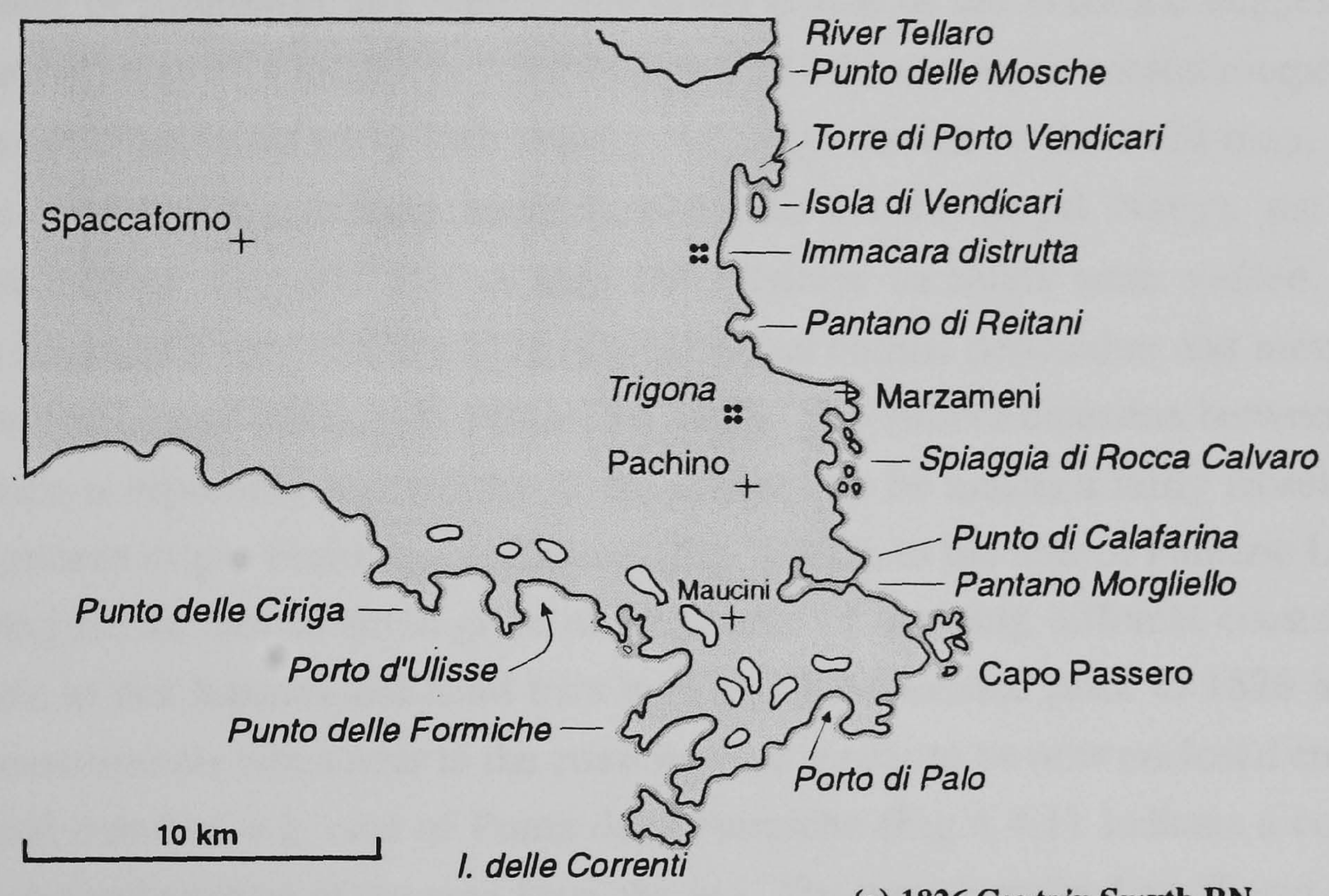

(a) 1826 Captain Smyth RN

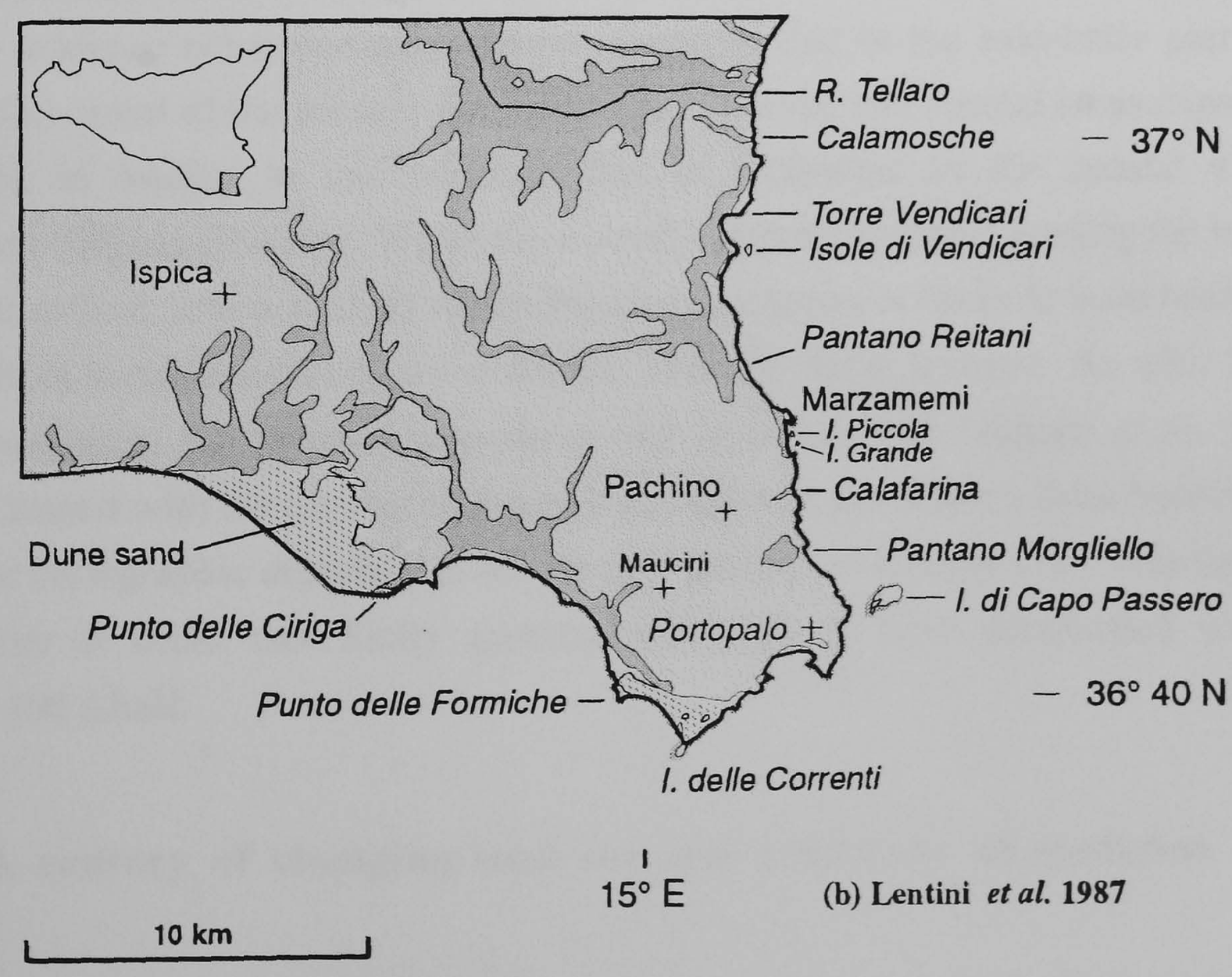

(b) Lentini *et al.* 1987

1963). Pantano Roveto and Pantano Piccolo can be identified apart with separate outlets into the bay containing the Isola di Vendicari.

(d) Captain Smyth RN 1826 AD (Fig.4.4./ Appendix I)

The number of soundings and represented detail drawn of the coastline suggest that this particular map may be a relatively reliable source of information on coastal morphology and shoreline positions in the early 19th century. Although similar to the 1720 map, in that the map was produced for military needs (constructed for the Royal Navy), the taking of fathom-soundings suggests that at least the offshore localities were visited. The map certainly suggests a very recent nature of widespread coastal deposition and morphological change within coastal settings in south east Sicily. The Ambra coastline between Pozzallo and Pachino is especially noteworthy as the outline can be matched fairly closely with the outcrop pattern of pre-Holocene sediments (Fig. 4.3.1.), to the rear of Pantano Longarini.
Accounting for the lack of detail given to the priority of mapping different coastal materials at the time, in that lagoons and sand bars may well have existed prior to 1826 in the area, depth measurements taken near to the coast in what appear to be now enclosed embayments and coastal marshes, e.g. east of Punta della Formiche (Fig.4.4.1) indicate a considerable infilling and reclamation of the area from the sea. The area described as *"Porto d'Ulisses"* is marked, though unclear as to whether it marks the present day Pantano Longarini-Cuba or the Marina della Marza (Fig. 4.4.1.)
On map evidence alone one may assume therefore that in the mid-latter part of the 19th century the extent of the present day "Holocene" alluvial and coastal areas expanded greatly in extent, in relation to the increased flux of sediments in the coastal zone, due to catchment-derived alluvium. With only a small catchment system feeding the lagoons of the Ambra coastline, sedimentation within Pantano Longarini is likely to have been accentuated by sediment transported along the coastline from the River Irminio. As with the Vendicari lagoon complex, fine-grained deposition and lagoonal infill (Amore *et al.* 1994) would have increased with the closure of the embayment by a developing dune barrier.
From the cartographic depiction alone the progradation of coastal dune and lagoon areas in this corner of south east Sicily appears, therefore, to have accelerated within the last century and a half.

4.10 A century of changing land use and landscape degradation

At the turn of the 19th-20th century, economic reforms and the industrialisation of the agriculture in northern Italy, was balanced in southern Italy and Sicily by mass emigration to Italian industrial areas and abroad. The relieved pressure on land use brought about by

abandonment often raised the living standards (in the form of wage increases) of those who remained, but in terms of the agricultural landscape, there was little change from previous centuries (Clark, 1984).

The twentieth century saw continuing efforts to reform the agricultural landscape of rural Sicily. The fascist government led by Benito Mussolini in the 1930's led a campaign of land reclamation to increase agricultural land for the cultivation of wheat as well as the political gain in dealing with the "southern problem" of the under-developed southern portion of Italy. In south east Sicily, the land reclamation of the Tellaro floodplain area commenced in 1933, while the Vendicari-Longarini areas were planned, but not commenced by the same date (Naval Intelligence Division, 1945). Although hindered by bureaucratic corruption and interrupted by the Second World War, these land drainage schemes also included improving mountain and upland areas to combat soil erosion. Other reclamation works of wetlands area in the region appear to have been conducted by municipal projects and imaginative individuals (Throckmorton & Throckmorton, 1973). Following Post-war land reforms (1950), remaining large uncultivated and badly uncultivated rural estates were expropriated by land reform agencies, in a sense breaking up the *latifondia* system after two thousand years of existence (Clark, 1989).

The present-day agricultural landscape of the low relief coastal area of south east Sicily consists of large tracts of intensive greenhouse cultivation for European markets, a diversity of crops being grown for local and foreign markets and continued goat and sheep grazing. The rural population remains concentrated around the coastal and inland market towns e.g. Pachino, Ragusa and Avola and the larger urban areas of Siracusa, Augusta and Catania, leaving a largely abandoned landscape between towns. Away from the fertile coastal plains the southern interior of the island presents a barren, treeless landscape. Human activity in the interior of the plateau remains largely involved with expansive agriculture. The characteristic landscape of the dry-stone field boundaries, separating pasture land and crops, is a preserved and largely maintained remnant of 18th century Spanish land reforms (Macadam, 1993).

Post-war industrialisation and urban expansion in south east Sicily has primarily been focused on the coastal urban stretch between Augusta to Siracusa (Mountjoy, 1970). The growth of the petrochemical industry from the 1950's in the Gulf of Augusta, occurred in conjunction with the discovery of offshore oil, has led to the largest, present-day concentration of chemical plants in Europe (Macadam, 1993). Coinciding with the industrialisation of the coastal zone, the last few decades has seen the widespread construction of secondary homes for urban populations and tourist resorts. Escaping the worst excesses of the Mediterranean riviera, new homes and tourist villages have spread into previously cultivated and coastal areas (e.g. *Lido di Noto*, *Lido di Avola*) as well as expanding the size of small ports and fishing villages (e.g. Portopalo di Capo Passero and Marzamemi). A number of nature reserves have been established within the coastline of

south east Sicily (Cavallaro, 1991), e.g. the *Oasi faunistica di Vendicari* near Noto and the *Fiume Ciana e saline di Irminio* near *Siracusa*, by the intervention of local and regional conservation bodies, i.e. the *Ispettorato Ripartimentale delle Forestale*. These are recent additions to the coastal landscape, occupying areas abandoned by industry and agriculture this century, allowing the regeneration of "natural" coastal landscapes and habitats.

4.11 Coastal wetlands in South East Sicily

Coastal wetlands developed on Holocene and recent sediments occur in a number of sheltered estuarine and lagoonal settings within the coastal zone of SE Sicily. Although having been extensively damaged by historical and recent phases of degradation, the remaining areas of coastal wetland environments provide settings where relationships and controls on wetland, coastal and fluvial environments may be investigated. As a consequence of the climate, hydrology and extent of human interaction, coastal marsh communities in south east Sicily are similar to other saline-brackish marshes developed in the coastal zone of the Mediterranean sea (e.g. Gimingham & Walton, 1959; Costa & Boira, 1981; Basset, 1986; Ortiz *et al.* 1995; Pacheco *et al.* 1996) and show many similarities with coastal wetlands in estuarine environments developed in California, U.S.A. (e.g. Zedler *et al.* 1986; Callaway *et al.* 1989; Davis, 1992; Cahoon *et al.* 1996; Niemi & Timothy-Hall, 1996) and Australia (e.g. Hodgkin & Hesp, 1998).

In the interior of Sicily, vegetation communities similar to those at the coast are also found where hydrological conditions, the geology in the local catchment and low rainfall totals, imitate low energy, saline coastal environments (Calvo *et al.* 1993, 1995).

At the coastline, due to the microtidal regime, often energetic wave environment and drainage catchment characteristics discussed above, wetlands in the coastal zone of SE Sicily have developed in a number of sheltered, low-energy coastal environments. Brullo & Furnari (1977) distinguished three main wetland vegetational systems, in relation to the substrate, hydrology and salinity of the wetland setting in south east Sicily (Table 4.3.). In both the larger (e.g. Vendicari, Pantano Longarini) and smaller confined wetland areas, for example at the mouth of the River Mulinello, near Augusta and the River Ciane near Siracusa, these associations are seen to form a complex vegetation mosaic in relation to localised physiographic and edaphic controls. The complexity of wetland vegetation is not just due to spatial differences but the response of plant communities to temporal differences in growing conditions.

A useful example of yearly-decadal temporal and spatial succession of halophyte wetland vegetation in south east Sicily, is provided by measured trends of vegetation communities around the Lago Pergusa, near Enna in central Sicily, approximately 50 km inland and 667

m above sea level (Calvo *et al.* 1995). A decrease in lake volume due to minimal rainfall over the previous decade (accompanied with increasing salinity), led to halophytic species migrating into the desiccating water body, developing a concentric zonation of species in relation to new hydrological gradients over the space of a few years (Calvo *et al.* 1995).

Table 4.2. Vegetation associations identified in coastal marshes of eastern Sicily. After Brullo & Fumari, (1977).

	A **Xerophytic association**	**B** **Sub-Xerophytic association**	**C** **Psammophytic association**
Substrate	Summer-desiccated sand and mud	Year-round wet mud	Semi-saturated dune sand or sandy mud
Coastal setting	Back barrier lagoon	Inland marshes	Rear dune-barrier
High Marsh	*Agropyron elongatum*	*Agropyron elongatum*	*Ammophila arenaria*
	Inula crithmoides	*Inula crithmoides*	*Imperata cylindrica*
⇧	*Juncus subulatus*	*Juncus maritimi*	*Juncus maritimi*
Typical species	*Arthrocnemum sp.*	*Arthrocnemum sp.*	*Scirpetum maritima*
⇩	*Suaeda maritimea*	*Salicornia subass.*	*Arthrocnemum sp.*
	Salicornia sp.		
Low Marsh			
Salinity	High salinity	Lower salinity	Low-brackish

Note: Both the Mulinello estuary and Pantano Piccolo sites (Ch.6) display characteristics of the Xerophytic, Sub-Xerophytic communities. Association C was observed to be more extensive in the rear dune environments at Vendicari and Pantano Longarini.

A common, almost intrinsic factor in coastal wetland landscapes of south east Sicily is the ubiquitous presence of either abandoned anthropogenic structures or the encroachment of modern developments. During the evolution of the coastal zone of south east Sicily, halophyte and other wetland plant communities have surely, by their present-day occupancy surrounded by past evidence of human activity, responded to long and short term disruption by hydrological-coastal processes and human activity. Either as a protracted or rapid response to anthropogenic or climatic variables, vegetation communities

have developed at rates of change and with a sufficient continuation of communities to ensure the continued colonisation of available sediment surfaces.

The palaeoenvironmental interpretation of geomorphological evidence and sediment sequences deposited within present-day coastal wetlands in south east Sicily, requires both human and natural factors to be considered. Long and short-term patterns of land use and dynamic environmental changes, in catchment areas supplying sediment to the coastal zone, have combined in developing a mosaic of interposed coastal and alluvial landforms and sediments.

An initial line of questioning during fieldwork, prior to the multi-proxy analysis of sediments from the settings chosen to be most suitable for recent palaeoenvironmental investigation, was to what extent do present-day wetland habitats reflect contemporary coastal wetland processes? How much of an effect have past anthropogenic and natural changes had? Are coastal wetlands a relic of a more active phase of coastal deposition currently adjusting to recent changes or have they been continually responsive, adjusting to dynamic environmental changes as they occurred?

Chapter Five

Techniques of Analysis

5.1 Sampling Methodology

Salt marsh and mudflat cores were taken from small wetlands in estuarine and lagoonal settings from south east Sicily by manual sampling techniques. The location of sites sampled are shown in Plates 6.3. and 6.6, with their respective environmental settings discussed in the following chapter. Core AMC was extracted by Dr. A. Cundy, using a hand driven 9 cm diameter PVC tube in September 1995. Cores PPA and PPB were manually extracted from the core sites using an open gouge (8 cm diameter) in October 1996. Care was taken to avoid compression of the core during sampling (e.g. Morton & White, 1997). The surface of the cores during the extraction of AMC, PPA and PPB did not alter during tube/gouge penetration. Recorded depths in the cores therefore relate to distance below sediment surface.

Sampling from the cores was either by dividing the core sections into consecutive 1-2 cm intervals or at intervals representing significant stratigraphic changes and horizons.Cores were described in the field and features added during the sub-sampling for individual analyses in the laboratory.

Core sites and their surroundings were levelled to an approximate sea level datum at the time of sampling. Because of the unavailability of official reference datum points in the field areas, a local datum relative to approximate sea level at the time was used. Local sea conditions made this occasionally difficult, for example on the gently shelving and exposed rock platforms in the locality of Vendicari. All levelling transects used during the study had closing errors less than 2 cm.

5.2 Radionuclide analysis

The activity of two radionuclides (^{137}Cs and ^{210}Pb) were determined with depth for the cores. ^{210}Pb was used for all cores, while ^{137}Cs was only used for the Augusta (AMC) core. ^{137}Cs and ^{210}Pb activities for core AMC was determined by Dr. A. Cundy. ^{137}Cs activities for AMC were determined by gamma spectrometry with a Canberra 30% P-type HPGe gamma ray spectrometer. Samples were counted for 18000 - 100000 seconds depending on their activity and maximum errors were typically in the order of 4% (1s). The detection limits for ^{137}Cs was 0.5 Bq kg^{-1}.

^{210}Pb activity for all cores was determined through the proxy measurement of its granddaughter ^{210}Po using alpha spectrometry. The method based on Flynn (1968) uses the auto-deposition of ^{210}Po onto Ag discs following a double acid (aqua regia and 6M HCl) leaching of the sediment sample. The addition of ^{209}Po as a "spike" was used as an internal standard during counting and analysis (See Appendix III for full methodology).

Supported ^{210}Pb activity was estimated using the value of constant total ^{210}Pb activity with depth. Without further radiometric analyses (i.e. the direct measurement of ^{226}Ra for example) the determination of the supported activity by this method is only an estimation. Unsupported ^{210}Pb activity was determined by subtracting total ^{210}Pb activity values by the estimated supported ^{210}Pb activity value. A minimum and maximum range of supported activity at depth was calculated by determining respectively:

- Min supported ^{210}Pb activity = STDEV- mean of activity totals above and below the interval of estimated supported activity at depth.
- Max supported ^{210}Pb activity = STDEV + mean of activity totals above and below the interval of estimated supported activity at depth.

Maximum and minimum unsupported values using these values were used in calculating the error bars for subsequent age depth calculations, using the ^{210}Pb dating models discussed in Chapter 2.

5.3 Loss on ignition analysis

An approximate measure of the organic and carbonate content in the cores was determined by loss on ignition (LOI) analysis. The procedure used for the analysis is shown in Appendix V. Oven-dried and powdered sediment samples extracted from the core at consecutive 1 or 2 cm intervals, were combusted in a ventilated furnace for 2 hours at 550°C and 12 hours at 850°C. Crucibles containing the samples were weighed prior to combustion and afterwards, once cooled in a moisture-free environment. A discussion of problems generated by this simple method and the quality of results obtained is given in a previous chapter (Chapter 2).

5.4 Major and trace element analysis

Major and trace element concentrations were determined using X-ray fluorescence on a Phillips PW1400 sequential X-ray spectrometer system under the supervision of Dr. I.W. Croudace from the Geosciences Advisory unit at the Southampton Oceanography Centre. Major elements were determined by a fused glass bead of sample and flux while trace elements were determined on a powdered and pressed sample of dried sediment. Sample preparation for trace and major elements are detailed in Appendix IV. Major element abundances are given as percentage abundance (%) of ashed sample. For major elements the precision by this procedure is nominally 1 % r.s.d. (relative standard deviation) while for trace elements it is 5 % r.s.d. A standard basalt powder sample was used for each

sample run as a control. Geochemical data for the cores was obtained using the same procedures as Cundy (1994). Major element abundance data was put into a Tilia (Grimm, 1991) spreadsheet, where chemostratigraphic zones were determined using the CONISS total sum of squares function for core zonation.

Trace element fluxes (see Section 6.1.13) were calculated for AMC using the following method:

$$TMf = \rho \times TMc \times Sacc$$

where:

Tmf = Trace element flux (mg/μg cm^2 a^{-1})

ρ = density of sediment horizon

TMc = measured trace element concentration (mg/μg)

Sacc = sediment accumulation rate (cm a^{-1})

Sediment accumulation rates used were at a higher resolution than those used for calculated trace element fluxes depicted in Cundy *et al.* (1998).

5.5 Pollen analysis

Samples were collected to determine the pollen content of recognisable sediment horizons and across boundaries within the cored sequences. Palynomorphs from the sediment samples were extracted using standard techniques (e.g. Moore *et al.* 1990), involving the removal of carbonate material by HCl, siliceous mineral matter by hydrofluoric acid and organic matter (cellulose) by acetolsyis and glacial acetic acid (See Appendix II).

As a consequence of the fine-grained mineral content of the cores, an extra procedure involving the washing of the sediment sample with sodium pyrophosphate (e.g. Bates et al. 1978) was used. Even with repeated washes by both HF and sodium pyrophosphate treatments the final slides often contained much minerogenic material. Fine sieving of the samples (10μm) was not carried out during sample preparation, which would have removed much of coarser material. *Lycopodium* spore tablets were added to the sediment samples (e.g. Stockmarr, 1971) to provide an estimate of absolute pollen concentrations (grains g^{-1}). Pollen concentrations per gram of dried sample were used instead of volumetric measures (g cm^3), due to the textural differences encountered in the cores (e.g. high shell content and muds containing coarse clastics). Pollen percentages were calculated by the formula:

$$p\% = (n/N) \times 100$$

where p% is percentage value; n is the count for an identified pollen type; and N is total count. For the study, N was taken to include all terrestrial pollen (arboreal and non-arboreal) taxa encountered. Aquatics and spores were not included in the total pollen sum.

Pollen concentrations (Pc) were determined as per dried sample mass:

$$Pc = \frac{(LYa / LYc * Pn)}{Sm}$$

where:

LYa = number of exotic grains added (one tablet containing approx. 10000 spores)
LYc = number of exotic grains counted
Pn = number of pollen grains counted
Sm = mass of dried sample used (g)

The exotic marker method and sediment accumulation rates determined by ^{210}Pb dating, enables the rate of pollen accumulation (Pa) to be calculated for the sample interval (e.g. Wang & Geurts, 1993):

$$Pa = Sacc/Pc^{c}$$

where:

Pa = pollen accumulation rate (grains cm^{-2} a^{-1})
Pc^{c} = pollen concentration (grains per cm^{-3} of sample)*
Sacc = sediment accumulation rate (time taken for 1 cm depth to accumulate)

*note the volumetric concentration of pollen in samples from PPA and PPB was determined by an estimated density (2.65 g cm^{3}) of sample and the already known sediment mass.

Pollen assemblages were examined using a Zeiss optical microscope at x400 and x 1000 magnification when necessary. Lower magnification was used for scanning the often sparsely concentrated slides. Pollen grain identification followed Moore *et al.* (1991) and a limited reference slide collection.

Pollen totals for each slide were almost entirely dominated by the super-abundance of Amaranthaceae-Chenopodiaceae pollen, only being replaced by Lactuceae pollen in a few sample intervals. Lactuceae is used in this study to include pollen types of the Asteraceae-Cichoridaeae family.

The abundance of Amaranthaceae-Chenopodiaceae and Lactuceae pollen led to lengthy counts (over 500 grains per slide) to identify less-well represented pollen types and to cover the diversity of pollen taxa in the sample. Consequently the relative abundance of these types were often dwarfed by the two to three main types. All the three types of pollen data presentation (relative abundance, pollen concentration and pollen accumulation rates) were used in the interpretation of depositional changes recognised in the core. In core AMC however due to low total pollen counts (< 100) only concentration and accumulation data was used for analysis and interpretation. In PPA and PPB where pollen totals for intervals were below 200 TP, the intervals were removed from the CONISS and percentage calculations.

Pollen data was initially entered into the Tilia program (Grimm, 1991) and attached statistical package (CONISS) to construct pollen diagrams and zone the reliable pollen data into Local Pollen Assemblage Zones (LPAZs). Other statistical analyses, for example the calculation of pollen concentrations and accumulation rates were determined on Excel™ spreadsheets.

In this study the term local pollen is used only in terms of vegetation once presumably found previously or currently above the core site, e.g. Amaranthaceae-Chenopodiaceae. Due to the estuarine and lagoonal nature of the core sites and the proximity of often ecologically-different plant communities at variable distances, "extra local" is used to describe pollen derived from plants in the vicinity or similar communities adjoined, for example by the same lagoon/estuarine system. A problem here occurs as for example at the northern margin of Pantano Piccolo, where ecologically diverse communities (halophytic community adjacent to ruderal species) occur within 1 m distance of each other.

Regional pollen is used to describe those types clearly derived from communities observed to be distant from the wetland area, e.g. *Pinus* and *Alnus* pollen grains were encountered in abundance within Pantano Piccolo sediments and nearby soils, even though trees were absent.

Chapter Six

RESULTS FROM MULTI-PROXY ANALYSES OF COASTAL WETLAND SEDIMENTS FROM SOUTH-EAST SICILY

6.1 RESULTS FROM THE MULINELLO ESTUARY

6.1.1 Site description

The River Mulinello (Fig. 6.1.) has its source approximately 15 km inland of Augusta Bay in Mid-Upper Pliocene-Pleistocene volcanic sequences, draining a catchment of Pliocene-Pleistocene limestone and sandstone sequences, deposited during successive Tertiary and Quaternary sea level high stands (Grasso & Lentini, 1982). Incision and erosion during phases of lower sea level and continued tectonic uplift has exposed older Miocene (Etnean) volcanic and limestone sequences along with later Quaternary alluvial materials (Fig. 6.1.1) (Bordonaro *et al.* 1984; Lentini, 1987). Transgressive sea level in the early Holocene and the subsequent highstand at *circa* 6 ka BP is likely to have initiated estuarine conditions in the embayment. Later Holocene deposition and the infilling of the sheltered embayment is likely to have occurred due to catchment erosion and the transport of alluvial materials into the microtidal coastline. As discussed in Chapter 4, the embayment is likely to have been greatly infilled during the last 1000 years, most recently as a consequence of expansive agriculture and soil erosion in the catchment during the last few centuries. The present day remains of salinas abandoned *circa* AD 1940-50 due to the expansion of larger scale operations in the west of the island (Naval Intelligence Division, 1945), are obvious features in the wetland landscape (Fig. 6.1.2, Plate 6.1.). The estuarine-wetland embayment (approx. 1.5 km^2) may also have been disturbed, previous to commercial salt production (late 19th to mid-20th century AD) in the past by smaller-scale salt panning operations, e.g. by the local community.

Its current condition is typical of many low lying coastal areas in south east Sicily and the Mediterranean, having experienced land use in the past (e.g. Basset, 1978; Delano-Smith, 1979) and currently being treated as low-value land, e.g. for refuse dumping on the marsh surface, for goat/cattle grazing and coastal re-development (Plate 6.2). The abandoned salina area to the north of the channel has been extensively landfilled for a new port access road and container storage depot for the expanding Augusta Bay harbour.

As well as local anthropogenic disturbance, the wetland/estuary is situated within the major petrochemical-industrial zone stretching between Augusta-Syracuse. Water quality within Augusta Bay enclosed by the Monte Tauro headland (Fig. 6.1) and harbour breakwater has shown signs of contamination from urban, shipping and industrial runoff (Magazzu *et al.* 1990) with elevated heavy metal concentrations recorded in marine organisms (Castagna *et al.* 1985). Elevated concentrations of chlorophyll-a in near shore

Figure 6.1. Location map of the River Mulinello Estuary

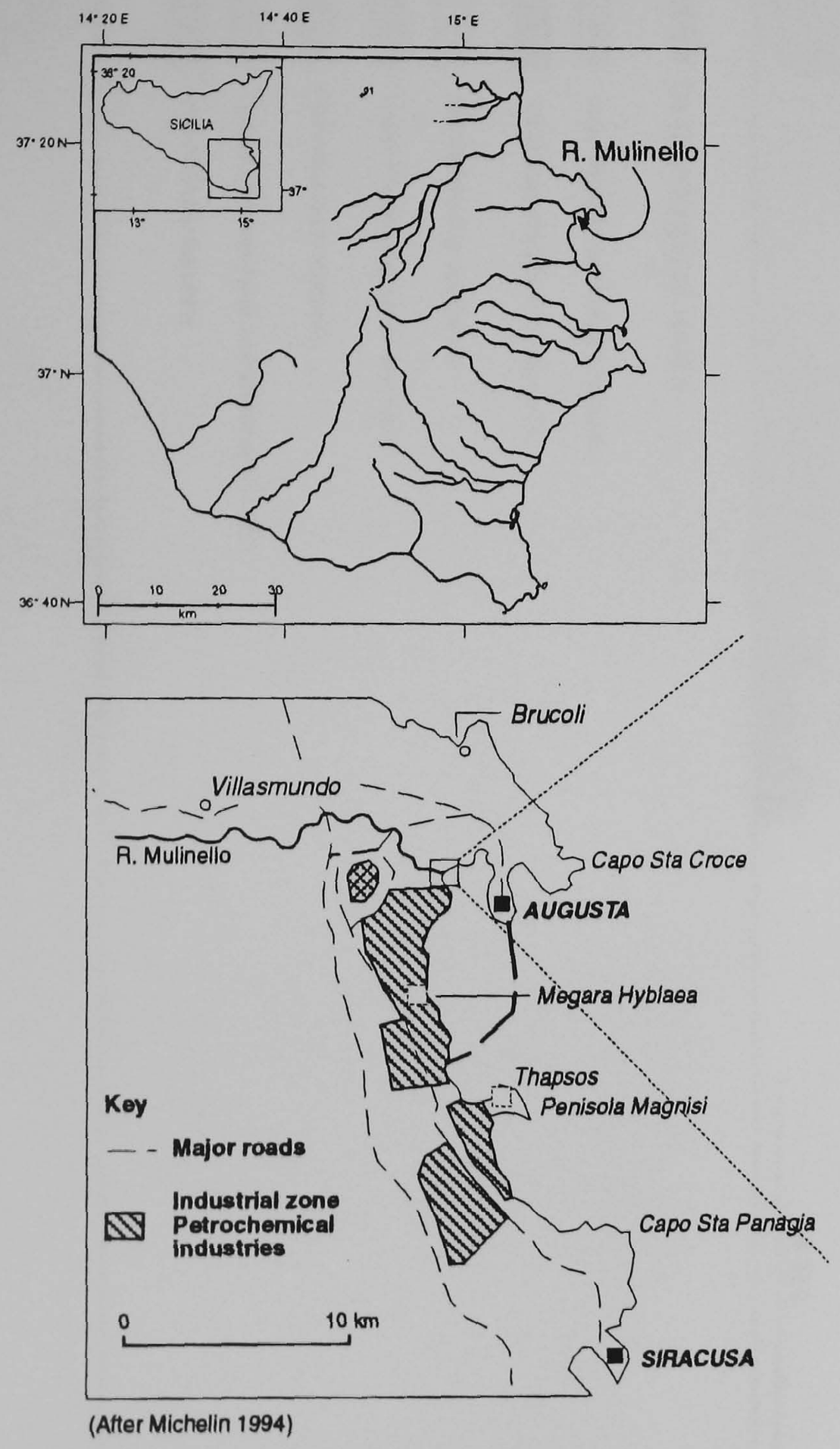

(After Michelin 1994)

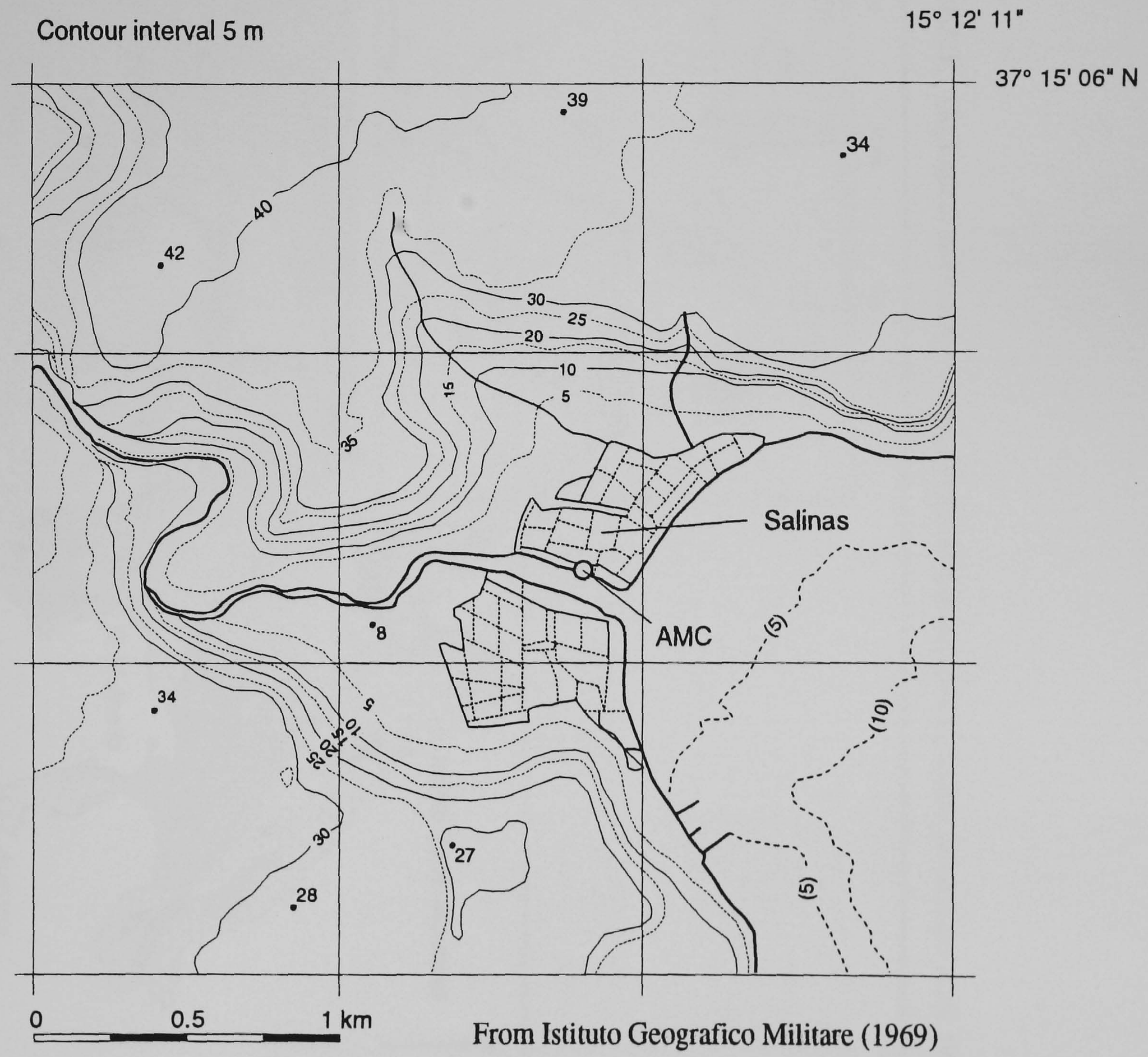

From Istituto Geografico Militare (1969)

Figure 6.1.1. Geological units in the vicinity of the Mulinello estuary (After Bordonaro *et al.* 1984)

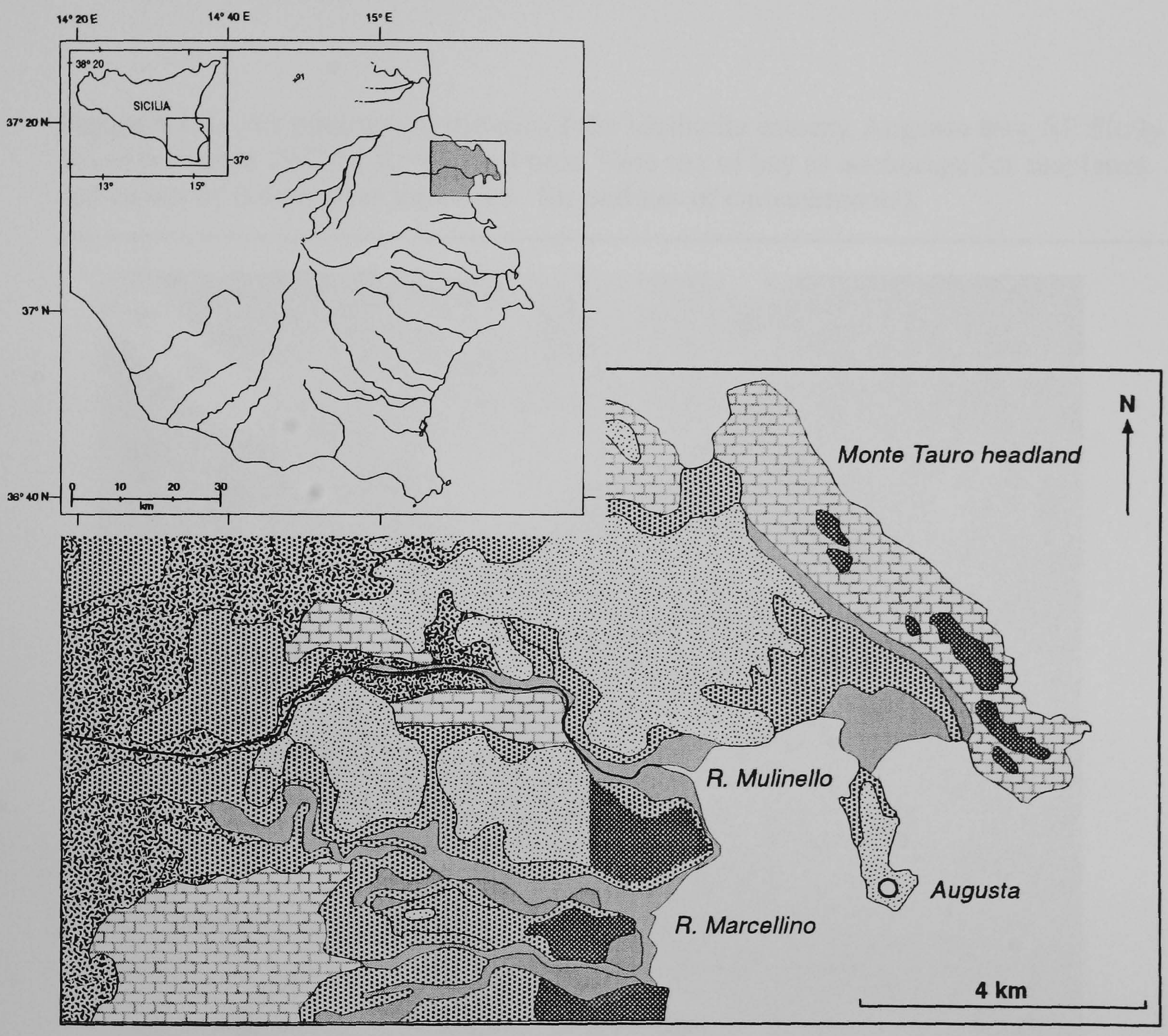

Figure 6.1.2. Air photograph mosaic of the Mulinello estuary, Augusta Bay, SE Sicily Taken 6 August 1942 by Royal Air Force. Note use of bay as anchorage for seaplanes and extent of salinas (See figure 6.1. for outlines of embankments).

□ Core site of AMC

MC River Mulinello channel

Figure 6.1.3. Topography of River Mulinello Estuary and locations of cores AMC and A1-3

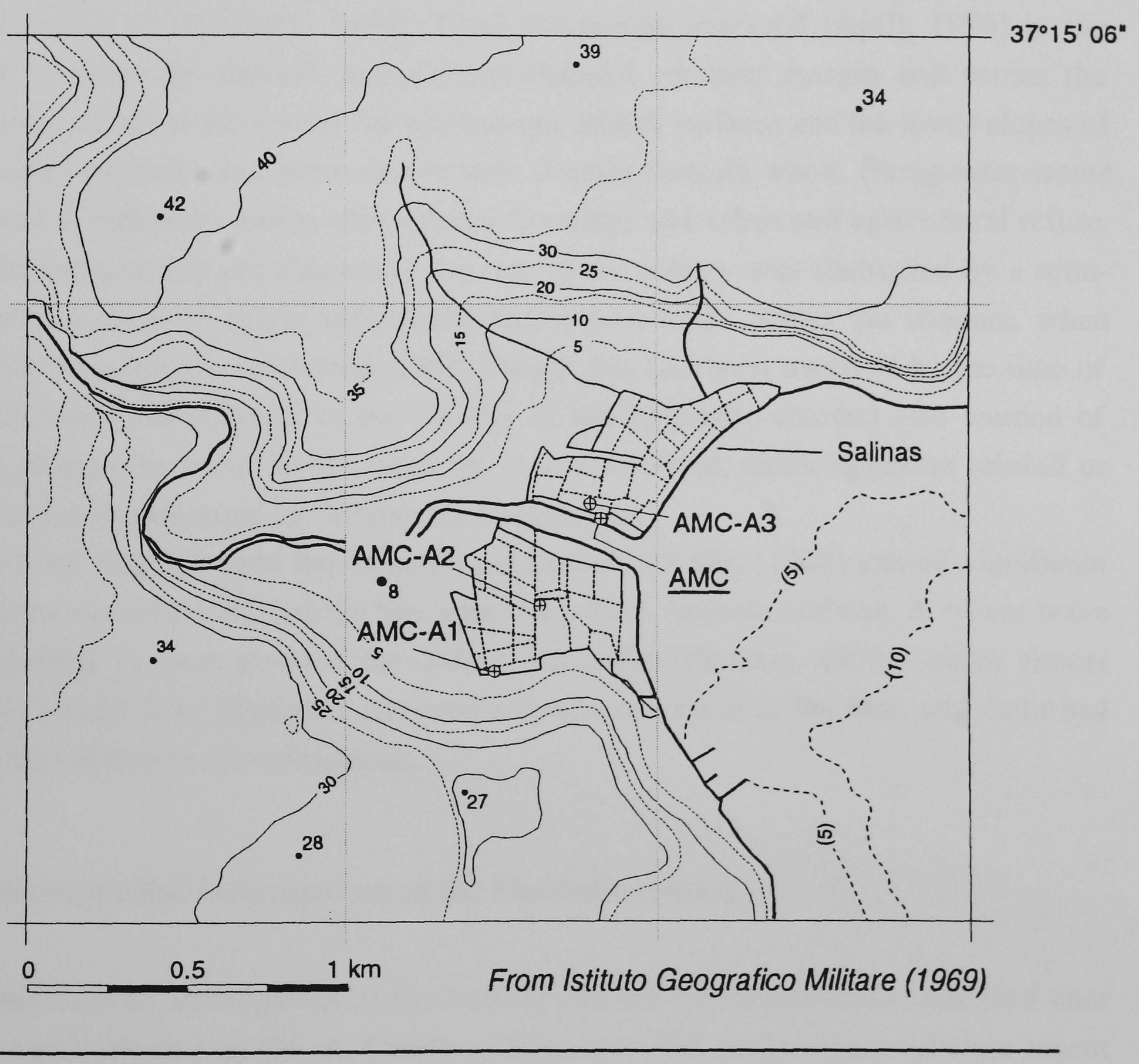

From Istituto Geografico Militare (1969)

waters also indicate an increased nutrient loading from urban and agricultural run-off (Khorram *et al.* 1991). Agriculture in the catchment of the Mulinello largely comprises citrus and olive plantations and intensively-cultivated market produce, which is likely not only to have required regular applications of pesticides and other agricultural chemicals in the past but to have altered the upstream hydrological regime.

Saltmarsh vegetation is established around the scattered remains of salinas, fringing the embanked estuarine channel of the Mulinello river (15°15'E 37°15'N; Fig. 6.1.) as it enters into the north-west corner of Augusta Bay. The mean tidal range in the area (based on tide gauge records at Catania 30 km N) is less than 30 cm (0.3 m springs, 0.1 neaps) (Hydrographer or the Navy, 1996). Tidal action was observed (April, 1998) in the locality to flood the narrow, halophyte-dominated, channel margin and across the abandoned salinas to the rear of the embayment. Marsh surfaces and the lower slopes of the channel embankments were strewn with flotsam (mainly wood, *Phragmites*-stems and plastics, reflecting recent alluvial/tidal flooding) and urban and agricultural refuse. The tidal influence in the channel to the rear of the estuary was obstructed by a semi-permeable barrage to allow agricultural traffic/goat herds across the channel, when fieldwork was initially conducted (1994) though this had been removed by the time of the final visit (1998). Signs in the vicinity of the Mulinello channel also warned of sudden changes in water level caused by, it was surmised, either upstream rainfall or bore-like waves generated by shipping in Augusta bay.
The tsunami that followed the Messina earthquake (28 Dec. 1908) caused significant water level variations around the bay area and within Augusta harbour. A 60 cm wave was reported to have flooded the *Salina Mulinello* (Platania, 1909), which almost certainly would have disrupted salt production in operation at the time and disturbed microtidal habitats in the embayment.

6.1.2 Stratigraphic investigations at the Mulinello estuary.

Sedimentological investigation at the locality and the collection of the analysed core AMC, was instigated by Dr. A. Cundy in February 1995 to determine whether recent contaminant records were preserved in these sediments (Cundy *et al.* 1998). On subsequent visits a number of additional cores were taken (December 1995, April 1998) in the vicinity of core site (AMC) and within the abandoned salinas area (Fig. 6.1.3). The aim of this was to provide a stratigraphic background to the high-resolution analyses conducted on AMC as well as exploring the potential of longer-term records existing within the Mulinello embayment. Core site locations were identifiable from air photographs (Figure 6.1.2.) and a 1:25000 map (Istituto Geografico Militare, 1969)

Table 6.1. Marsh sediment sequences determined at the Mulinello estuary, Augusta, SE Sicily

Core Site	*Core units (cm)*		*Unit description*	*Other core features*	
AMC-A1	00-05	G	Grey sand-silt. Coarse sand and *Betium* sp. gastropods		
	05-145	F	Dark brown mud. Dispersed shell material (*Hydrobia*).	81-84 118-119	sand layer sand layer
	145-195	E	Grey muddy sand. Fe-staining and shell fragments	164-166	sand layer
	193-220	D	Coarse shelly sand	193-204 204-209 209-220	sand layer grey clay shelly sand
	220-239	C	d.brown-black sand-silt and shell fragments		
	239-300	B	black shelly clay		
	300-310	A	blue-grey clay, grading into light brown.		

Core Site	*Core units (cm)*		*Unit description*	*Core features*	
AMC-A2	00-25	I	Black organic, fine silty clay	22-25	light grey clay
	25-51	H	Dark brown silty clay		
	51-150	G	Black-d.brown silty clay	60 72 120	shell horizon shell horizon shell horizon
	150-190	F	Brown-grey Fe-stained silty clay	162-165	sand horizon
	190-250	E	Grey silty mud	200-203 230-204	shell horizon reed stem
	250-300	D	Shell-rich sand*		
	300-365	C	Shell-rich grey silty mud		
	365-425	B	Coarse shelly sand	400	rounded pebbles
	425-432	A	Fine grained sand-silt and clay	425 428	grey silt sea-grass ball

depicting the layout of the salina embankments. Core sites were levelled into temporary bench marks relating to an assumed high-tide mark, providing an approximate sea level. Flotsam representing the most recent high-tide strandline was used, so measurements above sea level given here are only relative, due to neap-spring variation and wind-forcing effects in the bay-area. Access was restricted to the north of the Mulinello channel by recent port developments and so investigations were conducted in the area south of the Mulinello channel and the channel margins (Plates 6.2. & 6.3).

6.1.3 Mulinello Estuary: Core AMC-A1

Core AMC-A1 was extracted (29.04.98) in the south west corner of the Mulinello embayment, 10 m from the break of the surrounding slopes and adjacent to the rough grazing fields that adjoin the abandoned salinas. At the rear of the wetland area, the mud surface of the core site was covered by the incoming tide to a depth of a few centimetres during coring. A 3 metre sequence of sediments was recovered from the site using a wide (60 mm) open-chamber gouge (Table 6.1.). The sequence consisted within the upper 1.5 m, of grey silty clay, becoming increasingly dark brown and resistant to core penetration below 120 cm. Sand layers within the predominantly fine-grained sediments were observed at 84-81 cm and 119-118 cm. At 145 cm, this dark brown silty-clay was replaced by a dark grey-Fe mottled clay overlying a coarse, uncemented shelly grit which appeared at 195 cm. Hindered by this water saturated material, gouge collection was restricted until stiff, light blue-grey clay was encountered at 295 cm depth. The resistance of this compact basal clay to penetration and collection in the gouge, prevented further coring below 310 cm.

6.1.4 Mulinello Estuary: Core AMC-A2

The core site was situated in the centre of the abandoned salinas, approximately halfway between the Mulinello channel and surrounding embayment slopes (Fig. 6.1.3.). Coring took place (29.04.98) at the vegetated margin of one of the salinas. During coring, the tidal range and connection to the Mulinello channel/Augusta Bay was evident in the surrounding salinas, with water level increasing during core extraction, covering the core area finally to a depth of 15 cm. The core sequence comprised of dark organic mud and silts in the surface down to approximately 150 cm below the surface, followed by brown-grey silty clay with shells, organic material and sand horizons, overlying uncemented shelly marine sands and black organic mud (430 cm below the marsh surface). The blue-grey clay unit at the base of AMC-1 at the rear of marsh was not encountered.

The variety and depth of sediments found at the Mulinello estuary in cores AMC-A1 & AMC-A2, supports at least the primary assumption that significant sedimentation has occurred within the embayment. The depth of sediments extracted and stratigraphic changes encountered indicate a significant period of sediment supply and net deposition, within a predominantly low energy coastal environment. Shell-rich (*Cardium* sp.) sands at depth (containing marine organic remains, i.e. a wave rounded *Posidonia oceania* (sea-grass) accumulation), with organic mud and silts within the upper 1.5-2 m of the cores, suggests that the embayment has shifted in the past from more open to enclosed conditions most likely as a result of increased catchment-derived materials and restriction of the Mulinello river mouth (and subsequent lagoon-wetland formation). The fine-grained deposits encountered at depth indicate low energy estuarine-wetland conditions, interspersed with possibly higher energy deposits, e.g. coarse shell-rich sands (AMC-A1 unit D and AMC-A2 unit F). During the infilling of the embayment, the configuration of the Mulinello channel and bay-edge of alluvial-estuarine deposits can be expected to have moved over space and time, constructing the suite of channel, barrier (shell-rich sands) and more sheltered environments (organic mud). Shell horizons, e.g. between 50 and 150 cm depth in AMC-A2 (Table 6.1) may represent either short periods time conducive to expanding populations of sediment fauna (e.g. Tagliapietra *et al.*, 1998) or higher energy conditions which transported the larger bioclasts, while winnowing finer materials.

The absence of the blue-grey clay unit A (estuarine-mudflat) encountered at AMC-A1 and greater depth of sediment in the centre of the embayment found at AMC-A2, suggests that either the unit shelves towards the centre at a shallow gradient or has been eroded by channel activity/marine erosion. A more detailed stratigraphic and palaeoenvironmental investigation of the deposited sediments in the embayment was not conducted, due to the logistics of analysing multiple long cores in the time given and focus of this research on identifying recent environmental changes.

Although in the historical past the embayment has been greatly affected by salinas and continuing industrialisation, this surficial disturbance clearly overlies records of Holocene environmental change and deposition at the margin of Augusta Bay.

6.1.5 Channel-side accretion in the vicinity of core site AMC

On a levelled transect, using a narrow (3 cm) open-chamber gouge for greater penetration, a channel-perpendicular stratigraphy was carried out at the AMC core site. The local site stratigraphy and lithology is shown in Figure 6.1.4. and individual core descriptions (see below and Appendix VI). Stratigraphic boundaries identified by Cundy *et al.* (1998) and other units were recognisable in the nearby sediments from cores along

Figure 6.1.4 Channel margin stratigraphy and core locations at the Mulinello estuary, Augusta Bay, SE Sicily

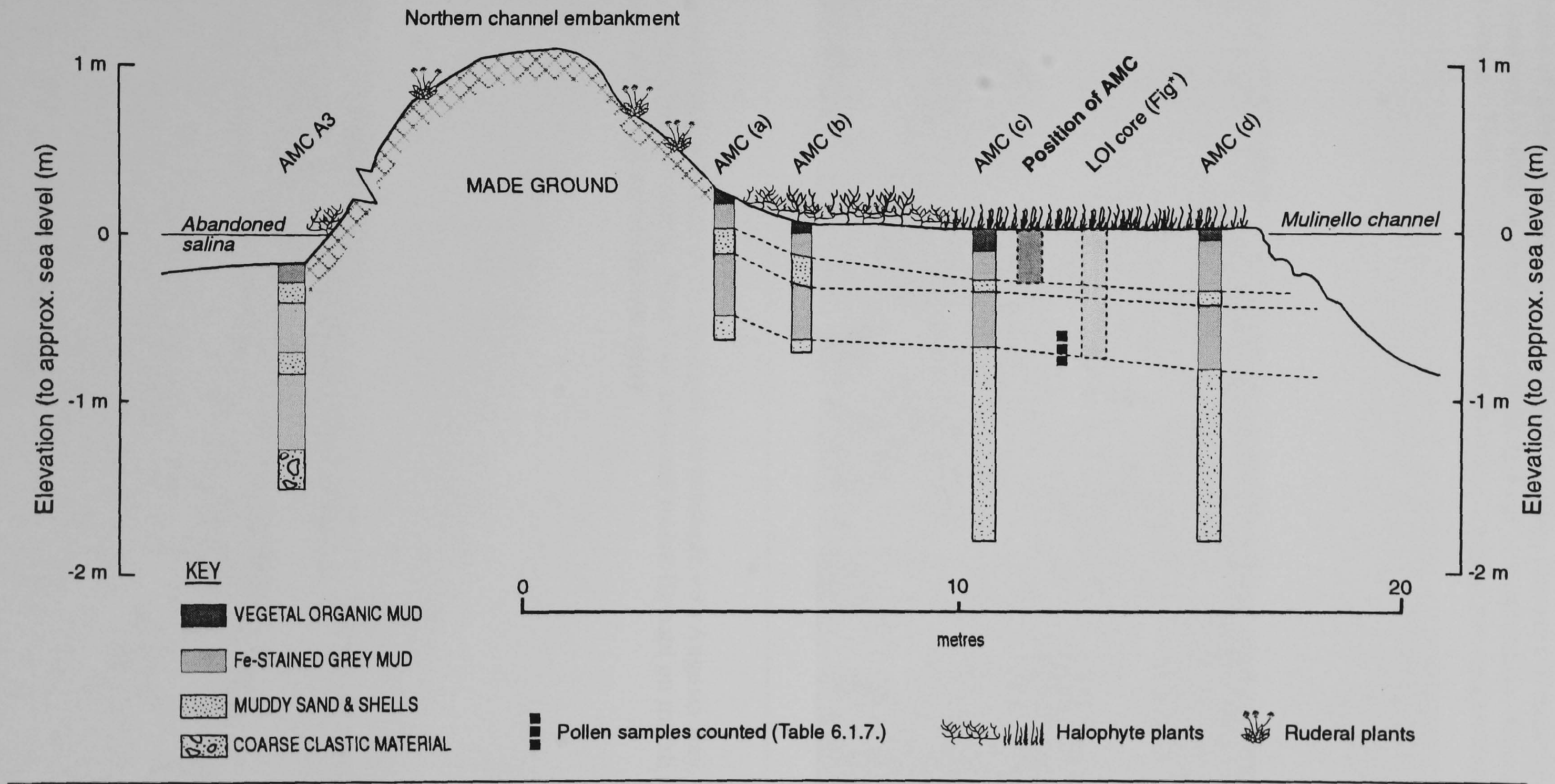

Plate 6.1. Remains of salina workings at the Mulinello estuary. Remains of rotary pumps to assist in the transport of water around pan network and aid in evaporation. View north from Mulinello channel. Note halophyte plant communities fringing pan embankments

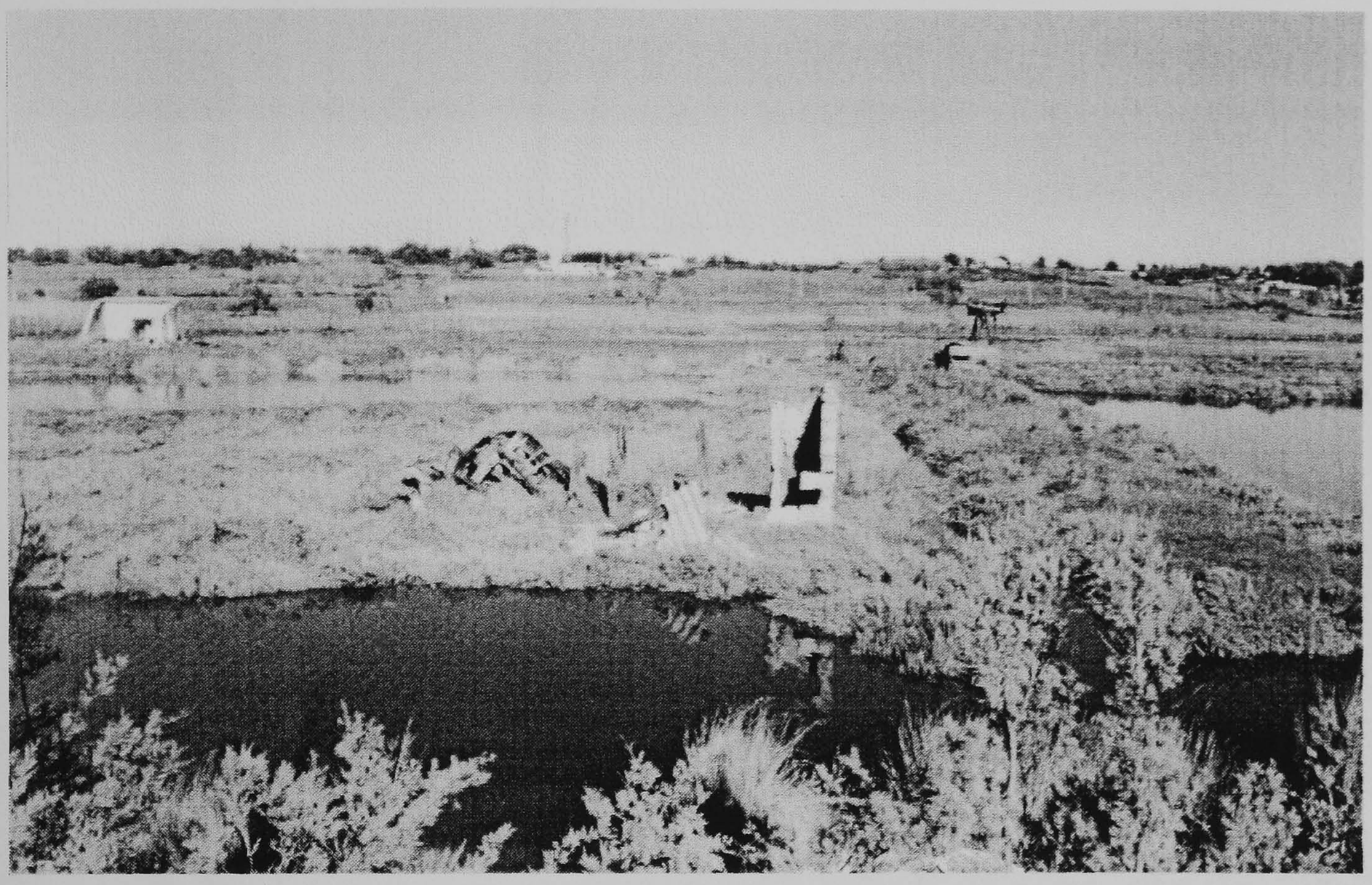

Plate 6.2. View east from north bank of the Mulinello river mouth into Augusta Bay. Salt marsh occupying channel margin. Note bare areas and recent flotsam on marsh surface. Modern port development and embankments (left)

Plate 6.3 Mulinello AMC core site (A) at northern margin of estuary channel. Photograph taken December 1995 looking west upstream. New road constructed for port development visible top right.

the transect (Fig. 6.1.4.). The core transect revealed that recent mud form a relatively thin horizon (<1 m) unconformably overlying water saturated, coarse shelly sand. A muddy-sand and shell-rich horizon divided the surface mud into upper (of which core AMC represents) and lower components.

Core retrieval below 70-80 cm near the core sampling site was prevented by water saturated shelly sand and so in comparison to cores AMC-A1 and AMC-A2, older sediments were not recoverable for examination at the site. An attempt at coring was halted at AMC-3 (Fig. 6.1.4.) (continuing on a transect vector from AMC-A1-AMC-A2) within the disused salinas by a considerable presence of rubble which appeared to be a remnant of an earlier construction, or hardcore dumped in the past for channel stabilisation to protect the area from flood damage.

The spatial extent of the intercalated mud and shelly-sands between the channel margin and the constructed embankment indicate at least two episodes of fine-grained accretion; that leading up to the present day on top of a thin shelly-sand and at depth with muddy-silt resting unconformably on top of a thicker unit (at least 1 m) of coarse shelly sand (Fig. 6.1.4.). As the embankment proved impenetrable to coring, it was difficult to determine which came first: the construction of the embankment or the fine-grained deposits ?

Outside of the area used for the industrial salinas at the unprotected channel margin, the site-stratigraphy suggests deposition has occurred at the site as a response to subsequent catchment/channel/estuarine processes rather than disturbance due to salina operations. It is also apparent that the core collected (AMC) is temporally and spatially representative of only the most recent sedimentation at the channel margin and of the Mulinello embayment.

6.1.6 AMC Core sedimentology

The principally fine-grained core sediments exhibited a clear stratification (Table 6.1.2.). Fe-oxy-hydroxide mottling was visible in the core associated with fine roots from the surface vegetation. The core was marked by significant darkening due to organic materials, especially between 14 and 4.5 cm depth, where black, oily streaks where also visible. Surface sediments were visibly organic, incorporating mollusca species typical of muddy saline-estuarine habitats e.g. *Hydrobia* sp. and *Bittium* sp. Within the sequence there was no clear evidence of abrupt depositional change, e.g. sand layers due to flooding/tsunami or rubble which may have been associated with embankment construction. The recent age of the sediments was indicated by the presence of plastic pellets (3-4 mm diameter) within a black organic layer at 7.5 cm.

6.1.5. Core description: AMC

The 30 cm core was subdivided into four stratigraphic horizons

	Depth (cm)	Sediment description
AMC-A	30 - 14	Dark brown/grey silt-clay with distinct Fe-oxyhydroxide mottling. Darker grey colouration observed from 25 cm down to the base of the core (sub-unit A1). Shell-rich, water saturated sand at base.
AMC-B	14 - 4.5	Dark brown silty clay with interspersed black, organic-rich layers.
AMC-C	4.5 - 2.5	Brown/grey silty clay mottled by distinct red/brown Fe-colouration. Fine roots from surface vegetation.
AMC-D	0 - 2.5	Surface humic peat comprising of roots and surface litter derived from *Sueda maritima* (L.) Dumort and *Atriplex portulacoides* (L.).The marsh surface was littered with *Hydrobia* sp. and conicular gastropod (*Bittium* sp.) shells, which also had been incorporated in unit D. Other surface materials included organic (driftwood, fragments of riparian vegetation) and inorganic (plastics) flotsam.

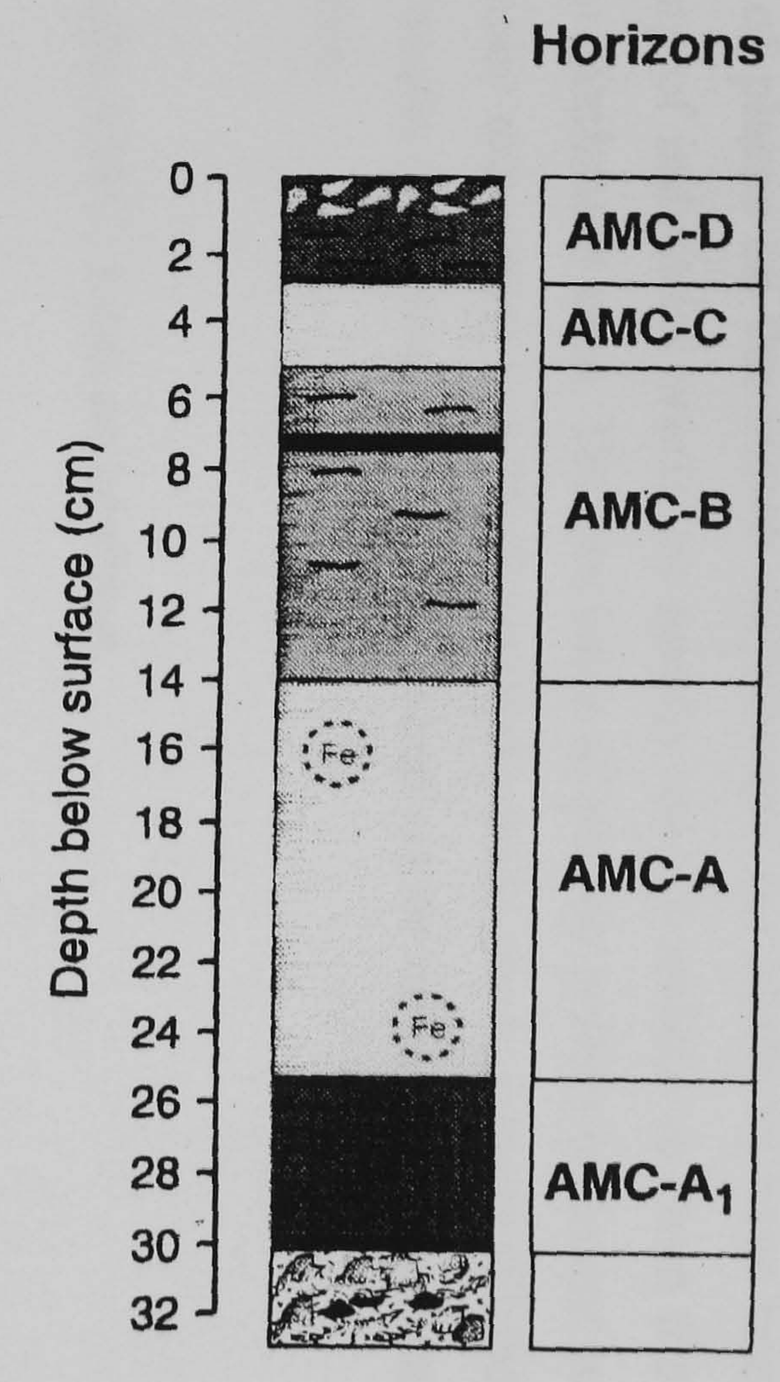

Beads of plastic (i.e. those used in packaging/plastic-injection moulding) were also found in a number of places on the marsh surface and are likely to have been derived from either dumping of industrial waste on nearby marsh surface or from the wider Augusta bay/Mulinello catchment area. The presence of plastic pellets in recent sediments (along with other plastic materials) is a Mediterranean-wide phenomenon (Shiber, 1982; Shiber 1987) symptomatic of industrial production and waste refuse in the coastal zone over the last few decades.

6.1.7 Mulinello AMC: Loss on ignition

Consecutive 1 cm intervals were sampled from AMC for loss on ignition analysis. Loss on ignition values were also determined for an exploratory core (AMC-1) collected during an initial investigative visit to the site (December 1995). Neither of the cores were subject to ignition at 850°C, limiting to some extent the interpretation of the cores by loss on ignition (Fig. 6.2).

LOI values show a marked decline from AMC A1 into AMC-A, declining until 20 cm (8% loss) when values increase to a mid-core peak at 14 cm (20 % loss). This occurs at the stratigraphic boundary (marked by an Fe-brown band) between an Fe-mottled grey silt-clay (AMC-A) and an increasingly darker brown, black-streaked horizon (AMC-B). Sediments with low combustion (8-9 %) values sit directly above this supposed organic horizon.

Combustion values AMC increase again to a broad peak at 8-6 cm. In Cundy *et al.* (1998) a peak at 8 cm depth was calculated at 50% loss. After the analysis of core AMC-1 (below) the combustion of a plastic pellet was assumed to have caused this aberrant peak, rather than being representative of the background sediment matrix. The replacement value of 25% loss at 8 cm, was obtained by plotting a two-point moving average curve on the remaining LOI profile with the 8 cm sample-horizon removed.

Another marked decrease in LOI values is observed between 5-3 cm (16% loss) before values increase in the surface humic and organic sediment of AMC-D.

Although sampled at a lower resolution of every 2 cm, LOI results from core AMC-1 (Fig. 6.2a), are similar to those observed in the upper 30 cm of AMC. The peak in ignition values at 6 cm was marked by the combustion of a plastic pellet left in the sediment matrix to estimate the subsequent loss. Below 30 cm, low LOI values of a grey silty clay (9-10 % loss) are interrupted by a minor ignition peak at 26 cm and more pronounced at 44 cm, before maintaining low values (12 % loss) through the shell-rich clastic material. The contact between silty clay and the basal shell and clastic unit is shown by the decline in combustion values (5-7 % loss) from 76 cm (Fig. 6.2a). Samples

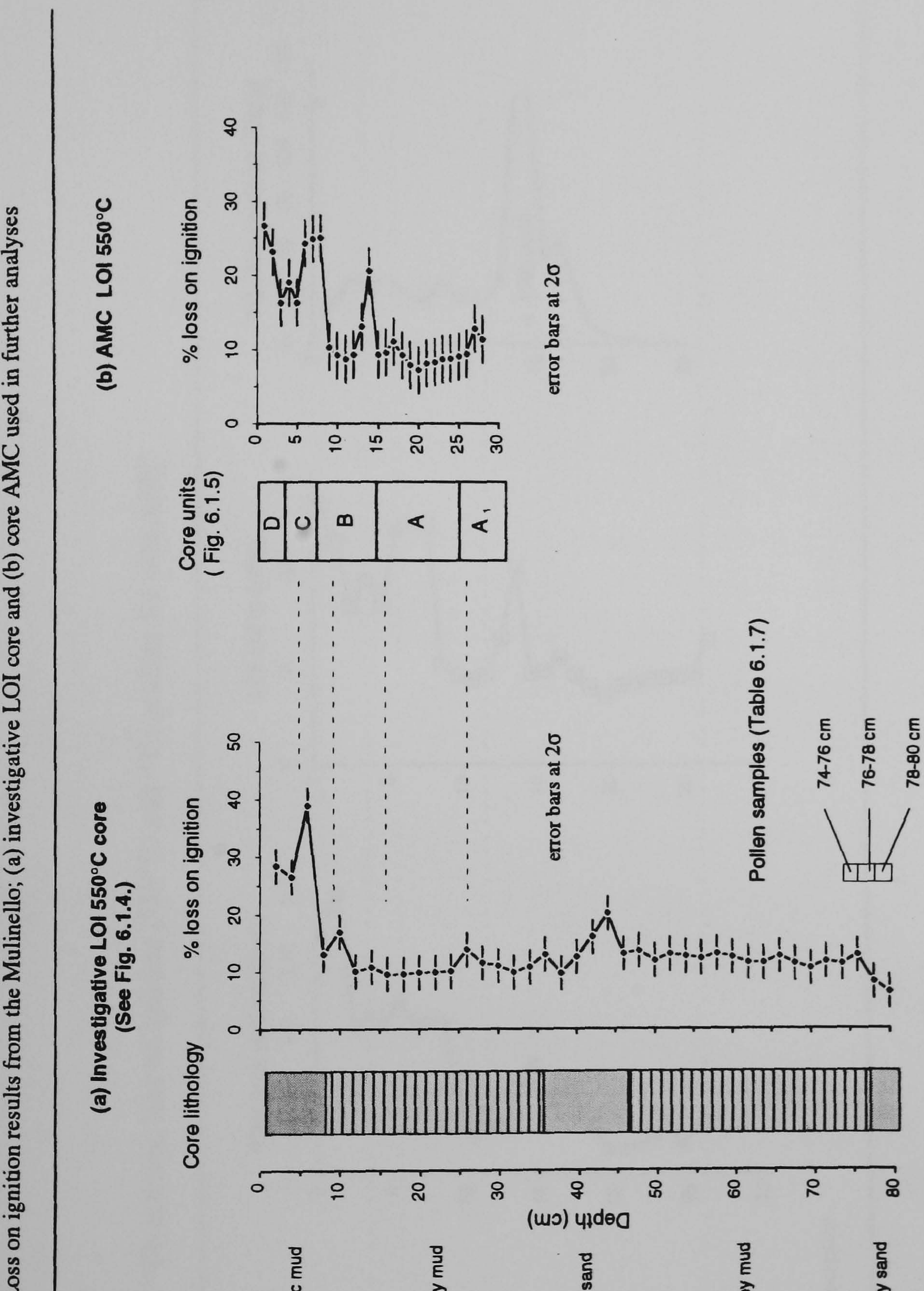

Figure 6.2. Loss on ignition results from the Mulinello; (a) investigative LOI core and (b) core AMC used in further analyses

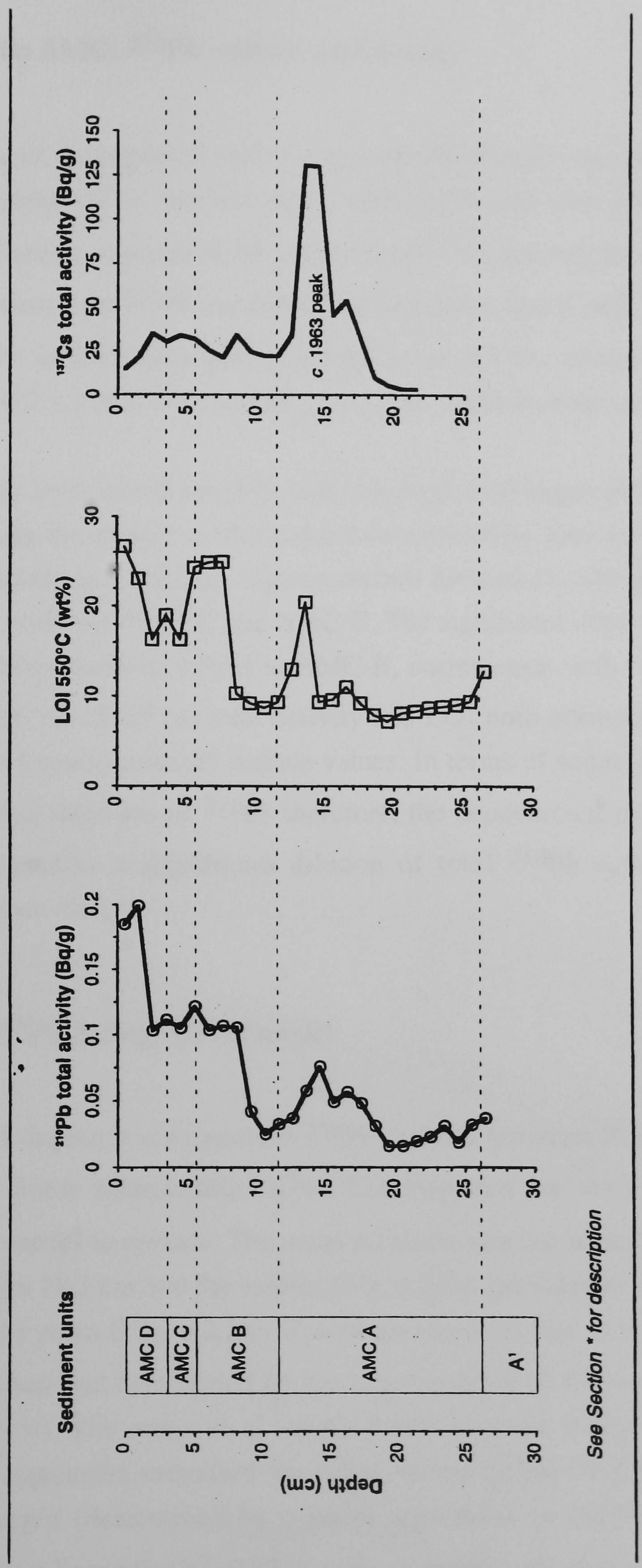

Figure 6.2.1. Total ^{210}Pb activity, loss on ignition (550°C) and ^{137}Cs profiles for core AMC

for pollen were taken across this boundary of channel-sands and estuarine muds (Table 6.1.7.).

6.1.8 Mulinello AMC: ^{210}Pb analysis and dating

The estimation of unsupported activity was calculated at 20 cm depth where total ^{210}Pb activity was observed to increase again with depth into unit AMC-A1, suggesting a change in sediment composition. Measured total ^{210}Pb activity decreases within AMC-A up to 20 cm, when total ^{210}Pb increases and develops a broad peak (14.5 cm). From 10.5 cm total ^{210}Pb activity increases abruptly up to 8.5 cm where it remains relatively constant (Fig. 6.2.1.) until 3-2 cm depth where the highest totals were encountered.

Profile changes correspond suitably with lithological changes observed at depth in the core, specifically the organic matter content determined by loss on ignition (Fig. 6.2.1.). The highest activities reflect the organic surface horizon D, which decline abruptly and remain low in horizons AMC-C and AMC-B. The significant departure between 13 and 8 cm from the fairly uniform values in AMC-B, corresponds with the sudden decrease in organic content. At 15-14 cm total activity and LOI both correlate as a peak, as ^{210}Pb activity makes a return towards surface values. In terms of sequence succession and the expected gradual decrease of ^{210}Pb therefore, the depositional period between ~15 cm and 9 cm represents a significant dilution of total ^{210}Pb activity, coinciding with decreased organic content.

6.1.9 AMC ^{210}Pb dating: CFCS model

The impact of depleted unsupported ^{210}Pb activity between 9 and 15 cm has clearly disrupted the linear relationship (R^2=0.522) required for the constant flux:constant sedimentation model to operate. The mean accretion rate calculated (0.275 cm/a^{-1}) for the interval between 19.5 cm and the surface (Fig. 6.2.2.), provides an approximate timescale over the last 90 years (Fig. 6.2.2b). The mean accretion rate determined by the CF:CS model is less than that determined for the cored interval (0.49 cm/yr^{-1}) by ^{137}Cs dating (described below). The removal of sample points between 9 and 15 cm depth from the CF:CS linear regression increased the effectiveness of the CF:CS model; reducing the 95% error margin (determined by a linear regression in ©SPSS for Windows) and providing a better linear fit (R^2=0.874), without greatly affecting the mean accretion rate (0.293 cm a^{-1}). This operation assumes that the 9-15 cm depth interval of low total

Figure 6.2.2. (a) ^{210}Pb total activity and CF:CS model linear plot of unsupported activity for Augusta-Mulinello AMC; (b) mean accretion rate discrepancy between ^{137}Cs and ^{210}Pb (accretion rates in brackets cm a^{-1})

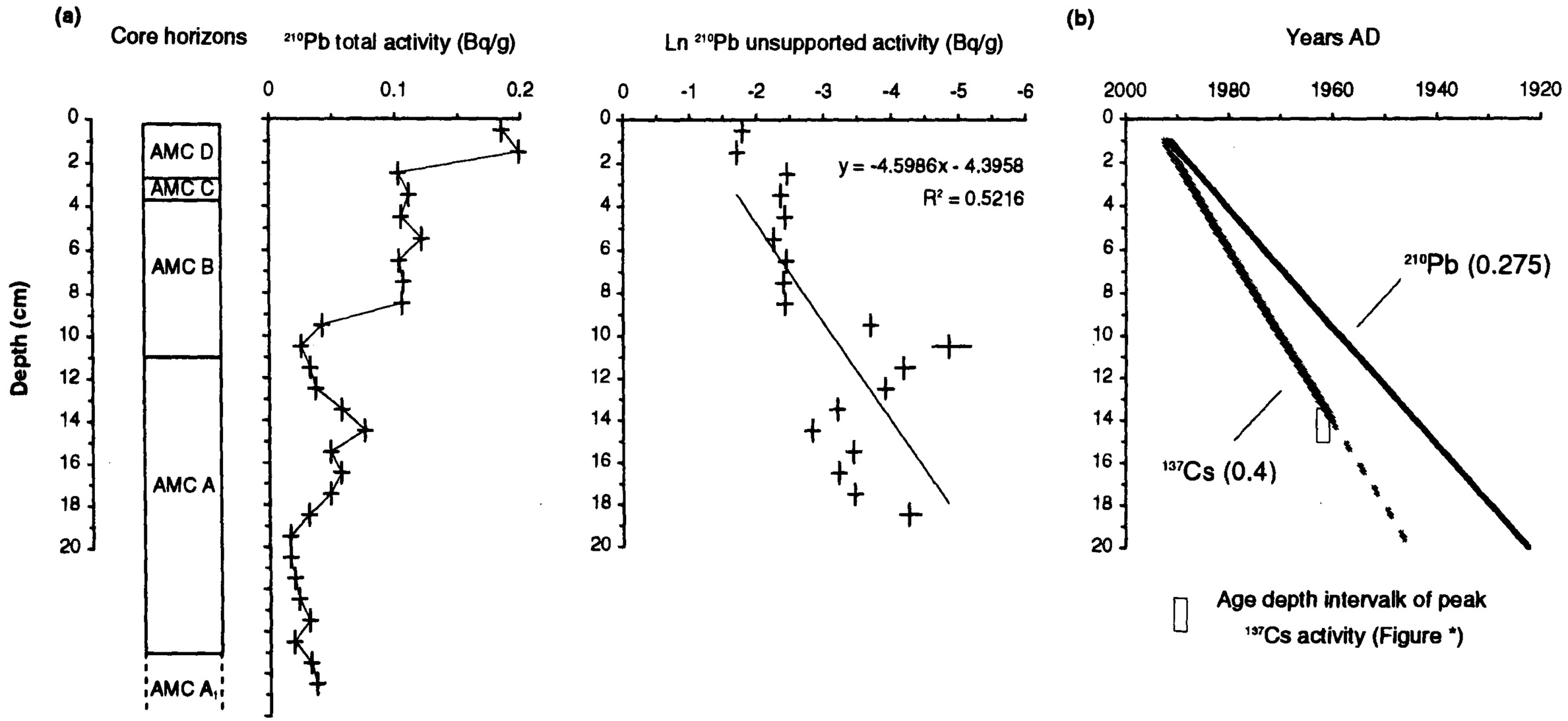

CF:CS model accretion rates (cm a^{-1}) determined by SPSS (95% Confidence linear regression)

Mean	**0.275**	$R^2 = 0.522$
Lower	0.184	
Upper	0.536	

x-axis error bars on CF:CS plot signify calculated maximum and minimum unsupported actvity totals; y-axis error bars indicate depth interval

activity and organic content represents an inwash of "older" materials. As a result, the linear regression calculated this as a non-phase or hiatus in sedimentation. The mean accretion rate determined by the CF:CS model for both scenarios however places the base of this ^{210}Pb depleted interval at 15 cm *circa* AD 1945-1950 (Fig. 6.2.2b).

6.1.10 AMC ^{210}Pb: variations in accretion determined by the CRS dating model

Calculated age depth relationships for core horizons, provided by the constant rate of supply (CRS) model, indicates that sedimentation at the core site has not been constant over the last 130 years. Although the mean accretion rate determined by the CRS model (0.26 cm a^{-1}) is only slightly less (0.27 cm a^{-1}) than the CF:CS model, the gradient of the age-depth curve indicates four successive phases of accretion: between the late 19th century up to *c.* 1940 AD (mean accretion rate 0.07 cm a^{-1}); between *c.* AD 1945 and *c.* AD 1956 (mean 0.39 cm a^{-1}); c. AD 1964 to c. AD 1986 (mean 0.21 cm a^{-1}) and between *c.* 1988 AD up to *c.* 1995 AD (0.39 cm a^{-1}) (Fig. 6.2.3.).

Significantly, the CRS model copes with the core section of low total ^{210}Pb activity (between 8.5 cm and 14.5 cm) by determining the period as one of higher accretion. If rapid accretion caused this change, by diluting the amount of available ^{210}Pbexcess from atmospheric deposition, rather than an inwash of old sediment, the argument for using the CRS model holds (e.g. Kirchner & Ehlers, 1998).

Accretion rates determined between sample intervals, plotted against depth and equivalent age emphasise these core changes (Table 6.1.3). The change between low, pre-20th century sedimentation rates and the highest recorded rate between c. AD 1951 and c. AD 1952 was initiated between 14.5 cm (c. AD 1940) and 13.5 cm (c. AD 1945). Increasing values from 14.5 cm culminate in the peak at 10.5 cm (0.79 cm a^{-1}) in line with the time difference between sample horizons. The rate of accretionary change and time difference between 11.5 cm (c. AD 1951±2) and 10.5 cm (c. AD 1952±2) would suggest a rapid, possibly instantaneous accretion event.

Decreasing soon after (c. 4 years) between 10.5 and 9.5 cm (0.28 cm a^{-1}), lowered accretion rates steadily increase, before abruptly increasing again (0.58 cm a^{-1}) over approximately two years, between 3.5 cm (c. AD 1986) and 2.5 cm (c. AD 1988). Rapid accretionary changes measured over 1 cm may be seen to occur beyond the limit of the error margins of the individual horizons determined by the ^{210}Pb CRS dating model.

Figure 6.2.3. Mulinello AMC ^{210}Pb CRS model Age-depth curves

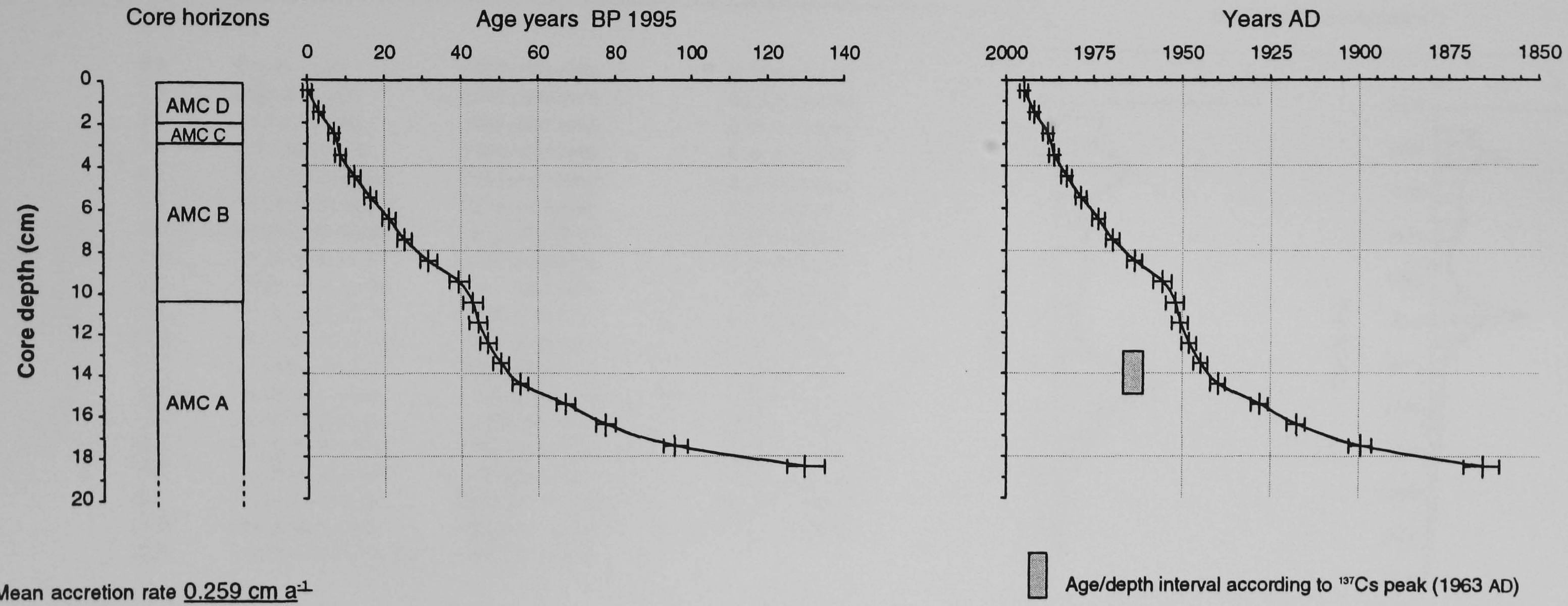

Mean accretion rate 0.259 cm a^{-1}

x error bars signify age range calculated by derived minimum and maximum unsupported activity at depth; y-axis error bars indicate depth interval

Table 6.1.1. Mulinello AMC: ^{210}Pb derived dates and sedimentation rates. Sedimentation rate plotted against core depth and time (Years AD)

Depth (cm)	Age BP	Years AD	Sedimentation rate (cm a^{-1})
0.5	0 (1.25- +1.20)	1995 (1994-1996)	0.34 (0.33-0.35)
1.5	2.95 (4.28-1.67)	1992 (1991-1993)	0.26 (0.25-0.26)
2.5	6.85 (8.30-5.46)	1988 (1987-1990)	0.58 (0.57-0.59)
3.5	8.56 (10.05-7.14)	1986 (1985-1988)	0.28 (0.27-0.28)
4.5	12.16 (13.74-10.65)	1983 (1981-1984)	0.25 (0.24-0.25)
5.5	16.24 (17.93-14.64)	1979 (1977-1980)	0.21 (0.20-0.21)
6.5	21.09 (22.94-19.33)	1974 (1972-1976)	0.24 (0.23-0.25)
7.5	25.20 (27.21-23.32)	1970 (1968-1972)	0.16 (0.15-0.17)
8.5	31.48 (33.75-29.35)	1964 (1961-1966)	0.13 (0.12-0.13)
9.5	39.44 (42.15-36.95)	1956 (1953-1958)	0.28 (0.28-0.27)
10.5	43.06 (45.74-40.59)	1952 (1949-1954)	0.79 (1.01-0.67)
11.5	44.33 (46.74-42.08)	1951 (1948-1953)	0.39 (0.42-0.36)
12.5	46.90 (49.11-44.83)	1948 (1946-1950)	0.30 (0.32-0.29)
13.5	50.18 (52.24-48.24)	1945 (1943-1947)	0.20 (0.20-0.20)
14.5	55.18 (57.30-53.20)	1940 (1938-1942)	0.08 (0.08-0.09)
15.5	66.95 (69.48-64.61)	1928 (1926-1930)	0.10 (0.09-0.10)
16.5	77.38 (80.03-74.94)	1918 (1915-1920)	0.06 (0.05-0.06)
17.5	95.50 (98.80-92.50)	1900 (1896-1903)	0.03 (0.03-0.03)
18.5	129.57 (134.92-124.99)	1865 (1860-1870)	-

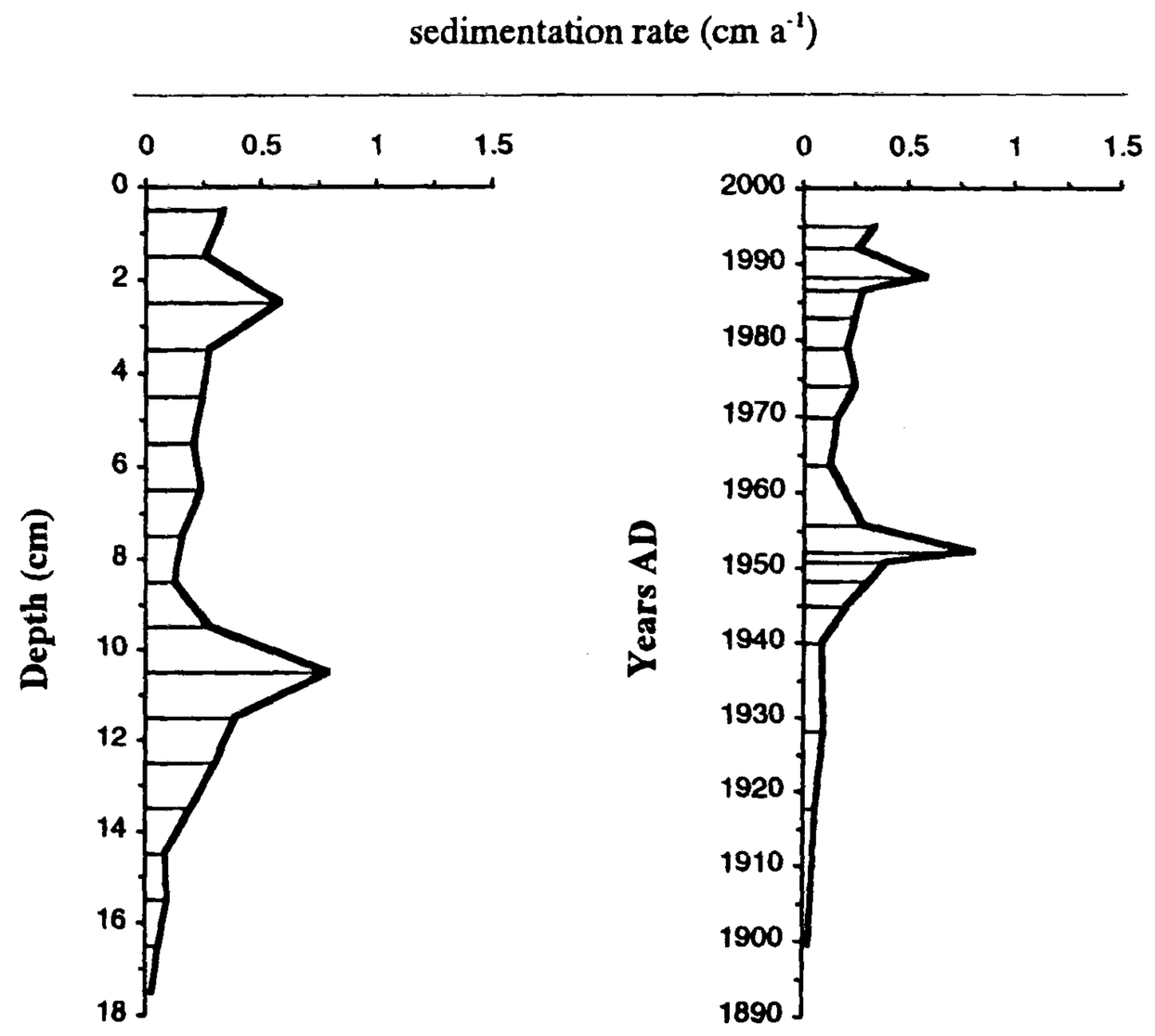

Sedimentation rate calculated between sample interval and one previous in cm a^{-1}

Figures in brackets derived from calculated maximum and minimum unsupported activity

6.1.11 AMC: ^{137}Cs dating

^{137}Cs activity shows a distinct maximum (130 Bq/g) at 13.5-14.5 cm depth (Fig. 6.2.1.). Assuming that this maximum represents the period of peak global atmospheric weapon testing (c. 1963-4 AD), an accretion rate of 0.4 cm a^{-1} can be estimated to have occurred since. A defined peak of ^{137}Cs activity in the core would normally suggest it has not been subsequently re-mobilised by mechanical bioturbation or diagenesis (e.g. DeLaune *et al.* 1978; Hatton *et al.,* 1983; Dumat *et al.* 1997).

The age-depth error between the 1963 AD ^{137}Cs peak at 13.5 cm and calculated ^{210}Pb age for the same depth (c. 1945 AD) is in the order of 16-20 years. This age-depth discrepancy near the ^{137}Cs peak may be explained by systematic errors in both radiometric techniques, though the greater error in age depth patterns below the ^{137}Cs peak (which wrongly suggests that measurable quantities of the isotope existed in the pre-nuclear age) raises considerable doubts about the precision of both radiometric dating techniques. The difficulty in comparing the results from both techniques is not assisted by the lack of a secondary peak attributable to a recent accidental release, i.e. Chernobyl (1986). Sicily's central Mediterranean position and distance (atmospheric and marine pathways) from point-source discharges, for example the River Rhône (Radakovitch *et al.* 1999) appears to have prevented this.

The peak in ^{137}Cs precedes stratigraphically the major disruption to both the ^{210}Pb and the LOI profile between 8.5 cm and 14.5 cm (Fig. 6.2.1.), highlighted by increased ^{210}Pb-derived accretion rates. Since the dominant peak, ^{137}Cs has remained relatively constant through the core, aside from a decrease in activity recognised within the surface 2 cm, inverse to the values of total ^{210}Pb activity and organic content.

As ^{137}Cs was not used in the other cores in this study, a thorough investigation of these discrepancies was not undertaken. It was felt ^{210}Pb in the case of AMC was more reliable than ^{137}Cs (not least due to the correspondence of core changes with identified documented climate and human impacts later) and could be used for cores taken from Pantano Piccolo (see below).

6.1.12 Mulinello AMC: Sediment geochemistry

Similar to LOI and ^{210}Pb, major element abundances were determined at consecutive centimetre intervals down the core, irrespective of sediment boundaries (Table. 6.1.2).

Table 6.1.2. Major element abundance (% ashed mass of oxides) from core AMC.

Depth (cm)	SiO2	Al2O3	CaO	Fe2O3	Na2O	MgO	TiO2	K2O	P2O5	MnO	LOI 550°C
	%	%	%	%	%	%	%	%	%	%	%
1	36.60	9.45	5.10	5.50	4.99	2.45	1.17	1.00	0.37	0.04	26.7
2	37.00	12.03	4.37	6.60	4.78	2.62	1.45	1.16	0.43	0.04	23.1
3	31.17	10.29	5.99	5.31	5.28	2.61	1.11	1.16	0.43	0.03	16.3
4	39.10	12.62	9.30	7.63	3.37	2.73	1.55	1.23	0.44	0.04	19
5	38.56	12.05	9.49	7.39	3.17	3.02	1.39	1.50	0.44	0.05	16.3
6	34.96	11.11	9.56	6.64	3.46	2.98	1.20	1.52	0.43	0.04	24.3
7	33.09	10.67	10.84	5.95	3.71	2.98	1.09	1.39	0.50	0.04	24.9
8	34.10	11.04	11.84	6.17	3.28	2.92	1.09	1.34	0.41	0.04	25
9	40.52	12.22	7.77	7.72	3.51	2.99	1.79	1.27	0.41	0.05	10.3
10	42.84	12.57	10.24	8.63	2.71	2.99	1.99	1.12	0.41	0.06	9.2
11	41.31	12.23	12.21	8.34	2.64	3.04	1.80	1.07	0.41	0.06	8.7
12	40.96	11.91	12.70	7.96	2.61	3.00	1.70	1.08	0.42	0.06	9.3
13	43.41	12.98	9.38	8.14	2.88	2.77	1.67	1.28	0.45	0.05	13
14	39.99	12.33	6.82	6.67	3.82	2.71	1.35	1.41	0.41	0.04	20.5
15	42.97	12.89	7.95	7.87	3.25	2.73	1.67	1.27	0.38	0.05	9.3
16	44.82	13.30	8.55	8.28	2.91	2.63	1.67	1.33	0.38	0.05	9.6
17	44.04	13.75	7.41	8.59	3.13	2.55	1.62	1.39	0.39	0.05	11
18	43.51	13.12	9.17	8.47	2.97	2.62	1.64	1.26	0.38	0.06	9.2
19	40.83	11.69	13.44	8.61	2.59	2.89	1.52	1.08	0.39	0.06	7.9
20	41.66	11.78	12.86	8.59	2.61	2.82	1.54	1.12	0.40	0.05	7.2
21	38.93	11.29	14.35	7.79	2.56	2.84	1.45	1.05	0.38	0.05	8.1
22	38.76	11.32	15.14	7.72	2.58	2.87	1.46	1.06	0.38	0.05	8.3
23	38.80	11.20	15.25	7.42	2.58	2.82	1.40	1.08	0.37	0.05	8.7
24	39.91	11.41	14.53	7.21	2.60	2.75	1.38	1.16	0.36	0.05	8.8
25	40.94	11.50	13.85	7.02	2.53	2.65	1.35	1.19	0.34	0.05	9
26	43.49	12.14	11.91	6.98	2.64	2.54	1.34	1.42	0.33	0.05	9.4
27	40.12	11.92	12.55	7.04	2.95	2.88	1.53	1.19	0.34	0.05	12.8
28	38.36	11.59	14.28	7.25	2.60	2.87	1.54	1.11	0.34	0.05	11.4
2σ	6.69	1.84	6.15	1.85	1.49	0.33	0.44	0.28	0.08	0.01	12.43

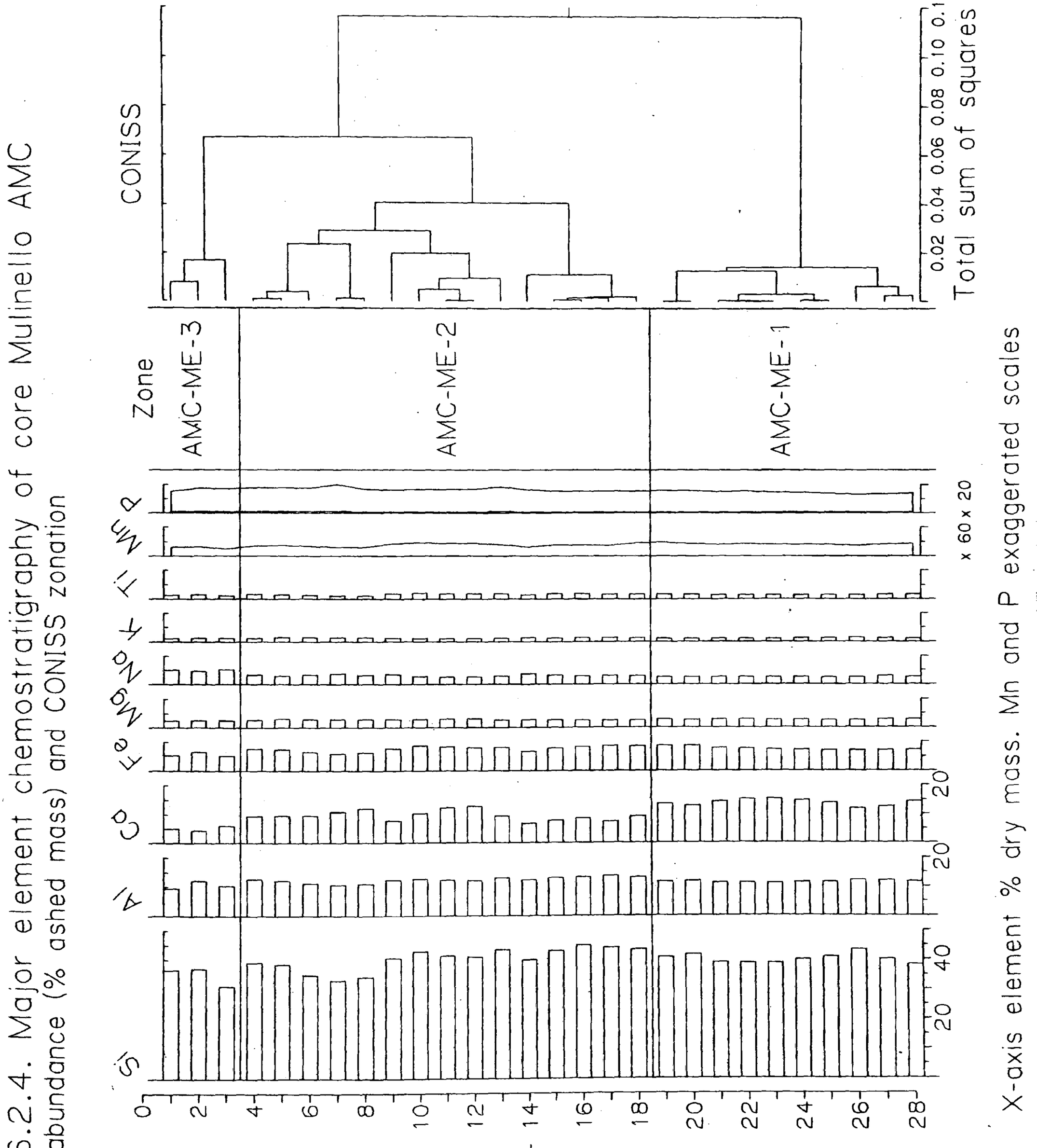

Figure 6.2.4. Major element chemostratigraphy of core Mulinello AMC
Element abundance (% ashed mass) and CONISS zonation

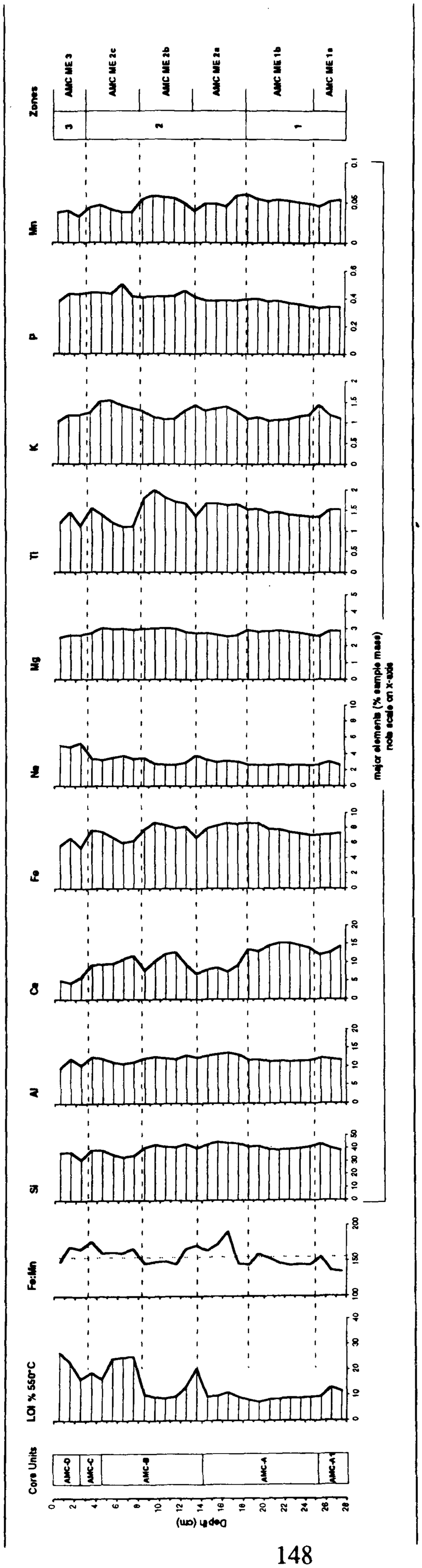

Figure 6.2.5. Mulinello AMC Loss on ignition, major element core profiles (Si to Mn in order of core abundance) and Fe:Mn ratio

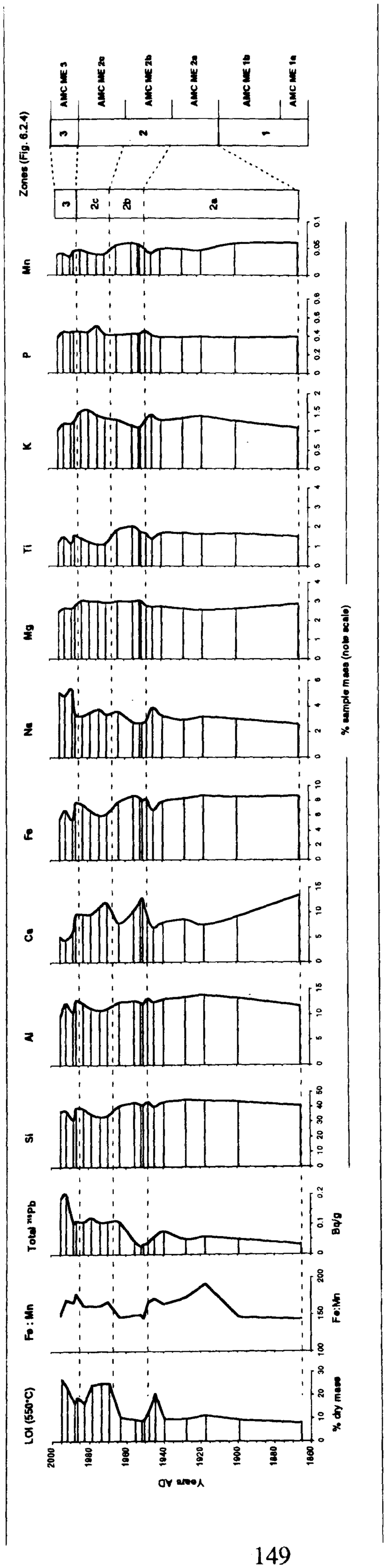

Figure 6.2.6. Mullinello AMC Major element core profiles, LOI, Fe:Mn ratio and ^{210}Pb total activity plotted against time (1 cm depth intervals)

Three main stratigraphic zones were identified by CONISS total sum of squares clustering (Fig. 6.2.4.) for the major element abundances; between 28 cm and 19-18 cm (AMC ME1), 18 cm and 4-3 cm (AMC ME2), and the surface 3-4 cm (AMC ME3). Zones AMC-ME1 and AMC-ME2 were also sub-divided into secondary zones (Fig. 6.2.4.).

Core-depth variations in the relative abundance of the group of major elements correspond well with the significant changes in composition marked by the 550°C loss on ignition profile (Fig. 6.2.5).

At the base of the sequence (AMC ME1a, corresponding to sediment unit A_1) Ca, Mg, Ti and Mn decrease towards the boundary with sediment unit A, while the abundance of Si, Al, Fe and K increase. Between 25 and 18 cm (AMC ME1b) values of Fe, Mg, Ti, P and Mn increase steadily with Ca, before a significant drop in the relative abundance of Ca (at 20-18 cm) appears to generate a marked increase of Si, Al, Fe, Mg, Ti, K and Mn towards the boundary with AMC ME2.

The upper 4 cm of core unit A (AMC-ME-2a) appears to be clearly influenced by increasing LOI up to the boundary with AMC-ME-2b. The drop in the Fe:Mn ratio between 20 and 18 cm is clearly linked to the relative increase of Mn, which suggests a less reduced conditions during deposition. Conversely the peak in the Fe:Mn ratio profile between 16-15 cm is apparently linked to the decline in Mn, which indicates that more reduced conditions existed either in the overlying water body or in the sediment due to the decomposition of organic matter. The mid-core LOI peak at 13-14 cm (20.5 % LOI) corresponds with a marked drop in Si, Fe and Ti abundance, while the reverse is seen by Na which is elevated over the same interval.

Decreased combustion losses in core unit AMC-B, between 14-8 cm (AMC-ME-2b), from the boundary of the lower sub-zone correspond to increased Ca, Ti, Fe and Mn. The drop in the Fe:Mn ratio for this intervals, is again caused by the increased abundance of Mn. Both K and Na show a marked decline in AMC-ME-2b. At 10 cm depth Ti begins to decline with the abrupt organic accumulation, corresponding to AMC-ME-2c.

At the beginning of AMC-ME-2c, increased organic content is coincident with a marked decrease in Si and Al and an increase in the ratio of Fe and Mn. The drop in Mn presumably resulting from the decreased minerogenic content and organic associated reduced-redox conditions which have led to its remobilisation. Having dropped to its lowest abundance in the sub-zone (1.09% at 7-8 cm), Ti is observed to increase with K towards the surface in AMC-ME-2c, as organic values decline in core unit AMC-C. Phosphorus also exhibits a minor peak apparently in association with the increased organic content at 7 cm.

Figure 6.2.6a. Major element abundance, Fe:Mn ratio and ^{210}Pb total activity plotted against proxy organic content (loss on ignition 550°C) from core AMC

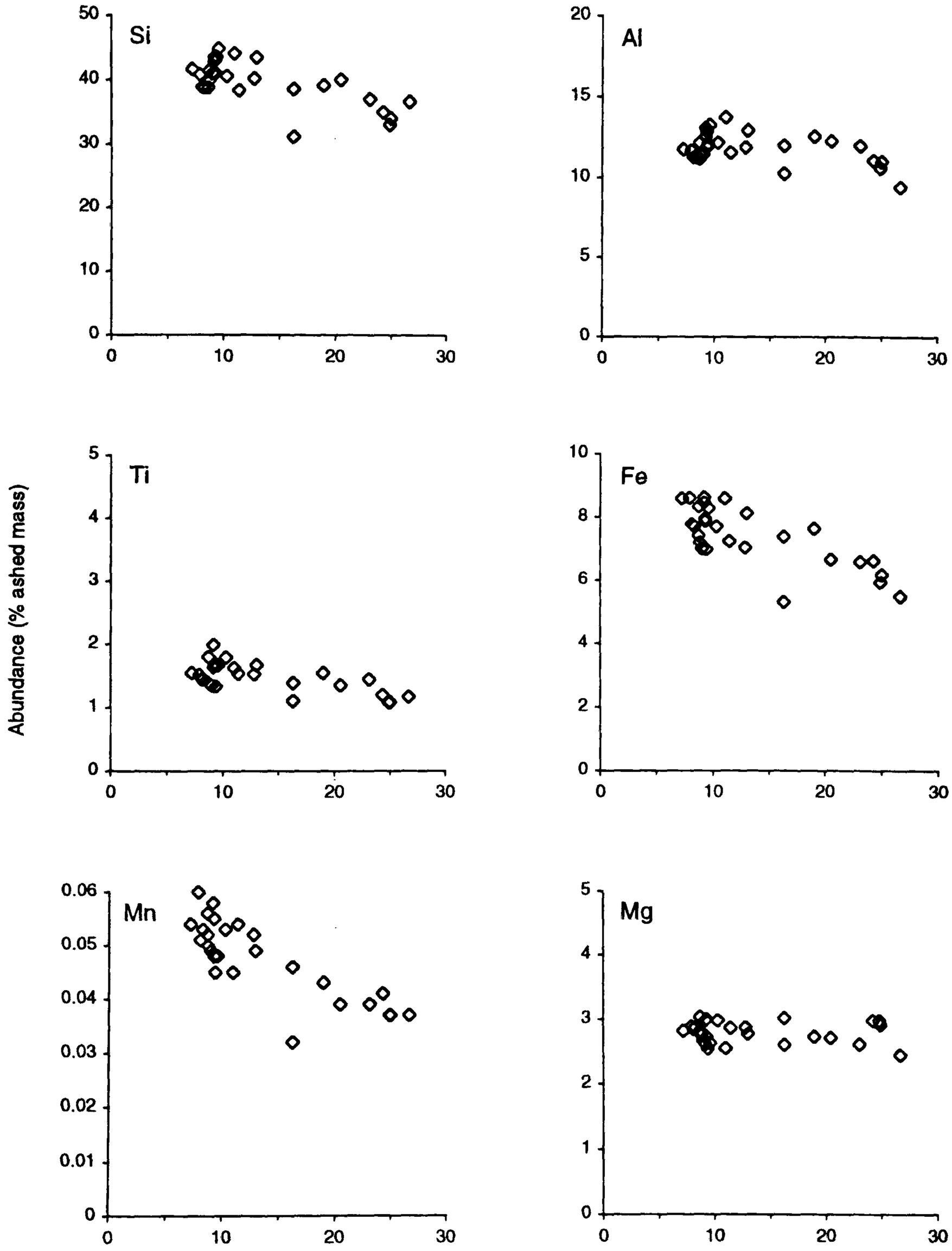

Figure 6.2.6b. Major element abundance, Fe:Mn ratio and ^{210}Pb total activity plotted against proxy organic content (loss on ignition 550°C) from core AMC

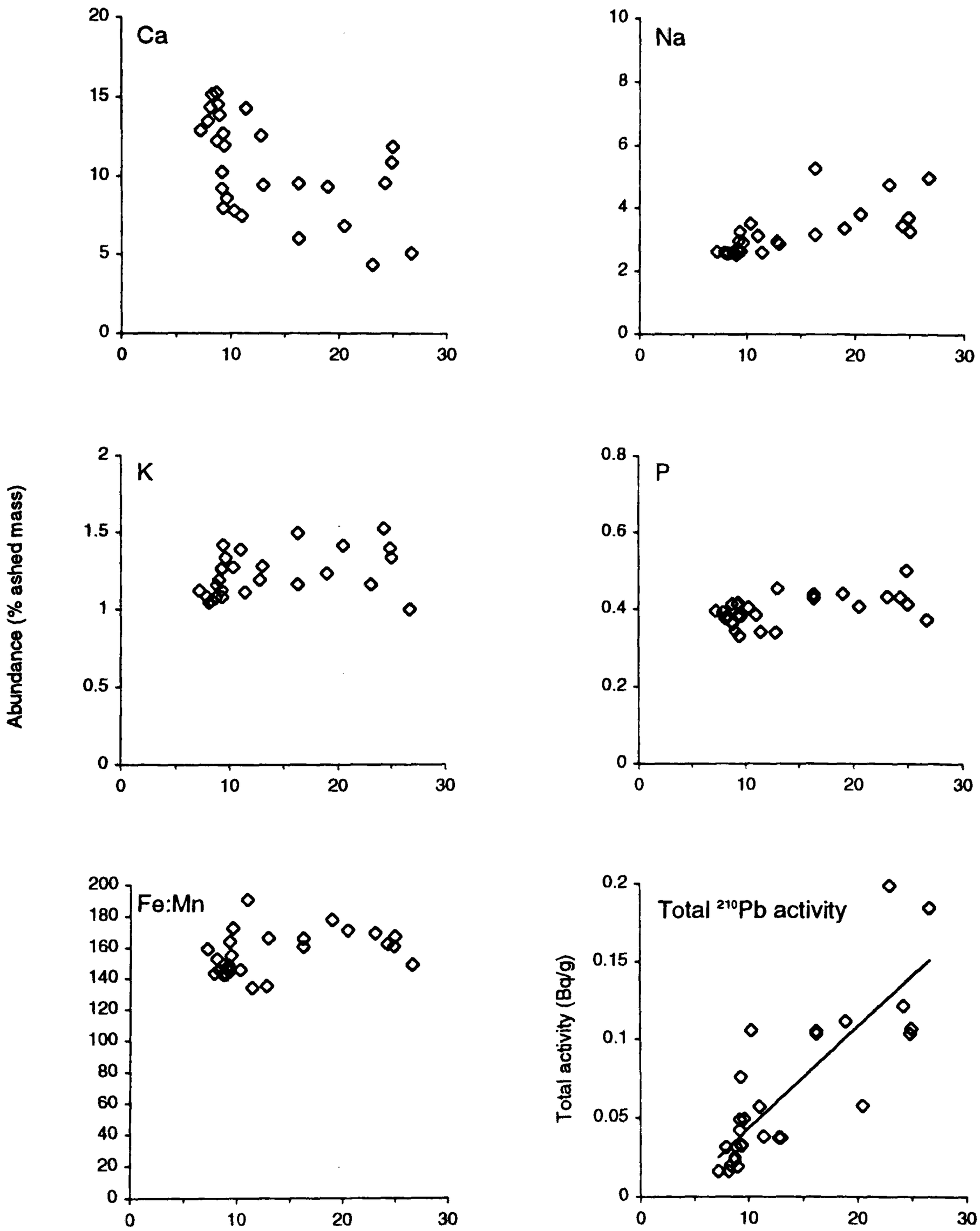

Figure 6.2.7. Core average abundances of major elements and correlation with; (a) LOI (550°C) and (b) Ti % ashed mass) from AMC

(a)

Element	Core average	(r) LOI
LOI	13.48	
Na_2O	3.17	0.73
P_2O_5	0.40	0.52
K_2O	1.22	0.37
MgO	2.79	-0.09
Al_2O_3	11.87	-0.44
CaO	10.60	-0.55
TiO_2	1.48	-0.65
SiO_2	39.67	-0.69
Fe_2O_3	7.41	-0.75
MnO	0.05	-0.82

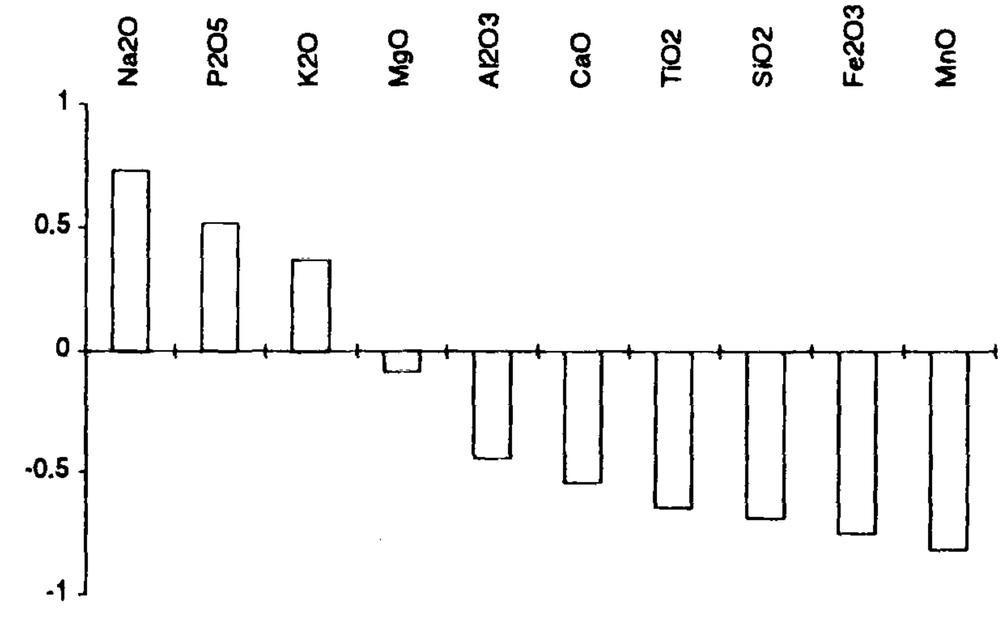

(b)

Element	Core average	(r) Ti
TiO_2	1.48	
Fe_2O_3	7.41	0.84
SiO_2	39.67	0.77
MnO	0.05	0.75
Al_2O_3	11.87	0.73
MgO	2.79	0.22
CaO	10.60	0.04
P_2O_5	0.40	-0.11
K_2O	1.22	-0.24
Na_2O	3.17	-0.47
LOI	13.48	-0.65

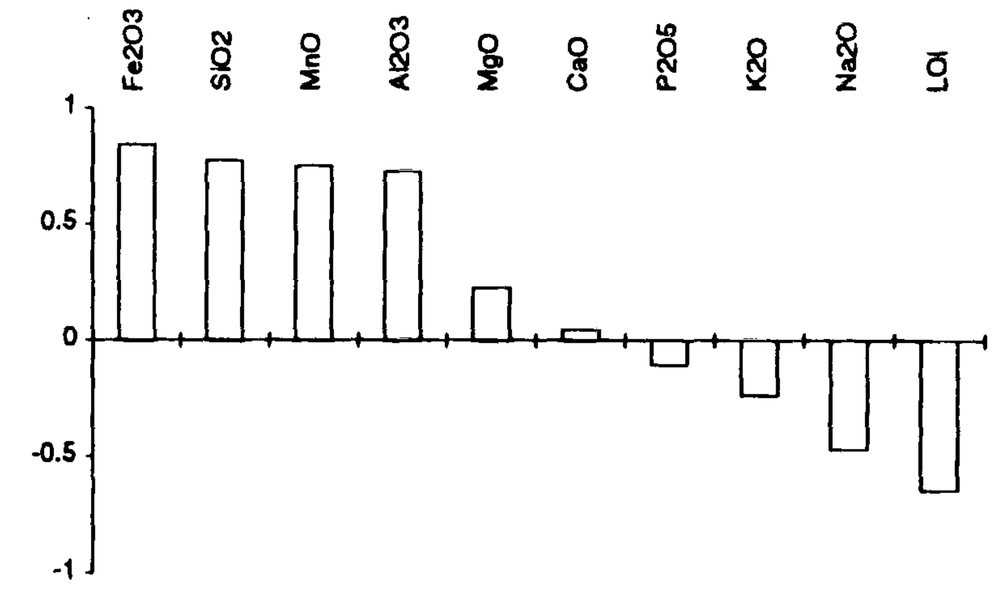

Elements ordered by correlation with LOI & TI

Within the upper 3-4 cm of the core, as organic content increases up to its maximum surface value (26.7 %), the abundance of Ca falls to its lowest value. The increase in Na, indicates its clear association with surface sediments of higher organic content. Due to the joint associations of elements with organic and inorganic sediment components and post-depositional processes, separating geochemical trends related to mineral and organic deposition in the shallow subsurface is complicated further by potentially mobile redox conditions.

Relationships between organic content and core composition is shown by the contrast in correlation between the individual elements (Fig. 6.2.7) and plots against organic content (Fig. 6.2.6a & 6.2.6b). A positive correlation is observed between Na, P and K reflecting their common association with vegetal litter and organic complexes and surface coincidence due to saline-evapotranspiration processes. The negative correlation of the other elements in the core suggests that the accumulation of organic material has been accompanied by reduced minerogenic input. The strong negative correlation of Ti, Si, Fe and Mn with LOI indicates that down-core variations appear largely due to changes in sediment provenance rather than the formation of post-depositional associations. Although the value of Fe:Mn ratios are concentrated (Fig. 6.2.6b) within sediments of low organic content (<15% loss on ignition), increased values also occur in higher organic sediments (>20% LOI) which indicates that the ratio can not be strictly used for core AMC as a proxy for either soil input or peat development (e.g. Brugam, 1978; Bennett *et al.* 1992). The abundances of Ca, Al and Mg in the sequence (Fig. 6.2.7.), all negatively correlating with LOI, possibly reflects both fine-grained minerogenic inputs (e.g. aluminosilicate minerals and carbonate clastic material) and inputs of shell material (biogenic carbonates).

The relationship between total ^{210}Pb activity and loss on ignition values (Fig. 6.2.6b) reflects the vertical distribution of ^{210}Pb activity and organic content in the core.

In Figure 6.2.6 the one centimetre sampling interval clearly indicates periods of enhanced and lower rates of accretion when plotted against age, rather than depth, with respective compositional changes. Prior to *circa* AD 1940 (14.5 cm) core composition in line with reduced accretion rates, remains relatively uniform. A marked reduction in the abundance of Ca is noticeable during this interval.

The increase in LOI at 13.5 cm (*circa* AD 1945) corresponds to a decrease in minerogenic elements (Si, Al, Ca, Fe, Ti and Mn) and increase in Na and K, presumably associated with organic materials or, as in the case of Na, possibly associated with a surface-saline environment. This horizon is also that associated with the peak in ^{137}Cs. Increased rates of accretion from *circa* AD 1945 up to *circa* AD 1952 are shown to

correspond with a return to previous abundances and a peak in Ca. Increasing Mn in the same interval, presumably associated with its input within the mineral fraction, reduces the Fe:Mn ratio at this juncture and remains reduced within AMC-ME-2b due to the increase in Mn through the interval.

Reduced accretion rates following the AD 1940 - 1950 transition and resultant relative increase in minerogenic elements is continued until the mid-1960's and early 1970's (8.5 cm - 7.5 cm), when accretion rates are associated with the enhanced accumulation of organic matter and subsequent change in sediment composition (AMC-ME-2c). Moving upwards through AMC-ME-2c, the abundance of minerogenic elements, i.e. Si, Al, Fe and Ti, increase to a slight peak at *circa* AD 1986. Conversely Ca is enhanced at the base of the organic layer, which may be due to the dissolution of carbonate in organic matter (Fig. 6.2.6) due to variations in pH.

At 2.5 cm (*circa* AD 1988) the secondary peak of accretion recorded in the core is associated with a relative drop in minerogenic elements, due to an apparent increase in Na. This peak in accretion is recognised as a major step in the total ^{210}Pb activity profile and minor peak in the Fe:Mn ratio. AMC-ME-3 (3.5 cm-0.5 cm) is the most recent period (post *circa* AD 1986) of organic accumulation which has followed an input of more minerogenic sediments. The abundance of Na and ^{210}Pb activity in the top 3 cm of the core indicates that the surface has remained relatively stable since c. AD 1988. Reducing conditions and raised pH due to the decomposition of surface organic matter appear to be reflected in the decrease in Ca and Fe:Mn ratio.

6.1.13 AMC Trace element geochemistry

Down core variations of trace element concentrations were also measured for core AMC to investigate historical patterns of trace metal contamination, and to provide further information on the cause of changes in core composition and sediment provenance. Trace metal concentrations (Table 6.1.3) in conjunction with ^{210}Pb-derived dating permits trace element fluxes (concentration of element to marsh surface over time) to also be determined (Table 6.1.4). As trace element information was not determined for the other cores in the study, only a summary is given here of trace element concentrations and fluxes obtained from AMC.

Observed patterns in major elements are continued between measured trace element concentration and LOI determined organic content. The correlation of trace elements to measured organic content (Table 6.1.3) indicates that the accumulation of organic material has biogeochemically (generation of organic-metal complexes) or temporally been preferential for the concentration of (in order) Pb, Zn, As, Hg and the halides, S, I,

Table 6.1.3. Mulinello AMC Trace element concentrations and (a) correlation of trace elements with LOI values (wt%) and Ti (%ashed mass)

												Halides			
Depth (cm)	Hg ppb	Pb ppm	Ti ppm	Zn ppm	Ni ppm	Cr ppm	V ppm	Ba ppm	La ppm	As ppm	Cu ppm	Cl ppm	Br ppm	I ppm	S ppm
0.5	44.2	106.9	11751.00	112.9	72.1	123	123	162	36.1	29.4	48.2	21.8	4.4	0.6	37.9
1.5	47.8	43	14436.00	120.1	88.3	143.9	143.1	177	46.3	21.9	52.4	13.9	4.3	0.4	26.3
2.5	66.0	76.9	11265.00	111	74.4	112.5	133.5	160.9	39.2	27.4	49.1	19.3	5.9	0.5	34.1
3.5	43.9	43.2	15560.00	109.8	83.4	146	156.9	198	48.3	9.8	46.7	7.9	2.4	0.2	13.5
4.5	41.3	56.7	13744.00	112.7	77.2	125	154.2	199.2	50.3	11.6	44.1	7.8	2.2	0.3	13.4
5.5	48.0	53.9	12249.00	114.3	76.7	117.4	150.1	181	48.1	13.9	45.1	7.8	2.6	0.3	20.6
6.5	95.2	55.6	11165.00	116	70.7	107.3	149.6	179.1	48.7	16.1	51	9.8	3.1	0.3	23.7
7.5	82.9	82.8	11201.00	93.1	62.5	108.5	152.1	188.6	42.3	12.5	41.5	9.2	3.0	0.2	20.0
8.5	77.2	85.4	18492.00	108.4	90.4	164.9	165.5	224.9	51.2	15.3	54.3	6.4	3.1	0.1	19.4
9.5	28.9	36.4	20671.00	98.2	94.9	184.5	184.6	286.4	47.8	3.9	53.9	2.6	1.3	0.1	9.4
10.5	32.8	20.4	18584.00	89	86.9	169.6	172.4	327.1	51.2	4.8	46.5	4.0	1.2	0.1	8.8
11.5	35.7	19.3	17883.00	92.4	85	171.2	177.3	354.5	47.8	5.1	46.3	2.8	1.2	0.1	9.4
12.5	43.5	24.3	16973.00	101.1	86.2	154.6	163.2	316.7	50.2	7	52.4	4.5	1.6	0.1	9.6
13.5	161.9	36.1	13556.00	104.6	78.2	128.9	150.8	251.6	47.2	17.5	54.2	10.8	4.1	0.3	21.9
14.5	76.7	26.5	16017.00	103.8	80.9	147.3	154.7	213.2	42.6	13.2	46.2	7.8	2.6	0.2	13.3
15.5	38.7	22.3	16632.00	106.3	82.1	152.4	176.7	221.3	50.4	10.4	45.9	6.3	1.7	0.1	8.8
16.5	34.7	22.6	16147.00	107.4	83.4	150.2	182.5	219.1	51.7	11.4	50.7	7.6	2.0	0.2	9.5
17.5	30.5	20	16405.00	96.3	83.1	150.1	168.8	232.6	49.1	12	50.5	7.0	1.6	0.2	8.6
18.5	19.3	16.3	15300.00	84	71.5	142.7	178.7	307.5	46.8	14	43.7	5.4	1.1	0.1	7.2
19.5	21.6	14.9	15643.00	80.1	73.5	144.6	170.3	368	48.1	13	43.5	2.6	0.9	0.1	6.0
20.5	20.0	16.2	15303.00	77.5	71.3	143.7	165.7	374.5	49	9	48.2	5.4	1.0	0.1	7.4
21.5	19.7	15.6	14894.00	74.1	69.7	149.3	157.5	360.5	45.3	9.2	47.8	5.9	0.9	0.1	7.7
22.5	26.7	16.2	14776.00	73.5	66.8	140.3	158.9	389.5	54.3	10.7	49.4	5.9	0.9	0.1	7.5
23.5	23.2	15.9	14436.00	74.9	64.2	134.8	161.7	371.2	43.6	9.1	52.3	5.4	0.9	0.0	7.6
24.5	24.0	17.4	14042.00	75.4	64.3	132.9	165.1	361.3	44.6	8.1	56.1	5.1	0.9	0.1	7.5
25.5		19.4	13687.00	77.1	61.4	131.6	162.2	307.3	47.3	8.6	59.4	4.6	1.0	0.1	7.3
26.5	23.7	19.7	15264.00	81.1	71.4	148.8	155	247.3	50.9	5.3	71.4	7.8	1.3	0.1	12.3
27.5		19	15473.00	78.2	70.2	155.7	162.8	223.1	52.6	3.5	58.3	5.8	1.0	0.1	13.3
2σ	31.1	25.04		15.12	8.84	18.48	13.75	74.70	3.97	6.20	6.01	4.36	1.30	0.14	8.29

(a)

Correlation of trace elements and LOI		Correlation of trace elements and TiO_2(wt%)	
Element	*r*	Element	*r*
Pb	0.735	Cr	0.9617497
Zn	0.673	V	0.7349113
As	0.599	Ni	0.7192163
Hg	0.545	La	0.4885657
Ni	-0.049	Ba	0.3045514
Cu	-0.122	Cu	0.1086011
La	-0.386	Zn	-0.1042544
Cr	-0.650	Hg	-0.3081886
Ba	-0.731	Pb	-0.4370734
V	-0.734	As	-0.5630572
S	0.814	Br	-0.4511449
I	0.745	I	-0.5399519
Br	0.726	S	-0.5540738
Cl	0.701	Cl	-0.5945431

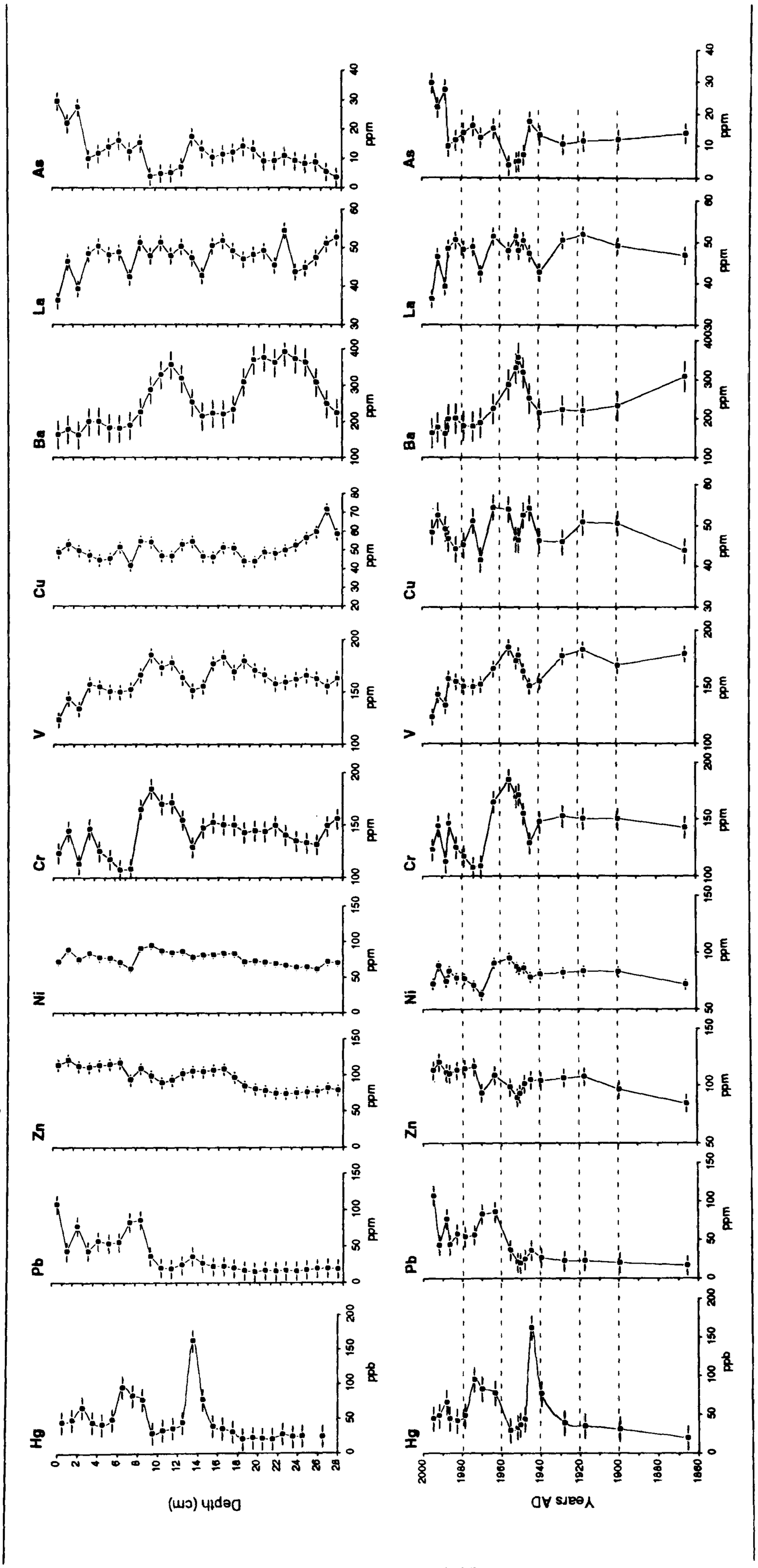

Figure 6.2.9. Mulinello AMC: Trace metal core concentrations against depth

Br and Cl. Conversely the negative correlation of V, Ba, Cr, La, Cu and Ni in the core with LOI values suggests that the variation of these elements has been due to phases of decreased organic accumulation.

The correlation of trace elements with Ti (as a proxy indicator of the minerogenic component of the sediments) corroborates this pattern of distribution (Table 6.1.3a). Elements positively associated with organic accumulation (Pb, Zn, As, Hg and the halides, S, I, Br and Cl) are negatively correlated with Ti; while Cr, V, Ni, La and Ba are all positively correlated with Ti. The poor correlation of Cu with both LOI and Ti values reflects the un-changing concentration of the element in the core.

These whole core correlations and element profiles indicate that the trace metal content of sediments deposited to form AMC has been a result of dominant phases of recent salt marsh development and channel-side accretion, i.e. shifting periods of organic enhanced sedimentation and low-organic phases of increased accretion.

The correlation of the halides (Cl, Br, I and S) with LOI-values ($r = 0.7$ to 0.8) and their down-core variation, indicates a close relationship with organic-associated accretion. Corresponding to organic values, increased halide values appear to be a consequence of salt marsh surface (evapo-transpirative) saline enrichment. The increased concentration of halides (associated with the minor LOI peak) at 13.5 suggests that prior to the distinct phase of rapid accretion, the core site surface was effectively similar to present day geochemical conditions.

The flux of trace metals (Fig. 6.3.) to the core site has clearly been affected by the accretionary episodes identified by ^{210}Pb-dating. Increased accretion rates between c. 1940 and the mid-1950's and the clear accretionary "pulse" c. 1951-2 AD is highly apparent in the trace element fluxes (Fig. 6.3). A distinction is visible between those elements associated with a higher organic content, specifically Hg, Pb and As, and those associated with a greater mineral component, e.g. Ni, Cr and Ti. Whereas the latter group closely parallels the rapid peak and decline pattern of low organic sediment accretion in the decade following the Second World War, the flux of Hg, Pb and As remain significantly higher up to the present (1995). Similar to the peak at 10.5 cm depth, in that influx rates of all calculated elements change, a lesser peak of trace element influx is noticeable between 2 and 4 cm (c. 1986-88 AD) also concurring with the increase in accretion rates at the time.

As discussed in Cundy *et al.* (1998) the increased flux of trace metals to the core site between c. 1945 and c.1956 AD represents the rapid accretion of catchment-sediment derived from the Mulinello catchment. The positive correlation of Cr, V, Ni, Ba, La and Cu with Ti and ante-correlation with organic content (Table 6.1.3.) suggests that the core site was dominated by channel processes and the deposition of sediments/soil material

Table 6.1.4. Mulinello AMC Trace element accumulation rates

												Halides			
	Hg	**Pb**	**Ti**	**Zn**	**Ni**	**Cr**	**V**	**Ba**	**La**	**As**	**Cu**	**Cl**	**Br**	**I**	**S**
	$\mu g\ cm^2\ a^{-1}$	$mg\ cm^2\ a^{-1}$													
Depth (cm)															
0.5	5.901	14.271	1568.751	15.072	9.625	16.420	16.420	21.627	4.819	3.925	6.435	2.907	0.583	0.076	5.065
1.5	5.289	4.755	1596.506	13.282	9.765	15.914	15.826	19.575	5.120	2.422	5.795	1.538	0.478	0.046	2.910
2.5	14.126	16.459	2411.036	23.757	15.924	24.078	28.573	34.437	8.390	5.864	10.509	4.128	1.271	0.117	7.303
3.5	7.894	7.768	2797.974	19.744	14.997	26.253	28.213	35.604	8.685	1.762	8.398	1.429	0.440	0.036	2.435
4.5	7.065	9.699	2351.076	19.279	13.206	21.383	26.378	34.076	8.604	1.984	7.544	1.334	0.370	0.047	2.289
5.5	6.021	6.761	1536.517	14.338	9.621	14.727	18.829	22.705	6.034	1.744	5.657	0.984	0.322	0.032	2.584
6.5	12.525	7.319	1469.691	15.270	9.307	14.124	19.692	23.576	6.411	2.119	6.713	1.285	0.414	0.033	3.116
7.5	8.951	8.938	1209.125	10.050	6.747	11.712	16.419	20.359	4.566	1.349	4.480	0.998	0.321	0.021	2.155
8.5	6.787	7.508	1625.817	9.531	7.948	14.498	14.551	19.773	4.502	1.345	4.774	0.567	0.277	0.011	1.704
9.5	7.567	9.524	5408.366	25.693	24.830	48.273	48.299	74.934	12.506	1.020	14.102	0.689	0.347	0.019	2.463
10.5	25.310	15.742	14340.423	68.677	67.057	130.873	133.033	252.408	39.509	3.704	35.882	3.124	0.911	0.053	6.776
11.5	13.352	7.212	6682.901	34.530	31.765	63.978	66.257	132.477	17.863	1.906	17.302	1.030	0.462	0.021	3.527
12.5	11.274	6.302	4401.926	26.220	22.356	40.095	42.326	82.136	13.019	1.815	13.590	1.166	0.418	0.023	2.479
13.5	18.238	4.067	1527.067	11.783	8.809	14.520	16.987	28.342	5.317	1.971	6.106	1.219	0.458	0.034	2.466
14.5	4.592	1.586	958.878	6.214	4.843	8.818	9.261	12.763	2.550	0.790	2.766	0.469	0.154	0.010	0.794
15.5	3.031	1.747	1302.604	8.325	6.430	11.936	13.839	17.332	3.947	0.815	3.595	0.491	0.133	0.009	0.692
16.5	1.406	0.916	654.207	4.351	3.379	6.085	7.394	8.877	2.095	0.462	2.054	0.310	0.080	0.009	0.384
17.5	0.720	0.472	387.243	2.273	1.962	3.543	3.985	5.491	1.159	0.283	1.192	0.166	0.038	0.004	0.204
18.5	0.147	0.124	116.695	0.641	0.545	1.088	1.363	2.345	0.357	0.107	0.333	0.041	0.008	0.001	0.055
2σ	12.24	9.57	6375.30	29.70	29.37	58.22	58.49	115.55	17.03	2.72	15.67	2.07	0.58	0.05	3.90

Figure 6.3. Mulinello AMC: Selected trace metal fluxes (μg/cm²/yr⁻¹) unless otherwise indicated

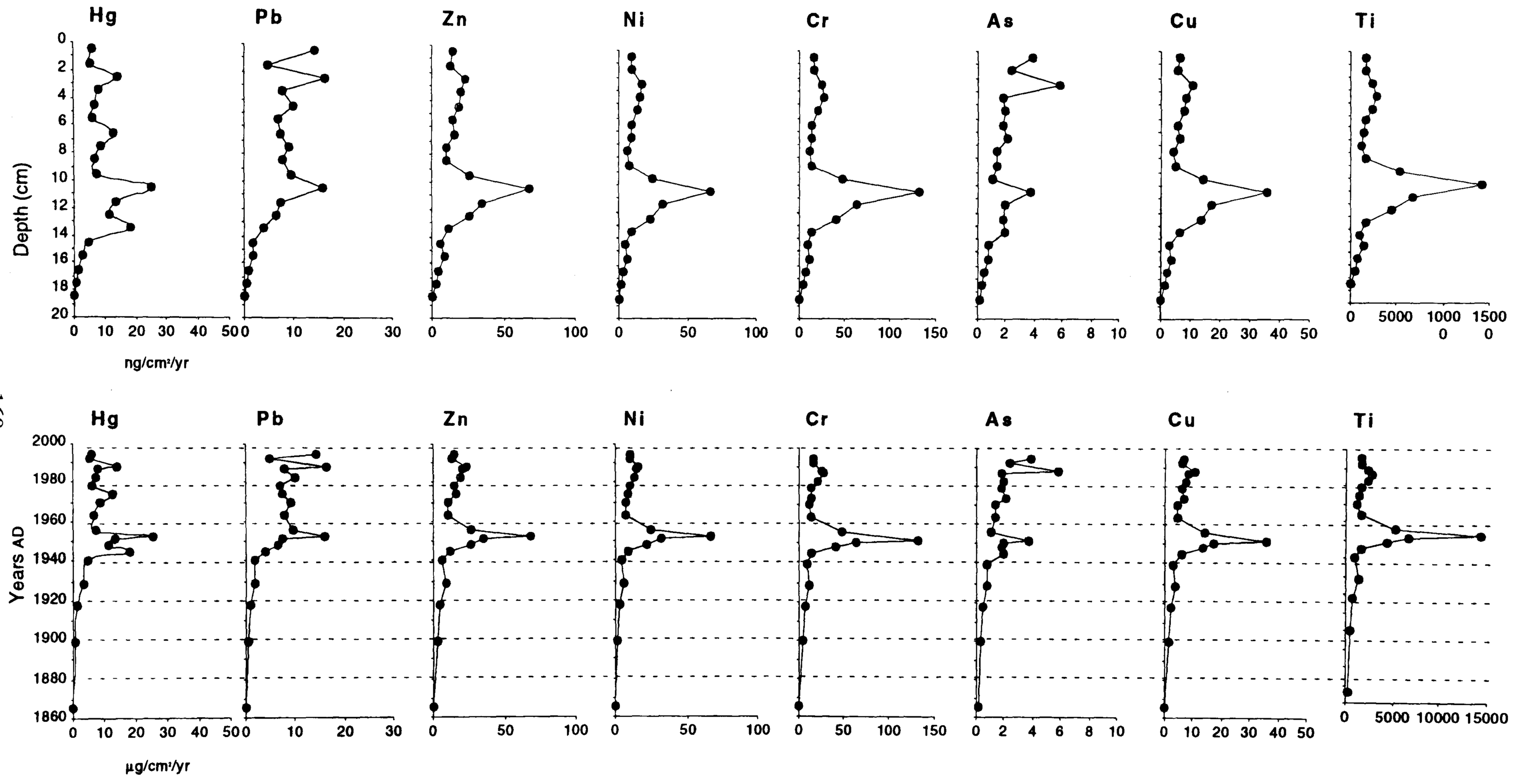

from eroded and weathered volcanic sequences (Fig. 6.1.1.). While catchment rocks were not directly characterised geochemically, the composition of similar Na-alkaline volcanics in Sicily (Cristofolini & Romano, 1982) would suggest to have been the primary source of detrital Ti, Fe, Cu, Ni, Zn and V. The concentration of Ti (1.5 - 1.8 %, wt% TiO_2) and Fe up to 10% (wt% Fe_2O_3 and FeO) in these lavas (Armienti *et al.* 1989) are comparable with abundance values observed in the cored sediment (Fig. 6.2.5.). Sediment derived from within the catchment overall (i.e. reworked alluvial sediments) rather than a single source is suggested by corresponding Ca and Ba values (Fig. 6.2.5. & 6.2.9) during this phase, representing the mineral fraction of sediment derived from carbonate-sequences in the catchment.

The negative correlation of Pb, Hg, Zn and As with Ti [compared to the positive r-values with LOI (Table 6.1.3.)] suggests their concentration in the core has not been due entirely to alluvial-detrital inputs from the catchment. Clearly during periods of organic associated accumulation, the stability of the wetland surface and preferential biogeochemical characteristics (e.g. Allen *et al.,* 1990; Bricker, 1993; Gambrell, 1994; Callaway *et al.* 1998) has enhanced Hg, Pb and As deposition. A low-energy aquatic or atmospheric transport pathway for these metals is suggested therefore to have caused the observed core patterns. Compared with the known period of industrial expansion in the area (see above) the flux of these potential pollutants to the core setting indicates that their presence (Hg and Pb) in the local environment has increased since the post-war period. The growth of the petrochemical and oil refinery industry in the Augusta Bay-Mulinello area, will also have combined with increased road transport (i.e. Pb-additive for petrol engines). As well as industrial contamination, post war intensive agriculture practices in the catchment, i.e. arsenic (arseno-phosphates) pesticide applications is suggested as the cause of the observed As flux rates and concentration in the core.

Trace element abundances confirm that hydrodynamic conditions affecting the depositional environment at AMC has greatly influenced the geochemical composition of sediments. Both catchment-hydrological changes (determining decadal and annual trends in sediment supply to the wetland setting) and the effect of *in situ* biogeochemical processes. The archival capacity of wetland soils developed at the mouth of the Mulinello river to retain geochemical signatures of depositional change and temporal patterns of potential contaminants dispersed in the local catchment/bay environment is clearly shown.

6.1.14 AMC Pollen

Pollen extraction and slide preparation for AMC was conducted by D. Horne and J. Firth of the Department of Geography, while pollen counts were determined by D. Horne and Dr. P.E.F. Collins. Prepared pollen slides from AMC were used to familiarise the author of common pollen types encountered. 19 horizons of 0.5 cm thickness were extracted from the short core AMC (Fig.6.1.5). Samples were taken to represent variations in core sedimentology and differences across marked boundaries. Total pollen counts varied in the sequence to compensate for the over-abundance of Amaranthaceae-Chenopodiaceae pollen and scarcity of grains in some of the horizons. None the less, pollen counts are too low to make a reliable interpretation using percentage abundance values. Pollen counts and calculated concentrations (grains/g) are shown in Tables 6.1.5 and 6.1.7.

Although the majority of pollen work for the core had been already accomplished prior to the start of this research, ^{210}Pb accretion data and pollen abundances had not been brought together in the form of pollen accumulation rates (Table 6.1.8.). A preliminary pollen analysis of basal sediments beneath AMC was also undertook (Table 6.1.6.), across the boundary of water saturated-shelly sands and alluvial muds above (Fig. 6.1.4.).

Accumulation rates of the most abundant tree (*Olea-Phyllirea, Pinus*), herb and aquatic types were determined for the upper 18 cm of the core (Table 6.1.8.) using ^{210}Pb-derived accretion values. The accumulation of pollen types at the site reflects the considerable variation of the nature and timing of sediment accretion, which has clearly influenced the pollen stratigraphy of AMC. Indicated by their relationship with sediment accretion rates (Fig. 6.3.3.), differences in the type of pollen accumulated have clearly been controlled by variable rates of sediment input and changing hydrodynamics of the wetland site.

Three local pollen assemblage zones (LPAZ's) were defined by CONISS using the concentration values of 40 pollen taxa in the core (Fig. 6.3.1.) and are numbered stratigraphically LPAZ AMC-1, AMC-2 and AMC-3, from the base of the core upward. Due to the low counts of pollen, only concentration values and pollen accumulation patterns are detailed below in relation to changing pollen-taphonomic patterns and potential nearby vegetational changes.

LPAZ AMC-1: 27 cm to 13.5 cm depth (pre-19th century to AD 1945)

Olea-Phyllirea, Pinus and *Quercus* undiff. concentrations indicate a significant atmospheric/water transport component to the pollen assemblage. Amaranthaceae-

Table 6.1.5. Pollen count data from core AMC (Mulinello). In order of counted abundance through core.

Sample depth (cm)	0.5 cm	1 cm	2.5 cm	3 cm	4 cm	5 cm	6.5 cm	7 cm	8 cm	9 cm	10 cm	11 cm	12 cm	13 cm	14 cm	15 cm	16 cm	17 cm	18 cm	23 cm	25 cm	27 cm
Aboreal pollen (AP)																						
Olea-Phyllirea	14	0	12	0	2	0	0	0	0	5	5	4	0	12	1	0	0	7	19	0	10	0
Pinus	2.5	2	2.5	0	0	1	0	0	0	0	1.5	0	1.5	0	0	0	0	0	2.5	1	1	0.5
Quercus undiff.	0	0	2	0	0	0	0	0	0	0	0	0	0	1	0	0	0	3	2	0	1	0
Alnus	6	0	0	0	0	0	0	0	0	0	0	0	0	0	0	0	2	0	0	0	0	0
Corylus	1	0	0	0	0	0	0	0	0	1	0	0	1	0	0	0	0	0	0	0	0	1
Carpinus undiff.	0	0	0	0	0	0	0	0	0	0	0	0	0	2	0	0	0	0	0	0	0	0
Castanea	0	0	0	0	0	0	0	0	0	0	0	0	0	0	0	0	0	0	0	0	1	0
Eucalyptus type	0	0	0	0	0	0	0	1	0	0	0	0	0	0	0	0	0	0	0	0	0	0
Populus	0	0	0	0	0	0	0	0	0	1	0	0	0	0	0	0	0	0	0	0	0	0
Aesculus type	0	0	0	0	0	0	0	0	0	0	0	0	0	0	0	1	0	0	0	0	0	0
Frangula	0	0	1	0	0	0	0	0	0	0	0	0	0	0	0	0	0	0	0	0	0	0
AP total	**23.5**	**2**	**17.5**	**0**	**2**	**1**	**0**	**1**	**0**	**7**	**6.5**	**4**	**2.5**	**15**	**1**	**1**	**2**	**10**	**23.5**	**1**	**13**	**1.5**
Non-arboreal (NAP) pollen																						
Amaranth.-Chenopodiaceae	162	75	244	79	92	95	96	86	108	28	17	3	18	16	138	79	68	103	46	11	7	23
Poaceae	32	14	6	14	0	4	2	10	1	10	14	2	39	10	1	3	32	13	22	34	10	46
Lactucae	3	7	6		4	1	1	2	0	19	20	8	26	31	0	11	4	9	31	38	25	14
Cyperaceae	2	1	1	1	0	0	0	0	0	9	10	4	0	17	1	6	1	9	13	0	4	1
Apiaceae	1	1	3	1	2	0	0	1	1	5	3	4	2	2	0	0	0	1	3	2	5	0
Asteraceae subf. Asteroideae	0	0	2	0	0	0	0	0	0	4	6	0	3	5	0	1	0	4	7	0	2	1
Sinapis type	0	0	6	1	0	1	0	0	1	0	2	0	2	2	0	1	1	0	0	1	4	0
Cirsium type	4	1	0	1	1	0	0	0	0	0	0	0	1	0	0	0	0	0	1	2	1	0
Linum	2	0	0	0	0	0	0	2	0	0	0	0	1	0	0	0	0	0	0	1	0	3
Filipendula type	1	2	0	1	0	0	0	1	0	0	0	0	0	0	0	0	1	0	0	0	0	2
Anthemis type	0	0	1	0	0	0	0	0	0	1	0	0	0	0	0	0	0	0	4	1	0	0
Centaurea type	0	0	0	0	0	0	0	0	0	0	0	0	1	1	0	0	3	0	0	1	0	0
Succisa	5	1	0	0	0	0	0	0	0	0	0	0	0	0	0	0	0	0	0	0	0	0
Urtica dioica	0	0	0	0	0	0	0	0	0	4	0	0	0	0	0	0	0	0	0	0	0	0
Rumex acetosa type	0	0	0	0	0	0	0	0	0	0	0	1	0	0	0	1	0	0	0	0	0	0
Plantago cf. coronopus	0	0	0	0	0	0	0	0	0	0	0	0	0	0	1	0	0	1	1	0	0	0
Scabiosa	0	0	0	0	0	0	0	0	0	0	0	0	0	1	0	0	0	0	0	0	0	1
Oxyria type	0	0	0	0	1	0	0	0	0	0	0	0	0	0	0	0	0	0	0	0	0	0
Ranunculus type	0	0	0	0	0	0	0	0	0	1	0	0	0	0	0	0	0	0	0	0	0	0
Scrophularia type	0	0	0	0	0	0	0	0	0	1	0	0	0	0	0	0	0	0	0	0	0	0
Hypericum perforatum type	0	0	0	0	0	0	0	0	0	1	0	0	0	0	0	0	0	0	0	0	0	0
Lotus type	0	0	0	0	0	0	0	0	0	0	0	0	0	1	0	0	0	0	0	0	0	0
Ononis type	0	0	0	0	0	0	0	0	0	0	0	0	0	0	0	1	0	0	0	0	0	0
Rumex undiff.	1	0	0	0	0	0	0	0	0	0	0	0	0	0	0	0	0	0	0	0	0	0
NAP total	**213**	**102**	**269**	**98**	**100**	**101**	**99**	**102**	**111**	**83**	**72**	**22**	**93**	**86**	**141**	**103**	**110**	**140**	**128**	**91**	**58**	**91**
Aquatics/Spores																						
Potamogeton coleogoton	5	2	1	3	0	0	0	2	2	4	0	1	5	2	0	0	1	2	2	7	2	3
Pteropsida monolete	0	0	0	1	0	0	0	0	0	0	0	0	0	0	0	0	0	2	1	0	4	0
Sparganium emersum type	2	0	1		0	0	0	0	0	0	0	0	0	0	0	0	0	0	2	0	0	0
Nymphaea	0	0	0	0	0	0	0	0	0	0	0	0	0	1	0	0	0	0	0	0	0	0
Aquatics/Spores total (not included in pollen sum)	**7**	**2**	**2**	**4**	**0**	**0**	**0**	**2**	**2**	**4**	**0**	**1**	**5**	**3**	**0**	**0**	**1**	**4**	**5**	**7**	**6**	**3**
Unideutified/deteriorated	1	0	12	0	8	0	0	0	1	26	13	9	0	11	5	11	1	16	25	1	20	3
Total Pollen sum (AP/NAP)*	**237.5**	**104**	**298.5**	**98**	**110**	**102**	**99**	**103**	**112**	**116**	**91.5**	**35**	**95.5**	**112**	**147**	**115**	**113**	**166**	**176.5**	**93**	**91**	**95.5**
Added Lycopodium	**43**	**23**	**68**	**33**	**44**	**3**	**5**	**13**	**5**	**250**	**262**	**80**	**52**	**80**	**7**	**149**	**52**	**161**	**26**	**80**	**15**	**49**

*too low pollen counts for statistically reliable % abundance data

Table 6.1.6. Preliminary pollen data from AMC core site (74cm to 80 cm depth). Concentrations in grains per g dried sediment

	Sample Horizon 74-76 cm		Sample Horizon 76-78 cm		Sample Horizon 78-80 cm	
	Count	conc.	Count	conc.	Count	conc.
Arboreal/Snrub pollen						
Olea-Phyllirea	17	726.50	7	221.52	5	259.61
Ericaceae	1	42.74	4	126.58	4	207.68
Quercus undiff.	6	256.41	3	94.94	0	0.00
Pinus	4	170.94	1	31.65	2	103.84
Betula	4	170.94	2	63.29	0	0.00
Non-arboreal (herb)						
Amaranth.-Chenopodiaceae	90	3846.15	66	2088.61	26	1349.95
Caryophyllaceae	15	641.03	4	126.58	12	623.05
Lactuceae	15	641.03	6	189.87	6	311.53
Poaceae	8	341.88	3	94.94	3	155.76
Rannunculus type	0	0.00	0	0.00	9	467.29
Artemesia	0	0.00	5	158.23	2	103.84
Cyperaceae	1	42.74	1	31.65	1	51.92
Asteraceae (Aster type)	1	42.74	0	0.00	1	51.92
Total Pollen	162	6923.08	102	3227.85	71	3686.40
Added Lycopodium	117		158		107	
Sediment mass (g)	2.0		2.0		1.8	

Count by S. Turner

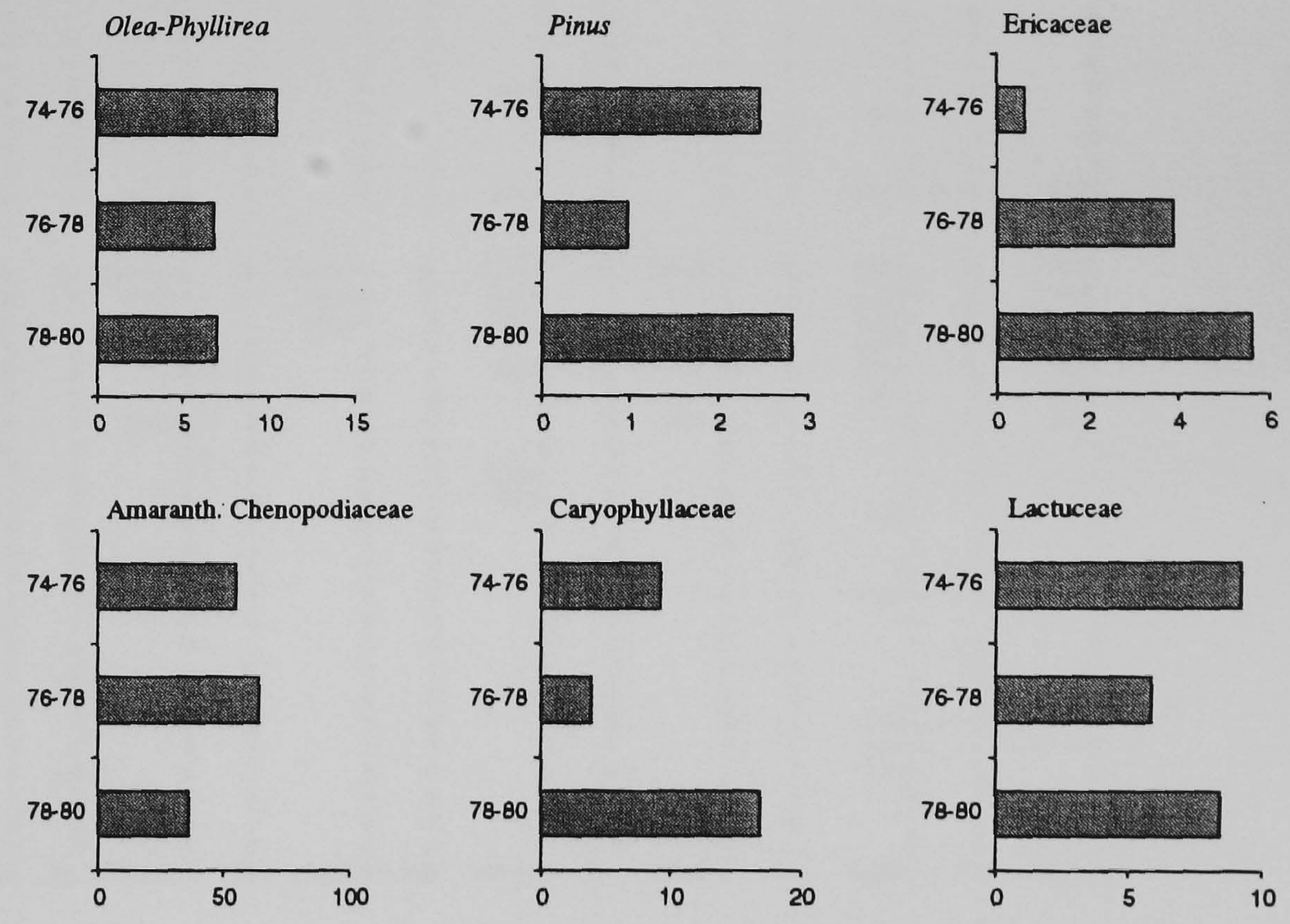

Note: Samples 74-76cm and 76-78cm from mud overlying shell-rich mud (78-80 cm).

Table 6.1.7. Pollen counts and concentration (grains per gram) data from core AMC (Mulinello). In order of count abundance through core.

	Sample horizon AMC 0.5 cm		Sample horizon AMC 1 cm		Sample horizon AMC 2.5cm		Sample horizon AMC 3cm		Sample horizon AMC 4cm		Sample horizon AMC 5cm		Sample horizon AMC 6.5cm		Sample horizon AMC 7cm		Sample horizon AMC 8cm		Sample horizon AMC 9cm		Sample horizon AMC 10cm	
	Count	gr/g	Count	gr/g	Count	gr/g	Count	gr/g	Count	gr/g	Count	gr/g	Count	gr/g	Count	gr/g	Count	gr/g	Count	gr/g	Count	gr/g
Aboreal pollen (AP)																						
Olea-Phyllirea	14	2457.22	0	0	12	3217.33	0	0	2	408.64	0	0	0	0	0	0	0	0	5	158.09	5	131.77
Pinus	2.5	438.79	2	619.13	2.5	670.28	0	0	0	0	1	2466.40	0	0	0	0	0	0	0	0	1.5	39.53
Quercus undiff.	0	0	0	0	2	536.22	0	0	0	0	0	0	0	0	0	0	0	0	0	0	0	0
Alnus	6	1053.09	0	0	0	0	0	0	0	0	0	0	0	0	0	0	0	0	0	0	0	0
Corylus	1	175.52	0	0	0	0	0	0	0	0	0	0	0	0	0	0	0	0	1	31.62	0	0
Carpinus undiff.	0	0	0	0	0	0	0	0	0	0	0	0	0	0	0	0	0	0	0	0	0	0
Castanea	0	0	0	0	0	0	0	0	0	0	0	0	0	0	0	0	0	0	0	0	0	0
Eucalyptus type	0	0	0	0	0	0	0	0	0	0	0	0	0	0	1	552.91	0	0	0	0	0	0
Populus	0	0	0	0	0	0	0	0	0	0	0	0	0	0	0	0	0	0	1	31.62	0	0
Aesculus type	0	0	0	0	0	0	0	0	0	0	0	0	0	0	0	0	0	0	0	0	0	0
Frangula	0	0	0	0	1	268.11	0	0	0	0	0	0	0	0	0	0	0	0	0	0	0	0
AP total	**23.5**	**4124.62**	**2**	**619.13**	**17.5**	**4691.94**	**0**	**0**	**2**	**408.64**	**1**	**2466.40**	**0**	**0**	**1**	**552.91**	**0**	**0**	**7**	**221.33**	**6.5**	**171.30**
Non-arboreal (NAP) pollen																						
Amaranth.-Chenopodiaceae	162	28433.52	75	23217.30	244	65419.06	79	17372.56	92	18797.22	95	234307.56	96	139332.37	86	47549.93	108	155256.06	28	885.31	17	448.01
Poaceae	32	5616.50	14	4333.90	6	1608.67	14	3078.68	0	0.00	4	9865.58	2	2902.76	10	5529.06	1	1437.56	10	316.18	14	368.95
Lactucae	3	526.55	7	2166.95	6	1608.67		0	4	817.27	1	2466.40	1	1451.38	2	1105.81	0	0	19	600.74	20	527.07
Cyperaceae	2	351.03	1	309.56	1	268.11	1	219.91	0	0	0	0	0	0	0	0	0	0	9	284.56	10	263.54
Apiaceae	1	175.52	1	309.56	3	804.33	1	219.91	2	408.64	0	0	0	0	1	552.91	1	1437.56	5	158.09	3	79.06
Asteraceae subf. Asteroideae	0	0	0	0	2	536.22	0	0	0	0	0	0	0	0	0	0	0	0	4	126.47	6	158.12
Sinapis type	0	0	0	0	6	1608.67	1	219.91	0	0	1	2466.40	0	0	0	0	1	1437.56	0	0	2	52.71
Cirsium	4	702.06	1	309.56	0	0	1	219.91	1	204.32	0	0	0	0	0	0	0	0	0	0	0	0
Linum	2	351.03	0	0.00	0	0	0	0.00	0	0	0	0	0	0	2	1105.81	0	0	0	0	0	0
Filipendula	1	175.52	2	619.13	0	0	1	219.91	0	0	0	0	0	0	1	552.91	0	0	0	0	0	0
Anthemis	0	0	0	0	1	268.11	0	0	0	0	0	0	0	0	0	0	0	0	1	31.62	0	0
Centaurea	0	0	0	0	0	0	0	0	0	0	0	0	0	0	0	0	0	0	0	0	0	0
Succisa	5	877.58	1	309.56	0	0	0	0	0	0	0	0	0	0	0	0	0	0	0	0	0	0
Urtica dioica	0	0	0	0	0	0	0	0	0	0	0	0	0	0	0	0	0	0	4	126.47	0	0
Rumex acetosa type	0	0	0	0	0	0	0	0	0	0	0	0	0	0	0	0	0	0	0	0	0	0
Plantago cf. coronopus	0	0	0	0	0	0	0	0	0	0	0	0	0	0	0	0	0	0	0	0	0	0
Scabiosa	0	0	0	0	0	0	0	0	0	0	0	0	0	0	0	0	0	0	0	0	0	0
Oxyria type	0	0	0	0	0	0	0	0	1	204.32	0	0	0	0	0	0	0	0	0	0	0	0
Ranunculus type	0	0	0	0	0	0	0	0	0	0	0	0	0	0	0	0	0	0	1	31.62	0	0
Scrophularia	0	0	0	0	0	0	0	0	0	0	0	0	0	0	0	0	0	0	1	31.62	0	0
Hypericum perforatum	0	0	0	0	0	0	0	0	0	0	0	0	0	0	0	0	0	0	1	31.62	0	0
Lotus type	0	0	0	0	0	0	0	0	0	0	0	0	0	0	0	0	0	0	0	0	0	0
Ononis type	0	0	0	0	0	0	0	0	0	0	0	0	0	0	0	0	0	0	0	0	0	0
Rumex undiff.	1	175.52	0	0	0	0	0	0	0	0	0	0	0	0	0	0	0	0	0	0	0	0
NAP total	**213**	**37384.818**	**102**	**31575.526**	**289**	**72121.83**	**98**	**21550.78**	**100**	**20431.76**	**101**	**249105.93**	**99**	**143686.50**	**102**	**56396.43**	**111**	**159568.73**	**83**	**2624.30**	**72**	**1897.46**
Aquatics/Spores																						
Potamogeton coleogoton	5	877.58	2	619.13	1	268.11	3	659.72	0	0	0	0	0	0	2	1105.81	2	2875.11	4	126.47	0	0
Pteropsida monolete	0	0	0	0	0	0	1	219.91	0	0	0	0	0	0	0	0	0	0	0	0	0	0
Sparganium emersum type	2	351.03	0	0	1	268.11		0	0	0	0	0	0	0	0	0	0	0	0	0	0	0
Nymphaea	0	0	0	0	0	0	0	0	0	0	0	0	0	0	0	0	0	0	0	0	0	0
Aquatics/Spores total (not included in pollen sum)	**7**	**1228.61**	**2**	**619.13**	**2**	**536.22**	**4**	**879.62**	**0**	**0**	**0**	**0**	**0**	**0**	**2**	**1105.81**	**2**	**2875.11**	**4**	**126.47**	**0**	**0**
Unidentified/deteriorated	1	175.52	0	0	12	3217.33	0	0	8	1634.54	0	0	0	0	0	0	1	1437.56	26	822.07	13	342.60
Total Pollen sum (AP/NAP)	**238**	**41684.95**	**104**	**32194.65**	**299**	**80031.10**	**98**	**21550.78**	**110**	**22474.94**	**102**	**251572.33**	**99**	**143686.50**	**103**	**56949.34**	**112**	**161006.29**	**116**	**3667.69**	**92**	**2411.36**
Added Lycopodium	**43**		**23**		**68**		**33**		**44**		**3**		**5**		**13**		**5**		**250**		**262**	
Sample mass (g)	2.65		2.81		1.10		2.76		2.22		2.70		2.76		2.78		2.78		2.53		2.90	

Table 6.1.7. Pollen counts and concentration (grains per gram) data from core AMC (Mulinello). In order of count abundance through core.

	Sample horizon AMC 11cm		Sample horizon AMC 12cm		Sample horizon AMC 13cm		Sample horizon AMC 14cm		Sample horizon AMC 15cm		Sample horizon AMC 16cm		Sample horizon AMC 17cm		Sample horizon AMC 18cm		Sample horizon AMC 23		Sample horizon AMC 25		Sample horizon AMC 27cm	
	Count	gr/g	Count	gr/g	Count	gr/g	Count	gr/g	Count	gr/g	Count	gr/g	Count	gr/g	Count	gr/g	Count	gr/g	Count	gr/g	Count	gr/g
Aboreal pollen (AP)																						
Olea-Phyllirea	4	1220.85	0	0	12	743.42	1	4617.23	0	0	0	0	7	321.79	19	3932.46	0	0.00	10	7821.51	0	0.00
Pinus	0	0	1.5	181.42	0	0	0	0	0	0	0	0	0	0.00	2.5	517.43	1	92.49	1	782.15	0.5	77.01
Quercus undiff.	0	0	0	0	1	61.95	0	0	0	0	0	0	3	137.91	2	413.94	0	0	1	782.15	0	0
Alnus	0	0	0	0	0	0	0	0	0	0	2	290.28	0	0	0	0	0	0	0	0	0	0
Corylus	0	0	1	120.95	0	0	0	0	0	0	0	0	0	0	0	0	0	0	0	0	1	154.02
Carpinus undiff.	0	0	0	0	2	123.90	0	0	0	0	0	0	0	0	0	0	0	0	0	0	0	0
Castanea	0	0	0	0	0	0	0	0	0	0	0	0	0	0	0	0	0	0	1	782.15	0	0
Eucalyptus type	0	0	0	0	0	0	0	0	0	0	0	0	0	0	0	0	0	0	0	0	0	0
Populus	0	0	0	0	0	0	0	0	0	0	0	0	0	0	0	0	0	0	0	0	0	0
Aesculus type	0	0	0	0	0	0	0	0	1	62.32	0	0	0	0	0	0	0	0	0	0	0	0
Frangula	0	0	0	0	0	0	0	0	0	0	0	0	0	0	0	0	0	0	0	0	0	0
AP total	**4**	**1220.85**	**2.5**	**302.37**	**15**	**929.28**	**1**	**4617.23**	**1**	**62.32**	**2**	**290.28**	**10**	**459.70**	**23.5**	**4863.83**	**1**	**92.49**	**13**	**10167.97**	**1.5**	**231.04**
Non-arboreal (NAP) pollen																						
Amaranth.-Chenopodiaceae	3	915.64	18	2177.07	16	991.23	138	637177.95	79	4923.63	68	9869.38	103	4734.87	46	9520.70	11	1017.39	7	5475.06	23	3542.55
Poaceae	2	610.43	39	4716.98	10	619.52	1	4617.23	3	186.97	32	4644.41	13	597.60	22	4553.38	34	3144.65	10	7821.51	46	7085.10
Lactucae	8	2441.70	26	3144.65	31	1920.50	0	0	11	685.57	4	580.55	9	413.73	31	6416.12	38	3514.61	25	19553.78	14	2156.33
Cyperaceae	4	1220.85	0	0.00	17	1053.18	1	4617.23	6	373.95	1	145.14	9	413.73	13	2690.63	0	0	4	3128.61	1	154.02
Apiaceae	4	1220.85	2	241.90	2	123.90	0	0	0	0	0	0	1	45.97	3	620.91	2	184.98	5	3910.76	0	0
Asteraceae subf. Asteroideae	0	0	3	362.84	5	309.76	0	0	1	62.32	0	0	4	183.88	7	1448.80	0	0	2	1564.30	1	154.02
Sinapis type	0	0	2	241.90	2	123.90	0	0	1	62.32	1	145.14	0	0	0	0	1	92.49	4	3128.61	0	0
Cirsium	0	0	1	120.95	0	0	0	0	0	0	0	0	0	0	1	206.97	2	184.98	1	782.15	0	0
Linum	0	0	1	120.95	0	0	0	0	0	0	0	0	0	0	0	0	1	92.49	0	0	3	462.07
Filipendula	0	0	0	0	0	0	0	0	0	0	1	145.14	0	0	0	0	0	0	0	0	2	308.05
Anthemis	0	0	0	0	0	0	0	0	0	0	0	0	0	0	4	827.89	1	92.49	0	0	0	0
Centaurea	0	0	1	120.95	1	61.95	0	0	0	0	3	435.41	0	0	0	0	1	92.49	0	0	0	0
Succisa	0	0	0	0	0	0	0	0	0	0	0	0	0	0	0	0	0	0	0	0	0	0
Urtica dioica	0	0	0	0	0	0	0	0	0	0	0	0	0	0	0	0	0	0	0	0	0	0
Rumex acetosa type	1	305.21	0	0	0	0	0	0	1	62.32	0	0	0	0	0	0	0	0	0	0	0	0
Plantago cf. coronopus	0	0	0	0	0	0	1	4617.23	0	0	0	0	1	45.97	1	206.97	0	0	0	0	0	0
Scabiosa	0	0	0	0	1	61.95	0	0	0	0	0	0	0	0	0	0	0	0	0	0	1	154.02
Oxyria type	0	0	0	0	0	0	0	0	0	0	0	0	0	0	0	0	0	0	0	0	0	0
Ranunculus type	0	0	0	0	0	0	0	0	0	0	0	0	0	0	0	0	0	0	0	0	0	0
Scrophularia	0	0	0	0	0	0	0	0	0	0	0	0	0	0	0	0	0	0	0	0	0	0
Hypericum perforatum	0	0	0	0	0	0	0	0	0	0	0	0	0	0	0	0	0	0	0	0	0	0
Lotus type	0	0	0	0	1	61.95	0	0	0	0	0	0	0	0	0	0	0	0	0	0	0	0
Ononis type	0	0	0	0	0	0	0	0	1	62.32	0	0	0	0	0	0	0	0	0	0	0	0
Rumex undiff.	0	0	0	0	0	0	0	0	0	0.00	0	0	0	0	0	0	0	0	0	0	0	0
NAP total	**22**	**6714.69**	**93**	**11248.19**	**86**	**5327.85**	**141**	**651029.64**	**103**	**6419.42**	**110**	**15965.17**	**140**	**6435.74**	**128**	**26492.37**	**91**	**8416.57**	**58**	**45364.78**	**91**	**14016.17**
Aquatics/Spores																						
Potamogeton coleogoton	1	305.21	5	604.74	2	123.90	0	0	0	0	1	145.14	2	91.94	2	413.94	7	647.43	2	1564.30	3	462.07
Pteropsida monolete	0	0	0	0	0	0	0	0	0	0	0	0	2	91.94	1	206.97	0	0	4	3128.61	0	0
Sparganium emersum type	0	0	0	0	0	0	0	0	0	0	0	0	0	0	2	413.94	0	0	0	0	0	0
Nymphaea	0	0	0	0	1	61.95	0	0	0	0	0	0	0	0	0	0	0	0	0	0	0	0
Aquatics/Spores total (not included in pollen sum)	**1**	**305.21**	**5**	**604.74**	**3**	**185.86**	**0**	**0**	**0**	**0**	**1**	**145.14**	**4**	**183.88**	**5**	**1034.86**	**7**	**647.43**	**6**	**4692.91**	**3**	**462.07**
Unidentified/deteriorated	9	2746.92	0	0	11	681.47	5	23086.16	11	685.57	1	145.14	16	735.51	25	5174.29	1	92.49	20	15643.03	3	462.07
Total Pollen sum (AP/NAP)	**35**	**10682.46**	**96**	**11550.56**	**112**	**6938.59**	**147**	**678733.03**	**115**	**7167.31**	**113**	**16400.58**	**166**	**7630.95**	**177**	**36530.49**	**93**	**8601.55**	**91**	**71175.77**	**96**	**14709.28**
Added Lycopodium	**80**		**52**		**80**		**7**		**149**		**52**		**161**		**26**		**80**		**15**		**49**	
Sample mass (g)	0.82		3.18		4.04		0.62		2.15		2.65		2.70		3.72		2.70		1.70		2.65	

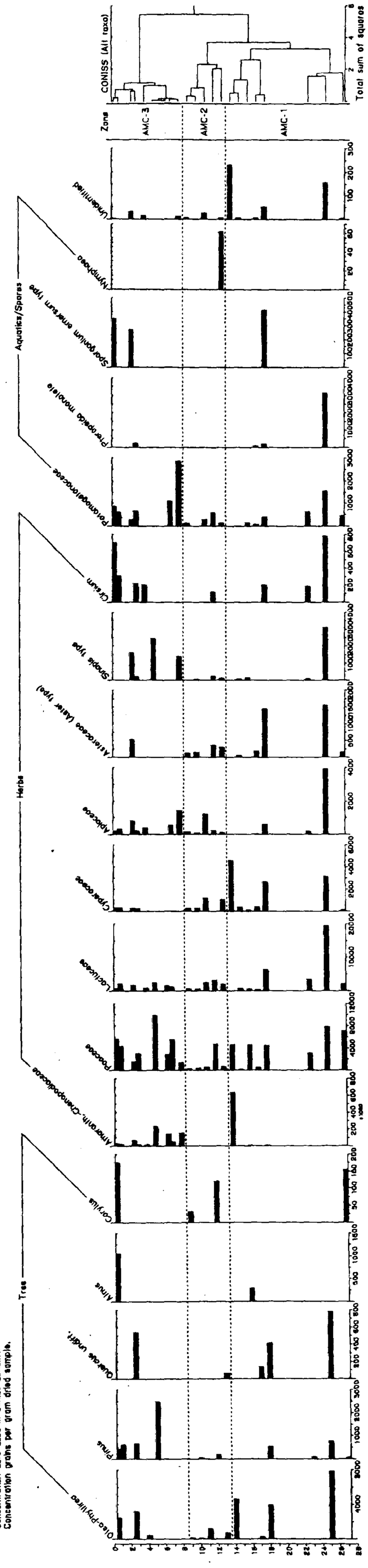

Figure 6.3.1. Concentrations of selected pollen taxa from core AMC
Concentration data used in Conlss zonation
Concentration grains per gram dried sample.

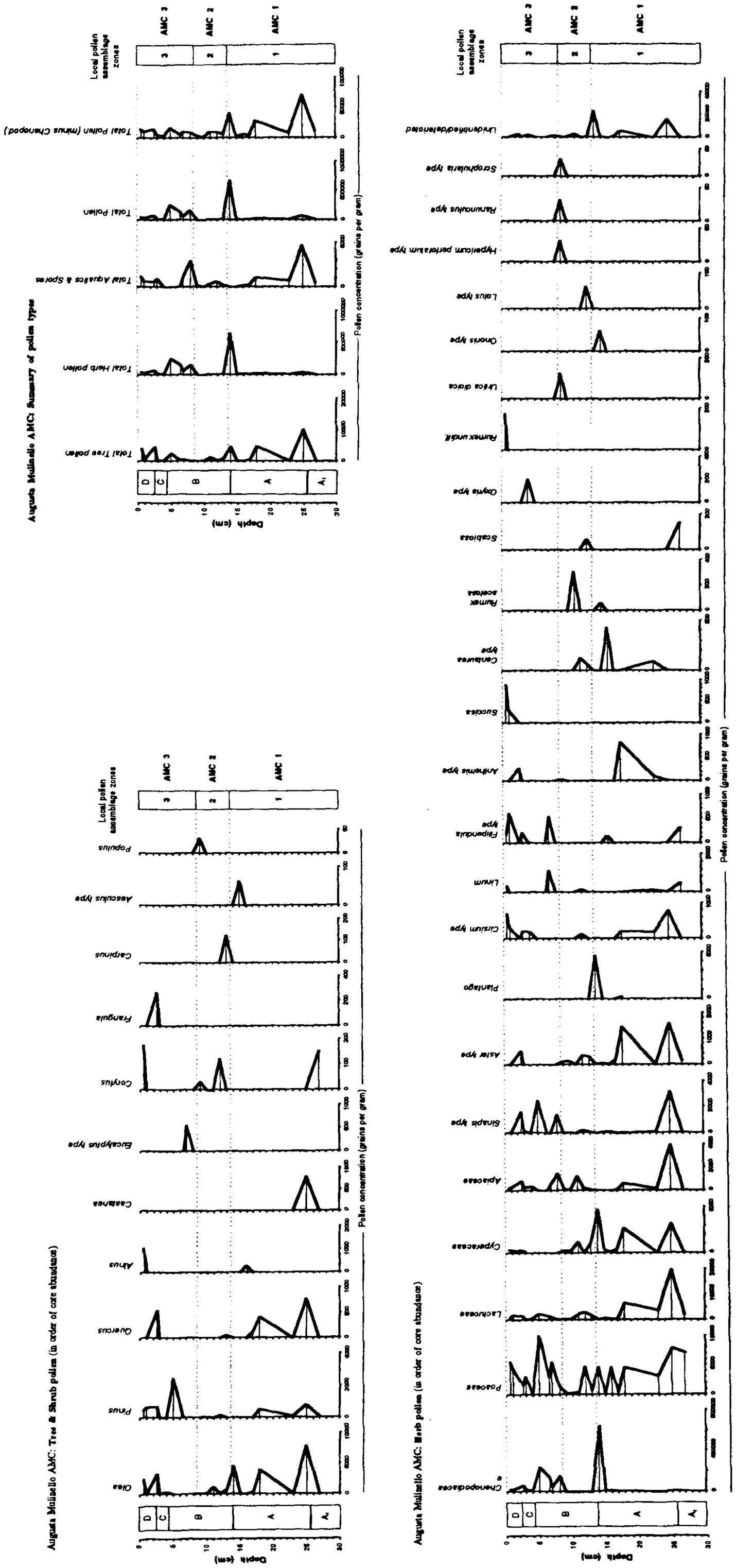

Figure 6.32. Augusta Mulinello AMC Pollen concentration diagram

Chenopodiaceae, Poaceae, Lactuceae and Cyperaceae are the dominant herb pollen types in the zone. Herb taxa apart from Amaranthaceae-Chenopodiaceae indicate a decrease in concentration from the lower samples of LPAZ AMC-1 up to AMC-2. Concentrations of Amaranthaceae-Chenopodiaceae (4.7 x 10^3 grains per gram) are checked between 16-17 cm (*circa* AD 1918) before increasing up to 14 cm (6.3 x 10^5 grains per gram).

This over-defined peak at 14 cm (*circa* AD 1945) is reflected in the increased concentrations of Cyperaceae and *Plantago* (4.6 x 10^3 grains per gram) and absence of Lactuceae. The magnitude and isolation of this solitary peak in Amaranthaceae-Chenopodiaceae pollen, coincidental with accelerated accretion, indicates that for a brief period deposition was preferential to the accumulation of organic materials and pollen deposition. As a single sample however, exhibiting a massive concentration, there is also a potential that the peak represents the incorporation of pollen-rich vegetal matter, such as a plant inflorescence.

Pollen accumulation rates in LPAZ-AMC-1 are similarly dominated by Amaranthaceae-Chenopodiaceae values. The apparent super-abundant accumulation of Amaranthaceae-Chenopodiaceae in the upper horizon of LPAZ AMC1 (3 x 10^5 grains cm^2 a^{-1}) is accompanied by increased accumulation of *Olea-Phyllirea*, Cyperaceae and unidentified/deteriorated grains (Table 6.1.8). The lower accumulation but remaining presence of Lactuceae, Poaceae, Asteraceae subf. Asteroideae and other herb pollen types in LPAZ AMC1, would indicate that the setting was in receipt of pollen from local/extra-local halophyte-ruderal plant communities *via* aquatic transport pathways.

LPAZ AMC-2: 13.5 cm to 8.5 cm depth (circa AD 1945 to circa AD 1964).

Amaranthaceae-Chenopodiaceae pollen is abruptly reduced over the transition of LPAZ AMC-1 into LPAZ AMC-2. Concentrations drop from 6.3 x 10^5 gr/g to 991 gr/g over 1 cm. Accumulation rates similarly drop (Fig. 6.3.3.). This rapid change occurs between c.1945 AD and c. 1948 AD, at the onset of increased accretion rates observed in the core up to c. 1964 AD. Lactuceae pollen responds inversely over this transition increasing from being absent at 14-13 cm to 1.9 x 10^3 at 13-12 cm. The relatively constant concentrations of Lactuceae, Poaceae, Cyperaceae and *Aster* type pollen suggest that the marsh surface was not directly replaced by distinctly different vegetation, rather local sources continued to supply pollen *via* atmospheric and aquatic transport. This period is marked by terrestrial extra local/local pollen derived from the catchment (e.g. *Olea-Phyllirea, Pinus, Poaceae*) and/or local, ruderal-disturbed ground vegetation (e.g. Lactuceae, Poaceae, Apiaceae, *Cirsium, Centaurea).*

LPAZ AMC-3: 8.5 cm to marsh surface (circa AD 1964 to AD 1995)

As rapidly as the relative abundance of Amaranthaceae-Chenopodiaceae collapsed at the LPAZ AMC-1/2 boundary, the transition to LPAZ AMC-3 is marked at 7.5 cm (*circa* AD 1970) by a return to Amaranthaceae-Chenopodiaceae concentrations observed in AMC-1. This transformation apparently occured over 1 cm or approximately 3-4 years (from *circa* AD 1964 to 1970 AD), occurring at the limit of the error margin of ^{210}Pb dates (Table 6.1.1.). This suggests that either the halophytic community responsible for local Amaranthaceae-Chenopodiaceae pollen production had recovered from prior disturbance or transport pathways supplying Amaranthaceae-Chenopodiaceae to the sediment surface had been re-established. Relatively constant and abundant pollen accumulation values of Amaranthaceae-Chenopodiaceae in the pollen zone suggests that the input of pollen was being derived from a colonising halophyte population above the core site or in the immediate locality of the core site. The abrupt transition between LPAZ AMC-2 and LPAZ AMC-3 which occurred *circa* AD 1964 and *circa.* AD 1970) is marked primarily by the increased accumulation of Chenopodiaceae, as well as the input of Apiaceae, *Sinapis* type and Potamogetonaceae, which disappeared during the period of enhanced input of Lactuceae and Asteraceae subf. Asteroideae in LPAZ-AMC-2.

Though Amaranthaceae-Chenopodiaceae dominates the pollen assemblage, concentration values of other taxa indicate more subtle variations. The increase in Amaranthaceae-Chenopodiaceae from 8 cm is mirrored by an increase in Poaceae, Lactuceae and *Sinapis* type, all of which decrease rapidly at 5 cm (*circa* AD 1983). At 5.5 cm depth (c. AD 1979) decreased accretion rates appear to have initiated a fall in Amaranthaceae-Chenopodiaceae accumulation rates. There is a significant decrease in the concentration of Amaranthaceae-Chenopodiaceae in the upper 5 cm of LPAZ AMC-3, which has seen an increase up to the surface in the concentrations of *Olea-Phyllirea*, Poaceae and other herb genera (e.g. *Cirsium*, *Filipendula and* Apiaceae).

In LPAZ AMC-3 the isolated accumulation peak in *Pinus* pollen at 9.5 cm, correlated with low accretion values (Fig. 6.3.3.) suggests an increased input of regional pollen or aquatic transport of buoyant grains unaccompanied by suspended sediment. The construction of a road-carrying barrage upstream of the site, or similar structures in the upstream channel (human-made or otherwise) may be expected to have periodically reduced sediment transport loads from the upstream catchment. Similarly this pattern may reflect some measure of marsh community maturity and surface elevation.

In the upper 4 cm of LPAZ AMC-3 a return of Amaranth.-Chenopodiaceae, Poaceae, *Olea-Phyllirea*, Lactuceae and Apiaceae is joined by a relatively constant accumulation

Table 6.1.8. Mulinello AMC: Sediment accretion and pollen accumulation rates for selected types

Depth interval	0.5	1	2.5	3	4	5	6.5	7	8	9	10	11	12	13	14	15	16	17	18
Cal. Years AD	1995	1995	1988	1988	1986	1983	1974	1974	1970	1964	1956	1952	1951	1948	1945	1940	1928	1918	1900
Accretion rate cm/a^{-1}	0.34	0.26	0.58	0.58	0.28	0.25	0.24	0.24	0.16	0.13	0.28	0.79	0.39	0.20	0.20	0.08	0.10	0.06	0.03
a) Pollen accumulation rate rates (grains/cm^2/a^{-1})																			
AP (Tree)																			
Olea	2207.05	0.00	4973.95	0.00	303.21	0.00	0.00	0.00	0.00	54.46	97.77	2555.85	0.00	393.92	2447.13	0.00	0.00	51.16	312.63
Pinus	394.12	421.05	1036.24	0.00	0.00	1633.99	0.00	0.00	0.00	0.00	29.33	0.00	187.50	0.00	0.00	0.00	0.00	0.00	41.14
NAP (Herb & Aquatic)																			
Amaranth. Chenopodiaceae	25538.75	15789.50	101136.95	26701.63	13947.54	155228.76	89669.77	30241.76	65828.57	304.99	332.42	1916.89	2250.00	525.22	337704.31	1043.81	2615.38	752.84	756.90
Poaceae	5044.69	2947.37	2486.97	4731.93	0.00	6535.95	1868.12	3516.48	609.52	108.92	273.76	1277.93	4875.00	328.26	2447.13	39.64	1230.77	95.02	361.99
Unidentified deteriorated	157.65	0.00	4973.95	0.00	1212.83	0.00	0.00	0.00	609.52	283.20	254.21	5750.67	0.00	361.09	12235.66	145.34	38.46	116.95	411.36
Lactuceae	472.94	1473.69	2486.97	0.00	606.41	1633.99	934.06	703.30	0.00	206.96	391.09	5111.71	3250.00	1017.62	0.00	145.34	153.85	65.78	510.08
Cyperaceae	315.29	210.53	414.50	338.00	0.00	0.00	0.00	0.00	0.00	98.03	195.54	2555.85	0.00	558.05	2447.13	79.28	38.46	65.78	213.91
Apiaceae	157.65	210.53	1243.49	338.00	303.21	0.00	0.00	351.65	609.52	54.46	58.66	2555.85	250.00	65.65	0.00	0.00	0.00	7.31	49.36
Potamogetonaceae	788.23	421.05	414.50	1013.99	0.00	0.00	0.00	703.30	1219.05	43.57	0.00	638.96	625.00	65.65	0.00	0.00	38.46	14.62	32.91
Sinapis type	0.00	0.00	2486.97	338.00	0.00	1633.99	0.00	0.00	609.52	0.00	39.11	0.00	250.00	65.65	0.00	13.21	38.46	0.00	0.00
Asteraceae (Aster type)	0.00	0.00	828.99	0.00	0.00	0.00	0.00	0.00	0.00	43.57	117.33	0.00	375.00	164.13	0.00	13.21	0.00	29.24	115.18
Cirsium	630.59	210.53	0.00	338.00	151.60	0.00	0.00	0.00	0.00	0.00	0.00	0.00	125.00	0.00	0.00	0.00	0.00	0.00	16.45
Total pollen influx	38544.59	22315.82	124555.96	34475.52	16676.41	166666.67	92471.95	36923.08	69485.71	1307.09	1789.23	23002.69	12562.50	3775.04	359728.51	1519.47	4384.62	1242.56	2986.45

b) Pollen accumulation rate rates (grains/cm^2/a^{-1}) Sorted by correlation values between sediment accretion and pollen accumulation rate (r) sed. accretion

AP (Tree)																				
Olea-Phyllirea	2207.05	0.00	4973.95	0.00	303.21	0.00	0.00	0.00	0.00	54.46	97.77	2555.85	0.00	393.92	2447.13	0.00	0.00	51.16	312.63	0.57
Pinus	394.12	421.05	1036.24	0.00	0.00	1633.99	0.00	0.00	0.00	0.00	29.33	0.00	187.50	0.00	0.00	0.00	0.00	0.00	41.14	0.18
NAP (Herb & Aquatic)																				
Apiaceae	157.65	210.53	1243.49	338.00	303.21	0.00	0.00	351.65	609.52	54.46	58.66	2555.85	250.00	65.65	0.00	0.00	0.00	7.31	49.36	0.81
Lactuceae	472.94	1473.69	2486.97	0.00	606.41	1633.99	934.06	703.30	0.00	206.96	391.09	5111.71	3250.00	1017.62	0.00	145.34	153.85	65.78	510.08	0.74
Cyperaceae	315.29	210.53	414.50	338.00	0.00	0.00	0.00	0.00	0.00	98.03	195.54	2555.85	0.00	558.05	2447.13	79.28	38.46	65.78	213.91	0.47
Potamogetonaceae	788.23	421.05	414.50	1013.99	0.00	0.00	0.00	703.30	1219.05	43.57	0.00	638.96	625.00	65.65	0.00	0.00	38.46	14.62	32.91	0.47
Asteraceae (Aster type)	0.00	0.00	828.99	0.00	0.00	0.00	0.00	0.00	0.00	43.57	117.33	0.00	375.00	164.13	0.00	13.21	0.00	29.24	115.18	0.37
Poaceae	5044.69	2947.37	2486.97	4731.93	0.00	6535.95	1868.12	3516.48	609.52	108.92	273.76	1277.93	4875.00	328.26	2447.13	39.64	1230.77	95.02	361.99	0.35
Sinapis type	0.00	0.00	2486.97	338.00	0.00	1633.99	0.00	0.00	609.52	0.00	39.11	0.00	250.00	65.65	0.00	13.21	38.46	0.00	0.00	0.32
Unidentified deteriorated	157.65	0.00	4973.95	0.00	1212.83	0.00	0.00	0.00	609.52	283.20	254.21	5750.67	0.00	361.09	12235.66	145.34	38.46	116.95	411.36	0.30
Cirsium	630.59	210.53	0.00	338.00	151.60	0.00	0.00	0.00	0.00	0.00	0.00	0.00	125.00	0.00	0.00	0.00	0.00	0.00	16.45	0.25
Amaranth. Chenopodiaceae	25538.75	15789.50	101136.95	26701.63	13947.54	155228.76	89669.77	30241.76	65828.57	304.99	332.42	1916.89	2250.00	525.22	337704.31	1043.81	2615.38	752.84	756.90	-0.04
Total pollen influx	38544.59	22315.82	124555.96	34475.52	16676.41	166666.67	92471.95	36923.08	69485.71	1307.09	1789.23	23002.69	12562.50	3775.04	359728.51	1519.47	4384.62	1242.56	2986.45	0.68

Figure 6.3.3. Accumulation rates of selected pollen genera; Mulinello AMC (0-17 cm depth). Ordered L-R by r - values determined between correlation of pollen accumulation rate and sediment accretion rate.

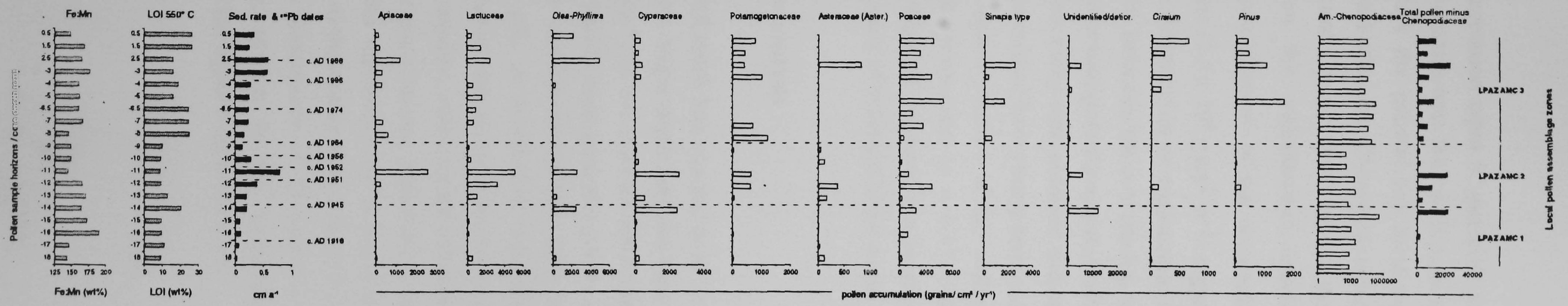

r - with accretion rate	r = 0.80	r = 0.73	r = 0.57	r = 0.47	r = 0.47	r = 0.37	r = 0.34	r = 0.32	r = 0.29	r = 0.25	r = 0.18	r = -0.04	r = 0.68

of wetland/aquatic vegetation types (Cyperaceae and Potamogetonaceae). As accretion remained relatively constant over the last 5 years up to AD 1995, pollen accumulation rates appear to reflect the present-day local vegetation and depositional setting. Dominated by Amaranthaceae-Chenopodiaceae, the accumulation of Poaceae, Lactuceae, Apiaceae and *Cirsium* types reflects the local ruderal and disturbed ground plant community on the embankment overlooking the site. A decrease in Amaranthaceae-Chenopodiaceae pollen accumulation between 2.5 cm (1.0×10^5 gr/cm^2/yr^{-1}) and 0.5 cm (2.5×10^4 g cm^2 yr^{-1}) suggests a local population decline (due to recent marsh surface degradation or taphonomic factors. Continued *Pinus* and *Olea-Phyllirea* accumulation indicates the core site has become preferential to the deposition of atmospheric and water-transported grains derived from the local catchment.

Indicated by their relationship with sediment accretion rates (Fig. 6.3.3.), differences in the type of pollen accumulated have clearly been controlled by variable rates of sediment input and changing hydrodynamics of the wetland site. The presence and positive correlation of Potamogetonaceae ($r = 0.47$) with accretion rates would support radiometric and geochemical evidence that [catchment-freshwater] channel processes have influenced the supply of sediment to the marsh setting during the last century.

6.1.15 AMC: Diatom analysis

Diatom analysis proved much less conclusive in terms of determining past depositional changes at the core site. Eight depth horizons were sampled and counts determined by Dr. P. Collins, of which only two (Surface and 6 cm) yielded identifiable valves (Cundy *et al.* 1998). Diatom valves were generally poorly preserved in samples from the core. Damage to the valves was determined as to have been caused by transport processes a change in sediment pH, or destructive ingestion by grazing molluscs and other invertebrates. The diatom assemblages found were indicative of a range of aquatic habitats and potential sources, reflecting the estuarine nature of the setting. A key finding however, was the absence of marine planktonic forms, reflecting the microtidal range of the setting. The greater representation of freshwater species (e.g. *Navicula angusta, Nitzschia perminuta*) at the surface than at depth (6 cm) may represent an increase in the last 20 years of the dominance of Mulinello channel-catchment controls on the depositional setting, similar to the accumulation of catchment pollen (e.g. Potamogetonaceae) in the upper 5 cm of the core.

CHAPTER SIX

RESULTS FROM PANTANO PICCOLO

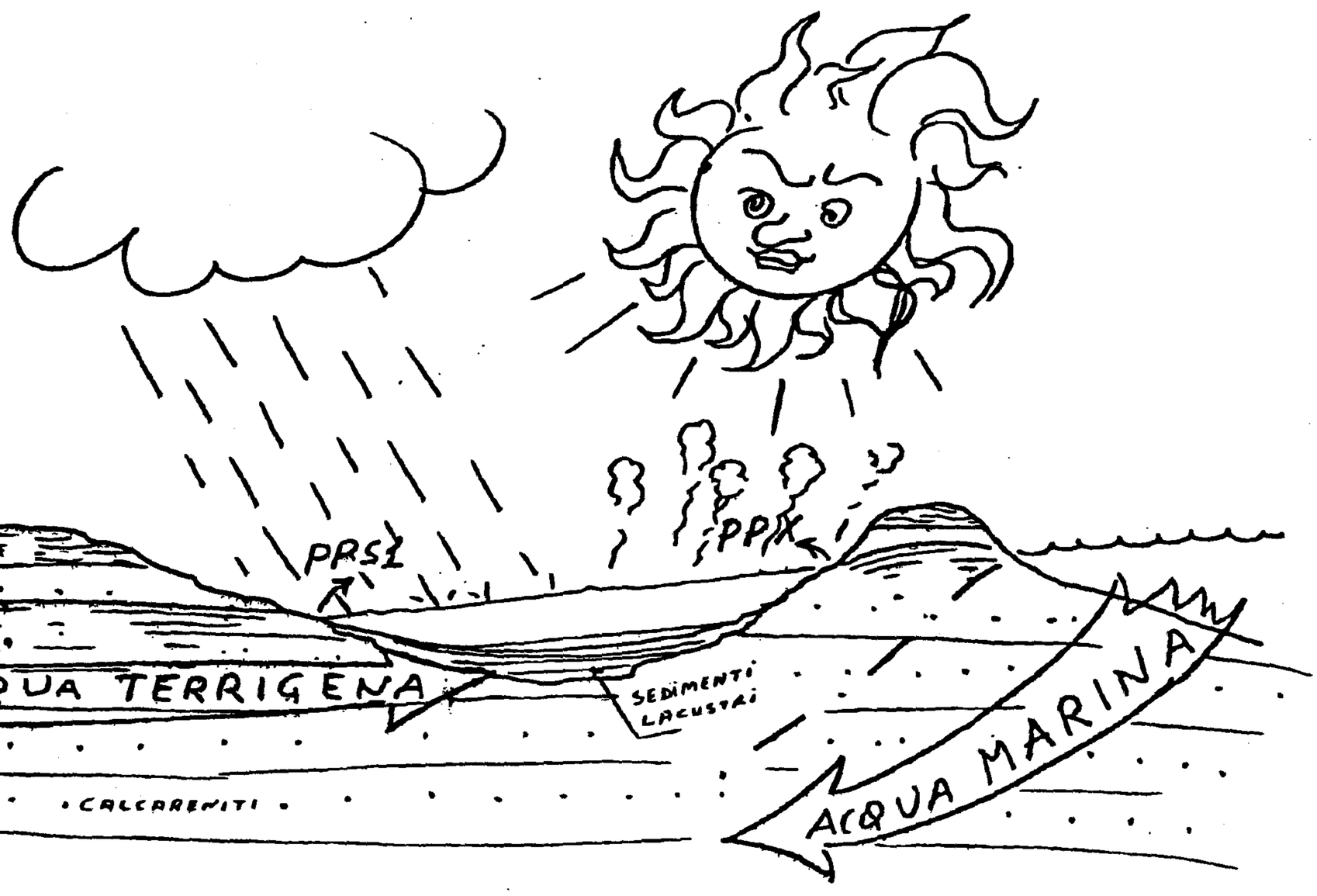

Diagram taken from Badalamenti *et al.* (1985).

6.2 RESULTS FROM PANTANO PICCOLO, VENDICARI

6.2.1 Site description

Pantano Piccolo is the smallest brackish lagoon (approx. 20 ha) of the Vendicari coastal lagoon system (Fig. 6.4.). The N-S oriented lagoon is enclosed on three sides by *garrigue-macchia* vegetation and historically cultivated fields, developed on Pliocene-Pleistocene shallow marine and coastal sediments (Fig.6.4.1./Plate 6.4.).

Forming a narrow fringe around the margin of the lagoon, brackish and salt tolerant (halophyte) vegetation has developed in response to local variations in growing conditions. Differences in hydrological-growing conditions are observable from plant communities around the lagoon. On the western margin stands of *Phragmites* and *Juncus* sp. are prevalent, whereas at the other margins more salt tolerant *Salicornia* sp and *Arthrocnemum glaucum* predominate.

Access to the sea is restricted by a narrow bedrock peninsula which parallels the eastern lagoon margin, dune barriers developed during the Holocene evolution of the Vendicari embayment and embankments constructed in the last 100-200 years for the local salina operations. Pantano Piccolo is separated from the adjoining Pantano Grande (Fig. 6.4.) by a rubble-earth barrier (approx. 6 m wide) at its southern end (Plate 6.3); constructed to utilise the lagoon as a reservoir for salt workings in Pantano Piccolo and to carry traffic for the now dis-used salinas and tuna fishery/processing plant.

Whereas water levels in the other lagoons of the Vendicari complex are greatly affected by seasonal discharge from the Saia-Scirbia river catchment, seasonal rainfall and the configuration of the *Foci del Pantano Sichilli* (Plate 4.3.), major water level variations in Pantano Piccolo are mediated by groundwater recharge. Freshwater springs at the margin of the lagoon occur at the interface between less permeable marls and permeable calcarenites (Dongarrà *et al.* 1985), which combined with the lagoons proximity to the sea indicates that the lagoon represents a local saline (seawater) and fresh groundwater mixing environment. Saline and fresh groundwater recharge into the lagoon, and the enhanced precipitation storage capacity caused by artificial impoundment, largely limits the extent of aerial exposure of benthic sediments during periods of low rainfall.

Previous measurements undertaken of lagoon water chemistry in Pantano Piccolo, indicate a clear relationship with seasonal climatic and hydrological conditions (Fig. 6.4.2.) (Dongarra *et al.* 1985). Measurements during the period November 1983 to November 1984, recorded minimum salinity in February (TDS = 49.5 gr/l) as a consequence of low evaporation and winter precipitation (Fig. 6.4.2). Maximum salinity was reached (total dissolved solid (TDS) = 168.8 gr/l) in September after steadily

Figure 6.4. Location map of Pantano Piccolo and the Vendicari lagoons, SE Sicily.

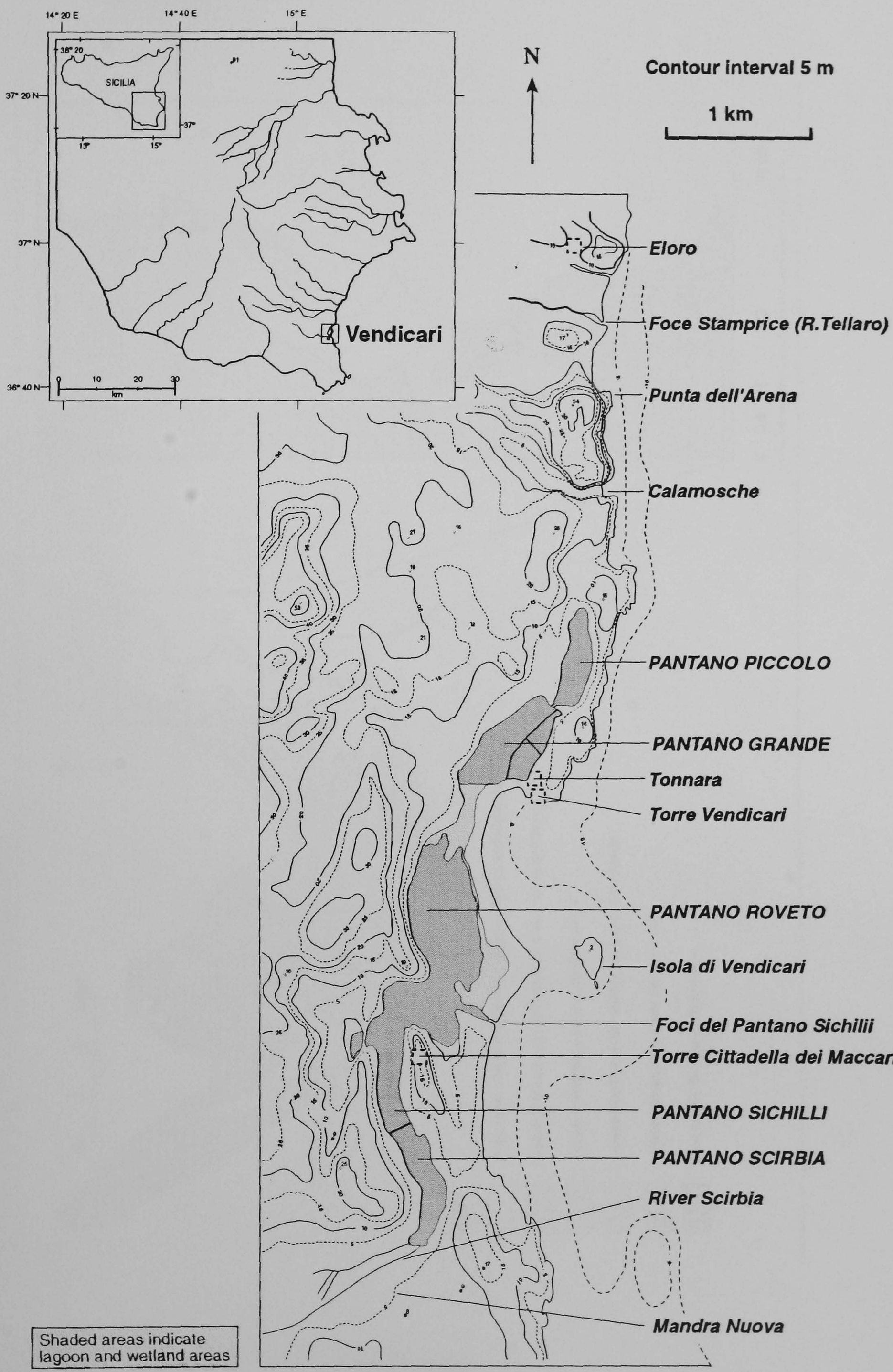

Topographic information from I.G.M (1969)

Figure 6.4.1. Geology of the Vendicari drainage catchment and coastline; (a) Geology of the River Scirbia (After Amore *et al.* 1994 and (b) Geological units at Vendicari (From Ruggieri, 1959)

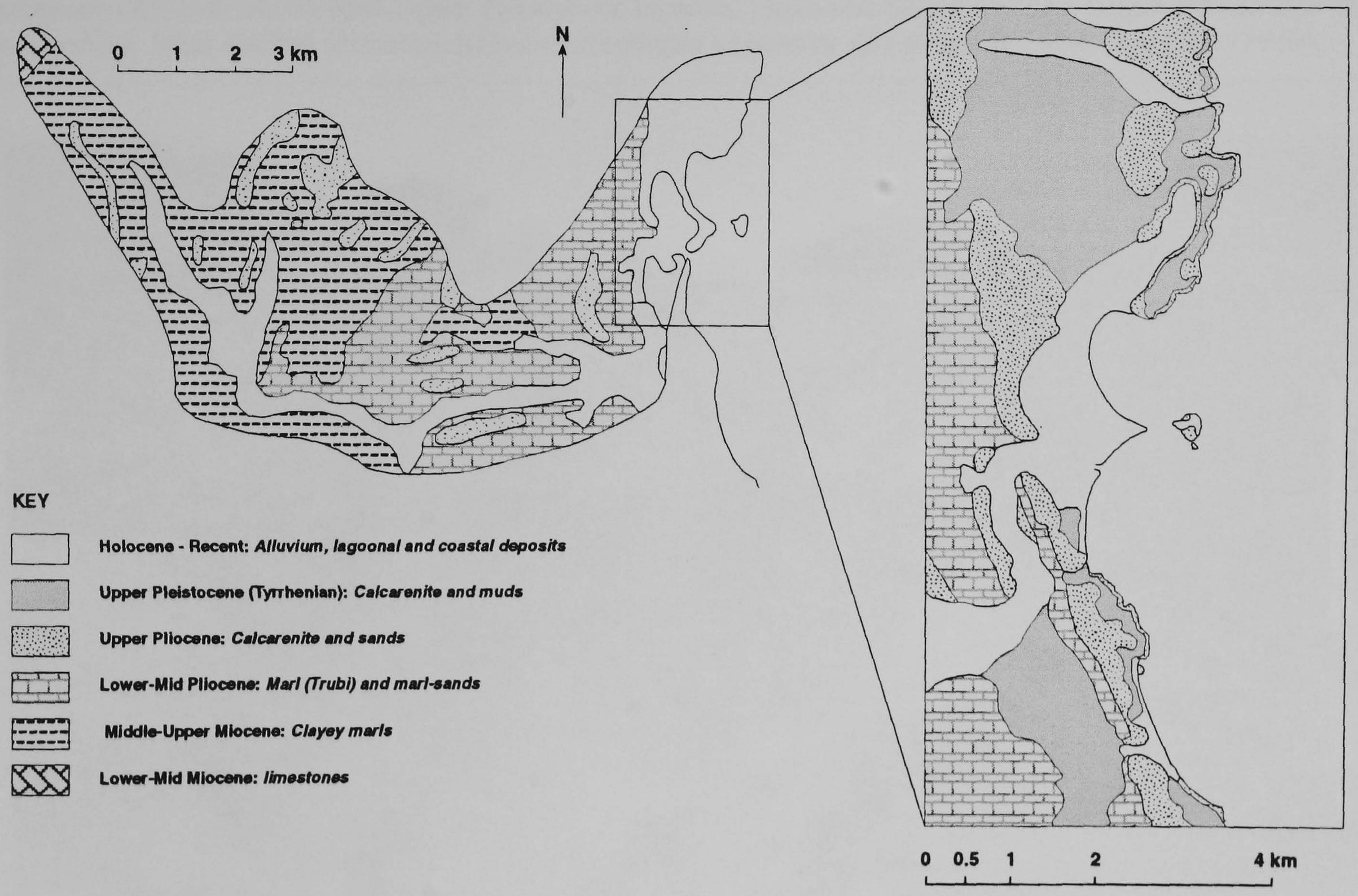

Plate 6.4. Coastal cliff section of geological units(450 m NE of Torre Vendicari) Ve ndicari. Upper Pliocene sandstone (A), overlain by Mid-Upper Pleistocene lagoonal muds and discordantly by Upper Pleistocene sand or *panchina.* Note infilled (dissolution) hollows/collapse structures (S) in unit B. After Ruggieri (1959).

increasing through the summer months of low or absent rainfall and increased evaporation (Dongarra *et al.* 1985).

As a result of seasonal salinity variations, periods of increased evaporation allow the formation of evaporitic minerals (predominantly gypsum and halite) in benthic sediments of the lagoon and as a surface crust at the lagoon margin. Fresh water inflow during the winter months has been observed to allow some re-dissolution of previously deposited evaporitic minerals, e.g. $CaSO_4$ [H_2O], NaCl and $CaCO_3$ (Dongarra *et al.* 1985; Badalamenti *et al.* 1985). Due to its enclosed nature and hydrological balance, the major ionic aquatic chemistry of Pantano Piccolo may be expected to have exerted a significant control on the major element geochemistry of recent sediments.

The lithology, macrofaunal content and spatial distribution of lagoon sediments in Pantano Piccolo has previously been described by Amore *et al.* (1994). As such only a summary of the findings from the study by Amore *et al.* (1994) are given here. Results from grain size analyses of recent sediments from Pantano Piccolo range between fine sands and very fine silts, which are poorly sorted to unsorted. The composition of the inorganic component was found to be quite uniform, formed of carbonate clasts, quartz and heavy minerals (Fig. 6.4.3.).

Macrofaunal remains dominate the organic fraction, with assemblages of bivalves, gastropods, echinoderms, ostracods and foraminifera. Molluscan remains are dominated by brackish-euryhaline species, i.e. *Hydrobia gr. ventrosa*, *Cerastoderma glaucum* and *Abra ovata*. Sediments at depth were observed to increase in inorganic content due to carbonate clasts, while decreasing in macrofossil content (Fig. 6.4.3.).

The bulk sampling technique and low resolution used by Amore *et al.* (1994) serves a useful purpose in suggesting an evolutionary background and contempoary sedimentology of Pantano Piccolo (and the other lagoons in the complex), but is clearly inadequate in discerning subtle depositional changes which may have been recorded in the lagoon sequences, on a scale of a few centimetres or less.

6.2.2 Historical land-use and occupation around Pantano Piccolo

Though the coastal landscape around Pantano Piccolo contains much evidence of long term past land-use and human activity, the principal causes influencing recent (over approximately the last two hundred years) lagoon deposition are expected to have forced changes to the hydrology of the lagoon and patterns of cultivation-abandonment of the surrounding slopes.

Within the lagoon itself, wall structures visible below the water surface on air photographs taken in AD 1943 are oriented west-east and traverse the water body (Fig.

Figure 6.4.2. Annual variation in water quality of Pantano Piccolo (Dongarra *et al.* 1985)

(a) pH and temperature (°C)

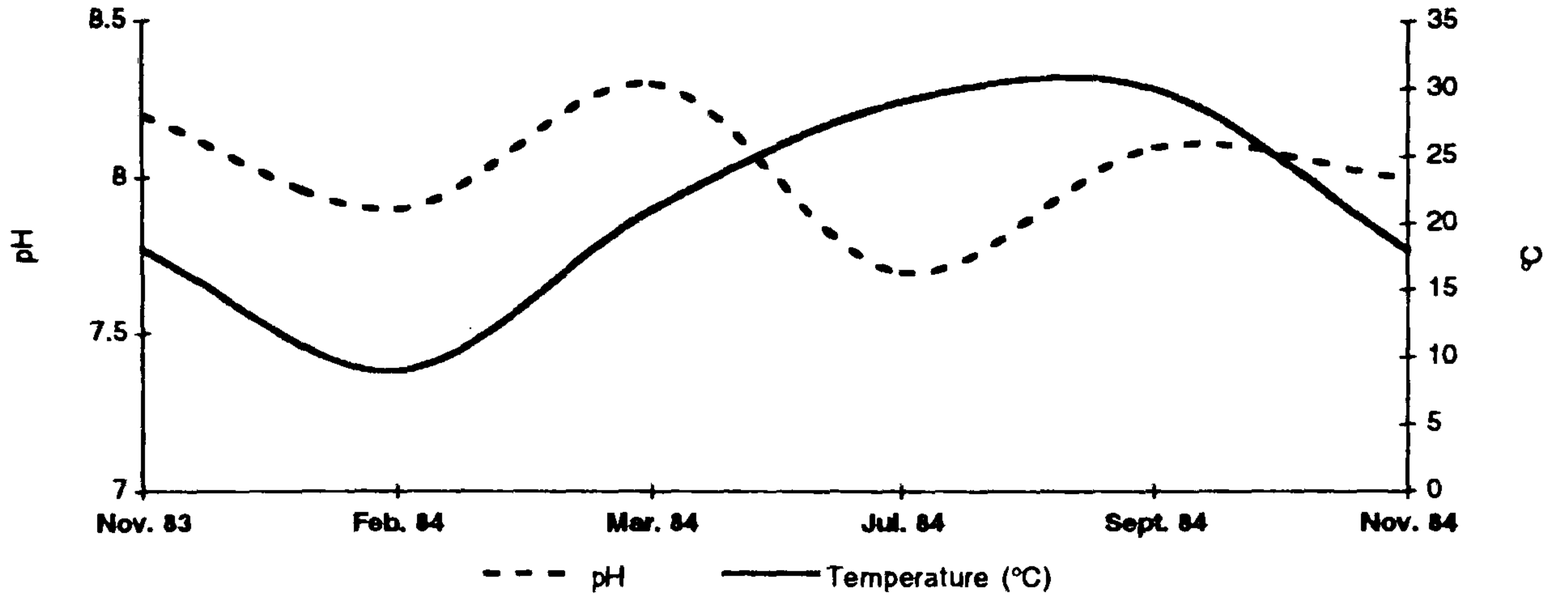

(b) dissolved Si and total dissolved solids (note scale differences)

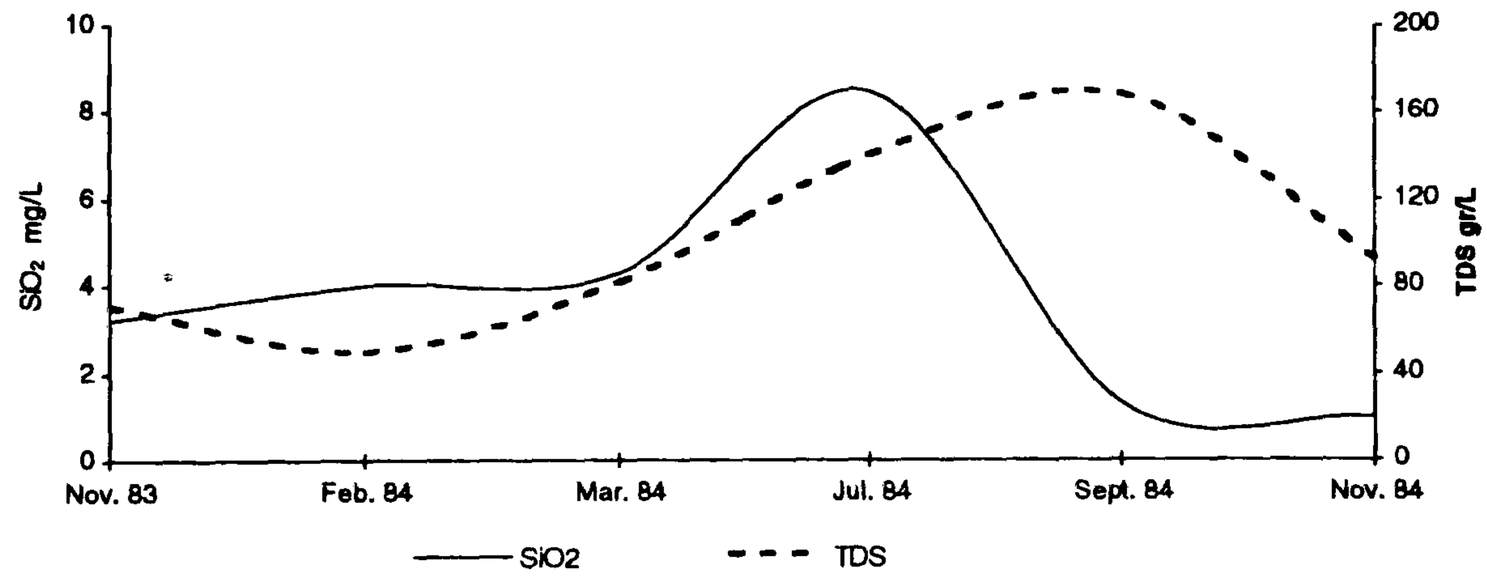

(c) Ionic chemistry of lagoon waters during period of years

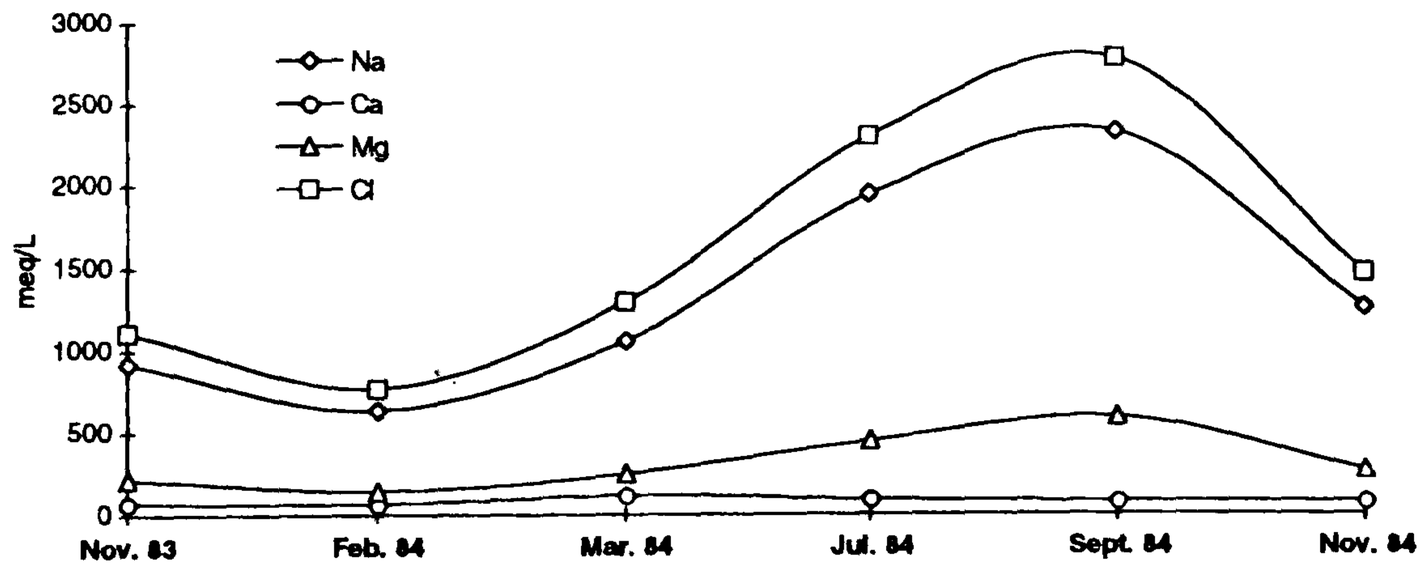

Figure 6.4.3 Sediment characteristics of Pantano Piccolo, Vendicari. Representative depth samples of lagoon stratigraphy: (1) Surface to 10 cm; (2) 10-20, 30 cm; (3) 20,30 - 50, 60 cm and (4) greater than 60 cm. (After Amore *et al.* 1994).

(a) Inorganic fraction of sample (mean %)

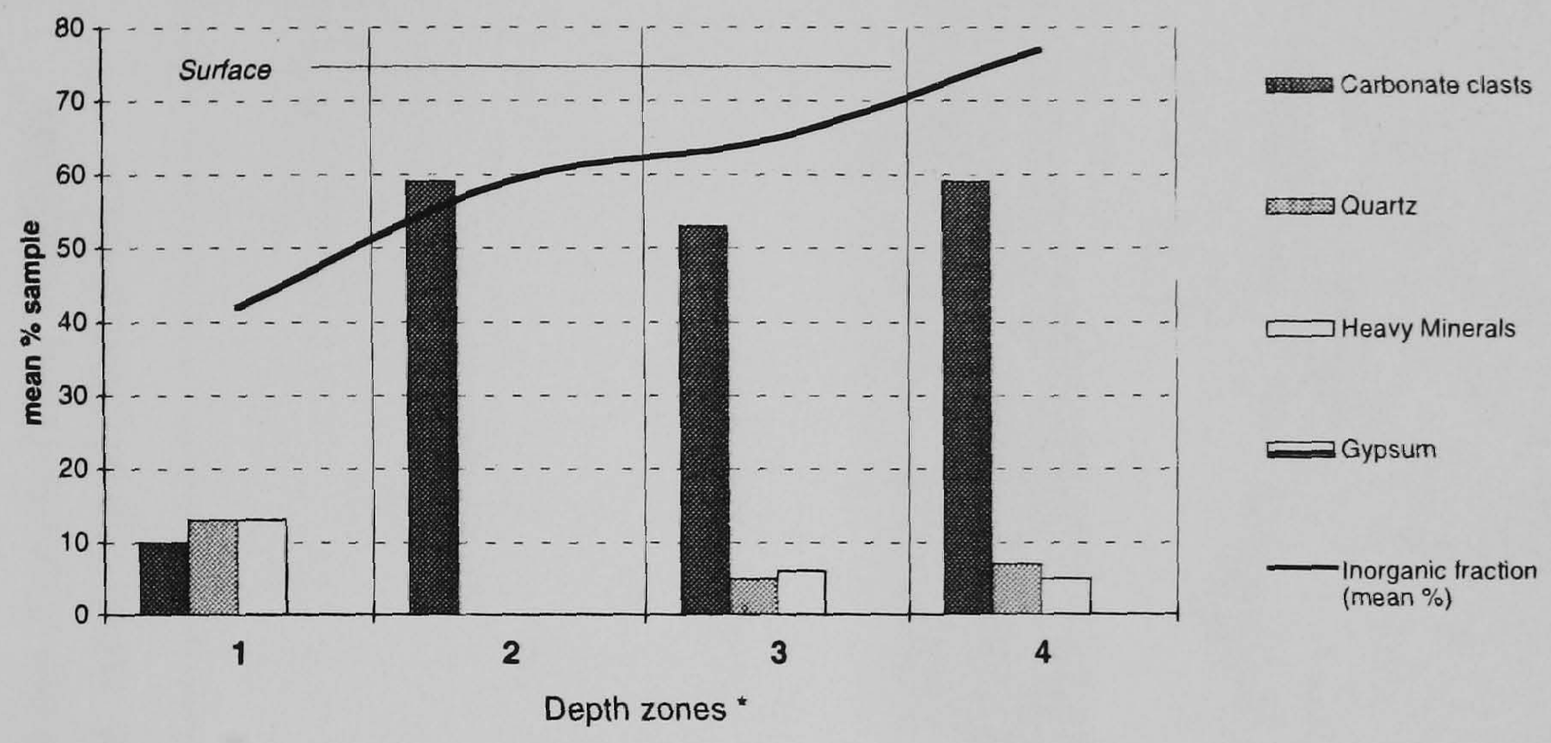

(b) Organic fraction of sample (mean %)

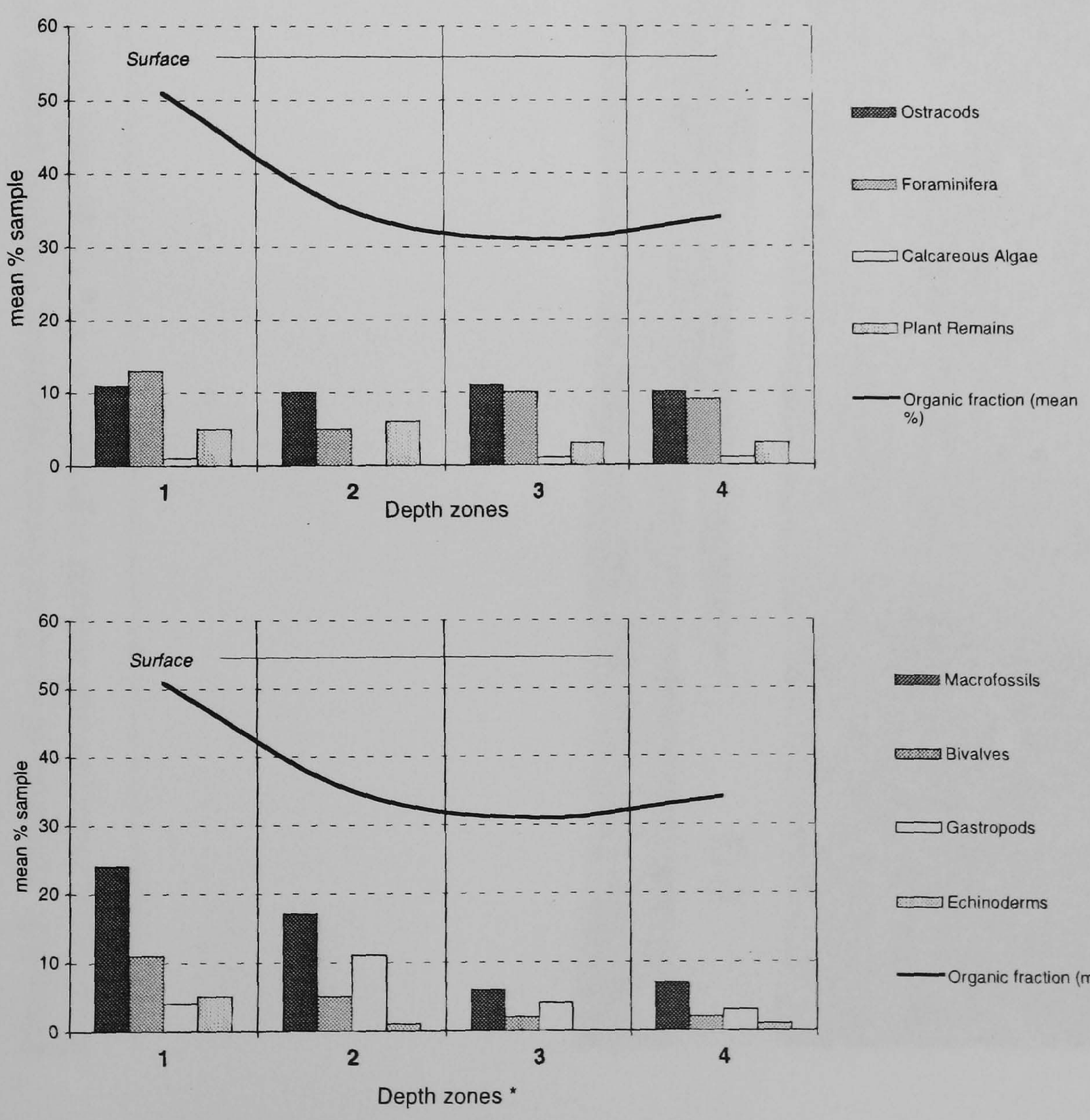

Plate 6.5. Remains of artificial barrier separating Pantano Grande (PG) and Pantano Piccolo (PP), Vendicari. Recovering *macchia* and ruderal vegetation in the foreground. View looking west from top of peninsula..

6.4.5.). The construction of these walls would have benefitted salina operations by impeding drainage from Pantano Piccolo into Pantano Grande, resulting in a more controllable supply of saline-brackish water during the summer months. Also clearly visible from air photographs at the time is the embankment constructed to separate Pantano Piccolo and Pantano Grande (Plate 6.5.) and the arterial network of channels and salt pans (Fig. 6.4.2.). The hydraulic gradient created by artificially raising water levels in Pantano Piccolo, with outflow controlled by a sluice, would clearly have been beneficial in transporting water to salt pans and where required in Pantano Grande.

Pantano Grande was used for salt panning, as a subsidiary industry of the nearby tuna fishery from the 18th century onwards. Both industries had finished by the mid-20th century, as a result of allied bombing in AD 1943 (destroying the tuna fishery) and irrecoverable flood damage to the salinas in AD 1951 (Amore *et al.* 1994). Pantano Piccolo and Pantano Grande were also utilised in the past by the local population for seasonal *Anguilla* (eel) fishing.

Subsistence-Peasant agriculture under the *latifondia* system (see Chapter 4) has probably typified the land use around Pantano Piccolo over the last 200-500 years, combining animal grazing with harvesting olives, vines, almonds and other cultivable crops (e.g. *Cichorium intybus*) managed by large familial farmhouses (*Masserie*). A number of these estates managed the land around Vendicari; the *Casa della Banca* to the east of Pantano Piccolo, the farmhouses of *Loreto-Messina* and *Santuccio* east of Pantano Grande and the *Casa dell'Cittadella* situated between Pantano Scirbia and the coast.
A network of stone-walled field boundaries surround the lagoon, running down to the lagoon edge and forming small enclosures on either side of the water body (Fig. 6.4.5.). Low walls (< 1 m) at the lagoon margin were almost certainly constructed to protect cultivated areas from high water levels, for example at the northern margin of the lagoon where the surrounding slope gradient is less and the fetch of waves has a greater potential distance to cause wave erosion than the western and eastern margins. Evidence of large scale and local rock quarrying is also apparent in the coastal and inland landscape around Pantano Piccolo (Fig. 6.4.5.). Rock surfaces on the calcarenite-marl peninsula to the east are pockmarked by quarries which may be of ancient or historical origin. Small-scale quarrying appears to have also occurred on the western slopes of Pantano Piccolo, indicated by cut surfaces on calcarenite outcrops.

Figure 6.4.4. Air photograph mosaic of Pantano Piccolo and Pantano Grande, Vendicari, SE Sicily. Taken 10 May 1943 by Royal Air Force.

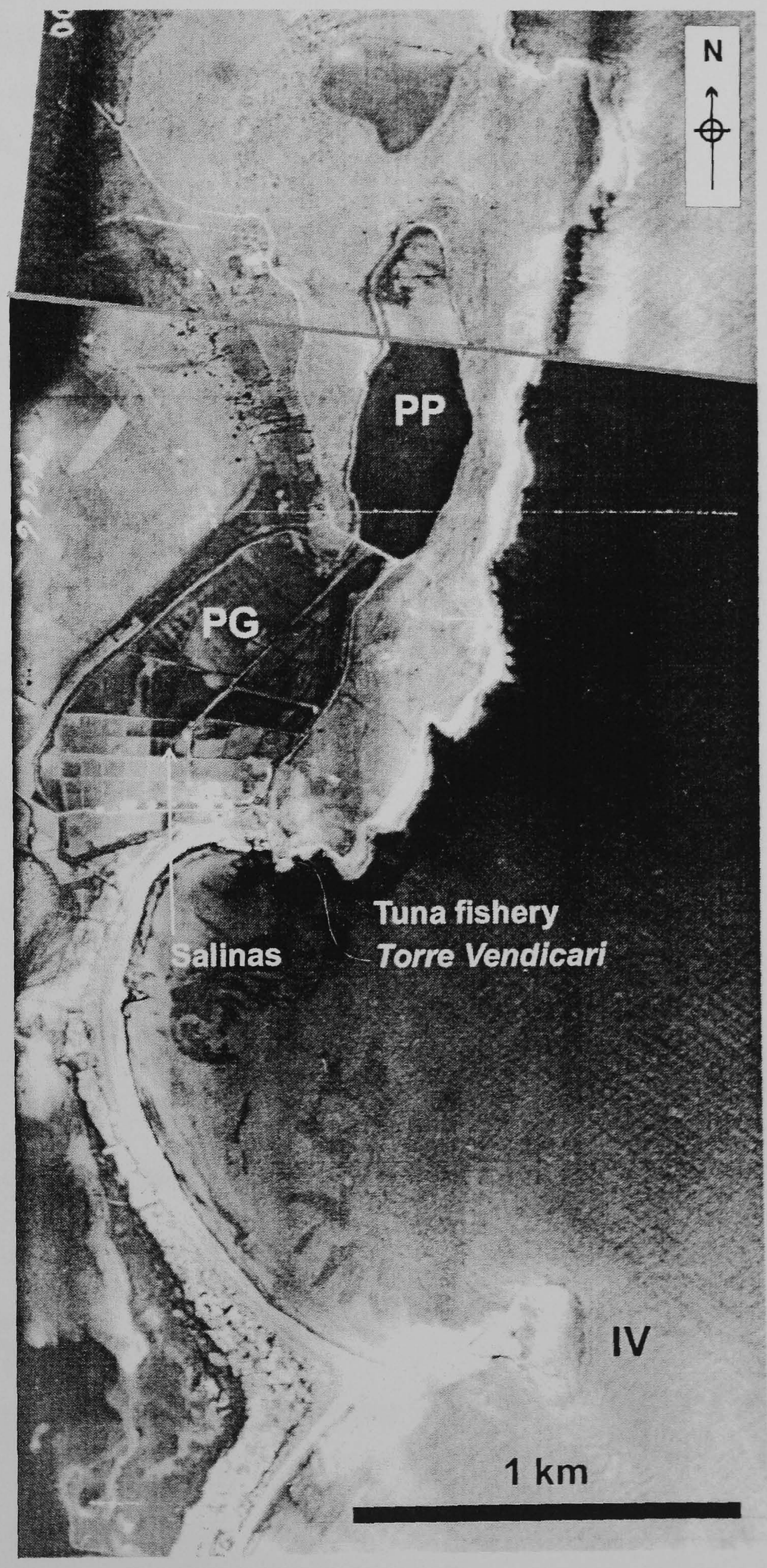

PP = Pantano Piccolo

PP = Pantano Grande

IV = Isola di Vendicari

Figure 6.4.5. Field boundaries and lagoon features around Pantano Piccolo, Vendicari

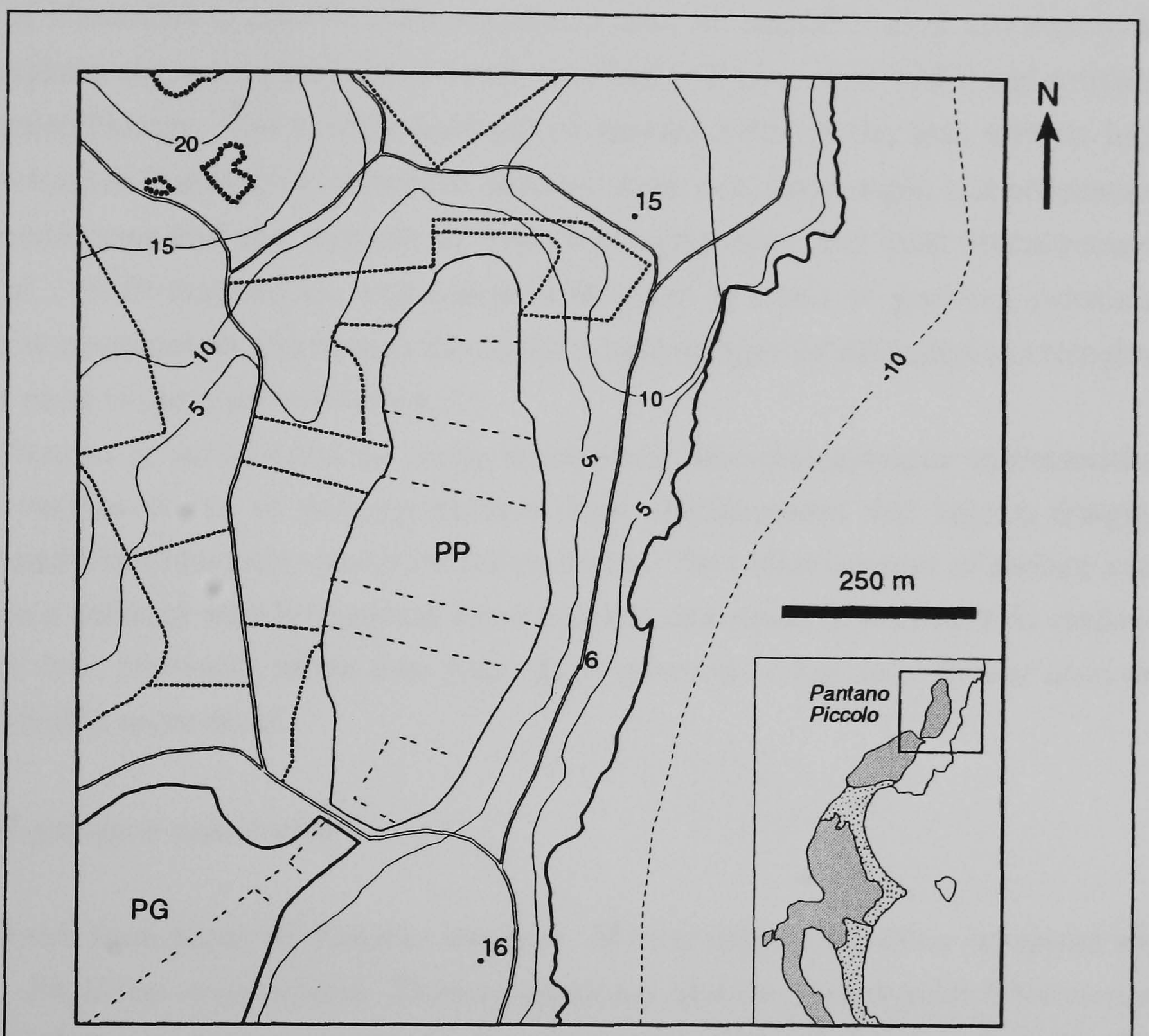

Key

salina embankments and submerged features observed in air photographs (1943)

stone wall field boundary

track-pathway

quarry

spot heights and contours (metres above sea level) (I.G.M. 1969)

PG Pantano Grande

PP Pantano Piccolo

6.2.3 Vegetation in the vicinity of Pantano Piccolo, Vendicari

The area of Vendicari is considered a conserved relic of natural coastal environments, once widespread along the coastline of south-east Sicily (Brullo *et al.* 1980) and southern Mediterranean Europe. The current diversity of species found in the area reflects local geomorphological features, i.e. substrate, distance from sea, slope angle and orientation, climatic conditions and the impacts of historical agriculture and land abandonment. Brullo *et al.* (1980) mapped the vegetation of the area in terms of growing substrate, hydrological environment and human disturbance, and recognised nine phytosociological vegetation units in the reserve (Table 6.2.).

Pantano Piccolo is surrounded by more established *Macchia-garrigue* communities, slopes in various stages of post-agricultural land abandonment and lagoon fringing halophyte and fresh-brackish vegetation communities. The pollen content of surface soils sampled on a transect which traversed these types is described in Section 6.5. (below). Because of their proximity to the core sites, the vegetation of the three former units are here described in more detail;

i) *Macchia-garrigue association*

The low shrub formations of *Pistacia lentiscus, Myrtus communis, Olea europaea* var. *sylvestris, Phyllirea angustifolia, Thymus capitatus* and the dwarf palm *Chamaerops humilis* are characteristic species of the *macchia-garrigue* vegetation found on the thin terra-rossa soils overlying the Plio-Pleistocene geology in the vicinity of Pantano Piccolo. The association includes *garrigue* forms of *macchia* species, found in the vicinity of the sea and in areas where less favourable growing conditions exist, e.g. in the vicinity of dis-used quarries. The association in the area represents what may be considered the climax or xero-mediterranean vegetation of the arid, south east corner of Sicily. This was likely to have developed early in the Holocene, compared to its more common place secondary role of succession from an *Ilex* association, which was degraded by early patterns of human occupation in the rest of the island (Chester *et al.* 1985).

On the seaward side of the rocky peninsula east of Pantano Piccolo *Myrtus communis* is unable to develop into higher shrubs due to the aridity and exposure of the coastal setting and occurs as low, anemomorphic forms (Plate 6.5.). On the lee slope of the peninsula, *macchia* and *garrigue* species have developed a dense blanket of vegetation extending down to the lagoon edge. Interspersed between *macchia* and *garrigue* species is a

Table 6.2. Phytosociological units recognised in Vendicari (Brullo *et al.* 1980).

Phytosociological Association	Environment	Species present
a) *Macchia* and Garrigue	Plio-Pleistocene solid geology Headlands and cliffed coastline.	*MACCHIA: Pistacia lentiscus, Myrtus communis, Olea europaea (var.sylvestris,) Myrtus communis, Phyllirea angustifolia, Chamaerops humilis,*
	Stabilised coastal sand areas	*MACCHIA: Juniperus macrocarpa, Ephedra fragilis, Pistacia lentiscus, Phyllirea angustifolia, Clematis cirrhosa.*
	More eroded-degraded areas	GARRIGUE: *Thymus capitatus, Sarcopoterium spinosum, Chamaerops humilis, Teucrium fruticans*
b) Salt tolerant cliff-shore species	Coastal cliffs and outcrops	*Limonium sp., Crithmum maritimum, Silene sedoides, Plantago macrorhiza, Cichorium spinosum.*
c) Xerophyllous herbs and ephemerals	Clearings in *Macchia* & Garrigue	*Desmazeria sicula, Catapodium marinum, Anthemis secundiramea, Plantago coronopus, Iris sisyrichium, Trifolium scabrum, Lotus edulis, Hyparrhenia hirta,* perennial *graminacea*
d) Psammophyllous ephemerals (halo-nitrophyllous)	Dune colonisation	*Cakile maritimae, Salsola kali, Atriplex tornabeni, Euphorbia peplis, Polygonum maritimum*
e) Psammophyllous perennials	Coastal Dunes	*Eryngium maritimum, Cyperus kallii, Cutandia maritima, Agropyron junceum, Sporobolus arenarius, Medicago marina, Ononis ramosissimae, Centaurea sphaerocephala, Scabiosa maritima, Lotus creticus*
f) Halophytic wetland vegetation	Lagoon margins	*Juncus acutus, Holoschoenus australis, Plantago crassifolia, Salicornia fruticosa, Arthrocnemum glaucum, Limonium sp., Triglochin bulbosum*
g) Fresh-brackish wetland vegetation	Submerged areas of fresh-slightly saline water. Variations in water depth. Rear dune-lagoon margins	*Phragmites australis, Schoenoplectus lacustre, Typha sp., Carex hispida, Sonchus maritimus, Cirsium polyantheum, Scirpus maritimus*
h) Aquatics	Submerged/floating in lagoons	*Ruppia spiralis, Lamprothamnium papulos, Potamogetum pectinatus*
i) Agricultural / abandoned	Margins of reserve and within	Vineyards, Orange and Olive, *Chrozophora tinctoria, Diplotaxis erucoides, Convolvulus arvensis, Chenopodium album, Hypericum xylosteifolium*

diversity of perennial grasses and xerophyllous herbs e.g. *Trifolium scabrum, Anthemis* sp. and *Plantago* sp., which are abundant early (Spring) in the year.
In terra-rossa and many other soils in the Mediterranean, the element phosphorus is often deficient due to climatic-pedogenic processes. To compensate for this deficiency, *garrigue* species such as *Sarcopoterium spinosum* may take up phosphorus at low concentrations in the soil solution via mycorrhizal symbionts (Berliner *et al.* 1987). It has also been shown that the addition of phosphorous on areas of *S. spinosum* dramatically changes the herbaceous vegetation, inducing the dominance of annual leguminous species rather than the *macchia-garrigue* association (Henkin *et al.* 1998). It is likely that the cultivated field areas around Pantano Piccolo may have had, at one time or another received phosphate-fertiliser treatment. The decline in usage may well be contributing to the re-expansion of *macchia-garrigue* into the once cultivated areas.

ii) *Agricultural / abandoned agricultural association*

Only the most inaccessible and exposed rock surfaces of the coastline in the vicinity of the lagoon are likely to have been unaffected by agriculture in the past, either by grazing animals (goats) or the cultivation of crops in the stone-walled enclosures.
Since abandonment, and while the area has been under conservation-protection, small-scale agriculture has continued in some areas, preventing the re-establishment of *macchia-garrigue* and coastal communities. Stands of *Opuntia* sp. are common at the southern end of the rock peninsula within stone-walled enclosures along with small-scale greenhouse cultivation, near to the site of the ruined tuna fishery.
Individuals of *Olea europaea* are scattered around the area, usually occurring at the margins of past cultivated fields and in sheltered positions. For example *Olea europaea* occurs at field margins to the north of Pantano Piccolo where it is associated with larger macchia species and *Ficus carica.*
The rapidity of colonisation by ruderal species was highlighted in the field next to the northern margin of the lagoon. Adjacent fields to the north of Pantano Piccolo had, on the initial field visit (08/1996), been recently ploughed. By the time of the next visit (05/98), the field was colonised by a weed community, dominated by *Chrysanthemum* and *Cirsium* species (Plate 6.6.). An association of exploitative, weed species with agricultural and physically disturbed land is common throughout Sicily, species present including: *Chrozophora tinctoria, Heliotropium europaeum, Diplotaxis erucoides, Chenopodium album* and *Amaranthus retroflexus* (Brullo *et al.* 1980).

iii) *Lagoon margin halophyte-brackish-wetland association*

Present-day halophytic and wetland vegetation occurs as a narrow margin (< 10 m width) around the periphery of Pantano Piccolo. Wetland vegetation is prevented from expanding "landward" by steep slopes and low walls constructed at the base of shallower gradient slopes surrounding the lagoon. The expansion and colonisation of fringing vegetation towards the interior of the lagoon is prevented by relatively constant groundwater-fed water levels.

Along the eastern lagoon margin, bare rock surfaces descend into the lagoon, supporting local stands of halophytic vegetation on rock benches where soil/sediment has been deposited. *Phragmites australis* and*Juncus* dominate the western margin, forming a wide sward (~10 m) of vegetation extending into the lagoon. At the northern margin of the lagoon an 8-10 m wide crescent of halophytic vegetation (*Salicornia -Arthrocnemum glaucum*) is established at the base of a stone wall which separates the lagoon from the adjoining recently cultivated, weed infested, south facing slope (Plate 6.9).

6.2.4 Stratigraphic investigations at the margins of Pantano Piccolo

The initial visit to the lagoon in September 1996 revealed an expanse (approx. 20 m at its widest point) of mudflat and emergent halophytic vegetation at the northern margin of Pantano Piccolo (Plate 6.6.). Fire had recently destroyed a sizeable portion of the marginal halophyte community, leaving only larger stems and a scorched surface. Both PPA and PPB were extracted during this low water period when the marsh surface at the PPA core site was emergent and PPB was extracted away from the lagoon margin in the exposed mudflat (Plate 6.6/6.7.).

In April 1998, high water levels in the lagoon had submerged the entire marsh area up to the surrounding wall. Two stratigraphic transects were achieved by coring along a taped line; from the surrounding lagoon wall into the lagoon and the margin of the vegetation into open water (through the PPA and PPB core locations respectively) (Fig. 6.4.7.). The water level of the lagoon in April 1998 was shown by a levelling transect (Fig. 6.4.6.) to be broadly comparable with sea level, though rough sea conditions on the exposed rocky coastline allowed only an approximate measurement.

Three main stratigraphic units were identified at the northern margin of Pantano Piccolo (Fig. 6.4.7.); a basal agglomerate of coarse clastics and fine grained mud, shell-rich sandy grey mud with a varying organic component and a surface accumulation of largely organic detritus derived from *in situ* plant growth and lagoon waters. The stratigraphy of the individual cores in the transects are described in Appendix VI. The description of

other cores investigated around Pantano Piccolo are described in Appendix VI. The location of core investigations from around the lagoon are shown in Figure 6.4.6. and Plate 6.6.

A coarse basal agglomerate occurred in almost every core sample taken only being absent in cores PPD and PPE (Fig. 6.4.6.) where a thin deposit (< 40 cm) of mud overlays solid calcarenite bedrock (Appendix VI). The coarse basal agglomerate at the base of the other cores proved impenetrable by gouge coring because of its compact and coarse clastic fabric. The outflow of water from some of the extracted core-holes and sedimentology of the unit led to the assumption that the basal clastic and fine-grained mud agglomerate formed a semi-permeable confining layer above the more porous calcarenite bedrock. Reflecting the same process of spring generation, which occurs around the periphery of Pantano Piccolo (i.e. Badalamenti *et al.* 1985; Dongarra *et al.* 1985), due to the contrasting permeablity of sediment units.

The contrasting lithology of this basal unit (reminiscent of nearby soil-slope products) overlain unconformably by lagoonal muds led to an initial assumption that this was representative of an earlier depositional phase in the valley-depression currently filled by Pantano Piccolo. It is likely that a significant hiatus exists (potentially 100's to 1000's of years) between the age of the basal clastic agglomerate and lagoonal deposits.

The dominant unit encountered in the lagoon margin sediment sequences, consisted of grey sandy and shell rich mud, not exceeding 45 cm in thickness. Significant lithological changes were observable in the unit; spatially correlatable *Cerastoderma glaucum* and *Hydrobia* gr.*ventrosa* shell concentrations (Fig. 6.4.7.), as well as organic horizons resembling those encountered at the surface (PPB 18-22 cm) and black organic smearing which occurred as a recognisable interval at the lagoon margin in cores PPA & PP3. The occurrence of shell material (intact valves and fragments of *Cerastoderma glaucum, Abra ovata, Bittium reticulatum, Hydrobia* and *Pirenella conica* etc.) within this unit was suggestive of a continued brackish-euryhaline lagoon environment during deposition. The traceable horizon of increased shell material between 30 and 40 cm (below aproximate sea level) suggests a temporally confined, though perhaps lagoon-wide period of macrofaunal (molluscan) activity.

Sediment structures associated with recent bioturbation, e.g. disturbed fine laminations were not visually observed, which indicated that either shelly lagoonal muds had not been bioturbated or the homogenous fabric meant that it had been well mixed. The abundance of shell material at depth in most horizons seemed to support the latter assumption of bioturbated sediments.

The surface thickness of the humic-organic material was greatest beneath the established halophyte community, forming a clear topographic high separating the perimeter wall from the mudflat-open lagoon water. Organic surface materials were less evident in the

Figure 6.4.6. Core locations of PPA and PPB and other cores around Pantano Piccolo

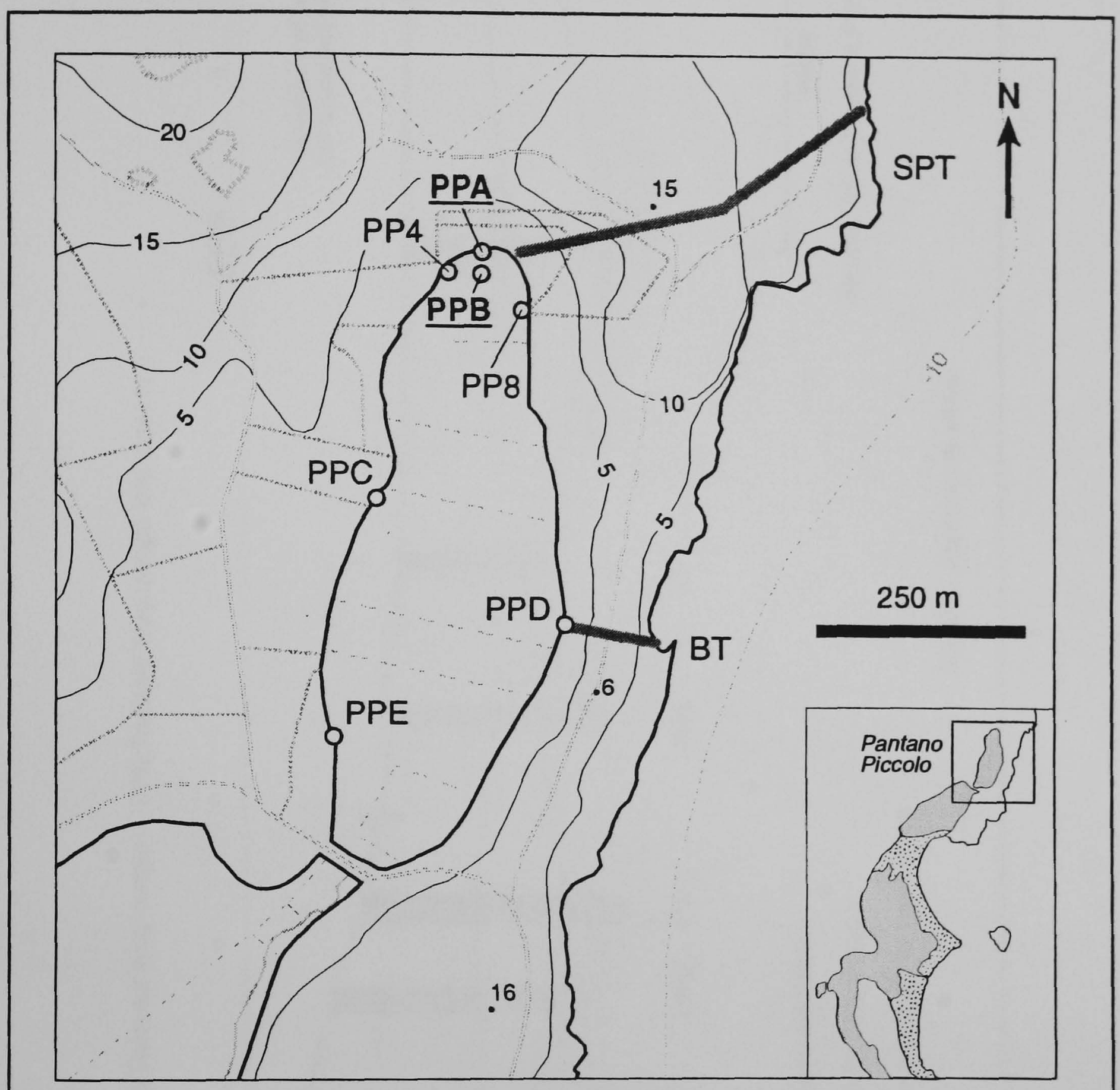

KEY

Levelled Transects

▬▬▬	SPT: Transect used for surface pollen samples (Section*)
▬▬▬	BT: Barrier Transect used to determine lagoon water level
○ PPE	Core site and label (See Appendix VI)
•16	Heights in metres. Contour interval 5 m

Photographs identifying the location of the PPA and PPB core sites are shown in Plates 6.6.& 6.7.

Figure 6.4.7. Composite representation of lagoon margin stratigraphy using transect data from PPA and PPB core sites

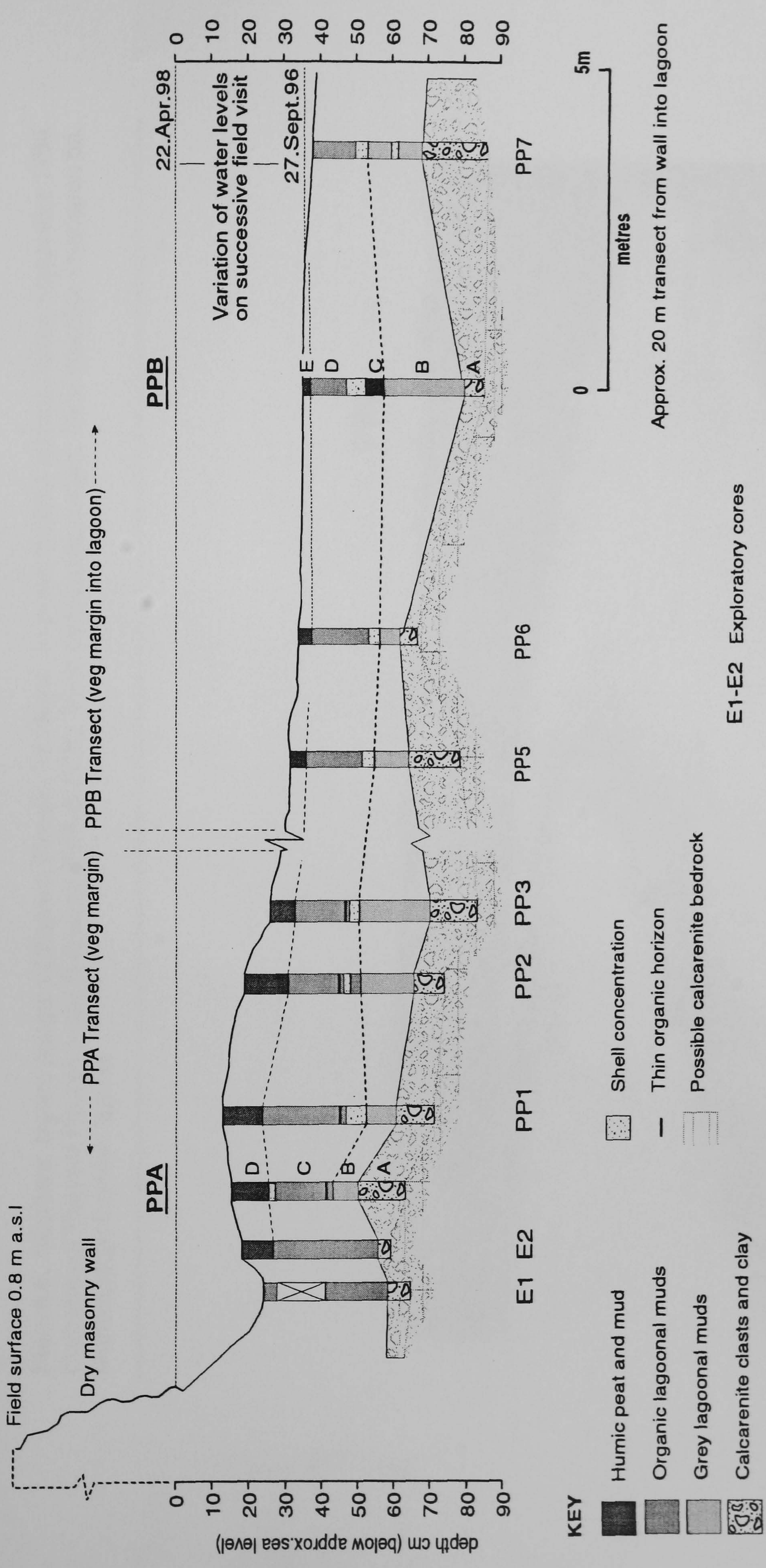

Plate 6.6. Northern lagoon margin of Pantano Piccolo, Vendicari. Exposed mudflat surface during September 1996. Core sites of Pantano Piccolo A and B marked (PPA & PPB). View west across margin. Note *macchia* vegetation on western slope beyond lagoon

Plate 6.7. Lagoon fringing halophytic wetland at northern margin of Pantano Piccolo, Vendicari. Core site of Pantano Piccolo A (PPA) marked. Core site PPB (off picture to right) covered by high water levels (April 1998). Water level to wall at rear of marsh (by person). Note degradation of marsh area in foreground. View north east across northern margin of lagoon.

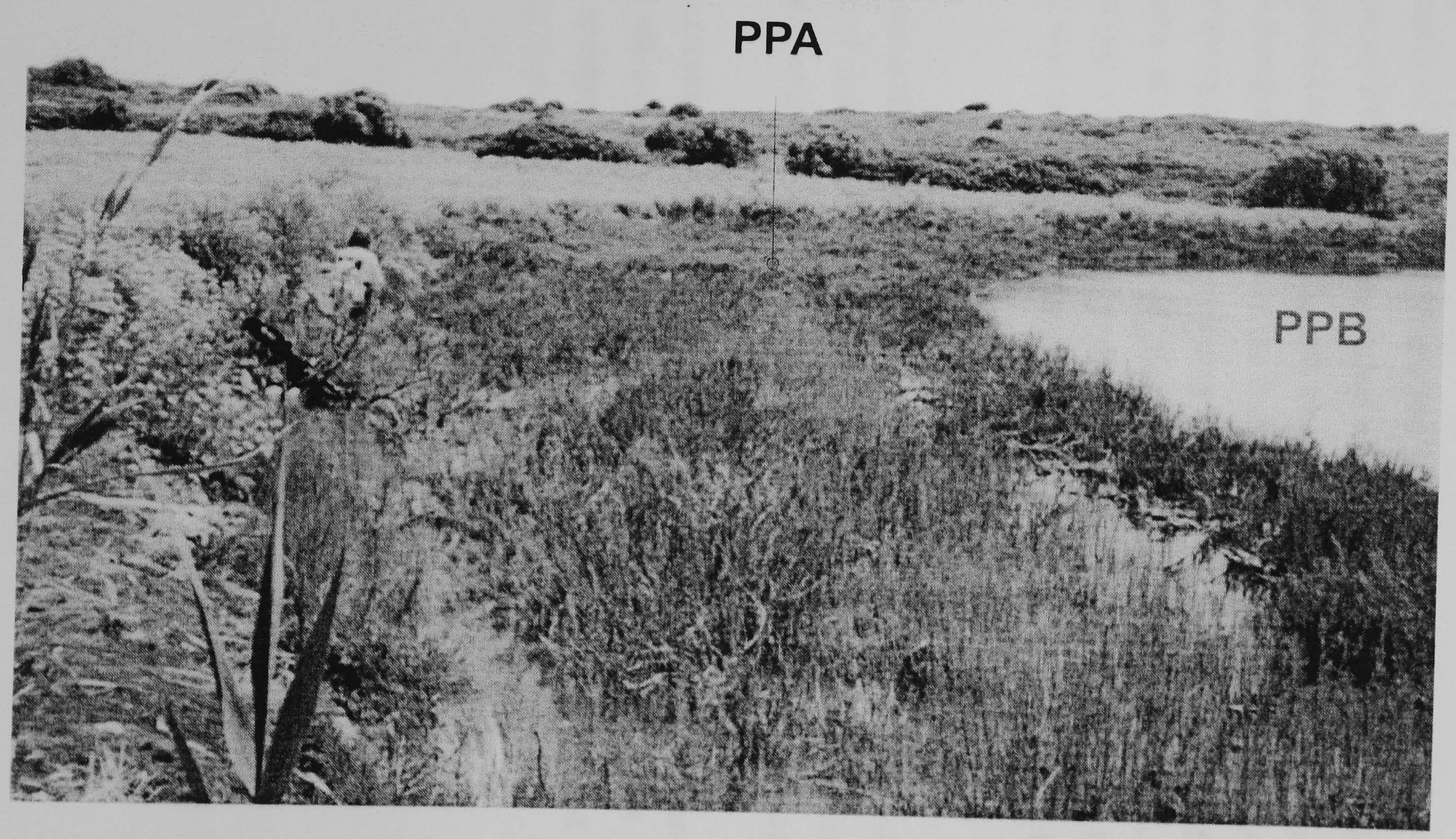

halophyte area which had been recently burnt and de-vegetated (Plate 6.7.). This surface peat/organic accumulation diminished towards the lagoon, being replaced by algal-material, as soon as the sediment surface was not covered by vegetation. At the rear of the halophyte community adjoining the wall, cores were diminished in surface organic material (E1-E2) and occurred in a greater depth of water, which may have been caused by the removal of material.

A more complex stratigraphy of organic accumulation was measured at core PPC (Fig. 6.4.6), taken from the *Juncus-Phragmites* vegetated western lagoon margin. A 90 cm sequence of vegetal organics and organic clay-silt overlying a clastic agglomerate was encountered at the lagoon margin sediments of the fringing vegetation. The depositional period represented by a low-organic brown-grey clay silt (Unit C) indicated a significant interruption to the *in situ* accumulation of plant organics derived from riparian (*Phragmites* sp. association) vegetation. A preliminary pollen analysis of the basal sediments from core PPC was abandoned, due to the near absence of palynomorphs in the prepared slides.

Physical evidence of human activity and disturbance was observed in the cores only in the form of small pieces of polystyrene and plastic sheeting found on the sediment surface, which was almost certainly derived from nearby cultivated fields and lagoon waters.

Core PPA therefore was extracted as a representative sequence of sediments from the high water inundated *Arthrocnemum glaucum*-vegetated margin, while PPB was extracted to characterise sediments deposited further in the lagoon, unvegetated and exposed as a mudflat during low water periods.

6.3 RESULTS FROM PANTANO PICCOLO A (PPA)

The core PPA was extracted from beneath growing stands of *Salicornia* sp. situated between the low wall adjacent to recently cultivated fields and open lagoon conditions of Pantano Picclo. The core was extracted during low lagoon water levels in September 1996 (Plate 6.6).

6.3.1 Pantano Piccolo PPA: Core sedimentology

Four horizons were recognised in the 48 cm core extracted intact from the halophyte vegetated lagoon margin (Fig. 6.4.8.). On extraction the core was divided into; a basal plastic clay with calcarenite clasts (48-35 cm), a grey lagoonal mud (35-9 cm) and a saline-crusted / surface-vegetation humic horizon (9-0 cm). At the base of the organic materials, between 9 and 7 cm, laminations (~4 mm thick) of light brown-whitish mud and darker humic peat were distinguishable when first extracted, though these were not visible when the core was sampled in the laboratory, possibly as a result of atmospheric exposure and dehydration. Other core features also became apparent during laboratory sampling e.g. the subdivision of the lagoonal muds into distinct lower and upper horizons (PPA-B & PPA-C respectively). The shell content in the core was marked by well-preserved articulated *Cerastoderma sp.* valves (e.g. at 18 cm) and shell-fragments (< 1 cm diameter). It was assumed that shells incorporated at depth represented both those that had been transported to the lagoon margin by wave action (as were present in strandlines around the lagoon) and individuals which had been incorporated in a life position.

6.3.2 Pantano Piccolo PPA : Loss on ignition results

1 cm depth intervals were consecutively sampled down the core for loss on ignition analysis. The visually determined stratigraphy was apparent in the % losses after combustion at 550°C, reflecting the basal (PPA-A) clastics and clay (av. 10.9 % loss, range 1.9%), grey muds of PPA-B between 35 and 28 cm (av. 14.2 %, range 2.8%), grey shelly muds between 27 cm and 10 cm (av. 18 %, range 6.6 %) in PPA-C and surface organics of PPA-D in the upper 9 cm (av. 32.7 % loss, range 27.8%) (Fig. 6.4.9.).
550°C ignition loss values in sediment unit PPA-A exhibit little variation. Above the boundary with unit PPA-B, combustion losses however increase gradually up to a small peak at 23 cm (22.8 % loss). This peak was coincidental with organic detritus observed in the core at the same depth. Above this peak, values decrease slowly up to PPA-D,

Table 6.3. Core description of Pantano Piccolo A

Horizons	Depth (cm)	Sediment description
PPA-D	00-09 cm	Surface humic muddy peat. Visible fragments of *Salicornia fruticosa* . Fibrous roots from *Arthrocnemum glaucum - Salicornia fruticosa* vegetation and stem-leaf fragments. Muddy-peat fabric containing intact *Hydrobia* gr. *ventrosa*. and *Truncatella subcylindrica* shells.
PPA-C	09-27 cm	Dark grey/brown shelly mud. Fragments and articulated valves of *Cerastoderma glaucum* (~0.4 cm) throughout horizon. Concentration of shell material directly underneath horizon D. Fine root material prevalent, with associated Fe-mottling around roots. Well preserved *Abra ovata and C. glaucum* at 24 cm. The intact valves contained none of the surrounding sediment.
PPA-B	27-35 cm	Merging transition of horizon C at 26 cm into lighter brown-grey brown mud. Occasional fine root material. interspersed *C. glaucum* fragments and intact valves. Gradual increase in Fe - terracotta colouring with depth to 35-36 cm.
PPA-A	35-48 cm	Fe-terracotta/brown clay silt and gravel-pebble clastics. *Cerastoderma glaucum* valve and fragments with 10-12 mm sub-angular gravel. Plastic and dry texture to compact clay matrix with small, sub-rounded calcarenite clasts encountered at 43 cm and 45-46 cm respectively. Irregular break of core at 48 cm depth.

Figure 6.4.8. Core sedimentology and stratigraphic horizons; Pantano Piccolo A

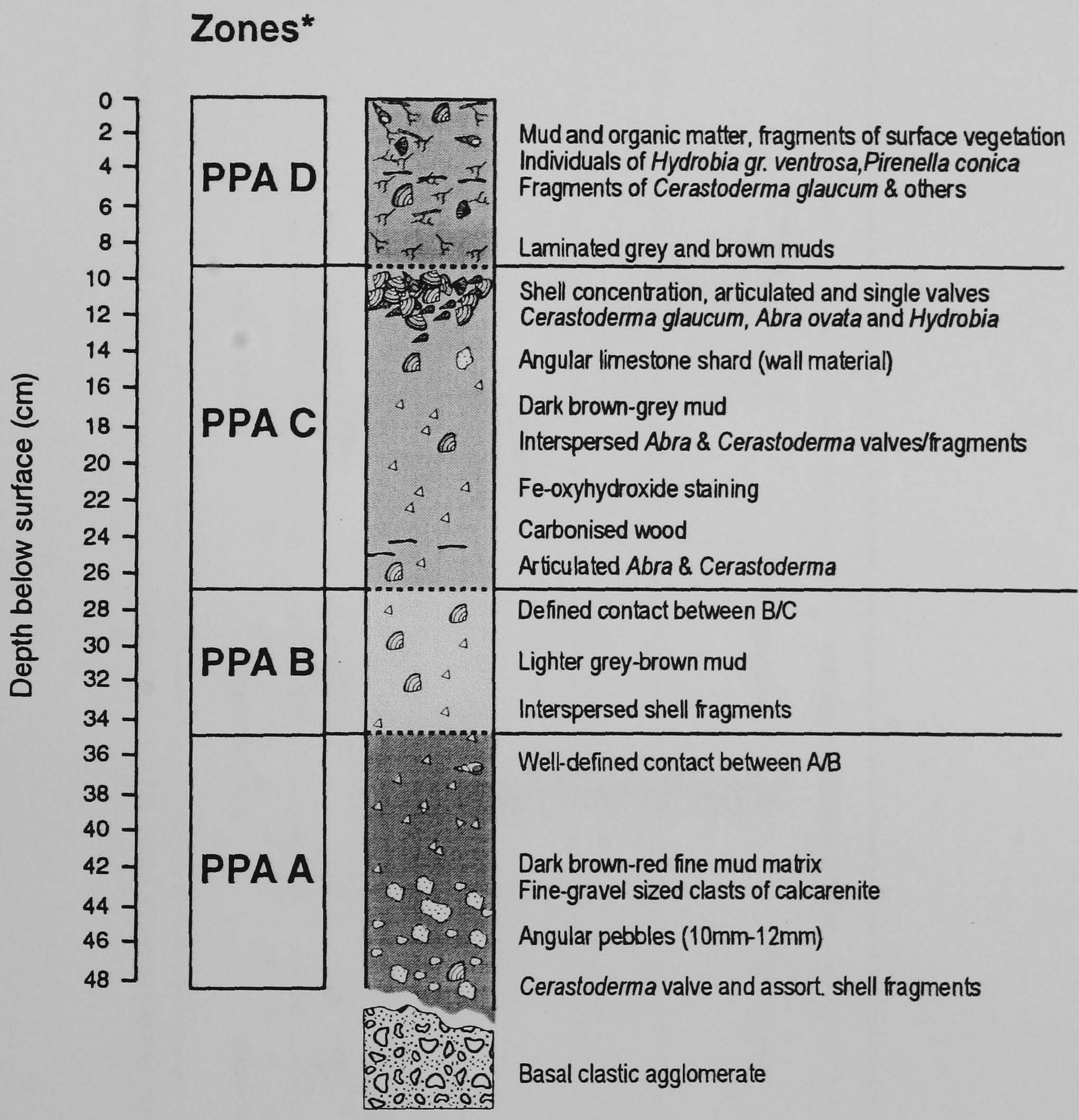

* PPA zones used in further references to core units

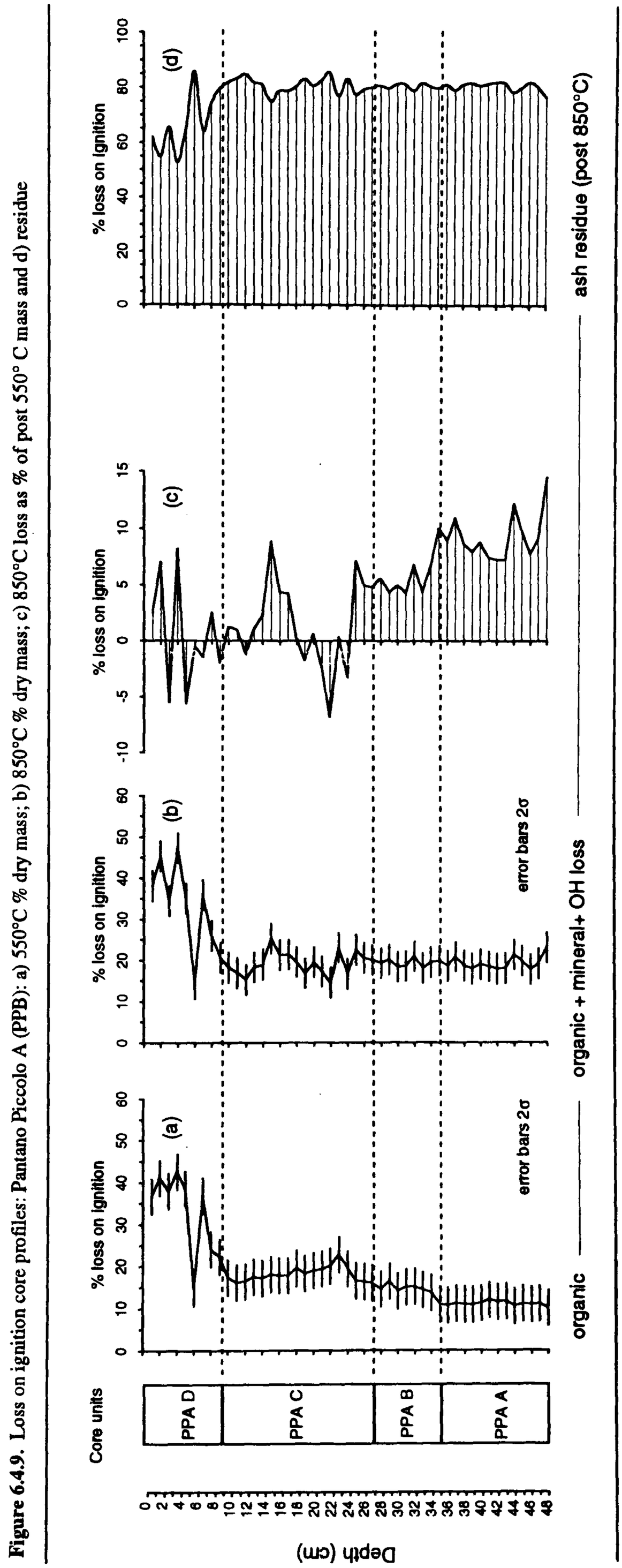

Figure 6.4.9. Loss on ignition core profiles: Pantano Piccolo A (PPB): a) 550°C % dry mass; b) 850°C % dry mass; c) 850°C loss as % of post 550° C mass and d) residue

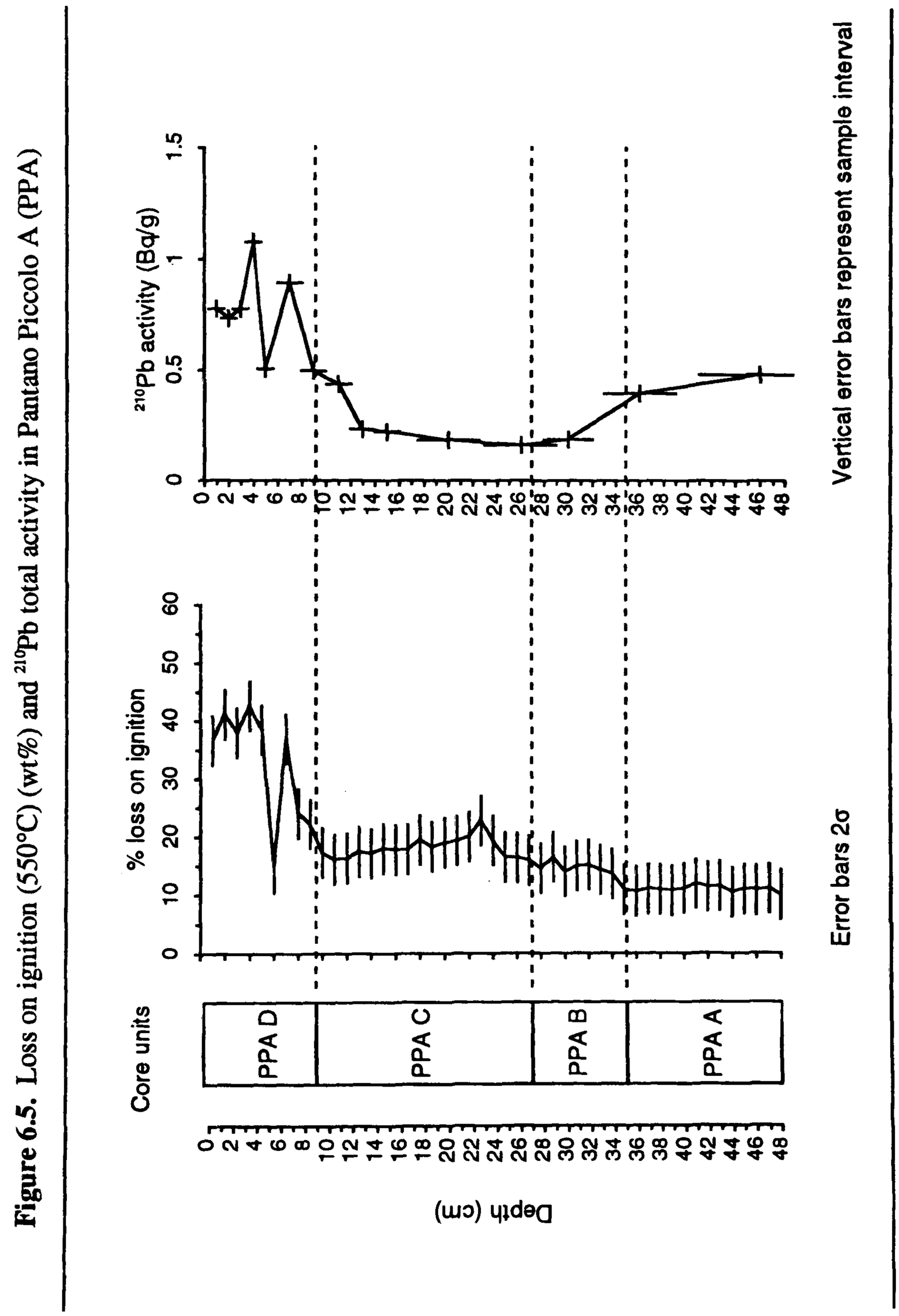

Figure 6.5. Loss on ignition (550°C) (wt%) and ^{210}Pb total activity in Pantano Piccolo A (PPA)

though remain higher than values encountered between 23 cm and 35 cm (av. 14.8 % loss).

The combustion of abundant organic-rich material at 550°C was apparent in PPA-D (av. 32.7 % loss). Only the sample interval spanning 5-6 cm led to a significant departure (14.1 % loss) within the unit. Closer inspection of the interval revealed the occurrence of small shell fragments (3-4 mm) in the organic-detrital mud. The LOI value also suggests that sediment from the lower horizon beneath (PPA-C) may have been incorporated into the interval, for example by an inwash of eroded sediment.

Losses following 850°C ignition were likely to have reflected both the total combustion of organic materials, carbonate ignition and water loss from hydrous minerals (e.g. $CaSO_4$ $2H_2O$). Consistent losses at 850°C occur below 26 cm, with the maximum loss at the base of the core (23% of dry mass or an additional 14.5 % post 550°C ignition). Further losses occur among 18cm and 12 cm depth, peaking at 15 cm (25.2% dry mass/8.9% post 550°C) and in the upper 10 cm of the core.

Another significant aspect of higher temperature combustion in the core was an apparent mass gain at some core intervals (Fig. 6.4.9b). The intervals that indicate an increase in mass during 850°C combustion occur as a distinct horizon between 17 and 25 cm, 7 and 5 cm and as isolated samples like that occurs at 3 cm. The increase in mass between 17 and 25 cm appears coincidental with the loss on ignition peak at 23 cm, though on inspection the actual interval only further decreased in mass by 0.3% dry mass. Sample contamination during combustion and weighing is unlikely, consequently these minor mass gains probably reflect oxide formation at high furnace temperatures.

The core therefore only contains a significant organic component within the upper 15 cm (Fig. 6.4.9d), within sediment horizon PPA-D, clearly representing a stage of organic accumulation at the core site. A minor peak at 23 cm depth, associated with observed humic material, would also appear to reflect a past period of enhanced organic accumulation.

6.3.3 Pantano Piccolo PPA ^{210}Pb analysis and dating

Fifteen samples (1 cm thick) were taken from the entire length of the core to assess longer term age-depth sediment relationships at the margin of the lagoon. Samples were taken at 1 cm intervals (Surface to 5 cm depth), every 2 cm (down to 15 cm) to characterise recent accretion at a high resolution, then at 20, 26, 30, 36 and 46 cm respectively. Activity totals are highest within the surface organic horizon PPA-D, from where they decrease slowly, before increasing in PPA-B & PPA-A at depth (Fig. 6.5.).

Figure 6.5.1. ^{210}Pb unsupported activity and CF:CS model linear plot and; (b) CF:CS age depth relationship, Pantano Piccolo A (PPA).

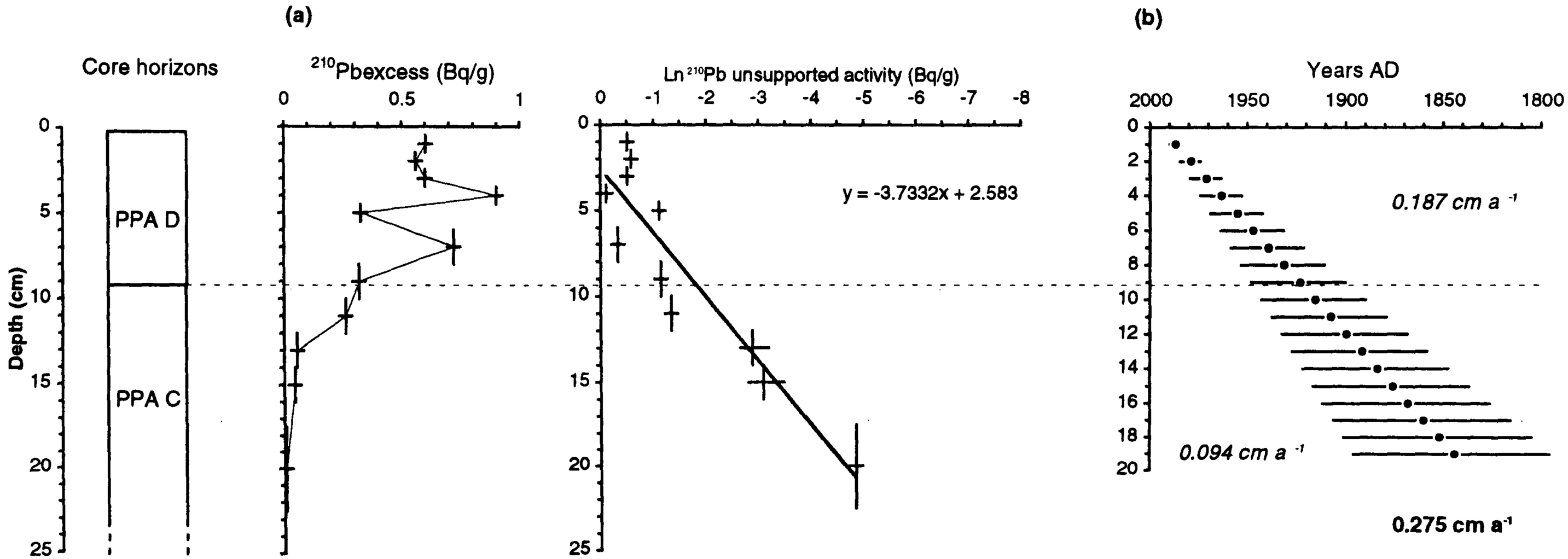

Mean accretion rates (cm/yr^{-1})determined by SPSS (95% Confidence linear regression)

Mean	0.126	R^2 = 0.841
Lower	0.094	
Upper	0.187	

Error bars signify calculated maximum and minimum unsupported actvity totals

The relationship between sediment composition (enhanced organic accumulation) and the age of materials is markedly apparent by the total activity profile. Autochthonous organic accumulation and the development of a vegetation protected depositional setting, appears to have been beneficial to the incorporation of ^{210}Pb; by continued atmospheric fallout or re-worked ^{210}Pb labile sediment.

Increased total activity in the base of the core (coincidental with PPA-A) appears unlikely to have been caused by recent mixing or the overturning of the sequence by dredging for example, within the last century. Elevated total activities at depth appear to be a consequence of the lithology of the basal sediments, either because of a higher ^{226}Ra content in the sediment matrix or possibly elevated ^{222}Rn in groundwater.

Increased ^{210}Pb activity below 25 cm (Fig. 6.5.) therefore limits the effectiveness of ^{210}Pb dating to the upper half (20 cm) of the core. Without further radiometric analyses to determine supported ^{226}Ra activity directly, unsupported activity at depth in PPA remains largely an estimate.

Total ^{210}Pb activity increases from 26 cm depth, signifying the transition from the sequence of lagoonal muds (horizon PPA-C) to surface organic mud. Although surface activity indicates considerable and abrupt variations, the possibly more gradual decline at depth in horizon PPA-C would indicate less disturbed and significantly older sediment. Gradually increasing ^{210}Pb activity in PPA-C suggests that the horizon PPA-C has been deposited sequentially and is older than 150-200 years. Activity totals increase rapidly from 13 cm depth.

In the surface 13 cm the expected pattern of decreased activity with depth from the surface however offset by the activity maximum (1.077 ± 1.21% Bq/g) occurring at 4 cm depth. This below-surface enrichment suggests that either downward mobilisation (mechanical or geochemical) or a variation in sediment composition or ^{210}Pb supply has affected the ^{210}Pb activity profile. At 5 cm an abrupt decline of total ^{210}Pb activity (0.504 ± 1.16 % Bq/g) occurs. Shell material and allochthonous sediments are capable of diluting ^{210}Pb activity profiles (e.g. Clark, 1986; Brezonik & Engstrom, 1998), and would appear to have also caused this sudden drop in activity. This pattern is supported by the drop in LOI 550° C values which occurred at 6 cm in the core (Fig. 6.5.), which was also related to the presence of shell material and minerogenic sediment.

Figure 6.5.2. Pantano Piccolo A (PPA) ^{210}Pb total activity CRS model age-depth curves

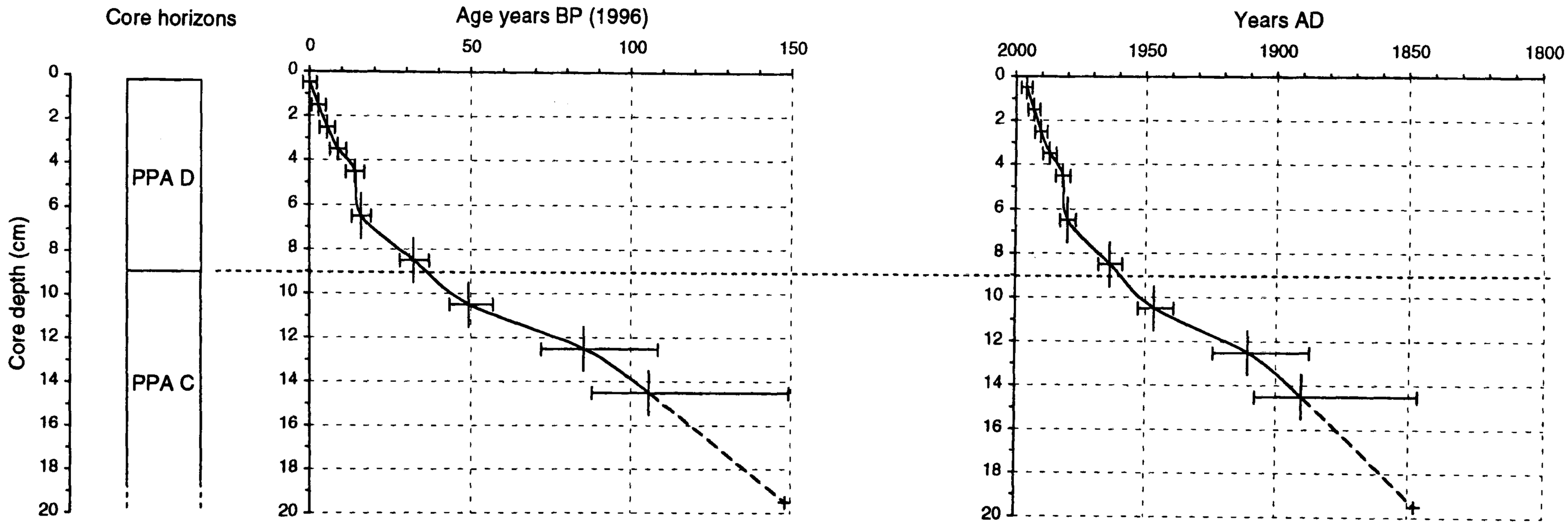

y error bars indicate sample interval

x error bars age range derived from minimum and maximum unsupported activity calculation

Mean accretion rate 0.275 cm/yr^{-1} for core interval

Table 6.3.1. Pantano Piccolo A: CRS model ^{210}Pb dates and sedimentation rates

Depth (cm)	Calculated Years BP 1996	Approximate Date AD	Sedimentation rate (cm/yr-1) *
0.5	0.0	1996 (1997-1995)	0.35 (0.19-1.32)
1.5	2.8	1993 (1991-1995)	0.38 (0.36-0.39)
2.5	5.5	1991 (1988-1993)	0.30 (0.29-0.32)
3.5	8.8	1987 (1985-1990)	0.19 (0.18-0.21)
4.5	14.0	1982 (1979-1985)	1.02 (0.97-1.07)
6.5	15.9	1980 (1977-1983)	0.12 (0.11-0.13)
8.5	32.1	1964 (1959-1968)	0.12 (0.10-0.13)
10.5	49.2	1947 (1939-1953)	0.06 (0.04-0.07)
12.5	85.2	1911 (1898-1924)	0.10 (0.05-0.12)
14.5	105.7	1890 (1847-1908)	0.12 (0.002-0.19)
19.5	148.3	1848 (-1682)	~

* Sedimentation rate calculated between upper and lower sample horizons (sample thickness / time)

Figures in brackets derived from calculated maximum and minimum unsupported activity and CRS model

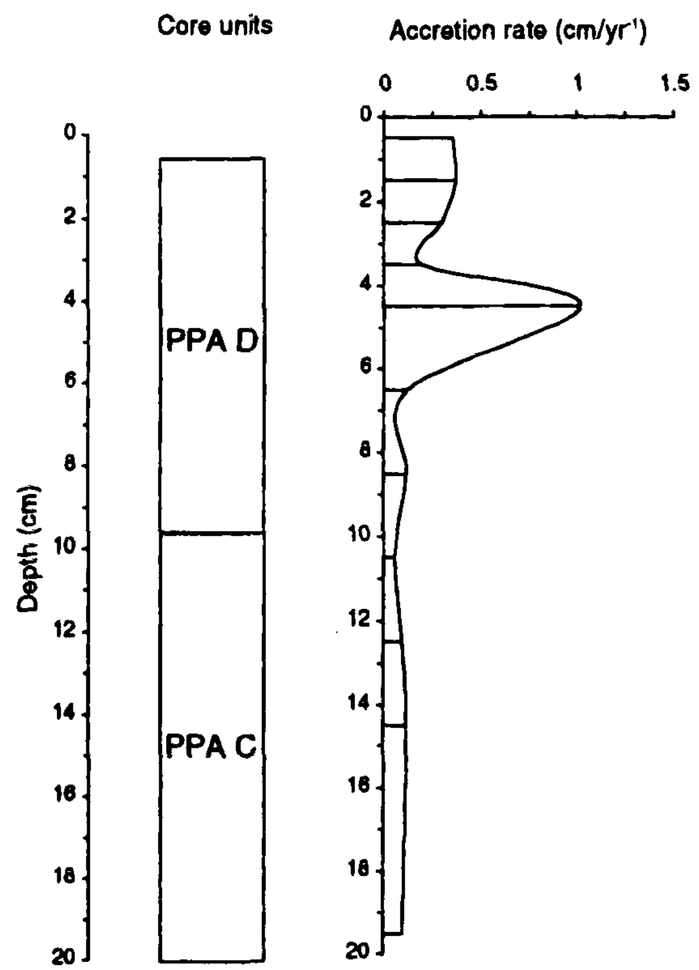

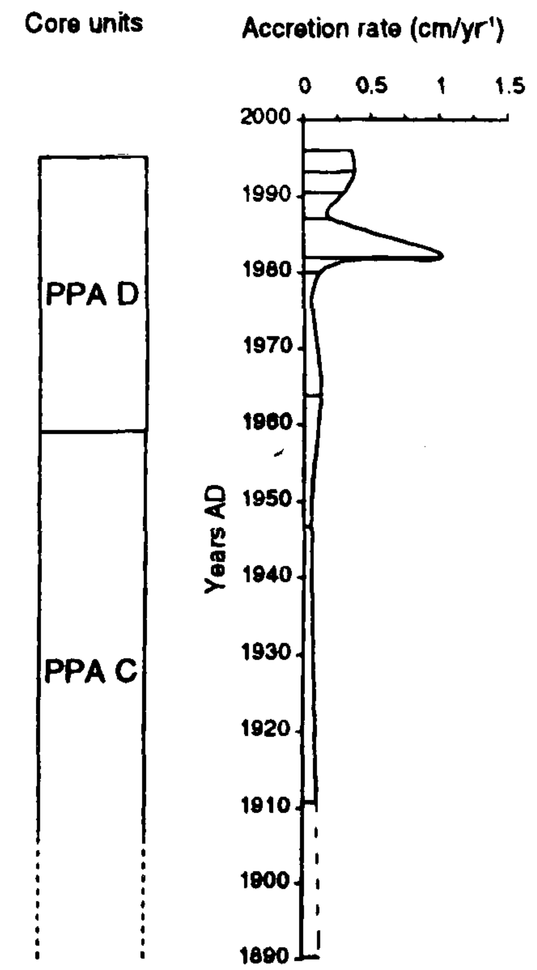

6.3.4 PPA : ^{210}Pb CF:CS dating model

The linear fit (R^2= 0.841) provided by the CF:CS model suggests that accretion at PPA has been fairly constant (Fig. 6.5.1.). The mean accretion rate determined (0.127 cm/a^{-1}) by the CF:CS model suggests that sedimentation changed, from lagoonal fine-grained shelly muds (PPA-C) to the accumulation of vegetal organics (Unit PPA-D), in the early twentieth century (*circa* 1920-1930 AD). At this rate of accretion, the upper 20 cm of the core represents deposition spanning approximately the last 150 years. Interpolation of accretion rates below this depth using the CF:CS model is speculative, due to the sedimentological differences and the ^{210}Pb activity profile (Fig. 6.5.). If an assumption is made that accretion remained relatively constant preceding 20 cm depth, a mean rate of 0.127 cm/a^{-1} suggests that the entire core may represent accretion over the last ~400 years (early 17th century onwards).

6.3.5 PPA: ^{210}Pb CRS dating model

The CRS age-depth curve (Fig. 6.5.2.) may be subdivided into two phases, corresponding with the sediment units PPA-C and PPA-D previously identified. Prior to ~AD 1980 (below 7 cm) accretion rates were constantly low (~0.1 cm a^{-1}). Accretion rates increase slightly (0.12 cm/a^{-1}) within the lower section of PPA-D, accompanied by increased organic content. The abrupt increase in accretion is clearly recognisable in the surface organic accumulation of PPA-D between 4.5 cm (*circa* AD 1982) and 6.5 cm (*circa* AD 1980) at 7 cm (*circa* AD 1981) (Fig. 6.5.2.). This pulse of rapid accretion is also coincidental with the drop in organic values determined by loss on ignition (Fig. 6.5.). Following this event, accretion has continued within the upper 4 cm of the core (~0.3 cm /a^{-1}) up to the present day at a greater rate, than before the peak at 7 cm. Calculated age-depth patterns and accretion rates plotted against both depth and age are shown in Table 6.3.1.

The accumulation of organic matter and enhanced accretion at the lagoon margin core site from *circa* AD 1950-1960, clearly reflects a profound change that occurred in the depositional environment. The causes and timing of this event are discussed in Chapter 7. The largest magnitude accretionary event has also occurred only in the last twenty years, with the deposition of 1-2 cm of material in approximately a year (*circa* AD 1981).

Accretion rates are calculated as having been higher in the core since this period, which indicates a continued positive accretionary response to the lagoon margin environment.

6.3.6 Pantano Piccolo PPA: Major element sediment geochemistry

Adjoining 1 cm thick samples were analysed for major elements along the entire length of the core (a total of 48 samples) (Table 6.3.2.). Down-core variations in the relative abundances of the ten major elements were grouped using CONISS into three main zones (Fig. 6.5.3); PPA-ME-1 between 48 cm and 25, PPA-ME-2 between 24 and 7 cm and PPA-ME-3 comprising the upper 6 cm of the core. Within the three major zones, further sub-zones were also recognised (Fig. 6.5.4.). The relationship between these chemostratigraphic zones and sedimentological horizons previously identified are shown also. Major element abundances are also plotted against ^{210}Pb derived ages (Fig. 6.5.5).

As combustion losses at 550°C indicated major inorganic-organic variations within the core, the association of major elements with either the organic or minerogenic component was deemed neccesary for the palaeoenvironmental interpretation of major element assemblages (Fig. 6.5.6.). Because of the major compositional variation between the upper 9 cm of the core (PPA-D) and the rest of the sequence, correlation values between element totals with LOI and Ti, differ between the total and sub-divided core sections (Table 6.3.3.).

The lower half of the core (PPA-ME-1) corresponds to a period when Ca was much more abundant. At the base of the core (PPA-ME-1a), decreased Ca corresponds to an increase in the Fe:Mn ratio and a small peak in P (0.29 wt %). At the boundary with PPA-ME-1b, an increase in Mn shifts the Fe:Mn ratio back. Ti decreases steadily in PPA-ME-1b up to the boundary with subzone PPA-ME-1*circa* The Fe:Mn ratio declines again at 33 cm with a reciprocal decline observed in Si and Al and an increase in Ca.

The base of PPA-ME-1c is marked by an increase in Si, Al, K and Ti and a decrease in Ca (Fig. 6.5.4.). Fe:Mn, Al, Na and Mg values increase throughout PPA-ME-1c as the abundance of Ca gradually decreases.

The transition between PPA-ME-1 and PPA-ME-2 (at 25 cm) is marked by the drop in Ca and Mn and an increase in Si (+ 4%), Al (+1%), Na, Mg, K and Ti at 24 cm depth. The LOI 550°C peak at 23 cm (22.8% wt. loss) follows this increase in detrital elements along with a minor peak observed in Ca abundance. The Fe:Mn ratio also suggests that during the deposition of PPA-ME-2a, the core setting was receiving a significant input of soil-derived-detrital materials (peaking at the boundary (19 cm) with PPA2b), as Ca declined to low levels which continued relatively uniformly throughout PPA ME 2.

Table 6.3.2. Major element abundance (% ashed mass of oxides) from core PPA

Depth (cm)	SiO_2	Al_2O_3	CaO	Fe_2O_3	Na_2O	MgO	K_2O	TiO_2	P_2O_5	MnO	LOI (550°C)
	%	%	%	%	%	%	%	%	%	%	%
1	42.73	11.92	20.82	6.31	8.14	6.48	2.39	0.61	0.54	0.06	36.62
2	45.28	14.17	13.50	7.59	8.99	6.81	2.08	0.75	0.77	0.07	41.12
3	49.38	18.58	5.04	7.50	9.63	5.32	3.05	0.95	0.50	0.05	37.89
4	50.26	17.35	3.37	7.79	10.88	5.68	3.15	0.94	0.53	0.05	42.57
5	52.74	16.07	3.20	7.67	10.15	5.44	3.29	0.93	0.46	0.05	38.42
6	52.03	16.16	3.32	8.93	9.38	5.62	3.08	0.94	0.47	0.05	14.67
7	52.61	16.92	5.63	8.65	6.64	4.93	3.25	0.94	0.37	0.05	36.86
8	51.44	17.25	8.22	8.67	5.50	4.77	2.90	0.92	0.30	0.05	24.06
9	55.78	15.74	7.93	8.66	4.23	3.46	2.93	0.96	0.25	0.04	22.17
10	57.17	16.66	6.02	8.64	3.91	3.06	3.27	1.00	0.23	0.04	17.30
11	57.10	16.22	7.26	8.43	3.73	2.85	3.14	1.00	0.22	0.04	16.16
12	57.94	16.60	5.89	8.34	3.87	2.85	3.24	1.00	0.22	0.04	16.32
13	58.05	16.33	6.83	7.71	3.78	2.76	3.26	1.01	0.23	0.04	17.45
14	58.11	16.65	5.78	7.99	4.05	2.78	3.31	1.04	0.25	0.04	17.15
15	56.94	16.42	7.63	8.11	3.56	2.70	3.33	1.01	0.25	0.04	17.99
16	58.06	16.97	6.54	7.41	3.57	2.71	3.41	1.05	0.25	0.04	17.79
17	58.21	17.53	5.90	6.97	3.66	2.81	3.54	1.08	0.25	0.04	17.82
18	57.77	17.20	6.50	6.71	4.35	2.87	3.26	1.06	0.25	0.04	19.49
19	54.76	17.07	7.55	9.16	3.88	2.89	3.40	0.98	0.27	0.04	18.24
20	56.43	17.83	6.48	7.21	4.14	3.03	3.54	1.05	0.25	0.04	19.02
21	55.83	17.55	7.76	7.05	4.05	2.97	3.47	1.03	0.25	0.04	19.28
22	55.15	17.65	8.62	7.31	3.69	2.89	3.42	1.00	0.22	0.04	20.00
23	53.88	16.64	11.08	7.82	3.41	2.90	3.08	0.96	0.20	0.05	22.79
24	55.20	17.79	8.32	6.76	4.28	3.05	3.35	1.01	0.21	0.04	19.31
25	51.95	16.01	15.07	7.04	3.22	2.98	2.56	0.92	0.18	0.06	16.49
26	52.39	14.29	16.53	7.90	2.87	2.61	2.31	0.86	0.16	0.07	16.40
27	52.06	14.61	16.70	7.42	2.97	2.76	2.38	0.87	0.16	0.07	15.94
28	53.76	15.02	15.55	6.63	2.86	2.61	2.44	0.90	0.16	0.07	14.51
29	53.26	14.56	16.75	6.91	2.61	2.60	2.22	0.88	0.15	0.07	16.45
30	53.00	14.03	17.85	6.78	2.59	2.56	2.11	0.86	0.14	0.08	14.01
31	52.61	14.21	18.66	6.14	2.64	2.53	2.12	0.87	0.15	0.08	14.96
32	55.49	14.56	15.81	6.07	2.27	2.34	2.30	0.94	0.15	0.08	15.16
33	51.18	12.65	21.08	6.70	2.55	2.53	2.02	0.82	0.15	0.12	14.29
34	53.30	12.66	19.28	7.02	2.45	2.25	1.97	0.85	0.14	0.09	13.60
35	55.10	13.45	16.35	7.46	2.33	2.15	2.05	0.88	0.14	0.09	10.93
36	55.31	13.15	16.37	7.52	2.32	2.09	2.12	0.88	0.14	0.09	10.59
37	54.34	13.01	17.31	7.78	2.40	2.11	1.92	0.89	0.14	0.10	11.06
38	56.34	13.83	16.16	6.13	2.31	2.04	2.07	0.92	0.12	0.09	10.90
39	55.21	13.40	17.50	6.14	2.55	2.05	2.03	0.89	0.13	0.11	10.75
40	54.21	13.94	17.32	6.70	2.41	2.09	2.19	0.92	0.13	0.10	11.12
41	54.62	13.72	18.21	5.79	2.36	2.07	2.10	0.91	0.12	0.10	11.94
42	55.18	14.69	15.77	6.25	2.52	2.61	1.77	0.96	0.15	0.10	11.40
43	54.56	13.92	18.42	5.71	2.33	2.18	1.61	1.01	0.13	0.13	11.56
44	55.84	14.03	16.75	5.49	2.76	2.14	1.82	0.93	0.13	0.12	10.44
45	56.19	14.48	15.74	5.73	2.67	2.12	1.86	0.96	0.14	0.09	11.03
46	56.48	15.16	14.96	5.89	2.32	2.12	1.89	0.97	0.13	0.09	10.84
47	56.53	15.18	14.17	6.28	2.35	2.09	2.03	0.99	0.29	0.09	11.09
48	57.74	15.22	13.23	5.99	2.49	2.13	1.96	1.01	0.14	0.10	10.04
2σ	6.18	3.31	10.81	1.90	4.57	2.45	1.23	0.17	0.27	0.05	17.18
Core average	54.36	15.40	12.10	7.18	4.01	3.07	2.62	0.94	0.24	0.07	18.25

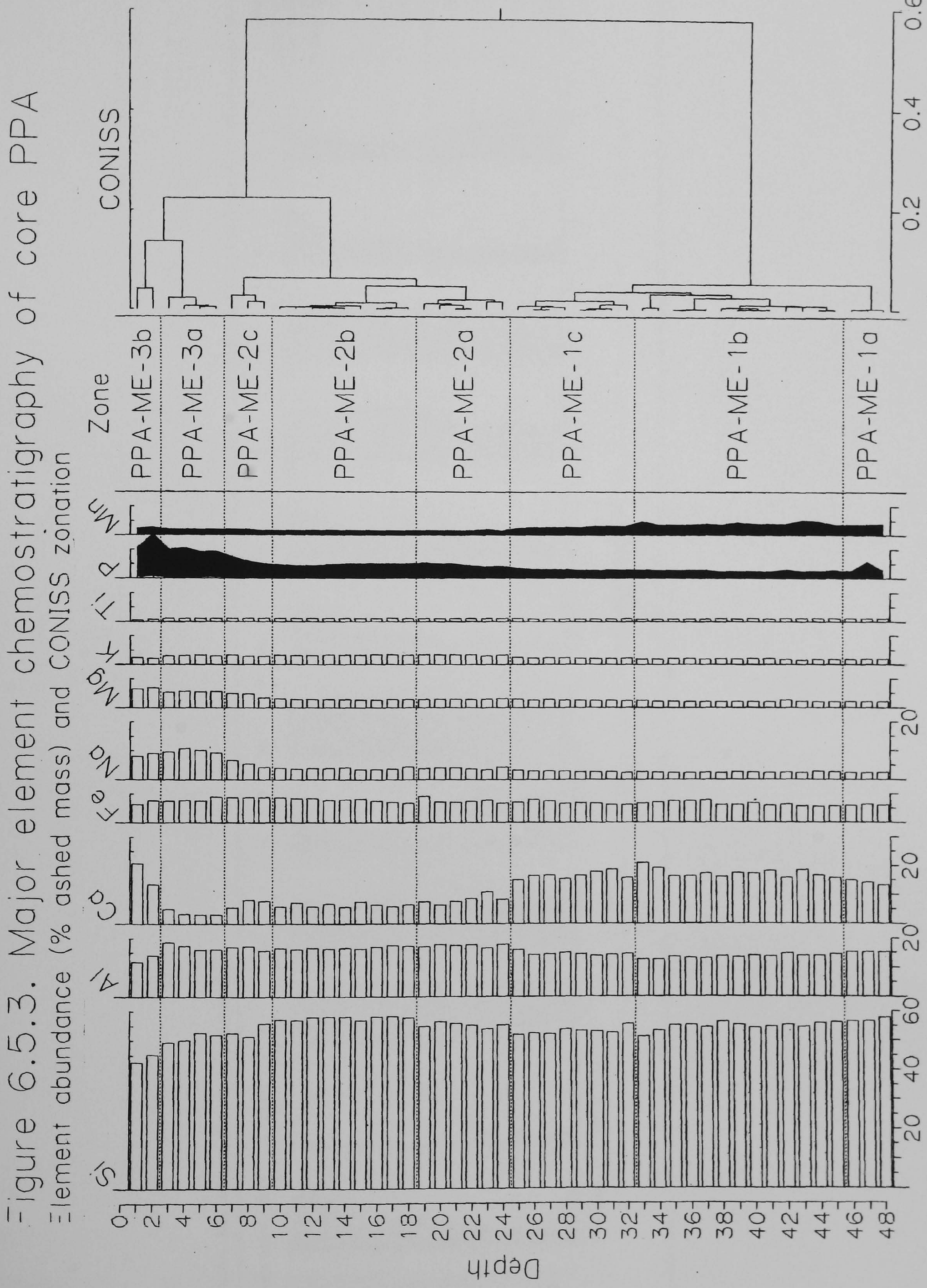

Figure 6.5.3. Major element chemostratigraphy of core PPA
Element abundance (% ashed mass) and CONISS zonation

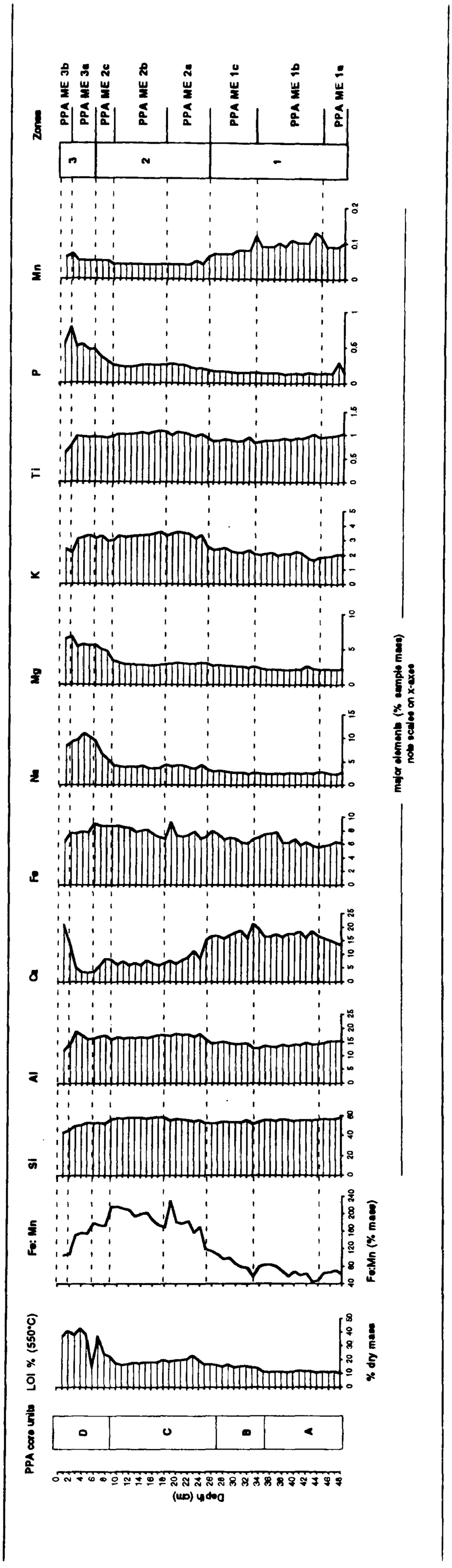

Figure 6.5.4. Pantano Piccolo A Major element core profiles (Si-Mn in order of abundance)

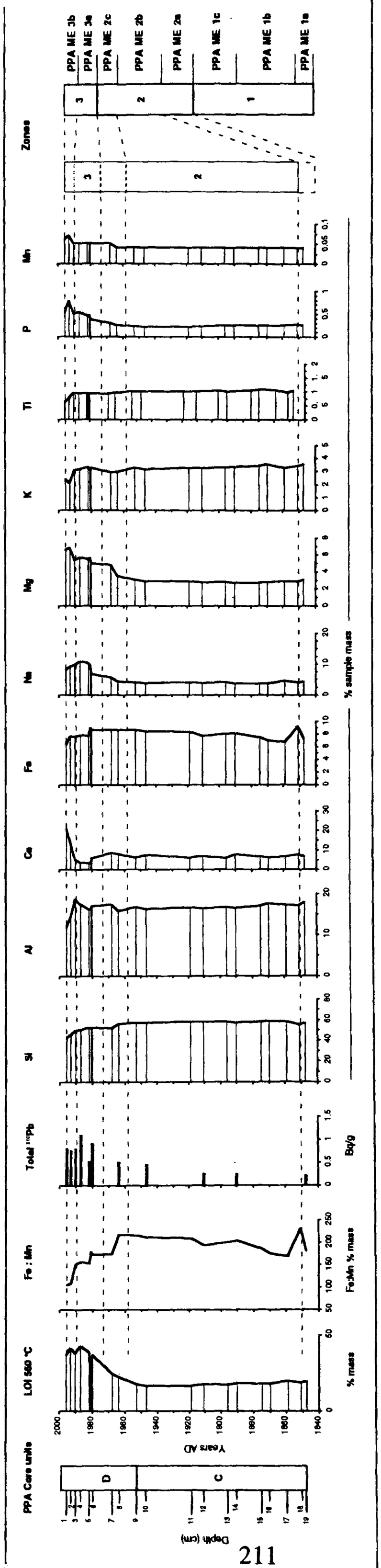

Figure 6.5.5. Pantano Piccolo A Major element core profiles plotted against time (1 cm depth and corresponding age intervals). Note Total ^{210}Pb activity.

Element abundances in PPA ME 2b indicate little change in sediment supply and composition over a time period of approximately 100 years (Fig. 6.5.5.). The subzone of PPA ME 2b corresponds at the base, to the late 19th century AD up to approximately the late 1950's (9-10 cm depth).

The abundance of all elements except Ca and Mn, indicate a positive correlation with loss on ignition at 550°C and Ti (Fig. 6.5.6.) below 10 cm depth. This relationship in the less obviously organic sediments of the core indicates that low organic combustion values are associated with the mineral component of the core. The exception of Ca and Mn reflects their down-core profiles, most significantly the change in the depositional environment represented between zones PPA-ME-1c and PPA-ME-2a (Fig. 6.5.4.), which dramatically reduced the amount of Ca and Mn incorporated into the lagoonal sequence.

Problems occur in the surface of the core with using the Fe:Mn ratio as a proxy for the input of soil detrital metals due to diagenetic re-mobilisation. Increased Mn in the upper core and a peak (0.07 %) at 2cm depth may represent a stable redox zone (water table) in relation to the lagoon margin hydrology, while increased Fe at depth (6 cm) may also represent diagenetic Fe enrichment at depth (e.g. Zwolsman *et al.* 1993).

The similar negative correlation between Fe and Ti (more stable and representative of fine-grained mineral sediments) between 0-9 cm and coincidental decrease in Ti, Si and Al in the surface 3-4 cm (Fig. 6.5.6.) suggests that there has been an actual decrease of minerogenic material in line with enhanced organic accumulation.

Subzone PPA ME 3a is conspicuous in the core by the abundance of Na and low Ca. The surface 3 cm of high organic content sediment, indicates a reduced minerogenic (Si, Al, Ti) input. The increase in Ca, Mg and abundance of P and Na in the surface 3 cm would certainly reflect the saline crust observed during core extraction and biomass (plant derived P) incorporation from the surface halophyte vegetation.

Above this horizon the geochemical composition of the sediment core (corresponding with organic accumulation in PPA-D) changes significantly as Si decreases in abundance to an extent not observed at any time before in the sequence. At 9 cm the Fe:Mn ratio starts to decline towards the surface as 550°C loss on ignition values increase with associated Na, Mg and P.

In horizon PPA-D a clear distinction exists between the association of elements with the minerogenic component (positive Ti correlation) and elements associated with increased combustion (organic) values (Table 6.3.3.). Elements P, Mg, Na, Mn and Ca in the core (Fig. 6.5.7) and their positive correlation with organic values, suggest surface concentration by saline-wetland soil vertical migration (e.g. McCaffrey & Thomson, 1980; Adam, 1990). The profile of Ca indicates a rapid decline from the surface to a core minimum (3 % ashed mass) at 5 cm, before recovering below 8cm (8.2%). This sub-

Table 6.3.3. Average major element abundances (% mass) in PPA and core correlation with LOI (550°C).

0-9 cm			**10-48 cm**			**Total core**		
Element	Av.	(*r*) LOI	Element	Av.	(*r*) LOI	Element	Av.	(*r*) LOI
LOI	32.71		LOI	14.91		LOI	18.25	
P_2O_5	0.47	0.572	MgO	2.54	0.906	MgO	3.07	0.895
MgO	5.39	0.502	K_2O	2.56	0.868	Na_2O	4.01	0.883
Na_2O	8.17	0.502	Na_2O	3.05	0.835	P_2O_5	0.24	0.871
MnO	0.05	0.478	Al_2O_3	15.25	0.791	K_2O	2.62	0.445
CaO	7.89	0.177	P_2O_5	0.18	0.703	Fe_2O_3	7.18	0.384
Al_2O_3	16.02	-0.074	Fe_2O_3	7.00	0.570	Al_2O_3	15.40	0.371
K_2O	2.90	-0.173	TiO_2	0.95	0.450	TiO_2	0.94	-0.236
TiO_2	0.88	-0.310	SiO_2	55.31	0.09	CaO	12.10	-0.469
SiO_2	50.25	-0.48	CaO	13.07	-0.698	MnO	0.07	-0.496
Fe_2O_3	7.97	-0.661	MnO	0.07	-0.861	SiO_2	54.36	-0.618

Elements ordered by correlation with LOI (wt%)

Major element abundances and correlation with Ti.

0-9 cm			**10-48 cm**			**Total core**		
Element	Av.	(*r*) Ti	Element	Av.	(*r*) Ti	Element	Av.	(*r*) Ti
TiO_2	0.88		TiO_2	0.95		TiO_2	0.94	
SiO_2	50.25	0.90	Al_2O_3	15.25	0.837	SiO_2	54.36	0.830
Al_2O_3	16.02	0.896	SiO_2	55.31	0.82	Al_2O_3	15.40	0.723
K_2O	2.90	0.825	P_2O_5	0.18	0.728	K_2O	2.62	0.533
Fe_2O_3	7.97	0.770	Na_2O	3.05	0.695	Fe_2O_3	7.18	0.138
Na_2O	8.17	-0.081	K2O	2.56	0.687	Na_2O	4.01	-0.172
LOI	32.71	-0.310	MgO	2.54	0.452	LOI	18.25	-0.236
P_2O_5	0.47	-0.564	LOI	14.91	0.450	P_2O_5	0.24	-0.243
MgO	5.39	-0.697	Fe_2O_3	7.00	0.173	MgO	3.07	-0.352
MnO	0.05	-0.766	MnO	0.07	-0.600	MnO	0.07	-0.382
CaO	7.89	-0.941	CaO	13.07	-0.857	CaO	12.10	-0.635

Elements ordered by correlation with Ti (wt%)

Figure 6.5.6. Correlation of major elements with (a) loss on ignition (550°C) and (b) Ti values: Pantano Piccolo A

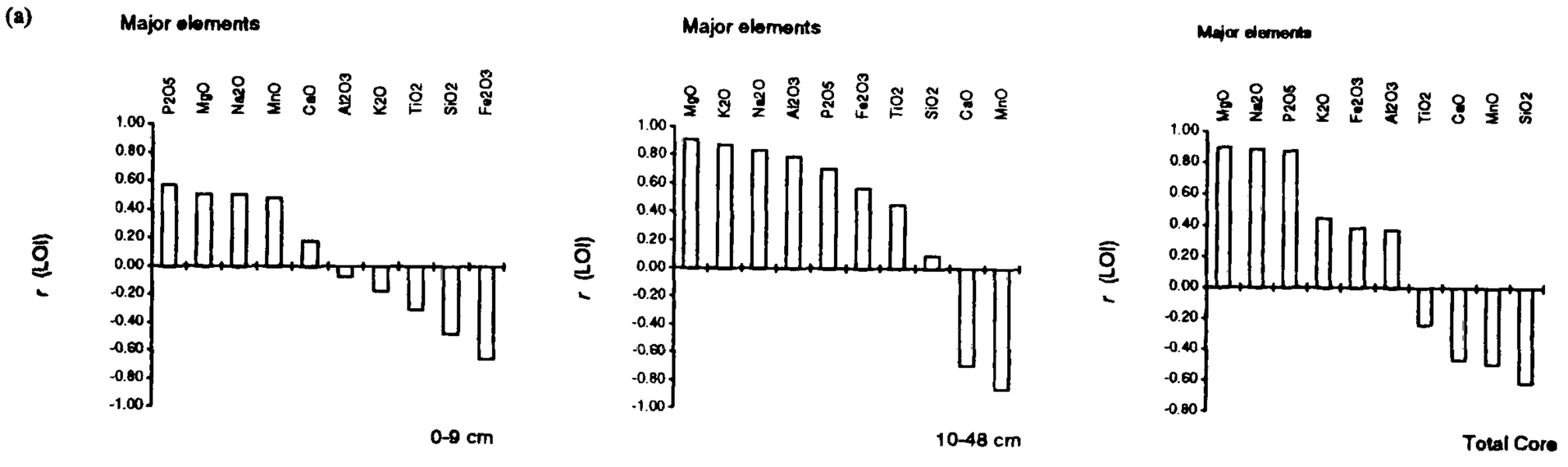

Figure 6.5.7a. Major element abundance, Fe:Mn ratio and ^{210}Pb total activity plotted against proxy organic content (loss on ignition at 550°C) from Pantano Piccolo A

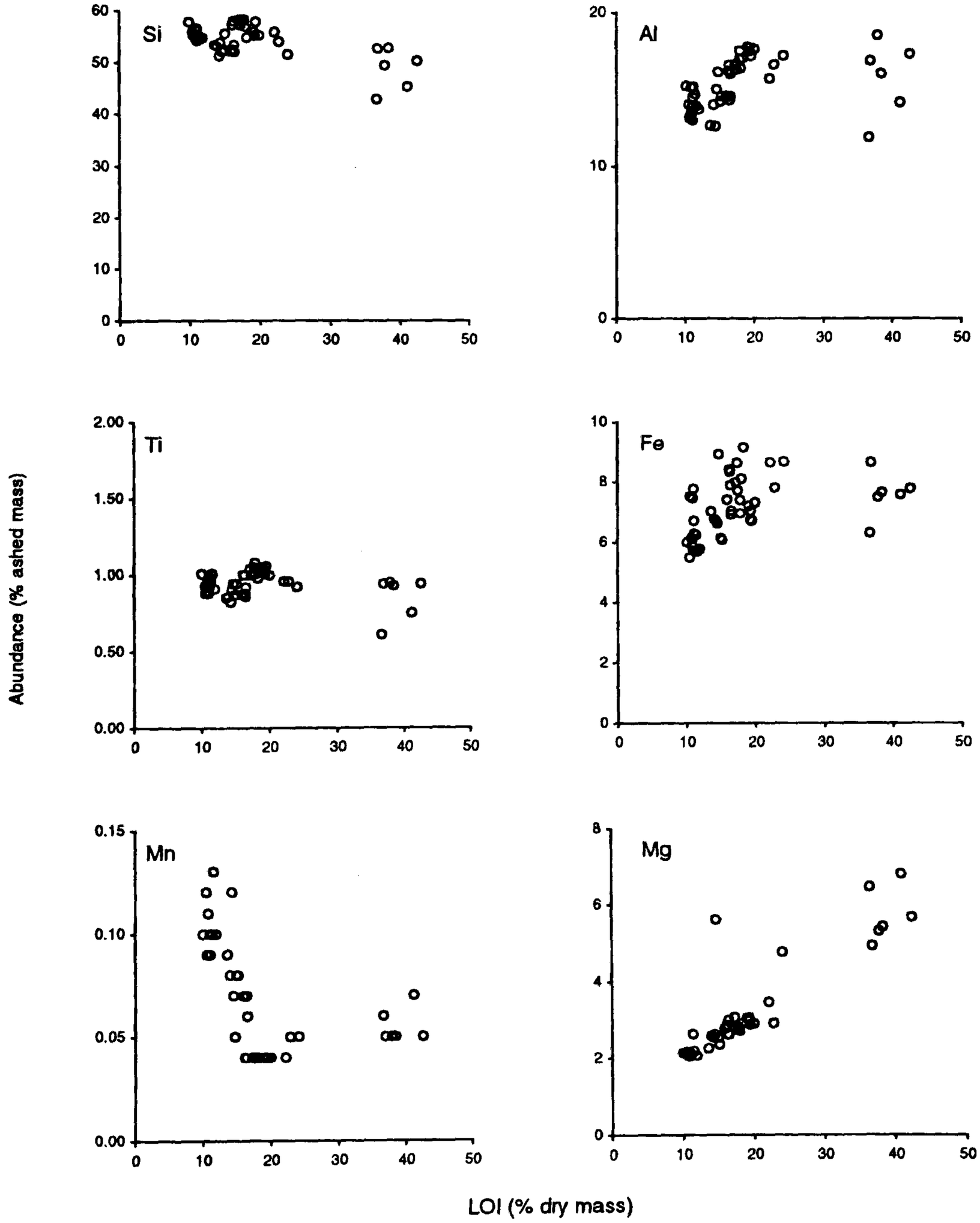

Figure 6.5.7b. Major element abundance, Fe:Mn ratio and ^{210}Pb total activity plotted against proxy organic content (loss on ignition at 550°C) from Pantano Piccolo A

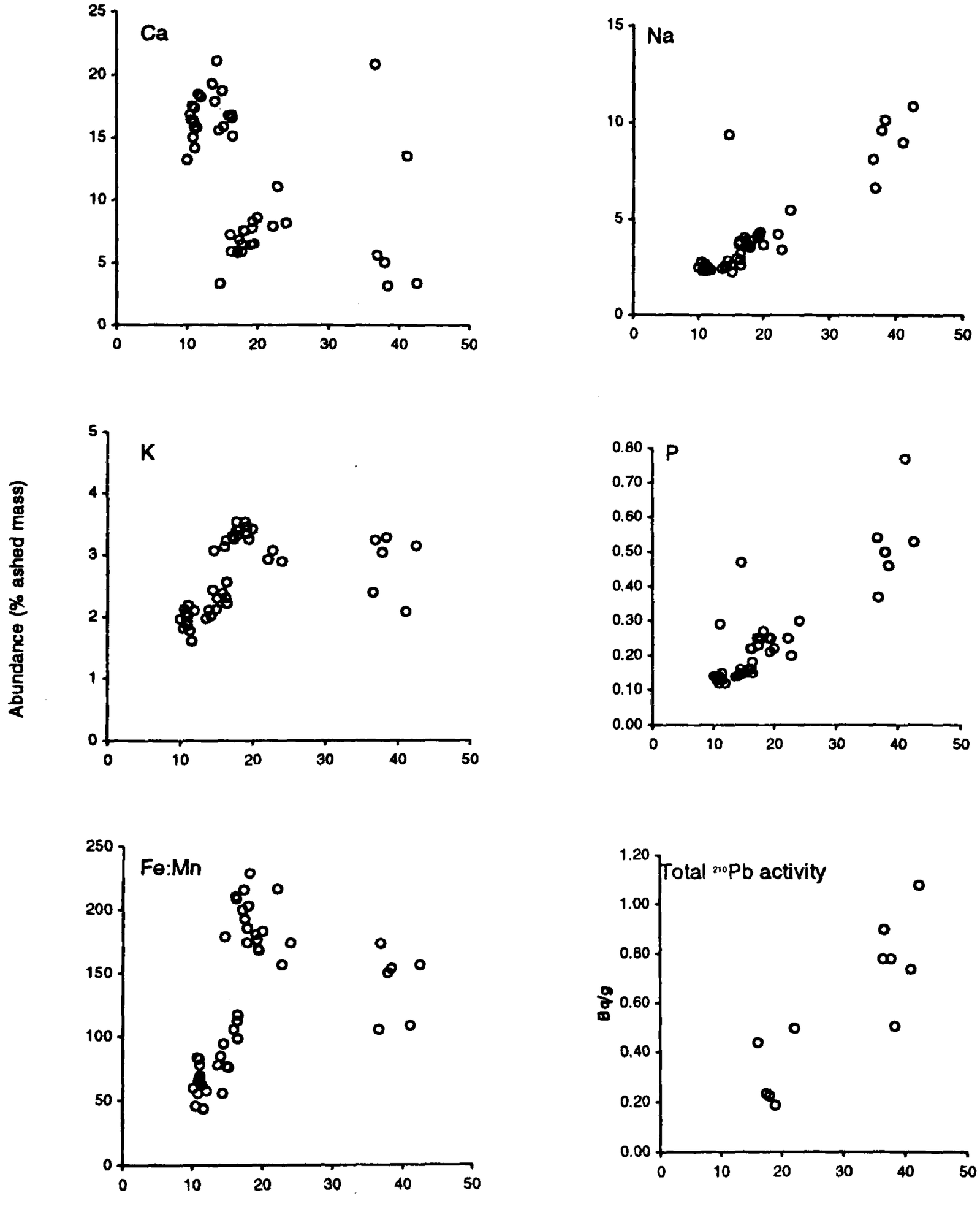

surface minima probably reflects the dissolution of carbonates due to a transient drop in pore water pH, caused by acidity generating processes (e.g. the decomposition of organic matter) in the oxic surface sediments (e.g. Zwolsman *et al.*, 1993). The banded light grey and brown sediments which were observed on extraction at the base of PPA-D (Fig. 6.4.8.) may have corresponded therefore to a zone of carbonate re-precipitation in a reduced environment. Their disappearance may have been due to being exposed to the atmosphere and/or a change in pH following extraction.

6.3.7 Pantano Piccolo A Pollen

Twenty-four 1 cm thick samples were extracted at 2 cm intervals through the core. Pollen totals in the core were dominated by Amaranthaceae-Chenopodiaceae and Lactuceae without which pollen totals would have been very low. Pollen grains were generally well preserved, though many Amaranthaceae-Chenopodiaceae and Lactuceae grains displayed evidence of mechanical stress.

Four local pollen assemblage zones using the CONISS total sum of squares function were defined (Fig. 6.5.8.) using all (28) pollen taxa. Relative abundance and total pollen concentrations were determined throughout the core (Figs. 6.5.8 and 6.5.9) and are tabulated in Tables 6.3.4. and 6.3.5. Due however to the low counts of pollen encountered (< 200 TP) in PPA at 40-39 cm, 34-33 cm, 28-27 cm, 26-25 cm 24-23 cm and 22-21 cm, these intervals were not used in the CONISS calculation or percentage diagram. Relative abundance values are only mentioned in the text below from reliable sample intervals. Pollen accumulation rates were also determined in samples within the upper 18 cm of the core (Table 6.3.6., Fig. 6.6.) using ^{210}Pb sedimentation rates derived from the CRS age-depth model.

LPAZ PPA-P1: 48-38.5 cm (Basal sediments and lagoonal deposits)

The lowest pollen zone is subdivided into upper (PPA-P1b) and lower (PPA-P1a) units. Pollen in the lower zone (PPA-P1a) is dominated by Amaranth.-Chenopodiaceae, Lactuceae, Cyperaceae, Poaceae, Asteraceae subf. Asteroideae and Apiaceae taxa. The relative abundance of Amaranthaceae-Chenopodiaceae remains relatively constant within PPA-P1, only increasing from 40 % at 47.5 cm up to 45 % at 41.5 cm, before declining into PPA-P2. Lactuceae similarly increases from 14.9 % at 47.5 cm up to 30.9% at 37.5 within PPA-P2.

An increase in pollen concentrations of tree, shrub, herb and aquatic types are observed within PPA-P1a. Increased concentrations of *Cirsium*, *Anthemis*, Caryophyllaceae, *Plantago* and *Serratula* indicate a nearby disturbed-ground community. An increase in

Table 6.3.4. Counts and pollen percentages of pollen types in sediment horizons of Pantano Piccolo A core (Surface - 24 cm depth) In order of number counted through core

	Sample horizon PPA 1-2cm		Sample horizon PPA3-4cm		Sample horizon PPA5-6cm		Sample horizon PPA7-8cm		Sample horizon PPA9-10cm		Sample horizon PPA 11-12cm		Sample horizon PPA 13-14cm		Sample horizon PPA 15-16cm		Sample horizon PPA 17-18cm		Sample horizon PPA 19-20cm		Sample horizon PPA 21-22cm		Sample horizon PPA 23-24cm	
	Count	%	Count	%	Count	%	Count	%	Count	%	Count	%	Count	%	Count	%	Count	%	Count	%	Count	%	Count	%
Arboreal pollen																								
Pinus	8	1.37	3	0.59	9	1.31	18	2.64	6	0.84	4	1.29	2	0.76	3	1.18	4	1.25	4	1.22	4	3.54	3	1.90
Quercus undiff.	7	1.20	6	1.18	4	0.58	4	0.59	5	0.70	4	1.29	6	2.27	5	1.97	2	0.63	7	2.13	4	3.54	1	0.63
Betula	1	0.17	3	0.59	3	0.44	0	0.00	0	0.00	0	0.00	0	0.00	0	0.00	2	0.63	0	0.00	0	0.00	4	2.53
Tilia	0	0.00	0	0.00	0	0.00	0	0.00	0	0.00	0	0.00	0	0.00	0	0.00	0	0.00	0	0.00	0	0.00	0	0.00
Alnus	0	0.00	0	0.00	0	0.00	0	0.00	0	0.00	0	0.00	0	0.00	0	0.00	0	0.00	0	0.00	1	0.88	0	0.00
Eucalyptus	1	0.17	0	0.00	0	0.00	0	0.00	0	0.00	0	0.00	0	0.00	0	0.00	0	0.00	0	0.00	0	0.00	0	0.00
Arboreal total	17	2.92	12	2.36	16	2.33	22	3.23	11	1.54	8	2.57	8	3.03	8	3.15	8	2.50	11	3.35	9	7.96	8	5.06
Olea-Phyllirea	19	3.26	10	1.97	22	3.20	38	5.57	14	1.97	8	2.57	12	4.55	19	7.48	9	2.81	11	3.35	7	6.19	6	3.80
Juniperus	3	0.52	3	0.59	0	0.00	6	0.88	0	0.00	0	0.00	2	0.76	0	0.00	0	0.00	8	2.44	0	0.00	0	0.00
Ericaceae	1	0.17	1	0.20	4	0.58	0	0.00	0	0.00	0	0.00	0	0.00	0	0.00	3	0.94	0	0.00	3	2.65	0	0.00
Ephedra fragilis	0	0.00	0	0.00	0	0.00	0	0.00	0	0.00	0	0.00	0	0.00	0	0.00	0	0.00	0	0.00	0	0.00	0	0.00
Corylus	0	0.00	0	0.00	0	0.00	0	0.00	0	0.00	1	0.00	0	0.00	0	0.00	0	0.00	0	0.00	0	0.00	2	1.27
Arboreal (Shrub) total	23	3.95	14	2.76	26	3.78	44	6.45	14	1.97	9	2.89	14	5.30	19	7.48	12	3.75	19	5.79	10	8.85	8	5.06
Non-Arboreal (Herb) pollen																								
Amaranth.-Chenopodiaceae	503	86.43	443	87.20	581	84.57	542	79.47	562	78.93	208	66.88	129	48.86	123	48.43	178	55.63	143	43.60	49	43.36	48	30.38
Lactuceae undiff.	5	0.86	2	0.39	5	0.73	12	1.76	62	8.71	42	13.50	61	23.11	69	27.17	86	26.88	92	28.05	27	23.89	63	39.87
Asteraceae subf. Asteroideae	4	0.69	4	0.79	17	2.47	12	1.76	15	2.11	7	2.25	22	8.33	12	4.72	9	2.81	24	7.32	5	4.42	9	5.70
Poaceae undiff.	13	2.23	14	2.76	16	2.33	21	3.08	8	1.12	9	2.89	8	3.03	7	2.76	8	2.50	13	3.96	4	3.54	3	1.90
Apiaceae undiff.	4	0.69	0	0.00	5	0.73	0	0.00	14	1.97	15	4.82	11	4.17	7	2.76	7	2.19	4	1.22	0	0.00	7	4.43
Cirsium	0	0.00	3	0.59	4	0.58	5	0.73	17	2.39	9	2.89	3	1.14	8	3.15	7	2.19	16	4.88	5	4.42	7	4.43
Anthemis	4	0.69	2	0.39	3	0.44	2	0.29	5	0.70	4	1.29	5	1.89	0	0.00	2	0.63	0	0.00	2	1.77	1	0.63
Cyperaceae	0	0.00	0	0.00	0	0.00	0	0.00	0	0.00	0	0.00	3	1.14	0	0.00	0	0.00	3	0.91	0	0.00	4	2.53
Lobelia type	0	0.00	0	0.00	9	1.31	19	2.79	0	0.00	0	0.00	0	0.00	0	0.00	0	0.00	0	0.00	0	0.00	0	0.00
Serratula	0	0.00	0	0.00	0	0.00	0	0.00	0	0.00	0	0.00	0	0.00	0	0.00	0	0.00	0	0.00	0	0.00	0	0.00
Plantago	8	1.37	7	1.38	3	0.44	3	0.44	0	0.00	0	0.00	0	0.00	0	0.00	0	0.00	0	0.00	0	0.00	0	0.00
Caryophyllaceae undiff.	0	0.00	0	0.00	0	0.00	0	0.00	0	0.00	0	0.00	0	0.00	1	0.39	2	0.63	3	0.91	0	0.00	0	0.00
Ranunculus type	0	0.00	0	0.00	0	0.00	0	0.00	0	0.00	0	0.00	0	0.00	0	0.00	0	0.00	0	0.00	1	0.88	0	0.00
Polygonaceae	0	0.00	0	0.00	0	0.00	0	0.00	4	0.56	0	0.00	0	0.00	0	0.00	1	0.31	0	0.00	0	0.00	0	0.00
Limonium type	0	0.00	0	0.00	0	0.00	0	0.00	0	0.00	0	0.00	0	0.00	0	0.00	0	0.00	0	0.00	0	0.00	0	0.00
Gentianella type	0	0.00	3	0.59	2	0.29	0	0.00	0	0.00	0	0.00	0	0.00	0	0.00	0	0.00	0	0.00	0	0.00	0	0.00
Fillipendula	1	0.17	4	0.79	0	0.00	0	0.00	0	0.00	0	0.00	0	0.00	0	0.00	0	0.00	0	0.00	0	0.00	0	0.00
NAP total	542	93.127	482	94.882	645	93.886	616	90.323	687	96.489	294	94.534	242	91.667	227	89.37	300	93.75	298	90.854	93	82.301	142	89.873
Total Pollen sum (AP/NAP)	582		508		687		682		712		311		264		254		320		328		113		158	
Aquatics																								
Potamogetonaceae	0	0.00	0	0.00	0	0.00	0	0.00	0	0.00	0	0.00	0	0.00	0	0.00	0	0.00	0	0.00	0	0.00	0	0.00
Nuphar	0	0.00	0	0.00	0	0.00	0	0.00	0	0.00	0	0.00	0	0.00	0	0.00	0	0.00	0	0.00	1	0.88	0	0.00
Nymphaeae	0	0.00	0	0.00	0	0.00	0	0.00	0	0.00	0	0.00	0	0.00	0	0.00	0	0.00	0	0.00	0	0.00	0	0.00
Aquatic total	0	0.00	0	0.00	0	0.00	0	0.00	0	0.00	1	0.32	0	0.00	0	0.00	0	0.00	0	0.00	1	0.88	2	1.27
(not included in pollen sum)																								
Added *Lycopodium*	116		43		68		104		109		82		122		108		127		128		195		163	

Table 6.3.4. Counts and pollen percentages of pollen types in sediment horizons of Pantano Piccolo A core (25 - 48 cm depth). In order of number counted through core

	Sample horizon PPA 25-26cm		Sample horizon PPA 27-28cm		Sample horizon PPA 29-30cm		Sample horizon PPA 31-32cm		Sample horizon PPA 33-34cm		Sample horizon PPA 35-36cm		Sample horizon PPA 37-38cm		Sample horizon PPA 39-40cm		Sample horizon PPA 41-42cm		Sample horizon PPA 43-44cm		Sample horizon PPA 45-46cm		Sample horizon PPA 47-48cm	
	Count	%	Count	%	Count	%	Count	%	Count	%	Count	%	Count	%	Count	%	Count	%	Count	%	Count	%	Count	%
Arboreal pollen																								
Pinus	10	5.24	9	4.81	14	6.97	15	6.61	3	2.24	5	2.12	7	2.78	7	4.38	5	1.92	8	3.39	8	2.40	7	2.76
Quercus undiff.	6	3.14	6	3.21	3	1.49	4	1.76	2	1.49	4	1.69	6	2.38	4	2.50	3	1.15	4	1.69	8	2.40	2	0.79
Betula	2	1.05	2	1.07	0	0.00	3	1.32	0	0.00	2	0.85	0	0.00	0	0.00	0	0.00	1	0.42	4	1.20	4	1.57
Tilia	2	1.05	1	0.53	0	0.00	0	0.00	0	0.00	0	0.00	0	0.00	0	0.00	0	0.00	0	0.00	0	0.00	0	0.00
Alnus	0	0.00	0	0.00	0	0.00	0	0.00	0	0.00	0	0.00	0	0.00	1	0.63	0	0.00	0	0.00	0	0.00	0	0.00
Eucalyptus	0	0.00	0	0.00	0	0.00	0	0.00	0	0.00	0	0.00	0	0.00	0	0.00	0	0.00	0	0.00	0	0.00	0	0.00
Arboreal total	20	10.47	18	9.63	17	8.46	22	9.69	5	3.73	11	4.66	13	5.16	12	7.50	8	3.08	13	5.51	20	6.01	13	5.12
Olea-Phyllirea	5	2.62	6	3.21	8	3.98	9	3.96	2	1.49	8	3.39	12	4.76	8	5.00	8	3.08	11	4.66	9	2.70	12	4.72
Juniperus	6	3.14	0	0.00	7	3.48	0	0.00	0	0.00	4	1.69	2	0.79	3	1.88	0	0.00	0	0.00	9	2.70	4	1.57
Ericaceae	6	3.14	0	0.00	0	0.00	0	0.00	0	0.00	0	0.00	0	0.00	0	0.00	0	0.00	0	0.00	2	0.60	0	0.00
Ephedra fragilis	0	0.00	4	2.14	2	1.00	2	0.88	0	0.00	0	0.00	3	1.19	0	0.00	0	0.00	0	0.00	2	0.60	0	0.00
Corylus	0	0.00	0	0.00	0	0.00	0	0.00	0	0.00	0	0.00	0	0.00	0	0.00	0	0.00	0	0.00	0	0.00	0	0.00
Arboreal (Shrub) total	17	8.90	6	3.21	15	7.46	9	3.96	2	1.49	12	5.08	14	5.56	11	6.88	8	3.08	11	4.66	20	6.01	16	6.30
Non-Arboreal (Herb) pollen																								
Amaranth-Chenopodiaceae	40	20.94	58	31.02	47	23.38	73	32.16	52	38.81	77	32.63	101	40.08	53	33.13	117	45.00	101	42.80	132	39.64	103	40.55
Lactuceae undiff.	92	48.17	57	30.48	78	38.81	77	33.92	43	32.09	86	36.44	78	30.95	38	23.75	67	25.77	48	20.34	54	16.22	38	14.96
Asteraceae subf. Aster	5	2.62	12	6.42	6	2.99	8	3.52	6	4.48	11	4.66	10	3.97	7	4.38	14	5.38	12	5.08	8	2.40	19	7.48
Poaceae	4	2.09	15	8.02	12	5.97	9	3.96	9	6.72	9	3.81	9	3.57	12	7.50	7	2.69	12	5.08	17	5.11	0	0.00
Apiaceae undiff.	5	2.62	5	2.67	10	4.98	5	2.20	8	5.97	9	3.81	9	3.57	9	5.63	4	1.54	7	2.97	13	3.90	12	4.72
Cirsium	1	0.52	3	1.60	7	3.48	5	2.20	4	2.99	7	2.97	6	2.38	4	2.50	13	5.00	6	2.54	18	5.41	11	4.33
Anthemis	0	0.00	3	1.60	3	1.49	4	1.76	0	0.00	3	1.27	4	1.59	0	0.00	6	2.31	8	3.39	9	2.70	4	1.57
Cyperaceae	2	1.05	0	0.00	0	0.00	1	0.44	1	0.75	0	0.00	0	0.00	7	4.38	0	0.00	0	0.00	20	6.01	32	12.60
Lobelia type	0	0.00	0	0.00	0	0.00	0	0.00	0	0.00	0	0.00	0	0.00	4	2.50	0	0.00	0	0.00	0	0.00	0	0.00
Serratula	2	1.05	0	0.00	0	0.00	2	0.88	0	0.00	3	1.27	4	1.59	3	1.88	3	1.15	3	1.27	4	1.20	3	1.18
Plantago	0	0.00	0	0.00	2	1.00	0	0.00	0	0.00	0	0.00	0	0.00	0	0.00	0	0.00	3	1.27	4	1.20	0	0.00
Caryophyllaceae undiff.	2	1.05	3	1.60	2	1.00	4	1.76	0	0.00	2	0.85	0	0.00	0	0.00	0	0.00	2	0.85	3	0.90	0	0.00
Ranunculus type	0	0.00	1	0.53	0	0.00	4	1.76	2	1.49	0	0.00	0	0.00	0	0.00	3	1.15	5	2.12	0	0.00	0	0.00
Polygonaceae	0	0.00	0	0.00	0	0.00	0	0.00	0	0.00	0	0.00	0	0.00	0	0.00	2	0.77	2	0.85	0	0.00	3	1.18
Limonium type	0	0.00	0	0.00	0	0.00	0	0.00	0	0.00	1	0.42	1	0.40	0	0.00	3	1.15	3	1.27	0	0.00	0	0.00
Gentianella type	0	0.00	0	0.00	0	0.00	0	0.00	0	0.00	0	0.00	0	0.00	0	0.00	0	0.00	0	0.00	1	0.30	0	0.00
Fillipendula	0	0.00	0	0.00	0	0.00	0	0.00	0	0.00	0	0.00	0	0.00	0	0.00	0	0.00	0	0.00	0	0.00	0	0.00
NAP(Herb) total	153	80.10	157	83.96	167	83.08	192	84.58	125	93.28	208	88.14	222	88.10	137	85.63	239	91.92	212	89.83	283	84.98	225	88.58
Total Pollen (AP/NAP)	191		187		201		227		134		236		252		160		260		236		333		254	
Aquatics																								
Potamogetonaceae	0	0.00	0	0.00	0	0.00	2	0.88	1	0.75	5	2.12	0	0.00	0	0.00	5	1.92	0	0.00	8	2.40	0	0.00
Nuphar	1	0.52	2	1.07	0	0.00	0	0.00	0	0.00	0	0.00	0	0.00	0	0.00	0	0.00	0	0.00	0	0.00	0	0.00
Nymphaeae	0	0.00	0	0.00	0	0.00	0	0.00	1	0.75	0	0.00	0	0.00	0	0.00	0	0.00	0	0.00	0	0.00	0	0.00
Aquatic total (not included in pollen sum)	1	0.52	2	1.07	0	0.00	2	0.88	2	1.49	5	2.12	0	0.00	0	0.00	5	1.92	0	0.00	8	2.40	0	0.00
Added *Lycopodium*	329		263		328		428		282		248		262		112		239		257		118		132	

Statistically unreliable low pollen totals for % underlined

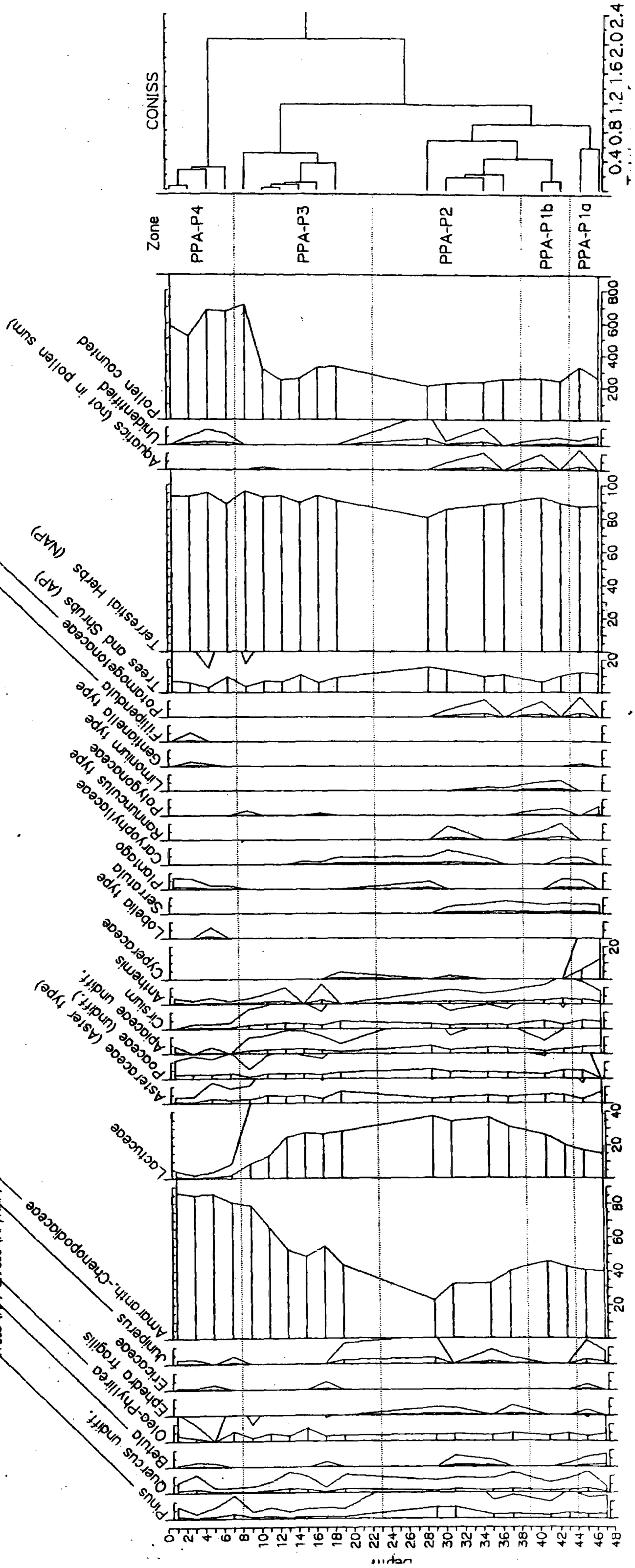

Figure 6.5.8. Pantano Piccolo A (PPA) Pollen percentage diagram
Note: due to low counts intervals 21-22, 23-24, 25-26, 27-28, 31-32 & 39-40 cm are absent from diagram and Coniss dendrogram calculation

anemophilous tree (*Pinus*, *Quercus undiff.*, *Betula*) and anemo/entomophilous macchia types (*Olea-Phyllirea*, *Juniperus*, Ericaceae) correspond with increased Cyperaceae (0.97 x 10^3 grains per gram at 45.5 cm) and Potamogetonaceae (0.39 x 10^3 grains/g) over the same interval.

Total pollen concentrations decline in PPA-P1b with a decrease in Cyperaceae and Potamogetonaceae pollen. A decline in the concentration of *Pinus*, *Quercus* undiff. and the disappearance of *Betula*, across the boundary of PPA-P1a and PPA-P1b is followed by a peak in tree pollen at 39.5 cm depth. A solitary *Alnus* grain was also counted at this horizon (0.05 x 10^3 grains/g). *Olea-Phyllirea* and *Juniperus* are seen also to decline from PPA-P1a and increase again in PPA-P1b.

Almost all herb pollen types decrease in concentration between PPA-P1a and PPA-P1b. Chenopodiaceae, Poaceae, *Anthemis*, *Cirsium*, Asteraceae subf. Asteroideae and to some extent, Apiaceae and *Serratula* type decline gradually into PPA-P2. The concentration of Lactuceae in PPA-P1b (av. 1.77 x 10^3 gr/g) increases slowly, before it too declines in PPA-P2 and sediment horizon PPA-B. PPA-P1 and its transition to PPA-P2 is marked in the core by the concentration of *Limonium* type pollen (0.72 x 10^2 grains/g at 43.5 cm down to 0.026 x 10^3 grains/g at 35.5 cm).

LPAZ PPA-P2: 38.5 to 22.5 cm (prior to the AD 19th - 20th century)

The continued decline in the relative abundance of Amaranthaceae-Chenopodiaceae reaches a minimum at 29.5 cm (23 %) commensurate with increasing Lactuceae which peaks at the same interval (38 %). Tree pollen concentrations increase in PPA-P2 up to the boundary with PPA-P3. The relative abundance of *Pinus* is also observed to increase measurably as Amaranthaceae-Chenopodiaceae declines.

Preceding a small peak in *Betula* concentration at 23.5 cm (454 grains/g), *Tilia* is represented in the core at 27.5 cm and 25.5 cm by only two grains and a solitary grain (34 grains/g and 52 grains/g respectively). Shrub pollen concentrations remain low in PPA-P2, with the re-appearance of Ericaceae at the upper boundary of the zone.

The recognisable peak in total pollen concentration at 23.5 cm (1.7 x 10^4 grains/g) is caused by an increase in the dominant herb types leading up to the top of PPA-P2 (including Cyperaceae). Only Poaceae and *Anthemis* continue at low concentrations into PPA-P3. Less abundant herb types (Caryophyllaceae,*Serratula* type and *Ranunculus* type) are also present in PPA-P2. These types decrease up to the boundary of PPA-P3 and disappear, with the exception of Caryophyllaceae which increases again in PPA-P3.

A greater element of extra-local transport or even marine influence is suggested by the abundance of foraminifera organic linings at 29-30 cm to 25-26 cm.

Table 6.3.5. Counts and pollen concentrations (grains per dry mass of sediment)of pollen types in sediment horizons of Pantano Piccolo A core (Surface - 24 cm depth)

	Sample horizon PPA 1-2cm		Sample horizon PPA3-4cm		Sample horizon PPA5-6cm		Sample horizon PPA7-8cm		Sample horizon PPA9-10cm		Sample horizon PPA 11-12cm		Sample horizon PPA 13-14cm		Sample horizon PPA 15-16cm		Sample horizon PPA 17-18cm		Sample horizon PPA 19-20cm		Sample horizon PPA 21-22cm		Sample horizon PPA 23-24cm	
	Count	Conc.	Count	Conc.	Count	Conc.	Count	Conc.	Count	Conc.	Count	Conc.	Count	Conc.	Count	Conc.	Count	Conc.	Count	Conc.	Count	Conc.	Count	Conc.
Arboreal pollen																								
Pinus	8	761.21	3	634.25	9	464.07	18	1176.59	6	301.13	4	206.70	2	69.00	3	268.13	4	359.13	4	119.32	4	134.86	3	340.83
Quercus undiff.	7	666.06	6	1268.50	4	206.25	4	261.47	5	250.94	4	206.70	6	206.99	5	446.88	2	179.57	7	208.81	4	134.86	1	113.61
Betula	1	95.15	3	634.25	3	154.69	0	0	0	0	0	0	0	0	0	0	2	179.57	0	0	0	0	4	454.44
Tilia	0	0	0	0	0	0	0	0	0	0	0	0	0	0	0	0	0	0	0	0	0	0	0	0
Alnus	0	0	0	0	0	0	0	0	0	0	0	0	0	0	0	0	0	0	0	0	1	33.72	0	0
Eucalyptus	1	95.15	0	0	0	0	0	0	0	0	0	0	0	0	0	0	0	0	0	0	0	0	0	0
Arboreal total	17	1617.57	12	2537.00	16	825.01	22	1438.06	11	552.06	8	413.39	8	275.98	8	715.00	8	718.27	11	328.13	9	303.44	8	908.88
Olea-Phyllirea	19	1807.87	10	2114.16	22	1134.39	38	2483.92	14	702.63	8	413.39	12	413.98	19	1698.13	9	808.05	11	328.13	7	236.01	6	681.66
Juniperus	3	285.45	3	634.25	0	0	6	392.20	0	0	0	0	2	69.00	0	0	0	0	8	238.64	0	0	0	0
Ericaceae	1	95.15	1	211.42	4	206.25	0	0	0	0	0	0	0	0	0	0	3	269.35	0	0	3	101.15	0	0
Ephedra fragilis	0	0	0	0	0	0	0	0	0	0	0	0	0	0	0	0	0	0	0	0	0	0	0	0
Corylus	0	0.00	0	0.00	0	0.00	0	0	0	0	1	52	0	0	0	0	0	0.00	0	0	0	0.00	2	227
Arboreal (Shrub) total	23	2188.48	14	2959.83	26	1340.65	44	2876.12	14	702.63	9	465.07	14	482.97	19	1698.13	12	1077.40	19	566.77	10	337.16	8	908.88
Non-Arboreal (Herb) pollen																								
Amaranth.-Chenopodiaceae	503	47861.00	443	93657.51	581	29958.34	542	35428.54	562	28205.49	208	10748.24	129	4450.24	123	10993.14	178	15981.47	143	4265.70	49	1652.08	48	5453.31
Lactuceae undiff.	5	475.76	2	422.83	5	257.82	12	784.40	62	3111.64	42	2170.32	61	2104.38	69	6166.88	86	7721.38	92	2744.37	27	910.33	63	7157.46
Asteraceae subf. Asteroideae	4	380.60	4	845.67	17	876.58	12	784.40	15	752.82	7	361.72	22	758.96	12	1072.50	9	808.05	24	715.92	5	168.58	9	1022.49
Poaceae undiff.	13	1236.96	14	2959.83	16	825.01	21	1372.69	8	401.50	9	465.07	8	275.98	7	625.63	8	718.27	13	387.79	4	134.86	3	340.83
Apiaceae undiff.	4	380.60	0	0	5	257.82	0	0	14	702.63	15	775.11	11	379.48	7	625.63	7	628.48	4	119.32	0	0.00	7	795.27
Cirsium	0	0	3	634.25	4	206.25	5	326.83	17	853.19	9	465.07	3	103.49	8	715.00	7	628.48	16	477.28	5	168.58	7	795.27
Anthemis	4	380.60	2	422.83	3	154.69	2	130.73	5	250.94	4	206.70	5	172.49	0	0	2	179.57	0	0	2	67.43	1	113.61
Cyperaceae	0	0	0	0	0	0	0	0	0	0	0	0	3	103.49	0	0	0	0	3	89.49	0	0	4	454.44
Lobelia type	0	0	0	0	9	464.07	19	1241.96	0	0	0	0	0	0	0	0	0	0	0	0	0	0	0	0
Serratula	0	0	0	0	0	0	0	0.00	0	0	0	0	0	0	0	0	0	0	0	0	0	0	0	0
Plantago	8	761.21	7	1479.92	3	154.69	3	196.10	0	0	0	0	0	0	0	0	0	0	0	0	0	0	0	0
Caryophyllaceae undiff.	0	0	0	0	0	0	0	0	0	0	0	0	0	0	1	89.38	2	179.57	3	89.49	0	0	0	0
Ranunculus type	0	0	0	0	0	0	0	0	0	0	0	0	0	0	0	0	0	0	0	0	1	33.72	0	0
Polygonaceae	0	0	0	0	0	0	0	0	4	200.75	0	0	0	0	0	0	1	89.78	0	0	0	0	0	0
Limonium type	0	0	0	0	0	0	0	0	0	0	0	0	0	0	0	0	0	0	0	0	0	0	0	0
Gentianella type	0	0	3	634.25	2	103.13	0	0	0	0	0	0	0	0	0	0	0	0	0	0	0	0	0	0
Filipendula	1	95.15	4	845.67	0	0	0	0	0	0	0	0	0	0	0	0	0	0	0	0	0	0	0	0
NAP total	542	51571.90	482	101902.75	645	33258.39	616	40265.65	687	34478.95	294	15192.23	242	8348.51	227	20288.15	300	26935.06	298	8889.37	93	3135.59	142	16132.70
Aquatics																								
Potamogetonaceae	0	0	0	0	0	0	0	0	0	0	0	0	0	0	0	0	0	0	0	0	0	0	0	0
Nuphar	0	0	0	0	0	0	0	0	0	0	0	0	0	0	0	0	0	0	0	0	1	33.72	0	0
Nymphaeae	0	0	0	0	0	0	0	0	0	0	0	0	0	0	0	0	0	0	0	0	0	0	0	0
Aquatic total	0	0	0	0	0	0	0	0	0	0	0	0	0	0	0	0	0	0	0	0	1	33.72	0	0.00
(not included in pollen sum)																								
Total Pollen sum (AP/NAP)	582	55377.94	508	107399.58	687	35424.06	682	44579.83	712	35733.64	311	16070.69	264	9107.47	254	22701.27	320	28730.73	328	9784.27	112	3776.19	158	17950.47
Foraminifera (undiff.)																					1	33.72		
Added Lycopodium	116		43		68		104		109		82		122		108		127		128		195		163	
Sample mass (g)	0.906		1.10		2.852		1.47		1.828		2.36		2.376		1.04		0.877		2.62		1.521		0.54	

Table 6.3.5. Counts and pollen concentrations (grains per dry mass of sediment)of pollen types in sediment horizons of Pantano Piccolo A core (25 - 48 cm depth)

	Sample horizon PPA 25-26cm		Sample horizon PPA 27-28cm		Sample horizon PPA 29-30cm		Sample horizon PPA 31-32cm		Sample horizon PPA 33-34cm		Sample horizon PPA 35-36cm		Sample horizon PPA 37-38cm		Sample horizon PPA 39-40cm		Sample horizon PPA 41-42cm		Sample horizon PPA 43-44cm		Sample horizon PPA 45-46cm		Sample horizon PPA 47-48cm	
	Count	Conc.	Count	Conc.	Count	Conc.	Count	Conc.	Count	Conc.	Count	Conc.	Count	Conc.	Count	Conc.	Count	Conc.	Count	Conc.	Count	Conc.	Count	Conc.
Arboreal pollen																								
Pinus	10	264.77	9	306.36	14	356.28	15	235.06	3	63.06	5	130.58	7	155.06	7	366.14	5	121.07	8	193.58	8	391.21	7	317.36
Quercus undiff.	6	158.86	6	204.24	3	76.35	4	62.68	2	42.04	4	104.46	6	132.91	4	209.22	3	72.64	4	96.79	8	391.21	2	90.67
Betula	2	52.95	2	68.08	0	0	3	47.01	0	0	2	52.23	0	0	0	0	0	0	1	24.20	4	195.60	4	181.35
Tilia	2	52.95	1	34.04	0	0	0	0	0	0	0	0	0	0	0	0	0	0	0	0	0	0	0	0
Alnus	0	0	0	0	0	0	0	0	0	0	0	0	0	0	1	52.31	0	0	0	0	0	0	0	0
Eucalyptus	0	0	0	0	0	0	0	0	0	0	0	0	0	0	0	0	0	0	0	0	0	0	0	0
Arboreal total	20	529.53	18	612.72	17	432.63	22	344.75	5	105.10	11	287.27	13	287.98	12	627.67	8	193.71	13	314.57	20	978.02	13	589.38
Olea-Phyllirea	5	132.38	6	204.24	8	203.59	9	141.03	2	42.04	8	208.93	12	265.82	8	418.45	8	193.71	11	266.18	9	440.11	12	544.04
Juniperus	6	158.86	0	0	7	178.14	0	0	0	0	4	104.46	2	44.30	3	156.92	0	0	0	0	9	440.11	4	181.35
Ericaceae	6	158.86	0	0	0	0	0	0	0	0	0	0	0	0	0	0	0	0	0	0	2	97.80	0	0
Ephedra fragilis	0	0	4	136.16	2	50.90	2	31.34	0	0	0	0	3	66.46	0	0	0	0	0	0	2	97.80	0	0
Corylus	0	0.00	0	0	0	0	0	0	0	0	0	0	0	0	0	0	0	0	0	0	0	0	0	0
Arboreal (Shrub) total	17	450.10	10	340.40	17	432.63	11	172.37	2	42.04	12	313.39	17	376.58	11	575.36	8	193.71	11	266.18	22	1075.83	16	725.39
Non-Arboreal (Herb) pollen																								
Amaranth.-Chenopodiaceae	40	1059.06	58	1974.33	47	1196.10	73	1143.94	52	1093.05	77	2010.91	101	2237.35	53	2772.20	117	2832.98	101	2444.01	132	6454.96	103	4669.68
Lactuceae undiff.	92	2435.85	57	1940.29	78	1985.02	77	1206.62	43	903.87	86	2245.95	78	1727.86	38	1987.61	67	1622.31	48	1161.51	54	2640.66	38	1722.79
Asteraceae subf. Asteroideae	5	132.38	12	408.48	6	152.69	8	125.36	6	126.12	11	287.27	10	221.52	7	366.14	14	338.99	12	290.38	8	391.21	19	861.40
Poaceae undiff.	4	105.91	15	510.60	12	305.39	9	141.03	9	189.18	9	235.04	9	199.37	12	627.67	7	169.49	12	290.38	17	831.32	0	0
Apiaceae undiff.	5	132.38	5	170.20	10	254.49	5	78.35	8	168.16	9	235.04	9	199.37	9	470.75	4	96.85	7	169.39	13	635.72	12	544.04
Cirsium	1	26.48	3	102.12	7	178.14	5	78.35	4	84.08	7	182.81	6	132.91	4	209.22	13	314.78	6	145.19	18	880.22	11	498.70
Anthemis	0	0	3	102.12	3	76.35	4	62.68	0	0	3	78.35	4	88.61	0	0	6	145.28	8	193.58	9	440.11	4	181.35
Cyperaceae	2	52.95	0	0	0	0	1	15.67	1	21.02	0	0	0	0	7	366.14	0	0	0	0	20	978.02	32	1450.77
Lobelia type	0	0	0	0	0	0	0	0	0	0	0	0	0	0	4	209.22	0	0	0	0	0	0	0	0
Serratula	2	52.95	0	0	0	0	2	31.34	0	0	3	78.35	4	88.61	3	156.92	3	72.64	3	72.59	4	195.60	3	136.01
Plantago	0	0	0	0	2	50.90	0	0	0	0	0	0	0	0	0	0	0	0	3	72.59	4	195.60	0	0
Caryophyllaceae undiff.	2	52.95	3	102.12	2	50.90	4	62.68	0	0	2	52.23	0	0	0	0	0	0	2	48.40	3	146.70	0	0
Ranunculus type	0	0	1	34.04	0	0	4	62.68	2	42.04	0	0	0	0	0	0	3	72.64	5	120.99	0	0	0	0
Polygonaceae	0	0	0	0	0	0	0	0	0	0	0	0	0	0	0	0	2	48.43	2	48.40	0	0	3	136.01
Limonium type	0	0	0	0	0	0	0	0	0	0	1	26.12	1	22.15	0	0	3	72.64	3	72.59	0	0	0	0
Gentianella type	0	0	0	0	0	0	0	0	0	0	0	0	0	0	0	0	0	0	0	0	1	48.90	0	0
Filipendula	0	0	0	0	0	0	0	0	0	0	0	0	0	0	0	0	0	0	0	0	0	0.00	0	0
NAP(Herb) total	153	4050.92	161	5480.46	169	4300.87	194	3040.05	125	2627.52	208	5432.06	225	4984.21	137	7165.87	239	5787.04	212	5129.99	285	13936.84	225	10200.75
Aquatics																								
Potamogetonaceae	0	0	0	0	0	0	2	31.34	1	21.02	5	130.58	0	0	0	0	5	121.07	0	0	8	391.21	0	0
Nuphar	1	26.48	2	68.08	0	0	0	0	0	0	0	0	0	0	0	0	0	0	0	0	0	0	0	0
Myrica	0	0	0	0	0	0	0	0	0	0	0	0	0	0	0	0	0	0	0	0	0	0	0	0
Nymphaeae	0	0	0	0	0	0	0	0	1	21.02	0	0	0	0	0	0	0	0	0	0	0	0	0	0
Aquatic total (not included in pollen sum)	1	26.48	2	68.08	0	0	2	31.34	2	42.04	5	130.58	0	0	0	0	5	121.07	0	0	8	391.21	0	0
Total Pollen sum (AP/NAP)	190	5030.55	185	6297.42	201	5115.23	225	3525.83	132	2774.66	231	6032.72	252	5582.31	160	8368.90	260	6295.52	236	5710.75	325	15892.89	254	11515.51
Foraminifera (undiff.)	5	132.38	3	79.43	9	238.29																		
Added *Lycopodium*	329		263		328		428		282		248		262		112		239		257		118		132	
Sample mass (g)	1.148		1.12		1.198		1.49		1.687		1.54		1.723		1.71		1.728		1.61		1.733		1.67	

Figure 6.5.9. Pantano Piccolo A: Pollen Concentration diagram (in order of core concentration)

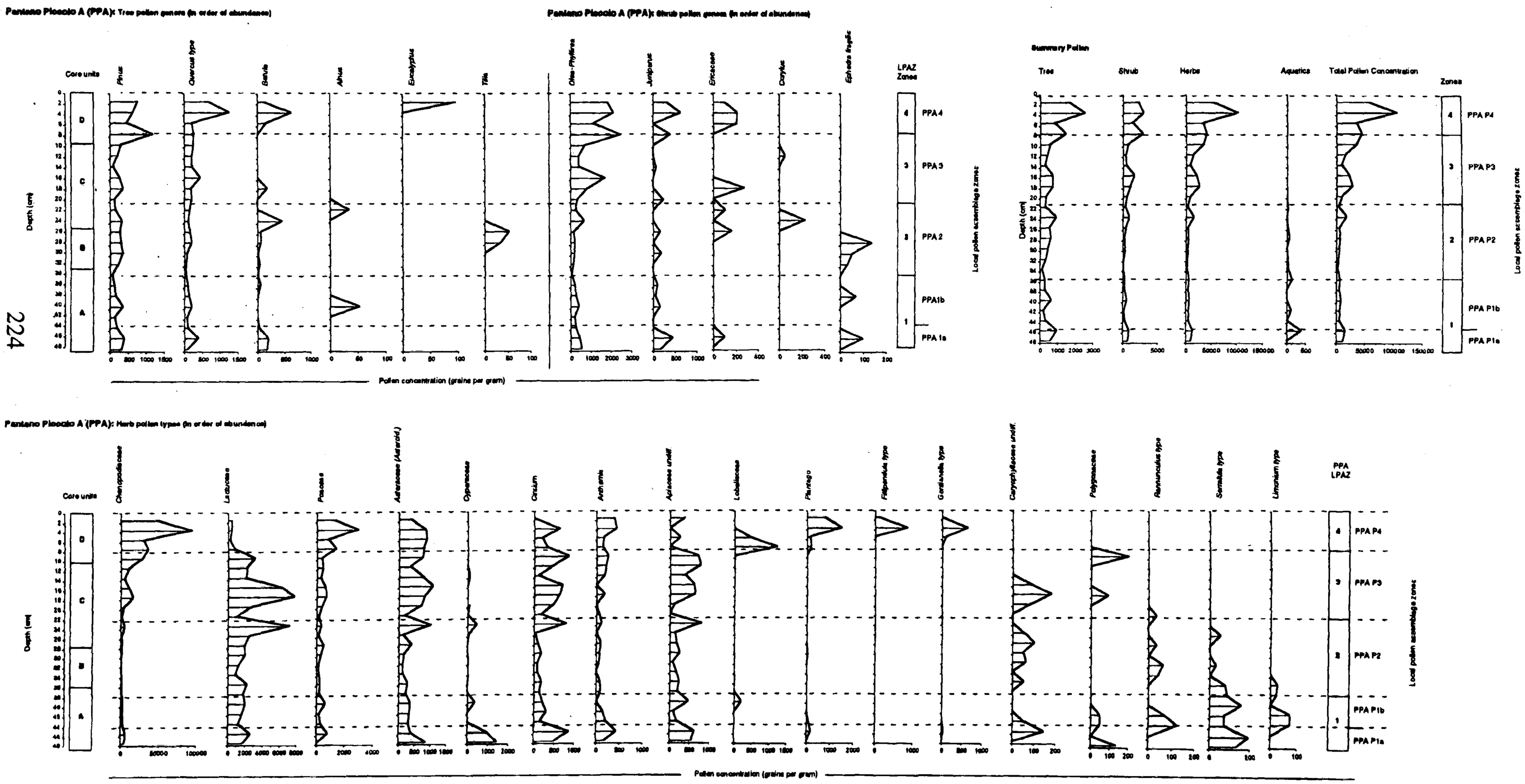

LPAZ PPA-P3: 22.5 cm to 8.5 cm (mid-late 19th century AD to circa AD 1964)

From the previously low relative abundance of Amaranthaceae-Chenopodiaceae and peak in Lactuceae at 29 cm, in LPAZ PPA 3 the abundance of Amaranthaceae-Chenopodiaceae increases steadily up to 78.9 % by 9.5 cm. The relative abundance of Lactuceae shows a corresponding decline through PPA-P3 to a low in PPA P4. Total pollen concentration increases through the zone from a low of 3.8 x 10^3 grains/g at 21.5 cm. Total pollen concentration (dominated by Chenopodiaceae) decreases at 13.5 cm (9.1 x 10^3 grains/g) before increasing steadily up to PPA P4.

Low values of *Pinus* and *Olea-Phyllirea* follow the pattern observed in the total pollen curve. *Pinus* concentration at 21.5 cm is at 0.13 x 10^3 grains/g and 0.069 x 10^3 grains/g at 13.5 cm. *Olea-Phyllirea* increases from 21.5 cm (0.23 x 10^3 grains/g) to a peak at 15.5 cm (1.6 x 10^3 grains/g) before decreasing again at 13.5 cm. *Olea-Phyllirea* increases again from this horizon to a peak (2.4 x 10^3 grains/g) at the base of PPA 4 (7.5cm). *Alnus* and *Betula* grains are also recorded at the base of PPA-P3.

Decreased pollen concentration at 21.5 cm is especially marked by the Lactuceae curve, having dropped from 7.1 x 10^3 grains/g at 23.5 cm down to 0.9 x 10^3 grains/g by 21.5 cm. The concentration of Lactuceae pollen recovers, however to a similar magnitude peak at 17.5 cm before decreasing in a step-like fashion into PPA P4 (See pollen accumulation rates below). The step in the Lactuceae curve at 13.5 cm is observed in the curves for *Cirsium*, Poaceae and Apiaceae, corresponding with the occurrence of Cyperaceae and the disappearance of Caryophyllaceae.

LPAZ PPA P4: 8.5 cm to surface (circa AD 1964 to AD 1996)

Amaranthaceae-Chenopodiaceae dominates the local pollen assemblage in PPA P4, with a maximum abundance (87 %) and concentration (9.3 x 10^4 grains/g) occurring at 3.5 cm. Tree and shrub types *(Pinus, Quercus undiff., Betula, Olea-Phyllirea, Juniperus* and Ericaceae) exhibit a marked increase in concentration in PPA P4. In the surface sample a single grain of *Eucalyptus* pollen was also found, which although insignificant statistically, was the only evidence of the many stands of the trees which occur inland to the west of Pantano Grande. The core interval marked by a decrease in LOI 550°C, at 5-6 cm was marked by the re-appearance of *Betula* and Ericaceae in the upper core as well as the lowest Lactuceae concentration in the core (0.25 x 10^3 grains/g). The interval only caused a slight decrease in the dominating increase of Amaranthaceae-Chenopodiaceae up to the surface.

The reduction of Lactuceae pollen in PPA P4 is coincident with the increase in Poaceae, *Anthemis*, Lobeliaceae, *Plantago*, *Filipendula* and *Gentianella* types. Apiaceae and *Cirsium* both decrease in concentration, contrasting with PPA-P3 while Asteraceae subf. Asteroideae remains relatively constant (approx. 0.8 x 10^3 grains per gram).

Total pollen concentration decreases in the near surface samples, similar to ^{210}Pb activity. An increase at depth in pollen concentration suggests that grains may have been washed (along with atmospheric unsupported ^{210}Pb) vertically down into the fibrous organic surface.

6.3.8 Pantano Piccolo A: Pollen accumulation rates

Pollen accumulation rates determined for sample intervals in Pantano Piccolo A are limited to the upper 18 cm of the core (Table 6.3.6.). Selected pollen types (Fig. 6.6.) were chosen as being representative of local vegetation, occurring in abundance within the ^{210}Pb dated profile and being potentially indicative of different pollen transport vectors to the site (Fig. 2.4). Accretion rates were calculated between each interval from the ^{210}Pb CRS model age-depth curve, giving slightly different accretion values for horizons than the original ^{210}Pb dating.

Three phases of accretion are recognised in the sequence which appear to have influenced pollen accumulation rates; (1) between 18 and 12 cm (prior to *circa* AD 1920) and (2) the steady increase in accretion up to *circa* AD 1987 (3-4 cm) and (3) a slight decrease in sediment accretion calculated between 4 cm and 2 cm pollen intervals, may also be observed to have affected pollen accumulation rates in the upper 2 cm of the core.

A close correlation of accretion and pollen accumulation rates in the core is observed in all types, except Apiaceae (r = 0.03), Caryophyllaceae (r = -0.25) and Lactuceae (r = -0.28). Tree/shrub types exhibit a close relationship between accretion and enhanced accumulation in LPAZ PPA-P4. In LPAZ PPA-P3 though, lower and more constant accretion rates suggests a relative increase in the initial amount of arboreal pollen production, rather than focusing of pollen by sediment transport.

Although dominating pollen accumulation in the upper 18 cm, Amaranthaceae-Chenopodiaceae is none the less reduced in LPAZ PPA-P3 and replaced to a considerable extent by the accumulation of types less related to accretion (Lactuceae, Apiaceae and Caryophyllaceae). The accumulation of *Anthemis*, Poaceae, Asteraceae subf. Asteroideae and *Cirsium* in PPA-P3 indicates a relatively constant supply of local

Table 6.3.6. Pantano Piccolo A: Sediment accretion and pollen accumulation rates for selected types

Depth Interval	1-2 cm (1.5)	3-4 cm (3.5)	5-6 cm (5.5)	7-8 cm (7.5)	9-10 cm (9.5)	11-12 cm (11.5)	13-14 cm (13.5)	15-16 cm (15.5)	17-18 cm (17.5)
Years BP	2.8	8.8	14	23	39	65	99	115	131
Cal.Years AD	1993	1987	1982	1973	1957	1931	1897	1881	1865
Accretion rate (cm/a^{-1})	0.33	0.40	0.22	0.13	0.08	0.06	0.13	0.13	0.12
a)Pollen accumulation rates (grains/cm²/a^{-1}) In order of core abundance									
AP (Tree & Shrub)									
Olea-Phyllirea	1596.95	2241.01	668.03	822.80	143.23	64.44	137.13	562.50	251.92
Pinus	672.40	672.30	273.29	389.75	61.38	32.22	22.85	88.82	111.97
Juniperus	252.15	672.30	0	129.92	0	0	22.85	0	0
Betula	84.05	672.30	91.10	0	0	0	0	0	55.98
Ericaceae	84.05	224.10	121.46	0	0	0	0	0	83.97
NAP (Herb)									
Amaranth.-Chenopodiaceae	42277.22	99276.96	17642.13	11735.70	5749.58	1675.46	1474.14	3641.48	4982.46
Lactuceae	420.25	448.20	151.83	259.83	634.30	338.31	697.07	2042.78	2407.25
Poaceae	1092.65	3137.42	485.84	454.70	81.84	72.50	91.42	207.24	223.93
Asteraceae (Asteroid.)	336.20	896.41	516.21	259.83	153.46	56.39	251.40	355.27	251.92
Quercus undiff.	588.35	1344.61	121.46	86.61	51.15	32.22	68.56	148.03	55.98
Plantago	672.40	1568.71	91.10	64.96	0	0	0	0	0
Cirsium	0	672.30	121.46	108.26	173.92	72.50	34.28	236.84	195.94
Apiaceae	336.20	0.00	151.83	0.00	143.23	120.83	125.70	207.24	195.94
Anthemis	336.20	448.20	91.10	43.31	51.15	32.22	57.14	0.00	55.98
Caryophyllaceae	0	0	0	0	0	0	0	29.61	55.98
	0								
Total Pollen	48917.18	113843.55	20860.83	14767.07	7284.17	2497.08	3016.85	7519.80	8957.23

b) Pollen accumulation rates (grains/cm²/a^{-1}) Sorted by correlation values between sediment accretion and pollen accumulation rates										(*r*) sed accretion
AP (Tree & Shrub)										
Olea-Phyllirea	1596.95	2241.01	668.03	822.80	143.23	64.44	137.13	562.50	251.92	0.951
Pinus	672.40	672.30	273.29	389.75	61.38	32.22	22.85	88.82	111.97	0.911
Ericaceae	84.05	224.10	121.46	0	0	0	0	0	83.97	0.860
Juniperus	252.15	672.30	0	129.92	0	0	22.85	0	0	0.859
Betula	84.05	672.30	91.10	0	0	0	0	0	55.98	0.800
NAP (Herb)										
Anthemis	336.20	448.20	91.10	43.31	51.15	32.22	57.14	0	55.98	0.948
Amaranth.-Chenopodiaceae	42277.22	99276.96	17642.13	11735.70	5749.58	1675.46	1474.14	3641.48	4982.46	0.917
Plantago	672.40	1568.71	91.10	64.96	0	0	0	0	0	0.906
Quercus undiff.	588.35	1344.61	121.46	86.61	51.15	32.22	68.56	148.03	55.98	0.903
Poaceae	1092.65	3137.42	485.84	454.70	81.84	72.50	91.42	207.24	223.93	0.888
Asteraceae (Asteroid.)	336.20	896.41	516.21	259.83	153.46	56.39	251.40	355.27	251.92	0.851
Cirsium	0.00	672.30	121.46	108.26	173.92	72.50	34.28	236.84	195.94	0.527
Apiaceae	336.20	0	151.83	0.00	143.23	120.83	125.70	207.24	195.94	0.032
Caryophyllaceae	0	0	0	0	0	0	0	29.61	55.98	-0.253
Lactuceae	420.25	448.20	151.83	259.83	634.30	338.31	697.07	2042.78	2407.25	-0.287
Total Pollen	48917.18	113843.55	20860.83	14767.07	7284.17	2497.08	3016.85	7519.80	8957.23	**0.917**

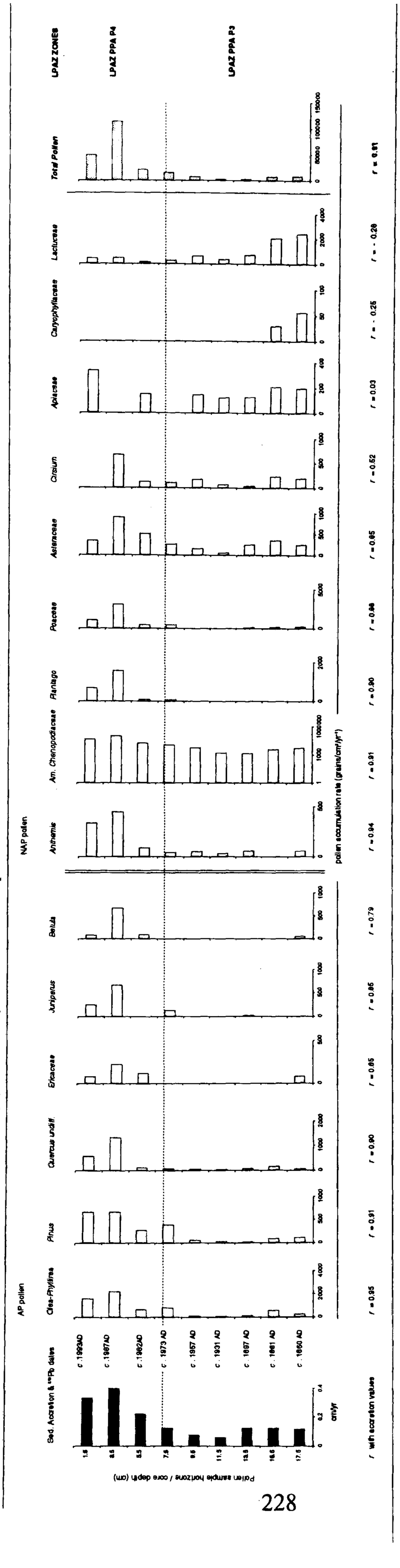

ure 6.6. Accumulation rates of selected pollen types: Pantano Piccolo A (0- 18 cm depth). Ordered L - R by correlation values between pollen accumulation and sediment accretion rate.

herb pollen, enhanced by increased sediment accretion, though perhaps not dependent on it to produce the observed accumulation rates.

The accumulation of some pollen types strongly correlated to accretion (*Olea-Phyllirea*, *Pinus*, *Quercus* undiff., *Anthemis*, Chenopodiaceae, Poaceae, Asteraceae subf. Asteroideae *and Cirsium*) are observed to have increased steadily in PPA-P3 from 11.5 cm depth (*circa* 1930 AD) to the boundary with PPA-P4 (*circa* AD 1970). Ericaceae, *Juniperus*, *Betula*, and *Plantago* appear to have only accumulated again once accretion had resumed within PPA-P4.

In PPA-P4 the relationship between sediment accretion and pollen accumulation is clear, repeating to a greater extent, the accretion/accumulation pattern observed between 14 and 18 cm. Maximum total pollen accumulation occurs in PPA-P4 at 3.5 cm (1.13×10^5 grains cm^2 a^{-1}) dominated by the peak accumulation of Amaranthaceae-Chenopodiaceae (9.9×10^4 grains cm^2 a^{-1}). A decrease in pollen accumulation is observed to have occurred with all types except *Pinus* (0.67×10^3 grains cm^2 a^{-1}) and Apiaceae (0.33×10^3 grains cm^2 a^{-1}) increasing in the surface sample interval. The accumulation rate of pollen in the core indicates that the accumulation of aerial-extra local pollen has clearly been enhanced by temporal and spatial patterns of sediment accretion.

6.4 RESULTS FROM PANTANO PICCOLO B (PPB)

Core PPB was taken from the mudflat exposed during low lagoon water levels (September 1996), approximately 15 m south (Plate 6.6.) from the core site of PPA (Fig. 6.4.7). The same number of multi-proxy analyses were conducted on the core PPB as the previous core (PPA) from Pantano Piccolo.

6.4.1 PPB-Core stratigraphy

Five horizons were identifiable in the extracted 49 cm core (Table 6.4.). The sequence (Fig. 6.6.1) was composed of dark grey lagoonal muds, with a well-defined shell rich horizon at 17-10 cm depth above a narrow vegetal organic horizon at 23-17 cm depth. Although a basal red/grey-brown clay and clastic agglomerate was encountered in the lower 3 cm of the core, the boundary with the overlying lagoonal muds was less defined than core PPA. Sub-rounded pebbles and gravel-sized material was encountered in the lagoonal muds from below 43 cm depth.

Shell material in PPB-B mainly occured as large (~8 mm) fragments and articulated valves of *Cerastoderma* sp., with smaller fragments of unidentifiable mollusc species. Within PPB-B, the well-preserved articulated valves of *Cerastoderma* sp. often did not contain any of the surrounding mud matrix. This suggests that individuals were actively bioturbating immediately/prior to death and were not subsequently reworked by wave-action.

Hydrobia ventrosa was encountered in abundance within PPB-C and PPB-E. In PPB-D (between 17 and 10 cm) the species was joined by an abundance of *Abra ovata, Cerastoderma glaucum, Pirenella conica* and *Bittium sp.,* which were predominantly well-preserved and articulated.

Evidence of Fe-oxyhydroxide staining was observed in the fine-grained grey mud (between 8 and 6 cm) above the shell rich layer (17-10 cm) on extraction. Fe-stained mottling had disapeared during transit and cold-storage. Although the core surface was unvegetated, organic material was apparent in the surface sediments, consisting of wood fragments (presumably flotsam from the lagoon fringe) and algal remains. Deposits of this surface accumulation occurred as a series of strand-lines at the northern margin of the lagoon (Plate 6.8.) caused by wave activity during falling (and presumably) rising water levels.

A saline crust was also evident at the surface of the core due to recent low water levels in the lagoon and surface exposure, leading to the surface migration and precipitation of saline-fluids.

Table 6.4. Core description of Pantano Piccolo B

Horizons	Depth (cm)	Sediment description
PPB E	00 - 03 cm	Dark grey brown mud. *Cardium glaucum, Bittium reticulatum* and *Hydrobia ventrosa* shells. Wood fragments and reed stems. Salt crust and algal matter
PPB D	17 - 03 cm	Dark grey mud. Fe-mottling in area of lower shell content (3-10 cm). Shell concentration of *C. glaucum, A. ovata* and conicular gastropods (*B. reticulatum*); predominantly articulated and well preserved. Increasingly organic, merging into horizon C from 15 cm.
PPB C	17 - 23 cm	Dark brown humic peat and organic mud. Woody material and abundant *Hydrobia* gr. *ventrosa* shells. Grading upwards into shell-rich interval (PPB-C)
PPB B	46 - 23 cm	Dark grey-brown mud. Large (0.8 mm) and interspersed fragments of *C. glaucum.* Black mottling and occasional carbonised wood fragments (42 and 24 cm). Increase in calcarenite clastic material and Fe/red-brown colouring between 40 and 46 cm. Large (30mm) sub-rounded calcarenite clast at 44 cm.
PPB A	46 - 49 cm	Fe-terracotta/brown clay silt and gravel and pebbles. Similar to basal unit in PPA (PPA-A).

Figure 6.6.1. Core sedimentology and stratigraphic zones; Pantano Piccolo B

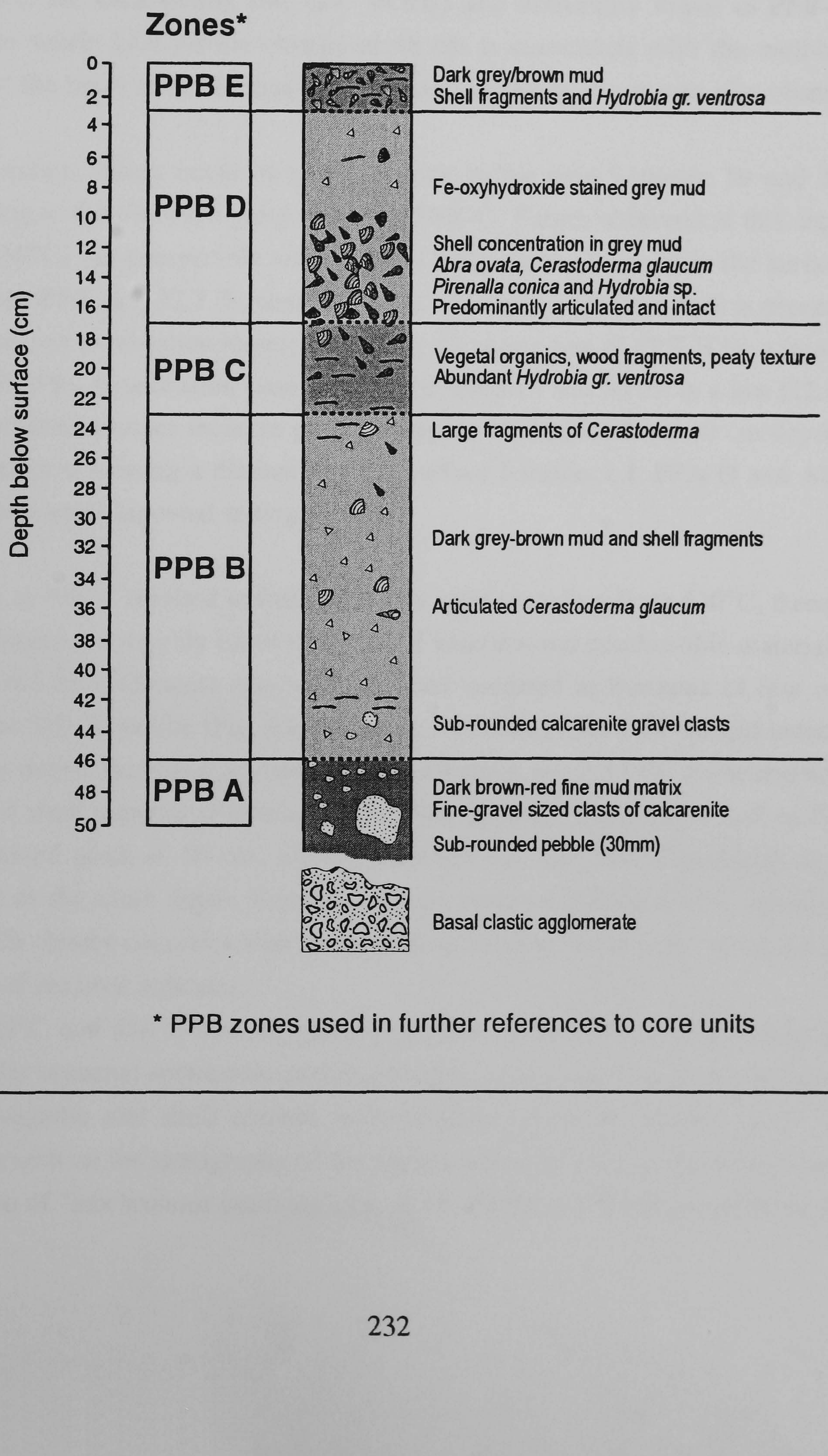

* PPB zones used in further references to core units

6.4.2 Pantano Piccolo B: Loss on ignition results

Consecutive 1 cm thick samples were sampled from the core for loss on ignition analysis at 550°C and 850°C (49 samples in total).

The previously identified core horizons were reflected to a large extent in combustion values at 550°C (Fig. 6.6.2.). Aside from the small peak at 26 cm, combustion losses below PPB-C are consistently low (av. 14.8%) and noticeably lower in PPB-A (av. 11.7%). The subtle LOI profile change at 46 cm is coincident with the well-defined boundary of the basal mud and gravel containing agglomerate, as was also observed in PPA.

Peak combustion values occur as a broad peak in the core between 19 and 16 cm, corresponding to the observed peaty mud unit PPB-C. Values observed at this depth (30 % loss at 550°C) are comparable with ignition loss values observed in the surface unit (D) from core PPA (av. 32.7 %, peak at 42 %). This mid-sequence peak is preceded by slightly increased combustion losses, starting in the upper part of PPB-B by a small peak at 26 cm (19.85%). Combustion losses decline between 16 and 10 cm to a low (12.6%) at 10 cm. Combustion losses increase gradually up to the surface from 10 cm depth even though the core is missing a distinct organic surface horizon, c.f. PPA-D and AMC-D, due to its open-water lagoonal setting.

Combustion at 850°C resulted in further loss on ignition values from 550°C, throughout the core, indicating a roughly linear decrease of volatiles and combustible materials with depth (Fig. 6.6.2b.). Greatest combustion losses occurred at horizons of low organic content in the 550 °C profile (Fig. 6.6.2c.), most noticeably below 24 cm and between 14 cm and 8 cm depth. Increased ignition between 14 and 8 cm at 850°C coincided with the abundance of shell material (*Bittium* sp., *Cardium* sp. etc.) in the lower half of PPB-D. The pronounced peak at 10 cm, closely matches the low 550°C combustion value encountered at the same depth. Increased losses incurred during 850°C ignition (Fig. 6.6.2.) in PPB clearly coincides with the carbonate content in the core; as the Ca profile (Fig. 6.6.7.) of the core indicates.

Both the 550°C and 850°C loss on ignition profiles from PPB identify stratigraphical changes in the lagoonal sediments, corroborating to an extent, though at a much higher resolution, organic and shell content measurements made by Amore *et al.* (1994). Previous research on the stratigraphy of the lagoon was with bulk samples taken as being representative of "isochronous intervals", i.e. at 10, 20-30 and 50-60 cm from the surface (Fig. 6.4.3.).

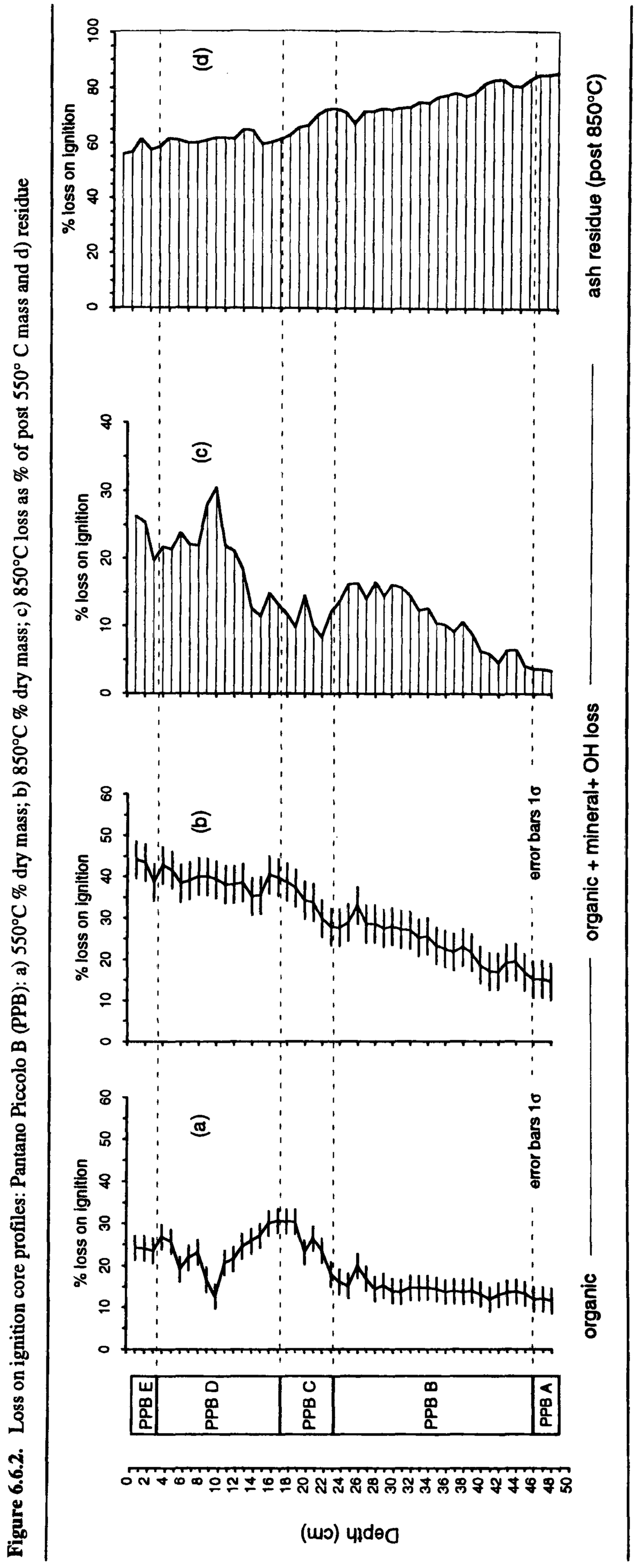

Figure 6.6.2. Loss on ignition core profiles: Pantano Piccolo B (PPB): a) 550°C % dry mass; b) 850°C loss as % of post 550° C mass and d) residue

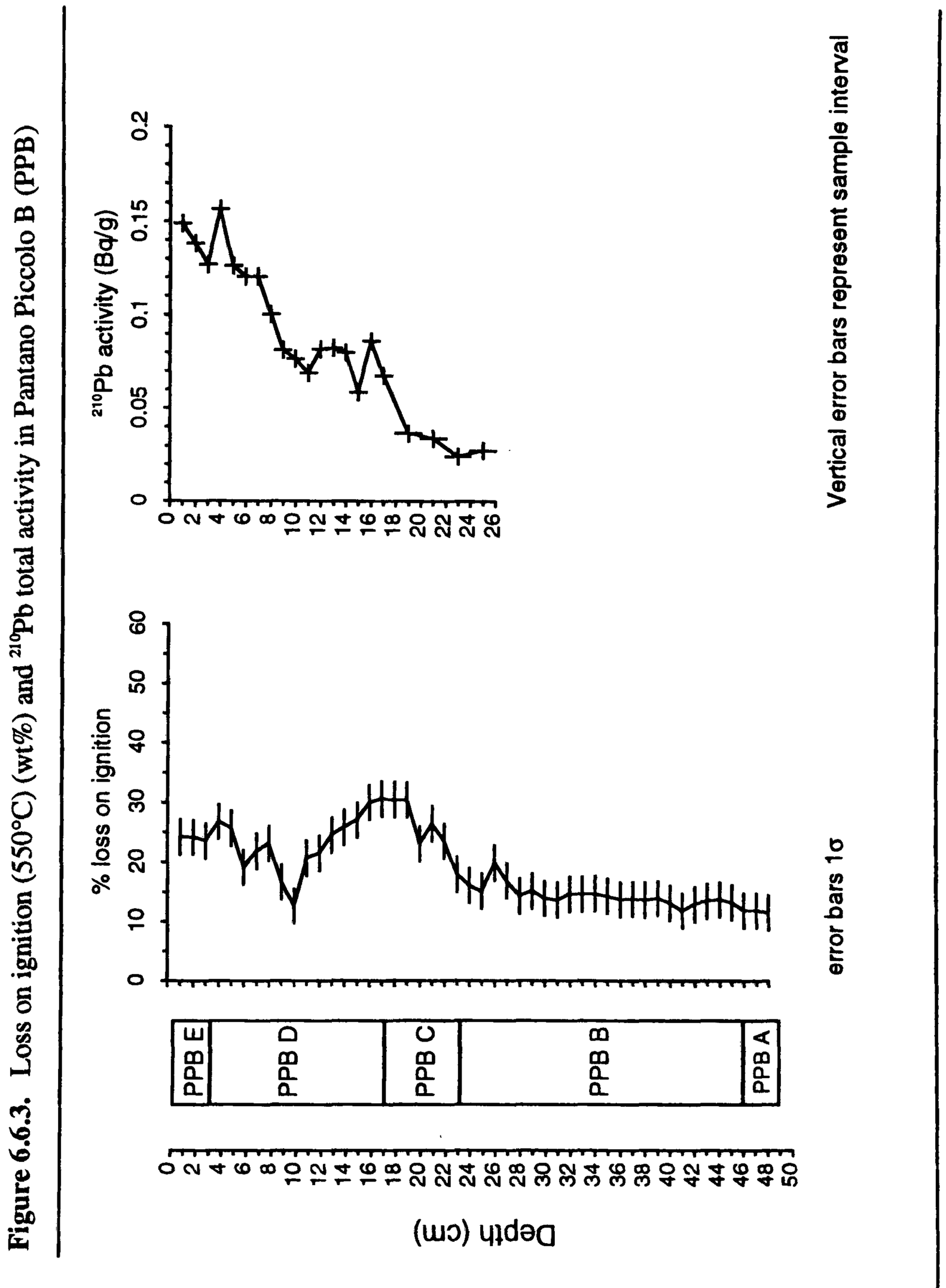

Figure 6.6.3. Loss on ignition (550°C) (wt%) and ^{210}Pb total activity in Pantano Piccolo B (PPB)

6.4.3 Pantano Piccolo PPB: ^{210}Pb analysis and dating

Twenty-one samples of one-centimetre thickness were taken from PPB at consecutive one-centimetre intervals, from the surface down to 17 cm and at 2 cm intervals down to 25 cm depth (Fig. 6.6.3). Sediments below 25 cm were not analysed due to the increased activity at depth previously measured in the basal lagoon units of PPA. The use of higher resolution sampling for PPB was to identify the timing of subtle accretion patterns in a more homogenous sequence.

From 16 cm, activity decreases to assumed supported ^{210}Pb activity at 21 cm. The slight increase which occurs in ^{210}Pb activity between 25 and 23 cm depth (upper section of PPB-B) was interpreted as having occurred due to a change in sediment composition, most likely due to a greater amount of ^{226}Ra in the older sediments. Between 19 and 11 cm increased ^{210}Pb activity appears to coincide in the core with increased organic matter (lower unit PPB-D and PPB-C). The single negative shift in activity at 15 cm would appear to be related to shell-carbonate material incorporated into the bulk sample (e.g. Brezonik & Engstrom, 1998).

From the apparent reversal in the expected decrease of total ^{210}Pb activity with depth, activity increases steadily from 11 cm up to a peak at 4 cm (0.15 Bq/g) (Fig. 6.6.3.). The decrease in total ^{210}Pb activity from the surface (1-3 cm) is reversed at 4 cm depth by a peak (0.16 Bq/g) in the shallow subsurface (outlining the contact between units PPB-D and PPB-E).

6.4.4 PPR: ^{210}Pb CF:CS dating model

Increased activity at depth was detrimental to the linear fit (R^2= 0.731) of values for the CF:CS model (Fig. 6.6.4.). The mean accretion rate determined (0.251 cm a^{-1}), provides a chronology of lagoonal accretion in the core (at least to the base of PPB-D) of approximately 50-60 years. Using this mean accretion rate, organic accumulation (PPB-C) was replaced by lagoonal mud deposits (PPB-D) *circa* AD 1930. Discounting variable accretion and hiatuses in the sequence, the mean rate of accretion calculated by the CF:CS model dates the base of the core (in PPB-A) to the early-19th century AD.

Figure 6.6.4. (a) ^{210}Pb unsupported activity and CF:CS model log-linear plot and: (b) CF:CS age depth relationship, Pantano Piccolo B (PPB)

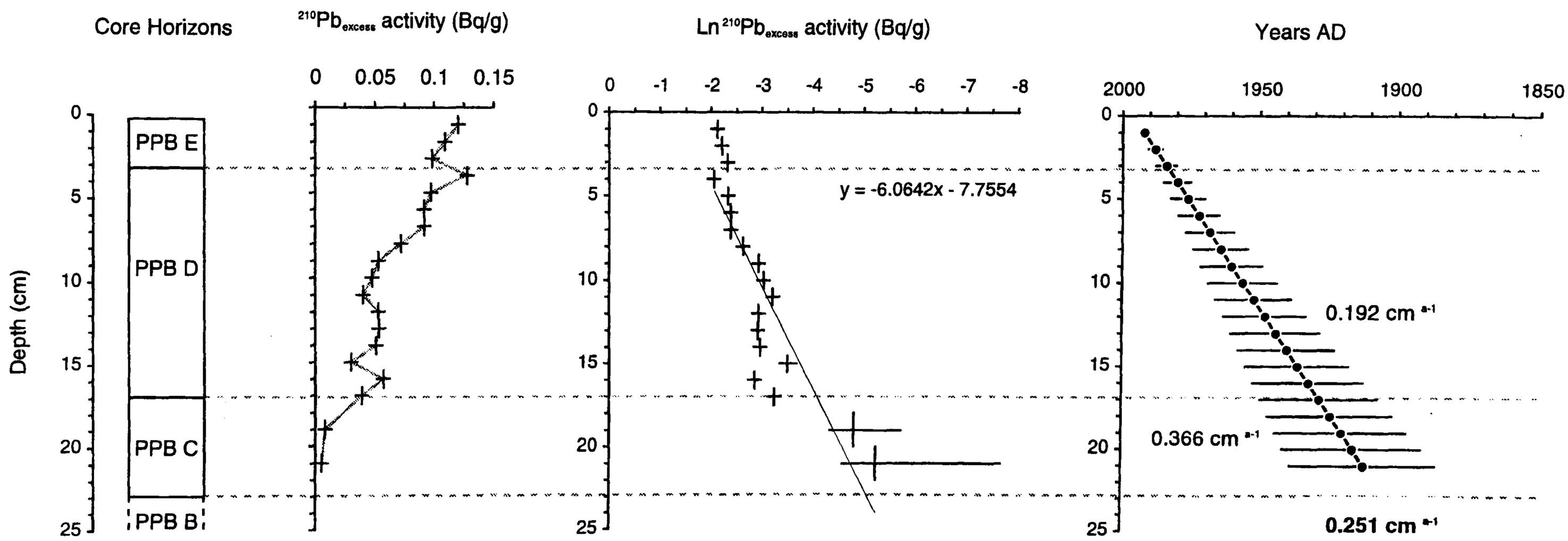

Mean accretion rates (cm/yr^{-1})determined by SPSS (95% Confidence linear regression)

Mean	0.251	$R^2 = 0.731$
Lower	0.192	
Upper	0.366	

Error bars signify calculated maximum and minimum unsupported actvity totals

Figure 6.6.5. Pantano Piccolo B (PPB) ^{210}Pb CRS model age depth curves

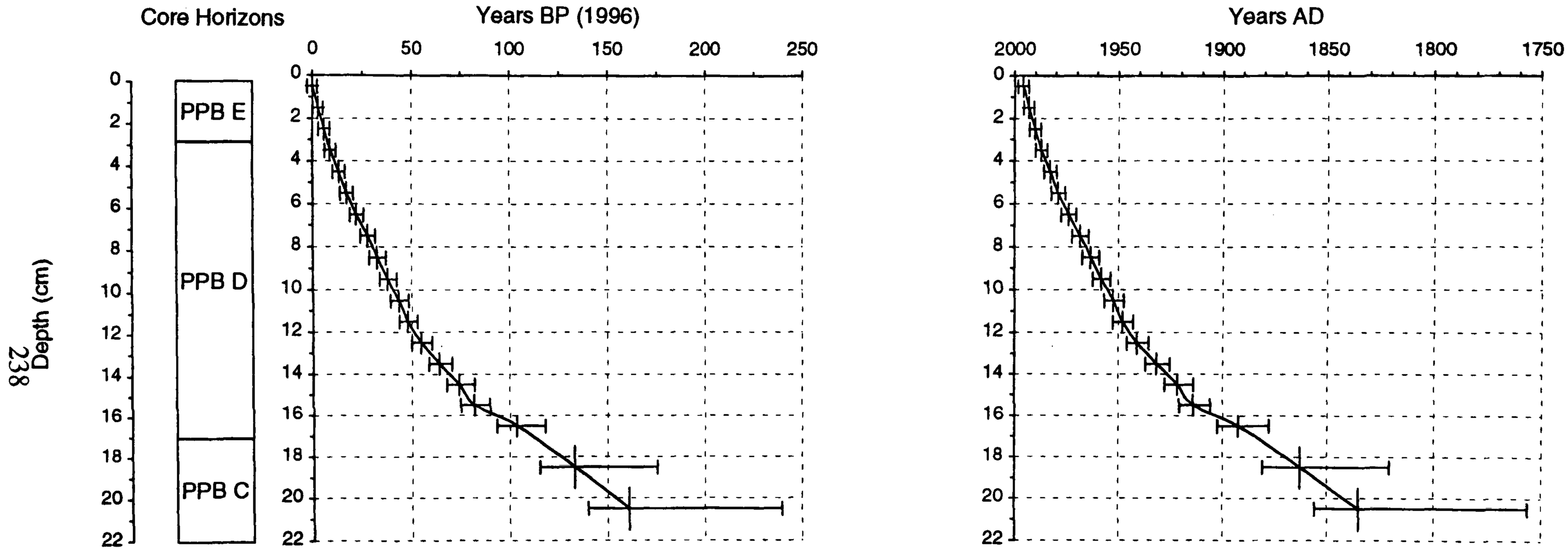

Mean accretion rate 0.187 cm/yr^{-1}

x- axis error bars signify age-range calculated maximum and minimum unsupported activity at depth; y-axis error bars indicate depth interval

Fig.6.4.1. Pantano Piccolo B: ^{210}Pb derived dates and sedimentation rates, plotted against depth and Years (AD)

*Depth (cm)	Age BP 1996	Years AD	Sedimentation rate (cm/yr^{-1})
0.5	0 (2.6 - +2.4)	1996 (1993-1998)	0.367 (0.352-0.381)
1.5	2.72 (5.4 - 0.2)	1993 (1991-1996)	0.324 (0.311-0.336)
2.5	5.81 (8.7 - 3.2)	1990 (1987-1993)	0.332 (0.319-0.344)
3.5	8.82 (11.8 - 6.1)	1987 (1984-1990)	0.233 (0.220-0.246)
4.5	13.1 (16.3 - 10.2)	1983 (1980-1986)	0.276 (0.262-0.288)
5.5	16.7 (20.2 - 13.6)	1979 (1976-1982)	0.199 (0.188-0.209)
6.5	21.7 (25.5 - 18.4)	1974 (1971-1978)	0.176 (0.165-0.186)
7.5	27.4 (31.6 - 23.8)	1969 (1964-1972)	0.204 (0.191-0.215)
8.5	32.3 (36.8 - 28.5)	1964 (1959-1968)	0.185 (0.176-0.192)
9.5	37.8 (42.5 - 33.7)	1958 (1954-1962)	0.176 (0.169-0.182)
10.5	43.4 (48.4 - 39.2)	1953 (1948-1957)	0.227 (0.221-0.231)
11.5	47.8 (52.9 - 43.5)	1948 (1943-1953)	0.142 (0.132-0.150)
12.5	54.9 (60.5 - 50.2)	1941 (1936-1946)	0.109 (0.099-0.116)
13.5	64.1 (70.5 - 58.7)	1932 (1925-1937)	0.098 (0.087-0.108)
14.5	74.2 (82.0 - 68.0)	1922 (1914-1928)	0.134 (0.125-0.141)
15.5	81.7 (90.0 - 75.1)	1914 (1906-1921)	0.046 (0.036-0.055)
16.5	103.4 (118.1 - 93.4)	1893 (1877-1902)	0.068 (0.035-0.091)
18.5	132.9 (175.2 - 115.4)	1863 (1821-1881)	0.072 (0.031-0.081)
20.5	160.9 (239.6 - 140.1)	1835 (1756-1856)	-

*mid sample depth

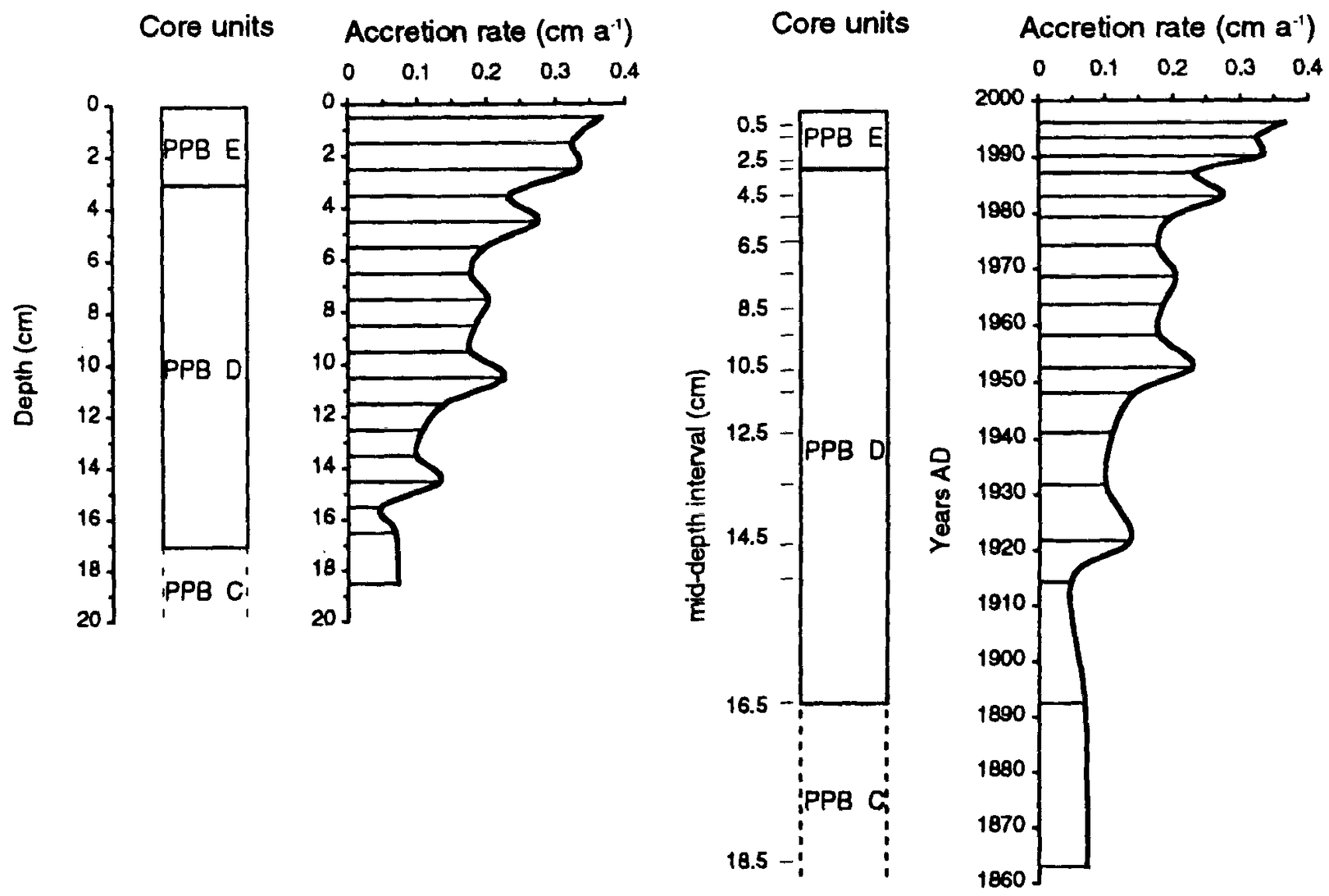

Sedimentation rate calculated between sample interval and one previous in cm a^{-1}

Figures in brackets derived from calculated maximum and minimum unsupported activity

6.4.5 PPB ^{210}Pb CRS dating model

The CRS age-depth curve for PPB indicates that the accretion of horizons PPB-E and PPB-D and the upper portion of PPB-C occurred within the last 150-200 years (Fig. 6.6.5.). The base of PPB-D (17 cm), representing the stratigraphic shift from organic accumulation (PPB-C) to lagoonal shell-rich muds (PPB-D), appears to have occurred at the end of the 19th century (c. AD 1890). Subtle variations in the curve indicate phases of enhanced accretion, more evident when accretion rates are plotted against time and depth (Table 6.4.1.). Following on from lowered accretion rates in the late 19th century, sedimentation rates in PPB have evidently periodically fluctuated over the last century, producing a step-like pattern of increasing accretion up to the present day (Table 6.4.1.). Intervals of increased accretion operating on this longer-term trend are recognisable in the core: at *circa* AD 1922 (AD 1914-1928), *circa* AD 1953 (AD 1948-1957), *circa* AD 1969 (1964-1972), *circa* AD 1983 (AD 1980-1986) and highest between AD 1990 and the surface. These recorded peaks appear to have therefore increased in frequency within the last 100 years, approximately from 31 years (AD 1922-1953), 16 years (AD 1953-1969), 14 years (AD 1969-1983) and 7 years (AD 1983-1990). The upper 3 cm of the core (PPB-E) has therefore accumulated at a greater rate (av. 0.33 cm a^{-1}), than the rest of the core following a slight decrease in accretion (0.23 cm a^{-1}) recorded between 4.5 cm and 3.5 cm (*circa* AD 1987).

Although the resolution of sampling at PPA hinders comparison, calculated accretion rates in PPB suggest that the lagoonal core (PPB) has received a more reliable source of sediment. Whether from re-worked lagoonal deposits or materials derived from the upstream catchment, the within-lagoon setting, i.e. covered by water for greater periods of time has certainly assisted the recording of subtle variations in sediment supply. The implications of these accretionary changes are discussed in Chapter 7.

6.4.6 Pantano Piccolo B: Major element geochemistry

Forty-nine consecutive 1 cm thick samples were extracted for XRF major element analysis (Table 6.4.2.). The percentage abundance of the ten elements in the core were grouped using the total sum of squares CONISS© function into three main chemostratigraphic zones (Fig. 6.6.6); PPB-ME-1 between 36 and 49 cm, PPB-ME-2 between 18 and 35 cm and PPB-ME-3 in the upper 17 cm of the core. Within these chemostratigraphic zones, further sub-zones were also recognised (Fig. 6.6.7).

Table 6.4.2. Major element abundances: Pantano Piccolo B (PPB)

	Major Elements (oxides % ashed mass)										% dry mass
Depth (cm)	**SiO_2**	**CaO**	**Al_2O_3**	**Fe_2O_3**	**MgO**	**Na_2O**	**K_2O**	**TiO_2**	**P_2O_5**	**MnO**	**LOI (550°C)**
1	30.98	48.48	7.83	3.81	5.76	1.41	0.64	0.44	0.30	0.11	24.21
2	34.45	43.49	8.60	4.01	5.72	1.73	0.89	0.49	0.25	0.10	24.14
3	36.32	38.77	9.76	4.50	5.92	2.42	1.03	0.54	0.27	0.11	23.57
4	35.47	38.96	9.39	4.37	6.95	2.49	1.12	0.53	0.24	0.13	26.82
5	35.35	37.77	9.41	4.47	7.60	2.73	1.33	0.52	0.26	0.16	25.71
6	35.30	40.14	8.78	4.16	7.17	2.31	0.94	0.51	0.24	0.15	19.15
7	34.75	39.63	8.85	4.41	7.31	2.94	0.95	0.51	0.25	0.15	21.86
8	33.54	42.95	8.54	4.15	6.89	1.94	0.90	0.48	0.23	0.14	23.19
9	26.20	58.59	6.00	2.84	5.37	0.08	0.04	0.36	0.17	0.12	16.70
10	26.34	58.07	6.08	3.14	5.36	0.04	0.04	0.36	0.16	0.12	12.66
11	34.26	42.20	8.68	4.95	5.97	2.04	0.76	0.49	0.19	0.11	20.68
12	33.32	42.65	8.56	5.06	6.23	2.28	0.84	0.48	0.20	0.11	21.50
13	33.02	42.19	8.53	5.65	5.93	2.52	1.12	0.47	0.18	0.10	24.53
14	38.67	28.20	10.40	7.34	6.98	4.97	2.17	0.58	0.21	0.14	25.81
15	46.52	27.68	11.35	5.42	3.40	3.02	1.21	0.69	0.16	0.10	27.09
16	38.22	31.64	11.02	6.11	5.60	4.40	1.77	0.60	0.25	0.08	30.00
17	41.62	22.99	12.48	8.20	5.89	5.42	1.99	0.71	0.28	0.09	30.61
18	46.31	16.02	14.17	7.74	5.35	6.57	2.30	0.80	0.26	0.08	30.46
19	45.93	13.76	20.55	6.55	4.45	5.52	1.97	0.69	0.22	0.07	30.40
20	47.95	22.66	13.25	5.36	3.76	4.27	1.29	0.77	0.21	0.05	23.11
21	53.14	14.75	14.87	5.45	3.86	4.31	2.00	0.88	0.24	0.04	26.42
22	52.28	16.84	15.02	5.09	3.43	4.19	1.47	0.89	0.22	0.04	23.53
23	50.01	23.19	13.20	4.73	3.05	3.11	1.20	0.80	0.17	0.05	17.93
24	47.47	27.66	11.89	4.79	3.10	2.78	0.92	0.73	0.16	0.07	16.10
25	45.34	31.52	11.15	4.68	3.20	2.08	0.63	0.71	0.16	0.08	15.14
26	45.71	29.91	11.34	5.13	3.40	2.42	0.77	0.71	0.16	0.08	19.85
27	47.78	27.64	11.63	5.26	3.07	2.42	0.78	0.72	0.16	0.07	16.86
28	46.31	27.27	11.63	4.92	3.02	4.56	0.86	0.71	0.14	0.08	14.33
29	46.34	28.74	12.21	4.99	3.00	2.52	0.81	0.74	0.15	0.08	15.18
30	46.65	30.47	11.21	4.50	2.85	2.14	0.79	0.71	0.15	0.10	13.92
31	48.04	28.18	11.45	4.83	2.78	2.41	0.89	0.73	0.14	0.10	13.65
32	46.23	28.06	11.44	5.48	3.47	2.91	1.08	0.71	0.16	0.10	14.65
33	48.40	26.40	11.79	5.26	2.93	2.67	1.12	0.74	0.14	0.10	14.63
34	48.64	26.15	12.00	5.12	2.92	2.66	1.06	0.74	0.14	0.10	14.72
35	46.08	29.69	11.81	4.98	2.75	2.45	0.86	0.74	0.14	0.10	14.30
36	47.90	26.57	11.92	5.30	2.80	2.80	1.28	0.73	0.13	0.10	13.72
37	51.95	18.98	13.78	6.08	2.94	3.11	1.59	0.84	0.14	0.10	13.83
38	49.95	21.64	13.21	6.01	3.07	3.07	1.49	0.80	0.14	0.12	13.66
39	49.76	22.03	13.45	6.03	2.88	2.94	1.42	0.81	0.13	0.13	13.93
40	51.57	19.06	13.99	6.41	2.82	2.96	1.62	0.86	0.13	0.12	13.12
41	53.36	16.31	14.66	6.49	2.84	2.88	1.71	0.89	0.14	0.16	11.84
42	51.57	18.85	13.92	6.39	3.03	3.09	1.59	0.83	0.12	0.14	12.93
43	54.18	14.65	14.84	6.85	2.83	2.71	2.31	0.91	0.13	0.10	13.48
44	54.99	13.10	15.15	6.92	2.81	2.67	2.63	0.93	0.13	0.11	13.73
45	56.55	10.24	15.72	7.03	2.69	3.01	2.98	0.96	0.18	0.07	13.22
46	57.80	7.95	16.26	7.37	2.61	3.00	3.25	0.99	0.12	0.08	11.87
47	56.44	9.88	15.95	7.45	2.60	2.91	2.99	0.96	0.12	0.19	11.92
48	56.99	9.44	16.15	6.97	2.64	2.86	3.05	1.00	0.12	0.22	11.53
49	58.99	5.70	17.36	7.35	2.45	2.98	3.29	1.05	0.13	0.17	11.46
2σ	16.95	24.68	5.88	2.41	3.22	2.34	1.56	0.35	0.10	0.07	11.93
Core average	45.00	27.51	12.07	5.51	4.15	2.93	1.42	0.71	0.18	0.11	18.65

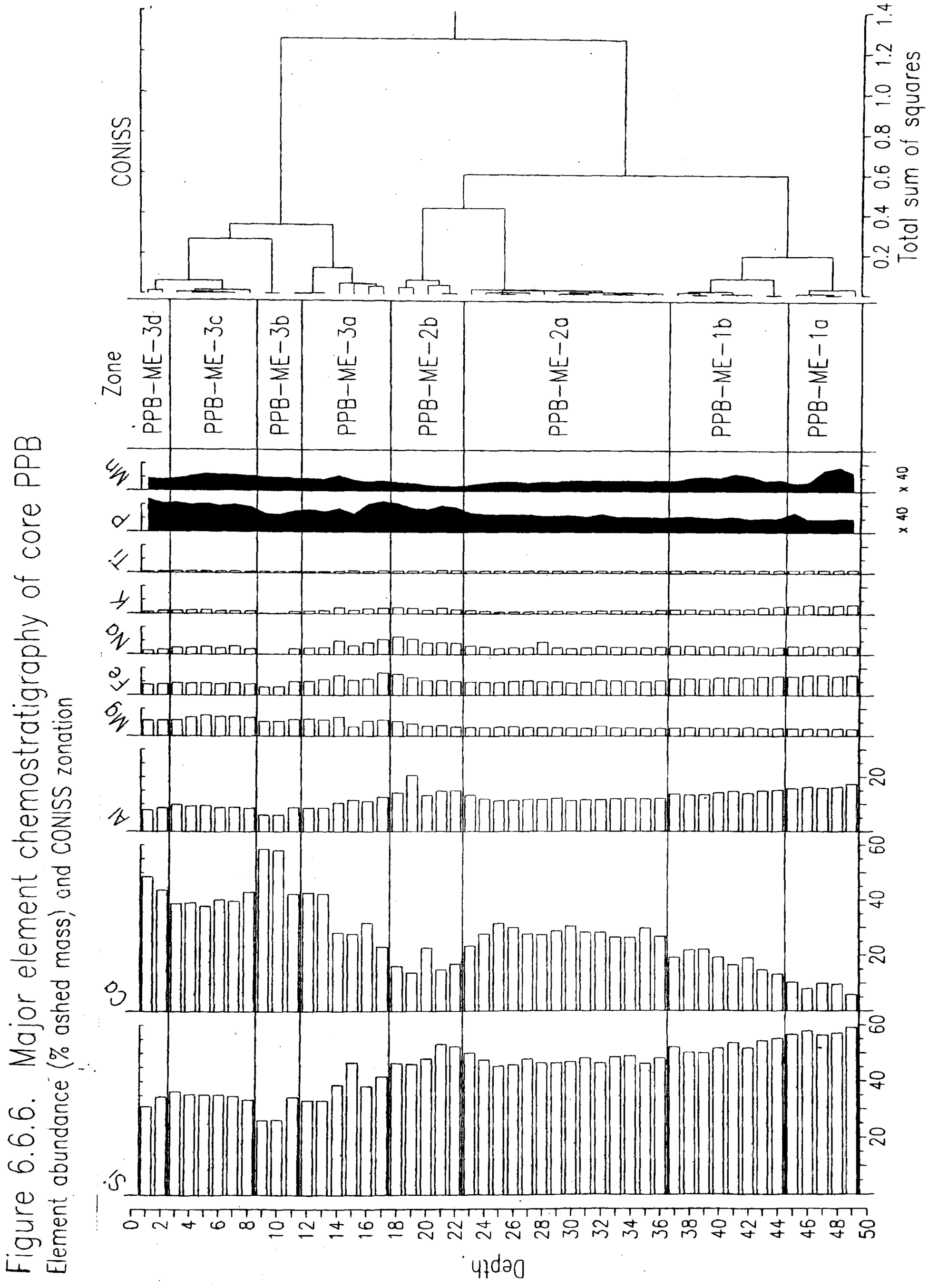

Figure 6.6.6. Major element chemostratigraphy of core PPB
Element abundance (% ashed mass) and CONISS zonation

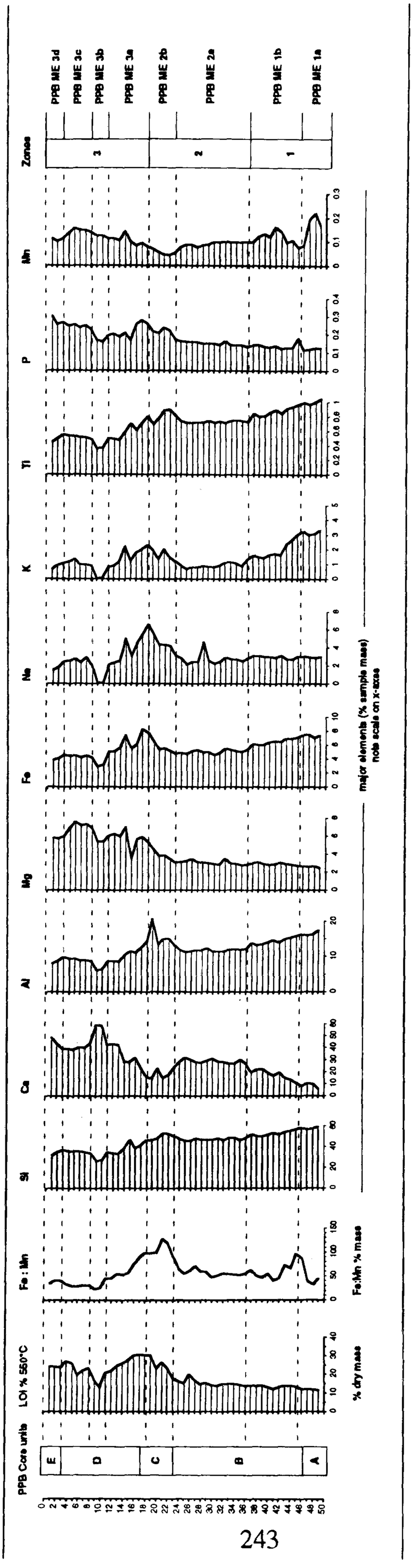

Figure 6.6.7. Pantano Piccolo B Major element core profiles (Si-Mn in order of abundance)

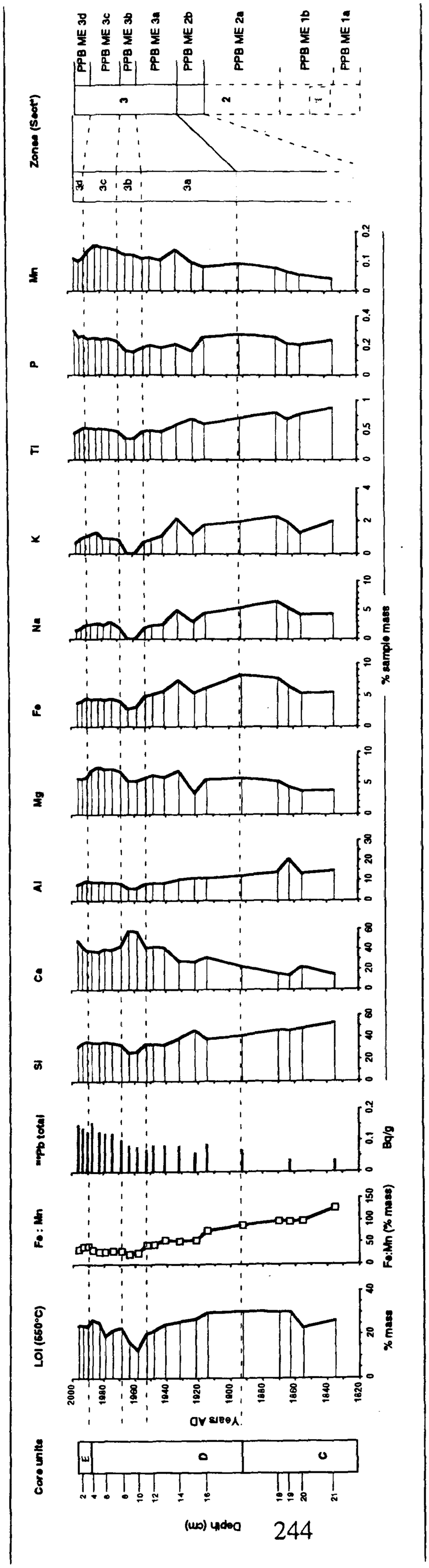

Figure 6.6.8. Pantano Piccolo B Major element core profiles plotted against ^{210}Pb-derived dates

The relationship between major element abundances, organic content and core depth (Fig. 6.6.9) are complicated in PPB by the absence of a distinct accumulation of vegetal material at the surface and the mixed association of organic materials, variable shell content and minerogenic sediments at depth. The surface association of elements in PPB would appear to clearly represent the sediment interface between physico-chemical properties of the overlying lagoon water body and atmosphere, unrestricted by wetland vegetation.

The positive correlation of P, Mg, Na with 550° C loss on ignition values in the core (Fig. 6.6.9.) reflects the increased abundance of the elements with vegetal organic content at depth (associated with the broad ignition peak) and increased combustion (though apparently less vegetal organic associated) losses at the surface. Although Ca abundance in the core varies greatly, a weak positive correlation with organic content (r = 0.28) represents the stratigraphic coincidence between shell content and the mid-depth organic accumulation (PPB-C). A less distinct relationship between element abundances and sedimentology is exhibited by Fe and K (Fig. 6.7.) which respond positively to the increased organic interval (PPB-C), as well as apparent mineralogical (low organic) variations at depth.

Elements associated with the inorganic component are shown by a correlation with Ti (Fig. 6.6.9.). By this correlation it may be observed that the two most abundant element species in the core (Si and Ca) are diametrically opposed. This indicates that the accumulation of sedimentary carbonate has occurred in relation to a reduction in mineral-detrital inputs. The apparent dichotomy of Mn with organic and inorganic components (Fig. 6.6.9) may be explained by the distribution of Mn in the core (Fig. 6.6.7.). This is reduced in the organic (PPB-C) interval while exhibiting an increased abundance at depth (PPB-ME-1a) corresponding to a low organic content. The distribution of both Fe and Mn in the core suggests that they are associated with minerogenic and organic sedimentation, which complicates a simple "soil wash-in" assumption of the Fe:Mn profile.

Two peaks in the Fe:Mn profile occur which would indicate a greater input of soil-Fe materials to the core site (Fig. 6.6.7.). The first occurs at the boundary of PPB-ME-1a and PPB-ME-1b, corresponding with the lagoon mud matrix-supported calcarenite clasts at the base of core unit PPB-B. Throughout PPB-B the Fe:Mn profile remains relatively constant, following a similar pattern to the 550°C loss on ignition profile. The second and more extensive peak in the Fe:Mn profile occurs with the increasing organic content in PPB-C. The peak itself precedes the highest organic values and the Fe:Mn profile is seen to decrease steadily to lower values caused by the peak in carbonate in PPB-ME-3b. A slight increase in the Fe:Mn profile is observed in the upper 10 cm.

Zone PPB-ME-1 is subdivided into two units: PPB-ME-1a (49-45 cm) and PPB-ME-1b (44-36 cm) (Fig. 6.6.7.). The basal sub-zone is marked by a peak in Mn (0.22 %) and the

Figure 6.6.9. Major element abundances and correlation with LOI (550°C) and Ti (wt%) values

(a) Correlation with LOI

Element	Av.	(*r*) LOI
LOI	18.65	
P_2O_5	0.18	0.86
MgO	4.15	0.70
Na_2O	2.93	0.46
CaO	27.51	0.28
Fe_2O_3	5.51	-0.05
K_2O	1.42	-0.11
Al_2O_3	12.07	-0.22
MnO	0.11	-0.28
TiO_2	0.71	-0.47
SiO_2	45.00	-0.49

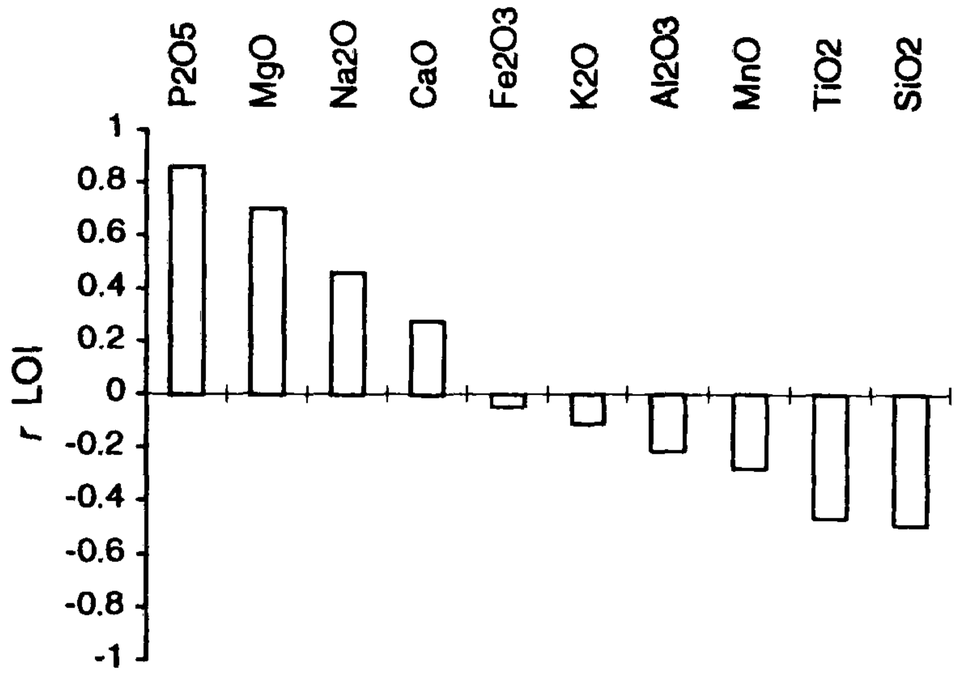

(b) Correlation with Ti

Element	Av.	(*r*) Ti
TiO_2	0.71	
SiO_2	45.00	0.99
Al_2O_3	12.07	0.89
K_2O	1.42	0.76
Fe_2O_3	5.51	0.72
Na_2O	2.93	0.41
MnO	0.11	-0.04
LOI	18.65	-0.47
P_2O_5	0.18	-0.56
MgO	4.15	-0.80
CaO	27.51	-0.96

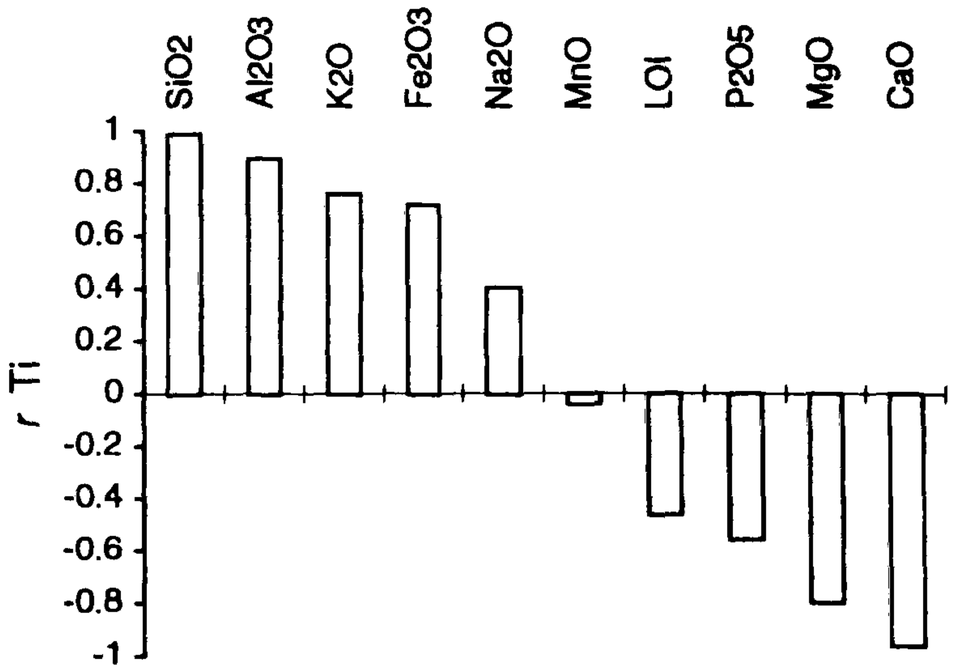

Figure 6.7a. Major element abundance, Fe:Mn ratio and ^{210}Pb total activity plotted against proxy organic content (loss on ignition at 550°C) from Pantano Piccolo B

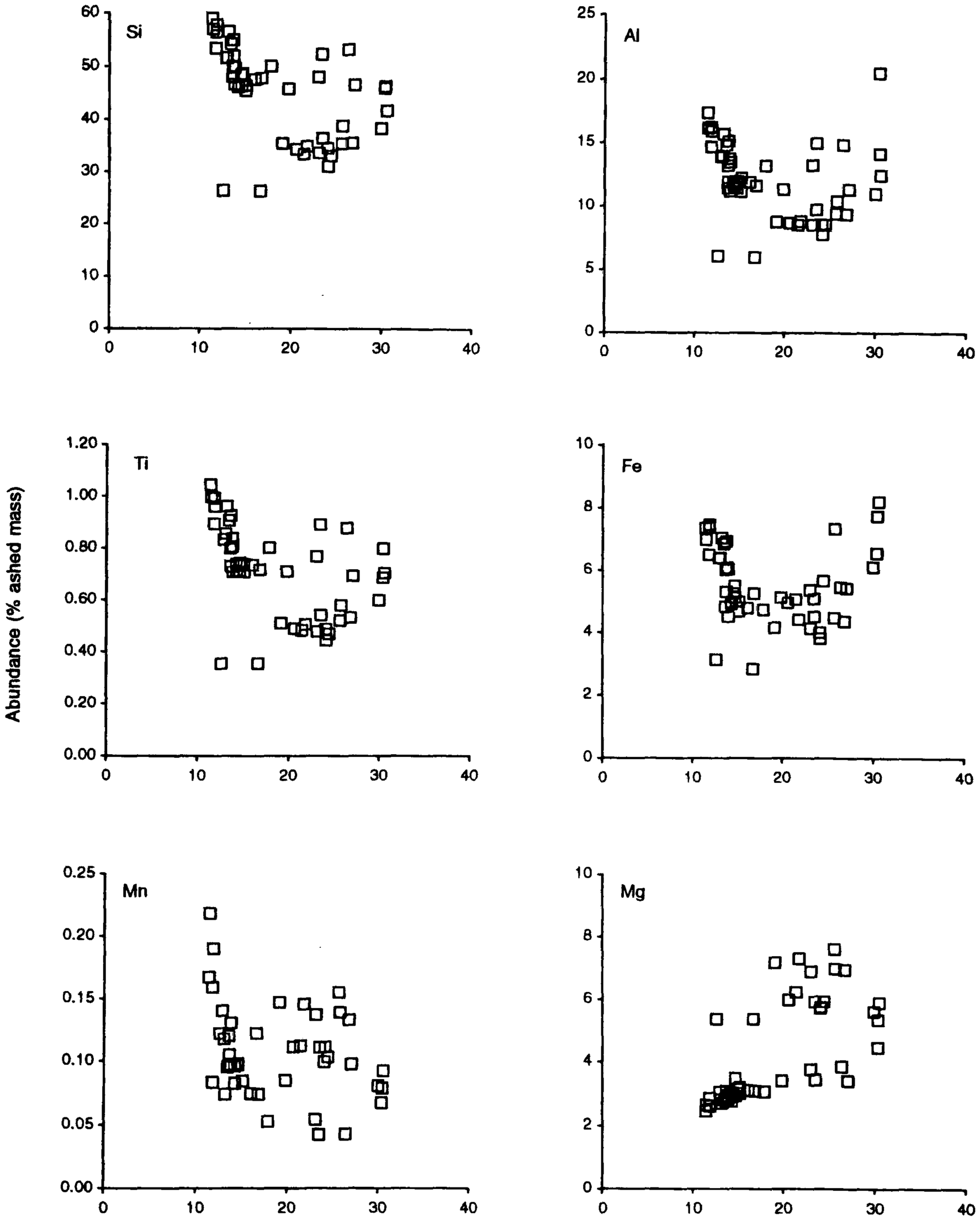

Figure 6.7b. Major element abundance, Fe:Mn ratio and ^{210}Pb total activity plotted against proxy organic content (loss on ignition at 550°C) from Pantano Piccolo B

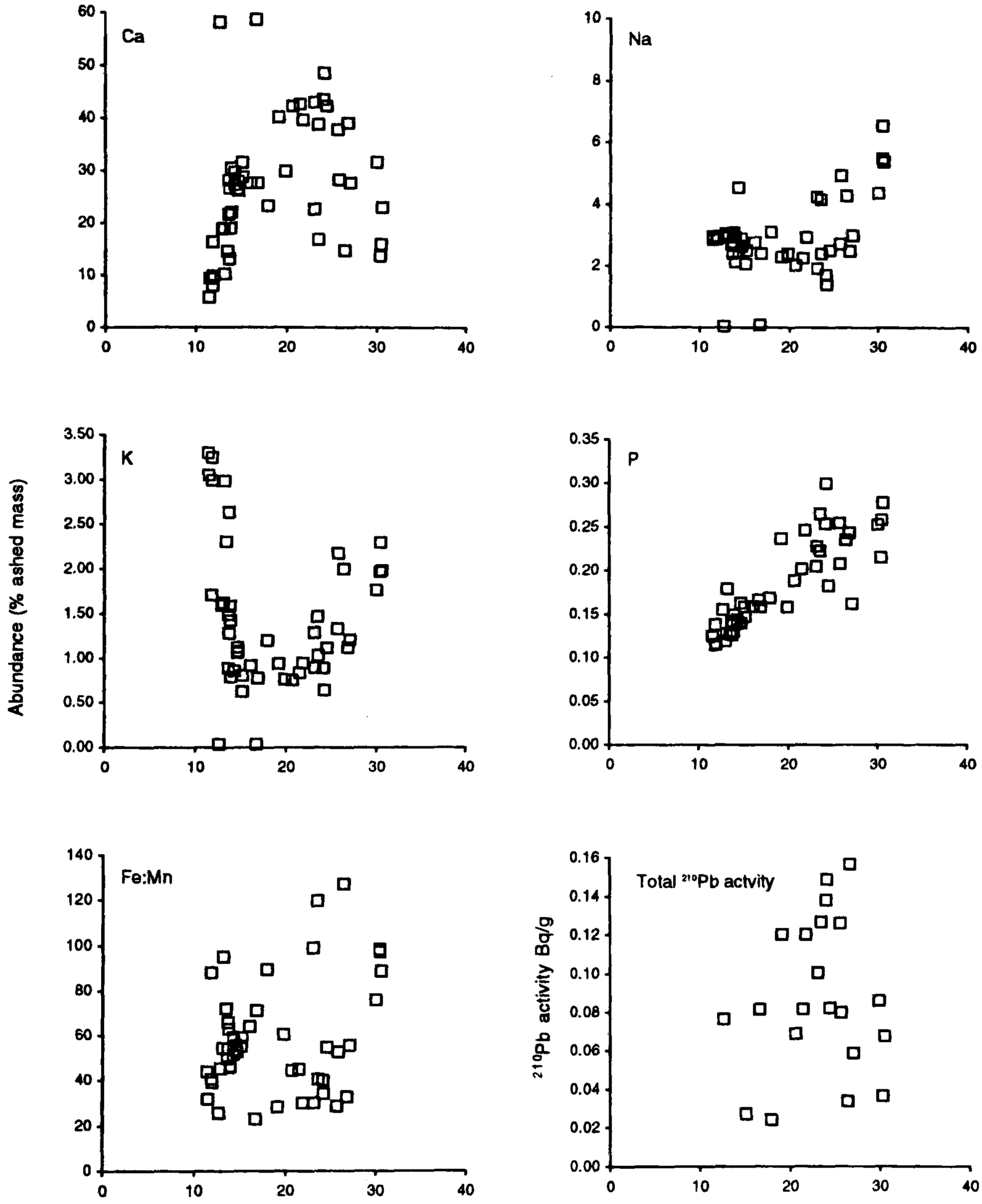

increased abundance of Si, Al, Fe, K and Ti to the detriment of Ca. Mn decreases again at the boundary with PPB-ME-1b. A small peak in P (0.18 %) is also recognised at the boundary. The abundance of Si, Al, Fe and Ti decrease steadily in PPB ME1b, K more abruptly between the boundary with PPB ME1a and 42 cm depth. Mn abundance in PPB ME1b recovers from the boundary at 45 cm to another peak at 41 cm before decreasing again into PPB-ME-2a.

The decreasing abundance of elements (Si, Al, Fe, K and Ti) in relation to steadily increasing Ca in PPB-ME-1, is met in PPB ME2a by a relatively stable period of sediment composition. Minor fluctuations are observed in Al, Mg and Fe, with a solitary peak in Na at 28 cm (4.5%). Throughout PPB-ME-1 and PPB-ME-2a, the abundances of Na, Mg and P exhibited little variability. As with all the analysed elements this pattern changes in PPB-ME-2b, corresponding to the organic unit (PPB-C) observed in the core. The peak of organic accumulation in PPB-C is preceded by an increase in the abundance of all elements, except Ca and Mn which decrease accordingly in the sub-zone. Although Si and Ti increase at the base of PPB-ME-2b, they are seen to decline before organic LOI values peak between 19 and 16 cm. Al (with a pronounced peak at 19 cm), Fe, Na and K are observed to increase concomitantly with the increased organic content in PPB-ME-2b, preceding PPB-ME-3 and the increased abundance of Ca. The ^{210}Pb-dated section of PPB-ME2b (*circa* AD 1835 to *circa* AD 1893) encompasses this broad peak in organic accretion and shift towards Ca-dominated lagoonal deposition. The association between P and biomass is evident across the boundary of PPB-ME-2b and PPB-ME-3a, corresponding with maximum organic content. This transition is also marked by the increased relative abundance of Mg in the upper half of the core.

PPB-ME-3 is entirely within the accretionary period dated by ^{210}Pb, its base corresponding to *circa* AD 1893 (Fig. 6.6.8.). Si, Al, Fe, Na, K and Ti decrease steadily through PPB-ME-3a, to marked lows in PPB-ME-3b as Ca subsequently peaks (*circa* AD 1958-1964). Subzone PPB-ME-3b reflecting this carbonate peak, spans a period of low accretion before *circa* AD 1953-1969 (11-8 cm).

Following the decline and low abundance of Si, Al, Fe, Na, K and Ti in PPB-ME-3a and PPB-ME-3b, the abrupt decline in Ca precedes PPB-ME-3c as a period of compositional homogeneity and increased minerogenic content (Fig. 6.6.8). The relative decrease in Ca in PPB-ME-3c is reflected by a comparitive increase in Mg, Mn, and P. The abundance of P is observed to increase in PPB-ME-3d along with increasing Ca as other minerogenic elements (Si, Al, Ti) decrease.

6.4.7 Pantano Piccolo B Pollen

Twenty-four 1 cm thick samples were extracted from PPB, representative of stratigraphic horizons and boundaries, especially the basal transition between PPB-A and PPB-B and the organic interval PPB-C. Similar to PPA the pollen counts from the core samples (Table 6.4.3.) were dominated by few taxa, namely Amaranthaceae-Chenopodiaceae, Lactuceae, Poaceae, *Cirsium*, *Olea-Phyllirea* and *Pinus*, without which pollen totals would have been extremely low. Compared to PPA, the diversity of pollen types found was greater which was assumed to reflect the cores setting, i.e. inundated for greater periods of time by the lagoon seston (reflecting extra-local/catchment sources). Mechanical damage was noticeable in many grains, especially the numbers of individual *Pinus* saccae, which may have been caused by enhanced bioturbation and ingestion by the sediment fauna (c.f. Chmura & Eisma, 1995).

Pollen counts (of 57 pollen taxa) were sub-divided into three local pollen assemblage zones using the CONISS© total sum of squares function (Fig. 6.6.6.). Relative abundance and pollen concentrations were determined through the core (Figs. 6.7.1, 6.7.2 & 6.7.3) and are tabulated here (Tables 6.4.3 & 6.4.4). Pollen counts were greater and more reliable in PPB compared with PPA and AMC, apart from the three basal samples (49-48 cm, 48-47 cm and 47-46 cm). These sample intervals were not used in the CONISS zonation or appear in the percentage diagram.

Pollen accumulation rates were also determined in samples within the upper 17 cm of the core (Table 6.4.5 / Fig. 6.7.4) using ^{210}Pb sedimentation rates derived from the CRS age-depth curve.

LPAZ PPB -P1: 49-29.5 cm (basal clay and pebble agglomerate and lagoonal muds)

The basal pollen zone is subdivided into upper (PPB-P1b) and lower (PPB-P1a) units. The lower subzone (49-46 cm) (corresponding with core unit PPB-A) is dominated by Amaranthaceae-Chenopodiaceae. Though total pollen counts in PPB-P1a were the lowest in the core, the subzone contained numerous grains of *Alnus*, *Betula*, *Corylus* and *Pinus*. From the base of the sequence the concentration of Lactuceae increases rapidly, from 0.067 x 10^3 grains/g at 49 cm up to 1.4 x 10^3 grains/g to the base of LPAZ PPB-P1b at 46 cm. Coincidental with the rise in Lactuceae is the increased concentration of Caryophyllaceae, *Plantago*, *Serratula*, Cyperaceae and a few grains of Lillaceae (*Tulipa* type).

PPB-P1b is a clearly defined subzone in which the greatest diversity of pollen taxa were encountered. Tree and shrub pollen abundance is dominated by a relatively constant concentration of *Pinus* and *Olea-Phyllirea* through the subzone, joined by *Alnus*, *Betula*

Table 6.4.3. Counts and pollen percentages of sediment horizons of Pantano Piccolo B core (Surface - 29 cm depth) Pollen types in order of count abundance

	Sample horizon PPB 0-1 cm		Sample horizon PPB 3-4cm		Sample horizon PPB 7-8cm		Sample horizon PPB 9-10cm		Sample horizon PPB 11-12cm		Sample horizon PPB 14-15cm		Sample horizon PPB 16-17cm		Sample horizon PPB 18-19cm		Sample horizon PPB 21-22cm		Sample horizon PPB 23-24cm		Sample horizon PPB 25-26cm		Sample horizon PPB 28-29cm	
	Count	%	Count	%	Count	%	Count	%	Count	%	Count	%	Count	%	Count	%	Count	%	Count	%	Count	%	Count	%
Arboreal pollen																								
Pinus	25	5.35	26	5.98	23.5	3.92	15.5	3.00	12.5	2.13	10	1.52	7.5	1.73	7	1.17	14	3.57	16.5	3.53	13	3.76	8	3.49
Alnus	7	1.50	2	0.46	3	0.50	9	1.74	6	1.02	7	1.06	4	0.92	11	1.84	0	0	4	0.86	0	0	8	3.49
Betula	7	1.50	0	0	3	0.50	7	1.35	2	0.34	4	0.61	3	0.69	2	0.34	0	0	7	1.50	2	0.58	3	1.31
Quercus undiff.	3	0.64	0	0	6	1.00	3	0.58	4	0.68	2	0.30	0	0	1	0.17	4	1.02	5	1.07	3	0.87	4	1.75
Picea	0	0	0	0	0	0	0	0	0	0	0	0	0	0	0	0	0	0	0	0	0	0	0	0
Juglans	0	0	0	0	1	0.17	0	0	0	0	0	0	0	0	0	0	0	0	0	0	0	0	0	0
Eucalyptus	0	0	1	0.23	0	0	0	0	0	0	0	0	0	0	0	0	0	0	0	0	0	0	0	0
AP total	42	8.99	29	6.67	36.5	6.09	34.5	6.67	24.5	4.18	23	3.49	14.5	3.34	21	3.52	18	4.59	32.5	6.95	18	5.20	23	10.04
Arboreal (Shrub) pollen																								
Olea-Phyllirea	68	14.56	64	14.71	79	13.18	61	11.79	78	13.32	55	8.35	29	6.67	61	10.22	32	8.16	57	12.19	63	18.21	28	12.23
Ericaceae	2	0.43	3	0.69	3	0.50	2	0.39	4	0.68	4	0.61	1	0.23	4	0.67	3	0.77	4	0.86	4	1.16	4	1.75
Juniperus	5	1.07	4	0.92	0	0	0	0	0	0	0	0	0	0	0	0	2	0.51	0	0	2	0.58	0	0
Ephedra fragilis	0	0	2	0.46	0	0	1	0.19	0	0	3	0.46	2	0.46	2	0.34	0	0	2	0.43	1	0.29	4	1.75
Corylus	0	0	0	0	0	0	0	0	0	0	0	0	0	0	0	0	0	0	0	0	0	0	0	0
Vitis vinifera	0	0	0	0	0	0	0	0	0	0	0	0	0	0	0	0	0	0	0	0	0	0	0	0
AP (Shrub) total	75	16.06	73	16.78	82	13.68	64	12.37	82	14.01	62	9.41	32	7.36	67	11.22	37	9.44	63	13.48	70	20.23	36	15.72
Non-arboreal pollen																								
Amaranth.-Chenopodiaceae	268	57.39	238	54.71	319	53.21	319	61.64	379	64.73	479	72.69	312	71.81	418	70.02	198	50.51	229	48.98	107	30.92	63	27.51
Lactuceae	5	1.07	9	2.07	11	1.83	5	0.97	3	0.51	3	0.46	3	0.69	4	0.67	9	2.30	24	5.13	33	9.54	43	18.78
Poaceae undiff.	34	7.28	22	5.06	32	5.34	31	5.99	22	3.76	27	4.10	14	3.22	7	1.17	13	3.32	3	0.64	14	4.05	9	3.93
Cirsium	7	1.50	3	0.69	13	2.17	14	2.71	8	1.37	11	1.67	11	2.53	17	2.85	22	5.61	38	8.13	22	6.36	11	4.80
Anthemis	6	1.28	7	1.61	11	1.83	13	2.51	4	0.68	7	1.06	12	2.76	14	2.35	24	6.12	17	3.64	15	4.34	0	0
Plantago undiff.	9	1.93	8	1.84	10	1.67	13	2.51	7	1.20	3	0.46	6	1.38	1	0.17	0	0	3	0.64	7	2.02	0	0
Apiaceae undiff.	10	2.14	4	0.92	13	2.17	6	1.16	4	0.68	7	1.06	8	1.84	9	1.51	5	1.28	8	1.71	11	3.18	6	2.62
Asteraceae subf. Aster	4	0.86	4	0.92	6	1.00	8	1.55	3	0.51	11	1.67	8	1.84	17	2.85	38	9.69	18	3.85	11	3.18	5	2.18
Caryophyllaceae	3	0.64	1	0.23	4	0.67	4	0.77	5	0.85	8	1.21	3	0.69	9	1.51	6	1.53	4	0.86	6	1.73	9	3.93
Filipendula	0	0	7	1.61	11	1.83	0	0	12	2.05	2	0.30	0	0.00	8	1.34	1	0.26	13	2.78	9	2.60	4	1.75
Lobelia type	0	0	2	0.46	7	1.17	0	0	3	0.51	0	0.00	0	0.00	0	0	9	2.30	9	1.93	8	2.31	1	0.44
Artemesia	0	0	0	0	0	0	0	0	0	0	0	0.00	0	0.00	0	0	0	0	0	0	0	0	0	0
Serratula	0	0	0	0	3	0.50	1	0.19	1	0.17	2	0.30	1	0.23	0	0	2	0.51	1	0.21	2	0.58	4	1.75
Mentha type	0	0	0	0	0	0	1	0.19	0	0	0	0	0	0	0	0	0	0	0	0	0	0	0	0
Gentianella	0	0	0	0	0	0	0	0	0	0	3	0.46	0	0	0	0	1	0.26	0	0	0	0	0	0
Medicago	0	0	0	0	3	0.50	0	0	0	0	0	0.00	0	0	0	0	0	0	0	0	0	0	0	0
Saxifraga type	0	0	4	0.92	10	1.67	0	0	2	0.34	3	0.46	0	0	0	0	4	1.02	0	0	0	0	0	0
Euphorbia	0	0	0	0	0	0	0	0	8	1.37	0	0	0	0	0	0	0	0	0	0	0	0	0	0
Centaurea	0	0	0	0	0	0	0	0	0	0	0	0	0	0	0	0	0	0	0	0	0	0	0	0
Polygonaceae	0	0	2	0.46	0	0	0	0	0	0	0	0	1	0.23	0	0	0	0	2	0.43	0	0	2	0.87
Cyperaceae	0	0	0	0	0	0	0	0	0	0	0	0	0	0	0	0	0	0	2	0.43	1	0.29	0	0
Pteridium undiff.	0	0	0	0	0	0	0	0	0	0	0	0	0	0	0	0	0	0	0	0	0	0	0	0
Erodium	0	0	0	0	0	0	0	0	0	0	0	0	0	0	0	0	0	0	0	0	0	0	2	0.87
Rumex	0	0	5	1.15	0	0	0	0	0	0	0	0	0	0	0	0	0	0	0	0	0	0	0	0
Primula type	0	0	2	0.46	2	0.33	0	0	0	0	0	0	0	0	0	0	0	0	0	0	0	0	0	0
Scabiosa	0	0	2	0.46	2	0.33	0	0	2	0.34	0	0	1	0.23	0	0	0	0	0	0	1	0.29	0	0
Liliaceae	0	0	0	0	0	0	0	0	0	0	0	0	0	0	0	0	0	0	0	0	0	0	0	0
Sorbus	0	0	0	0	0	0	0	0	0	0	0	0	0	0	0	0	0	0	0	0	0	0	0	0
Ranunculus type	0	0	0	0	0	0	0	0	0	0	0	0	0	0	0	0	4	1.02	0	0	0	0	0	0
Stachys type	0	0	4	0.92	0	0	0	0	0	0	0	0	0	0	0	0	0	0	0	0	0	0	0	0
Lotus type	0	0	0	0	0	0	3	0.58	0	0	0	0	0	0	0	0	0	0	1	0.21	0	0	0	0
Armeria maritima	0	0	0	0	0	0	0	0	0	0	0	0	0	0	0	0	0	0	0	0	0	0	0	0
Hypericum type	0	0	0	0	0	0	0	0	0	0	0	0	0	0	0	0	0	0	0	0	0	0	0	0
Vicia type	0	0	0	0	0	0	0	0	0	0	0	0	0	0	0	0	0	0	0	0	0	0	0	0
Astragalus	0	0	0	0	0	0	0	0	0	0	0	0	0	0	0	0	1	0.26	0	0	0	0	0	0
Linum	0	0	0	0	0	0	0	0	0	0	0	0	0	0	0	0	0	0	0	0	0	0	0	0
Eryngium maritimum	0	0	0	0	0	0	0	0	0	0	0	0	0	0	0	0	0	0	0	0	0	0	0	0
Marrubium vulgare	0	0	0	0	0	0	0	0	0	0	0	0	0	0	0	0	0	0	0	0	0	0	0	0
Rhinanthus	0	0	0	0	0	0	0	0	0	0	0	0	0	0	0	0	0	0	0	0	0	0	0	0
NAP total	350	74.31	333	75.00	461	77.15	419	80.81	479	79.53	574	86.06	388	87.66	509	84.55	337	85.97	372	79.57	258	72.27	170	70.83
Unidentified/deteriorated	4	0.86	9	2.07	24	4.00	1	0.19	16	2.73	8	1.21	6	1.84	5	0.84	0	0.00	0	0.00	11	3.18	11	4.80
Total Pollen (AP/NAP)	467		435		599.5		517.5		585.5		659		434.5		597		392		467.5		346		229	
Aquatics																								
Butomus	0	0	0	0	0	0	0	0	0	0	0	0	0	0	0	0	0	0	0	0	0	0	0	0
Myriophyllum	0	0	0	0	0	0	3	0.58	0	0	2	0.30	0	0	2	0.34	0	0	0	0	0	0	0	0
Nuphar	0	0	0	0	0	0	0	0	0	0	0	0	0	0	0	0	0	0	0	0	0	0	0	0
Potamogetonaceae	0	0	0	0	0	0	0	0	0	0	0	0	0	0	0	0	4	1.02	0	0	0	0	0	0
Total aquatics (as % TP) (not included in total pollen sum)	0	0	0	0	0	0	3	0.58	0	0	2	0.3035	0	0	2	0.335	4	1.0204	0	0	0	0	0	0
Counted Lycopodium	79		112		132		118		69		89		39		83		84		228		234		184	

Statistically unreliable low pollen totals for % are underlined

Table 6.4.3. Counts and pollen percentages of sediment horizons of Pantano Piccolo B core (30 - 49 cm depth) Pollen types in order of count abundance

	Sample horizon PPB 30-31cm		Sample horizon PPB 32-33cm		Sample horizon PPB 34-35cm		Sample horizon PPB 36-37cm		Sample horizon PPB 38-39cm		Sample horizon PPB 40-41cm		Sample horizon PPB 42-43cm		Sample horizon PPB 44-45cm		Sample horizon PPB 45-46cm		Sample horizon PPB 46-47cm		Sample horizon PPB 47-48cm		Sample horizon PPB 48-49cm	
	Count	%	Count	%	Count	%	Count	%	Count	%	Count	%	Count	%	Count	%	Count	%	Count	%	Count	%	Count	%
Arboreal pollen																								
Pinus	23	5.64	9	2.36	9.5	2.52	8	2.22	15	3.50	12.5	3.54	16.5	4.07	21	5.80	24.5	8.40	16	9.09	2.5	4.42	6.5	9.22
Alnus	11	2.70	5	1.31	2	0.53	1	0.28	3	0.70	1	0.28	3	0.74	6	1.66	2	0.69	5	2.84	6	10.62	0	0
Betula	7	1.72	4	1.05	0	0	7	1.94	2	0.47	2	0.57	4	0.99	3	0.83	0	0	2	1.14	4	7.08	1	1.42
Quercus undiff.	2	0.49	2	0.52	1	0.26	2	0.55		0	2	0.57	6	1.48	3	0.83	2	0.69	0	0	0	0	0	0
Picea	0	0	1	0.26	1	0.26	0	0	1	0.23	0	0	3	0.74	1	0.28	1	0.34	0	0	0	0	0	0
Juglans	1	0.25	0	0	1	0.26	0	0	0	0	0	0	2	0.49	2	0.55	1	0.34	0	0	0	0	0	0
Eucalyptus	0	0	0	0	0	0	0	0	0	0	0	0	0	0	0	0	0	0.00	0	0	0	0	0	0
Arboreal total	**44**	**10.78**	**21**	**5.51**	**14.5**	**3.84**	**18**	**4.99**	**21**	**4.94**	**17.5**	**4.95**	**34.5**	**8.51**	**36**	**9.94**	**30.5**	**10.46**	**23**	**13.07**	**12.5**	**22.12**	**7.5**	**10.64**
Arboreal (Shrub) pollen																								
Olea-Phyllirea	27	6.62	39	10.24	33	8.74	31	8.59	55	12.82	42	11.88	26	6.41	19	5.25	13	4.46	6	3.41	0	0	0	0
Ericaceae	6	1.47	4	1.05	1	0.26	3	0.83	3	0.70	4	1.13	5	1.23	0	0	0	0	0	0	0	0	0	0
Juniperus	7	1.72	2	0.52	3	0.79	4	1.11	8	1.86	0	0	1	0.25	0	0	4	1.37	0	0	0	0	2	2.84
Ephedra fragilis	6	1.47	0	0	2	0.53	4	1.11	0	0	0	0	8	1.97	0	0	2	0.69	0	0	0	0	0	0
Corylus	7	1.72	1	0.26	1	0.26	0	0	0	0	0	0	0	0	4	1.10	0	0.00	0	0	1	1.77	1	1.42
Vitis vinifera	0	0	0	0	2	0.53	0	0	0	0	0	0	1	0.25	0	0	0	0	0	0	0	0	0	0
Arboreal (Shrub) total	**53**	**12.99**	**48**	**12.67**	**42**	**11.13**	**42**	**11.63**	**66**	**15.38**	**48**	**13.01**	**41**	**10.11**	**23**	**6.36**	**19**	**6.52**	**6**	**3.41**	**1**	**1.77**	**3**	**4.26**
Non-arboreal pollen																								
Am.-Chenopodiaceae	77	18.87	74	19.95	60	15.89	85	23.55	80	18.65	69	19.52	102	25.15	72	19.89	94	32.25	55	31.25	28	49.56	40	56.74
Lactaceae	61	14.95	58	15.22	69	18.28	72	19.94	56	13.05	79	22.35	76	18.74	77	21.27	40	13.72	43	24.43	5	8.85	4	5.67
Poaceae undiff.	14	3.43	40	10.50	35	9.27	23	6.37	19	4.43	17	4.81	27	6.66	28	7.73	35	12.01	23	13.07	4	7.08	5	7.09
Cirsium	17	4.17	11	2.89	19	5.03	26	7.20	16	3.73	17	4.81	16	3.95	18	4.97	7	2.40	6	3.41	0	0	0	0
Anthemis	14	3.43	17	4.46	12	3.18	15	4.16	28	6.53	19	5.37	13	3.21	8	2.21	5	1.72	0	0	0	0	0	0
Plantago	19	4.66	11	2.89	28	7.42	15	4.16	23	5.36	28	7.92	21	5.18	18	4.97	11	3.77	2	1.14	3	5.31	3	4.26
Apiaceae undiff.	14	3.43	22	5.77	21	5.56	17	4.71	20	4.66	22	6.22	16	3.95	14	3.87	1	0.34	0	0	0	0	0	0
Asteraceae subf. Aster	14	3.43	10	2.62	9	2.38	10	2.77	18	4.20	9	2.55	16	3.95	8	2.21	8	2.74	0	0	0	0	1	1.42
Caryophyllaceae	9	2.21	8	2.10	9	2.38	3	0.83	8	1.86	4	1.13	6	1.48	11	3.04	3	1.03	3	1.70	0	0	5	7.09
Pilliperdalia	12	2.94	7	1.84	8	2.12	7	1.94	6	1.40	8	2.26	0	0	11	3.04	0	0	0	0	0	0	0	0
Lobelia type	6	1.47	1	0.26	0	0	1	0.28	0	0	0	0	4	0.99	0	0	0	0	0	0	0	0	0	0
Artemisia	9	2.21	6	1.57	7	1.85	3	0.83	15	3.50	4	1.13	0	0	0	0	2	0.69	0	0	0	0	0	0
Serratula type	4	0.98	1	0.26	1	0.26	2	0.55	3	0.70	0	0	1	0.25	4	1.10	6	2.06	2	1.14	0	0	2	2.84
Mentha type	3	0.74	4	1.05	6	1.59	0	0	7	1.63	3	0.85	3	0.74	1	0.28	1	0.34	0	0	0	0	0	0
Gentianella	2	0.49	3	0.79	5	1.32	3	0.83	3	0.70	3	0.85	2	0.49	4	1.10	0	0	0	0	0	0	0	0
Medicago	4	0.98	2	0.52	1	0.26	0	0	0	0	0	0	4	1.48	9	2.49	0	0	0	0	0	0	0	0
Saxifraga type	0	0	0	0	0	0	0	0	0	0	0	0	0	0	0	0	0	0	0	0	0	0	0	0
Euphorbia	1	0.25		0	0	0	8	2.22		0	2	0.57	0	0	0	0	0	0	0	0	0	0	0	0
Centaurea	4	0.98	1	0.26	4	1.06	0	0	8	1.86	0	0	0	0	0	0	0	0	0	0	0	0	0	0
Polygonaceae	0	0	0	0	0	0	2	0.55	0	0	1	0.28	2	0.49	3	0.83	0	0	1	0.57	0	0	0	0
Cyperaceae	2	0.49	2	0.52		0	2	0.55	0	0	0	0		0	2	0.55	3	1.03	0	0	0	0	0	0
Pteridium undiff.	2	0.49	1	0.26	3	0.79	0	0	0	0	0	0	1	0.25	0	0	3	1.03	0	0	0	0	0	0
Erodium	2	0.49	2	0.52	0	0	0	0	1	0.23	1	0.28	0	0	1	0.28	0	0	0	0	0	0	0	0
Rumex	3	0.74	0	0	0	0	0	0	0	0	0	0	0	0	0	0	0	0	0	0	0	0	0	0
Primula type	0	0	0	0	4	1.06	0	0	0	0	0	0	0	0	0	0	0	0	0	0	0	0	0	0
Scabiosa	0	0	0	0	0	0	0	0	0	0	0	0	0	0	0	0	0	0	0	0	0	0	0	0
Liliaceae (Tulipa)	2	0.49	1	0.26	1	0.26	0	0	0	0	0	0	0	0	0	0	2	0.69	1	0.57	0	0	0	0
Sorbus	0	0	0	0	3	0.79	2	0.55	0	0	0	0	0	0	2	0.55	0	0	0	0	0	0	0	0
Ranunculus type	2	0.49	0	0	1	0.26	0	0	0	0	0	0	0	0	0	0	0	0	0	0	0	0	0	0
Stachys type	0	0	0	0	2	0.53	0	0	0	0	0	0	0	0	0	0	0	0	0	0	0	0	0	0
Lotus type	0	0	0	0	0	0	0	0	0	0	0	0	0	0	0	0	1	0.34	0	0	0	0	0	0
Armeria maritima	0	0	3	0.79	0	0	0	0	1	0.23	0	0	0	0	0	0	0	0	0	0	0	0	0	0
Hypericum type	0	0	0	0	0	0	0	0	0	0	3	0.85	0	0	0	0	0	0	0	0	0	0	0	0
Vicia type	0	0	1	0.26	1	0.26	0	0	0	0	0	0	0	0	0	0	0	0	0	0	0	0	0	0
Astragalus	0	0	1	0.26	0	0	0	0	0	0	0	0	0	0	0	0	0	0	0	0	0	0	0	0
Linum	0	0	0	0	0	0	0	0	2	0.47	0	0	0	0	0	0	0	0	0	0	0	0	0	0
Eryngium maritimum	0	0	1	0.26	0	0	0	0	0	0	0	0	0	0	0	0	0	0	0	0	0	0	0	0
Marrubium vulgare	0	0	1	0.26	0	0	0	0	0	0	0	0	0	0	0	0	0	0	0	0	0	0	0	0
Rhinanthus	0	0	0	0	0	0	0	0	1	0.23	0	0	0	0	0	0	0	0	0	0	0	0	0	0
NAP total	**307**	**73.64**	**306**	**77.27**	**315**	**82.14**	**259**	**82.34**	**329**	**74.27**	**289**	**81.75**	**326**	**77.71**	**299**	**80.81**	**242**	**77.49**	**146**	**79.49**	**43**	**72.27**	**69**	**88.31**
Unidentified	14	3.43	23	6.04	12	3.18	5	1.39	27	6.29	1	0.28	18	4.44	12	3.31	20	6.86	11	6.25	3	5.31	0	0
Total Pollen (AP/NAP)	**408**	**100**	**381**	**100**	**377.5**	**100**	**361**	**100**	**429**	**100**	**353.5**	**100**	**405.5**	**100**	**362**	**100**	**291.5**	**100**	**176**	**100**	**56.5**	**100**	**78.5**	**100**
Aquatics																								
Butomus	2	0.49	0	0	0	0	0	0	1	0.23	3	0.85	9	2.22	0	0	0	0	0	0	0	0	0	0
Myriophyllum	0	0	0	0	0	0	1	0.28	0	0	0	0	0	0	0	0	0	0	0	0	0	0	0	0
Nuphar	0	0	1	0.26	0	0	0	0	0	0	0	0	0	0	0	0	0	0	0	0	0	0	0	0
Potamogetonaceae	0	0	0	0	0	0	0	0	0	0	0	0	0	0	0	0	0	0	0	0	0	0	0	0
Total aquatics total	**2**	**0.4902**	**1**	**0.2625**	**0**	**0**	**1**	**0.277**	**1**	**0.2331**	**3**	**0.8487**	**9**	**2.2196**	**0**	**0**	**0**	**0**	**0**	**0**	**0**	**0**	**0**	**0**
Counted Lycopodium	248		223		177		192		234		249		294		248		499		441		243		288	

Statistically unreliable low pollen totals for % are underlined

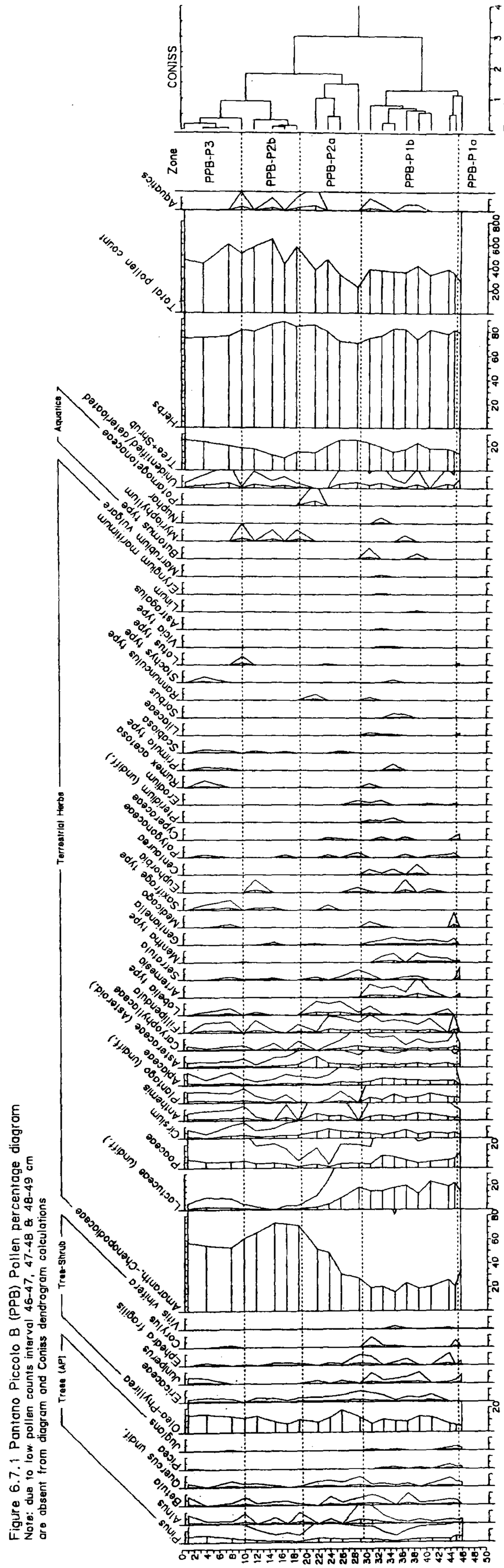

Figure 6.7.1 Pantano Piccolo B (PPB) Pollen percentage diagram
Note: due to low pollen counts interval 46-47, 47-48 & 48-49 cm
are absent from diagram and Coniss dendrogram calculations

and *Quercus* undiff. taxa. Less abundant in PPB-P1b is the occurrence of *Juglans*, *Corylus*, *Picea* and a single grain of *Vitis* at 43.5 (0.24 %) and two at 34.5 cm (0.52 % or 0.05 x 10^3 grains/g). Frequently under-represented, values of *Vitis* pollen exceeding 0.1% of total pollen have been used as an indicator that vines have been growing nearby at the time of deposition (Bottema & Woldring, 1990; Atherden *et al.* 1993).

Low values of Ericaceae appear at the base of PPB-P1b (0.08 x 10^3 grains/g or 1.2%) and remain fairly constant (through the subzone into PPB-P2a). *Juniperus* type also reappears in PPB-P1b, at a greater abundance than in PPB-P1a, before decreasing at the boundary with PPB-P2a.

Although throughout the core Amaranthaceae-Chenopodiaceae dominates the relative abundance of pollen, in PPB-P1b the concentration of Lactuceae approximately equals Chenopodiaceae, exceeding it in concentration at depths of 44.5, 40.5 and 34.5 cm (Fig. 6.7.3.).

The correspondence of Lactuceae, *Cirsium*, Poaceae, *Anthemis*, Apiaceae, *Plantago undiff.*, Caryophyllaceae and *Artemisia* in PPB-P1b indicates that lagoonal sediments at the time were receiving pollen from a local or extra-local disturbed-ruderal community. The diversity of less-abundant types in PPB-P1b (e.g. *Gentianella*, *Mentha*, *Medicago*, *Centaurea*, Cyperaceae, *Butomus* and *Erodium*) also reflect local-extra local terrestrial and aquatic sources. The occurrence of *Eryngium maritimum*, *Marrubium vulgare* and *Armeria maritima* suggests the core site was receiving extra-local pollen at the time from the coastal or dune and back barrier habitats towards the seaward margin of the lagoon/s. An increased marine or saline influence is also suggested by the concentrations of foraminifera organic linings which were recorded in PPB-P1b (Table 6.4.4.).

LPAZ PPB-P2: 29.5 to 9.5 cm (pre-19th century AD*to circa* AD *1958)*

The pollen zone represents a clear transformation in the supply of pollen to the core site, initiated by a marked negative shift in total pollen concentration and herb pollen diversity before being replaced by an environment conducive to the deposition of arboreal pollen species and abundant Amaranthaceae-Chenopodiaceae pollen. A marked decrease in the concentration of abundant pollen types (Fig. 6.7.3.), e.g. *Anthemis*, Asteraceae subf. Asteroideae, Poaceae, Apiaceae, Amaranthaceae-Chenopodiaceae, Caryophyllaceae and *Plantago undiff.* is observed at the boundary of PPB-P2a. These types along with Lactuceae however are observed to have already been in decline from ~35 cm depth within PPB-P1b.

Horizon PPB-P2a is marked by the reduction of total pollen concentration between 30 and 24 cm, corresponding with the upper portion of core unit PPB-B, preceding the accumulation of organic matter (PPB-C). Following this low, an increase in total pollen

Table 6.4.4. Counts and pollen concentrations of sediment horizons of Pantano Piccolo B core (Surface - 29 cm depth) Pollen types in order of count abundance

	Sample horizon PPB 0-1 cm		Sample horizon PPB 3-4cm		Sample horizon PPB 7-8cm		Sample horizon PPB 9-10cm		Sample horizon PPB 11-12cm		Sample horizon PPB 14-15cm		Sample horizon PPB 16-17cm		Sample horizon PPB 18-19cm		Sample horizon PPB 21-22cm		Sample horizon PPB 23-24cm		Sample horizon PPB 25-26cm		Sample horizon PPB 28-29cm	
	Count	grains/g	Count	grains/g	Count	grains/g	Count	grains/g	Count	grains/g	Count	grains/g	Count	grains/g	Count	grains/g	Count	grains/g	Count	grains/g	Count	grains/g	Count	grains/g
Arboreal pollen																								
Pinus	25	2485.90	26	1893.50	23.5	1297.60	15.5	1009.65	12.5	1365.18	10	1070.09	7.5	1534.78	7	638.92	14	1041.02	16.5	296.23	13	208.86	8	138.55
Alnus	7	696.05	2	145.65	3	165.65	9	586.25	6	655.29	7	749.06	4	818.55	11	1004.02	0	0	4	71.81	0	0	8	138.55
Betula	7	696.05	0	0	3	165.65	7	455.97	2	218.43	4	428.04	3	613.91	2	182.55	0	0	7	125.67	2	32.13	3	51.96
Quercus undiff.	3	298.31	0	0	6	331.30	3	195.42	4	436.86	2	214.02	0	0	1	91.27	4	297.43	5	89.77	3	48.20	4	69.28
Picea	0	0	0	0	0	0	0	0	0	0	0	0	0	0	0	0	0	0	0	0	0	0	0	0
Juglans	0	0	0	0	1	55.22	0	0	0	0	0	0	0	0	0	0	0	0	0	0	0	0	0	0
Eucalyptus	0	0	1	72.83	0	0	0	0	0	0	0	0	0	0	0	0	0	0	0	0	0	0	0	0
AP total	42	4176.32	29	2111.98	36.5	2015.42	34.5	2247.29	24.5	2675.75	23	2461.21	14.5	2967.24	21	1916.76	18	1338.45	32.5	583.48	18	289.18	23	398.34
Arboreal (Shrub) pollen																								
Olea-Phyllirea	68	6761.66	64	4660.92	79	4362.13	61	3973.48	78	8518.72	55	5885.50	29	5934.48	61	5567.73	32	2379.47	57	1023.33	63	1012.15	28	484.94
Ericaceae	2	198.87	3	218.48	3	165.65	2	130.28	4	436.86	4	428.04	1	204.64	4	365.10	3	223.07	4	71.81	4	64.26	4	69.28
Juniperus	5	497.18	4	291.31	0	0	0	0	0	0	0	0	0	0	0	0	2	148.72	0	0	2	32.13	0	0
Ephedra fragilis	0	0	2	145.65	0	0	1	65.14	0	0	3	321.03	2	409.27	2	182.55	0	0	2	35.91	1	16.07	4	69.28
Corylus	0	0	0	0	0	0	0	0	0	0	0	0	0	0	0	0	0	0	0	0	0	0	0	0
Vitis vinifera	0	0	0	0	0	0	0	0	0	0	0	0	0	0	0	0	0	0	0	0	0	0	0	0
AP (Shrub) total	75	7457.71	73	5316.36	82	4527.79	64	4168.89	82	8955.58	62	6634.56	32	6548.39	67	6115.37	37	2751.26	63	1131.05	70	1124.61	36	623.49
Non-arboreal pollen																								
Am.-Chenopodiaceae	268	26648.90	238	17332.79	319	17614.19	319	20779.32	379	41392.27	479	51257.36	312	63846.77	418	38152.61	198	14722.94	229	4111.28	107	1719.04	63	1091.11
Lactuceae	5	497.18	9	655.44	11	607.39	5	325.69	3	327.64	3	321.03	3	613.91	4	365.10	9	669.22	24	430.88	33	530.17	43	744.73
Poaceae undiff.	34	3380.83	22	1602.19	32	1766.94	31	2019.31	22	2402.72	27	2889.25	14	2864.92	7	638.92	13	966.66	3	53.86	14	224.92	9	155.87
Cirsium	7	696.05	3	218.48	13	717.82	14	911.95	8	873.72	11	1177.10	11	2251.01	17	1551.66	22	1635.88	38	682.22	22	353.45	11	190.51
Anthemis	6	596.62	7	509.79	11	607.39	13	846.81	4	436.86	7	749.06	12	2455.64	14	1277.84	24	1784.60	17	305.20	15	240.99	0	0
Plantago undiff.	9	894.93	8	582.61	10	552.17	13	846.81	7	764.50	3	321.03	6	1227.82	1	91.27	0	0	3	53.86	7	112.46	0	0
Apiaceae undiff.	10	994.36	4	291.31	13	717.82	6	390.83	4	436.86	7	749.06	8	1637.10	9	821.47	5	371.79	8	143.63	11	176.72	6	103.92
Asteraceae subf. Aster	4	397.74	4	291.31	6	331.30	8	521.11	3	327.64	11	1177.10	8	1637.10	17	1551.66	38	2825.61	18	323.16	11	176.72	5	86.60
Caryophyllaceae	3	298.31	1	72.83	4	220.87	4	260.56	5	546.07	8	856.07	3	613.91	9	821.47	6	446.15	4	71.81	6	96.39	9	155.87
Filipendula	0	0	7	509.79	11	607.39	0	0	12	1310.57	2	214.02	0	0	8	730.19	1	74.36	13	233.39	9	144.59	4	69.28
Lobelia type	0	0	2	145.65	7	386.52	0	0	3	327.64	0	0	0	0	0	0	9	669.22	9	161.58	8	128.53	1	17.32
Artemisia	0	0	0	0	0	0	0	0	0	0	0	0	0	0	0	0	0	0	0	0	0	0	0	0
Serratula	0	0	0	0	3	165.65	1	65.14	1	109.21	2	214.02	1	204.64	0	0	2	148.72	1	17.95	2	32.13	4	69.28
Mentha type	0	0	0	0	0	0	1	65.14	0	0	0	0	0	0	0	0	0	0	0	0	0	0	0	0
Gentianella	0	0	0	0	0	0	0	0	0	0	3	321.03	0	0	0	0	1	74.36	0	0	0	0	0	0
Medicago	0	0	0	0	3	165.65	0	0	0	0	0	0	0	0	0	0	0	0.00	0	0	0	0	0	0
Saxifrage type	0	0	4	291.31	10	552.17	0	0	2	218.43	3	321.03	0	0	0	0	4	297.43	0	0	0	0	0	0
Euphorbia	0	0	0	0	0	0	0	0	8	873.72	0	0	0	0	0	0	0	0	0	0	0	0		0
Centaurea	0	0	0	0	0	0	0	0	0	0	0	0	0	0	0	0	0	0	0	0	0	0	0	0
Polygonaceae	0	0	2	145.65	0	0	0	0	0	0	0	0	1	204.64	0	0	0	0	2	35.91	0	0	2	34.64
Cyperaceae	0	0	0	0	0	0	0	0	0	0	0	0	0	0	0	0	0	0	2	35.91	1	16.07	0	0
Erodium	0	0	0	0	0	0	0	0	0	0	0	0	0	0	0	0	0	0	0	0	0	0	2	34.64
Rumex	0	0	5	364.13	0	0	0	0	0	0	0	0	0	0	0	0	0	0	0	0	0	0	0	0
Primula type	0	0	2	145.65	2	110.43	0	0	0	0	0	0	0	0	0	0	0	0	0	0	0	0	0	0
Scabiosa	0	0	2	145.65	2	110.43	0	0	2	218.43	0	0	1	204.64	0	0	0	0	0	0	1	16.07	0	0
Liliaceae	0	0	0	0	0	0	0	0	0	0	0	0	0	0	0	0	0	0	0	0	0	0	0	0
Sorbus	0	0	0	0	0	0	0	0	0	0	0	0	0	0	0	0	0	0	0	0	0	0	0	0
Ranunculus type	0	0	0	0	0	0	0	0	0	0	0	0	0	0	0	0	4	297.43	0	0	0	0	0	0
Stachys type	0	0	4	291.31	0	0	0	0	0	0	0	0	0	0	0	0	0	0	0	0	0	0	0	0
Lotus type	0	0	0	0	0	0	3	195.42	0	0	0	0	0	0	0	0	0	0	1	17.95	0	0	0	0
Armeria maritima	0	0	0	0	0	0	0	0	0	0	0	0	0	0	0	0	0	0	0	0	0	0	0	0
Hypericum type	0	0	0	0	0	0	0	0	0	0	0	0	0	0	0	0	0	0	0	0	0	0	0	0
Vicia type	0	0	0	0	0	0	0	0	0	0	0	0	0	0	0	0	0	0	0	0	0	0	0	0
Astragalus	0	0	0	0	0	0	0	0	0	0	0	0	0	0	0	0	1	74.36	0	0	0	0	0	0
Linum	0	0	0	0	0	0	0	0	0	0	0	0	0	0	0	0	0	0	0	0	0	0	0	0
Eryngium maritimum	0	0	0	0	0	0	0	0	0	0	0	0	0	0	0	0	0	0	0	0	0	0	0	0
Marrubium vulgare	0	0	0	0	0	0	0	0	0	0	0	0	0	0	0	0	0	0	0	0	0	0	0	0
Rhinanthus	0	0	0	0	0	0	0	0	0	0	0	0	0	0	0	0	0	0	0	0	0	0	0	0
NAP total	346	34404.92	324	23595.90	457	25234.12	418	27228.08	463	50566.28	566	60567.15	340	77762.09	504	46002.19	337	25058.74	372	6678.59	247	3968.25	159	2753.76
Unidentified/deteriorated	4	397.74	9	655.44	24	1325.21	1	65.14	16	1747.43	8	856.07	8	1637.10	5	456.37	0	0.00	0	0.00	11	176.72	11	190.51
Total Pollen (+unident)	467	46436.7	435	31679.68	599.5	33102.53	517.5	33709.4	585.5	63943.04	659	70518.99	434.5	88914.81	597	54490.69	392	29148.45	467.5	8393.12	346	5538.77	229	3966.11
Aquatics																								
Butomus	0	0	0	0	0	0	0	0	0	0	0	0	0	0	0	0	0	0	0	0	0	0	0	0
Myriophyllum	0	0	0	0	0	0	3	195.42	0	0	2	214.02	0	0	2	182.55	0	0	0	0	0	0	0	0
Nuphar	0	0	0	0	0	0	0	0	0	0	0	0	0	0	0	0	0	0	0	0	0	0	0	0
Potamogetonaceae	0	0	0	0	0	0	0	0	0	0	0	0	0	0	0	0	4	297.43	0	0	0	0	0	0
Total aquatics	0	0	0	0	0	0	3	195.42	0	0	2	214.02	0	0	2	182.55	4	297.43	0	0	0	0	0	0
Foraminifera (undiff.)															7	764.50	6	655.29					8	873.72
Counted Lycopodium	79		112		132		118		69		89		39		83		84		228		234		184	
Dried sample mass (g)	1.273		1.226		1.372		1.301		1.327		1.05		1.253		1.32		1.601		2.443		2.66		3.138	

Table 6.4.4. Counts and pollen concentrations of sediment horizons of Pantano Piccolo B core (30 - 49 cm depth) Pollen types in order of core abundance

	Sample horizon PPB 30-31cm		Sample horizon PPB 32-33cm		Sample horizon PPB 34-35cm		Sample horizon PPB 36-37cm		Sample horizon PPB 38-39cm		Sample horizon PPB 40-41cm		Sample horizon PPB 42-44cm		Sample horizon PPB 44-45cm		Sample horizon PPB 45-46cm		Sample horizon PPB 46-47cm		Sample horizon PPB 47-48cm		Sample horizon PPB 48-49cm	
	Count	grains/g	Count	grains/g	Count	grains/g	Count	grains/g	Count	grains/g	Count	grains/g	Count	grains/g	Count	grains/g	Count	grains/g	Count	grains/g	Count	grains/g	Count	grains/g
Arboreal pollen																								
Pinus	23	465.34	9	200.19	9.5	264.14	8	205.46	15	319.24	12.5	251.00	16.5	278.11	21	390.42	24.5	245.12	16	180.32	2.5	47.48	6.5	109.93
Alnus	11	222.55	5	111.22	2	55.61	1	25.68	3	63.85	1	20.08	3	50.57	6	111.55	2	20.01	5	56.35	6	113.95	0	0
Betula	7	141.62	4	88.97	0	0	7	179.77	2	42.56	2	40.16	4	67.42	3	55.77		0	2	22.54	4	75.97	1	16.91
Quercus type	2	40.46	2	44.49	1	27.80	2	51.36		0	2	40.16	6	101.13	3	55.77	2	20.01	0	0	0	0	0	0
Picea	0	0	1	22.24	1	27.80	0	0	1	21.28	0	0	3	50.57	1	18.59	1	10.01	0	0	0	0	0	0
Juglans	1	20.23	0	0	1	27.80	0	0	0	0	0	0	2	33.71	2	37.18	1	10.01	0	0	0	0	0	0
Eucalyptus	0	0	0	0	0	0	0	0	0	0	0	0	0	0	0	0	0	0	0	0	0	0	0	0
Arboreal total	**44**	890.21	**21**	467.12	**14.5**	403.15	**18**	462.28	**21**	446.93	**17.5**	351.41	**34.5**	581.50	**36**	669.30	**30.5**	305.15	**23**	259.22	**12.5**	237.41	**7.5**	126.85
Arboreal (Shrub) pollen																								
Olea-Phyllirea	27	546.27	39	867.50	33	917.52	31	796.15	55	1170.53	42	843.37	26	438.23	19	353.24	13	130.07	6	67.62	0	0	0	0
Ericaceae	6	121.39	4	88.97	1	27.80	3	77.05	3	63.85	4	80.32	5	84.28	0	0	0	0	0	0	0	0	0	0
Juniperus	7	141.62	2	44.49	3	83.41	4	102.73	8	170.26	0	0	1	16.86	0	0	4	40.02	0	0	0	0	2	33.83
Ephedra fragilis	6	121.39	0	0	2	55.61	4	102.73	0	0	0	0	8	134.84		0	2	20.01	0	0	0	0	0	0
Corylus	7	141.62	1	22.24	1	27.80	0	0	0	0	0	0	0	0	4	74.37	0	0	0	0	1	18.99	1	16.91
Vitis vinifera	0	0.00	0	0.00	2	55.61	0	0	0	0	0	0	1	16.86	0	0	0	0	0	0	0	0	0	0
Arboreal (Shrub) total	**53**	1072.30	**46**	1023.20	**42**	1167.76	**42**	1078.65	**66**	1404.64	**46**	923.69	**41**	691.06	**23**	427.61	**19**	190.10	**6**	67.62	**1**	18.9924	**3**	50.74
Non-arboreal pollen																								
Art.-Chenopodiaceae	77	1557.87	76	1690.51	60	1668.22	85	2182.98	80	1702.59	69	1385.54	102	1719.22	72	1338.60	94	940.47	55	619.86	28	531.79	40	676.52
Lactuceae	61	1234.16	58	1290.13	69	1918.46	72	1849.11	56	1191.81	79	1586.35	76	1280.99	77	1431.56	40	400.20	43	484.62	5	94.96	4	67.65
Poaceae undiff.	14	283.25	40	889.74	35	973.13	23	590.69	19	404.37	17	341.37	27	455.09	28	520.57	35	350.18	23	259.22	4	75.97	5	84.56
Cirsium	17	343.95	11	244.68	19	528.27	26	667.74	16	340.52	17	341.37	16	269.68	18	334.65	7	70.04	6	67.62	0	0	0	0
Anthemis	14	283.25	17	378.14	12	333.64	15	385.23	28	595.91	19	381.53	13	219.12	8	148.73	5	50.03	0	0	0	0	0	0
Plantago undiff.	19	384.41	11	244.68	28	778.50	15	385.23	23	489.50	28	562.25	21	353.96	18	334.65	11	110.06	2	22.54	3	56.98	3	50.74
Apiaceae undiff.	14	283.25	22	489.36	21	583.88	17	436.60	20	425.65	22	441.77	16	269.68	14	260.28	1	10.01	0	0	0	0	0	0
Asteraceae subf. Aster	14	283.25	10	222.44	9	250.23	10	256.82	18	383.08	9	180.72	16	269.68	8	148.73	8	80.04	0	0	0	0	1	16.91
Caryophyllaceae	9	182.09	8	177.95	9	250.23	3	77.05	8	170.26	4	80.32	6	101.13	11	204.51	3	30.02	3	33.81	0	0	5	84.56
Filipendula	12	242.79	7	155.71	8	222.43	7	179.77	6	127.69	8	160.64	0	0	11	204.51	0	0	0	0	0	0	0	0
Lobelia type	6	121.39	1	22.24	0	0	1	25.68	0	0	0	0	4	67.42	0	0	0	0	0	0	0	0	0	0
Artemisia	9	182.09	6	133.46	7	194.63	3	77.05	15	319.24	4	80.32	0	0	0	0	2	20.01	0	0	0	0	0	0
Serratula	4	80.93	1	22.24	1	27.80	2	51.36	3	63.85	0	0	1	16.86	4	74.37	6	60.03	2	22.54	0	0	2	33.83
Mentha type	3	60.70	4	88.97	6	166.82	0	0	7	148.98	3	60.24	3	50.57	1	18.59	1	10.01	0	0	0	0	0	0
Gentianella	2	40.46	3	66.73	5	139.02	3	77.05	3	63.85	3	60.24	2	33.71	4	74.37	0	0	0	0	0	0	0	0
Medicago	4	80.93	2	44.49	1	27.80	0	0	0	0	0	0	6	101.13	9	167.32	0	0	0	0	0	0	0	0
Saxifrage type	0	0	0	0	0	0	0	0	0	0	0	0	0	0	0	0	0	0	0	0	0	0	0	0
Euphorbia	1	20.23		0	0	0	8	205.46		0	2	40.16	0	0	0	0	0	0	0	0	0	0	0	0
Centaurea	4	80.93	1	22.24	4	111.21	0	0	8	170.26	0	0	0	0	0	0	0	0	0	0	0	0	0	0
Polygonaceae	0	0	0	0	0	0	2	51.36	0	0	1	20.08	2	33.71	3	55.77	0	0	1	11.27	0	0	0	0
Cyperaceae	2	40.46	2	44.49		0	2	51.36	0	0	0	0		0	2	37.18	3	30.02	0	0.00	0	0	0	0
Erodium	2	40.46	2	44.49	0	0	0	0	1	21.28	1	20.08	0	0	1	18.59	0	0	0	0	0	0	0	0
Rumex	3	60.70	0	0	0	0	0	0	0	0	0	0	0	0	0	0	0	0	0	0	0	0	0	0
Primula type	0	0	0	0	4	111.21	0	0	0	0	0	0	0	0	0	0	0	0	0	0	0	0	0	0
Scabiosa	0	0	0	0	0	0	0	0	0	0	0	0	0	0	0	0	0	0	0	0	0	0	0	0
Liliaceae	2	40.46	1	22.24	1	27.80	0	0	0	0	0	0	0	0	0	0	2	20.01	1	11.27	0	0	0	0
Sorbus	0	0	0	0	3	83.41	2	51.36	0	0	0	0	0	0	2	37.18	0	0	0	0	0	0	0	0
Ranunculus type	2	40.46	0	0	1	27.80	0	0	0	0	0	0	0	0	0	0	0	0	0	0	0	0	0	0
Stachys type	0	0	0	0	2	55.61	0	0	0	0	0	0	0	0	0	0	0	0	0	0	0	0	0	0
Lotus type	0	0	0	0	0	0	0	0	0	0	0	0	0	0	0	0	1	10.01	0	0	0	0	0	0
Armeria maritima	0	0	3	66.73	0	0	0	0	1	21.28	0	0	0	0	0	0	0	0	0	0	0	0	0	0
Hypericum type	0	0	0	0	0	0	0	0	0	0	3	60.24	0	0	0	0	0	0	0	0	0	0	0	0
Vicia type	0	0	1	22.24	1	27.80	0	0	0	0	0	0	0	0	0	0	0	0	0	0	0	0	0	0
Astragalus	0	0	1	22.24	0	0	0	0	0	0.00	0	0	0	0	0	0	0	0	0	0	0	0	0	0
Linum	0	0	0	0.00	0	0	0	0	2	42.56	0	0	0	0	0	0	0	0	0	0	0	0	0	0
Bryonia maritimum	0	0	1	22.24	0	0	0	0	0	0	0	0	0	0	0	0	0	0	0	0	0	0	0	0
Marrubium vulgare	0	0	1	22.24	0	0	0	0	0	0	0	0	0	0	0	0	0	0	0	0	0	0	0	0
Rhinanthus	0	0	0	0	0	0	0	0	1	21.28	0	0	0	0	0	0	0	0	0	0	0	0	0	0
Non-arboreal total	**297**	6008.93	**291**	6472.88	**309**	8591.35	**296**	7601.91	**315**	6703.95	**289**	5803.21	**312**	5258.79	**291**	5410.17	**223**	2221.12	**136**	1532.75	**40**	759.70	**60**	1014.78
Unidentified/deteriorated	14	283.25	23	511.60	29	806.31	5	128.41	27	574.62	1	20.08	18	303.39	12	223.10	20	200.10	11	123.97	3	56.98	0	0.00
Total Pollen (+unident)	**408**	8254.7	**381**	8474.8	**394.5**	10968.57	**361**	9271.24	**459**	9130.15	**353.5**	7096.39	**405.5**	6834.75	**362**	6730.18	**291.5**	2916.47	**176**	1983.86	**56.5**	1073.07	**70.5**	1192.36
Aquatics																								
Butomus	2	40.46	0	0	0	0	0	0	1	21.28	3	60.24	9	151.70	0	0	0	0	0	0	0	0	0	0
Myriophyllum	0	0	0	0	0	0	1	25.68	0	0	0	0	0	0	0	0	0	0	0	0	0	0	0	0
Nuphar	0	0	1	22.24	0	0	0	0	0	0	0	0	0	0	0	0	0	0	0	0	0	0	0	0
Potamogetonaceae	0	0	0	0	0	0	0	0	0	0	0	0	0	0	0	0	0	0	0	0	0	0	0	0
Total aquatics total	**2**	40.46	**1**	22.24	**0**	0	**1**	25.68	**1**	21.28	**3**	60.24	**9**	151.70	**0**	0	**0**	0	**0**	0	**0**	0	**0**	0
Foraminifera (undiff.)	2	218.43	1	109.21	2	218.43	3	327.64	2	218.43	3	327.64			2	218.43								
Counted Lycopodium	248		223		177		192		234		249		294		268		499		441		263		288	
Dried sample mass (g)	1.993		2.016		2.032		2.028		2.008		2		2.018		2.007		2.003		2.012		2.002		2.053	

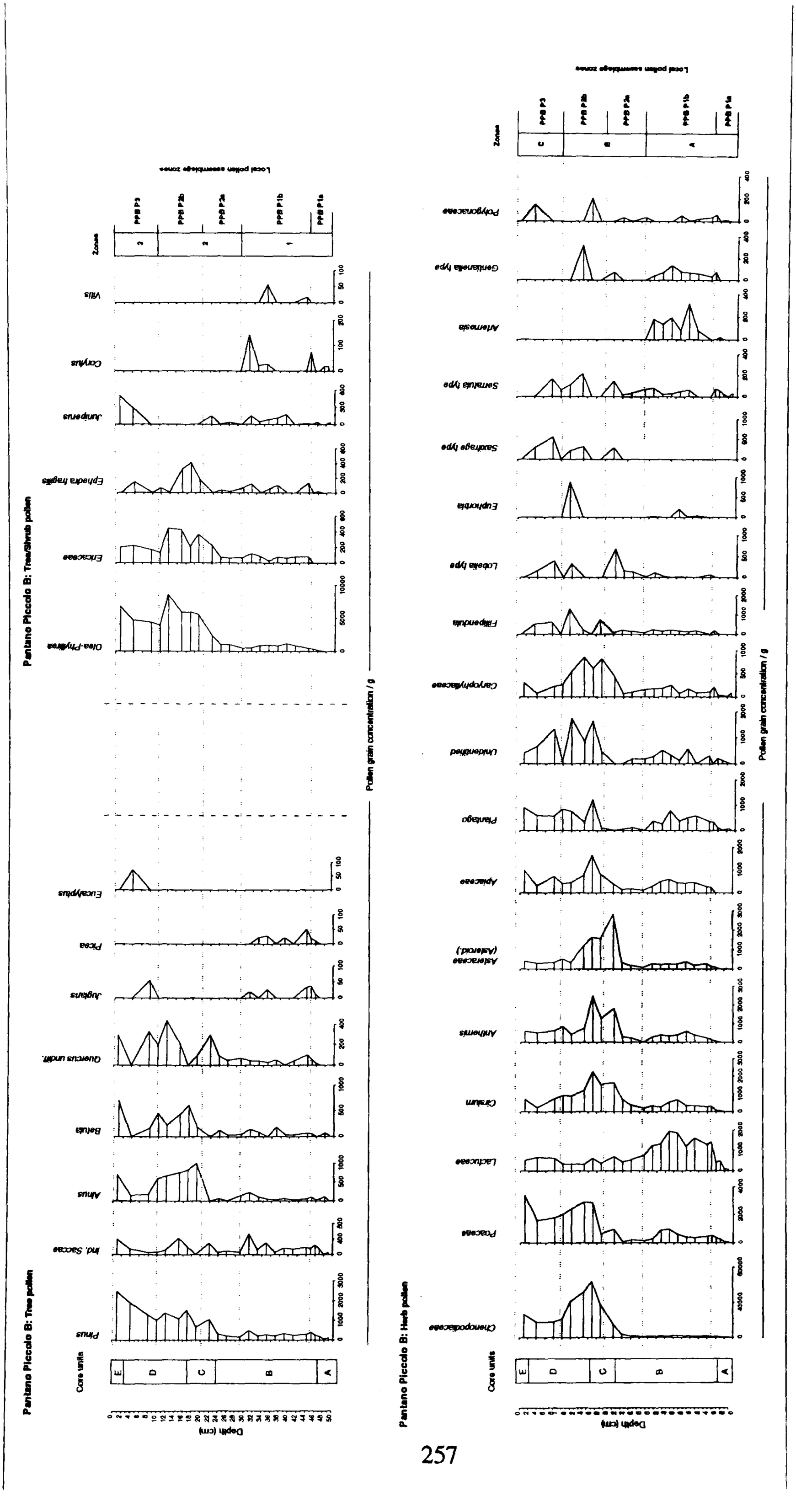

Figure 6.7.2. Pantano Piccolo B: Pollen concentration diagrams. Ordered L-R in order of core abundance

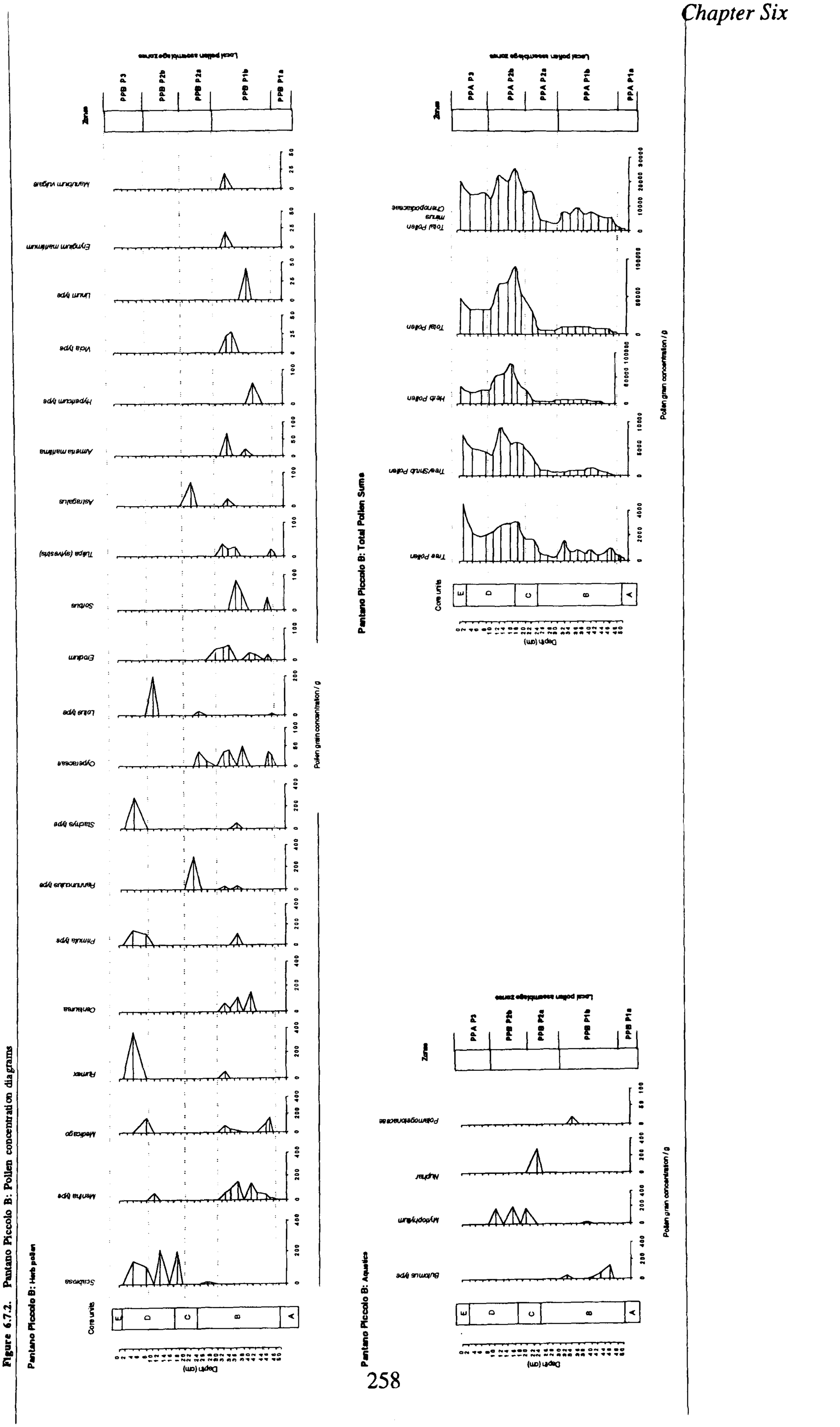

Figure 6.7.2. Pantano Piccolo B: Pollen concentration diagrams

Figure 6.7.3. Summary diagram of main pollen types in Pantano Piccolo B. Pollen taxa arranged L-R alphabetically

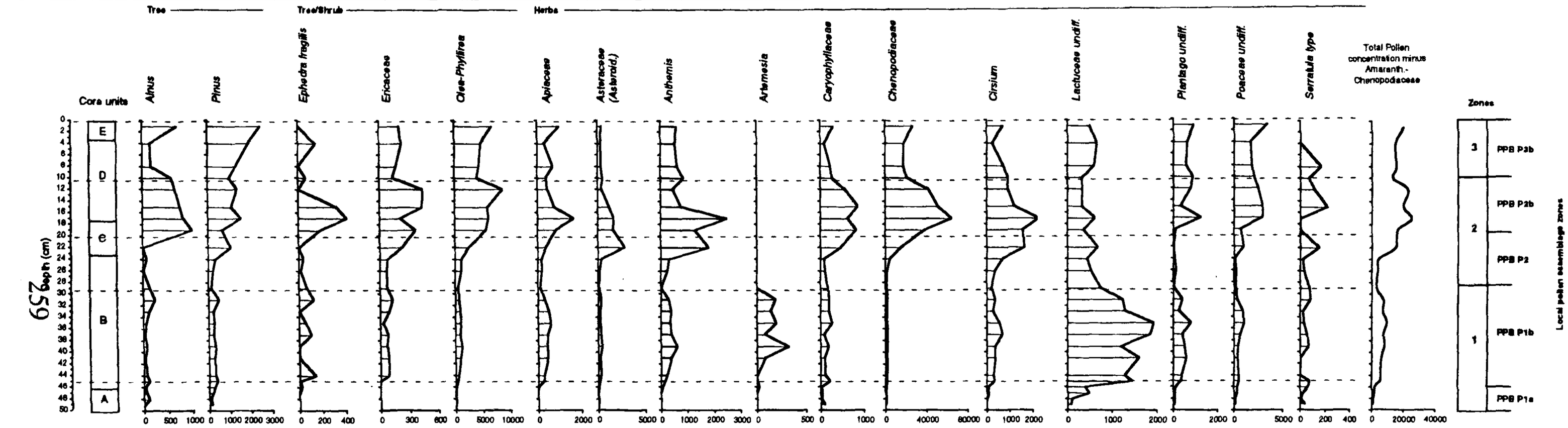

concentration, appears coincidental with increased organic content in the core (PPB-C) (Fig. 6.7.3.). PPB-P2a represents the start of a common increase in the accumulation of pollen, peaking in the subzone above. Only Asteraceae subf. Asteroideae, *Lobelia* and *Ranunculus* types are observed to peak preceding the pollen-abundant sediments of PPB-P2b. An increase in the concentration of arboreal tree and shrub pollen is clearly indicated in PPB-P2; increasing gradually from 29 cm, e.g. *Pinus* and *Quercus undiff.* or more rapidly in association with the peak organic content and repeat of lagoon sedimentation (PPB-D), i.e. *Alnus*, *Betula*, *Olea-Phyllirea* and Ericaceae. The age of the peak in *Olea-Phyllirea* at 11.5 cm (8.5 x 10^3 grains/g) corresponds to the calculated date *c.* AD 1948.

Amaranthaceae-Chenopodiaceae pollen concentration closely follows the pattern of organic content in PPB-C (compare with Fig. 6.6.2) and dominates the herb pollen, as well as the total pollen content of the sediments in PPB-P2. Progressively increasing from the base of the sediment unit (48 % TP or 4.0 x 10^3 grains/g at 23.5 cm) up to a peak at the upper boundary (17 cm depth or *circa* AD 1893) of PPB-C (70 % TP or 6.3 x 10^4 grains/g).

Amaranthaceae-Chenopodiaceae abundance decreases above this, again in conjunction with decreasing organic content. Other abundant herb types are seen to have responded with greater variation, e.g. Poaceae, *Plantago* are seen to have rapidly increased in concentration in conjunction with Amaranthaceae-Chenopodiaceae, though decreasing in abundance more gradually towards PPB-P3. *Cirsium* and *Anthemis* both peak (2.2-2.4 x 10^3 grains/g) in conjunction with Apiaceae (1.6 x 10^3 grains/g) and Amaranthaceae-Chenopodiaceae (6.3 x 10^4 grains/g) at 17 cm before decreasing rapidly in the basal section of PPB-D. An increase in Caryophyllaceae, *Filipendula*, *Euphorbia*, *Ephedra fragilis*, *Serratula* type, *Gentianella* and *Scabiosa* values is also noticeable within PPB-P2b.

LPAZ PPB-P3: 9.5 cm to Surface (circa AD *1958 to circa* AD*1996)*

The lower boundary of PPB-P3 coincides with the upper limit of the shell concentration in sediment horizon PPB-D. The transition from shell-rich lagoonal muds to a more homogenous grey lagoonal mud occurred (10-9 cm) *circa* AD 1958 and is marked by a significant drop in Amaranthaceae-Chenopodiaceae, Ericaceae, *Olea-Phyllirea* and total pollen concentration (Fig. 6.7.3.).

Decreasing in concentration from the base of PPB-P2b, *Alnus* and *Betula* values drop in PPB-P3 recovering towards the surface. Although indicating a drop in concentration at the boundary of PPB-P3, *Pinus* increases through the zone up to the surface. The re-appearance of *Juglans* in the zone (c. AD 1969) and occurrence of *Eucalyptus* (*c.* AD

1987) may be a reflection of recent tree growth in the catchment, e.g. for field boundaries around the landward margin of the Vendicari lagoon system. *Olea-Phyllirea*, Ericaceae and *Juniperus* pollen recover from the drop in concentration at the lower boundary of PPB-P3 and increase towards the surface.

Compared with PPB-P2, the abundance of herb pollen types is reduced in PPB-P3. Having remained low and relatively constant from PPB-P1, Lactuceae pollen recovers to a higher concentration in PPB-P3. Chenopodiaceae, Poaceae, and Caryophyllaceae, all having decreased at the beginning of the zone, slowly recover towards the surface. *Anthemis* and Asteraceae subf. Asteroideae taxa develop a small peak at the boundary with PPB-P2b (coincidental with *Plantago*) before remaining constantly low in the zone.

6.4.7.1 Pantano Piccolo B: Pollen accumulation rates

Pollen accumulation rates for selected types were determined for the upper seven sample intervals in the core, spanning approximately the last 150 years of sedimentation in the upper 19 cm of the core. Pollen taxa were chosen to represent the most frequent and abundant grains as well as their use in indicating significantly different vegetational changes and pollen provenance transport vectors.

Pollen accumulation rates are tabulated in order of abundance and their individual correlation with the ^{210}Pb-derived accretion rate at the time of deposition (Table 6.4.5.). Because of the low resolution of pollen sampling in the upper core and the variability of accretion rates determined over the same interval (Table 6.4.1.), pollen influx rates were determined using accretion rates determined for the individual horizon, rather than between the pollen sample intervals (the approach used in PPA previously).

The samples used for pollen accumulation rates may be seen therefore to have been extracted from horizons which were not exclusively periods of peak or decreased accretion rates, following the same increasing trend of accretion rates. Pollen accumulation rates from the core therefore only represent a broad picture of the relationship between accretionary changes and pollen deposition at the core site.

A close correlation between accretion and pollen accumulation rates in the core is recognised in the core sequence (Table 6.4.5.) for the selected pollen taxa, apart from *Ephedra fragilis* (r = -0.035) and *Serratula* type (r = -0.241) (Fig. 6.7.3). *Pinus*, *Olea-Phyllirea*, *Betula* and *Quercus undiff.* pollen accumulation rates follow the trend in accretion rates indicating that although being primarily transported within the atmosphere, lagoon-sediment transport pathways and depositional kinetics have certainly controlled the final incorporation to the core setting of well-dispersed types. Ericaceae pollen indicates higher accumulation rates occurring c. AD 1922 and c. AD 1948. The

Table 6.4.5. Pantano Piccolo B: Sediment accretion and pollen accumulation rates for selected pollen types

Depth interval (cm)	0.5	3.5	7.5	9.5	11.5	14.5	16.5	18.5
Years BP	0.00	8.82	27.44	37.76	47.84	74.28	103.45	132.99
Cal. Years BP	1996	1987	1969	1958	1948	1922	1893	1863
Accretion Rate (cm a^{-1})	0.37	0.23	0.20	0.18	0.14	0.13	0.07	0.07

a) Pollen accumulation rates (grains/cm^2/a^{-1}) In order of sample abundance

AP (Tree & Shrub)								
Olea-Phyllirea	6583.49	2883.83	2354.38	1857.80	3202.34	2090.84	1064.48	1056.35
Pinus	2420.40	1171.56	700.35	472.06	513.20	380.15	275.30	121.22
Alnus	677.71	90.12	89.41	274.10	246.33	266.11	146.83	190.49
Betula	677.71	0.00	89.41	213.19	82.11	152.06	110.12	34.63
Ericaceae	193.63	135.18	89.41	60.91	164.22	152.06	36.71	69.27
Quercus undiff.	290.45	0.00	178.81	91.37	164.22	76.03	0.00	17.32
Ephedra fragilis	0.00	90.12	0.00	30.46	0.00	114.05	73.41	34.63
NAP (Herb)								
Amaranth.-Chenopodiaceae	25946.70	10724.25	9506.94	9715.38	15560.09	18209.34	11452.38	7238.57
Poaceae	3291.74	1502.38	1854.17	2009.34	2438.64	2320.32	2745.60	645.05
Cirsium	677.71	135.18	387.43	426.38	328.45	418.17	403.77	294.39
Unidentified	387.26	405.54	715.26	30.46	656.89	304.12	293.65	86.59
Anthemis	580.90	315.42	327.83	395.92	164.22	266.11	440.48	242.44
Apiaceae (Umbillifferae)	968.16	180.24	387.43	182.73	164.22	266.11	293.65	155.85
Plantago	871.34	360.48	298.02	395.92	287.39	114.05	220.24	17.32
Asteraceae subf. Aster	387.26	180.24	178.81	243.65	123.17	418.17	293.65	294.39
Lactuceae	484.08	405.54	327.83	152.28	123.17	114.05	110.12	69.27
Caryophyllaceae	290.45	45.06	119.21	121.82	205.28	304.12	110.12	155.85
Serratula type	0.00	0.00	89.41	30.46	41.06	76.03	36.71	0.00
Total Pollen	45213.08	19601.04	17866.50	15852.21	24038.08	25128.12	15948.90	10372.97

a) Pollen accumulation rates (grains/cm^2/a^{-1}) Sorted by correlation values between sediment accretion and pollen accumulation rates

									(*r*) sed accretion
AP (Tree & Shrub)									
Pinus (Total)	2420.40	1171.56	700.35	472.06	513.20	380.15	275.30	121.22	0.96
Olea europea L.	6583.49	2883.83	2354.38	1857.80	3202.34	2090.84	1064.48	1056.35	0.91
Betula L.	677.71	0.00	89.41	213.19	82.11	152.06	110.12	34.63	0.75
Quercus type	290.45	0.00	178.81	91.37	164.22	76.03	0.00	17.32	0.73
Ericaceae	193.63	135.18	89.41	60.91	164.22	152.06	36.71	69.27	0.67
Alnus	677.71	90.12	89.41	274.10	246.33	266.11	146.83	190.49	0.66
Ephedra fragilis	0.00	90.12	0.00	30.46	0.00	114.05	73.41	34.63	-0.35
NAP (Herb)									
Lactuceae	484.08	405.54	327.83	152.28	123.17	114.05	110.12	69.27	0.92
Plantago	871.34	360.48	298.02	395.92	287.39	114.05	220.24	17.32	0.92
Apiaceae (Umbillifferae)	968.16	180.24	387.43	182.73	164.22	266.11	293.65	155.85	0.79
Amaranth.-Chenopodiaceae	25946.70	10724.25	9506.94	9715.38	15560.09	18209.34	11452.38	7238.57	0.65
Anthemis	580.90	315.42	327.83	395.92	164.22	266.11	440.48	242.44	0.60
Cirsium	677.71	135.18	387.43	426.38	328.45	418.17	403.77	294.39	0.48
Poaceae	3291.74	1502.38	1854.17	2009.34	2438.64	2320.32	2745.60	645.05	0.45
Unidentified	387.26	405.54	715.26	30.46	656.89	304.12	293.65	86.59	0.28
Caryophyllaceae	290.45	45.06	119.21	121.82	205.28	304.12	110.12	155.85	0.25
Asteraceae subf. Aster	387.26	180.24	178.81	243.65	123.17	418.17	293.65	294.39	0.12
Serratula type	0.00	0.00	89.41	30.46	41.06	76.03	36.71	0.00	-0.24
Total Pollen	45213.08	19601.04	17866.50	15852.21	24038.08	25128.12	15948.90	10372.97	0.81

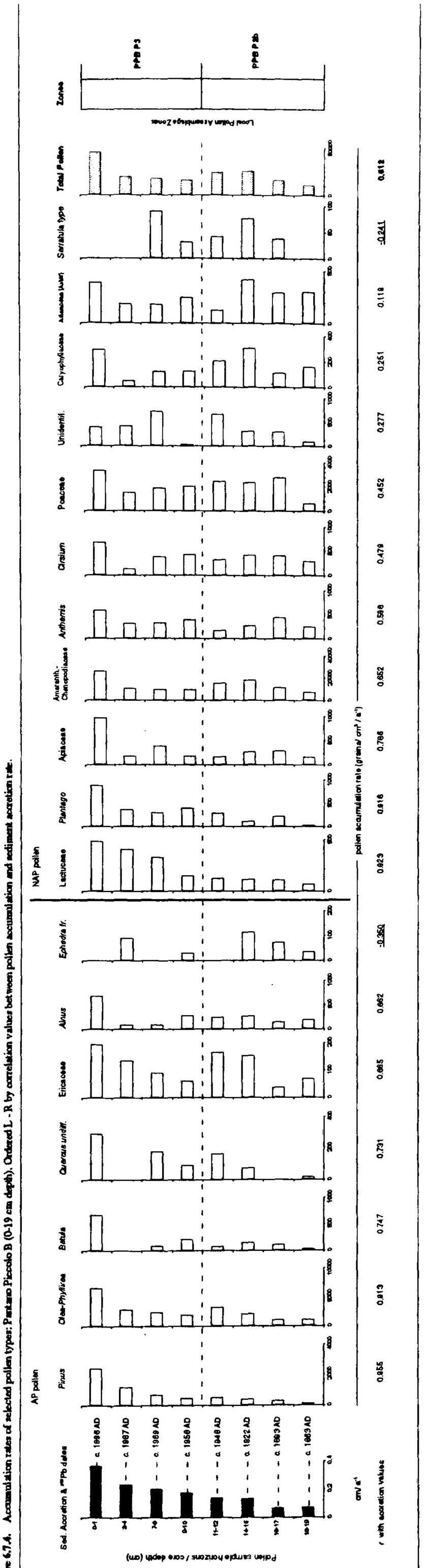

Figure 6.7.4. Accumulation rates of selected pollen types: Pantano Piccolo B (0-19 cm depth). Ordered L - R by correlation values between pollen accumulation and sediment accretion rate.

accumulation rate of Ericaceae is also seen to have increased steadily with accretion from around AD 1958. Remaining relatively constant in the cored section *Alnus* pollen accumulation shows an apparent decrease at 7.5 and 3.5 cm (AD 1969 and AD 1987) preceding the surface interval peak (0.6 x 10^3 grains cm^2 a^{-1}).

Herb pollen accumulation rates show a broader affinity and variation with sedimentation rates (Fig. 6.7.4.). Due to the reduced input of local atmospheric fallout to the core site, the accumulation of herb pollen types have depended on aquatic transport/sediment inputs. Lactuceae, *Plantago* and Apiaceae accumulation rates have parallelled increasing accretion rates over the last century (Fig. 6.7.4.).

Amaranthaceae-Chenopodiaceae, *Anthemis*, *Cirsium* and Poaceae accumulation rates over the same period have remained relatively constant. Caryophyllaceae and Asteraceae subf. Asteroideae accumulation rates appear to have been less associated with lower accretion (PPB-P2b) with the eruption of surface sample. Changing rates of accretion appear not to have affected the accumulation of *Ephedra fragilis*, while increased accretion in PPB-P3 coincides with the disappearance of *Serratula* type.

Without surface vegetation during the recorded sequence, pollen accumulation rates have apparently responded to trends in lagoonal sediment transport, reflecting the mudflat-benthic setting of the core site during the depositional period. The accumulation of pollen taxa suggests that vegetation fringing the lagoon generated a reservoir (decreased concentration-higher diversity) of pollen available to be incorporated in the sediment. Once deposited on the lagoon sediment surface, pollen grains may be expected to have been re-mobilised and re-distributed by wave activity and variable water levels.

6.5 SURFACE POLLEN RELATIONSHIPS AROUND PANTANO PICCOLO

6.5.1 Introduction

In the absence of detailed monitoring studies of the changing spatial distribution of plant communities, the reconstruction of past vegetation patterns has relied heavily on pollen grains and other plant materials being incorporated into datable sediment sequences (e.g. Pennington, 1979; Planchais, 1987; Stevenson & Battarbee, 1991; Rhodes & Davis, 1995). Due to the variability in pollen production and dispersal mechanisms between individual species and differences in pollen assemblages caused by variable transport pathways, surface pollen assemblages may not simply reflect surface vegetation at a point in time. This is especially the case in coastal wetlands due to a diversity of pollen sources and transport vectors between plant and sediment burial (see Chapter 2). As a result, if sediment sequences (pollen assemblages) are to be used to determine former vegetational changes of an area, fossil pollen assemblages should be compared with modern day vegetation-pollen associations (e.g. Wright, 1967; Stevenson, 1985; Woo *et al.* 1998) to assist palaeoenvironmental reconstructions.

Although a study of the vegetation communities in the Vendicari area surrounding Pantano Piccolo had already been determined by Brullo *et al.* (1980), it was considered necessary to investigate the relationship between surface vegetation and soil-surface pollen in the vicinity of Pantano Piccolo. The present-day vegetation associations between the coastline and Pantano Piccolo were felt to represent spatially, the temporal changes in vegetation that may have occurred in the vicinity in the past, i.e. coastal vegetation patterns due to "natural" conditions, "natural" coastal vegetation in recovery from long-term degradation, recently cultivated areas and local halophytic communities. Pollen from these vegetation associations may be expected to have been incorporated successively into the lagoon sediments, due to temporal changes in shifting patterns of land-use.

Studies in the Mediterranean of modern pollen rain in relation to vegetation communities have identified that the floristic composition of the surface is a determining factor on the vegetation community inferred by the pollen spectra of nearby depositional environments and soil surfaces (e.g. Stevenson, 1985; Diaz-Fernandez, 1994; Carrión *et al.* 1995). Open communities such as dry grassland and *macchia-garrigue* communities have been observed to contain an increased relative abundance of extra-local, well dispersed pollen types (e.g. *Alnus, Betula, Pinus*) due to the local presence of low pollen producing, often insect-pollinated, species (e.g. Petanidou & Vokou, 1990).

Figure 6.8. Surface pollen transect. Vegetation communities and land use near Pantano Piccolo, Vendicari

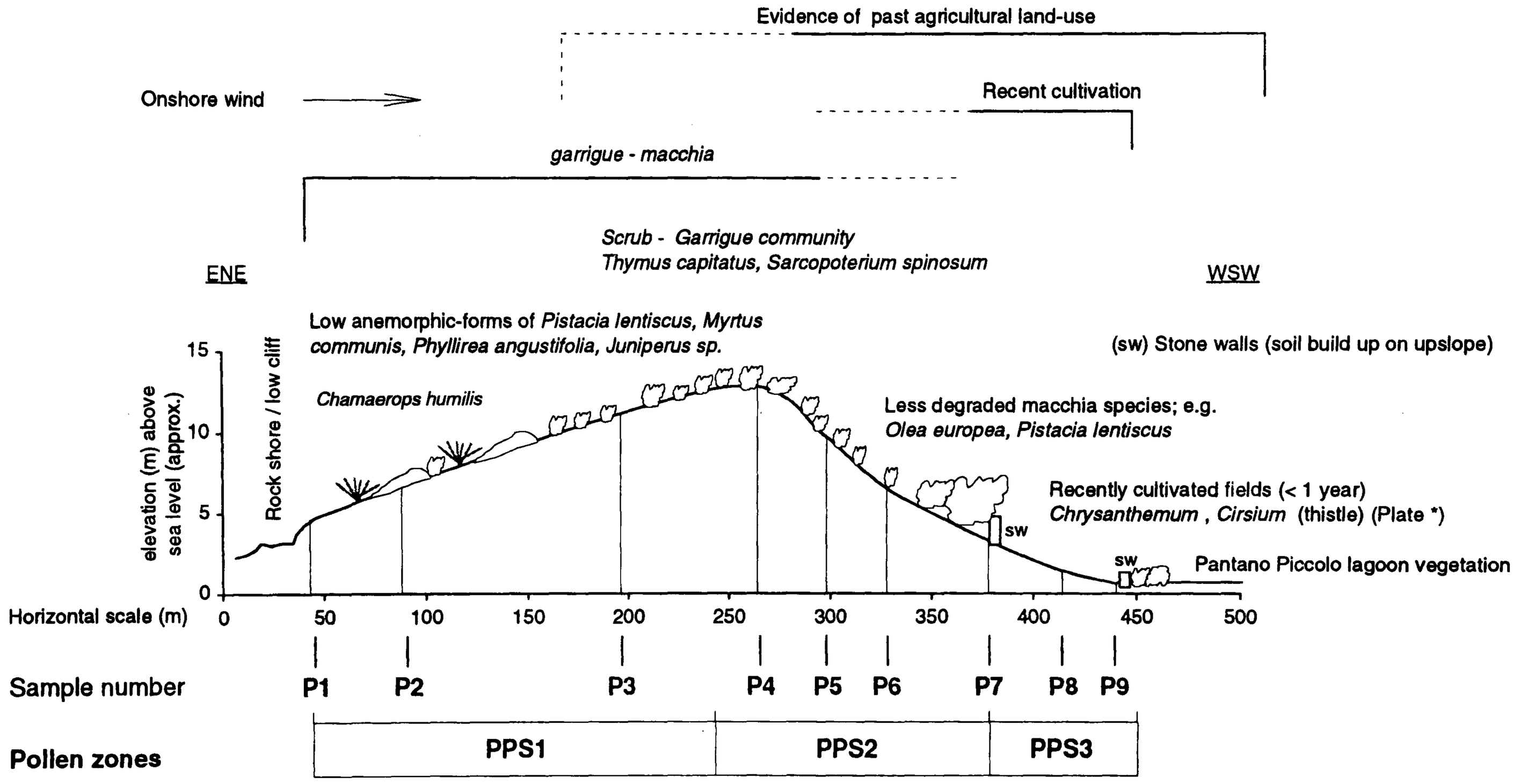

6.5.2 Site description and sampling methodology

Soil-surface samples were collected on a measured and levelled transect (Fig. 6.8.) from the storm-ridge at the rear of the rock-platform shoreline NE of Pantano Piccolo, traversing both the seaward and lagoon-facing slopes of the marl-calcarenite peninsula. Vegetation communities encountered along the transect were those identified by Brullo *et al.* (1980). These communities were found to be controlled by distance and increased altitude from the sea/lagoon, growing conditions (soil-climate) and extent of human activity (Table 6.5.). An initial reason for the orientation of the transect was to test a hypothesis that the deposition of pollen derived from aerial-transported *macchia-garrigue* species, i.e. *Phillyrea angustifolia, Pistacia lentiscus, Chamaerops humilis, Erica scoparia* (Herrera, 1988) may be enhanced in the lee of the calcarenite barrier, on the slopes surrounding the lagoon. It was observed during fieldwork that onshore wind velocity was considerably lower in the lee of the barrier and at the lagoon margin.

The sample taken at each site comprised of ~1 cm depth of soil and organic detritus scraped from an area approximately 5 cm^2. Soil surfaces directly beneath large trees or shrubs were not sampled, to avoid over-representation of single species by direct gravity fallout. At sample sites P1 - P6 the soil comprised of a thin, exposure hardened, *terra-rossa* type soil developed on the calcarenite-limestone. On inspection the bare soil was often covered by a dried-lichen crust, which was considered potentially advantageous in trapping recent pollen and stabilising the soil surface (e.g. Alexander & Calvo, 1990). The surface of P7 showed evidence of recent surface water movement and sediment transport. Soil samples from within the recently (< 1.5 years) ploughed area (P8 and P9) were distinctly darker and more humic. Pollen assemblages extracted from the surface samples were expected therefore, not to wholly reflect modern pollen fallout (i.e. surface vegetation at the time of sampling), but the recent incorporation of pollen into the thin soil, derived from local plant communities and aerial transport over the last few years.

Plate 6.8. Macchia-garrigue plant community at sample position P3 on surface pollen transect (SPT). Sarcopoterium spinosum and Juniperus macrocarpa in foreground. Annual species filling gaps on thin terra-rossa soil and calcarenite bedrock. NE of Pantano Piccolo, Vendicari. Photo taken April 1998.

Plate 6.9. Boundary between ruderal and halophyte communities at the northern margin of Pantano Piccolo, Vendicari (April, 1998). Overhanging *Chrysanthemum* anthers approx. 2 m directly above salt marsh surface. View south down western margin of Pantano Piccolo

Table 6.5. Surface pollen samples and vegetation zones: Pantano Piccolo, Vendicari

Sample No.	Altitude (m)*	Vegetation communities†
P 1	4.6	Salt tolerant cliff-shore species: *Limonium sp., Crithmum maritimum, Silene sedoides, Plantago macrorhiza, Cichorium spinosum, Euphorbia sp.*
P 2	6.7	Macchia-xerophyllous herbs and ephemerals: *Pistacia lentiscus, Juniperus macrocarpa, Myrtus communis, Olea europaea, Phyllirea angustifolia, Chamaerops humilis, Ephedra fragilis*
P 3	11.2	Absence of trees
P 4	12.8	Macchia-garrigue-xerophyllous herbs and ephemerals: *Thymus capitatus, Sarcopoterium spinosum, Chamaerops humilis, Teucrium fruticans, Anthyllis barba-jovis*
P 5	9.7	Trees in sheltered positions (*Ficus carica, Olea europea*)
P 6	6.5	Long term abandoned: *Olea europaea, Pistacia lentiscus, Juniperus macrocarpa,*
P 7	3.3	Trees-large *macchia* shrubs at field boundary
P 8	1.4	Recent cultivated/disturbed: *Chrozophora tinctoria, Diplotaxis erucoides, Convulvulus arvensis, Chenopodium album, Hypericum triquetrifolium, Chrysanthemum sp., Cirsium sp.*
P 9	0.6	Absence of trees

* Sea level approximated by upper shore limit of *Ulvaceae* (Sea Lettuce) on exposed rock platform.

† After Brullo *et al.* 1980.

6.5.3 Pollen results from soil surface samples on Transect T1

Due to the physical characteristics of the soil samples, pollen counts were not expected to be high. None the less fairly reliable pollen totals were achieved apart from in P1 and P2. Pollen counts were sub-divided into three local pollen assemblage zones using the CONISS© total sum of squares function (Fig. 6.8.1.), using all available pollen count data. Relative abundance (% total land pollen) and more reliable pollen concentrations were determined for the samples (Tables 6.5.1 & 6.5.2.). Concentrations of pollen types from the samples across the transect are shown in four parts in Figure 6.8.2. Changes in the pollen assemblages encountered are described from P1 to P9, along the direction taken during sample collection.

i) PPS 1: (P1 to P3 Seaward facing slopes of macchia and garrigue)

The maximum abundance of low values of *Alnus* (1.5% / 0.095 x 10^3 grs/g) and more abundant *Pinus* (17.3% / 1.0 x 10^3 grs/g) occurs in P1 at the foot of the seaward slope. *Betula* pollen also occurs at P1 (1.0%) with a greater abundance than P3 (0.4 %). *Quercus undiff.* type and *Picea* pollen also occur in P3. An increase in *Olea-Phyllirea* pollen is observed at PPS-P1 (4.6% / 0.28 x 10^3 grs/g) though remaining below 5% within LPAZ PPS1. *Juniperus* is first recorded along the transect in P3 (2% / 0.047 x 10^3 grs/g) while a single grain of Ericaceae (0.5 % / 0.017 x 10^3 grs/g) was encountered in P2.

Poaceae pollen occurs at its greatest abundance on the transect in P1 (11.2 % / 0.7 x 10^3 grs/g), while a landward decrease is also observed from P1 by Asteraceae subf. Asteroideae , *Plantago* and *Serratula* pollen types. An increase in the relative abundance in *Cirsium* (10% / 0.35 x 10^3 grs/g) is observed at P2, which along with *Anthemis* values remain relatively uniform across the peninsula until within LPAZ PPS 3. Lactuceae similarly, although dominating the pollen assemblage in PPS1 occurs relatively constant through PPS1 and into PPS 2. Dry and open growing conditions in between the low shrub vegetation is represented in the pollen assemblage at P3 by the presence of *Marrubium vulgare* and *Erodium* pollen grains. Salt-tolerant Amaranthaceae-Chenopodiaceae and Caryophyllaceae are only represented by single grains in P1, even though the sample site is in the close vicinity of potential upper-shore pollen sources (e.g. *Silene maritima*).

Table 6.5.1. Counts and pollen percentages of pollen types in surface sediment samples on Pantano Piccolo transect. Pollen types ordered as abundance total spanning transect

Sample Sites	P1		P2		P3		P4		P5		P6		P7		P8		P9	
	Count	%	Count	%	Count	%	Count	%	Count	%	Count	%	Count	%	Count	%	Count	%
Arboreal genera																		
Pinus	34	17.3	20	10.0	32	12.4	34	9.3	21	9.3	29	8.7	28	8.1	25	7.1	5	1.4
Olea-Phyllirea	9	4.6	2	1.0	9	3.5	54	14.8	4	1.8	6	1.8	38	11.0	89	25.2	17	4.7
Quercus undiff.	0	0.0	0	0.0	1	0.4	0	0.0	0	0.0	0	0.0	4	1.2	11	3.1	4	1.1
Juniperus	0	0.0	0	0.0	2	0.8	5	1.4	3	1.3	2	0.6	3	0.9	2	0.6	0	0.0
Alnus	3	1.5	2	1.0	0	0.0	3	0.8	1	0.4	0	0.0	3	0.9	3	0.8	0	0.0
Betula	2	1.0	0	0.0	1	0.4	0	0.0	3	1.3	0	0.0	4	1.2	1	0.3	0	0.0
Platanus	0	0.0	0	0.0	0	0.0	7	1.9	0	0.0	0	0.0	0	0.0	0	0.0	0	0.0
Picea	0	0.0	0	0.0	3	1.2	3	0.8	0	0.0	0	0.0	0	0.0	0	0.0	0	0.0
Ephedra fragilis	1	0.5	0	0.0	1	0.4	1	0.3	0	0.0	0	0.0	1	0.3	0	0.0	0	0.0
Corylus	0	0.0	0	0.0	0	0.0	0	0.0	0	0.0	0	0.0	2	0.6	0	0.0	0	0.0
Tilia	0	0.0	0	0.0	0	0.0	0	0.0	0	0.0	1	0.3	0	0.0	0	0.0	0	0.0
Ericaceae	0	0.0	1	0.5	0	0.0	0	0.0	0	0.0	0	0.0	1	0.3	0	0.0	0	0.0
Non-arboreal genera																		
Lactuceae	102	51.8	129	64.5	153	59.1	133	36.3	154	68.4	219	65.8	176	51.0	58	16.4	52	14.5
Cirsium	0	0.0	20	10.0	8	3.1	13	3.6	6	2.7	9	2.7	8	2.3	57	16.1	76	21.2
Anthemis	8	4.1	4	2.0	14	5.4	15	4.1	14	6.2	8	2.4	6	1.7	12	3.4	92	25.6
Poaceae	22	11.2	8	4.0	17	6.6	21	5.7	7	3.1	11	3.3	16	4.6	7	2.0	3	0.8
Amaranth.-Chenopodiaceae	1	0.5	0	0.0	0	0.0	8	2.2	0	0.0	4	1.2	12	3.5	13	3.7	42	11.7
Caryophyllaceae	1	0.5	0	0.0	3	1.2	8	2.2	4	1.8	10	3.0	5	1.4	6	1.7	30	8.4
Asteraceae (Aster type)	7	3.6	8	4.0	3	1.2	10	2.7	0	0.0	0	0.0	4	1.2	11	3.1	8	2.2
Aplaceae undiff.	0	0.0	0	0.0	4	1.5	4	1.1	3	1.3	8	2.4	0	0.0	11	3.1	5	1.4
Saxifrage type	0	0.0	0	0.0	0	0.0	12	3.3	0	0.0	0	0.0	0	0.0	11	3.1	12	3.3
Ranunculus type	0	0.0	2	1.0	0	0.0	8	2.2	0	0.0	12	3.6	0	0.0	3	0.8	0	0.0
Plantago	1	0.5	1	0.5	0	0.0	4	1.1	1	0.4	4	1.2	3	0.9	8	2.3	2	0.6
Centaurea	0	0.0	0	0.0	2	0.8	6	1.6	0	0.0	0	0.0	10	2.9	3	0.8	1	0.3
Serratula type	4	2.0	3	1.5	0	0.0	4	1.1	4	1.8	3	0.9	1	0.3	3	0.8	0	0.0
Medicago type	0	0.0	0	0.0	0	0.0	0	0.0	0	0.0	1	0.3	7	2.0	0	0.0	3	0.8
Sinapis type	0	0.0	0	0.0	0	0.0	2	0.5	0	0.0	3	0.9	0	0.0	3	0.8	0	0.0
Erodium	0	0.0	0	0.0	1	0.4	6	1.6	0	0.0	0	0.0	0	0.0	0	0.0	0	0.0
Filipendula	0	0.0	0	0.0	3	1.2	0	0.0	0	0.0	0	0.0	0	0.0	4	1.1	0	0.0
Gentianella	1	0.5	0	0.0	0	0.0	0	0.0	0	0.0	0	0.0	5	1.4	0	0.0	1	0.3
Lotus type	0	0.0	0	0.0	0	0.0	1	0.3	0	0.0	0	0.0	0	0.0	0	0.0	6	1.7
Solanum	0	0.0	0	0.0	0	0.0	0	0.0	0	0.0	0	0.0	0	0.0	7	2.0	0	0.0
Astragalus	0	0.0	0	0.0	0	0.0	0	0.0	0	0.0	0	0.0	5	1.4	0	0.0	0	0.0
Artemesia	0	0.0	0	0.0	0	0.0	0	0.0	0	0.0	0	0.0	1	0.3	3	0.8	0	0.0
Marrubium vulgare	0	0.0	0	0.0	2	0.8	0	0.0	0	0.0	0	0.0	1	0.3	0	0.0	0	0.0
Mentha type	0	0.0	0	0.0	0	0.0	2	0.5	0	0.0	1	0.3	0	0.0	0	0.0	0	0.0
Polygonum	1	0.5	0	0.0	0	0.0	2	0.5	0	0.0	0	0.0	0	0.0	0	0.0	0	0.0
Euphorbia	0	0.0	0	0.0	0	0.0	0	0.0	0	0.0	2	0.6	0	0.0	0	0.0	0	0.0
Chelidonium	0	0.0	0	0.0	0	0.0	0	0.0	0	0.0	0	0.0	1	0.3	0	0.0	0	0.0
Cyperaceae	0	0.0	0	0.0	0	0.0	0	0.0	0	0.0	0	0.0	0	0.0	1	0.3	0	0.0
Scrophularia type	0	0.0	0	0.0	0	0.0	0	0.0	0	0.0	0	0.0	0	0.0	1	0.3	0	0.0
Total Pollen	197		200		259		366		225		333		345		353		359	
Added *Lycopodium*	123		224		166		189		173		122		248		268		158	

Unreliable total pollen counts for % abundances are underlined

Table 6.5.2. Counts and pollen concentration of pollen types in surface sediment samples on Pantano Piccolo transect. Pollen types ordered as abundance total spanning transect

Sample Sites	P1		P2		P3		P4		P5		P6		P7		P8		P9	
	Count	grains/g	Count	grains/g	Count	grains/g	Count	grains/g	Count	grains/g	Count	grains/g	Count	grains/g	Count	grains/g	Count	grains/g
Arboreal genera																		
Pinus	34	1086.6	20	356.7	32	765.6	34	719.3	21	482.5	29	930.7	28	450.7	25	368.4	5	123.2
Olea-Phyllirea	9	287.6	2	35.7	9	215.3	54	1142.4	4	91.9	6	192.6	38	611.7	89	1311.6	17	419.0
Quercus undiff.	0	0.0	0	0.0	1	23.9	0	0.0	0	0.0	0	0.0	4	64.4	11	162.1	4	98.6
Juniperus	0	0.0	0	0.0	2	47.8	5	105.8	3	68.9	2	64.2	3	48.3	2	29.5	0	0.0
Alnus	3	95.9	2	35.7	0	0.0	3	63.5	1	23.0	0	0.0	3	48.3	3	44.2	0	0.0
Betula	2	63.9	0	0.0	1	23.9	0	0.0	3	68.9	0	0.0	4	64.4	1	14.7	0	0.0
Platanus	0	0.0	0	0.0	0	0.0	7	148.1	0	0.0	0	0.0	0	0.0	0	0.0	0	0.0
Picea	0	0.0	0	0.0	3	71.8	3	63.5	0	0.0	0	0.0	0	0.0	0	0.0	0	0.0
Ephedra fragilis	1	32.0	0	0.0	1	23.9	1	21.2	0	0.0	0	0.0	1	16.1	0	0.0	0	0.0
Corylus	0	0.0	0	0.0	0	0.0	0	0.0	0	0.0	0	0.0	2	32.2	0	0.0	0	0.0
Tilia	0	0.0	0	0.0	0	0.0	0	0.0	0	0.0	1	32.1	0	0.0	0	0.0	0	0.0
Ericaceae	0	0.0	1	17.8	0	0.0	0	0.0	0	0.0	0	0.0	1	16.1	0	0.0	0	0.0
Non-arboreal genera																		
Lactuceae	102	3259.7	129	2300.8	153	3660.4	133	2813.7	154	3538.1	219	7028.5	176	2833.0	58	854.7	52	1281.6
Cirsium	0	0.0	20	356.7	8	191.4	13	275.0	6	137.8	9	288.8	8	128.8	57	840.0	76	1873.1
Anthemis	8	255.7	4	71.3	14	334.9	15	317.3	14	321.6	8	256.7	6	96.6	12	176.8	92	2267.4
Poaceae	22	703.1	8	142.7	17	406.7	21	444.3	7	160.8	11	353.0	16	257.5	7	103.2	3	73.9
Amaranth.-Chenopodiaceae	1	32.0	0	0.0	0	0.0	8	169.2	0	0.0	4	128.4	12	193.2	13	191.6	42	1035.1
Caryophyllaceae	1	32.0	0	0.0	3	71.8	8	169.2	4	91.9	10	320.9	5	80.5	6	88.4	30	739.4
Asteraceae (Aster type)	7	223.7	8	142.7	3	71.8	10	211.6	0	0.0	0	0.0	4	64.4	11	162.1	8	197.2
Apiaceae undiff.	0	0.0	0	0.0	4	95.7	4	84.6	3	68.9	8	256.7	0	0.0	11	162.1	5	123.2
Saxifrage type	0	0.0	0	0.0	0	0.0	12	253.9	0	0.0	0	0.0	0	0.0	11	162.1	12	295.8
Ranunculus	0	0.0	2	35.7	0	0.0	8	169.2	0	0.0	12	385.1	0	0.0	3	44.2	0	0.0
Plantago	1	32.0	1	17.8	0	0.0	4	84.6	1	23.0	4	128.4	3	48.3	8	117.9	2	49.3
Centaurea	0	0.0	0	0.0	2	47.8	6	126.9	0	0.0	0	0.0	10	161.0	3	44.2	1	24.6
Serratula type	4	127.8	3	53.5	0	0.0	4	84.6	4	91.9	3	96.3	1	16.1	3	44.2	0	0.0
Medicago type	0	0.0	0	0.0	0	0.0	0	0.0	0	0.0	1	32.1	7	112.7	0	0.0	3	73.9
Sinapis type	0	0.0	0	0.0	0	0.0	2	42.3	0	0.0	3	96.3	0	0.0	3	44.2	0	0.0
Erodium	0	0.0	0	0.0	1	23.9	6	126.9	0	0.0	0	0.0	0	0.0	0	0.0	0	0.0
Fillipendula	0	0.0	0	0.0	3	71.8	0	0.0	0	0.0	0	0.0	0	0.0	4	58.9	0	0.0
Gentianella	1	32.0	0	0.0	0	0.0	0	0.0	0	0.0	0	0.0	5	80.5	0	0.0	1	24.6
Lotus type	0	0.0	0	0.0	0	0.0	1	21.2	0	0.0	0	0.0	0	0.0	0	0.0	6	147.9
Solanum	0	0.0	0	0.0	0	0.0	0	0.0	0	0.0	0	0.0	0	0.0	7	103.2	0	0.0
Astragalus	0	0.0	0	0.0	0	0.0	0	0.0	0	0.0	0	0.0	5	80.5	0	0.0	0	0.0
Artemesia	0	0.0	0	0.0	0	0.0	0	0.0	0	0.0	0	0.0	1	16.1	3	44.2	0	0.0
Marrubium vulgare	0	0.0	0	0.0	2	47.8	0	0.0	0	0.0	0	0.0	1	16.1	0	0.0	0	0.0
Mentha type	0	0.0	0	0.0	0	0.0	2	42.3	0	0.0	1	32.1	0	0.0	0	0.0	0	0.0
Polygonum	1	32.0	0	0.0	0	0.0	2	42.3	0	0.0	0	0.0	0	0.0	0	0.0	0	0.0
Euphorbia	0	0.0	0	0.0	0	0.0	0	0.0	0	0.0	2	64.2	0	0.0	0	0.0	0	0.0
Chelidonium	0	0.0	0	0.0	0	0.0	0	0.0	0	0.0	0	0.0	1	16.1	0	0.0	0	0.0
Cyperaceae	0	0.0	0	0.0	0	0.0	0	0.0	0	0.0	0	0.0	0	0.0	1	14.7	0	0.0
Scrophularia type	0	0.0	0	0.0	0	0.0	0	0.0	0	0.0	0	0.0	0	0.0	1	14.7	0	0.0
Total Pollen	197	6295.7	200	3567.1	259	6196.4	366	7742.9	225	5169.2	333	10687.2	345	5553.4	353	5202.1	359	8847.9
Added *Lycopodium*	123		224		166		189		173		122		248		268		158	
Sample dry mass (g)	2.5		2.5		2.5		2.5		2.5		2.6		2.5		2.5		2.6	

Figure 6.8.1. Pollen percentage diagram of surface soil samples
Transect between sea and Pantano Piccolo, Vendicari
Terrestrial pollen count data used in Coniss zonation

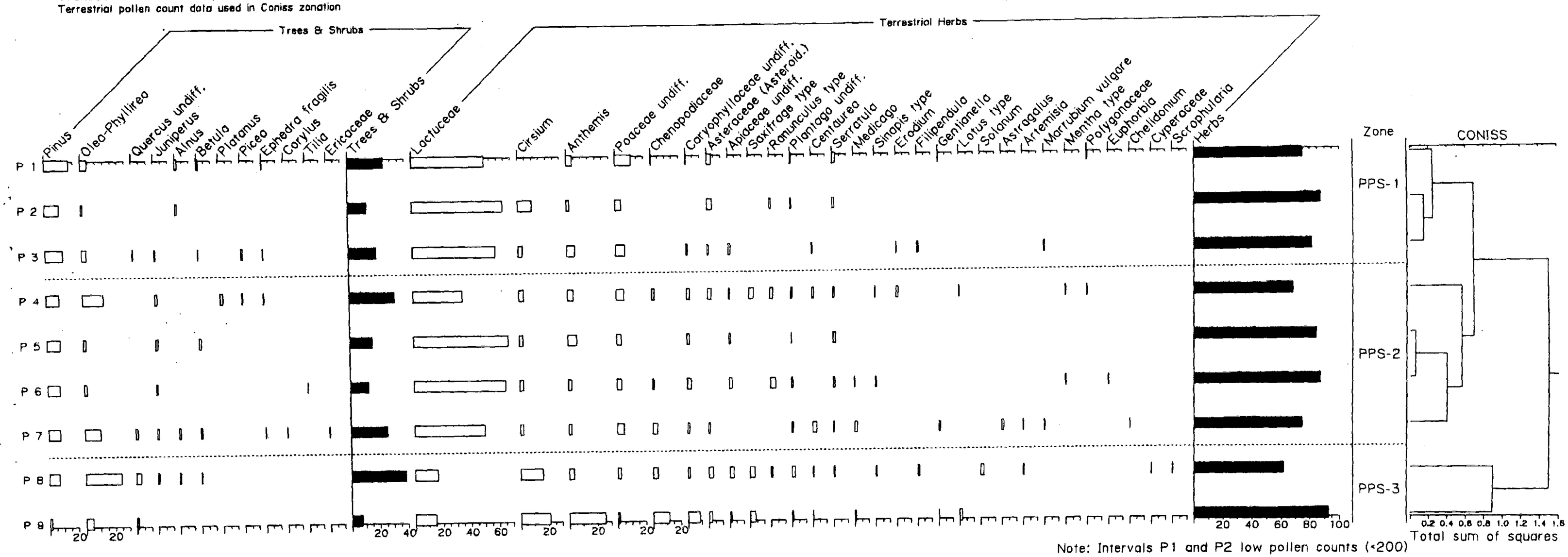

Note: Intervals P1 and P2 low pollen counts (<200)

ii) PPS 2: (P4 to P7 Abandoned agricultural land / regenerating macchia)

Pinus values are distributed fairly evenly between the four samples in the zone (av. 8.8%) though a peak in *Pinus* pollen concentration occurs at P6 (930 grs/g). *Alnus* and *Betula* occur in the zone at a continued low abundance (< 1.3 %) along with *Platanus*, *Picea*, *Corylus* (P7) and *Tilia* (0.3 % / 32 grs/g).

A peak in *Olea-Phyllirea* at P4 (14.8% / 1.1 x 10^3 grs/g) coincidental with a peak in *Juniperus* (1.4 % / 0.10 x 10^3 grs/g) precedes a drop in values which recover gradually in LPAZ PPS2. The peak in *Juniperus* is followed by gradually decreasing values towards LPAZ PPS 3. A solitary grain of Ericaceae was found in P7. Lactuceae pollen is at its highest concentration (7.0 x 10^3 grs/g) in PPS 2, coinciding in P6 with a peak in Apiaceae (0.25 x 10^3 grs/g, Caryophyllaceae (0.3 x 103 grs/g), *Plantago* (0.12 x 10^3 grs/g), and *Ranunculus* type (0.38 x 10^3 grs/g). *Anthemis* and *Cirsium* values follow from LPAZ PPS 1 with little variation through LPAZ PPS2, with a marked drop of Poaceae and absence of Amaranthaceae-Chenopodiaceae and Asteraceae subf. Asteroideae pollen at P5.

iii) PPS 3: (P8 to P9 Recently cultivated land surfaces)

Sample points P8 and P9 see Lactuceae at its lowest relative abundance, with a concomitant increase in *Olea-Phyllirea*, *Cirsium*, *Anthemis*, Asteraceae subf. Asteroideae, Caryophyllaceae and Amaranthaceae-Chenopodiaceae. Decreasing *Pinus* across the transect reaches its lowest point at P9 (1.4 % / 120 grs/g) combined with an absence of *Alnus* and *Betula* and other tree species. *Quercus undiff.* however increases in P8 (3.1 % / 160 grs/g).

Olea-Phyllirea is the most abundant pollen type (25.2 % / 1.3 x 10^3 grs/g) in P8 though by P9 is more than halved. *Juniperus* pollen is absent in P9, having decreased steadily from P4.

The massive increase in herb pollen in herb pollen in LPAZ PPS 3 is skewed towards the base-of-slope/lagoon margin sample P9. In P8 Lactuceae values are comparable with *Cirsium* (16 % / 0.8 x 10^3 grs/g), before in P9 both *Cirsium* and *Anthemis* exceed Lactuceae. The decrease in Lactuceae in LPAZ PPS3 is accompanied by lowered Poaceae, *Centaurea*, *Serratula* and *Ranunculus* type. The zone is also marked by the low abundance/occurrence of Cyperaceae, *Saxifraga* type, *Artemisia*, *Scrophularia* and *Solanum* pollen types.

Figure 6.8.2. Pollen concenntrations in surface samples along transect T1 and lagoon samples

Tree pollen genera

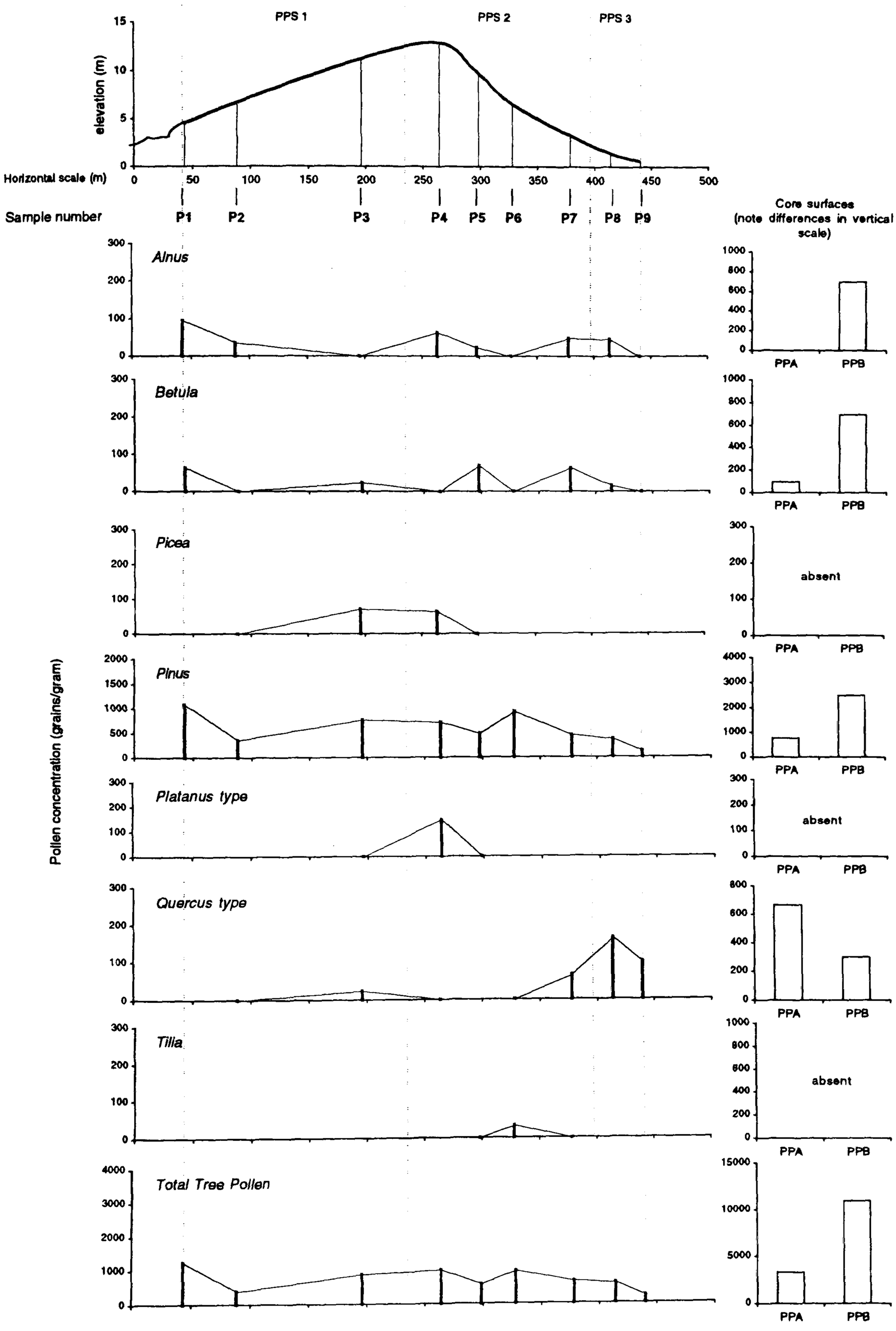

Figure 6.8.2. Pollen concenntrations in surface samples along transect T1 and lagoon samples

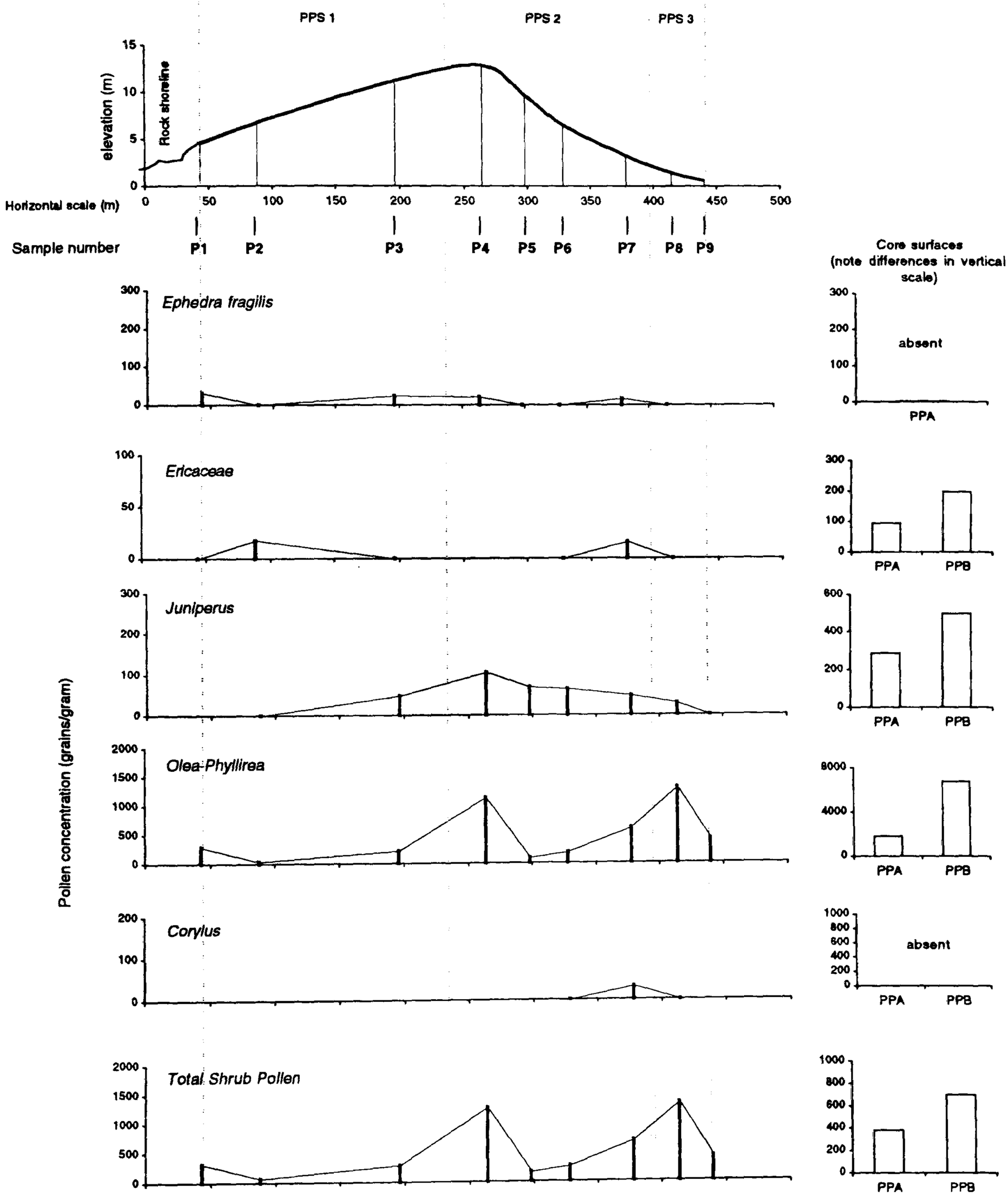

Figure 6.8.2. Pollen concentrations in surface samples along transect T1 and lagoon samples

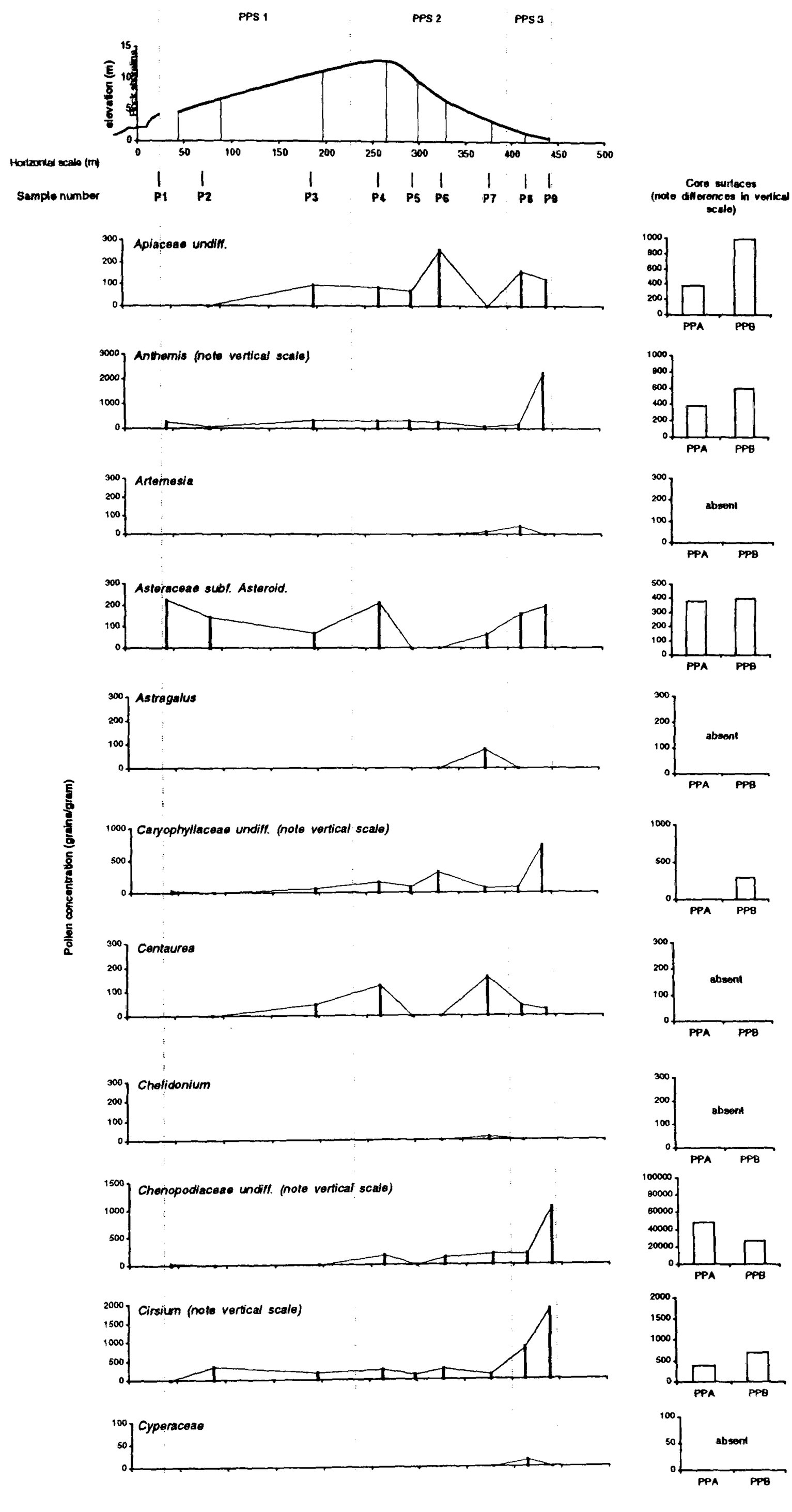

Figure 6.8.2. Pollen concentrations in surface samples along transect T1 and lagoon samples

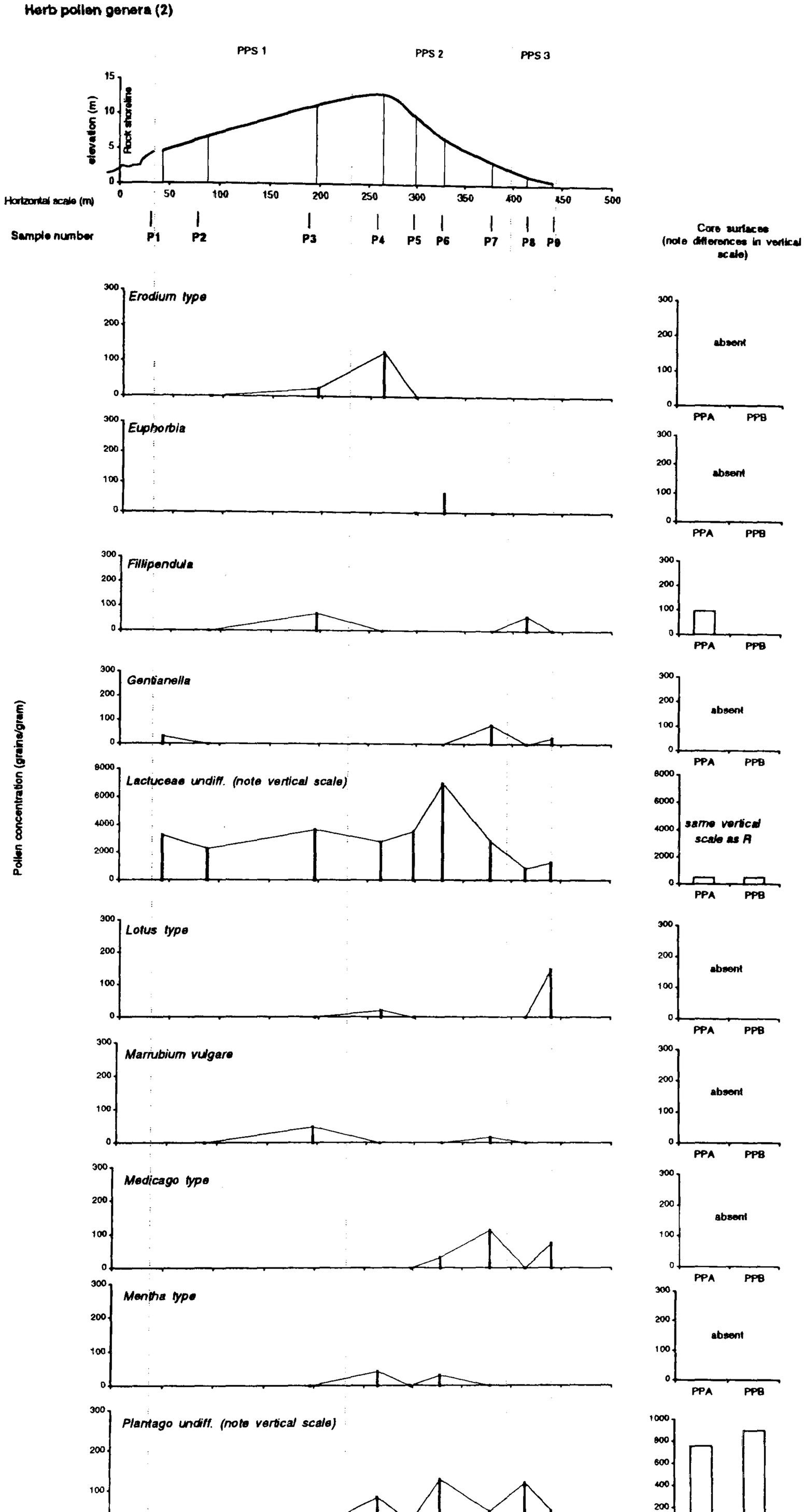

Figure 6.8.2. Pollen concenntrations in surface samples along transect T1 and lagoon samples

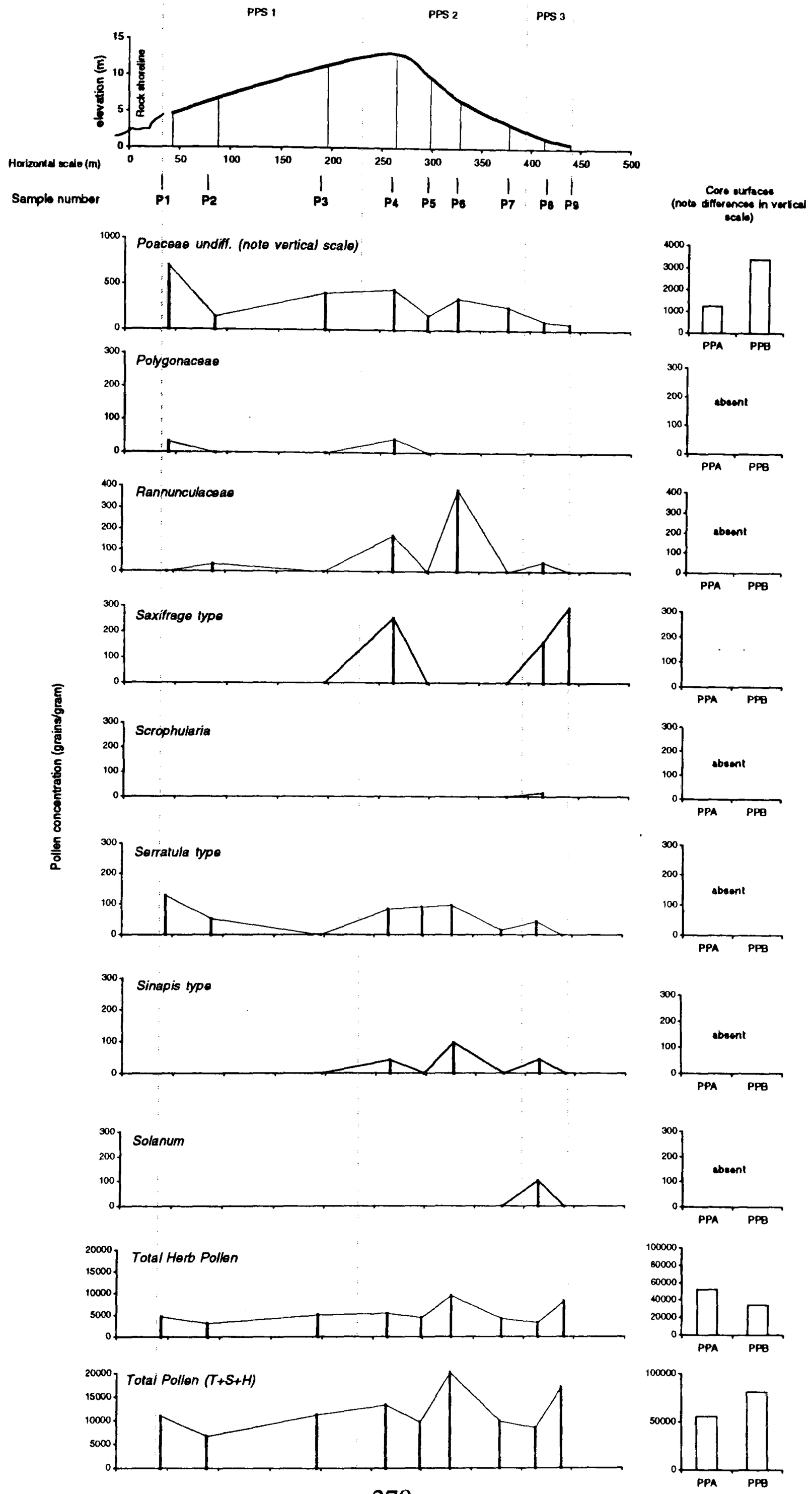

Compared to the abundance of pollen types typical of disturbed ground across the rest of the transect, the large increase in *Anthemis*, Caryophyllaceae, Amaranthaceae-Chenopodiaceae and *Cirsium*, apparently reflects local pollen production in the vicinity of P8-P9.

6.5.4 Comparison with surface samples from cores PPA and PPB

For comparison the concentration of the same pollen types found in the surface intervals of PPA (1-2 cm) and PPB (0-1 cm) are shown to the right of the transect pollen profiles (Fig. 6.8.2.).

Plate 6.6. shows clearly the abrupt boundary between salt marsh vegetation and local ruderal plant populations at the northern margin of lagoon. The field surface surrounding the lagoon, fronted by a stone wall is in the picture approximately 1 m higher than the water surface. Additionally the height of the vegetation (0.5-1 m) means that flower anthers are *approx.* 1-2 m above the marsh surface. Although contrasting growing conditions were closely juxtaposed at the waters edge, the introduction of pollen by gravity fallout and local aerial transport onto the marsh surface was therefore expected to have occurred (Chapter 2, Fig. 2.4.).

Arboreal pollen occurs at a greater concentration in the lagoon surface-sediment samples, compared to the surrounding soil, with the exception of *Quercus undiff.* type pollen. *Pinus* and *Betula* pollen in the surface of PPA are comparable with pollen concentrations in the soil transect surface samples.

Shrub pollen types also show a clear concentration of pollen grains in lagoonal sediments, particularly in PPB. The difference between PPA and PPB is especially apparent with *Olea-Phyllirea* pollen, which shows a two-three fold increase between open lagoon sediments and those beneath the vegetated margin. Differences in the abundance of herb pollen and possible transport pathways to recent lagoon sediments and soil samples are exemplified by the spatial patterns of Amaranthaceae-Chenopodiaceae and Lactuceae pollen.

The concentration of Lactuceae in the surface sediments of PPA and PPB is lower, compared with its peak total (7.0×10^3 grs/g) in the transect (P6). The low values of Lactuceae at the lagoon margin appear to be a continuation of decreasing values encountered in the surface samples following P6. Decreased values in the surface of both PPA and PPB would suggest that Lactuceae pollen transport from terrestrial sources to the lagoon is limited.

Conversely, Amaranthaceae-Chenopodiaceae pollen which dominates the pollen assemblage of surface sediments in the lagoon is poorly represented across the transect, aside from in soils adjacent to the lagoon (P9). Halophyte vegetation (*Salicornia-*

Arthrocnemum sp.) at the margin of the lagoon is the clear source of Amaranthaceae-Chenopodiaceae pollen at the core sites. The pollen content of P9 adjacent to the halophyte vegetation may well reflect both the local growth of salt-tolerant/disturbed ground vegetation and outward pollen transport from the lagoon fringe, i.e. by high water wave activity or local wind-dispersal.

The local abundance of *Anthemis*, Caryophyllaceae and *Cirsium* in P9 are not matched in the nearby lagoon fringing or mud flat sediments. Surface concentrations in PPA and PPB are however higher than preceding transect values, which would indicate a significant amount of transport to the lagoon and/or sediment focusing of grains. This pattern is continued in herb types encountered in the lagoon and the transect, with PPB generally containing a greater concentration than PPA. Amaranthaceae-Chenopodiaceae in PPA is the marked exception to this, due no doubt to the presence of surface halophyte vegetation above the core site.

A problem with the identification of pollen at the generic level is highlighted with the transect patterns of Poaceae and *Plantago*. Across the transect, Poaceae and *Plantago* types however may be more representative of dry-grassland species, e.g. *Plantago arenaria*, whereas the pollen types in the lagoon may be more representative of wetland/ coastal habitats, e.g. *Phragmites australis, Plantago maritima*. This has clear implications in the palaeoenvironmental interpretation of core sequences.

Pollen concentrations in land-surface assemblages are dominated by local pollen production, gravity fallout and local wind dispersal. Lagoon sediment concentrations however indicate that either transport to the surface has been enhanced (e.g. by expanding plant communities) or pollen grain concentrations have been increased by aquatic processes. As mentioned in Chapter 2, wave activity in a shallow-depth water body can be particularly important for re-suspending and transport pollen grains previously deposited or maintaining grains in the seston. The linear form and orientation of the lagoon would suggest that wave action is more pronounced at the northern and southern margin. Pollen deposited on the exposed mudflat (during low water levels) may be expected to have been re-mobilised with rising water levels.

It is also clear that the greater abundance of pollen grains in lagoon surface sediments (and those incorporated in the past) highlights the greater preservation potential of the aquatic depositional environment.

6.5.5 Summary points of results from surface pollen samples

• *Alnus*, *Betula* and *Pinus* occur in surface soil samples in the absence of local tree populations, indicating long range aerial transport and possibly a uniform deposition on the peninsula.Greater concentration of pollen types in unvegetated/regularly inundated

mudflat surface sediments suggest significant aquatic transport and accretion-related deposition.

• *Macchia*-associated pollen types (i.e. *Juniperus*, *Quercus undiff.*, Ericaceae, *Olea-Phyllirea*, *Ephedra fragilis*) occur, with the exception of *Olea-Phyllirea*, at low abundances in surface sediments spanning the transect. Evidence that local wind direction and velocity across the peninsula have influenced pollen abundances in surface transect soils, appears to be negated by local fallout from nearby vegetation. The peak in *Olea-Phyllirea* in the recently cultivated area (surface sample P8) may be attributed to being downwind of an *Olea europea* stand at the field margin (approx. 50 m distant).

• Lactuceae was the most abundant pollen type found in surface soil materials. The concentration of Lactuceae in PPS1 and PPS2 ranged between 2.3 to 7.0 x 10^3 grs/g (av. 3.6 x 103 grs/g). It is perhaps noteworthy that the peak concentration of Lactuceae occurred in an area of relic cultivation (P6). Potential cultivable species grown in Mediterranean pasture/grassland/weed species (Delano-Smith, 1979) producing Lactuceae pollen include; *Cichorium intybus* (Chicory), *Lactuca* (Lettuces) and *Taraxacum* (Dandelions) which may have been grown in the area, either as a perennial crop or by irrigation. Pollen concentrations of Lactuceae were however observed to drop in the area of most recent cultivation and within the surface lagoon sediments.

• Coinciding with Lactuceae, the temporal and spatial intensity of disturbance appears to be recognisable in the distribution of ruderal pollen types across the transect. Indicator types (e.g. Asteraceae subf. Asteroideae, Amaranth.-Chenopodiaceae, *Cirsium*) occur across the transect and are observed to increase significantly in areas of relic cultivation (PPS2) and recent disturbance (PPS3).

• Differences in the pollen content of surface samples in the lagoon with surface samples from the nearby slopes, confirm the importance of aquatic pollen transport and accretionary influenced deposition, in the lagoon pollen sequences from cores PPA and PPB.

• It is apparent that the initial hypothesis of pollen deposition being enhanced on slopes facing the lagoon due to local atmospheric conditions, is unclear due to the local variation and dominating control of vegetation types in the area.

• The data on surface pollen accumulation here may only provide a partial insight into the spatial distribution of pollen due to taphonomic processes; and could be greatly

improved by real-time/seasonal monitoring of air movement and pollen content and surface traps other than soil. The results do however give an idea as to the extent that vegetational changes have on the pollen content of a nearby depositional setting.

Chapter Seven

Analysis & Discussion

7.1 Introduction

Due to the direct influence of anthropogenic activity on terrestrial and coastal systems in the coastal zone of south east Sicily, the accretion of coastal wetland sediment sequences deposited in the archaeo-historical past has been punctuated by phases of disturbance. Spanning a particularly intensive period of land-use changes, sediment sequences used in this study are an archive of information reflecting multiple phases of wetland disturbance and recovery over the last 100-200 years and more.

The advantage of using recent sediment sequences is that they have a greater potential of having been affected by documented phases of disturbance (either due to human activity or natural factors). Subsequently much less ambiguous statements may be made between the depositional record and actual environmental changes. Obviously disturbed settings are usually avoided for determining broad spatial and temporal palaeoenvironmental trends as local forcing factors often dominate. Recognising the impact of these local controlling factors is however imperative for understanding the recent evolution of small, marginal coastal wetlands.

A recurrent problem in the interpretation of geomorphological change and Holocene sediment sequences in the Mediterranean region (either a dominance of natural or anthropogenic controls) appears to have been repeated in the sediment cores analysed. Although situated in settings heavily influenced by historical patterns of human activity, the dominant forcing factor in depositional trends has been due to inherent natural factors characteristic of the Mediterranean environment.

Distinguishing between human and natural factors in sediment sequences is limited by the availability and quality of proxy data reflecting environmental changes. In younger sequences this problem should theoretically be alleviated by documented records of environmental change affecting the area under study, which can be matched to identifiable sediment changes. Where this is achievable and historical patterns of sediment deposition can be measured, an important historical context for present day settings and future impacts of environmental change are capable of being determined.

The previous chapter provides new evidence of dynamic depositional changes that have occurred in coastal wetland environments in south east Sicily during the 20th century. The cored stratigraphy of shallow sequences used for multi-proxy analyses, indicate that abrupt environmental changes have caused deposition to shift between recognisable organic, biogenic and minerogenic phases. The magnitude and timing of these events recognised in the individual cores, along with the known environmental history of the settings, suggest that these stratigraphic changes have occurred primarily as a response to anthropogenic alteration of coastal and hydrological processes.

Local spatial and temporal correlations identified between the lagoon cores PPA and PPB indicate that although broader scale controls on deposition are identifiable by comparing adjoining records, the difference in stratigraphy between two close cores questions the validity of using single core sequences/stratigraphic units (especially in older sediments) as being representative of environmental conditions at the time.

7.2 Recent environmental changes in the coastal zone of south east Sicily

In this chapter the depositional record of each core is determined, drawing from the multi-proxy lines of evidence, then compared with each other and the recent environmental history of the core sites, to determine the sensitivity, response and relationship of the wetland settings to direct anthropogenic and environmental controls on sedimentation.

7.2.1 Environmental change recorded in core AMC, River Mulinello, SE Sicily.

Core AMC represents the most recent phase of fine-grained minerogenic and organic associated accretion, at the estuarine river mouth of the River Mulinello as it enters the north west corner of Augusta Bay, south east Sicily. The stratigraphy at the core site (summarised in Fig. 7.1.) indicates that the site has fluctuated between more active (deposition of coarse grained shelly-silts) and lower energy phases (brown organic-grey muds), reflecting variations in estuarine channel/river mouth dynamics and the impact of industrial development on the coastal wetland.

From the base of the core (27 cm) up to the earliest ^{210}Pb dated interval at 18.5 cm (*circa* AD 1865), the setting appears to have been in the early stages of estuarine salt marsh evolution. Pollen assemblages from this period (Fig. 6.3.1.) indicate a progressive increase in the relative frequency of Amaranthaceae-Chenopodiaceae pollen, to the detriment of Lactuceae, Poaceae and other ruderal pollen types. While being dominated by local halophyte-ruderal populations, the occurrence of well-dispersed, regional to extra-local pollen grains (*Pinus, Alnus, Olea-Phyllirea*) in the section suggests that the core setting was also receiving a fairly constant supply of pollen from the estuarine catchment. Unvegetated mud areas surrounded by *Salicornia-Arthrocnemum* and ruderal species within close proximity (1 to 0.5 m) due to recent flooding and surface disturbance, which existed during fieldwork nearer the exit of the river into the bay, possibly serve as a modern example of the core site at the time.

By *circa* AD 1918 (17 cm depth) an established halophyte dominated salt marsh appears to have been present at the core site, formed presumably by the gradual expansion of channel-side/ embankment-fringing halophyte vegetation. This is expressed in the sediment

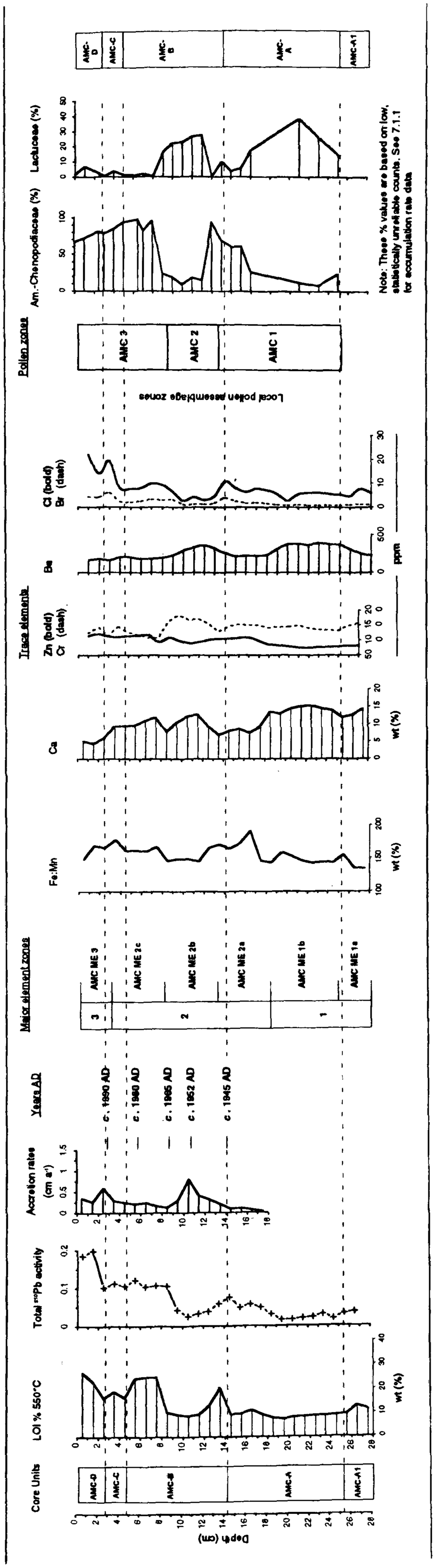

Figure 7.1. Stratigraphic summary of Mulinello core (AMC). Note inverse relationship between Amaranth.-Chenopodiaceae and Lactuceae

sequence not only by pollen content, but by increasing loss on ignition values (Fig. 7.1.). Minerogenic sediment accretion associated with the growth of halophyte vegetation and salt marsh soil conditions appear to have existed up to *circa* AD 1940 (14.5 cm). An abrupt change to the depositional setting then occurred within the ^{210}Pb-calculated timespan of 4-5 years (Fig. 7.1.1.).

Over a centimetre depth in the sequence, i.e. by *circa* AD 1945 (13.5 cm), Amaranthaceae-Chenopodiaceae pollen values reach estimated accumulation rate of 3.3 x 10^5 grains cm^2 a^{-1}. Associated with this is an increase in accretion rate (0.2 cm a^{-1}) an increased organic content (20%) and change in composition shown by sediment geochemistry.

Amaranthaceae-Chenopodiaceae accumulation would appear to reflect a localised focusing of transported grains, as a consequence of the sudden change in accretion and marsh surface disturbance. The envisaged scenario is that the incorporation of pollen and vegetal matter from local stands of *Salicornia-Arthrocnemum* was supplemented by additional material, i.e. plant stems and inflorescences, uprooted during bank collapse or channel erosion and washed onto the marsh surface. This would also account for a minor peak in LOI at the same interval and noticeable drop (apparently Na-associated) in the abundance of major elements. An influx of catchment-alluvial sediment associated or contemporaneous with this "event" is highlighted by trace element data by which the interval represents the base horizon of increased trace element inputs derived from upstream geological sequences (e.g. Cr and Ba in Fig. 7.1.1.).

This transformation of the marsh surface initiated a marked difference in depositional conditions at the core site. By *circa* AD 1948 a reduction in the accumulation of Amaranthaceae-Chenopodiaceae pollen at *circa* AD 1945 was counteracted by an increase in Lactuceae (Fig. 7.1.1), Apiaceae, and Asteraceae subf. Asteroideae and a higher diversity of (extra-local) pollen types. Within this short time scale (between 1 and 3 years) plant communities (or at least contributing individuals) in the local area, underwent a dramatic transformation. Such a rapid and magnitudinal change in Amaranthaceae-Chenopodiaceae abundance, suggests that the growing environment for salt marsh plants was suddenly stressed (i.e. by flooding or burial) which led to a catastrophic decline in the local halophyte population.

From 13.5 cm to 8.5 cm the combined evidence of accretion rates, pollen data, major and trace element data from the interval is supportive of a salt-marsh destructive phase that was initiated *circa* AD 1945 and continued until *circa* AD 1964. The coincidental peak and decline pattern of Ca (wt %), the accumulation of catchment-derived trace metals (i.e. Cr, V, Ti, Ba) and sediment accretion rates indicates a period of maximum sediment inwash onto the degraded salt marsh surface to have occured *circa* AD 1951-2. (see Fig. 7.1.1.).

Figure 7.1.1. Selected sedimentological features from AMC and monthly annual rainfall totals at Catania and Piazza Armerina, SE Sicily for the period 1900-1980 AD (Also see Figure 7.1.).

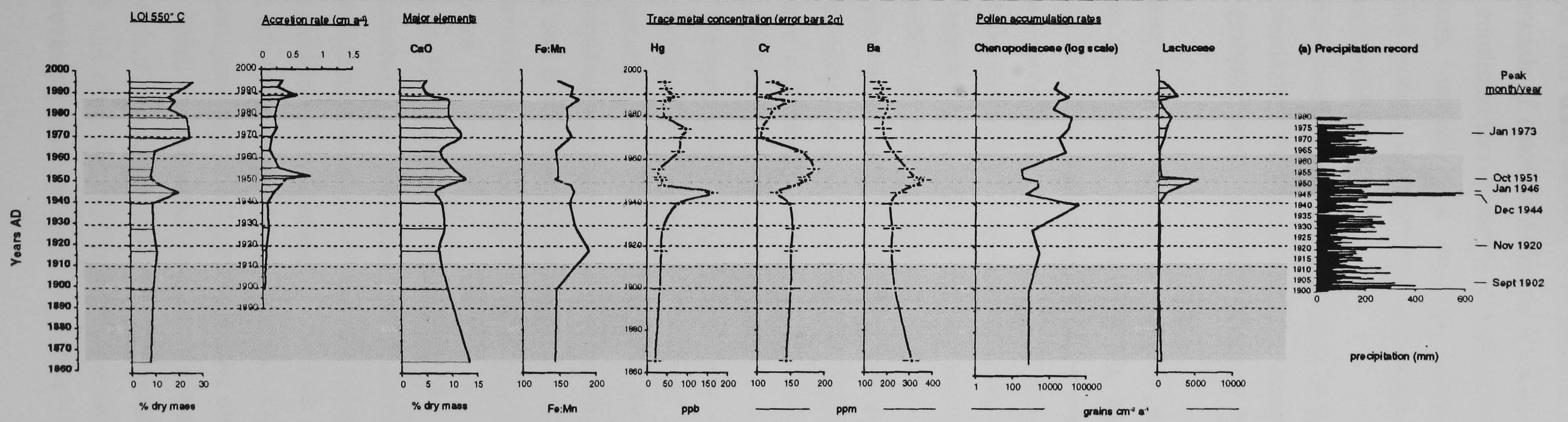

Phases interpreted as channel-alluvial dominated sedimentation. Note coincidental decrease in LOI, Fe:Mn ratio, Hg and Chenopodiaceae with increased Ca, Cr, Ba and Lactuceae.

Although major and trace element concentration data from sampled intervals certainly supports an inwash of catchment-channel derived materials, coinciding with a peak in accretion, the continued incorporation of pollen derived from local, channel-side ruderal-riparian habitats, including a depleted source of salt marsh (Amaranthaceae-Chenopodiaceae) pollen, suggests that disturbance to the marsh surface and growing conditions were localised.

It is conceivable however, that during a phase of high discharge, the active channel also affected (i.e. inundated) the higher elevation marginal areas (between the channel and human-made embankments) currently occupied by rough grazing land and ruderal vegetation.

The marked drop in the Fe:Mn ratio for the interval between *circa* AD 1945 and *circa* AD 1964 highlights the enhanced abundance of Mn. Most likely the core pattern reflects an enhanced input of alluvium-associated Mn (along with other trace metals) rather than post-depositional processes having contributed to the geochemical redistribution of Fe.

Following the peak intensity of accretion rates *circa* AD 1951-2, decreased flooding of the marsh surface appears to account for the declining catchment-derived trace element values and ruderal pollen content, as successive phases of inundation were less capable of transporting minerogenic sediment and decreased estuarine-channel discharge rates had a lesser effect on pollen transport from channel-margin ruderal communities.

Equally as major a vegetation change as the previous apparent catastrophic decline in halophyte vegetation and subsequent input of ruderal-riparian pollen, was the establishment between *circa* AD 1964 and *circa* AD 1970 of a significant salt marsh community at the core site. Responding to a change in hydrodynamic conditions (indicated by decreased accretion rates following on from the *circa* AD 1951-2 peak) the return of high relative frequencies of Amaranthaceae-Chenopodiaceae pollen and relative decrease in Si, Al, Fe, Ti and a decrease in catchment trace metal flux indicates that allochthonous minerogenic accretion was supplanted by enhanced organic sedimentation over a period of around four years.

Between *circa* AD 1970 and until *circa* AD 1979 (5.5 cm depth), when core site vegetation was again disturbed, the abundance of Amaranthaceae-Chenopodiaceae and distinct organic texture indicates that the formation of a salt marsh peat sediment fabric was able to develop for a limited time (approximately a decade).

Between *circa* AD 1979 and *circa* AD 1983 the drop in LOI values is concomitant with increasing minerogenic major and catchment trace metal contents. The Fe:Mn ratio peak at 3.5 (*circa* AD 1986) cm, the small peak in trace metal accumulation recognised at 2.5cm (*circa* AD 1988) and increased sediment accretion rates between these, suggest that between *circa* AD 1979 and *circa* AD 1988 a lower magnitude repeat of depositional conditions, documented previously between *circa* AD 1945 and AD 1964, existed at the site.

A decrease in the relative abundance and flux of Amaranthaceae-Chenopodiaceae pollen within the upper 4 cm of the core would appear to reflect the modern degradation of nearby marsh surfaces due to rough grazing, the dumping of waste refuse and the large scale port and road development (smothering existing halophyte communities) to the north of the core site. The accumulation of wetland, freshwater and ruderal pollen types (e.g. Cyperaceae, Potamogetonaceae, Poaceae, *Cirsium*) in the surface 4 cm (mid-AD 1980 onwards) indicates that the salt marsh surface has continued to be influenced by channel-inputs and the local growth of disturbed communities at the terrestrial margin of the salt marsh.

7.2.2 Controlling factors on wetland development identified in core AMC during the last century.

From the past record it is apparent that the salt marsh margin of the Mulinello channel has been subject to rapid colonisation and degradation of halophyte communities, in response to dynamic estuarine and alluvial sedimentation over the last century. The rate at which these changes have occurred effectively shadows the effect of longer term neotectonic trends on relative sea level. The effect of seismological events in the Mulinello catchment and Augusta bay area, documented for the period covered by the dated core were not identified in the sediment sequence. Accretionary, geochemical or palynological evidence of the 1908 Messina earthquake and associated tsunami which was reported to have flooded areas of the Mulinello estuary (Platania, 1909) was not found. The event which in the core sequence should exist between 17.5 and 16.5 cm depth (approximately 18 years of accretion, *circa* AD 1900 to *circa* AD 1918) was unable to be distinguished from the decadal-scale changes identified in the sequence. However a preliminary investigation of sediments from the related core depth for foraminifera (S. Kortekaas, Coventry University, *pers comm.*) found an increase in deep water marine species. This would suggest that the tsunami event was significant, though not enough to dramatically affect plant communities or estuarine sedimentation.

Evidence of historical tectonic activity in the Mulinello landscape affecting the catchment hydrology, i.e. landslide damming of narrow valleys, temporary lake formation and subsequent drainage, e.g. Nicoletti *et al.* (1999), were also unidentified.

Exposed shoreline wave activity may be expected to have had only a limited effect on the core setting, due primarily to the sheltered position of the river mouth in Augusta bay. The setting may however have been affected by local wave conditions, set up by local wind patterns and shipping movements within the harbour. Shallow-depth, flooded sediment surfaces at the margin of the channel are likely to have been the most affected areas, especially when un-vegetated. Low wave activity within the microtidal range may be

expected to have almost continually re-mobilised fine-grained clastic, shell and organic detritus when sediment surfaces were covered by water. The importance of reducing the impact of wave activity is clear therefore for the continued accumulation of organic materials. The effectiveness of wave energy dissipation by vegetation was observed in the present-day dense stands of *Salicornia* to be almost total within 1 m of the channel edge. Organic-enhanced accretion phases in the core would appear to have been caused by physiographic changes to the surrounding setting, either physically protecting the core site from wave action or allowing conditions to develop capable of retaining organic detritus (e.g the accumulation of sediment and elevation of the wetland surface).

The overall sedimentology of the core sequence indicates that channel side deposition for the last 100 years has been dependent on the balance of accretion and erosion, created by the interaction of low-energy microtidal estuarine-channel conditions and the inflowing Mulinello river. Although lacking a hydrographic record of past channel discharge patterns, the exchange of water between the Mulinello catchment basin and Augusta Bay will almost certainly have been determined by the seasonally skewed pattern of winter precipitation and high summer temperatures, typical of the region. Seasonal runoff from the catchment is likely to have led to the estuarine water mass alternating between net dilutive and net evaporative states typical of Mediterranean-climate estuaries (e.g. Largier *et al.* 1997). The biophysical stresses imposed by this regime on plant communities, even those adapted to salinity variations, more than likely provided thresholds which led to the rapid breakdown or encouraged re-colonisation of local vegetation. The timescales of halophyte re-colonisation identified in the core fall well within the time taken for experimental and natural halophyte populations to re-establish themselves (approx. 1-3 years) (See Chapter 2) following sediment surface disturbance and salinity induced stresses (e.g. Bertness & Ellison, 1987; Pennings & Callaway, 1992; Allison, 1995, 1996).

As a result of having developed channel-side of the anthropogenic embankments, the core site may be expected to have been subjected to more extreme variations of flow dynamics. Compared with a broad wetland-floodplain surface where flow rates dissipate due to surface resistance and deposition is encouraged, flow rates within confined channels (i.e. between embankments) have a greater erosion and sediment transport potential. Lower magnitude channel discharge rates when confined therefore may be expected to have a greater erosional potential than similar magnitude flood events in broader channels. The construction of embankments therefore to protect the industrial salinas and the operation of the salina operations itself, separated the wetland area at the mouth of the Mulinello area into two zones; one affected by salina operations and cut-off from only the most extreme hydrological conditions and a wetland area governed by the new hydraulic regime imposed

by anthropogenic channel modifications. It is apparent therefore that the cored section is a clear record of wetland colonisation and response to the modified 19th-20th century channel-side hydraulic regime.

As discussed in Chapter 4, climate records from south east Sicily document a number of high magnitude rainfall events and above average wet years which have occurred over the last century. Monthly patterns of precipitation totals plotted against the major core changes are shown (Figure. 7.1.1.). It is apparent from this that the timing of some peak precipitation events are coincidental with major temporal, compositional and palaeoecological changes in core AMC. Between *circa* AD 1900 and *circa* AD 1940, the resolution and sample ages of ^{210}Pb dating precludes any real chance of correlating a particular monthly peak of precipitation to core changes. The AD 1900's, 1930's and 1940's appear to have been particularly wet (Fig. 4.2.3.), interrupted by peak monthly rainfall totals greater than 400 mm (Fig.4.2.2.). The pollen content of horizons covering this period indicate a greater catchment component, in line with an expanding Amaranthaceae-Chenopodiaceae population. Lower accretion rates would suggest that the site was not affected by large influxes of sediment due to catchment flooding, but gradual accretion and elevation of the sediment surface, allowing the establishment of nearby halophyte communities.

Significantly the large magnitude monthly rainfall totals recorded at Catania in December AD 1944 and January AD 1946 coincide (at least in terms of the resolution and accuracy of ^{210}Pb dating of the intervals) with the changing rate in accretion recorded at 13.5 cm (*circa* AD 1945) and 12.5 cm (*circa* AD 1948). The consequent peak in accretion (0.79 cm a^{-1}) recorded between 11.5 cm (*circa* AD 1951) and 10.5 cm (*circa* AD 1952) corresponds with the peak monthly rainfall total of October AD 1951. An increase in accretion between 7.5 cm and 6.5 cm (*circa* AD 1974) is also recognised which appears to be coincidental with the January AD 1973 precipitation peak. The lack of rainfall data for the period recognised between 3.5 cm and 2.5 cm (*circa* AD 1988) prevents a comparison (at the present time) with the calculated increase in accretion.

The geochemistry of sediments derived from Mulinello core AMC contains an important catchment-derived signature of periodic flooding, being the primary control on sediment input and subsequent variations in core composition. It is apparent that the major change in sediment material influx recognised as to have occurred between *circa* AD 1940 and *circa* AD 1964 (14.5 cm and 8.5 cm depth respectively) was due to a dynamic change in channel margin hydrodynamics caused by successive flood events brought about by intense rainfall in the Mulinello catchment. Though the recorded rainfall amounts in December AD 1944 and January AD 1946 were both greater than the precipitation total for October AD 1951, the impact of the 1951 event, i.e. 11-12 October 1951 (see Section 4.4.) on accretion rates

may have been due to more available alluvial sediment, i.e. that which had been temporarily stored in the local catchment from the previous mid-1940's high rainfall events.

A slight increase in the rate of accretion would also appear to occur between *circa* AD 1970 and *circa* AD 1974, coincidental with a peak in rainfall during January AD 1973. Following this another peak in accretion between *circa* AD 1986 and *circa* AD 1988 occurs, which at the present time (due to the lack of climatic data) cannot be ascribed to a particular precipitation event.

7.3 Environmental changes recorded in core PPA, Pantano Piccolo, Vendicari

Core PPA represents the most recent phase of accretion at the northern-most lagoonal margin of the Vendicari lagoon complex in south east Sicily, deposited at the juncture of surrounding calcarenite slopes and the lagoonal environment of Pantano Piccolo.

Clastic material within the red-brown basal clay PPA-A (48-35 cm) measurably fined from the base of the core, containing numerous sub-rounded gravel-pebble clasts, up to the boundary with PPA-B, in which only coarse sand size grains were found in the plastic clay matrix. The difference in the size of clastic materials in the horizon suggests that deposition was initially rapid with little time for sorting, before either the supply of coarse materials were reduced or better sorting occurred in the depositional setting. The intact *Cerastoderma* sp. valve and other shell fragments incorporated within the matrix suggests that PPA-A was deposited within or at the margin of a brackish-lagoonal environment. The horizon is low in organic content (av. 10.9 %) and exhibits only minor variations in abundance of the dominant major elements. Dominated by Amaranthaceae-Chenopodiaceae (which along with the few grains of *Limonium* encountered would certainly suggest a nearby halophytic plant community) at the time, the pollen assemblage of the horizon also contains well-dispersed pollen types (i.e. *Pinus, Betula, Alnus*, *Quercus* undiff., *Olea-Phyllirea*) along with higher concentrations of disturbed ground/ruderal pollen types (i.e. *Anthemis*, Asteraceae subf. Asteroideae, Apiaceae, Caryophyllaceae and *Serratula* type). The latter types appear to have been associated more with the deposition of the coarser clastic material at depth.

In addition to the obvious lithological similarity between sediments at the base of PPA and soil-slope products collected for surface pollen analysis (Chapter 6), pollen abundances are also similar. The most apparent similarity with PPA-A are surface samples P4 to P7 (LPAZ PPS-2) from the least recently cultivated area (of expanding *macchia* vegetation) on the slopes facing the lagoon.

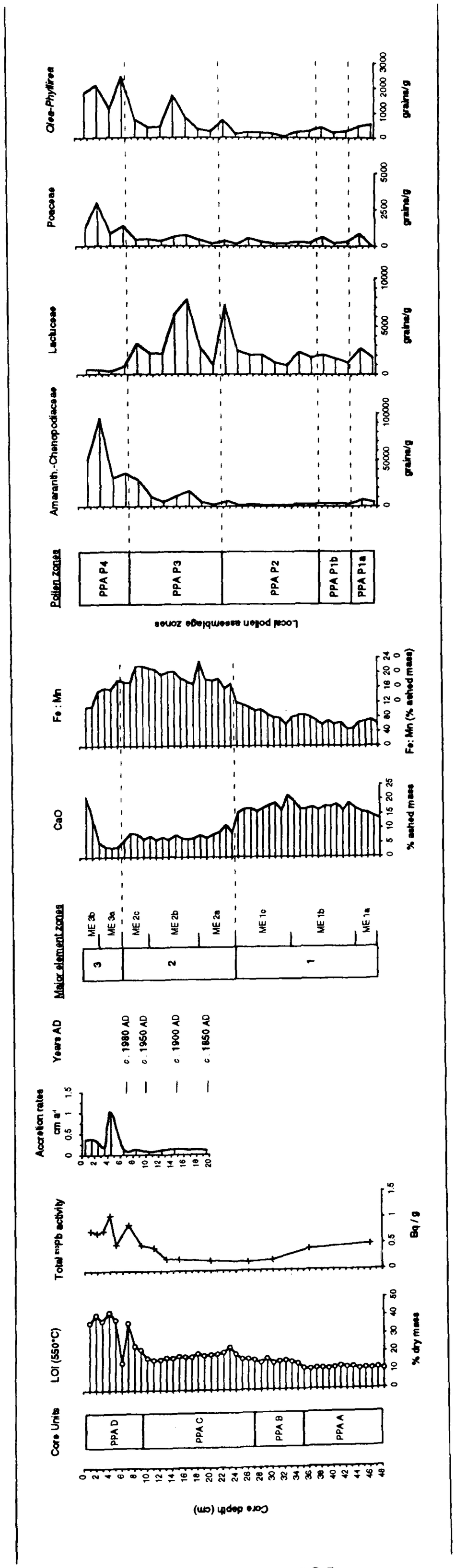

Figure 7.2. Stratigraphic summary of Pantano Piccolo A core (PPA)

In the core PPA the transition between horizons PPA-A and PPA-B was visible as a distinct change in colour, from clastic-rich red-brown clay to grey, shell-rich lagoonal muds. The transition is less apparent however, from the multi-proxy sources of evidence (Fig. 7.2.). The subtle increase in LOI 550°C was not measurably associated with increased organic content, rather losses appear to have been more associated with hydrous mineral water loss in the matrix.

Major element values from the horizon (corresponding approximately with PPA-ME-1c) indicates a fairly uniform composition, while the pollen content in PPA-B also suggests a continuation of fine-grained minerogenic-bioclastic sedimentation following PPA-A. An increase in the relative abundance of potentially long range transported *Pinus* pollen between 36 and 26 cm, peaking at 30-29 cm (6.9 % TP) would also suggest that the horizon represents a past phase of open lagoonal conditions, enhancing the deposition of aquatically transported grains. Again more open lagoonal conditions, possibly due to a connection with the sea, are suggested by the presence of foraminifera organic linings up to the boundary with PPB-C.

Although the visible boundary between PPA-B and PPB-C (35 cm) was not particularly marked by the multi-proxy analyses, the basal sediments of horizon PPB-C above, represents both a significant textural and temporal transformation of the depositional setting in the historical past. The decrease of Ca from 26-24 cm marks the division between a relatively Ca-abundant phase (horizons PPA-A and PPA-B) and the Ca-depleted phase in the upper half of the core between approximately 25 cm depth and the enrichment of Ca in the surface 3 cm. The Fe:Mn ratio increases likewise at this depth (Fig. 7.2.), due to the depletion of Mn. Geochemical evidence indicates that sediment horizons PPA-A and PPA-B were primarily deposited in more aerobic, alkaline conditions. Although sediment conditions became increasingly reduced from 34 cm depth (basal PPA-B) the abrupt increase in the Fe:Mn ratio from 25 cm to 24 cm represents a rapid change to more reducing conditions. Below the limit of ^{210}Pb dating in this study, only estimated dates can be assigned to these changes, using the last determined accretion rate at 20 cm (0.12 cm a^{-1}). Horizon PPA-B (perhaps *circa* AD 1725-1790) therefore spans the previous period of increasing Fe:Mn ratio values and the start of the decline in Ca, before the marked Fe:Mn ratio increase and concomitant drop in Ca within PPA-C between 25 cm (perhaps *circa* AD 1807) and 24 cm (perhaps *circa* AD 1815).

These abrupt changes at the base of PPA-C are simultaneous in the core with increased Lactuceae at 25-6 cm and low concentrations of Amaranthaceae-Chenopodiaceae. Pollen concentration values increase for types indicative of disturbance (i.e. Lactuceae,*Cirsium*, *Anthemis*) at 23-4 cm, coinciding with the Fe:Mn ratio increase at the same depth and up to the transition with PPA-D.

The large drop in absolute concentrations of these types relatively soon after the peak at 22-21 cm (estimated at *circa* AD 1840) may be a consequence of a short-lived decrease in local

pollen production due for example to grazing or surface burial, or a temporary cessation of pollen transport to the site caused by low-water levels.

Palynological and geochemical data indicate therefore that sedimentation at PPA from the beginning of the 18th century (26 cm) at least up to *circa* AD 1950-1960 (~10 cm), occurred within a brackish, possibly reducing, stagnant environment. The coincidental change in geochemical conditions, reflecting a rapid change of sediment conditions and pollen content suggestive of disturbance at the base of PPA-C, indicates that lagoon conditions changed as nearby, freshly-disturbed soil-sediment surfaces were colonised by ruderal-type vegetation. The end of this period inversely, saw the decline of Lactuceae pollen (superseded by the expanding Amaranthaceae-Chenopodiaceae population) and another shift in the depositional environment leading to the accumulation of vegetal organic matter (PPA-D). The concentration of brackish-hypersaline shell species at the boundary of PPA-C with PPA-D (12-10 cm) may represent a death assemblage of *in situ* organisms which dwelled in the surface of the reduced sediment. The abundance of shells would indicate that some lagoonal process concentrated the assemblage, either due to an expanded population which took advantage of the depositional environment at the time or due to high energy sediment transport from the inner lagoon.

The abrupt transformation of the sediment sequence from one almost entirely minerogenic in nature to a visible and measurably organic phase in PPA-D occurs as the Fe:Mn ratio drops suddenly, after its relatively steady increase from the base of PPA-B (Fig. 7.2.). An increase in the relative abundance of Mn and the parallel decrease in Fe and the Fe:Mn ratio within PPA-D indicate control by soil redox processes. The surface-organic control on sediment chemistry is also highlighted in PPA-D by the two-fold increase in Na, Mg and P and the fluctuation of Ca in the surface 10 cm (Fig.6.5.4.).

Over a relatively short time period (approximately the last 40 years) organic-associated accretion surpasses any rates measured previously in the core. Judging by the lithology of the horizon, sediment accretion rates and the Amaranthaceae-Chenopodiaceae dominated pollen assemblage, organic accumulation and the elevation of the marsh surface has responded positively to changes that occurred in hydrological-lagoonal conditions following the deposition of PPA-C. Estimated pollen flux rates for the period (Fig. 6.6.) exhibit a similar tendency with sediment accumulation rates, indicating that the establishment of salt marsh vegetation has been advantageous to pollen deposition. When the site was visited during high water levels (Spring AD 1998) semi-submerged halophytic vegetation was acting as an efficient baffle against wave activity.

The flux to the sediment surface and incorporation of anemophilous-aquatic transported pollen types, e.g. *Olea-Phyllirea, Pinus*, Ericaceae, *Betula* and Poaceae, would appear to be directly attributable to this factor.

The pulse of accretion (1.02 cm a^{-1}) that occurred between 7 cm (*circa* AD 1980) and 5 cm (*circa* AD 1982) and the drop in LOI 550°C values at 6 cm cannot be dismissed as

coincidental. Although not differentiated by geochemical or palynological analyses, only by loss on ignition and visual inspection which both suggest a carbonate (shell content) cause, the accretionary "event" appeared not to have a dramatic effect on the setting. An event involving localised inwash of shell-rich sediment onto the marsh surface, derived from the inner lagoon, caused by wave activity and high water levels, at the lagoon margin is a realistic scenario.

7.4 Environmental changes recorded in PPB, Pantano Piccolo, Vendicari

Situated approximately 15 m south of the northern lagoon margin of Pantano Piccolo, the sediment sequence of core PPB was extracted in an attempt to quantify the most recent period of accretion from the seasonally/low water exposed mudflat setting. Although the sequence was, on extraction, clearly dominated by lagoonal sediments, evidence of significant depositional changes were also recognised that prompted further investigation.

The basal clay and gravel/pebble deposit in core PPB occurred only as a thin horizon (49-46 cm) overlying the solid calcarenite bedrock. An assessment of the coarse clastic horizon, with its increased relative abundance of minerogenic elements (particularly Si, Al, Fe, K, Ti and Mn) and low organic content (av. 11.7 % 550 ℃ LOI) suggests that deposition at the time was dominated by dynamic physical processes, such as wave action. An increased relative abundance of well-dispersed, long range-atmospheric transport grains of *Pinus, Alnus* and *Corylus* occurs in the base as a result of the low pollen content of the sediment; though their abundance suggests a greater presence of nearby tree stands or the efficient focusing of well-dispersed taxa from nearby land-surfaces. Even more than PPA-A, the pollen assemblage and lithology of PPB-A is clearly similar to the soil-surface samples taken from the lagoon margin slopes (Figure 6.8.2.).

The concentration of Lactuceae pollen is seen to expand rapidly through PPB-A into PPB-B, overtaking Amaranthaceae-Chenopodiaceae which although dominating the relative abundance of pollen in the lowest sample (49-48 cm) declines constantly towards PPB-B. Concentration values of Amaranthaceae-Chenopodiaceae in PPB-A are the lowest in the core (< 680 grains/g). The increase in Lactuceae pollen at the boundary with PPB-B and the shift into lagoonal muds is also observed to coincide with a peak in the ratio of Fe:Mn, suggestive of a soil in-wash phase or event. Associated with this peak (which spans LPAZ's PPB-1a and PPB-1b) is the first occurrence of *Olea-Phyllirea* (67 grains/g 47-46 cm) and *Juglans* (45 grains/g at 46-45 cm).

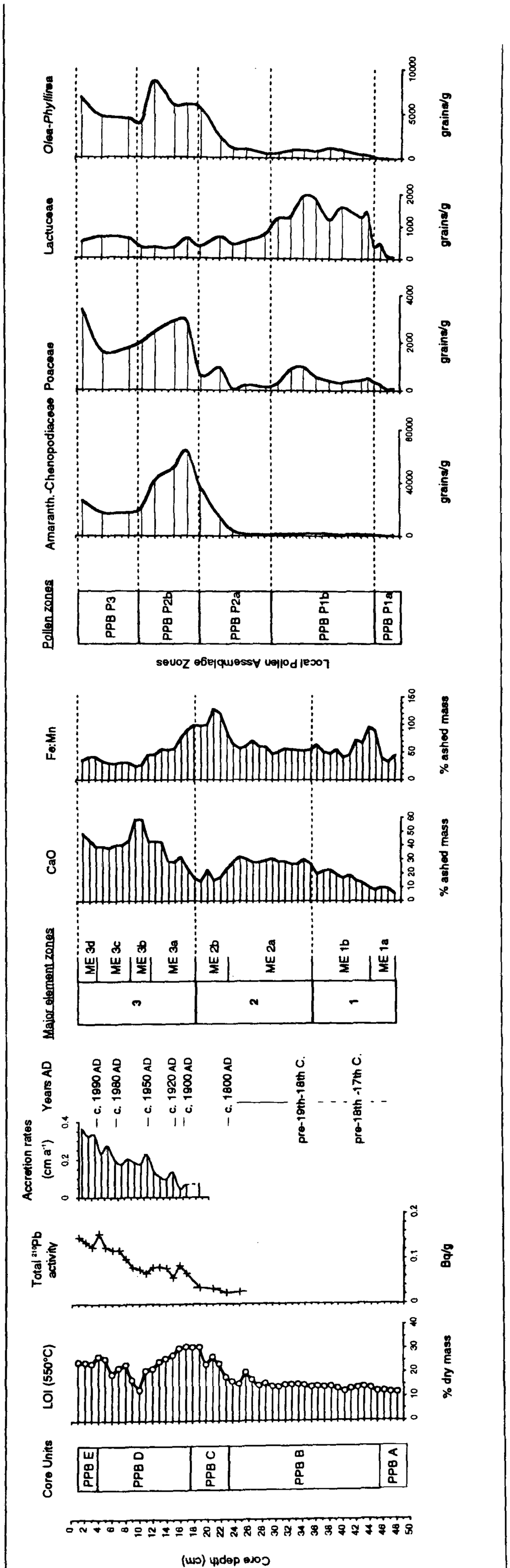

Figure 7.3. Stratigraphic summary of Pantano Piccolo B core (PPB)

The unconformably overlying sedimentology of PPB-B (46-23 cm) is characterised by grey fine-grained muds containing brackish-marine molluscan fauna. These muds exhibited a gradual increase in CaO from the boundary with PPB-A (highlighted by post-LOI 850°C loss) and a pollen content in which the abundance of Amaranthaceae-Chenopodiaceae grains is comparable with Lactuceae (Fig. 7.3.). The assemblage also contains pollen indicative of extra-local ruderal sources and possibly arboreal cultivation in the catchment area (e.g. *Olea-Phyllirea*, *Vitis*, *Juglans* and other ruderal types including Apiaceae, *Artemisia*, Asteraceae subf. Asteroideaeand *Cirsium*). This suggests that during the period represented by LPAZ PPB-1b (45-29 cm depth) local halophyte communities were inundated by elevated water levels, allowing lagoon-brackish accretion and less abundant pollen grains from extra-local sources to be incorporated into the sediment. Similarly the abundance of foraminifera organic linings in the pollen slides during this phases suggests a more open-lagoonal, possibly marine influenced depositional setting.

This CaO and Lactuceae pollen zone of the core stratigraphy is replaced at 23 cm by an accumulation of organic matter (PPB-C), an increase in minerogenic materials and a massive increase in the abundance of Amaranthaceae-Chenopodiaceae. The earliest ^{210}Pb-dated horizon at 20.5 cm (*circa* AD 1835) in PPB-C suggests that this shift in the environment of deposition occurred at the turn of the AD 18th-19th century (*circa* AD 1800).

Beneath the depth of greatest organic content (19-16 cm), the relative increase in Si, Al, Fe and Ti would indicate that the accumulation of humic mud/peat followed accumulation of catchment-derived sediment (24-20 cm). Some caution exists as to whether this increase in minerogenic elements represents a true influx of Ca-depleted materials or a relative increase, due to Ca-reduction in the organic horizon due to pH-related dissolution. An associated increase in Amaranthaceae-Chenopodiaceae, *Cirsium*, Asteraceae subf. Asteroideae, *Anthemis* and Caryophyllaceae pollen with the increase in minerogenic elements does however suggest that disturbed ground and ruderal vegetation communities were in the vicinity at the time.

It is plausible that the accretion of sediment, either soil material derived from local slopes or as a result of increased sediment loads in the lagoon water body elevated the sediment surface, changing the hydrology of the core site and growing conditions for local vegetation. The peak abundance of Amaranthaceae-Chenopodiaceae in the upper part of horizon PPB-C is similar to that in the surface sample of PPA beneath a well-established community, which would indicate that the organic horizon PPB-C represents the gradual development of a halophyte community rather than a more rapid accumulation of organic matter, i.e. plant material washed in from more disturbed settings (e.g. Bertness & Ellison, 1987). According to the ^{210}Pb dates obtained, this organic-phase (23-17 cm) existed for almost the entire 19th century. The boundary of PPB-C and PPB-D at 17 cm depth was dated by ^{210}Pb to *circa* AD 1893. PPB-C deposited in the early-mid nineteenth century

represents a juncture in the sediment stratigraphy of core PPB, largely separating two significantly different depositional regimes, especially in pollen content, that have occupied the same setting.

In PPB-D the mass-abundance of well-preserved bivalves, gastropod shells and organic matter incorporated within the lower half of PPB-D (17-10 cm) suggest that the depositional environment following the accumulation of organic enhanced PPB-C was a conducive habitat to benthic and surface-grazing mollusca fauna. Bioturbation may be expected to have been intense, as the ^{210}Pb activity profile suggests, with relatively constant ^{210}Pb activity totals with depth. Conditions allowing the accumulation of organic matter appear not only to have provided an abundant food source for sediment fauna at the time (from the turn of the 20th century to *circa* AD 1953) but beneficial for the preservation of extra-local, well dispersed pollen types, e.g. *Alnus*, *Pinus*, *Betula*, *Olea-Phyllirea*, Ericaceae and Poaceae).

This period associated with a high shell content (between 17 and 10 cm) sees steadily increasing accretion rates interrupted by two minor peaks: between 15.5 cm and 14.5 cm (*circa* AD 1922) and between 11.5 cm and 10.5 cm (*circa* AD 1953). The peak in accretion *circa* AD 1922 corresponds to a relative increase in the abundance of Si and Ti, which would suggest an input of minerogenic material. The latter accretion peak at 10.5 cm (*circa* AD 1953) precedes the shell-associated Ca peak at 10-9 cm (*circa* AD 1958), which ended this increased Ca phase and resulted in the deposition of grey muds with a visibly lower shell and organic content up to *circa* AD 1990 (2-3 cm).

Local pollen assemblage zones PPB P2b and PPB P3 also divide horizon PPB-D in two (Fig. 6.7.1). Accumulation patterns of the commonest pollen types (Fig. 6.7.3.) are depleted within PPB P2b, apart from Ericaceae, Poaceae, Caryophyllaceae, Asteraceae subf. Asteroideae, *Serratula* type and *Ephedra fragilis*. The accumulation of tree/shrub pollen types (i.e. *Pinus*, *Olea-Phyllirea*, *Betula*, *Quercus* type and *Alnus*) and halophyte-ruderal types in PPB P2b, suggests a low energy environment suitable for the incorporation of well-dispersed pollen and a nearby local source of disturbed-saline ground. The increased flux of both well-dispersed, atmospheric pollen (i.e. *Pinus*, *Olea-Phyllirea*, Ericaceae, Poaceae) and ruderal/halophyte-wetland herb (e.g. Lactuceae, *Anthemis*, Asteraceae subf. Asteroideae, *Plantago*) pollen types, coinciding with increased sediment accretion rates, suggests that from *circa* AD 1958 the setting became more open to lagoonal sediment transport.

The most recent surficial sediments (PPB-E) unsurprisingly exhibit current mudflat conditions, marked by increased Ca and P and a relative reduction in other minerogenic elements. The salt and algal crusted mudflat surface has also incorporated the greatest totals of tree pollen.

7.5 Environmental change at the northern margin of Pantano Piccolo, Vendicari, SE Sicily.

It is clear that the northern margin of Pantano Piccolo has undergone significant environmental changes, represented by the sedimentology of cores PPA and PPB, within a relatively confined physiographic setting. The local stratigraphy identified by a series of cores and transects into the lagoon (Fig. 6.4.3.) also revealed that the different horizons are relatively consistent. The dating of PPA (outer lagoon) and PPB (inner lagoon) allows an interpretation of broader-scale stratigraphic changes at the northern margin.
Lithological differences between two cores and their time-depth relationships are shown in Figure 7.4. and Figure 7.4.1. summarises the two cores sedimentological differences and major element zones and local pollen assemblages. A cartoon outlining the main changes discussed here, which have occurred at the lagoon margin and generated the present day stratigraphy is shown in Figure 7.6.

The deposition of the basal horizon PPA-A/PPB-A at the northern margin of Pantano Piccolo, appears to have been crucial for continued lagoonal deposition at the site as it acted as an aquitard by separating lagoon waters from the permeable calcarenite bedrock/clastic deposit below. In their study of the south east Sicilian coastline, Basile *et al.* (1986) postulate that the formation of coast parallel lagoons enclosed by clastic materials was favoured in shelly limestone hollows "by the presence of a thin clayey cover". Without the necessary dating control to ascertain the true age of the deposit, it can only be assumed that the horizon PPA-A/PPB-A represents a pre-18th palaeosol or other fine-grained deposit which initiated lagoonal sedimentation at the site. Brackish-saline conditions were, it appears, already in existence during the deposition of PPA-A (indicated by incorporated *Cerastoderma* fragments). The low organic content and potential errors created by "old" carbonate material and marine-fresh groundwater exchange between the lagoon and sea suggest that the use of other dating methods would be more suitable than ^{14}C.

Pollen assemblages from the fine-grained matrix of both cores revealed a surprising amount of well-dispersed, regional extra local tree pollen (*Pinus, Betula, Corylus* and *Alnus*) along with more expected ruderal-halophyte and wetland pollen types (Fig. 7.4.3.). This suggests that the same physical processes which deposited the fine-grained matrix of the basal agglomerate also transported pollen from nearby ruderal-halophyte plant communities while incorporating regional or extra-local pollen which had been deposited

Figure 7.4. Temporal and spatial relationships between cores PPA & PPB, Pantano Piccolo.

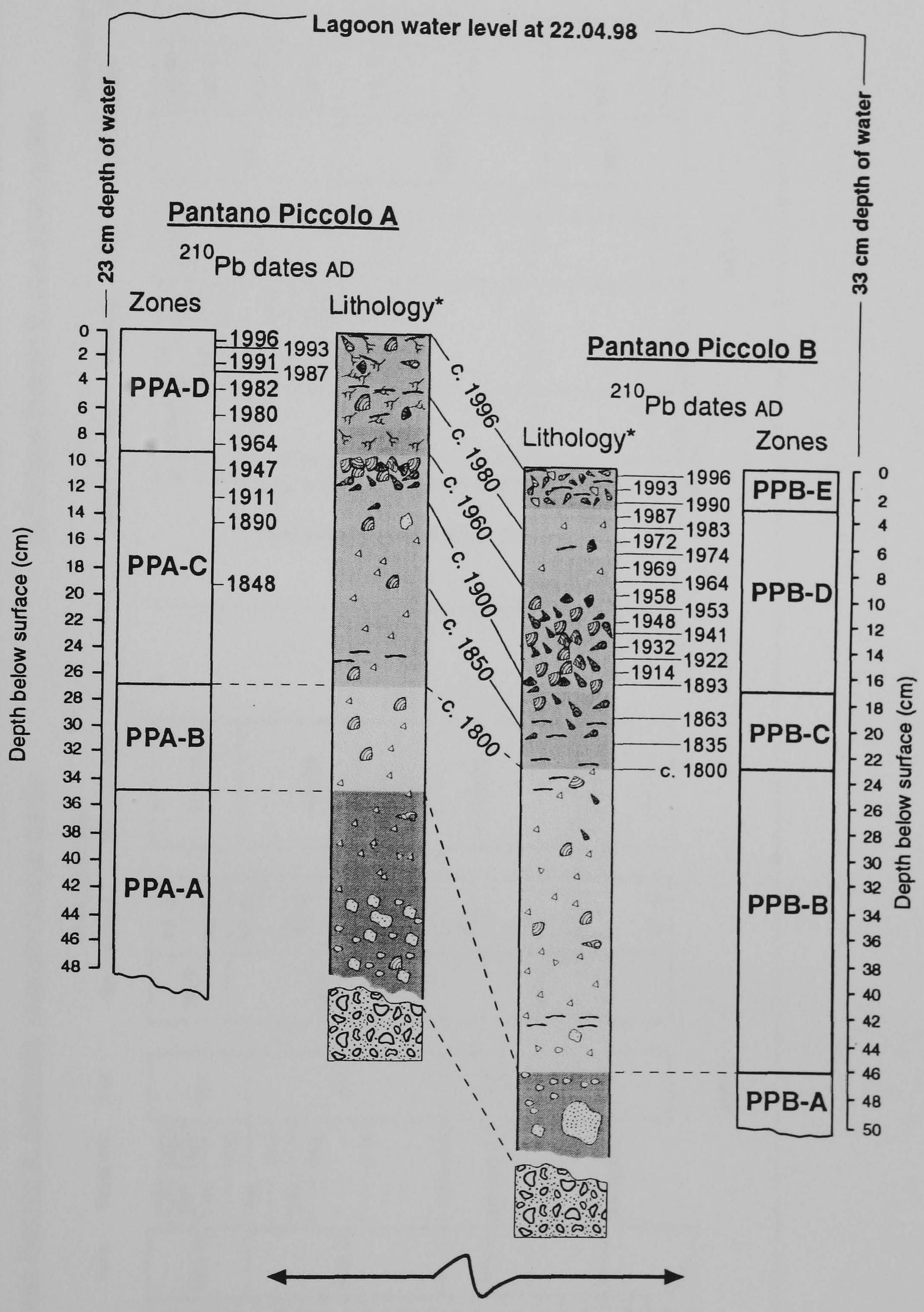

Figure 7.4.1. Comparison between cores PPA and PPB by depth and age of sample below sediment surface, LOI, chemostratigraphy and pollen assemblage zones

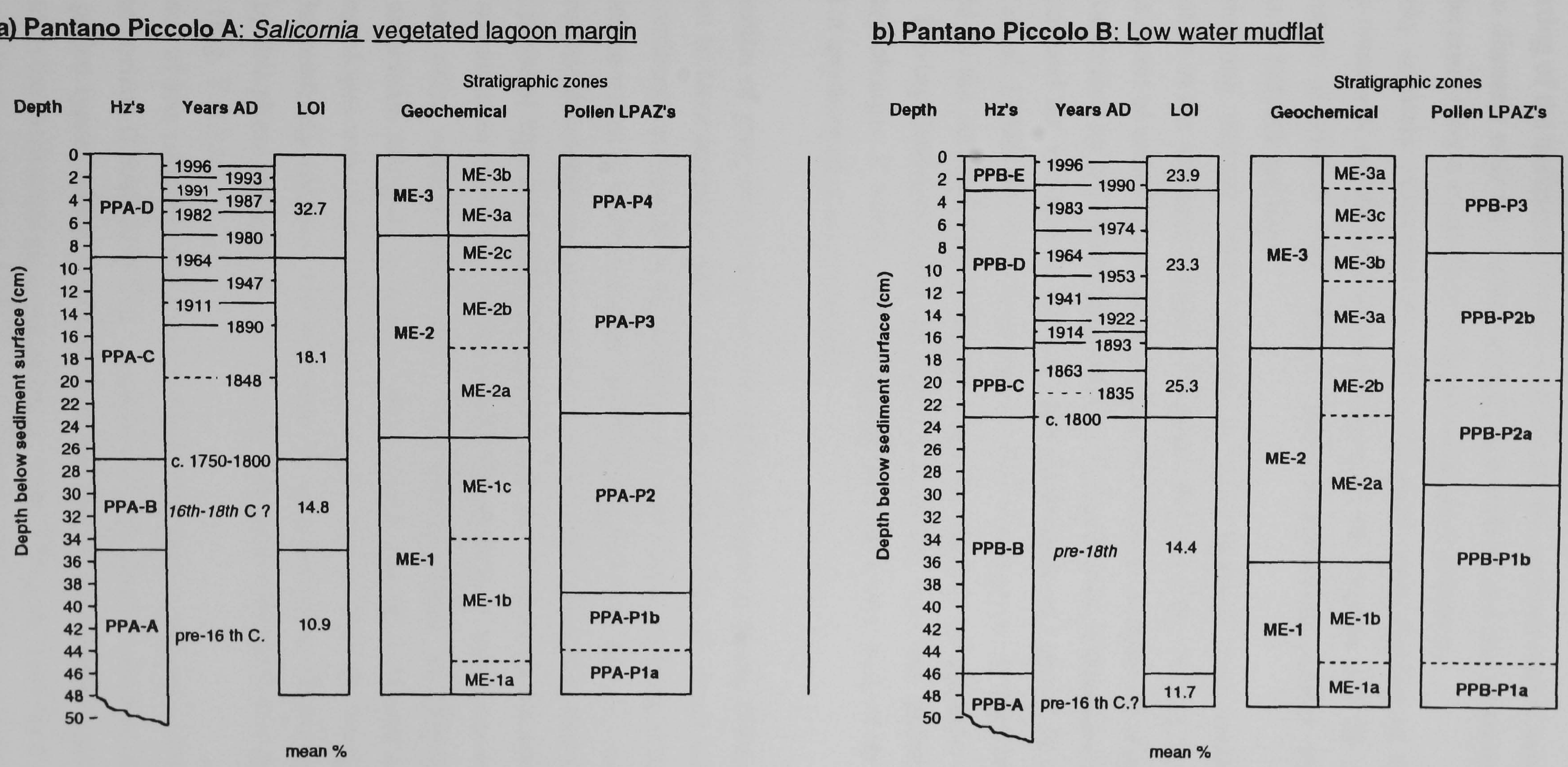

on nearby land-surfaces or were in the seston of the water body that may have been in existence at the foot of the slope.

Some sorting of the horizon is observed, with both the coarser clastic material, which was smaller in diameter near the contact with PPA-B/PPB-B and the observed shift from the base of the core, from a more clast to matrix-supported sediment.

A similarity certainly exists between the pedological characteristics of the contemporary thin terra-rossa soil on the surrounding slopes of the lagoon and the sedimentological characteristics of PPA-A and PPB-A. Both incorporating gravel and pebble sized fragments of bedrock geology.

This underlying deposit which appears to have initiated and maintained lagoonal sedimentation at the northern margin of Pantano Piccolo (Fig. 7.4.2.) is interpreted as a result of a phase of soil-slope product inwash, possibly as a result of slope instability and soil erosion caused by land-use/climate change. A significant comparison may be had with this horizon and the terreginous red silts and mud-supported gravel facies described by Pacheco *et al.* (1996) in the *Albufereta de Pollença* lagoon in Mallorca, which were interpreted as the siliclastic input brought into the lagoon by episodic local catchment flooding. Having determined that the upper half of the core has undergone significant accretionary changes it would appear unlikely that the lower half of the core has been deposited at anything near a constant rate.

The deposition of grey silts and mud with brackish lagoonal fauna (PPA-B and PPB-B) appears not to have occurred after a significant hiatus from the basal sediment horizon, with the continued incorporation of possibly reworked clastic material at the base of PPB-B. The horizon varies in thickness at the northern margin of the lagoon, smoothing out the irregular surface developed in the calcarenite bedrock and subsequent drape of clastics and clay. This phase of lagoonal sedimentation (PPA-B and PPB-B) is recorded by almost 50 % of the sequence in core PPB, while only 16 % of PPA. Concentrations of Lactuceae, Poaceae and other ruderal pollen types, including *Artemisia* in PPB-B suggests that sediment-associated transport of grains from ruderal-disturbed ground communities on surrounding slopes was more effective to the inner lagoon than the margin (PPA) (Fig. 7.4.3). The relatively constant concentration of Amaranthaceae-Chenopodiaceae in both cores during this phase suggests that salt marsh vegetation remained at a distance from the core sites (Fig. 7.4.3.).

The presence of less common tree and shrub pollen types (i.e. *Juglans*, *Corylus*, *Picea* and *Vitis*) in the horizon (LPAZ PPB-P1b) suggests not only that the site was in receipt of well dispersed pollen types, which would support the idea of more open lagoonal conditions, but also that in the extra-local area, arboriculture-viticulture may have been practised.

Although similar in respect of mean organic content (14-15 %), a comparison of major element abundances in the two horizons PPA-B and PPB-B of the two cores, highlights

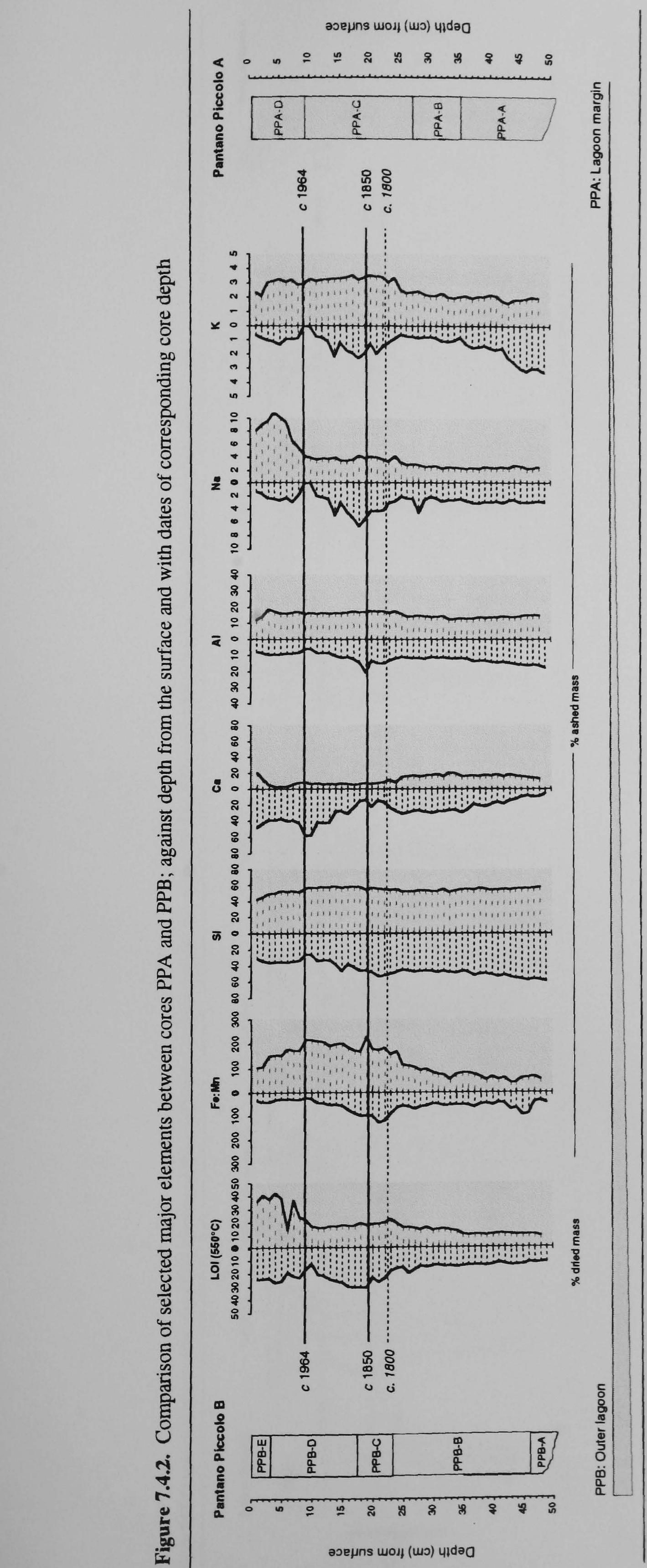

Figure 7.4.2. Comparison of selected major elements between cores PPA and PPB; against depth from the surface and with dates of corresponding core depth

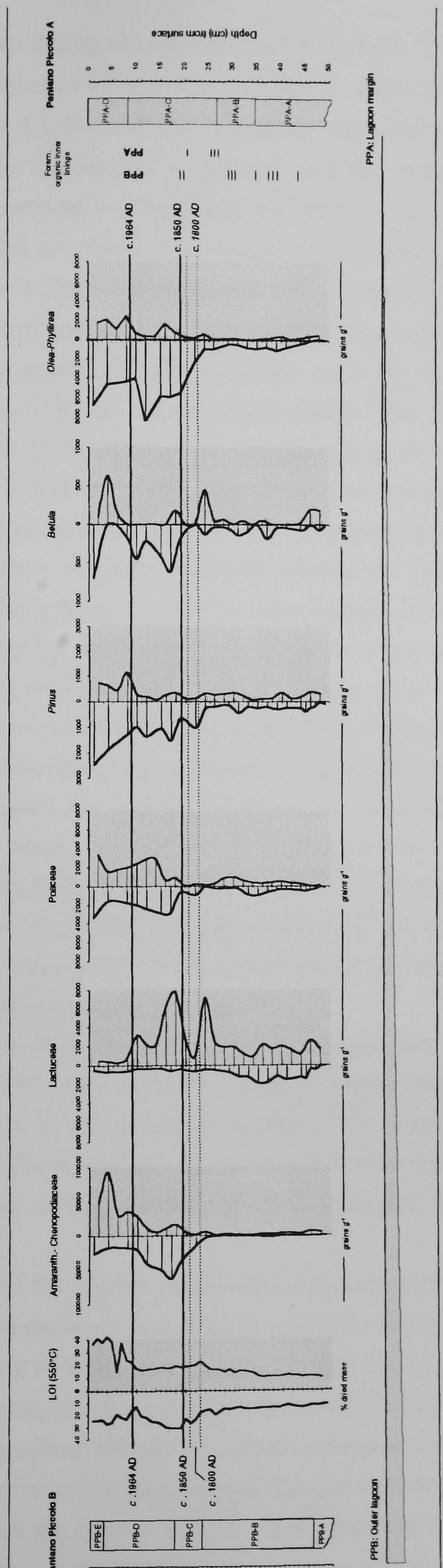

Figure 7.4.3. Comparison of selected pollen types and LOI between cores PPA and PPb: against depth from the surface and corresponding dates. Pollen concentrations in grains g^{-1}. Note lines indicating presence of Foraminifera organic linings

spatial differences during the same depositional phase. The abundance of Si, Al, K, Fe and Mn is slightly higher in PPA-B than in PPB-B, while Ca abundance is more enhanced in PPB-B (Fig. 7.4.2.). Na and Mg indicates a very similar depositional environment, most likely due to the submerged conditions and the chemistry of lagoon waters during deposition. If continually submerged, the increase of mineral elements may have been caused by physical processes at the margin of the lagoon, i.e. a winnowing effect of wave action in shallower depths. The horizon (PPB-B and PPA-B) would appear therefore to represent a phase of open and possibly more alkaline lagoonal sedimentation.

Either due to increased sediment accretion, or a fall in water level, halophyte-wetland vegetation and subsequent organic accumulation was initiated at the position of PPB, approximately 20-25 m south of the marginal fringe of halophyte vegetation found at the present. The estimated age of this change (*circa* AD 1800) and the development of PPB-C would appear to be diachronistic with the estimated age of the base of horizon PPA-C, suggestive of more stagnant lagoonal conditions. An expansion of lagoon margin vegetation outwards from the east or west margin, possibly tracing a bar of lagoonal sediments formed by wave action or an isolated mound in the lagoon, rather than a complete regression of the northern lagoon margin would appear to have occurred.

The depositional environment to the north of this vegetated barrier may therefore have been protected from disturbance by wave activity, allowing more anoxic conditions to develop and enhanced organic accumulation. The minor peak at 23 cm depth in PPA-C along with visible signs of black, organic streaking observed at the same depth and at a similar elevation in cores PP1, PP2 and PP3 (Fig. 6.4.3.) appears therefore to be more than coincidental, but reflective of this anoxic/organic preservation phase. An enhanced supply of plant matter, transported from the marsh front into the rear lagoon environment, may have also have been a contributory factor.

The concentration of shells encountered stratigraphically beneath this potential episode of anoxia in PPA, PP1, PP2 and PP3, suggests that molluscan fauna which took advantage of organic matter in the sediment (*Bittium* sp.) were also detrimentally affected by continuous or perhaps seasonal phases of extreme anoxicity as observed at the margin of Pantano Vendicari during low water levels in September 1996.

By *circa* AD 1890 the organic accumulation period represented by PPB-C was overtaken by lagoonal sedimentation, becoming an attractive setting for prolific molluscan activity, while conditions at PPA remained as before. The change of lagoon conditions at this time and the previous major change recognised at *circa* AD 1800 in both the cores would appear to correspond therefore with the increased anthropogenic control on the hydrology of the lagoon related to the salina operations in Pantano Grande (Chapter 6.). The construction of walls W-E across the lagoon and the sluice-controlled, 6 m wide embankment at the southern connection with Pantano Grande (Plate 6.4.) appears therefore to be recorded in

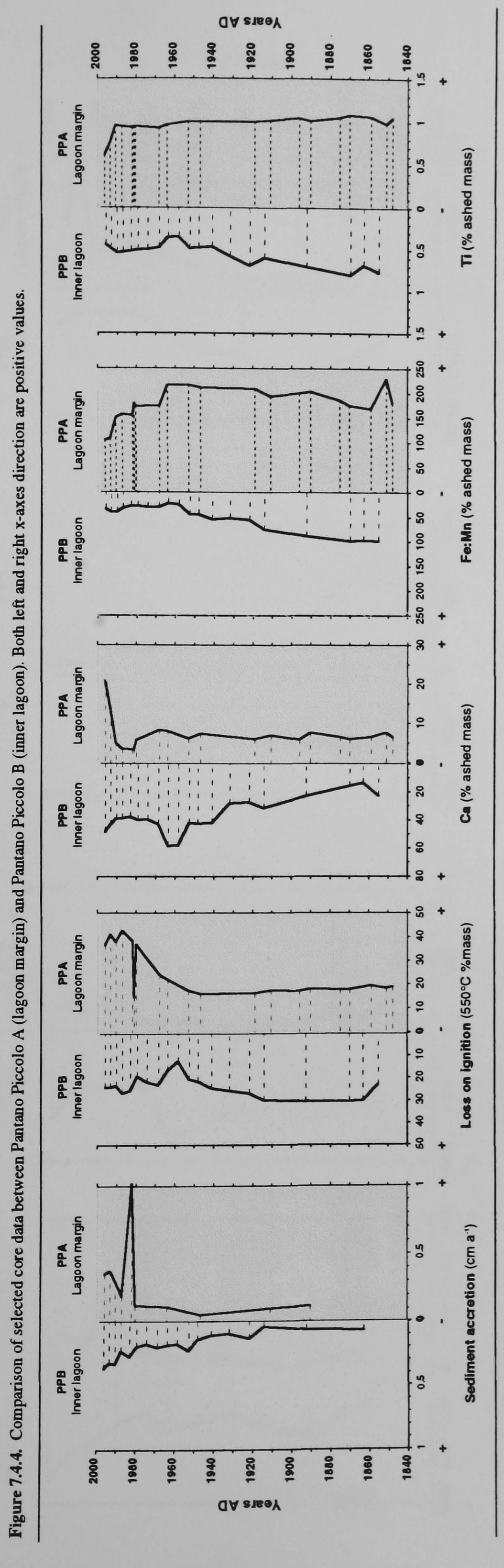

Figure 7.4.4. Comparison of selected core data between Pantano Piccolo A (lagoon margin) and Pantano Piccolo B (inner lagoon). Both left and right x-axes direction are positive values.

Figure 7.4.5. Comparison of selected pollen concentration data between Pantano Piccolo A (lagoon margin) and Pantano Piccolo B (inner lagoon). Both left and right x-axes direction are positive values.

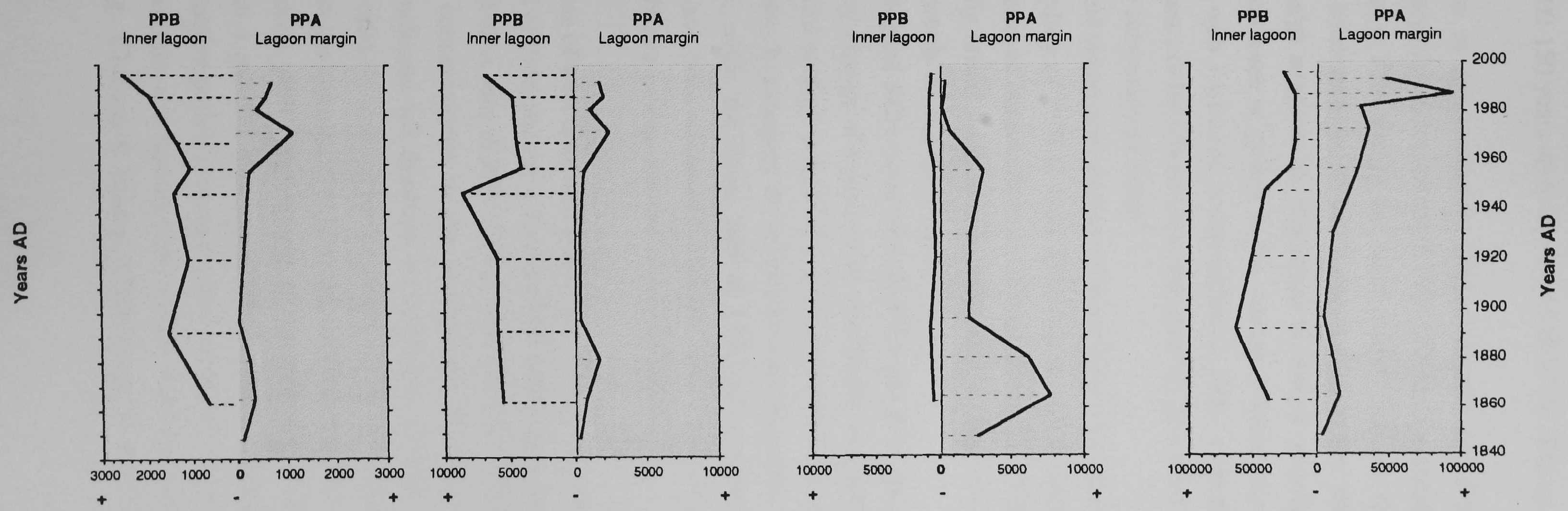

the northern margin lagoon sediments as the beginning of a stagnant lagoonal phase that lasted for 100-150 years up to the latter half of the 20th century.

The increase in Amaranthaceae-Chenopodiaceae and Poaceae pollen, concomitant with increasing organic accumulation in PPB-C/PPB-D, coincides with increased concentrations of Lactuceae in PPA during the same period *circa* AD 1800-1850 (Fig. 7.4.3.). Widely fluctuating concentrations of Lactuceae in PPA in this time period (ranging from 900 to 7700 grains/g) suggests an expansion of ruderal populations or variable transport and incorporation rates of pollen to the margin (relative abundances show a gradual peak). Compared with Lactuceae concentration in PPB, ruderal plant expansion in the lagoon margin appears to have been localised, possibly generated by the construction of low walls and nearby cultivation of fields.

The peak and subsequent decline of Amaranthaceae-Chenopodiaceae pollen concentrations at the boundary of PPB-C with PPB-D is matched relatively temporally, though with a lesser increase of Amaranthaceae-Chenopodiaceae in PPA. It is suggested that as a result of artificially raised water levels, halophyte populations were beginning to be forced to relocate towards the lagoon margins.

Sedimentological differences between PPA and PPB suggest that following the early-mid 19th century change of lagoon-wide conditions, local differences in the physiography of the individual settings remained a dominant control on pollen accumulation and sediment geochemistry. In summary the major element composition of PPA-C was dominated by Si, Al and Fe, while the lower half of PPB was dominated by Ca. Mineral matter may therefore have been winnowed from the inner lagoon area and transported to the margin, leaving behind a greater amount of shell material.

The increase of well dispersed pollen, e.g. *Pinus*, *Olea-Phyllirea, Alnus* and Poaceae (Fig. 7.4.3.) and of local and extra-local ruderal pollen types following the transition from PPB-C into PPB-D is seen in PPB (LPAZ PPB-P2b). In PPA (LPAZ PPA-P3) a similar change in pollen concentrations is also recognised. Restricted lagoonal conditions created by artificial enclosure led therefore to conditions suitable for the accumulation of pollen. Accretion rates determined for the period for the two cores (7.4.4.) prior to *circa* AD 1965 suggest that the increase in pollen concentration was less of a record of a dramatic increase in local ruderal plant communities, or an expansion of nearby *Alnus-Pinus-Olea-Phyllirea* stands than a product of a depositional regime conducive to pollen incorporation. It is likely that active pollen scavenging and subsurface incorporation of pollen grains from the sediment surface and lagoon water seston was also enhanced by the production of faecal pellets (e.g. Chmura & Eisma, 1995) by the *in situ* mollusc fauna (i.e. bivalve filter-feeders).

Pollen accumulation rates calculated for LPAZ PPA-P3 and PPB-P2b indicate an enhanced accumulation of ruderal pollen types, particularly in PPA with noticeably higher values in Lactuceae accumulation at the latter half of the nineteenth century (Fig. 6.5.9.). Lactuceae pollen accumulation at PPB during the same period was however much lower.

Enhanced Lactuceae-Caryophyllacae-Apiaceae accumulation in PPA during this time would appear therefore, to have been a continuation of the main period of disturbance, i.e. the re-establishment/expansion of salt marsh and ruderal communities at the margin of the lagoon due to the artificial change in water levels and nearby wall construction-cultivation of nearby fields.

The much lower accumulation rates of Lactuceae pollen in PPB within LPAZ P2b (Fig. 6.7.4.) appears to reflect the low transport potential of Lactuceae pollen away from the main area of production at the lagoon fringe.

Accretion rates were determined at a much lower resolution in PPA-C for the last century, than the same period in PPB-D. As a result, although subtle changes to the rate of accretion are likely to have occurred during the deposition of PPA-C, they are not recorded to the same detail as in PPB-D. Separated from the supply of sediments brought in by the Saia Scirbia catchment and Pantano Grande by an artificial embankment with continually controlled water levels, it is no surprise that accretion rates at the northern margin of Pantano Piccolo were low.

In effect without a direct local catchment input to influence the supply of sediment to the core sites (cf. core AMC at the Mulinello estuary) varying accretion rates may be assumed to effectively have only occurred by three ways:

- the input of catchment or local soil-sediment due to a high magnitude event in the *Saia-Scirbia*-catchment/Pantano Vendicari lagoon complex capable of exceeding the hydrological restrictions imposed by embankment construction;

- hydrological variations within the enclosed lagoon capable of re-suspending, transporting and focusing sediment at the core site or;

- biogenic-geochemical autochthonous accumulation that may have been dependent on the local hydrological environment.

A moderating factor for meteorologically caused hydrological changes must have been that the lagoon was protected against severe hydrological variations by water levels being maintained by marine-fresh groundwater discharge.

A comparison of monthly rainfall totals and accretion rates for the period AD 1900-1980 would indicate a significant correspondence between precipitation and accretion recorded in PPB. Significant peaks in accretion rates within PPB-D, preceding the apparently identical

Figure 7.6. Cartoon of sedimentation phases at the northern margin of Pantano Piccolo, Vendicari.

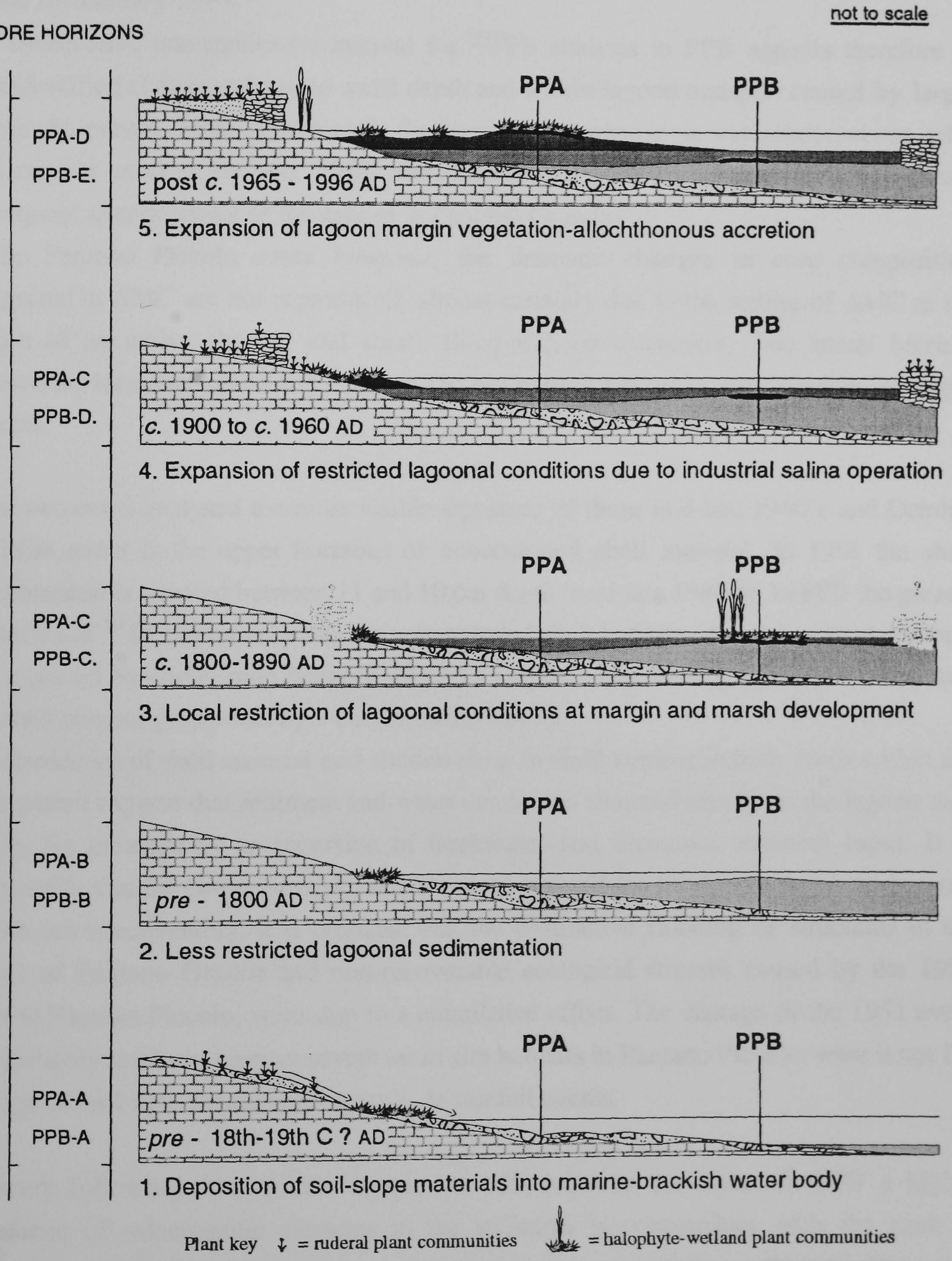

post-1980's increase recognised in both PPA and PPB, appear to correspond with recorded highs in monthly rainfall totals (Fig. 7.7.). Pronounced peaks in accretion are recognised in PPB between 16 and 15 cm depth (*circa* AD 1922), 12 and 11 cm (*circa* AD 1953) and at 6-5 cm (*circa* 1983 AD) which (taking into account error margins) appear to reflect high rainfall totals recorded in November 1920 and the close run of wet winters, December 1944, January 1946 and October 1951. A slight increase in accretion is also visible for January 1973.

The consecutive one-centimetre interval for ^{210}Pb analysis in PPB appears therefore to have identified changes related to water depth and within-lagoon transport caused by larger magnitude events. Most significantly the accretionary change is contemporaneous with high rainfall totals in October 1951, the documented year of destructive flooding and subsequent abandonment of the salinas in Pantano Grande.

In the Pantano Piccolo cores however, the dramatic changes in core composition recognised in AMC are not reproduced, almost certainly due to the setting of AMC at the margin of an active channel and small, flood-affected catchment. Too many barriers between the local catchment and Pantano Piccolo existed for major compositional changes to occur.

In the two cores analysed the most visible signature of these mid-late 1940's and October AD 1951 event is the upper horizons of concentrated shell material. In PPA the shell concentration is situated between 11 and 10 cm depth (mid-late 1940's). In PPB the greater resolution of ^{210}Pb dating indicates the concentrated shell horizon (with a low mud content) was replaced by shelly mud between 12 to 11 cm (mid-late 1940's to early 1950's) and low shell content grey muds by 9 cm (*circa* AD 1965).

The abundance of shell material and sudden drop in shell content in both cores within the same period suggest that sediment and water conditions changed rapidly in the lagoon as a whole, for example by an incursion of freshwater and increased sediment input. It is conceivable that the two prior peak rainfall events stressed the local ecology of the lagoon, though not irrecoverably. It is probable that the destructive flooding of structures in the salinas of Pantano Grande and non-recoverable ecological stresses caused by the 1951 event in Pantano Piccolo, were due to a cumulative effect. The damage of the 1951 event may possibly not have been so severe on *in situ* habitats in Pantano Piccolo, were it not for damage caused by previous high magnitude rainfall events.

Recovery following these events appear two-fold between the cores. In PPB a higher abundance of minerogenic elements in the sediment is concomitant with the start of enhanced pollen accumulation rates of well-dispersed types (e.g. *Pinus*, *Olea-Phyllirea* and Ericaceae) and local ruderal-halophyte types (i.e. Lactuceae). Following the abandonment of the salinas, the gradual deterioration of walls and embankments by wave activity

(possibly the breaching of the barrier between Pantano Piccolo and Pantano Grande) may be expected to have released a considerable amount of sediment and previously deposited pollen, i.e. the expansion of the potential catchment area of pollen sources.

Conversely at the core setting of PPA, the change in lagoonal conditions initiated the phase of *in situ* plant-derived (Amaranthaceae- Chenopodiaceae) organic accretion resembling (at least palynologically) the early-mid 19th century phase of Amaranthaceae-Chenopodiaceae dominated organic sediments in PPB (Fig. 7.6.). The continued increase (% and concentration) in Amaranthaceae-Chenopodiaceae observed suggests that without the water-level stability afforded by artificially controlled water levels, the expansion of the fringing vegetation was likely to have been limited by the range of seasonal water level fluctuations. Although marsh growth apparently stabilised organic accumulation at the margin, the setting continued to be influenced by minerogenic sedimentation and local disturbance, e.g. the order of magnitude increase in accretion *circa* AD 1982. This event appears to have been caused by the marsh surface being rapidly inundated by minerogenic-shell carbonate material, having either been derived from the fronting mudflat or from material dumped on the surface from the field/wall above. The event though appears not to have had much impact on the established salt marsh community.

The surface 10 cm of PPA and PPB represents the most recent phase of sedimentation at the northern margin of Pantano Piccolo and may be viewed as a period that saw the recovery of natural mudflat and marsh communities, after the phase of disturbance created by industrial salina operations. However the most recent and apparently indiscrimanate destruction of the salt marsh population at the northern margin of Pantano Piccolo had occurred very recently before core sample collection in September 1996. The removal of a large portion (approx. 10 m^2) of the present day marsh by fire and excavation had resulted in a severely degraded marsh community (open to wave action during high water levels) adjacent to one remaining in good condition. The impact of this event on Amaranthaceae-Chenopodiaceae pollen content in surface samples was not clear in PPA or PPB, because of the continued supply of local pollen from undisturbed communities above the core surface (discussed below in next section).

In both cores therefore from Pantano Piccolo, the recorded trend of sedimentation has been one of continued accretion. The concern held by local conservation workers, that the lagoons (especially Pantano Grande) have been progressively silting up would appear to be supported by the increased accretion rates observed over the last century in PPA and PPB, especially since industrial activity ceased and conservation efforts began. Clearly in confined shallow lagoon areas any increase in sedimentation at the margin effectively reduces the feeding area capable of supporting migratory and resident wildfowl. Much greater multi-disciplinary work is however required, to determine whether trends observed are typical of the Vendicari lagoon system or just Pantano Piccolo.

7.5.1 Recorded environmental change at the margin of Pantano Piccolo: implications for longer-term records

The rapidity of vegetational and depositional changes identified in this study would not have been identified without the high-resolution sequential sampling for many of the analyses. Although physical disturbance caused great differences to the depositional setting, it may be considered not to be a limiting factor on the quality of records potentially available. With repeat sampling in the core locality and at a higher resolution within horizons previously identified as periods of dynamic environmental change, greater detail may have been achieved.

Though the combined data generated by the two cores PPA and PPB has allowed an effective interpretation of past depositional changes at the northern margin of Pantano Piccolo, it is clear that if only one core were used for high resolution analysis the broader scale interpretation of environmental changes would have been much reduced. Although in this example, inferred "lagoon-wide" interpretations made by the analysis of either PPA or PPB, would have been effectively checked by the basic identification of local stratigraphic differences.

The timing of events and the apparent dominance of local controlling factors on depositional records identified at Pantano Piccolo, raise many questions regarding older sediment sequences and palaeoecological records, particularly coastal wetland records of relative sea level change over longer term timescales recorded in marine, estuarine and salt marsh sequences. Longer-term records of Late Quaternary sea level change and coastal development invariably sacrifice higher-resolution sedimentological analyses for determining larger-scale geomorphological trends by breaking down dating and palaeoecological analyses into a series of index horizons. Similarly the spatial resolution of sampling over an area is kept broad to identify larger-scale patterns of coastal landform development. It is however seen that even over the last century, subtle changes in water levels (less than 0.5 m) can lead to very different depositional conditions within 20 m distance of each other.

As an analogy, if lagoonal sediments were removed from Pantano Piccolo (the space occupied by PPB) by erosion, leaving behind only marginal sediments, then the interpreted sequence (PPA) would be much less representative of the setting and less capable of revealing subtle differences in palaeoenvironmental records that existed prior to erosion. Over the Late Quaternary timescale, disturbance caused by human activity and dynamic environmental changes has almost certainly continually generated conditions in coastal wetland environments, for multiple phases of erosion, deposition and mobile configurations of sediment facies.

Although usually a question of logistics and effort required to conduct high-resolution studies (especially at the resolution used in this study) on long and multiple sediment cores, it is clear that the timespan of changes recognised in this study would easily fit into the error range typical of precise radiocarbon dating and resolution of sampling used in longer term/greater depth stratigraphic investigations. Understandably, interpreting recent and shallow depths of sediments does account for much of the freedom possible for high resolution investigation. The implication remains however that many of the changes recognised in longer-term sequences, assumed as representative of the environment at the time, may be a preserved record of either short term or near instantaneous events of local environmental change.

7.6 The effectiveness of coastal wetland sediments in south-east Sicily as an archive of historical environmental change in the region

Microtidal and lagoonal depositional settings and coastal marsh plant communities in the study areas are shown to have been highly sensitive and responsive to broader hydrological changes during the previous 100-200 years in south east Sicily. Phases of organic and inorganic accretion are recognised in terms of hydrological events and patterns of human occupation.

The industrial expansion of low lying coastal-estuarine environments for the purpose of salina operations in the 19th century was a definitive phase for the development of marsh settings in the study areas. At the Mulinello core site (AMC) for example, as a response to the construction of channel-side embankments (for upstream access-wharfage and salina protection) this was a period of channel-dominated processes and the gradual establishment of salt marsh vegetation. At Pantano Piccolo the same socio-economic causes for the industrialisation of low-lying coastal areas accelerated the slow evolutionary process of lagoon enclosure by the construction of a human-made embankment, effectively separating the lagoon from its main connection to the Vendicari lagoon complex. The shutting-off of inland catchment controls on sediment supply water levels shifted marginal salt marsh communities and dramatically changed *in situ* lagoonal environments.

The period following this industrial period up to the present has been a response of channel and lagoonal environments to local and larger scale variations in catchment hydrology and dynamic wetland vegetation communities. The local variations in sedimentology and cause of depositional changes have been discussed, highlighting the influential role of regional climate (precipitation events) patterns over the last century.

The assumption that regional precipitation events should be identifiable in appropriately dated and located sediment sequences dispersed around the area, appears to hold true at

least for the mid-late AD 1940's and 1951 sequence of events (Fig. 7.7.). In both AMC and PPB a distinguishable peak in accretion is recognised in relation to this phase. The impact of this sequence of events has been observed to have affected the individual settings differently (though in both cases destructive flooding of salt marsh communities occurred) and preserved a different palaeoenvironmental signature. The 1951 rainfall event which saw totals greater than 400 mm fall across much of SE Sicily on the 11 October (Figure 4.2.4.) and localised centres of higher totals (+ 600 mm) in upland areas may clearly be considered a regional signature. Certainly the signature of this event should be identifiable in other recent sediment sequences in SE Sicily.

Although coastal wetlands in south east Sicily clearly represent only a small component of the land-ocean-atmosphere system in the central Mediterranean, the correspondence of elevated sea temperatures in the mid-1940's - 1950 (Fig. 3.7.) and recorded alluvial inputs during the same period, suggest they are capable of recording complex and broader scale environmental interactions.

It is apparent that the relatively rapid re-establishment of salt marsh vegetation (3-4 years) following the collapse of local comunities by sediment-laden floodwater, as recorded in AMC, or raised lagoon water levels between PPB-PPA, was aided by the expansion of unaffected salt marsh communities. Amaranthaceae-Chenopodiaceae and other salt marsh pollen types do not disappear from the depositional sequences following both hydrological events, indicating the continued local presence of salt marsh vegetation. Rapid re-colonisation of the AMC core site is likely to have occurred as nearby communities expanded by rhizospheric shooting and seedling growth, as well as seed transport from upstream riparian communities.

Although there is a time gap between the collapse of the halophyte community at the base of PPB-D and similar conditions prior to collapse, at the base of PPA-D of at least 100 years, the accumulation of Amaranthaceae-Chenopodiaceae in both cores during this period indicates that substantial stands of salt marsh vegetation continued to exist around the lagoon.

The spatial extent of destruction required to generate the decreased abundance of Amaranthaceae-Chenopodiaceae pollen observed in core PPB during the 19th century is highlighted by recent destruction of marsh vegetation at Pantano Piccolo. Amaranthaceae-Chenopodiaceae pollen accumulation in the upper 2 cm of PPA appears to have declined within the last five years, perhaps as a consequence of recent degradation, whereas in PPB the accumulation of Amaranthaceae-Chenopodiaceae has continued apace in the last few years.

Because of the proximity of the core PPA to the degraded area this decline may be real or an effect of decreased accretion. The relative abundance of Amaranthaceae-Chenopodiaceae would suggest that the change in accretion rate would account for much of the change. The continued rate of Amaranthaceae-Chenopodicaceae pollen accumulation at PPB would

Figure 7.7. Comparison of ^{210}Pb derived accretion rates between cores AMC, PPA & PPB and combined rainfall data* for the period 1900 to 1980

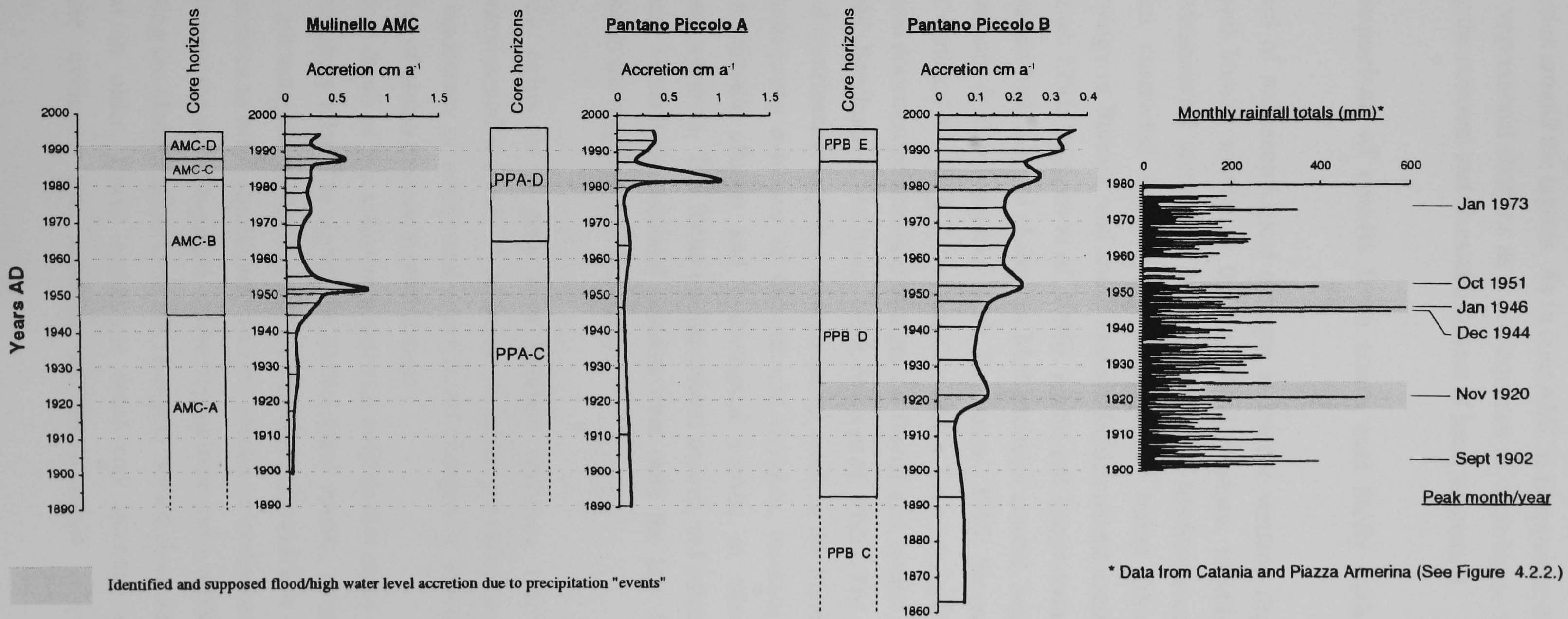

appear to not have been affected by local destruction, receiving its supply from unaffected communities around the lagoon. As in core AMC it is apparent that the sediment record of dramatic vegetational changes as a consequence of disturbance is a very localised event, involving the removal and re-establishment of local vegetation.

7.7 Comparison of results from south east Sicily with other similar studies

The record of sedimentological changes in coastal wetland deposits related to climatic change and human activity in the last 100-150 years, identified here by multi-proxy palaeoenvironmental techniques are a rarity in the Mediterranean. Aspects of this study have been conducted before, for example the recent (though un-dated) physical sedimentology of Balearic and south eastern Sicilian recent coastal wetland deposits (e.g. Amore *et al.* 1994; Pacheco *et al.* 1996), recent and longer-term palynological records of vegetation and hydrological change in Mediterranean coastal, lagoonal and deltaic settings (e.g. Planchais & Parravergara, 1984; Stevenson, 1985; Stevenson *et al.* 1993; Leroy, 1992) as well as, the long list of studies which have attempted to relate the impact of climatic and documented land-use changes on fluvial and coastal sedimentation (e.g. Vita-Finzi, 1969; Brückner & Hoffman, 1992; Maas *et al.* 1998). The strength of this work and its original contribution to palaeoenvironmental work in the Mediterranean comes from its use of multi-proxy evidence of depositional changes, resulting in the identification of short-term climatic change and hydrological events, in otherwise human-dominated depositional systems. The focus on interrelated human and natural environmental change and coastal wetland depositional patterns over only the last 100-150 years is of key importance to the originality of this study.

This study exists in a grey area between real-time monitoring and longer-term palaeoenvironmental records. A situation therefore providing a critical viewpoint of the potential inaccuracy of interpreted depositional changes in low-temporal resolution long-term studies of global environmental change.

The physical depth of the sediment sequences used in this study and the subtle variations of sedimentology related to significant hydrological events, identified by high resolution sampling, are testament to the fact that a potential exists with low-resolution, index-horizon dated sequences to miss significant changes related to environmental change. Clearly in older sediments the actual logistics of identifying these more subtle trends is a major factor in preventing the identification of subtle changes. Nonetheless when dramatic changes are recognised in older, lower resolution dated and sampled sequences, the lack of intermediate evidence can produce an interpretation which automatically infers

environmental change *via* high magnitude, low frequency events than unobserved precursory gradual changes.

Depositional changes identified in Holocene salt marsh sequences in California identified by Davis *et al.* (1992) serves as a suitable example. Although indisputable that long term global climatic change and Late Holocene climatic instability caused excessive amounts of freshwater (bringing in non-local land pollen) to enter coastal marsh areas, the resolution of ^{14}C-dating and subsequent pollen accumulation rates provide little information as to the actual rate of change, i.e. is the record that of a single flood or the preserved record of one of a number of floods that occurred successively over a period of 10-100 years or less.

It is hardly surprising that factors identified in this research, such as the importance of local environmental changes and the fact that nearby, similarly aged deposits may infer a different sequence of events are naturally glossed over in the interpretation of longer-term, broader-scale records of global environmental change due primarily to the logistics of interpreting multiple sediment sequences. Although to the detriment of interpreting longer-term trends in environmental change, this study at least provides an example of the spatial and temporal variability of deposition in predominantly low energy, mixed organic/inorganic coastal sediments, which commonly occur in long term sequences recording relative sea level change and coastal sedimentation.

The rate of changes identified in this study when compared to measurements of actual changes in Mediterranean coastal wetlands affected by alluvial flooding or erosion (e.g. e.g. the Rhône delta, France (Hensel *et al.* 1998) and the Venice lagoon, Italy (Day *et al.* 1999) are comparable, i.e. the same order of magnitude in changes of accretion on marsh surfaces. These recent monitoring studies also clearly out-do recent depositional histories by their measurement of the spatial variability of coastal wetland dynamics.

In particular findings in this study complement those few studies which have been conducted in Mediterranean catchments on recent geomorphological changes and changes over the last two centuries as discussed in Chapter 3. This study provides a necessary progression from recording changes following on from the climatically unstable period of the Little Ice Age, to those that have occurred within the last century. For example the study by Maas *et al.* (1998) identified three alluvial units which were deposited in Crete since the late 19th century. The first apparently due to increased precipitation in the Eastern Mediterranean from AD 1871 to 1947, the next two apparently related to single flood events which occurred during the period AD 1968 to 1989. These most recent coarse-grained deposits were identified by air photographs rather than ^{14}C and lichenometric dating which had been used on older sediments. The radionuclide dating of downstream sediments in this study would be a natural progression from the above example, to compare the timing of upstream and downstream changes in erosion and sedimentation with coastal sedimentation. Achieving a high-resolution dating timescale allows a tighter

interpretation to be made between "locally" recorded climatic data and sedimentological evidence suggestive of high magnitude flood events or other dynamic processes. It is clear that to identify linkages between recent climatic change, catchment processes and sediment transport/deposition over time a holistic approach is vital.

Compared with other multi-proxy sedimentological studies conducted to determine the relationship between the historical human modification of catchment areas and hydrological/climatic variability over the last century (e.g. Stevenson & Batterbee, 1991; Heathwaite, 1993; Gale *et al.* 1995; Rhodes & Davis, 1995; Sheffield *et al.* 1995; Wohlfarth *et al.* 1998; Cronin *et al.* 2000), it is regrettable that, for the catchments used in this study, there was a lack of smaller-scale and more gradualistic evidence of environmental change. The interpretation of recognised depositional changes at the Mulinello salt-marsh and from Pantano Piccolo would have greatly benefited from more historical data regarding land-use from the upstream catchments and the lagoon complex, as for example the multi-proxy records of land-use used in the study of deposition in Slapton Ley, Devon, UK (Heathwaite, 1993).

Thus the main regret lies in the fact that in this study it was not that depositional changes could not be identified or temporally constrained within human-disturbed settings, rather subtle sedimentological differences proved difficult to relate to "actual" historical environmental changes.

Analogous to a coarse resolution sampling strategy which identifies only major changes, documentary evidence of land-use changes and environmental change over the last hundred years in this study have been related to large magnitude events, i.e. floods, which warranted attention largely because of their destructive impact on socio-economic systems.

7.8 Coastal wetlands in south-east Sicily as a threatened environment: implications for the Mediterranean

It is clear that the salt marsh communities encountered in this study have been able to respond and recover positively to major changes that affected the coastal wetland settings in the last two centuries, and would also not be in their current state were it not for historical anthropogenic disturbance and the irregular inputs of sediment material. Their continued presence indicating their resilience to environmental change and adaptive capability to survive dramatic environmental changes.

An important concern for the future vulnerability and spatial pattern of coastal wetlands in south east Sicily, and microtidal wetlands in the Mediterranean as a whole, is highlighted by the past temporal and spatial patterns of disturbance and recovery recorded in the cores studied. Organic accretion and local communities of halophyte vegetation were seen to

have been rapidly recoverable only when detrimental stresses were removed and re-colonisation could occur. However when suitable growing conditions are prevented by continued ecological-physical stresses and potential communities capable of re-colonising the area are reduced (as is occurring at the present day at the Mulinello site), the potential of wetland regeneration is greatly reduced.

Already confined by the narrow spatial margin of microtidal-hydrological conditions, local relief and existing anthropogenic structures, the future existence of coastal wetlands in south east Sicily outside of areas afforded room for landward regression or refuge from disturbance appears unpromising, especially in light of predicted future sea level trends for the next century and the rapidity of seemingly unchecked coastal development and destruction of coastal wetland areas in the Mediterranean.

Chapter Eight

Conclusions

8.1 Conclusions

The deposition of coastal wetland sediment sequences in south east Sicily has been particularly effective in recording environmental changes caused by human activity and significant precipitation events during the last century. Industrial-agricultural development in the study areas has locally dominated controls on deposition since at least the mid-19th century. Significant phases of disturbance and recovery caused by alluvial flooding events however, remained the major control in the development and status of present-day microtidal-lagoonal coastal wetlands.

The successful application of gathering multi-proxy palaeoenvironmental data from short-core coastal wetland sequences in microtidal estuarine and lagoonal settings have allowed local anthropogenic changes to be differentiated against local and catchment-scale controls on sediment transport and deposition. Regional changes due to sea level rise and tectonic activity over this short timescale are not identified, due to the dominance of local controls, e.g. the artificial raising of lagoon water levels for the local salt industry.

The importance of alluvial flooding to marsh dynamics and maintenance of brackish-saline water levels in Mediterranean microtidal estuarine-lagoonal settings was demonstrated in the analysed core sequences from the Mulinello estuary, Augusta and Pantano Piccolo, nr. Noto in south east Sicily. For the immediate post war period, i.e. 1945-1951 AD, accretionary and compositional changes recognised can be seen to coincide with documented peaks in precipitation and associated episodes of high channel discharge/water levels.

^{210}Pb was used successfully for dating recent depositional sequences which have been affected by considerable variations in sedimentation over the last century and a half. Resulting compositional variations and accretion rates greatly affected the radionuclide profiles determined for each core, though without too significant an effect on existing dating models. The significant discrepancy between ^{210}Pb and ^{137}Cs when used in combination for dating AMC, highlighted a significant potential for errors using radionuclide dating in disturbed microtidal sediment sequences of variable composition.

Shifts between organic-associated and more minerogenic sediments were identifiable with historical patterns of local hydrodynamics as a result of the close interaction between intra-estuarine/lagoonal processes and responsive local salt marsh communities.

Pollen concentrations and accumulation rates indicate the importance of sediment supply and accretion on the final assemblage of grains in a horizon, with temporal and spatial trends of surrounding vegetation communities. Pollen assemblages of salt marsh and terrestrial soil surfaces were dominated by pollen types derived primarily by gravity fallout. Organic-enhanced sediments/peats are shown to have been clearly related with conditions supporting the growth of Chenopodiaceae-pollen producing plants, i.e. salt marsh vegetation.

Pollen assemblages from estuarine and lagoonal sediments were dominated by a few recognisable pollen types, namely Chenopodiaceae, Poaceae, Lactuceae, *Olea* and *Pinus*. Periods of organic accumulation reflecting the stabilisation of sediment surfaces and growth of halophytic vegetation (e.g. *Salicornia* sp.) are dominated by Chenopodiaceae pollen. Abrupt and lowered values of Chenopodiaceae pollen are met by enhanced Lactuceae, Poaceae and ruderal pollen types. Disturbance to marsh communities are therefore recognised by the influx of extra-local ruderal pollen.

Abundances of major and trace elements in core sequences were greatly influenced by the presence of organic matter, either plant derived or biogenic (shell material). The geochemical trends identified were primarily a result of stratigraphic variations, reflecting palaeo-hydrological influences. Major element abundances associated with contemporary surface environments (i.e. elevated phosphorous) were preserved, to an extent, in buried salt marsh soils.

The use of multi-proxy palaeoenvironmental evidence in coastal wetland settings has indicated the importance of using independent sources of sedimentological data to justify and assist in the interpretation of changes in recent sedimentation.

8.2 Proposals for further research

Although much work has been carried out on the use of salt marsh and recent depositional environments as archives for environmental change, a number of themes identified during this study require further attention.

(i) *Within disturbed or artificially created coastal wetland settings, conditions exist for the preservation of local and external signatures of environmental change.*

A basis for the re-evaluation of existing data and detailed sediment investigation of coastal wetland sequences, integrated with archaeological and historical information, is provided by the findings of this study. While sedimentological studies may have done much to characterise pre-anthropogenic disturbance phases and following historical patterns of

recovery, depositional patterns during an "occupational" phase (at least the last 100-150 years in the example of this study) are seen to have been sensitive to both anthropogenic and inherent environmental processes.

Palaeoenvironmental differences, recognised spatially (< 20 m) between cores in Pantano Piccolo and in sediment sequences (on a centimetre scale) from cores used in this study suggest that much more detailed palaeoenvironmental reconstructions are obtainable from archaeological and historical sites in coastal areas around the Mediterranean.

As tectonic, climatic and ecological differences in the Mediterranean are recognised to have been detrimental in the identification of synchronous alluvial and coastal sedimentation phases over longer timescales, this study would suggest that more detailed sediment investigations (i.e. higher resolution core-sampling and greater spatial density of core sites) are able to identify significant (perhaps un-recognised) events attributable to either local or regional environmental changes.

A "bottom-up" approach to determining regional similarities by increased local coverage presents nonetheless an enormous task for associated workers, especially when greater depths of sequences are required to be analysed. It is advocated here that due to the greater existence of documented records of environmental change during this century, research should be focused on coastal wetland sediments deposited in the last hundred years.

Linkages over the same timescale between upstream catchment changes and coastal settings should also be identified by geomorphological mapping, historical documentation and sediment analyses. Ideally linkages related to annual-decadal scale sedimentation patterns should also be identified offshore.

(ii) *The use of wetland sediments in SE Sicily as an archaeological-historical archive of the vectoral transmission of malaria.*

Coastal wetland areas in Sicily have been in the past central to both the proliferation of malaria and the controlled eradication of the disease in 1947 AD. As it is clear that coastal wetland sediments in the region have been responsive to hydrological and anthropogenic changes, a potential may exist for recording the incidence of the disease by the preserved remains of *Anopheles* sp. Efforts being made by the author of this work, in conjunction with Italian workers (P. Nicoletti, *Istituto di Ricerca per la Protezione Idreologica, Cosenza*, pers comm.) to the viability of research, to investigate an extremely important aspect of the relationship between society, malaria and coastal wetland areas.

As has been shown by work in south east Sicily, this incidence of malaria in previously unaffected areas, was due to the effect of seismically triggered landslide, it is clear that the effect of expanding coastal wetlands due to enhanced, catchment-derived sedimentation

must have had a dramatic effect on historical patterns of population and land-use in the coastal zone.

The generation of data examining the relationship between the incidence of malaria and environmental changes (i.e. the expansion-contraction of wetland areas due to damming or climate change) has much significance for areas still affected by malaria, for example the highlands of Ethiopia (Ghebreyesus *et al.* 1999) and those areas which may start to show a higher incidence (or even return, as in southern England) due to predicted future climate changes/reduction in malaria control methods.

(ii) *The study of deeper sequences encountered during fieldwork should provide an archive of longer term coastal evolution in south east Sicily.*

Deeper sediment sequences identified during fieldwork at the Mulinello estuary and at the Tellaro floodplain and Calamosche inlet in the Vendicari reserve, indicate a considerable archive of depositional changes. These sequences should also be analysed at a resolution and with the same techniques as used in this study, to provide a longer term background of the impact and interaction of anthropogenic activity in upstream catchments and coastal processes. Certainly a focus should be identfying periods of sedimentation contemporaneous with the known historical occupation of the local area/catchment.

Questions remain concerning Holocene relative sea level changes and coastal evolution that have occurred in the region. These preliminary investigations of deeper sequences suggest that they may contain much information on the geomorphological and anthropogenic evolution of south-east corner of Sicily. A concern for future investigation of coastal wetlands in the region is that continued development (exemplified at the Augusta site) will cause many problems requiring future study.

REFERENCES

Abbot, J. T. and Valastro, Jr., S. (1995). The Holocene alluvial records of the chorai of Metapontum, Basilicita and Croton, Calabria, Italy. *In*: Lewin, J., Macklin, M.G. and Woodward, J.C. (eds.), *Mediterranean Quaternary River Environments*. A.A. Balkema, Rotterdam, 195-205.

Abdel-Razik, M. S. and Ismail, A. M. A. (1990). Vegetation composition of a maritime salt marsh in Qatar in relation to the edaphic features. *Journal of Vegetation Science*, **1**, 85-88.

Adam, P. (1990). *Saltmarsh ecology*. Cambridge University Press, Cambridge.

Adorni, G. and Carveni, P. (1993). Geomorphology and seismotectonic elements in the Giarre area, Sicily. *Earth Surface Processes and Landforms,* **18**, 275-283.

Agnesi, V., Macaluso, T. and Masini, F. (1998). L'Ambiente e il clima della Sicilia nell'ultimo milione di anni. *In*: Agnesi, V., Macaluso, T. and Masini, F. (eds.) *Prima Sicilia: alle origini della società siciliana (Vol I)*. Palermo, 31-56.

Alexander, C. R., Smith, R. G., Calder, F. D., Schropp, S. J. and Windom, H. L. (1993). The historical record of metal enrichment in two Florida estuaries. *Estuaries*, **16**, 627-637.

Alexander, R. W. and Calvo, A. (1990). The influence of lichens on slope processes in some Spanish badlands. *In*: Thornes, J. B. (ed.), *Vegetation and Erosion.*, John Wiley and Sons Ltd., Chichester, 385-398.

Allen, J. R. L., Rae, J. E. and Zanin, P. E. (1990). Metal speciation (Cu, Zn, Pb) and organic matter in an oxic salt marsh, Severn Estuary, South-west Britain. *Marine Pollution Bulletin*, **21**, 574-580.

Allen, J. R. L., Rae, J. R., Longworth, G., Hasler, S. E. and Ivanovich, M. (1993). A comparison of the 210-Pb dating technique with three other independent dating methods in an oxic estuarine salt-marsh sequence. *Estuaries,* **16**, 670-677.

Allen, J. R. M., Brandt, U., Brauer, A., Hubberten, H-W., Huntley, B., Keller, J., Kraml, M., Mackensen, A., Mingram, J., Negendank, J. F. W., Nowaczyk, N. R., Oberhänsli, H., Watts, W. A., Wulf, S. and Zolitschka, B. (1999). Rapid environmental changes in southern Europe during the last glacial period. *Nature,* **400**, 740-743.

Allison, S. K. (1995). Recovery from small-scale anthropogenic disturbances by Northern California salt marsh plant assemblages. *Ecological Applications,* **5**, 693-701.

Allison, S. K. (1996). Recruitment and establishment of salt marsh plants following disturbance by flooding. *American Midland Naturalist*, **136**, 232-247.

Altunel, E. (1999). Geological and geomorphological observations in relation to the 20 September 1899 Menderes earthquake, Western Turkey. *Journal of the Geological Society,* **156**, 241-246.

Alvisi, F. and Frignani, M. (1996). ^{210}Pb-derived sediment accumulation rates for the central Adriatic Sea and crater lakes Albano and Nemi (central Italy). *Mem. Ist. Ital. Idrobiol.*, **55**, 303-320.

Amiaud, B., Bouzille, J. B., Tournade, F. and Bonis, A. (1998). Spatial patterns of soil salinities in old embanked marshlands in western France. *Wetlands*, **18**, 482-494.

Amore, C., D'Alessandro, L., Giuffrida, E., Lo Giudice, A., Randazzo, G. and Zanini, A. (1990). *First data about shoreline evolution along the coasts of eastern Sicily*. Littoral 1990 Eurocoast Conference Proceedings, Marseille, p.284-292

Amore, C., Costa, B., Di Geronimo, S., Giuffrida, E., Randazzo, G. and Zanini, A. (1994). Temporal evolution, sediments and fauna of the Vendicari lagoons. *In*: Matteucci *et al.* (eds.), *Studies on Ecology and Palaeoecology of Benthic communities.* Modena, Boll. Soc. Paleontol. Ital, **2**, 1-15.

Amore, C., Costa, B., Randazzo, G. and Zanini, A. (1997). Environmental evolution of the Longarini and Cuba lagoons (southeastern Sicily). *Rivista Italiana di Paleontologia é stratigrafia*, **103**, 3-14.

Amore, C. and Randazzo, G. (1997). First data on the coastal dynamics and the sedimentary characteristics of the area influenced by the River Irminio basin (SE Sicily). *Catena*, **30**, 357-368.

Andreu, V., Rubio, J. L. and Cerni, R. (1995). Effect of Mediterranean shrub on water erosion control. *Environmental Monitoring and Assessment*, **37**, 5-15.

Andrews, R. and Brown, J. (1993). *Sicily: The Rough Guide*. Rough Guides Ltd. London.

Appleby, P. G. and Oldfield, F. (1978). The calculation of Pb-210 dates assuming a constant rate of supply of unsupported Pb-210 to the sediment. *Catena,* **5**, 1-8.

Appleby, P. G. and Oldfield, F. (1992). Application of 210-Lead to sedimentation studies. *In*: M. Ivanovich and Harmon, R.S. (eds.), *Uranium series disequilibrium applications to earth, marine and environmental sciences*. Oxford Science, 2nd Ed, Oxford, 731-783.

Argenti, N. (1998) Dati pluviometrici stazione di Piazza Armerina. *http://www.ggg.it/geologia/pluviometrie/ARMERINA.htm*. Accessed: 12/17/98.

Armentano, T. V. and Woodwell, G. M. (1975). Sedimentation rates in a Long Island marsh determined by ^{210}Pb dating. *Limnology and Oceanography*, **20**, 452-456.

Armienti, P., Innocenti, F., Petrini, R., Pompilio, M. and Villari, L. (1989). Petrology and Sr-Nd isotope geochemistry of recent lavas from Mt. Etna: bearing on the volcano feeding system. *Journal of Volcanology and Geothermal Research,* **39**, 315-327.

Arndt, J. L. and Richardson, J. L. (1993). Temporal variations in the salinity of shallow groundwater from the periphery of some North Dakota wetlands, U.S.A. *Journal of Hydrology,* **141**, 75-105.

Arnaud-Fasseta, G. and Provansal, M. (1999). High frequency variations of water flux and sediment discharge during the Little Ice Age (AD 1586-1725) in the Rhône Delta (Mediterranean France): Relationship to the catchment basin. *Hydrobiologia*, **410**, 241-250.

Atherden, M., Hall, J. and Wright, J.C. (1993). A pollen diagram from the northeast Peloponnese, Greece: implications for vegetation history and archaeology. *The Holocene*, **3, 4**, 351-356.

Bacci, G. (1982-3). Antico stabilimento per la pesca e la lavorazione del tonno presso Portopalo. *Kokalos,* **28-29**, 343-347.

Badalementi, F., Calandra, V. and Dongarrà, G. (1985). L'approccio idrogeochemico nell'analisi di un ecosistema naturale: La zona umida di Vendicari, Sicilia. *Natura,* **76**, 3-17.

Baeteman, C. (1985). Late Holocene geology of the Marathon Plain. *Journal of Coastal Research,* **1**, 173-185.

Baldwin, A. H. and Mendelssohn, I. A. (1998). Effects of salinity and water level on coastal marshes: an experimental test of disturbance as a catalyst for vegetation change. *Aquatic Botany,* **61**, 255-268.

Ballais, J.-L. (1995). Alluvial Holocene terraces in eastern Maghreb: climate and anthropogenica controls. *In*: Lewin. J., Macklin, M. G. and Woodward, J. C. (eds.), *Mediterranean Quaternary River Environments*. A.A. Balkema, Rotterdam, 183-205.

Ballouche, A. and Carruesco, C. (1986). Holocene evolution of a lagoon ecosystem, Qualidia, Morocco. *Revue de Géologie dynamique et de Géographie Physique,* **27**, 113-118.

Barber, K. E., Battarbee, R. W., Brooks, S. J., Eglington, G., Haworth, E. Y., Oldfield, F., Stevenson, A. C., Thompson, R., Appleby, P. G., Austin, W. E. N., Cameron, N. G., Ficken, K. J., Golding, P., Harkness, D. D., Holmes, J. A., Hutchinson, R., Lishman, J. P., Maddy, D., Pinder, L. C. V., Rose, N. L. and Stoneman, R. E. (1999). Proxy records of climate change in the UK over the last two millenia: documented change and sedimentary records from lakes and bogs. *Journal of the Geological Society,* **156**, 369-380.

Barker, G. W. and Hunt, C.O. (1995). Quaternary valley floor erosion and alluviation in the Biferno Valley, Molise, Italy: The role of tectonics, climate, sea level change, and human activity. *In:* Lewin, J., Macklin, M. G. and Woodward, J. C. (eds.) *Mediterranean Quaternary River Environments*. A. A. Balkema, Rotterdam, 145-157.

Barrata, M. (1910). *La catastrofe sismica calabro messinese (28 dicembre 1908).* II Vols. Palermo.

Basile, B., Di Stefano, G. and Lena, G. (1986). Landings, Ports, Coastal Settlements and Coastlines in Southeastern Sicily from Prehistory to Late Antiquity. *British Archaeological Reports, International Series,* **404**, 15-33.

Basset, P. A. (1976). The vegetation of a Camargue pasture. *Journal of Ecology,* **66**: 803-827.

Bates, C. D., Coxon, P. and Gibbard, P.L. (1978). A new method for the preparation of clay-rich sediment samples for palynological investigation. *New Phytologist,* **81**, 459-463.

Battiston, G. A., Degetto, S., Gerbasi, R., Sbrignadello, G. and Tositti, L. (1988). The use of Pb-210 and Cs-137 in the study of sediment pollution in the Lagoon of Venice. *Science of the Total Environment,* **77**, 15-23.

Beeftink, W. G. (1979). The structure of salt marshes in relation to environmental disturbances. *In*: Jeffries, R. L. and Davy, A. J. (eds.), *Ecological processes in coastal environments*. Blackwell Scientific Publications, Oxford, 77-94.

Bell, A. G. (1982). The effects of land-uses and climate on valley sedimentation. *In*: A. F. Harding (ed.), *Climatic change in later Prehistory*. University Press, Edingburgh, 127-147.

Bellotti, P., Milli, S. Totora, P. and Valeri, P. (1995). Physical stratigraphy and sedimentology of the Late Pleistocene-Holocene Tiber delta depositional sequence. *Sedimentology,* **42**, 617-634.

Benito, G., Machado, M. J., & P_rez-Gonz‡lez, A. (1996). Climate change and flood sensitivity in Spain. *In*: A. G. Brown, J. Branson & Gregory, K. J. (eds.)*Global Continental Changes: the Context of Palaeohydrology*. Geological Society Special Publication, **115**, 85-98.

Bennett, K. D., Boreham, S., Sharp, M. J. and Switsur, V. R. (1992). Holocene history of environment, vegetation and human settlement on Catta Ness, Lunnasting, Shetland. *Journal of Ecology,* **80**, 241-273.

Benninger, L. K., Aller, R. C., Cochran, J. K. and Turekian, K. K. (1979). Effects of biological sediment mixing on the ^{210}Pb chronology and trace metal distribution in a Long Island Sound sediment core. *Earth and Planetary Science Letters,* **43**, 241-259.

Benson, B. E., Grimm, K. A., Clague, J. J. (1997). Tsunami deposits beneath tidal marshes on northwestern Vancouver Island, British Columbia. *Quaternary Research,* **48**, 192-204.

Berliner, R., Jacoby, B. and Zamski, E. (1987). Mycorrhiza is essential for phosphate supply to *Cistus incanus* L. on native soils in northern Israel. *Journal of Plant Nutrition*, **10**, 1323-1330.

Berner, R. A. (1981). A new geochemical classification of sedimentary environments. *Journal of Sedimentary Petrology,* **51**, 359-365.

Bertness, M. D. and Ellison, A., M. (1987). Determinants of pattern in a New England salt marsh plant community. *Ecological Monographs,* **57**, 129-147.

Bhiry, N. and Filion, L. (1996). Characterization of the soil hydromorphic conditions in a paludified dunefield during the Mid-Holocene Hemlock Decline near Québec City, Québec. *Quaternary Research,* **46**, 281-297.

Bierman, P., Lini, A., Zehfuss, Church, A, Thompson-Davis, P., Southton, J. and Baldwin, L. (1997). Postglacial ponds and alluvial fans: Recorders of Holocene landscape history. *GSA Today,* **7**, 1-8.

Bintliff, J. (1981). Archaeology and the Holocene evolution of coastal plains in the Aegean and Circum-Mediterranean. *In*: D. Brotherwell and Dimbleby, G. (eds.), *Environmental aspects of Coasts and Islands*. Oxford, British Archaelogical Reports International Series,**94**, 11-31.

Bintliff, J. L. (1975). Mediterranean alluviation: new evidence from archaeology. *Proceedings of the Prehistorical Society*, **41**, 78-84.

Boccone, P. (1697). Intorno il terremoto della Sicilia, seguito l'anno 1693. *In*: *Museo di fisica e di esperienze variato, e decorato di Osservazioni naturali, Note medicinali, e Ragionamenti secondo i Principij de'Moderni.*

Boër, B. (1996). Plants as soil indicators along the Saudi coast of the Arabian Gulf. *Journal of Arid Environments*, **33**, 417-423.

Bonfiglio, L. and Piperno, M. (1996). Early Faunal and Human Populations. *In*: R. Leighton (ed.), *Early Societies in Sicily: new developments in archaeological research.* Accordia Research Centre, University of London, London, **5**, 21-31.

Bonfiglio, L. and Insacco, G. (1992). Paleoenvironmental, Paleontological and stratigraphic significance of vertebrate remains in Pleistocene limnic and alluvial deposits from Southeastern Sicily. *Palaeogeography, Palaeoclimatology, Palaeoecology,* **95**, 195-208.

Bonny, A. P. (1976). Recruitement of pollen to the seston and sediment of some Lake District lakes. *Journal of Ecology,* **64**, 859-887.

Bordonaro, S., Di Grande, A., Raimondo, W. (1984). Lineamenti geomorfostratigrafici pleistocenici tra Melilli, Augusta e Lentini, (Siracusa). *Boll. Acc. Gioenia. Sci. Nat.,* **17**, 65-88.

Bordoni, P. and Valensise, G. (1998). Deformation of the 125 ka marine terrace in Italy: tectonic implications. *In*: Stewart, I. S. and Vita-Finzi, C. (eds.), *Coastal Tectonics.* Geological Society of London Special Publication,**146**, 71-110.

Bottema, S. (1980). Palynological investigations on Crete. *Review of Palaeobotany and Palynology,* **31**, 193-217.

Bottema, S. (1982). Palynological investigations in Greece with special reference to pollen as an indicator of human activity. *Palaeohistoria*, **24**, 257-289.

Bottema, S. and Woldring, H. (1990). Anthropogenic indicators in the pollen record of the Eastern Mediterranean. *In*: S. Bottema, Entjes-Nieborg, G. and Van Zeist, W. (eds.), *Man's role in the shaping of the Mediterranean landscape*. A. A. Balkema, Rotterdam, 231-264.

Bressolierbousquet, C. (1991). Geomorphological effects of land reclamation in the 18th century at the mouth of the Leyre River, Arcachon Bay, France. *Journal of Coastal Research,* **7**, 113-126.

Brezonik, P. L. and Engstrom, D. R. (1998). Modern and historic accumulation rates of phosphorous in Lake Okeechobee, Florida. *Jouranl of Paleolimnology,* **20**, 31-16.

Bricker, S. B. (1993). The History of Cu, Pb and Zn inputs to Narragansett Bay, Rhode Island as recorded by salt marsh sediments. *Estuaries,* **16**, 589-607.

Brückner, H. (1986). Man's impact on the evolution of the physical environment in the Mediterranean Region in historical times. *Geojournal,* **13.1**, 7-17.

Brückner, H. and Hoffman, G. (1992). Human induced erosion processes in Mediterranean countries-evidence from archaeology, pedology and geology. *Geökoplus,* **3**, 97-110.

Brugam, R. B. (1978). Human disturbance and the historical development of Linsley Pond. *Ecology,* **59**, 19-36.

Brullo, S., and Furnari, F. (1977). *La vegetazione palustre in Sicilia.* Atti II Congresso Siciliano di Ecologia, Noto, Istituto di Botanica, Universita di Catania.

Brullo, S., Fagotto, F. and Marceno. (1980). *Carta della vegetazione di Vendicari, Sicilia.* Consiglio Nazionale delle Richerche, Roma.

Brush, G. S. and DeFries, R. S. (1981). Spatial distributions of pollen in surface sediments of the Potomac estuary. *Limnol. Oceanogr.,* **26**, 295-309.

Bull, L. J., Kirkby, M. J., Shannon, J. and Hooke, J. M. (1999). The impact of rainstorms on floods in ephemeral channels in southeast Spain. *Catena*, **38**, 191-209.

Butler, R. W. H., Grasso, M., and La Manna, F. (1992). Origin and deformation of the Neogene-Recent Maghrebian foredeep at the Gela Nappe, SE Sicily. *Journal of the Geological Society,* **149**, 547-556.

Caçador, I., Vale, C. and Catarino, F. (1996). Accumulation of Zn, Pb, Cu, Cr and Ni in sediments between roots of the Tagus Estuary salt marshes, Portugal. *Estuarine, Coastal and Shelf Science*, **42**, 393-403.

Cahoon, D. R., Lynch, J.C. and Powell, A.N. (1996). Marsh vertical accretion in a southern California estuary, U.S.A. *Estuarine Coastal and Shelf Science,* **43**, 19-32.

Cahoon, D. R. and Lynch, J. C. (1997). Vertical accretion and shallow subsidence in a mangrove forest of southwestern Florida, USA. *Mangroves and Salt Marshes,* **1**, 173-186.

Callaway, J. C., DeLaune, R.D. and Patrick Jr, W.H. (1998). Heavy metal chronologies in selected coastal wetlands from Northern Europe. *Marine Pollution Bulletin,* **36**, 82-96.

Callaway, R. M., Jones, S. and Parikh, A. (1990). Ecology of a Mediterranean-climate estuarine wetland at Carpinteria, California: Plant distributions and soil salinity in the upper marsh. *Canadian Journal of Botany,* **68**, 1139-1146.

Calvo, S., Barone, R., NaselliFlores, L., Frada Orestano, C., Dongarra, G., Lugaro, A. and Genchi, G. (1993). Limonological studies on lakes and reservoirs of Sicily. *Il Naturalista Sicilia*, **17**, 1-292.

Calvo, S., Marceno, C., Ottonello, D., Orestano, C. F., Romano, S., Longo, A. (1995). Osservazioni Naturalistiche ed Ecologiche intorno al lago Pergusa. *Il Naturalista Siciliano,* **14**, 63-84.

Campbell, I. D. and Campbell, C. (1994). Pollen preservation: Experimental wet-dry cycles in saline and desalinated sediments. *Palynology,* **18**, 5-10.

Cannarozzo, M., Dasaro, F. and Ferro, V. (1995). Regional rainfall and flood frequency analysis for Sicily using the 2-component extreme value distribution. *Hydrological Sciences Journal,* **40**, 19-42.

Carbone, S., Di Geronimo, I., Grasso, M., Iozzia, S. and Lentini, F. (1982). I terrazi marini dell'area Iblea (Sicilia Sud-Orientale): Contributi conculsivi per la realizzazione delle carta Neotettonica d'Italia. *Publ. Consigli Nazionale delle Ricerche,* **506**, 1-35.

Carrión, J. S., Dupré, M., Pilar-Fumanal, M., Montes, R. (1995). A palaeoenvironmental study in semi-arid southeastern Spain: the palynological and sedimentological sequence at Perneras Cave (Lorca, Murcia). *Journal of Archaeological Science,* **22**, 355-367.

Carruesco, C. and Lapaquellerie, Y (1985). Heavy metal pollution in the Arcachon Basin (France): bonding states. *Marine Pollution Bulletin,* **16**, 493-497.

Cartaxana, P. and Lloyd, D. (1999). N_2, N_2O and O_2 profiles in a Tagus estuary salt marsh. *Estuarine, Coastal and Shelf Science,* **48**, 751-756.

Castagna, A., Sinatra, F., Castagna, G., Stoli, A. and Zafarana, S. (1985). Trace element evaluations in marine organisms. *Marine Pollution Bulletin,* **16**, 416-419.

Catalano, R., Di Stefano, P., and Vitale, F. P. (1995). Structural trends and palaeogeography of the central and western Sicily belt: new insights. *Terra Nova,* **7**, 179-188.

Cavallaro, C. (1991). Parcs et reserves naturelles en Sicilie; Un parimoine culturel, economique et social. *Mediterranee,* **72**, 57-68.

Cencini, C. (1998). Physical processes and human activities in the evolution of the Po delta, Italy. *Journal of Coastal Research,* **14**, 774-793.

Cerda, A. (1997). Soil erosion after land abandonment in a semi arid environment of southeastern Spain. *Arid Soil research and Rehabilitation,* **11**, 163-176.

Cerda, A. (1998). The influence of geomorphological position and vegetation cover on the erosional and hydrological processes on a Mediterranean hillslope. *Hydrological Processes,* **12**, 661-671.

Cerda, A. (1998). Soil aggregate stability under different Mediterranean vegetation types. *Catena*, **32**, 73-86.

Chambers, R. M. and Odum, W. E. (1990). Porewater oxidation, dissolved phosphate and the iron curtain: Iron-phosphorous relations in tidal freshwater marshes. *Biogeochemistry,* **10**, 37-52.

Chapman, V. J. (1960). *Saltmarshes and Salt Deserts of the World.* Leonard Hill, London.

Chester, D. K., Duncan, A. M., Guest, J. E. and Kilburn, C. R. J (1985). *Mount Etna, the anatomy of a volcano*. London, Chapman and Hall.

Chester, D. K. and Duncan, A. M. (1982). The interaction of volcanic activity in Quaternary times upon the evolution of the Alcantara and Simeto Rivers, Mount Etna, Sicily. *Catena*, **9**, 319-342.

Chmura, G. L. and Eisma, D. (1995). A palynological study of surface and suspended sediments on a tidal flat: implications for pollen transport and deposition in coastal waters. *Marine Geology,* **128**, 183-200.

Church, T. M., Lord, C.J. and Somayajulu, B. L. K. (1981). Uranium, Thorium and Lead nuclides in a Delaware salt marsh sediment. *Estuarine, Coastal and Shelf Science,* **13**, 267-275.

Clark, J. S., and Patterson, W. A. (1985). The development of a tidal marsh: upland and oceanic influences. *Ecological Monographs,* **55**, 189-217.

Clark, J. S. (1986a). Late Holocene vegetation and coastal processes at a Long Island tidal marsh. *Journal of Ecology,* **74**, 561-578.

Clark, J. S. (1986b). Dynamism in the barrier-beach vegetation of Great South Beach, New York. *Ecological Monographs,* **56**, 97-126.

Clark, M. (1989). *Modern Italy 1871-1982*. Longman, London.

Cochran, J. K., Hirschberg, D. J., Wang, J. and Dere, C. (1998). Atmospheric deposition of metals to coastal waters (Long Island Sound, New York U.S.A.): Evidence from Saltmarsh deposits. *Estuarine, Coastal and Shelf Science,* **46**, 503-522.

Colacicchi, R. (1963). Geologia del territorio di Pachino (Sicilia Orientale). *Geologia Romana,* **2**, 343-404.

Collier, R. E. L., Leeder, M.R., Rowe, P.J. and Atkinson, T.C. (1992). Rates of tectonic uplift in the Corinth and Megara Basins, Central Greece. *Tectonics,* **11**, 1159-1167.

Coltorti, M. (1997). Human impact in the Holocene fluvial and coastal evolution of the Marche region, Central Italy. *Catena,* **30**, 311-335.

Cooper, A. (1982). The effects of salinity and waterlogging on the growth and cation uptake of salt marsh plants. *New Phytologist,* **90**, 263-275.

Corre, J. (1992). The coastline of the Gulf of Lions: Impact of a warming of the atmosphere in the next few decades. *In*: M. J. Tooley and S. Jelgersma (eds.), *Impacts of Sea-level rise on European Coastal wetlands*. Blackwell, Oxford, 124-135.

Costa, M. and Boira, H. (1981). La vegetaciòn costera Valencia: los saladares. *Anal. Jard. Bot. Madrid,* **38**, 233-244.

Craft, C. B., Seneca, E.D. and Broome, S.W. (1991). Loss on ignition and Kjedhal digestion for estimating organic carbon and total nitrogen in estuarine marsh soils: Calibration with dry combustion. *Estuaries,* **14**, 175-179.

Craft, C. B., Seneca, E. D. and Broome, S. W. (1993). Vertical accretion in microtidal regularly and irregularly flooded estuarine marshes. *Estuarine Coastal and Shelf Science,* **37**, 371-386.

Cremers, A., Elsen, A., De Preter, P. and Maes, A. (1988). Quantitative analysis of radiocaesium retention in soils. *Nature,* **335**, 247-249.

Cristofolini, R. and Romano, R. (1982). Petrological features of Etnean volcanic rocks. *Memoir of the Italian Geological Society,* **23**, 99-116.

Cronin, T., Willard, D., Karlsen, A., Ishman, S., Verardo, S., McGeehin, J., Kerhin, R., Holmes, C., Colman, S. and Zimmerman, A. (2000). Climatic variability in the eastern United States over the past millennium from Chesapeake Bay sediments. *Geology,* **28**, 3-6.

Cundy, A. B. (1994). Radionuclide and geochemical studies of recent sediments from the Solent Estuarine System. University of Southhampton Thesis.

Cundy, A. B. and Croudace, I.W. (1995). Physical and chemical associations of radionuclides and trace metals in estuarine sediments: an example from Poole Harbour, Southern England. *Journal of Environmental Radioactivity,* **35**,191-211.

Cundy, A. B. and Croudace, I.W. (1995). Sedimentary and geochemical variations in a salt marsh/mud flat environment from the mesotidal Hamble estuary, southern England. *Marine Chemistry,* **51**, 115-132.

Cundy, A. B. and Croudace, I. W. (1996). Sediment accretion and recent sea level rise in the Solent, Southern England: Inferences from radiometric and geochemical studies. *Estuarine, Coastal and Shelf Science,* **43**, 449-467.

Cundy, A. B., Collins, P. E. F., Turner, S. D., Croudace, I. W. and Horne, D. (1998). 100 years of environmental change in a coastal wetland, Augusta Bay, southeast Sicily: evidence from geochemical and palaeoecological studies. *In*: K. S. Black D. M. Paterson and A. Cramp (eds.), *Sedimentary Processes in the Intertidal Zone*. Geological Society of London Special Publication,**139**, 243-254.

Cundy, A. B., Kortekaas, S., Dewez, T., Stewart, I. S., Collins, P. E. F., Croudace, I. W., Maroukian, H., Papanastassiou, D., Gaki-Papanastassiou, P., Pavlopoulos, K. and Dawson, A. (1999). Coastal wetlands as recorders of earthquake subsidence in the Aegean: a case study of the 1894 Gulf of Atalanti earthquakes, central Greece. *Marine Geology **in press***:

Daoust, R. J., Moore, T. R., Chmura, G. L., and Magenheimer, J. F. (1996). Chemical evidence of environmental changes and anthropogenic influences in a Bay of Fundy saltmarsh. *Journal of Coastal Research,* **12**, 520-533.

Davis, O. K. (1992). Rapid climatic change in coastal Southern California inferred from pollen anaiysis of San Joaquin marsh. *Quaternary Research,* **37**, 89-100.

Day, J. W., Scarton, F., Rismondo, A. and Are, D. (1998). Rapid deterioation of a salt marsh in Venice Lagoon, Italy. *Journal of Coastal Research*, **14**, 583-590.

Day, J. W., Rybczyk, J., Scarton, F., Rismondo, A., Are, D. and Cecconi, G. (1999). Soil accretionary dynamics, sea level rise and the survival of wetlands in Venice Lagoon: A field and modelling approach. *Estuarine Coastal and Shelf Science*, **49**, 607-628.

De Casabianca, M.-L., Laugier, T. and Marinho-Soriano, E. (1997). Seasonal changes of nutrients in water and sediment in Mediterranean lagoon with shellfish farming activity (Thau Lagoon, France). *ICES Journal of Marine Science,* **54**, 905-916.

Debussche, M., Lepart, J. and Dervieux, A. (1999). Mediterranean landscape changes: evidence from old postcards. *Global Ecology and Biogeography,* **8**, 3-15.

Delano-Smith, C. (1979). *Western Mediterranean Europe: A Historical Geography of Italy, Spain and Southern France since the Neolithic.*Academic Press, London

DeLaune, R. D., Patrick, Jr.,W.H. and Buresh, R.J. (1978). Sedimentation rates determined by 137Cs dating in a rapidly accreting salt marsh. *Nature,* **275**, 532-533.

DeLaune, R. D., Nyman, J. A. and Patrick Jr., W. H. (1994). Peat collapse, ponding and wetland loss in a rapidly submerging coastal marsh. *Journal of Coastal Research,* **10**, 1021-1030.

Di Castri, F. and Mooney, H. A. (1973). *Mediterranean type ecosystems: origin and structure.* Chapman and Hall Ltd. London

Di Grande, A., and Raimondo, W. (1982). Linee di costa Plio-Pleistocene è Schema Liostratigrafico del Quaternario Siracusano. *Estratto da Geologica Romana,* **11**, 279-309.

Di Grande, A., Raimondo, W. (1983). Lineamenti geologici del territorio siracusano tra Palazzolo, Noto e Siracusa (Sicilia sud-orientale). *Bolletino Societa Geologica Italiana* **102**, 241-260.

Dijkema, K. S. (1987). Geography of salt marshes in Europe. *Zeitschrift für Geomorphologie,* **31**, 489-499.

Dominik, J. and Stanley, D. J. (1993). Boron,beryllium and sulfur in Holocene sediments and peats of the Nile delta, Egypt: Their use as indicators of salinity and climate. *Chemical Geology,* **104**, 203-216.

Dongarra, G., Azzaro, E., Bellanca, A., Macaluso, A., Parello, F. and Badalamenti, F. (1985). Carrateristiche geochimiche di alcuni laghi ipersalini della Sicilia sud-orientale. *Rendiconti della Societa Italiana di Mineralogia e Petrologia,* **40**, 317-332.

Douglas, I. (1990). Sediment Transfer and Siltation. *In*: Turner, J. *et. al.* (eds.) *The Earth as transformed by human action: Global and regional changes in the Biosphere over the past 300 years.* Cambridge University Press, 215-234.

Douglas, T., Critchley, D., & Park, G. (1996). The deintensification of terraced agricultural land near Trevélez, Sierra Nevada, Spain. *Global Ecology and Biogeography Letters*, **5**, 258-270.

Dubar, M. and Anthony, E.J. (1995). Holocene environmental change and river mouth sedimentation in the Baie des Anges, French Riviera. *Quaternary Research,* **43**, 329-343.

Duchafour, P. (1977). *Pedology: pedogenesis and classification.* Allen & Unwin, London.

Dumas, B., Gueremy, P., Lhenaff, R., and Raffy, J. (1993). Rapid uplift, stepped marine terraces and raised shorelines on the Calabrian coast of Messina Strait, Italy. *Earth Surface Processes and Landforms,* **18**, 241-256.

Dumat, C., Cheshire, M. V., Fraser, A. R., Shand, C. A. and Staunton, S. (1997). The effect of removal of soil organic matter and iron on the adsorption of radiocaesium. *European Journal of Soil Science,* **48**, 675-683.

Dupré, M., Fumanal, M. P., Sanjaume, E., Santisteban, C., Usera, J. and Viñals, M. J. (1988). Quaternary evolution of the Pego coastal lagoon (Southern Valencia, Spain). *Palaeogeography, Palaeoclimatology, Palaeoecology,* **68**, 291-299.

Durbin, C. S. and. Henderson-Sellers, A. (1981). Meteorological importance of the volcanic activity of Mount Etna. *Weather,* **36**, 284-291.

Ehlers, J., Nagorny, K., Scmidt, P., Stieve, B. and Zietlow, K. (1993). Storm surge deposits in North Sea salt marshes dated by ^{134}Cs and ^{137}Cs determination. *Journal of Coastal Research,* **9**, 698-701.

Eisma, D. (1964). Stream deposition in the Mediterranean area in historical times. *Nature,* **23**, 1061.

Eisma, D. (1978). Stream deposition and erosion by the eastern shore of the Aegean. *In*: Brice, C. W. (ed.), *The environmental history of the near and Middle East since the Last Ice Age*. London, 67-81.

El-Daoushy, F. and Eriksson, M. G. (1998). Radiometric dating of recent lake sediments from a highly eroded area in semi-arid Tanzania. *Journal of Paleolimnology,* **19**, 377-384.

Ellison, J. C. (1996). Pollen evidence of Late Holocene mangrove development in Bermuda. *Global Ecology and Biogeography Letters,* 5, 315-326.

Ely, L. L., Webb, R. H. and Enzel, Y. (1992). Accuracy of post-bomb 137-Cs and 14-C in dating fluvial deposits. *Quaternary Research,* **38**, 196-204.

Emery, K. O., Aubrey, D. G. and Goldsmith, V. (1988). Coastal neotectonics of the Mediterranean from tide-gauge records. *Marine Geology,* **81**, 41-52.

Esselink, P., Dijkema, K.S., Reents, S. and Hageman, G. (1998). Vertical accretion and profile changes in abandoned man-made tidal marshes in the Dollard estuary, the Netherlands. *Journal of Coastal Research,* **14**, 570-580.

Facaros, D. and Pauls, M. (1986). *Italian Islands*. London, Cadogan Books.

Farmer, J. G. (1991). The perturbation of historical pollution records in aquatic sediments. *Environmental Geochemistry and Health,* **13**, 76-83.

Fernández, P. M. D. (1994). Relations between modern pollen rain and Mediterranean vegetation in Sierra-Madrona, Spain. *Review of Palaeobotany and Palynology,* **82**, 113-125.

Ferreri, G. B. and Ferro, V. (1990). Short duration rainfalls in Sicily. *Journal of Hydraulic Engineering-ASCE,* **116**, 430-435.

Firth, C., Stewart, I., McGuire, W. J., Kershaw, S. and Vita-Finzi, C. (1996). Coastal elevation changes in eastern Sicily: implications for volcano instability at Mount Etna. *In*: W. J. McGuire, Jones, A. P. and Neuberg, J. (eds.), *Volcano Instability on the Earth and Other Planets*. London, Geological Society Special Publication, **110**, 153-167.

Flemming, N. C. and Webb, C. O. (1986). Tectonic and eustatic coastal changes during the last 10, 000 years derived from archaeological data. *Zeitschrift für Geomorphologie,* **Suppl-Bd. 62**, 1-29.

Flemming, N. C. (1998). Archaeological evidence for vertical movement on the continental shelf during the Palaeolithic, Neolithic and Bronze Age periods. *In*: Stewart, I. S. and Vita-Finzi, C. (eds.), *Coastal Tectonics*. London, Geological Society Special Publication, **146**, 129-146.

Flohn, H. (1984). Climate variability and its time changes in European countries, based on instrumental observations. *In*: H. Flohn & Fantechi, R. (eds.) *The Climate of Europe Past, Present and Future. Natural and Man-induced climatic changes: a European perspective*. D. Reidel Publishing Company, Dordrecht, 65-118.

French, J. R., Spencer, T. and Stoddart, D. R. (1990). Backbarrier salt marshes of the North Norfolk coast: geomorphic development and response to rising sea-levels. *UCL Discussion Papers in Conservation,* **54**.

French, J. R. and Stoddart, D. R. (1992). Hydrodynamics of salt marsh creek systems:implications for marsh morphological development and material exchange. *Earth Surface Processes and Landforms,* **17**, 235-252.

French, J. R. and Spencer, T. (1993). Dynamics of sedimentation in a tide dominated back barrier salt marsh, Norfolk, UK. *Marine Geology,* **110**, 315-331.

Gabrielides, G. P., Golik, A., Loizides, L., Marino, M.G., Bingel, F. and Torregrossa, M.V. (1991). Man-made garbage pollution on the Mediterranean coastline. *Marine Pollution Bulletin,* **23**, 437-441.

Gale, S. J., Haworth, R. J. and Pisanu, P. C. (1995). The 210-Pb chronology of Late Holocene deposition in an Eastern Australian lake basin. *Quaternary Science Reviews,* **14**, 395-408.

Gallego-Fernandez, J. B., Garcia-Mora, M. R. and Garcia-Novo, F. (1999). Small wetlands lost: a biological conservation hazard in Mediterranean landscapes. *Environmental Conservation*, **26**, 190-199.

Gambrell, R. P. (1994). Trace and toxic metals in wetlands: a review. *Journal of Environmental Quality,* **23**, 883-891.

Gardner, L. R., Sharma, P., and Moore, W.S. (1987). A regeneration model for the effect of bioturbation by fiddler crabs on ^{210}Pb profiles in salt marsh sediments. *Journal of Environmental Radioactivity,* **5**, 25-36.

Ghebreyesus, T. A., Haile, M., Witten, K. H., Getachew, A., Yohannes, A. M., Yohannes, M., Teklehaimanot, H. D., Lindsay, S. W. and Byass, P. (1999). Incidence of malaria among children living near dams in northern Ethiopia: community based incidence survey. *British Medical Journal,* **319**, 663-666.

Gimingham, C. H. and Walton, K. (1954). Environment and the structure of scrub communities on the limestone plateaux of Northern Cyrenaica. *Journal of Ecology,* **42**, 505-520.

Goy, J. L. and Zazo, C. (1986). Synthesis of the Quaternary in the Almeria littoral; Neotectonic activity and its morphologic features, Western Betics, Spain. *Tectonophysics,* **130**, 259-270.

Grasso, M. and Lentini, F. (1982). Sedimentary and Tectonic evolution of the eastern Hyblean Plateau (south eastern Sicily) during late Cretaceous to Quaternary time. *Palaeogeography, Palaeoclimatology, Palaeoecology,* **39**, 261-280.

Grimm, E. (1991). TILIA and TILIA.GRAPH. Illinois State Museum, Illinois.

Grimshaw, H. M. (1989). Loss on ignition. *In*: Allen, S. E. (ed.), *Chemical Analysis of Ecological materials*. Blackwell Scientific Publications, Oxford, 15-16.

Grousset, F. E., Jouanneau, J. M., Castaing, P., Lavaux, G. and Latouche, C. (1999). A 70 year record of contamination from Industrial activity along the Garonne River and its tributaries (SW France). *Estuarine, Coastal and Shelf Science,* **48**, 401-414.

Grove, J. M. and Conterio, A. (1995). The climate of Crete in the 16th-Century and 17th-Century. *Climatic Change*, **30**, 223-247.

Grüger, E. (1977). Pollenanalytische Untersuchung zur wurmzeitlichen Vegetations Geschicte von Kalabrian (Suditalien). *Flora,* **166**, 475-489.

Guidoboni, E. and Traina, G. (1996). Earthquakes in Medieval Sicily. *Annali di Geofisica,* **XXXIX**, 1201-1225.

Guntenspergen, G. R., Cahoon, D. R., Grace, J., Steyer, G. D., Fournet, S., Towson and Foote, A. L. (1995). Disturbance and Recovery of the Louisiana coastal marsh landscape from the impacts of Hurricane Andrew. *Journal of Coastal Research,* **21**, 324-339.

Gutiérrez-Elorza, M. and Peña-Monnè, J. L. (1998). Geomorphology and late Holocene climatic change in Northeastern Spain. *Geomorphology,* **23**, 205-217.

Guzzardi, L. (1996). Insediamenti preistorici costieri nel Siracusano. *http://www.millecose.it/corleone/archeo/rela35.htm.* Accessed: 03/11/1997

Hardaway, C., Sheu, W, Meriwether, J. R., Sneddon, J. and Beck, J. N. (1998). The effect of diagenetic processes on the radiochronology of soft sediments using ^{210}Pb and ^{137}Cs. *Microchemical Journal,* **58**, 127-134.

Harrison, S. P., Yu, G. and Tarasov, P.E. (1996). Late Quaternary Lake-Level record from Northern Eurasia. *Quaternary Research,* **45**, 138-159.

Harvey, A. M., Miller, S.Y. and Wells, S.G. (1995). Quaternary soil and river terrace sequences in the Aguas/Feos river systems: Sorbas basin, southeast Spain. *In:* Lewin, J., Macklin, M. G. and Woodward, J. C. (eds.), *Mediterranean Quaternary River Environments*. A.A. Balkema, Rotterdam, 263-281.

Harvey, J. W., Chambers, R. M. and Hoelscher, J. R. (1995). Preferential flow and segregation of porewater solutes in wetland sediment. *Estuaries,* **18**, 568-578.

Hatton, R. S., DeLaune, R. D. and Patrick Jr.,W. H. (1983). Sedimentation, accretion, and subsidence in marshes of Barataria Basin, Louisiana. *Limnol. Oceanography,* **28**, 494-502.

Havinga, A. J. (1984). A 20-year investigation into the differential corrosion susceptibility of pollen and spores in different soil types. *Pollen et spores*, **26**, 541-548.

He, Q. and Walling, D. E. (1996). Use of fallout ^{210}Pb measurements to investigate longer-term rates and patterns of overbank sediment deposition on the floodplains of lowland rivers. *Earth Surface Processes and Landforms,* **21**, 141-154.

Heathwaite, A. L. (1993). Catchment controls on the Recent sediment history of Slapton Ley, south west England. *In*:: D. S. G. Thomas & R. J. Allison (eds.) *Landscape Sensitivity*. John Wiley & Sons Ltd., Chichester, 241-259.

Heijnis, H., Berger, G. W. and Eisma, D. (1987). Accumulation of estuarine sediment in the Dollard area: comparison of ^{210}Pb and pollen influx methods. *Netherlands Journal of Sea Research,* **21**, 295-301.

Henkin, Z., Seligman, N.G., Kafkafi, U. and Noy-Meir, I. (1998). "Effective growing days": a simple predictive model of the response of herbaceous plant growth in a Mediterranean ecosystem to variation in rainfall and phosphorous availability. *Journal of Ecology,* **86**, 137-148.

Hensel, P. F., Day, Jr., J. W. and Pont, D. (1999). Wetland vertical accretion and soil elevation change in the Rhône River delta, France: The importance of riverine flooding. *Journal of Coastal Research,* **15**, 668-681.

Hill, J., Hostert, P., Tsioutlis, G., Kasapidis, P., Udelhoven, Th. and Diemer, C. (1998). Monitoring 20 years of increased grazing impact on the Greek island of Crete with earth observation satellites. *Journal of Arid Environments,* **39**, 165-178.

HMSO (1964). *Weather in the Mediterranean.* Meteorological Office, London.

HMSO (1972). *Tables of temperature, relative humidity, precipitation and sunshine for the world (Pt.III, Europe and the Azores).* Meteorological Office, London.

Hodgkin, E. P. and Hesp, P. (1998). Estuaries to salt lakes: Holocene transformation of the estuarine ecosystems of south-western Australia. *Marine and Freshwater Research,* **49**, 183-201.

Hölzer, A. and Hölzer, A. (1998). Silicon and titanium in peat profiles as indicators of human impact. *The Holocene,* **8**, 685-696.

Hunt, C. O., Gilbertson, D. D. and Donahue, R. E. (1992). Palaeoenvironmental evidence for agricultural soil erosion from late Holocene deposits in the Montagnola Senese, Italy. *In*: Bell, M. and Boardman, J. G. (eds.), *Past and Present Soil Erosion: Archaeological and Geographical Perspectives*, Oxbow Monographs, Oxford, **22**, 163-174.

Hunt, C. O. and Gilbertson, D. D. (1995). Human activity, landscape change and valley alluviation in the Feccia Valley, Tuscany, Italy. *In*: Lewin, J., Macklin, M. G. and Woodward, J. C. (eds.), *Mediterranean Quaternary River Environments*. A.A. Balkema, Rotterdam, 167-176.

Huntley, B. (1988). Europe; Glacial and Holocene vegetation history-20 ky to Present. *In*: Huntley, B. and Webb, T. (eds.), *Vegetation History*. Kluwer Academic Publishers, Amsterdam, 341-383.

Hutchinson, S. M. and Prandle, D. (1994). Siltation in the salt marsh of the Dee Estuary derived from ^{137}Cs analysis of shallow cores. *Estuarine, Coastal and Shelf Science,* **38**, 471-478.

Issar, A. S. and Makover-Levin, D. (1996). Climate changes during the Holocene in the Mediterranean region. *In*: Issar, A. S. and Angelakis A. N. (eds.), *Diachronic climatic impacts on water resources: with emphasis on the Mediterranean region*.Springer, Barcelona, 55-75.

Istituto Geografico Militare (1969). Melilli 1:25000. Rome, Istituto Geografico Militare.

Istituto Geografico Militare (1969). Vendicari 1:25000. Rome, Istituto Geografico Militare.

Jalut, G., Amat, A.E., Mora, S.R.I., Fontugne, M., Mook, R., Bonnet, L. and Gauquelin, T. (1997). Holocene climatic changes in the Western Mediterranean: installation of the Mediterranean climate. *Comptes Rendus De L'Académie des Sciences Série II Fascicule A-Sciences de la Terre et des Planétes,* **325**, 327-334.

Jefferies, R. L. and Perkins, N. (1977). The effect on the vegetation of the additions of inorganic nutrients to salt marsh soils at Stiffkey, Norfolk. *Journal of Ecology,* **65**, 867-882.

Jenne, E. A. and Zachara, J. M. (1987). Factors influencing the sorption of metals. *In*: Dickson, K. L., Maki, A. W. and Brungs, W. A. (eds.), *Fate and effects of sediment bound chemicals in aquatic systems*. Pergammon Press, 83-97.

Jennings, S. C., Carter, R. W. G. and Orford, J. D. (1993). Late Holocene salt marsh development under a regime of rapid relative sea level rise: Chezzetcook Inlet, Nova Scotia. Implications for the interpretation of palaeomarsh sequences. *Canadian Journal of Earth Sciences,* **30**, 1374-1384.

Judson, S. (1963). Erosion and deposition of Italian stream valleys during historic times. *Science,* **140**, 898-899.

Kelly, M. G. and Huntley, B. (1991). An 11000-year record of vegetation and environment from Lago di Martignano, Latium, Italy. *Journal of Quaternary Science,* **6**, 209-224.

Kelsey, H. M., Witter, R. C. and Hemphill-Haley, E. (1998). Response of a small Oregon estuary to coseismic subsidence and postseismic uplift in the past 300 years. *Geology,* **26**, 231-234.

Khorram, S., Cheshire, H., Geraci, A.L. and Larosa, G. (1991). Water quality mapping of Augusta Bay, Italy from Landsat TM data. *International Journal of Remote Sensing,* **12**, 803-808.

King, R. (1973). *Sicily*. David and Charles, Newton Abbot.

Kirchner, G. and Ehlers, H. (1998). Sediment geochronology in changing coastal environments: Potentials and limitations of the Cs-137 and Pb-210 methods. *Journal of Coastal Research,* **14**, 483-492.

Kjerfve, B. and Magill, K. E. (1989). Geographic and hydrodynamic characteristics of shallow coastal lagoons. *Marine Geology,* **88**, 187-199.

Klimek, K., and Zawilinska, L. (1985). Trace elements in alluvia of the Upper Vistula as indicators of palaeohydrology. *Earth Surface Processes and Landforms,* **10**, 273-280.

Kosmas, C., Danalatos, N., Cammeraat, L.H., Chabart, M., Diamantopoulos, J., Farand, R., Gutierrez, L., Jacob, A., Marques, H., Martinez-Fernandez, J., Mizara, A., Moustakas, N., Nicolau, J. M., Oliveros, C., Pinna, G., Puddy, R., Puigdefabregas and Roxo, J. (1997). The effect of land use on runoff and soil erosion rates under Mediterranean conditions. *Catena,* **29**, 45-59.

Kraft, J. C., Rapp Jr., G. and Aschenbrenner, S.E. (1975). Late Holocene palaeogeography of the coastal plain of the Gulf of Messenia, Greece, and its relationships to archaeological settings and coastal change. *Geological Society of America Bulletin,* **86**, 1191-1208.

Kraft, J. C., Aschenbrenner, S.E. and Rapp, Jr., G. (1977). Palaeogeographic reconstructions of coastal Aegean archaeological sites. *Science,* **195**, 941-947.

Kraft, J. C., Kayan, I. and Erol, O. (1980). Geomorphic reconstructions in the environs of Ancient Troy. *Science,* **209**, 776-782.

Krishnaswamy, S., Lal, D., Martin, J. M. and Meybeck, M. (1971). Geochronology of lake sediments. *Earth and Planetary Science Letters,* **11**, 407-414.

Kutiel, H., Maheras, P. and Guika, S. (1996). Circulation and extreme rainfall conditions in the Eastern Mediterranean during the last century. *International Journal of Climatology,* **16**, 73-92.

Kutiel, H. and Maheras, P. (1998). Variations in the temperature regime across the Mediterranean during the last century and their relationship with circulation.*Theoretical and Applied Climatology*, **63**, 39-53.

Lamb, H. F., Gasse, F., Benkaddour, A., Elhamouti, N., Vanderkaars, S., Perkins, W.T., Pearce, N.J. and Roberts, C.N. (1995). Relation between century-scale Holocene arid intervals in tropical and temperate zones. *Nature,* **373**, 134-137.

Lamb, H. H. (1977). *Climate: Present, Past and Future: Climatic History and the Future.* Methuen, London.

Lamb, H. H. (1984). Climate in the last thousand years: natural climatic fluctuations and change. *In*: H. Flohn & Fantechi, R. (eds.), *The Climate of Europe Past, Present and Future. Natural and Man-induced climatic changes: a European perspective*. Dordrecht, D. Reidel Publishing Company, 25-64.

Lamb, H. H. (1995). *Climate, History and the Modern World.* Routledge, London.

Lambeck, K. (1996). Sea level change and shore-line evolution in Aegean Greece since upper Paleolithic time. *Antiquity,* **70**, 588-611.

Lampedusa, G. d. (1960). *The Leopard (Il Gattopardo).* Collins and Harvill, London.

Largier, J. L., Hollibaugh, J. T. and Smith, S.V. (1997). Seasonally hypersaline estuaries in Mediterranean-climate regions. *Estuarine, Coastal and Shelf Science,* **45**, 789-797.

Lasanta, T., Garca-Ruiz, J. M., Pérez-Rontomé C., & Sancho-Marcón, C. (2000). Runoff and sediment yield in a semi-arid environment: the effect of land management after farmland abandonment. *Catena,* **38**, 265-278.

Lekkas, E., Lozios, S., Skourtsos, E. and Kranis, H. (1996). Liquefaction, ground fissures and coastline change during the Egio earthquake (15 June 1995; Central Western Greece). *Terra Nova,* **8**, 648-654.

Lena, G. and Basile, B. (1986). Coastal Geomorphology and Exploitation of Lithic Resources (Latomies and Limekilns) in the Territory of Siracusa in Ancient Time.*Thalassa,* XX.

Lentini, F. (1987). Carta Geologica della Sicilia sud orientale 1:100000. Societa Elaborazioni Cartografiche, Florence.

Leroux, M. (1998). Climatic evolution in the North Atlantic/Europe/Mediterranean space. *In* Leroux, M (ed.), *Dynamic Analysis of Weather & Climate.*, John Wiley & Sons Ltd, Chichester, 304-322.

Leroy, S. A. G. (1992). Palynological evidence of *Azolla nilotica* Dec. in recent Holocene of the eastern Nile Delta and palaeoenvironment. *Vegetation History and Archaeobotany,* **1**, 43-52.

Leroy, S., Ambert, P. and Suc, J.P. (1994). Pollen record of the Saint-Macaire maar (Herault, Southern France)-A Lower Pleistocene glacial phase in the Languedoc coastal plain. *Review of Palaeobotany and Palynology,* **80**, 149-157.

Lipschitz, N. and Biger, G. (1990). Ancient dominance of the *Quercus calliprinos - Pistacia palaestina* association in Mediterranean Israel. *Journal of Vegetation Science*, **1**, 67-70.

López-Avilés, A., Ashworth, P. J. and Macklin, M. G. (1998). Floods and Quaternary sedimentation style in a bedrock-controlled reach of the Bergantes river, Ebro basin, Northeast Spain. *In*: G. Benito, V. R. Baker & Gregory K. J. (eds.) *Palaeohydrology & Environmental Change*., John Wiley & Sons Ltd, Chichester, 181-196.

Lord, C. J. and Church, T. M. (1983). The geochemistry of salt marshes: Sedimentary ion diffusion, sulfate reduction and pyritization. *Geochima et Cosmochimica Acta.* **47**, 1381-1391.

Lund-Hansen, L. C., Valeur, J., Pejrup, M., Jensen, A. (1997). Sediment fluxes, re-suspension and accumulation rates at two wind-exposed coastal sites and in a sheltered bay. *Estuarine, Coastal and Shelf Science.* **44**, 521-531.

Lyrintzis, G. and Papanastasis, V. (1995). Human activities and their impact on land degradation-Psilorites mountain in Crete: a historical perspective. *Land Degradtion and Rehabilitation.* **6**, 79-93.

Maas, G. S., Macklin, M. G. and Kirkby, M. J. (1998). Late Pleistocene and Holocene river development in Mediterranean steepland environments, southwest Crete, Greece. *In*: G. Benito, V. R. Baker & Gregory K. J. (eds.) *Palaeohydrology & Environmental Change*, John Wiley & Sons Ltd., Chichester, 153-165

Macadam, A. (1993). *Sicily*. A & C Black, London.

Mackereth, F. J. H. (1965). Chemical investigations of lake sediments and their interpretation. *Proceedings of the Royal Society.* **B161**, 295-309.

Mackereth, F. J. H. (1966). Some chemical observations of post-glacial lake sediments. *Philosophical Transactions of the Royal Society, B* **250**, 165-213.

Macklin, M. G., Lewin, J. and Woodward, J.C. (1995). Quaternary fluvial systems in the Mediterranean basin. *In*: Lewin, J., Macklin, M. G. and Woodward, J. C. (eds.), *Mediterranean Quaternary River Environments*. A.A. Balkema, Rotterdam, 1-25.

Macleod, D. A. and Vita-Finzi, C. (1982). Environment and provenance in the development of recent alluvial deposits in Epirus, northwest Greece. *Earth Surface Processes and Landforms,* **7**, 29-43.

Magazzu, G., Romeo, G., Azzaro, F., Decembrini, F., Oliva, F. and Piperno, A. (1995). Chemical pollution from urban and industrial sewages in Augusta Bay, Sicily. *Water Science and Technology,* **32**, 221-229.

Maheras, P. (1988). Changes in precipitation conditions in the Western Mediterranean over the last century. *Journal of Climatology,* **8**, 179-189.

Malatesta, A. (1985). Geologia e paleobiologia dell'era glaciale. *La Nuova Italia Scientifica,* **XX**

Manso, M. L. M. and Andres, I. M. (1993). Pollinic characters in Mediterranean salt marsh plants in relation to their pollination mechanism. *Acta Botanica Gallica,* **140**, 263-274.

Marinello, O. (1899). Spostamento della foce del Simeto (Sicilia). *Rivista Geografica Italiana,* **10**, 284-290.

Marino, M. G. (1992). Carbon Dioxide increase, Sea level rise and impacts on the Western Mediterranean: The Ebro delta case. *In*: M. J. Tooley and S. Jelgersma (eds.), *Impacts of Sea-level rise on European Coastal wetlands*. Blackwell, Oxford, **27**, 124-135.

Martin, J. and Meybeck, M. (1979). Elemental mass balance of material carried by major world rivers. *Marine Chemistry,* **7**, 173-206.

Martìn-Consuegra, E., Chisvert, N., Cáceres, L. and Ubera, J. L. (1998). Archaeological , Palynological and Geological contributions to landscape reconstructions in the alluvial plian of the Guadalquivir river at San Bernardo, Sevilla (Spain). *Journal of Archaeological Science,* **25**, 521-532.

Martinez-Fernandez, J., Lopezbermudez, F., Martinez-Fernandez, J. and Romerodiaz, A. (1995). Land-use and soil-vegetation relationships in a Mediterranean ecosystem; El Ardal, Murcia, Spain. *Catena,* **25**, 153-167.

Marty, D., Esnault, G., Caumette, P., Ranaivosonrambeloarisoa, E. and Bertrand, J. C. (1990). Denitrification, sulfate reduction and methanogenesis in the upper sediments of a Mediterranean coastal lagoon. *Oceanologica Acta,* **13**, 199-210.

Mathers, S., Brew, D. S. and Arthurton, R. S. (1999). Rapid Holocene evolution and neotectonics of the Albanian Adriatic coastline. *Journal of Coastal Research,* **15**, 345-354.

McCaffrey, R. J. and Thomson, J. (1980). A record of the accumulation of sediment and trace metals in a Connecticut salt marsh. *Advances in Geophysics,* **22**, 165-236.

McNeill, J. R. (1992). *The Mountains of the Mediterranean world: an environmental history*. Cambridge, Cambridge University Press.

Megiér, J., Folving, S. and Paracchini, M. L. (1997). Atti della giornata di studio "POP Sicilia-cartografia tematica, morfologia delle coste, erosione del suolo e gestione dei sedimenti. *EUR Report* No. 17262 IT.

Metaxas, D. A., Bartzokas, A. and Vitsas, A. (1991). Temperature fluctuations in the Mediterranean area during the last 120 years. *International Journal of Climatology,* **11**, 897-908.

Michelin (1994). *Sicilia: carte routière et touristique*. Michelin, Paris.

Money, D. C. (1965). *Climate, Soils and Vegetation.*, University Tutorial Press Cambridge.

Moore, P. D. (1990). Soils and ecology: Temperate wetlands. *In*: M. Williams (eds.), *Wetlands: A threatened landscape*. Blackwell, Oxford, 95-114.

Moore, P. D., Webb, J. A. and Collinson, M. E. (1991). *Pollen Analysis 2nd Ed.*, Blackwell Scientific Publications, Oxford.

Mourtzas, N. D. and Marinos, P.G. (1994). Upper Holocene sea level changes: Paleogeographic evolution and its impact on coastal archaeological sites and monuments. *Environmental Geology,* **23**, 1-13.

Mulargia, F., Broccio, F., Achilli, V. and Baldi, P. (1985). Evaluation of a seismic quiescence pattern in southeastern Sicily. *Tectonophysics,* **116**, 335-364.

Mulargia, F., Broccio, F., Achilli, V. and Baldi, P. (1991). Is a destructive earthquake imminent in southeastern Sicily? *Tectonophysics,* **188**, 399-402.

Naval Intelligence Division (1945). *Italy.* Naval Intelligence Division, Report No. BR.517B.

Naveh, Z. (1975). The evolutionary significance of fire in the Mediterranean region. *Vegetatio,* **29**, 199-208.

Hydrogapher of the Navy (1996). Admiralty Tide Tables (1. European Waters), HMSO London

Neboit, R. (1984). Erosion des sols et colonisation grecque en Sicile et en Grande Gréce. *Bulletin Association Géografie Français,* **499**, 5-13.

Nelson, A. R., Shennan, I., and Long, A.J. (1996). Identifying coseismic subsidence in tidal wetland stratigraphic sequences at the Cascadia subduction zone of western North America. *Journal of Geophysical Research,* **101**, 6115-6135.

Nicholls, R. J. and Hoozemans, F. M. J. (1996). The Mediterranean: vulnerability to coastal implications of climate change. *Ocean and Coastal Management* , **31**, 105-132.

Nicoletti, P. G. and Scalzo, A. (1998). Ancient landslide-dammed lakes in southeastern Sicily and their presumable contribution to malaria development: a poorly known effect of local seismicity. *International Journal of Anthropology,* **13**, 201-210.

Nicoletti, P. G. and Terranova, O. (1998). Duration of lakes dammed by old, earthquake-triggered landslides in southeastern Sicily. *Eigth International Congress International Association for Engineering Geology and the Environment*, A. A. Balkema. Vancouver, 2135-2142

Niemi, T. M. (1990). Paleoenvironmental history of submerged ruins on the northern Euboean Gulf coastal plain, Central Greece. *Geoarchaeology: An international journal,* **5**, 323-347.

Niemi, T. M. and Timothy-Hall, N. (1996). Historical changes in the tidal marsh of Tomales Bay and Olema Creek, Marin County, California. *Journal of Coastal Research,* **12**, 90-102.

Nixon, S. W., Oviatt, C. A., Garber, J. and Lee, V. (1976). Diel metabolism and nutrient dynamics in a salt marsh embayment. *Ecology,* **57**, 740-750.

Norton, S. A., Hess, C. T., Blake, G.M., Morrison, M.L. and Baron, J. (1985). Excess unsupported ^{210}Pb in lake sediment from Rocky Mountain lakes: A groundwater effect. *Canadian Journal of Fisheries and Aquatic Science,* **42**, 1249-1254.

Nozaki, Y., DeMaster, D.J., Lewis, D.M. and Turekian, K.K. (1978). Atmospheric ^{210}Pb fluxes determined from soil profiles. *Journal of Geophysical Research,* **83**, 4047-4051.

Nyman, J. A., Carloss, M., DeLaune, R. D. and Patrick, Jr., W. H. (1994). Erosion rather than plant dieback as the mechanism of marsh loss in an estuarine marsh. *Earth Surface Processes and Landforms,* **19**, 69-84.

Oenema, O. and DeLaune, R. D. (1988). Accretion rates in salt marshes in the Eastern Scheldt, south-west Netherlands. *Estuarine, Coastal and Shelf Science,* **26**, 379-394.

Orme, A. R. (1990). Wetland morphology, hydrodynamics and sedimentation. *In*: M. Williams (ed.), *Wetlands: a threatened landscape*. Blackwell, Oxford, 42-94.

Orson, R. A., Warren, R. S. and Niering, W. A. (1998). Interpreting sea level rise and rates of vertical marsh accretion in a southern New England tidal salt marsh. *Estuarine, Coastal and Shelf Science,* **47**, 419-429.

Ortiz, R., Rogel, J.A. and Alcara, F. (1995). Soil vegetation relationships in 2 coastal salt marshes in south eastern Spain. *Arid Soil Research and Rehabilitation,* **9**, 481-493.

Pacheco, P., Sintes, E. and Fornos, J. J. (1996). Geomorphology and biosedimentological characterisation of a lagoon system in a microtidal western Mediterranean embayment (Albufereta de Pollenca, Balaeric Islands). *Zeitschrift für Geomorphologie,* **40**, 117-130.

Paepe, R. R., Hadziotis, M. E. and Van Overloop, E. S. (1995). Twenty cyclic pulses of drought and humidity during the Holocene. *In*: C. W. Finkl Jr. (ed.),

Journal of Coastal Research Special Issue No. 17: Holocene Cycles: Climate, Sea Levels, and Sedimentation. CERF,**17**, 55-61.

Papazachos, B. C. and Papazachou, C.B. (1997). *The Earthquakes of Greece*. P. Ziti and Co., Athens.

Parizzi, M. G., Salgado-Labouriau, M. L. and Kohler, H. C. (1998). Genesis and environmental history of Lago Santa, southeastern Brazil. *The Holocene*, **8**, 311-321.

Patrick, W. H. and DeLaune, R. D. (1972). Characterisation of the oxidised and reduced zones in flooded soil. *Proceedings of the American Soil Science Society*, **36**, 573-576.

Pavese, M. P., Banzon, V., Colacino, M., Gregori, G. P. and Pasqua, M. (1995). Three historical data series on floods and anomalous climatic events in Italy. *In*: R. S. Bradley and Jones P. D. (eds.), *Climate since AD 1500.*, Routledge, London, 155-170.

Pecora, A. (1968). *Sicilia: Le regione d'Italia*. Unione Tipografico Editice Torinese.

Pennings, S. C. and Callaway, R. M. (1992). Salt marsh plant zonation: the relative importance of competion and physical factors. *Ecology*, **73**, 681-690.

Pennington, W. (1974). The origin of pollen in lake sediments: an enclosed lake compared with one receiving inflow streams. *New Phytologist*, **83**, 189-213.

Pennington, W., Cambray, R.S., Eakins, J.D and Harkness, D. D. (1976). Radionuclide dating of the recent sediments of Blelham Tarn. *Freshwater Biology*, **6**, 317-331.

Perez, A. S. and Remmers, G. G. A. (1997). A landscape in transition: An historical perspective on a Spanish latifundist farm. *Agriculture Ecosystems & Environment* , **63**, 91-105.

Perry, A. (1981). Mediterranean climate-a synoptic reappraisal. *Progress in Physical Geography*, **5**, 105-113.

Peyron, O., Guliot, J., Cheddadi, R., Tarasov, P., Reille, M., De Beaulieu, J, Bottema, S. and Andrieu, V. (1998). Climatic reconstruction in Europe for 18000 yrs BP from pollen data. *Quaternary Research*, **49**, 183-196.

Piatanesi, A. and Tinti, S. (1998). A Revision of the 1693 eastern Sicily earthquake and tsunami. *Journal of Geophysical Research-Solid Earth,* **103**, 2749-2758.

Pickard, G. L. and Emery, W. J. (1990). *Descriptive Physical Oceanography: An Introduction*. Pergammon Press, Oxford.

Pirazzoli, P. A. (1987). Sea-level changes in the Mediterranean. *In*: M. J. Tooley. and I. Shennan (eds.), *Sea Level Changes*. Blackwell Scientific Publications, Oxford,152-181.

Pirazzoli, P. A., Stiros, S.C., Laborel, J. and Laborel-Deugen, F. (1994). Late Holocene shoreline changes related to palaeoseismic events in the Ionian Islands, Greece. *The Holocene,* **4**, 397-405.

Planchais, N. and Parravergara, I. (1984). Pollen analysis of lagoonal and coastal sediments in the Languedoc Rousillon and in the Province of Castellon (Spain). *Bulletin de la Société Botanique de France- Actualitiés Botaniques,* **1984**, 2-4.

Platania, G. (1908-1909). Il maremoto dello Stretto di Messina del 28 dicembre 1908. *Bollettino della Societa geologica italiana,* **13**, 369-458.

Plater, A. J. and Shennan, I. (1992). Evidence of Holocene sea-level change from the Northumberland coast, eastern England. *Proceedings of the Geologists Association,* **103**, 201-216.

Poli, E. (1965). *La vegetazione altomontana dell' Etna*. Sondrio.

Prentice, I. C., Guiot, J. and Harrison, S.P. (1992). Mediterranean vegetation, lake levels and palaeoclimate at the last glacial maximum. *Nature,* **360**, 658-660.

Procelli, E. (1996). Sicily between the Early and Middle Bronze Ages: a brief survey. *In*: R. Leighton (eds.), *Early Societies in Sicily: new developments in archaeological research*. Accordia Research Centre, University of London, London, **5**, 89-101.

Provansal, M. (1995). Holocene sedimentary sequences in the Arc River delta and the Etang de Berre in Provence, southern France. *In*: Lewin, J., Macklin, M. G. and Woodward, J. C. (eds.), *Mediterranean Quaternary River Environments*. A. A. Balkema, Rotterdam, 159-165.

Purer, E. A. (1942). Plant ecology of the Coastal salt marshlands of San Diego County, California. *Ecological Monographs,* **12**, 81-111.

Puigdefábregas, J., and Mendizabal, T. (1998). Perspectives on desertification: western Mediterranean. *Journal of Arid Environments,* **39**, 209-224.

Pye, K. (1991). Aeolian dust transport and deposition over Crete and adjacent parts of the Mediterranean Sea. *Earth Surface Processes and Landforms,* **17**, 271-288.

Quine, T. A., Navas, A., Walling, D.E. and Machin, J. (1994). Soil erosion and redistribution on cultivated and uncultivated land near Las-Bardenas in the Central Ebro river basin, Spain. *Land Degradation and Rehabilitation,* **5**, 41-55.

Rackham, O. (1990). The greening of Myrtos. *In*: S. Bottema Entjes-Nieborg, G. and Van Zeist, W. (eds.), *Man's role in the shaping of the Mediterranean landscape.* A.A. Balkema, Rotterdam, 341-348.

Radakovitch, O., Charmasson, S., Arnaud, M. and Bouisset, P. (1999). ^{210}Pb and Caesium accumulation in the Rhône Delta sediments. *Estuarine, Coastal and Shelf Sciences,* **48**, 77-92.

Rae, J. E. and Allen, J. R. L. (1993). The significance of organic matter degradation in the interpretation of historical pollution trends in depth profiles of estuarine sediment. *Estuaries,* **16**, 678-682.

Ranwell, D. S. (1964). Spartina Salt Marshes in southern England: III. Rates of establishment, succession and nutrient supply at Bridgewater Bay, Somerset. *Journal of Ecology,* **52**, 95-105.

Ranwell, D. S. (1972). *Ecology of Saltmarshes and Sand Dunes.* Chapman and Hall, London.

Reboredo, F. H. S. and Ribeiro, C. A. G (1984). Vertical distribution of Al, Cu, Fe and Zn in the soil salt marshes of the Sado estuary, Portugal. *International Journal of Environmental Studies,* **23**, 249-253.

Reddaway, J. M. and Bigg, G. R. (1996). Climatic change over the Mediterranean and links to the more general atmospheric circulation. *International Journal of Climatology*, **16**, 651-661.

Reddy, K. R. and D'Angelo, E. M. (1994). Soil processes regulating water quality in wetlands. *In*: W. J. Mitsch (eds.), *Global wetlands: Old World and New*. Amsterdam, Elsevier Science, 309-324.

Redfield, A. C. (1972). Development of a New England salt marsh. *Ecological Monographs*, **42**, 201-237.

Reille, M. and Lowe, J. J. (1993). A re-evaluation of the vegetation history of the eastern Pyrenees (France) from the end of the Last Glacial to the present. *Quaternary Science Reviews*, **12**, 47-77.

Rhodes, T. E. and Davis, R. B. (1995). Effects of Late Holocene forest disturbance and vegetation change on Acidic Mud Pond, Maine, USA. *Ecology*, **76**, 734-746.

Riding, R., Braga, J.C., Martin, J.M., Sanchez-Almazo, I. M. (1998). Mediterranean Messinian Salinity cris: Constraints from a coeval marginal basin, Sorbas, southeastern Spain. *Marine Geology*, **146**, 1-20.

Ritchie, J. C., McHenry, J. R. and Gill, A. C. (1974). Fallout ^{137}Cs in the soils and sediments of three small watersheds. *Ecology*, **55**, 887-890.

Ritchie, J. C., Eyles, C.H. and Haynes, C.V. (1985). Sediment and pollen evidence for an early to mid-Holocene humid period in the eastern Sahara. *Nature*, **314**, 352-355.

Robbins, J. A., Edgington, D.N. and Kemp, A.L.W. (1978). Comparitive 210-Pb, 137-Cs, and pollen geochronologies of sediments from Lakes Ontario and Erie. *Quaternary Research*, **10**, 256-278.

Roberts, N. (1989). *The Holocene: An Environmental History*. Blackwell, Oxford.

Roberts, N. (1990). Human-induced landscape change in South and Southwest Turkey during the later Holocene. *In*: S. Bottema Entjes-Nieborg, G. and Van Zeist, W (eds.), *Man's role in the shaping of the Mediterranean landscape*. A. A. Balkema, Rotterdam, 53-67.

Robinson, C. (1994). A long record of environmental change illustrated by sediment geochemistry, Lago-Grande di Monticchio, Southern Italy. *Chemical Geology,* **118**, 235-254.

Roman, C. T., Peck, J.A., Allen, J.R., King, J.W. and Appleby, P.G. (1997). Accretion of a New England (USA) Salt marsh in response to inlet migration, storms and sea level rise. *Estuarine Coastal and Shelf Science,* **45**, 717-727.

Romero, R., Guijarro, J. A., Ramis, C. and Alonso, S. (1998). A 30-year (1964-1993) daily rainfall database for the Spanish Mediterranean regions: First exploratory study. *International Journal of Climatology*, **18**, 541-560.

Rose, J., Meng, X. and Watson, C. (1999). Palaeoclimate and palaeoenvironmental responses in the western Mediterranean over the last 140ka: evidence from Mallorca, Spain. *Journal of the Geological Society,* **156**, 435-448.

Rossignol-Strick, M., Planchais, N., Paterne, M. and Duzer, D. (1992). Vegetation dynamics and climate during the deglaciation in the south Adriatic basin from a marine record. *Quaternary Science Reviews,* **11**, 415-423.

Rossignol-Strick, M. (1995). Sea-Land correlation of pollen records in the Eastern Mediterranean for the glacial-interglacial transition: Biostratigraphy versus radiometric time-scale. *Quaternary Science Reviews,* **14**, 893-915.

Rozan, T. F., Hunter, K.S. and Benoit, G. (1994). Industrialisation as recorded in floodplain deposits of the Quinnipiac River, Connecticut. *Marine Pollution Bulletin,* **28**, 564-569.

Ruecker, G., Schad, P., Alcubilla, M. M. and Ferrer, C. (1998). Natural regeneration of degraded soils and site changes on abandoned agricultural terraces in Mediterranean Spain. *Land Degradation and Development,* **9**, 179-188.

Ruggieri, G. (1959). Geologia della zona costiera di Torre Vendicari (Sicilia sud-orientale). *Rivista Mineraria Siciliana,* **55**, 12-14.

Rull, V., Vegas-Vilarrœbia, T. and Espinoza de Pern'a, N. (1999). Palynological record of an early-mid Holocene mangrove in Eastern Venezuela.

Implications for sea-level rise and disturbance history. *Journal of Coastal Research,* **15**, 496-504.

Runnels, C. N. (1995). Environmental degradation in ancient Greece. *Scientific American,* **272**, 96-99.

Sabater, F., Sabater, S. and Armengol, J. (1990). Chemical characteristics of a Mediterranean river as influenced by land-uses in the watershed. *Water Research,* **24**, 143-155.

Sadek, L. A. and El-Darier, S. M. (1995). Cyclic vegetational change and pattern in a community of Arthrocnemum macrostachyum in Mediterranean coastal desert of Egypt. *Journal of Arid Environments,* **31**, 67-76.

Sanchez, J. M., Otero, X. L., Izco, J. (1998). Relationships between vegetation and environmental characteristics in a salt-marsh system on the coast of Northwest Spain. *Plant Ecology,* **136**, 1-8.

Schmidt, J. (1862). Sur le grand tremblement de terre qui a eu lieu en Grèce le 26 décembre 1861. *C. R. Acad. Sci. Paris,* **54**, 669-671.

Schminke, H. U., Behncke, B., Grasso, M. and Raffi, S. (1997). Evolution of the northwestern Iblean Mountains, Sicily: uplift, Pliocene/Pleistocene sea level changes, palaeoenvironment and volcanism. *Geologische Rundschaü,* **86**, 637-669.

Schumm, S. A. (1981). Evolution and response of the fluvial system; sedimentologic implications. *SEPM Special Publication,* **31**, 19-29.

Schütt, B. (1998). Reconstruction of palaeoenvironmental conditions by investigation of Holocene playa sediments in the Ebro Basin, Spain: preliminary results. *Geomorphology* **23**, 273-283.

Serra, A. (1973). Meteorological situations associated with Autumn floods in S. Italy during the 50 year period 1920-70. *Rivista di Meteorologia Aeronautica,* **33**, 43-53.

Sestini, G. (1992). The impact of climatic changes and sea-level rise on two deltaic lowlands of the Eastern Mediterranean. *In*: M. J. Tooley and Jelgersma, S. (eds.), *Impacts of Sea-level rise on European Coastal wetlands*. Blackwell, Oxford, **27**, 124-135.

Shackelton, J. C., and van Andel, T.H. (1980). Prehistoric shell assemblages from Franchthi cave and evolution of the adjacent coastal zone. *Nature,* **288**, 357-9.

Sheffield, A. T., Healy, T.R. and McGlone, M.S. (1995). Infilling rates of a steepland catchment estuary, Whangamata, New Zealand. *Journal of Coastal Research,* **11**, 1294-1308.

Shiber, J. G. (1982). Plastic pellets on Spain's "Costa del Sol" beaches. *Marine Pollution Bullettin,* **13**, 409-412.

Shiber, J. G. (1987). Plastic pellets and tar on Spain's Mediterranean beaches. *Marine Pollution Bulletin,* **18**, 84-86.

Siegel, F. R., Gupta, N., Shergill, B., Stanley, D.J. and Gerber, C. (1995). Geochemistry of Holocene sediments from the Nile Delta. *Journal of Coastal Research,* **11**, 415-431.

Silander, J. A. and Antonovics, J. (1982). Analysis of interspecific interactions in a coastal plant community-a perturbation approach. *Nature,* **298**, 557-560.

Simpson, G. C., Mossman, R. G., Walker, G., Clayton, F. L. and Exner, F., Ed. (1927). World Weather records pre-1921. *Smithsonian Miscellaneous Collections.* Smithsonian Institution, Washington.

Simpson, G. C., Mossman, R. G., Walker, G. and Clayton, F. L. (1934). World Weather records 1921-1930. *Smithsonian Miscellaneous Collections*. Smithsonian Institution, Washington.

Sneh, Y. and Klein, M. (1984). Holocene sea level changes at the Coast of Dor, South east Mediterranean. *Science,* **26**, 831-832.

Soter, S. (1998). Holocene uplift and subsidence of the Helike Delta, Gulf of Corinth, Greece. *In*: Stewart, I. S. and Vita-Finzi, C. (eds.), *Coastal Tectonics*. London, Geological Society of London Special Publication,**146**, 41-56.

Soter, S. (1999). Macroscopic seismic anomalies and submarine pockmarks in the Corinth-Patras rift, Greece. *Tectonophysics,* **308**, 275-290.

Stansell, J. (1990). A Mediterranean holiday from pollution. *New Scientist*, **126**, 28-29.

Stevenson, A. C. (1985). Studies in the vegetational history of S.W. Spain: II. Palynological investigations at Laguna de Las Madres S.W. Spain. *Journal of Biogeography*, **12**, 293-314

Stevenson, A. C. and Battarbee, R. W. (1991). Paleocological and documentary records of recent environmental change in Garaet el Ichkeul - a seasonally saline lake in NW Tunisia. *Biological Conservation*, **58**, 275-295.

Stewart, I. S., Cundy, A., Kershaw, S. and Firth, C. (1997). Holocene coastal uplift in the Taormina area, Northeastern Sicily: Implications for the southern prolongation of the Calabrian Seismogenic belt. *Journal of Geodynamics*, **24**, 37-50.

Suc, J. P. (1984). Origin and evolution of the Mediterranean vegetation and climate in Europe. *Nature*, **307**, 429-432.

Szeicz, J. M., Zeeb, B. A., Bennett, K. B. and Smol, J. P. (1998). High resolution paleoecological analysis of recent disturbance in a southern Chilean *Nothofagus* forest. *Journal of Paleolimnology*, **20**, 235-252.

Tadjiki, S. and Erten, H.N. (1994). Radiochronology of sediments from the Mediterranean Sea using natural Pb-210 and fallout Cs-137. *Journal of Radioanalytical and Nuclear Chemistry*, **181**, 447-459.

Tagliapietra, D., Pavan, M. and Wagner, C. (1998). Macrobenthic community changes related to eutrophication in Palude della Rosa (Venetian Lagoon, Italy). *Estuarine Coastal and Shelf Science*, **47**, 217-226.

Tarasov, P. E., Cheddadi, R., Guiot, J., Bottema, S., Peyron, O., Belmonte, J., Ruiz-Sanchez, V., Saadi, F. and Brewer, S. (1998). A method to determine warm and cool steppe biomes from pollen data; application to the Mediterranean and Kazakhastan regions. *Journal of Quaternary Science*, **13**, 335-344.

Thirgood, J. V. (1981). *Man and the Mediterranean Forest: A history of resource depletion*. Academic Press, London.

Thorndycraft, V., Hu, Y., Oldfield, F., Crooks, P.R.J. and Appleby, P.G. (1998). Individual flood events detected in the recent sediments of the Petit Lac d'Annecy, eastern France. *The Holocene,* **8**, 741-746.

Throckmorton, P. and Throckmorton, J. (1973). The Roman wreck at Pantano Longarini. *International Journal of Nautical Archaeology,* **2.2**, 243-266.

Tivy, J. (1993). *Biogeography: A Study of Plants in the Ecosphere*. Longman, London.

Tomczak, M. and Godfrey, J. S. (1994). Regional Oceanography: An Introduction. Pergamon Press, 300-309.

Tooley, M. J. and Jelgersma, S. (1992). The future of the European coastal lowlands. *In*: M. J. Tooley and Jelgersma, S. (eds.), *Impacts of sea-level rise on European Coastal lowlands*. Blackwell, Oxford, **27**, 219-250.

Tsimplis, M. N. (1997). Collection and analysis of monthly mean sea level data in the Mediterranean and the Black sea. *Journal of Coastal Research,* **13**, 534-544.

Tzedakis, P. C. (1993). Long-term tree populations in northwest Greece through multiple Quaternary climatic cycles. *Nature,* **364**, 437-440.

Ulzega, A. and Hearty, P. J. (1986). Geomorphology, stratigraphy and geochronology of late Quaternary marine deposits in Sardinia. *Zeitschrift für Geomorphologie,* **62**, 119-129.

U.S. Department of Commerce (1959). *World Weather Records 1941-1950.* Washington D. C.

Vallettesilver, N. J., Bricker, S. B. and Salomons, W. (1993). Historical trends in contamination of estuarine and coastal sediments: an introduction to the dedicated issue. *Estuaries,* **16**, 575-576.

Van Andel, T. H. (1989). Late Quaternary sea-level changes and archaeology. *Antiquity,* **63**, 733-745.

Van Andel, T. H., Zangger, E. and Demitrack, A. (1990). Land Use and soil erosion in Prehistoric and Historical Greece. *Journal of Field Archaeology,* **17**, 379-96.

Victor, R., Victor, J. R. and Clarke, N. V. (1997). Physical and chemical environment of Khawr Mugsayl, a coastal lagoon in southern Oman. *Journal of Arid Environments,* **36**, 1-14.

Viles, H. and Spencer, T. (1995). *Coastal Problems: Geomorphology, ecology and society at the coast.* Arnold, London.

Viñals, M. J. and Fumanal, M. P (1995). Quaternary development and evolution of the sedimentary environments in the Central Mediterranean Spanish coast. *Quaternary International,* **29/30**, 119-128.

Vita-Finzi, C. (1964). Synchronous stream deposition throughout the Mediterranean area in historical times. *Nature,* **202**, 1324.

Vita-Finzi, C. (1964). Stream deposition in the Mediterranean area in historical times. *Nature,* **204**, 1061.

Vita-Finzi, C. (1969). *The Mediterranean Valleys.* Cambridge University Press, Cambridge.

Vita-Finzi, C. (1976). Diachronism in Old World alluvial sequences. *Nature* **263**, 218-219.

Vita-Finzi, C. (1986). *Recent Earth Movements: an introduction to neotectonics.* University Press, Cambridge.

Waller, M. P. (1998). An investigation into the palynological properties of fen-peat through multiple pollen profiles from south-eastern England. *Journal of Archaeological Science,* **25**, 631-642.

Walling, D. E., Quine, T.A., and Rowan, J.S. (1992). Fluvial transport and redistribution of Chernobyl fallout radionuclides. *Hydrobiologia,* **235/236**, 231-246.

Williams, T. P., Bubb, J.M. and Lester, J.N. (1994). Metal accumulation within salt marsh environments: a review. *Marine Pollution Bulletin,* **28**, 277-290.

Wilson, R. J. A. (1996). *Archaeology in Sicily 1988-95.* Council of the Society for the Promotion of Hellenic Studies/British School at Athens. Report No, **42**, 59-123.

Windom, H. L., Schroop, S. S., Calder, F. D., Ryan, J. D., Smith, R. G. and Rawlinson, C. H. (1989). Natural trace metal concentrations in estuarine and coastal marine sediments of the southeast United States. *Environmental Science and Technology,* **23**, 314-320.

Windom, H. L., Niencheski, L. F. and Smith, Jr., R. G. (1999). Biogeochemistry of nutrients and trace metals in the estuarine region of the Patos lagoon (Brazil). *Estuarine, Coastal and Shelf Science,* **48**, 113-123.

Wise, S. M. (1980). Caesium-137 and Lead-210: A review of the techniques and some applications in geomorphology. *In*: Cullingford, R. A., Davidson, D. A. and Lewin, J. (eds.), *Timescales in Geomorphology*. John Wiley & Sons Ltd, Chichester, 109-127.

Wohlfarth, B., Holmquist, B., Cato, I. and Linderson, H. (1998). The climatic significance of clastic varves in the Ångermanälven Estuary, northern Sweden, AD 1860 to 1950. *The Holocene* **8**, 521-534.

Woo, H. J., Oertel, G. F., Kearney, M. S. (1998). Distribution of pollen in surface sediments of a barrier-lagoon system, Virginia, USA. *Review of Palaeobotany and Palynology,* **102**, 289-303.

Woodward, J. C. (1995). Patterns of erosion and suspended sediment yield in Mediterranean river basins. *In*: I. D. L. Foster, Gurnell, A. M. and Webb, B. W. (eds.) *Sediment and Water Quality in River Catchments*. John Wiley and Sons Ltd., Chichester, 365-389.

Woolf, S. (1979). *A history of Italy 1700-1860; The social constraints of political change*. London, Methuen and Co Ltd.

Wright, J., H. E., McAndrews, J. H. and van Zeist, W. (1967). Modern pollen rain in western Iran and its relation to plant geography and Quaternary vegetational history. *Journal of Ecology,* **55**, 415-443.

Yaalon, D. H. (1997). Soils in the Mediterranean region: What makes them different?. *Catena,* **28**, 157-169.

Yll, E., Perez-Obiol, R., Pantaleon-Cano, J. and Roure, J. M. (1997). Palynological evidence for Climatic and Human activity during the Holocene on Minorca (Balearic Islands). *Quaternary Research,* **48**, 339-347.

Zalidis, G. C., Mantzavelas, A. L. and Gourvelou, E. (1997). Environmental impacts on Greek Wetlands. *Wetlands,* **17**, 339-345.

Zedler, J. B., Covin, J., Nordby, C. and Williams, P. (1986). Catastrophic events reveal the dynamic nature of salt-marsh vegetation in Southern California. *Estuaries,* **9**, 75-80.

Zhang, X., Quine, T. A. and Walling, D. E. (1998). Soil erosion rates on sloping cultivated land on the Loess Plateau near Ansai, Shaanxi Province, China: An investigation using Cs-137 and rill measurement. *Hydrological Processes,* **12**, 171-189.

Zonneveld, K. A. F. (1996). Palaeoclimatic reconstruction of the last deglaciation (18-8ka BP) in the Adriatic Sea region; A land-sea correlation based on palynological evidence. *Palaeogeography, Palaeoclimatology, Palaeoecology,* **122**, 89-106.

Zwolsman, J. J. G., Berger, G. W. and Van Eck, G. T. M. (1993). Sediment accumulation rates, historical input, post-depositional mobility and retention of major elements and trace metals in salt marsh sediments of the Scheldt estuary, SW Netherlands. *Marine Chemistry,* **44**, 73-94.

Zwolsman, J. J. G., van Eck, G.T.M. and Burger, G. (1996). Spatial and temporal distribution of Trace metals in sediments from the Scheldt Estuary, South-west Netherlands. *Estuarine, Coastal and Shelf Science,* **43**, 55-79.

APPENDIX I

Historical Maps of South-East Sicily

Appendix I (i).
Map of south east Sicily (1700) Hubert Iaillot.

no scale

Appendix I (ii)
Map of south east Sicily (1720) German Military

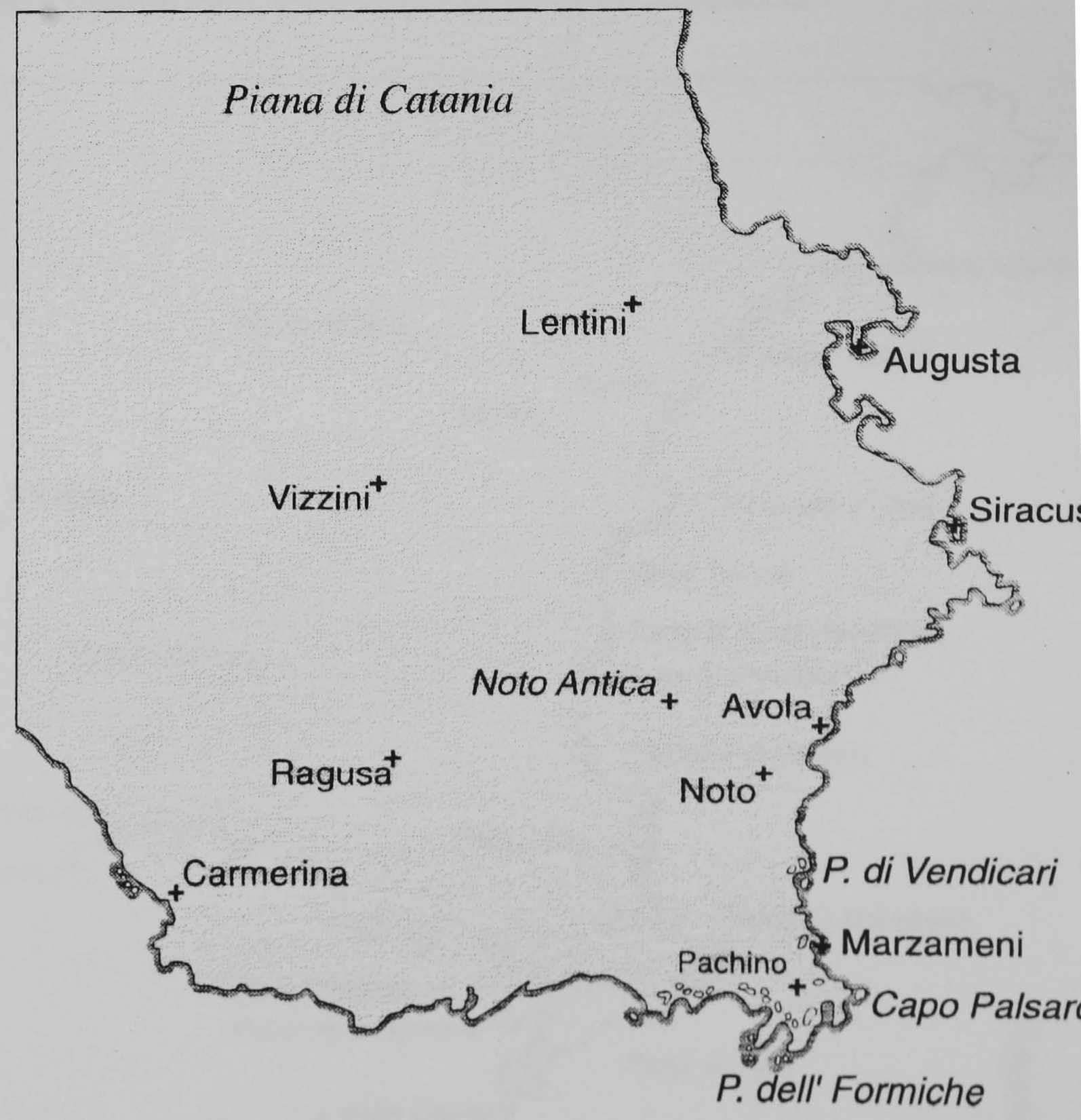

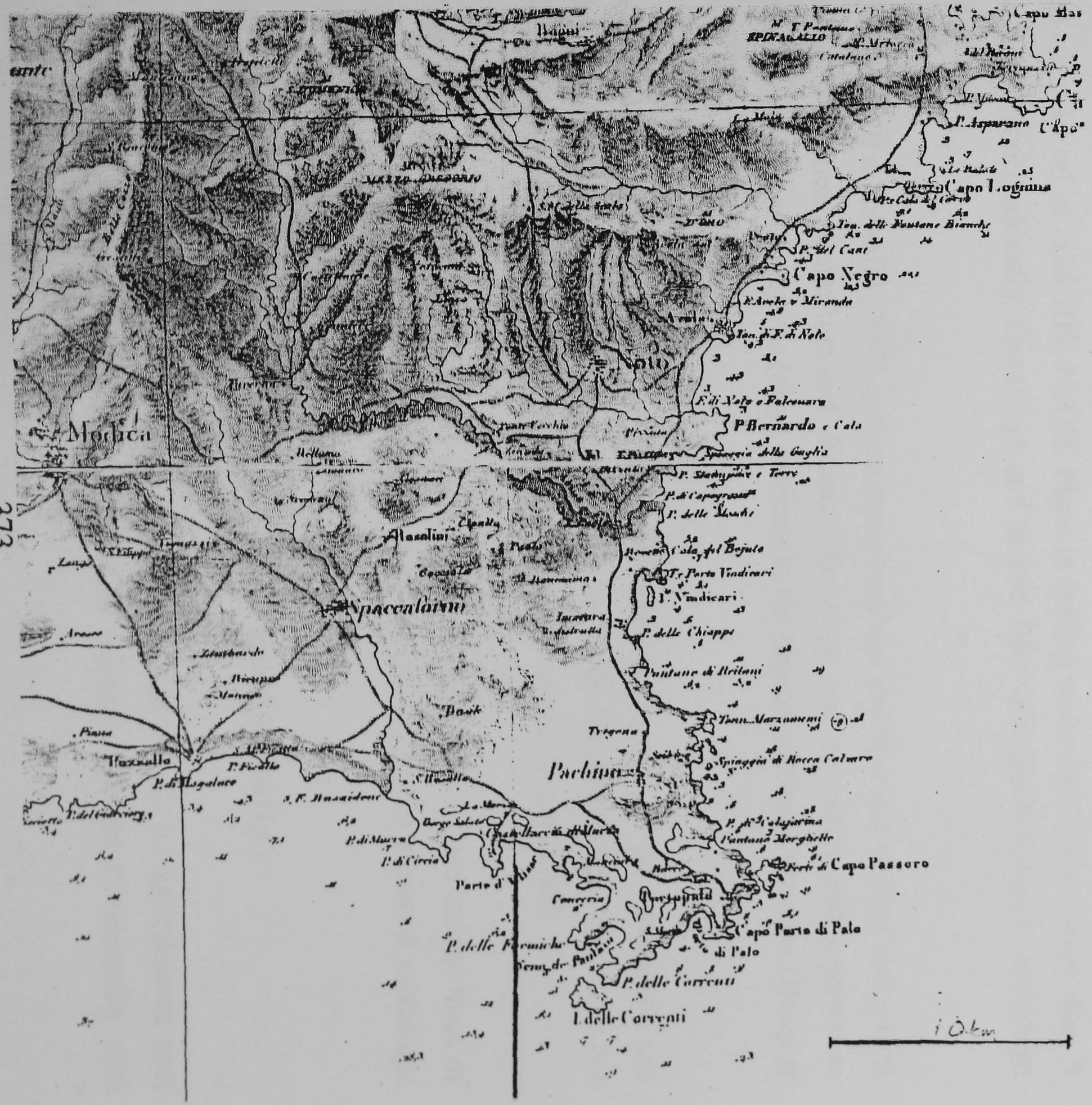

Appendix I (iii)
Map of south east Sicily (1826) Captain Smyth RN

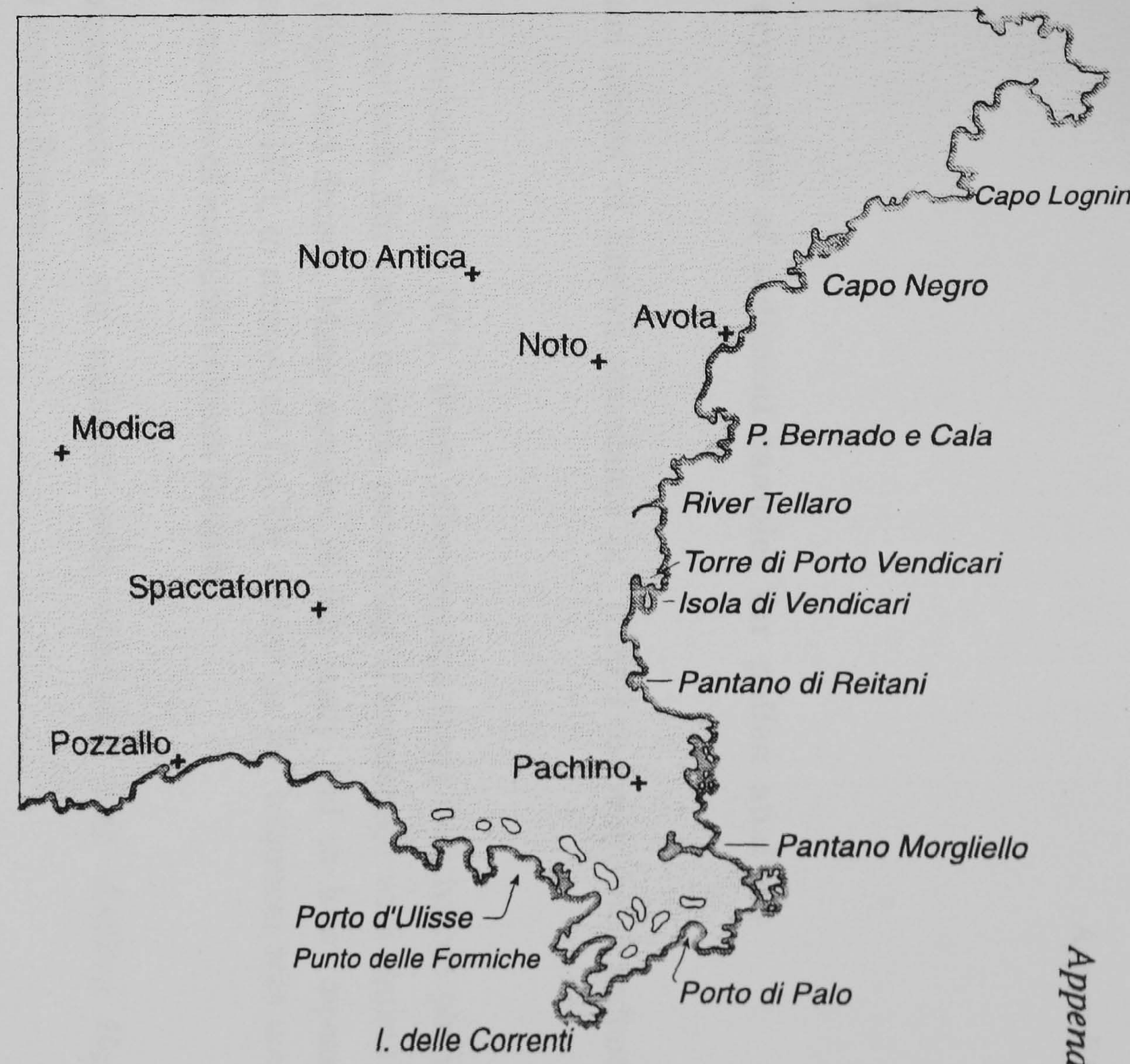

APPENDIX II

Procedure for preparation of sediment samples for pollen analysis

1. Add *Lycopodium* tablets of known abundance (c. 10000) to oven dried sediment samples.

2. Add *circa* 10% solution of cold HCl. When effervescence stops, stir before placing tube in boiling water bath. Stir again in bath, preventing effervescence with squirts of acetone. Centrifuge and decant. Many samples in this study had to have repeated additions of fresh 10% HCl, to remove all $CaCO_3$ before the HF treatment was used, to prevent the formation of insoluble calcium fluoride.

3. Decant HCl supernatent and stir sediment with whirlymix with distilled H_2O. Centrifuge and decant. Repeat.

4. Add *circa* 10 ml of cold 10% NaOH. Place in boiling water bath for no more than 5 minutes. Stir occasionally. Centrifuge and decant. Mix with distilled water, centrifuge and decant.

5. Add *circa* 10 ml of mild (10%) sodium pyrophosphate and heat in a boiling water bath for 10-20 minutes, centrifuge and decant. This stage was necessary and repeated to remove very fine minerogenic (clay) particles in the lagoon sediment samples (Bates *et al.* 1978).

6. Strain and wash sample through a fine mesh screen (150 μm) into polypropylene test tube (20 ml). Wash residue on screen thoroughly with distilled water, and store for analysis under binocular microscope. Ensure wash of sample is contained.

7. Wash strained sample with distilled water at least 5 times until brown colour trace of organic material removed. Mix thoroughly with whirlymix before repeated centrifuge and decanting.

8. Add 10% HCl, stir, centrifuge and decant. Repeat with distilled H_2O.

9. In fume cupboard, wearing full protective clothing add *ca.* 10 ml hydrofluoric acid (HF). Place tube in boiling water bath for 20 minutes, stirring occasionally with

polythene rods. Centrifuge and decant HF supernatent into neutralising sodium carbonate solution. Refill tube with 10% HCl and place in boiling water bath for about 20 minutes, stirring occasionally. Centrifuge and decant. Stage 9 may be repeated one or more times if sediment is very minerogenic

10. Add *circa* 10 ml distilled H_2O, stir, centrifuge and decant.

11. Add *circa* 10 ml glacial acetic acid, stir, centrifuge and decant.

12. Add 9:1 ratio of acetic anhydride and concentrated sulphuric acid (Erdtmans acetolysis solution), stir and place tube in boiling water bath for 3 minutes, stirring after 1.5 minutes. Remove tube from bath and fill with glacial acetic acid, centrifuge and decant.

13. Add *circa* 10 ml glacial acetic acid, stir, centrifuge and decant.

14. Add 10% NaOH to obtain correct pH for subsequent staining, stir, centrifuge and decant.

15. Add distilled H_2O, stir, centrifuge and decant.

16. Add 1 or 2 drops of fuchsin to fluid glycerol. Add stained glycerol to warmed sediment sample in test tube. Stir. Using pipette add drops of mixture to warmed microscope slide. Add glass coverslip and allow to cool and set on flat surface. Label slide for storage and counting.

    Large coverslips (50mm x 20 mm) were used due to low pollen numbers and the dominance of single types in samples, i.e. Chenopodiaceae and Lactuceae. The entire slide area was often covered during counting.

APPENDIX III

Laboratory procedure and methodology for determining ^{210}Pb activity

Proxy method using alpha spectrometric determination of ^{210}Po following acid leaching and auto-deposition onto Ag discs (After Flynn, 1968).

1. Weigh 1-3 g of dry, powdered sediment accurately, into a 250ml beaker. Tare scales to zero. Add ca. 0.5 ml tracer (4.86 dpm/ml) and record mass of tracer added immediately.

2. Add 50 ml aqua regia (3:1 HCl:HNO_3). Add slowly to avoid vigorous reaction with organic material in sample. Leave for 3-5 hours.

3. Decant excess acid off from sediment and retain. Reapply aqua regia or add 30 ml 6M HCl. Cover and reflux on a hotplate for 4 hours.

4. Allow to cool and then filter. Strain residue 3 times with distilled H_2O. After this stage the sediment residue may be disposed of.

5. Collect supernatant in a 250 ml conical flask and carefully evaporate to dryness, without excessive boiling.

6. Re-dissolve in a small volume of concentrated HCl and evaporate to dryness. Repeat.

7. Re-dissolve in 5.5 ml 6M HCl. Transfer to a polonium plating cell (thoroughly cleaned 100 ml beaker). Wash the conical flask several times with distilled H_2O and add washings to cell. Make volume of liquid in cell up to 40 ml (using H_2O) at which point the molarity of the acid will be approximately 0.8 M.

8. Add approximately 1.5 g ascorbic acid (reducing agent) to the cell and stir until solution changes to a pale yellow/green colour.

9. Add freshly cleaned and polished Ag disc in plastic disc holder.

10. Leave to plate for 36 hours on a warm hot plate with cover glass.

11. Inspect cell during early stages of plating to ensure disc is not discolouring (i.e. turning black). Replace if necessary with fresh disc.

12. At end of plating, remove disc and wash with distilled H_2O, followed by acetone and leave covered by a crystallising dish for minimum of 24 hours before counting.

13. Counting was performed on an ORTEC alpha spectrometer (576A) with a multi-channel analyser, with samples under vacuum to prevent energy loss of alpha particles. Samples were counted for at least 80,000 seconds, giving a maximum error of 5% for the cores. Longer sample runs were occasionally used (160000-240000 seconds) for samples of increased depth/age to reduce count error. Total ^{210}Pb activity was determined for each sample by measuring the peak differences between ^{209}Po and ^{210}Po thus:

$$= \left(\frac{\text{210Po peak}}{\text{sample mass}} \right) \Big/ \left(\frac{\text{209Po peak}}{\text{sample mass}} \times \left(\frac{\text{209Po spike}}{60} \right) \right.$$

APPENDIX IV

Determination of major and trace elements of sediment samples.

(a) Sample preparation for major element determination

1. Oven dried sediment samples were powdered by a motorised agate pestle and mortar for 2 minutes.

2. Sediment samples were combusted at 850°C for 24 hours to remove carbonates. Sediment samples from core PPB were combusted at 900°C for 24 hours to ensure the removal of carbonate-shell material.

3. Accurately weigh 0.8 g (within error of ± 0.0005) of powdered and combusted sample and add to exactly 4 g of general purpose "eutectic" flux (4 lithium metaborate : 1 lithium tetraborate).

4. Fuse flux and powdered sample by melting sample at 1150°C in platinum crucible and pour in to platinum mould. Allow to cool ready for XRF.

(b) Sample preparation for trace element determination

1. Oven dried sediment samples powdered by a Tema gyratory swing mill (motorised pestle and mortar) for 20 seconds.

2. Powdered sample made into 20g pressed powder pellets and inserted into XRF.

APPENDIX V

Proxy measurement of organic content by using loss on ignition

- Consecutive 1 cm depth sediment samples were extracted from cores by a clean scalpel blade, removing approximately 1 cm^3 of the sediment. Shell and coarse clastic materials were not removed prior to combustion.

- Sediment samples were oven dried (50°C for 24 hours) and powdered by pestle and mortar.

- Powdered sediment was then added to ceramic crucibles and re-weighed. Sediment samples were combusted; first at 550°C for 2 hours then 12 hours at 850°C in a vented furnace.

- Crucibles were weighed immediately, after sufficient cooling in a dry atmosphere. Loss on ignition was then calculated as a percentage of mass lost during combustion (e.g. Grimshaw, 1989):

$$\text{Loss on ignition (\%)} = \left(\frac{\text{post combustion loss (g)}}{\text{pre - combustion mass (g)}} \right) \times 100$$

APPENDIX VI

Core descriptions from field areas and transects

Marsh sediment sequences determined at the Mulinello estuary, Augusta, SE Sicily

Core Site	*Core units (cm)*		*Unit description*	*Other core features*	
Mulinello AMC (a)	00-06	**D**	Organic mud	Abundance of shells on top	
	06-35	**C**	Fe-stained brown-grey silty mud	16 17-18 22-30 30-35	0.5 cm sand layer fine silver sand shelly sand and silt red-brown colour
	35-75	**B**	Grey clay silt interspersed with black organic "smears"	72	black, wood fragment
	75-84	**A**	Dark grey mud and shell framents. Sand at base		

Core Site	*Core units (cm)*		*Unit description*	*Core features*	
Mulinello AMC (b)	00-09	**D**	Surface organic rich mud		
	09-36	**C**	Brown-grey silty mud	17 22-22 26 34-35	thin sand layer thin sand layer thin sand layer sand layer
	36-82	**B**	Fe-mottled, grey silt clay	40 54 70	Fe-staining wood fragments sea grass ball
	< 82	**A**	No collection in shelly-sand	82	shelly sand

Core Site	*Core units (cm)*		*Unit description*	*Core features*	
Mulinello AMC A3	00-13	**E**	Dark black silty mud		
	13-23	**D**	Grey sand-silt	16	Fe-mottling
	23-60	**B**	Grey silty mud	40 54	shell concentration wood fragments
	60-115	**A**	Grey, compact silt mud	70-73 82	increasing sand coarse clastics at base

Marsh sediment sequences determined at the Mulinello estuary, Augusta, SE Sicily

Core Site	*Core units (cm)*		*Unit description*	*Other core features*
Mulinello AMC (c)	00-03	**E**	Surface organic mud	
	03-30	**D**	Dark grey-brown mud	4 laminated clays 22 Fe staining 30 smooth clay horizon
	30-70	**C**	plastic, grey clay-silt	30-45 grey-brown colour 55 large gastropod shell
	70-75	**B**	grey clay-shelly sand	75 clay-sand contact
	75-1.85	**A**	shelly sand	fragmentary collection

Core Site	*Core units (cm)*		*Unit description*	*Core features*
Mulinello AMC (d)	00-08	**D**	Surface organics	05-08 Grey-d.brown laminae
	08-40	**C**	Grey-brown clay-silt	35-40 clay and sand mix
	40-110	**B**	Dark brown clay silt and increasing shell content	50 shell horizon 55 shell horizon 60 shell fragments 65 compact clay horizon 80 *Cerastoderma* valve 100 Crab carapace
	110-165	**A**	Shell and grey silt	160 Shell fragments and strong H_2S aroma.

Sediment sequences determined at Pantano Piccolo, Vendicari, SE Sicily

Core Site	*Core units (cm)*		*Unit description*	*Other core features*
Pantano Piccolo (PP1)	00-12	E	Vegetal-rich organic detritus	
	12-35	D	Brown-grey silty-clay	33 Black organic horizon
	35-40	C	Shell-rich grey mud	37 Whole *Cerastoderma*
	40-49	B	Low shell content, grey clay/silt	
	50-58	A	Orange-brown clay. Dry and compact. Gravel clasts	Abrupt A/B contact

Core Site	*Core units (cm)*		*Unit description*	*Other core features*
Pantano Piccolo (PP2)	00-06	D	Vegetal-rich organic detritus	*Pirenella conica / Hydrobia*
	06-35	C	Grey silty-clay	26 brown organic horizon 29 shell horizon 33 smooth clay layer
	35-48	B	Lighter grey-yellow silty clay	Abrupt AB contact
	48-55	A	Orange-brown clay. Dry and compact. Lighter mottling.	49 3 cm calcarenite clast

Core Site	*Core units (cm)*		*Unit description*	*Other core features*
Pantano Piccolo (PP 3)	00-07	D	Vegetal-rich organic detritus	Strong H_2S aroma
	07-44	C	Dark grey silty-clay	22 Thin organic horizon 23 Shell concentration 36 *Cerastoderma* valve
	25-44	B	Lighter grey shelly mud	44 *Hydrobia* conc.
	44-58	A	Orange-brown clay. Dry and compact. Gravel clasts	52 Angular gravel clasts 58 Solid basal strata

Sediment sequences determined at Pantano Piccolo, Vendicari, SE Sicily

Core Site	*Core units (cm)*	*Unit description*		*Other core features*
Pantano Piccolo (PP 4)	00-05	**C**	Vegetal-rich organic detritus	
	05-25	**B**	Dark grey silty-clay	20-23 Saturated silty sand
	25-37	**A**	Orange-brown clay. Dry and compact. Gravel clasts	25 Gravel clasts 30 Angular gravel clasts 58 Solid basal strata

Core Site	*Core units (cm)*	*Unit description*		*Other core features*
Pantano Piccolo (PP 5)	00-04	**D**	Vegetal-rich organic detritus	
	04-33	**C**	Dark grey silty-clay	20 - 22 shell concentration
	22-33	**B**	Lighter grey silt-mud	25 Gravel clasts 30 Grey-orange colour
	33-48	**A**	Orange-brown clay. Dry and compact. Gravel clasts	48 Solid basal strata

Core Site	*Core units (cm)*	*Unit description*		*Other core features*
Pantano Piccolo (PP 6)	00-04	**D**	Vegetal-rich organic detritus	
	04-28	**C**	Dark grey silty-clay and shells	6 Thin sand horizon
	20-28	**B**	Lighter grey shelly mud	20 *Cerastoderma* valve
	28-32	**A**	Orange-brown clay. Dry and compact. Gravel clasts	29 Gravel fragments 32 Solid basal strata

Sediment sequences determined at Pantano Piccolo, Vendicari, SE Sicily

Core Site	*Core units (cm)*		*Unit description*	*Other core features*	
Pantano Piccolo (PP 7)	00-15	**C**	Grey sand-silt	No surface organic 12-15	Clay horizon
	15-30	**B**	Grey silty-clay and shells	21	Shell horizon
				26	Shell horizon
				29	Shell horizon
	30-49	**A**	Orange-brown clay. Dry and compact. Gravel clasts	32	rounded pebble
				49	impenetrable base

Core Site	*Core units (cm)*		*Unit description*	*Other core features*	
Pantano Piccolo (PP 8)	00-06	**C**	Vegetal-rich organic detritus		
	06-36	**B**	Dark grey silty-clay and shells	19	Shell concentration
	36-46	**A**	Orange-brown clay. Dry and compact. Gravel clasts	38	Angular gravel clasts

Core Site	*Core units (cm)*		*Unit description*	*Other core features*	
Pantano Piccolo (PPC)	00-11	**E**	Saturated silt-vegetal organics		
	11-19	**D**	Brown silt and vegetal organics	19-20	grey-yellow clay
	19-63	**C**	Brown-grey, clay-silt	63	Sand horizon
	63-78	**B**	Fibrous plant material with low grey mud content	91	impenetrable clastics
	78-91	**A**	Sand and vegetal fragments Calcarenite clasts Reed and root stems		